Rhino-Orbito-Cerebral Mucormycosis

Nishi Gupta
Santhosh G. Honavar
Editors

Springer

Rhino-Orbito-Cerebral Mucormycosis

Nishi Gupta • Santhosh G. Honavar
Editors

Rhino-Orbito-Cerebral Mucormycosis

Springer

Editors
Nishi Gupta
Department of Otorhinolaryngology
& Head & Neck Surgery
Dr Shroff Charity Eye Hospital
Daryaganj, Delhi, India

Santhosh G. Honavar
Department of Ophthalmic Plastic
Surgery and Orbital Diseases
Centre for Sight, Banjara Hills
Hyderabad, India

ISBN 978-981-16-9728-9 ISBN 978-981-16-9729-6 (eBook)
https://doi.org/10.1007/978-981-16-9729-6

This Springer imprint is published by the registered company Springer Nature Singapore Pte Ltd. The registered company address is: 152 Beach Road, #21-01/04 Gateway East, Singapore 189721, Singapore

Dedicated to all those who have perished as a result of this dreadful disease, as well as the families who have borne the anguish of mutilating treatments on their loved ones while staying strong.

Foreword

This book authored and edited by Drs Nishi Gupta and Santhosh Honavar provides invaluable information on Rhino-Orbital-Cerebral Mucormycosis (ROCM). Not commonly encountered in most developed countries, ROCM labelled as "Black Fungus" made headlines all over the world, as it blazed, fast and furious, through the sub-continent of India, creating an avalanche of cases, during the second wave of Covid-19 pandemic, that took place for several months in 2021. Almost 50000 cases were reported in three months ending July 2021.

This book is a compilation of personal and institutional experiences of several authors who risked their lives to fight this deadly disease. The challenges faced were insurmountable, but they fought valiantly. The battle is far from over and the fight against Covid-19 related mucormycosis continues.

The large number of cases led to a better understanding of this disease and its management which is expressed in this book. Each individual chapter provides invaluable up-to-date information on all aspects of ROCM including aetiology, pathophysiology, clinical behaviour, clinical features, diagnostic modalities, histopathology and treatment.

A debate on classification and prognostic guidance for ROCM has also been proposed. All chapters are accompanied with images and illustrations to provide for a better understanding. As an example, the chapter on histopathol-

ogy is accompanied with excellent pictures showing some rarely seen histological features.

The vital role of imaging, such as computed tomography (CT) scan, magnetic resonance imaging (MRI) and its various sequences, such as DWI, T1, T2, STIR, FLAIR, CISS and FIESTA, in making an early diagnosis, assessment of the extent of the disease, staging and surgical planning and subsequent follow-up evaluation has been well discussed.

The chapters on treatment, including medical treatment ranging from traditional Amphotericin to newer Azoles and adjunctive treatments are very well written. The pharmacodynamics, dosage and methods on administration and their role in the management of ROCM are discussed and easy to understand.

Surgical debridement of ROCM is, undoubtedly, challenging. Familiarity to how it spreads and the anatomical regions involved, guided by imaging studies, is the key to surgical debridement. This can be achieved both by endo-nasal and open approaches. Indications for surgery, both endo-nasal and open approaches have been discussed and illustrated by several case reports, in this book.

Each article has several learning points and clinical pearls to offer. These collectively become a treasure trove of information for physicians and surgeons interested in this disease. My congratulations to all the contributors for an excellent work!

Dharambir S. Sethi
NUS-Duke Graduate Medical School, Singapore, Singapore
Novena ENT – Head & Neck Surgery Centre, Singapore, Singapore

Preface

There was a definite goal in mind when developing a textbook on Rhino-Orbito-Cerebral Mucormycosis (ROCM) at the time. The desire evolved as a result of a dreadful disease that claimed the lives of those who were impacted by it.

The unexpected surge in cases, the disease's aggressiveness, its unpredictable course, and acute shortages of pharmaceuticals and equipment accessories made it seem as if the entire universe had come down to put our endurance, talent, and courage to the test in the face of this unique situation.

Every day was a new learning experience, with new approaches being investigated and discoveries being documented and compared. In summary, every effort was made to pick up as soon as feasible and to save as much as possible. As a result of this, several forums with all of the essential skills to treat ROCM were developed.

This book captures the essence of all we learnt during the outbreak. Pathogenesis, diagnosis, and an emphasis on culture-independent diagnostic techniques, as well as required surgical processes and specific advancements, are all presented. As a result of our interactions with those patients, several debates have erupted on a variety of topics. This publication was written with the help of clinicians from several specialties. The topic of future directions was explored. Invasive fungal diseases, particularly in rhino-orbito-cerebral areas, require much greater attention.

Daryaganj, Delhi, India — Nishi Gupta
Hyderabad, India — Santhosh G. Honavar

Contents

About the Editors

Nishi Gupta is currently the Associate Medical Director and Head, Department of Otorhinolaryngology & Head & Neck Surgery at Dr Shroff's Charity Eye and ENT Hospital, New Delhi, India.

Dr Nishi Gupta obtained her MS degree in Otorhinolaryngology from Nagpur University in 1992 and trained at Great Ormond Street Hospital for Children, London. She popularized the technique of endoscopic dacryocystorhinostomy in the country.

She has 28 years of experience in Otorhinolaryngology and is a Founder of Tele otology services in India in collaboration with Medtronic USA, Inc in 2013. Her special area of interest includes endoscopic sino-orbital, skull base and lacrimal surgeries. She has published five projects on trans-nasal endoscopic procedures with the current book on ROCM with Springer being the sixth one.

These projects include three books published by her on Endoscopic Dacryocystorhinostomy, first in 2006, the second edition in 2011 and the third in 2020 with Springer. A video series on a variety of techniques of endoscopic DCR in 1999 and an advanced version of the video series of various endoscopic procedures related to the lacrimal drainage system is under publication with Springer since 2021.

The Ranbaxy award, Wolf endoscopic session winner award, Academic excellence award, Best paper award, KAIZEN Achievement Award and various state orations are among the honours she has received.

Santhosh G. Honavar, MD, FACS, FRCOphth received residency training in Ophthalmology, followed by senior residency in Ophthalmic Plastic Surgery and Ocular Oncology at the Dr Rajendra Prasad Centre for Ophthalmic Sciences, AIIMS, New Delhi. He further trained in Ocular Oncology and was mentored by Prof Jerry A Shields and Prof Carol L Shields at the Wills Eye Hospital, Philadelphia, PA, USA. He thereafter established the Ocular Oncology Service at LV Prasad Eye Institute, Hyderabad, the first such facility in the country. He was the Associate Director of LVPEI. Dr Honavar currently heads the Department of Ophthalmic Plastic Surgery and Ocular Oncology and National Retinoblastoma Foundation at Centre for Sight, Hyderabad and leads the Medical Services team and CFS Education. He is also the Editor of Indian Journal of Ophthalmology. Some of the major awards and honours to his credit include Col Rangachari Gold Medal by the AIOS, 1992; Dr Siva Reddy International Award by the AIOS, 2007; Shanti Swarup Bhatnagar Award by the Government of India, 2010; Prof MA Matin Award by the Bangladesh Academy of Ophthalmology, 2013; Jerry Shields International Award by APAO, 2013; APAO Distinguished Service Award 2018; Peters Rogers Oration ANZSOPS, 2019; Lifetime Achievement Award by the American Academy of Ophthalmology, 2019; and Honorary Fellowship, the highest award of the Royal College of Ophthalmologists, 2020.

1 Introduction

Nishi Gupta

Rhino-orbital-cerebral-mucormycosis (ROCM) was earlier known as orbital zygomycosis due to prominent ocular symptoms resulting from fungal infections caused by fungi in the order Mucorales with *Rhizopus oryzae* as the most common species [1, 2]. ROCM is a life-threatening fungal infection that usually occurs in an immunocompromised host and presents initially as vision loss, ptosis, diplopia, and ophthalmoplegia. If left untreated, ROCM can progress to complete vision loss and death [1, 2]. However, since the COVID pandemic, ROCM has been affecting an increasing number of immunocompetent individuals who have substantial ocular symptoms.

Rhizopus oryzae is a fast growing aseptate filamentous fungi that causes 90% of rhino-orbito-cerebral infections. It possesses angioinvasive properties and has a mortality rate of up to 50% [2, 3].

The first case of mucormycosis was described by Friedrich Küchenmeister in 1855 [4]. The term "*Mycosis Mucorina*" was first coined by Arnold Paltauf in 1885 in a case involving the sinuses, brain, and gastrointestinal tract, following which the term "mucormycosis" became popular [4]. In 1955, Harris described the first case of a patient with Cerebro-rhino-orbital mucormycosis [3, 5].

Mucormycosis is becoming more common around the world, but it is especially prevalent in India due to untreated diabetes mellitus [6–11]. The prevalence of mucormycosis in India before the COVID-19 pandemic was approximately 0.14 cases per 1000 population, which is 80 times more than the prevalence in developed countries [12, 13]. The number of instances of ROCM infection has increased dramatically during the second wave of the COVID-19 pandemic [12–14]. The Indian Council of Medical Research issued guidelines for recognizing and treating COVID-19-associated mucormycosis [15]. In India on Jun 28, 2021, there were 40,845 confirmed cases of mucormycosis, with 3129 mortalities. From these cases, 85.5% (34,940) had a history of being infected with SARS-CoV-2, and 52.69% (21,523) were on steroids; also 64.11% (26,187) had diabetes [15, 16]. The progression has been aggressive needing mutilating surgeries like orbital exenteration, palatal resection, and intracranial intervention. Therefore, establishing an early diagnosis of mucormycosis is crucial for initiating aggressive antifungal medication and is linked to improved survival [17, 18]. The correction of the underlying systemic condition and surgical debridement is equally important [17].

Although tissue culture aids diagnosis, non-culture methods like quantitative polymerase chain reaction are also required for quick diagnosis [19–21]. A real-time PCR assay was developed

N. Gupta (✉)
Dr Shroff's Charity Eye Hospital, New Delhi, India

N. Gupta, S. G. Honavar (eds.), *Rhino-Orbito-Cerebral Mucormycosis*,
https://doi.org/10.1007/978-981-16-9729-6_1

for Rhizopus, mucor, and Cunninghamella species targeting 28SrRNA gene [22].

Computed tomography reveals only pansinusitis in patients with rhino-orbital-cerebral illness, therefore, lack of soft tissue delineation or absence of deeper infection on computed tomography does not rule out mucormycosis. Magnetic resonance imaging (MRI) is more sensitive than computed tomography for the detection of orbital and intracranial structures [23].

Advanced radiological techniques involving multiple MRI sequences such as T1W, T2W fat-suppressed, T1W contrast-enhanced, Diffusion-weighted, and MR angiography are required to distinguish mucormycosis from other infections during the significant spike of ROCM patients imaging has emerged to be the most crucial investigation in COVID pendemic. The findings on MRI were pathognomonic of the invasive fungal infection even before the microbiological diagnosis. Even if hyphae are not visible on microscopy, and the culture fails to grow them due to their fragility, MRI can help confirm the diagnosis and begin treatment. However, a histopathological diagnosis is required for major resections such as orbital exenteration.

In most cases unique ocular signs were the first symptom, and typical MRI findings were the highlights in cases with ROCM during this mucor epidemic. The spread of mucor in ROCM was irregular, unrelated to the immunocompetent or immunocompromised condition, and did not follow a predictable course. There were aggressive cases where patients had no nasal signs but presented with an intracranial infarct with pustules on the skin, unilateral facial pain, and so on. The treating team of otorhinolaryngologists, radiologists, ophthalmologists, neurosurgeons, and microbiologists was always battling to come up with the best techniques for dealing with these cases.

MRI is the most informative approach for mapping the disease prior to any surgical intervention. It has greatly improved the result by identifying the extent of resection based on MRI and for postoperative follow-up, it has significantly improved the outcome. Making MRI accessible to majority of the centers will undoubtedly aid in improving patient outcomes.

Since there is thrombosis and necrosis of the blood vessels resulting in tissue necrosis, surgical debridement of the necrotic tissue is necessary. Patients who did not have surgical debridement had a higher mortality rate than those who were operated on and underwent surgical debridement [24–32]. At the same time rectifying the underlying systemic problems with the help of a multidisciplinary team is critical to patient's long term survival. The detailed pathogenesis of the COVID-related mucormycosis which has been discussed in subsequent chapters enables for the identification and management of these predisposing factors.

The care of ROCM cases presents a number of obstacles, including quick diagnosis and complete management, which requires the involvement of a multidisciplinary team. This book discusses numerous approaches to dealing with ROCM cases in order to obtain an optimal outcome. Various microbiological approaches including molecular methods for the quick diagnosis of mucormycosis, have been described. For further confirmation of the diagnosis, histopathological procedures have been detailed separately.

The profile of patients returning with residual/recurrent disease was analysed in a separate chapter, and the useful insights acquired were highlighted. A detailed chapter on classification dilemma is included in ROCM that shows that a prognostic-based strategy rather than a stage-based resection is most suited. Surgical debridement, antifungal medicine dose as well as switch therapy, must all be done correctly.

Aggressive debridement and use of combination antifungals were explored. A chapter on future directions in the management of mucormycosis has been written based on our findings. More research on the sensitivity and susceptibility of antifungal drugs as well as the development of freely available molecular methods for mucormycosis is required.

As a result, future directions must be well and properly defined, given the rising number of

patients, long waiting periods, and critical demand for equipment and accessories. A team of otorhinolaryngologists, radiologists, neurosurgeons, ophthalmologists, faciomaxillary surgeons, and microbiologists are needed for comprehensive management of ROCM. As noted in coming chapters advanced equipment with training facilities as well as additional research in the field of mucormycosis with cost regulation of antifungal medications, would aid in the better manage ROCM.

References

1. Mukherjee B, Raichura ND, Alam MS. Fungal infections of the orbit. Indian J Ophthalmol. 2016;64(5):337–45.
2. Roden MM, Zaoutis TE, Buchanan WL, Knudsen TA, Sarkisova TA, Schaufele RL, et al. Epidemiology and outcome of zygomycosis: a review of 929 reported cases. Clin Infect Dis. 2005;41(5):634–53.
3. Ma L-J, Ibrahim AS, Skory C, Grabherr MG, Burger G, Butler M, et al. Genomic analysis of the basal lineage fungus Rhizopus oryzae reveals a whole-genome duplication. PLoS Genet. 2009;5(7):e1000549. https://doi.org/10.1371/journal.pgen.1000549.
4. Chander J. Mucormycosis. In: Textbook of medical mycology, vol. 26. 4th ed. New Delhi: Jaypee Brothers Medical Publishers; 2018. p. 534–96.
5. Harris J. Mucormycosis: report of a case. Pediatrics. 1955;16:857–67.
6. Torres-Narbona M, Guinea J, Martínez-Alarcón J, Muñoz P, Gadea I, Bouza E. Impact of zygomycosis on microbiology workload: a survey study in Spain. J Clin Microbiol. 2007;45:2051–3. https://doi.org/10.1128/JCM.02473-06.
7. Bitar D, Van Cauteren D, Lanternier F, Dannaoui E, Che D, Dromer F, Desenclos JC, Lortholary O. Increasing incidence of zygomycosis (mucormycosis), France, 1997–2006. Emerg Infect Dis. 2009;15:1395–401. https://doi.org/10.3201/eid1509.090334.
8. Ambrosioni J, Bouchuiguir-wafa K, Garbino J. Emerging invasive zygomycosis in a tertiary care center: epidemiology and associated risk factors. Int J Infect Dis. 2010;14:e100–3. https://doi.org/10.1016/j.ijid.2009.11.024.
9. Saegeman V, Maertens J, Meersseman W, Spriet I, Verbeken E, Lagrou K. Increasing incidence of Mucormycosis in university hospital, Belgium. Emerg Infect Dis. 2010;16:1456–8. https://doi.org/10.3201/eid1609.100276.
10. Kontoyiannis DP, Yang H, Song J, Kelkar SS, Yang X, Azie N, Harrington R, Fan A, Lee E, Spalding JR. Prevalence, clinical and economic burden of mucormycosis-related hospitalizations in the United States: a retrospective study. BMC Infect Dis. 2016;16:730. https://doi.org/10.1186/s12879-016-2023-z.
11. Guinea J, Escribano P, Vena A, Muñoz P, Martínez-Jiménez MDC, Padilla B, Bouza E. Increasing incidence of mucormycosis in a large Spanish hospital from 2007 to 2015: epidemiology and microbiological characterization of the isolates. PLoS One. 2017;12:e0179136. https://doi.org/10.1371/journal.pone.0179136.
12. Skiada A, Pagano L, Groll A, Zimmerli S, Dupont B, Lagrou K, et al. Zygomycosis in Europe: analysis of 230 cases accrued by the registry of the European Confederation of Medical Mycology (ECMM) working group on zygomycosis between 2005 and 2007. Clin Microbiol Infect. 2011;17(12):1859–67. https://doi.org/10.1111/j.1469-0691.2010.03456.x.
13. Arunaloke C. Fungal infections in Asia: eastern frontier of mycology. Elsevier; 2013.
14. Prakash H, Ghosh AK, Rudramurthy SM, Singh P, Xess I, Savio J, Pamidimukkala U, Jillwin J, Varma S, Das A, et al. A prospective multicenter study on mucormycosis in India: epidemiology, diagnosis, and treatment. Med Mycol. 2018; https://doi.org/10.1093/mmy/myy060.
15. India reports 40,854 cases of black fungus so far. Mint; 28 Jun 2021. Accessed 16 Jul 2021.
16. Delhi has more black fungus infections than active Covid-19 cases: govt data. Mint; 14 Jul 2021. Retrieved 16 Jul 2021.
17. Spellberg B, Walsh TJ, Kontoyiannis DP, Edwards J Jr, Ibrahim AS. Recent advances in the management of mucormycosis: from bench to bedside. Clin Infect Dis. 2009;48(12):1743–51. https://doi.org/10.1086/599105.
18. Chamilos G, Lewis RE, Kontoyiannis DP. Delaying amphotericin B–based frontline therapy significantly increases mortality among patients with hematologic malignancy who have zygomycosis. Clin Infect Dis. 2008;47:503–9.
19. Kontoyiannis DP, Chamilos G, Hassan SA, Lewis RE, Albert ND, Tarrand JJ. Increased culture recovery of zygomycetes under physiologic temperature conditions. Am J Clin Pathol. 2007;127:208–12.
20. Francesconi A, Kasai M, Harrington SM, et al. Automated and manual methods of DNA extraction for *aspergillus fumigatus* and *Rhizopus oryzae* analyzed by quantitative real-time PCR. J Clin Microbiol. 2008;46:1978–84.
21. Hata DJ, Buckwalter SP, Pritt BS, Roberts GD, Wengenack NL. Real-time PCR method for detection of zygomycetes. J Clin Microbiol. 2008;46:2353–8.
22. Kasai M, Harrington SM, Francesconi A, et al. Detection of a molecular biomarker for zygomycetes by quantitative PCR assays of plasma, bronchoalveolar lavage, and lung tissue in a rabbit model of experimental pulmonary zygomycosis. J Clin Microbiol. 2008;46:3690–702.

23. Reed C, Bryant R, Ibrahim AS, et al. Combination polyene-caspofungin treatment of rhino-orbital-cerebral mucormycosis. Clin Infect Dis. 2008;47:364–71.
24. Kontoyiannis DP, Wessel VC, Bodey GP, Rolston KV. Zygomycosis in the 1990s in a tertiary-care cancer center. Clin Infect Dis. 2000;30:851–6.
25. Nithyanandam S, Jacob MS, Battu RR, Thomas RK, Correa MA, D'Souza O. Rhino-orbito-cerebral mucormycosis: a retrospective analysis of clinical features and treatment outcomes. Indian J Ophthalmol. 2003;51:231–6.
26. Peterson KL, Wang M, Canalis RF, Abemayor E. Rhinocerebral mucormycosis: evolution of the disease and treatment options. Laryngoscope. 1997;107:855–62.
27. Khor BS, Lee MH, Leu HS, Liu JW. Rhinocerebral mucormycosis in Taiwan. J Microbiol Immunol Infect. 2003;36:266–9.
28. Petrikkos G, Skiada A, Sambatakou H, et al. Mucormycosis: ten-year experience at a tertiary-care center in Greece. Eur J Clin Microbiol Infect Dis. 2003;22:753–6.
29. Tedder M, Spratt JA, Anstadt MP, Hegde SS, Tedder SD, Lowe JE. Pulmonary mucormycosis: results of medical and surgical therapy. Ann Thorac Surg. 1994;57:1044–50.
30. Pavie J, Lafaurie M, Lacroix C, et al. Successful treatment of pulmonary mucormycosis in an allogenic bone-marrow transplant recipient with combined medical and surgical therapy. Scand J Infect Dis. 2004;36:767–9.
31. Reid VJ, Solnik DL, Daskalakis T, Sheka KP. Management of bronchovascular mucormycosis in a diabetic: a surgical success. Ann Thorac Surg. 2004;78:1449–51.
32. Asai K, Suzuki K, Takahashi T, Ito Y, Kazui T, Kita Y. Pulmonary resection with chest wall removal and reconstruction for invasive pulmonary mucormycosis during antileukemia chemotherapy. Jpn J Thorac Cardiovasc Surg. 2003;51:163–6.

2 Clinical Presentation of Cases with Rhino-Orbito-Cerebral Mucormycosis

Nidhi Dhawan and Nishi Gupta

Rhino-Orbito-Cerebral mucormycosis (ROCM) is an angioinvasive mycosis that carries high morbidity and mortality risks. With the current pandemic's growing patterns, the grave clinical and pathogenetic complex has been brought into sharper light. During the second wave of the COVID-19 pandemic, a surge of rhino-orbito-cerebral mucormycosis was noted in patients a few weeks after recovery [1, 2].

Despite other nations have documented COVID-associated mucormycosis, India has the highest number of cases due to its reputation as the world's diabetic capital [2, 3]. ROCM is the commonest type of mucormycosis, and it includes the entire spectrum of mucormycosis from sino-nasal disease to rhino-orbital disease that may progress to rhino-orbital-cerebral disease [2, 4, 5]. A high rate of mortality is associated with ROCM [1, 6].

2.1 Background

Mucormycosis, has long been regarded as a dreaded clinical diagnosis and a disease of the immunocompromised. The comorbidities usually associated with both increased incidence and poorer outcomes are diabetes Mellitus, hematological malignancies, chemotherapy, organ transplant, and severe injuries [7]. Mucormycosis is caused by the Mucorales group of fungi. These fungi are present in the environment and on inhalation in an immune-competent host; Mucor is rejected from the surface by the mucosal barrier itself. It is in the immune-compromised host that the fungus can cross this immune barrier and invade the tissues due to uncontrolled diabetes mellitus, steroids intake, or those on immunosuppressants [1, 8].

The patients with hematological malignancies are more prone to pulmonary mycoses, while diabetic acidotic patients more commonly suffer from progressive and unrelenting rhino-orbito-cerebral disease. The interaction between the spore coat protein CotH3 and the Glucose Related Protein 78 (GRP78) on nasal epithelial cells may be the fundamental pathogenetic event in diabetics. Expression of both proteins is significantly increased by diabetic ketoacidosis chemistry, increased blood glucose, and increased circulating ketones. It facilitates invasion of the epithelium and cascades into often lethal rhino-orbito-cerebral disease [7].

The COVID-19 Pandemic has resulted in an explosion of cases of ROCM, referred to as COVID-Associated Mucormycosis (CAM). Nearly 50,000 cases were reported from India in 3 months of the second wave of the pandemic, ending July 2021 [9]. The sudden surge of cases was probably due to the immune disabling nature of COVID-19 and the use of steroids that

N. Dhawan · N. Gupta (✉)
Dr Shroff's Charity Eye Hospital, New Delhi, India

N. Gupta, S. G. Honavar (eds.), *Rhino-Orbito-Cerebral Mucormycosis*,
https://doi.org/10.1007/978-981-16-9729-6_2

precipitated diabetes in COVID-19 patients. These patients rarely develop pulmonary mucormycosis, which involves different receptors and fungal ligands (CotH7 and Integrin β1) [7].

2.2 Clinical Features

ROCM begins in the nasal passages and sinuses, spreads to the orbit and eye, and eventually reaches the brain. Angioinvasion and spreading ischemia are a hallmark of the disease. In the 1950s, Smith and Krichner established criteria for clinical diagnosis of Mucormycosis [10]: These include black necrotic turbinates, blood-tinged nasal discharge with or without ipsilateral facial pain, soft peri-orbital or peri-nasal swelling/discoloration or induration (Figs. 2.1 and 2.2), ptosis with drooping of eyelid lid edema, proptosis (Figs. 2.3, 2.4, 2.5, 2.6, 2.7, 2.8, 2.9, 2.10, and 2.11), and ophthalmoplegia (Fig. 2.12). There may be associated multiple cranial nerve palsies unrelated to documented lesions [7].

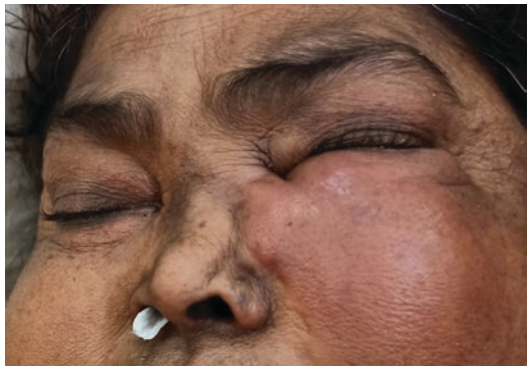

Fig. 2.1 Clinical photograph of a patient showing edema of the paranasal area involving cheek skin

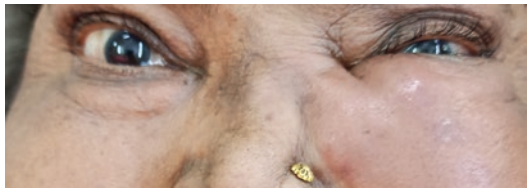

Fig. 2.2 Clinical photograph showing facial edema on the left side

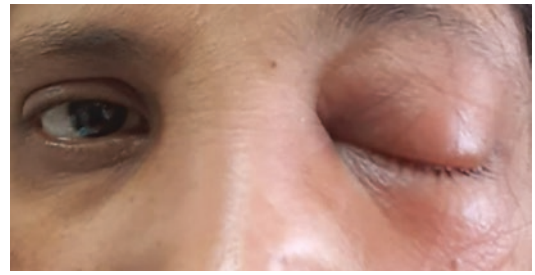

Fig. 2.3 Clinical photograph showing ptosis with partial proptosis left (Photo Courtesy: Dr. Manisha Singh, RML Delhi)

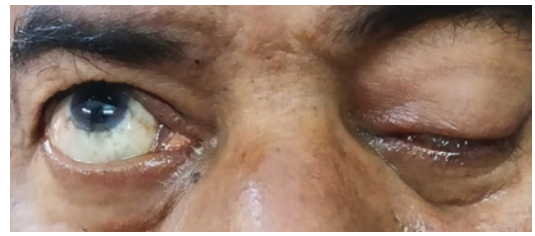

Fig. 2.4 Clinical photograph showing left ptosis

Fig. 2.5 Clinical photograph showing left lid edema and proptosis

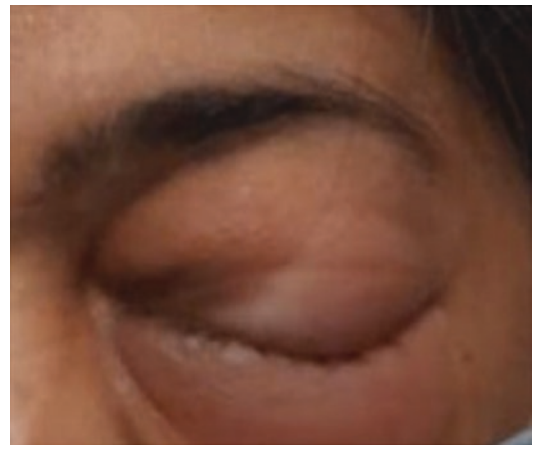

Fig. 2.6 Clinical photograph showing left lid edema

Fig. 2.7 Clinical photograph showing left periorbital cellulitis

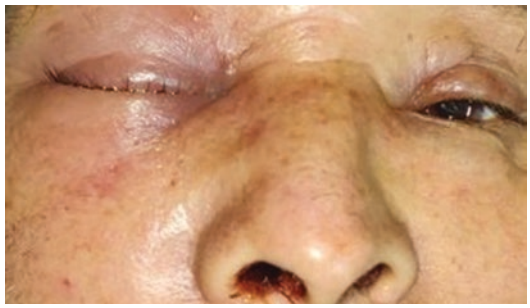

Fig. 2.8 Clinical photograph showing right lid edema (Photo Courtesy: Dr. Bibhu Pradhan TDMC Kathmandu)

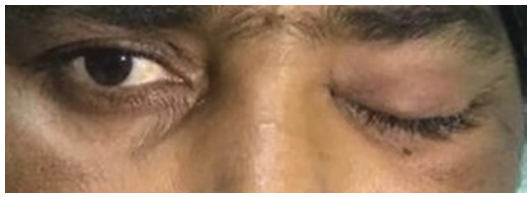

Fig. 2.9 Clinical photograph showing left ptosis (Photo Courtesy: Dr. Bibhu Pradhan TDMC Kathmandu)

Palatal lesions (Figs. 2.13, 2.14, and 2.15), loosened teeth, fistulae in the region of cheek and palpebral area, blackened areas of eschar, and necrosis developing and extending on the skin of the face are also common clinical presentations (Figs. 2.16, 2.17, and 2.18).

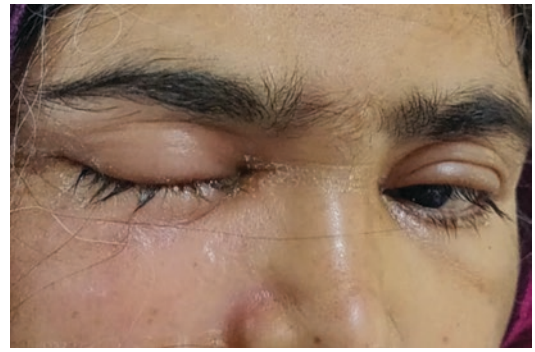

Fig. 2.10 Clinical photograph showing right ptosis (Photo Courtesy: Dr. Aparna; Fortis Faridabad)

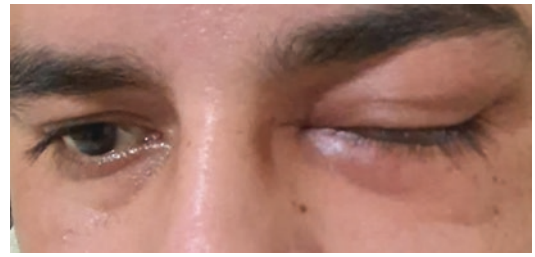

Fig. 2.11 Clinical photograph showing left lid edema (Photo courtesy; Dr. Manisha Singh, RML Delhi)

Loss of vision, eye pain, and altered sensation in the infraorbital area are common and ominous as this indicates invasion of the infraorbital nerve. Involvement of the anterior parts of the eye, including cornea and conjunctiva, indicates orbital exenteration (Figs. 2.19, 2.20, 2.21, and 2.22). If the anterior structures are preserved, globe sparing orbital exenteration or an endoscopic orbital debridement can be performed based on the extent of the disease. Early symptoms of stuffiness and nasal discharge, sometimes blood stained, maybe missed. In late cases, a nasal endoscopy may demonstrate the presence of eschar or slough (Figs. 2.23, 2.24, and 2.25). These may rapidly evolve into the orbital and intracranial compartment symptoms of severe pain in the eyes and head.

All the progressive symptoms and signs are the result of extending thrombosis and associated ischemia and tissue necrosis. The sudden blindness seen in complicated ROCM can be due to several pathogenetic mechanisms like central retinal artery

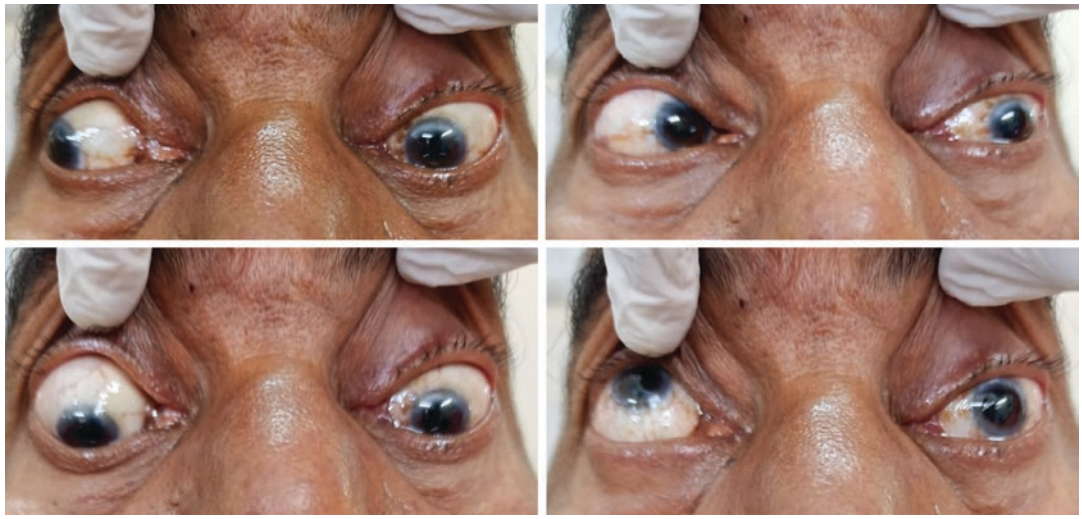

Fig. 2.12 Clinical photograph showing Ophthalmoplegia, restricted eye movements

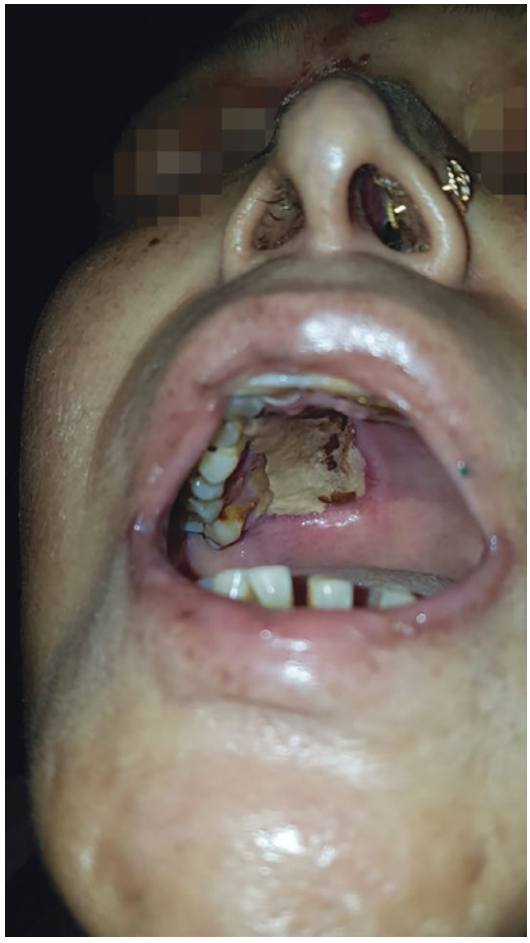

Fig. 2.13 Clinical photograph showing palatal necrosis (Photo Courtesy: Dr. Rajeev Pachauri Agra)

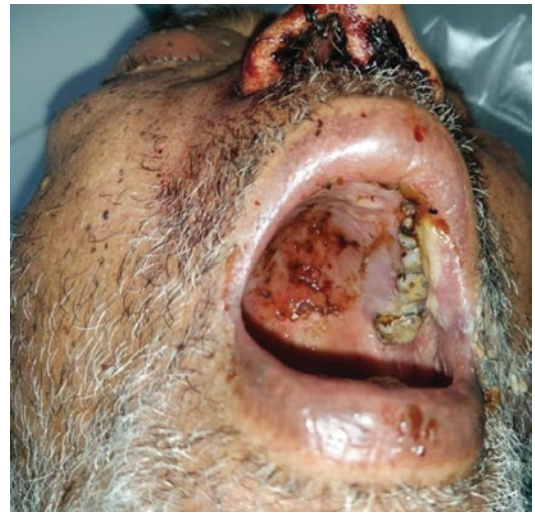

Fig. 2.14 Clinical photograph showing palatal bogginess (Photo Courtesy: Dr. Rajeev Pachauri Agra)

occlusion, thrombosis of the posterior ciliary artery, optic nerve infarction in the intraorbital course, direct fungal invasion of the optic nerve in the intracranial part or even optic chiasm [11].

2.3 When to Suspect COVID-Associated Mucormycosis

A patient presenting with the symptoms of ROCM described above and the history of COVID with deterioration of vision, unrelenting sharp head-

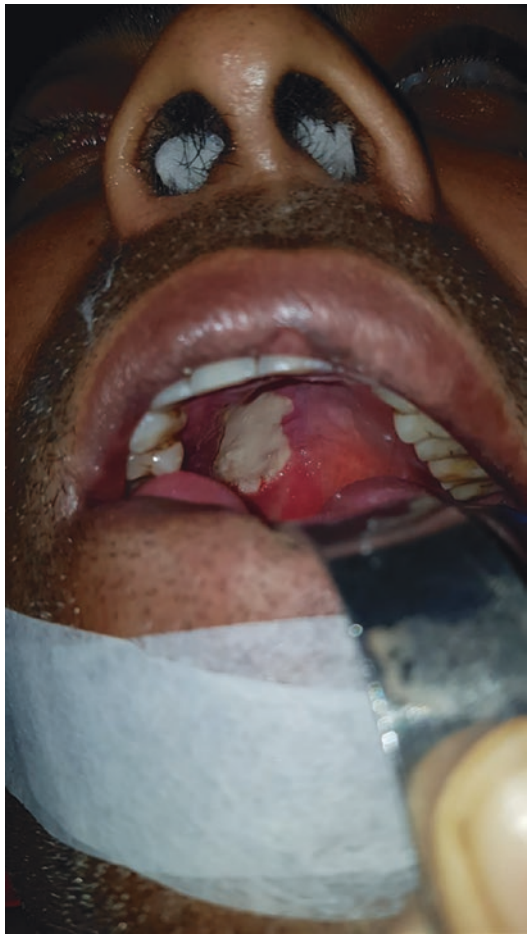

Fig. 2.15 Clinical photograph showing palatal necrosis (Photo Courtesy: Dr. Rajeev Pachauri Agra)

ache, and facial pain/numbness. There may be an associated history of nose block/blood-stained nasal discharge with or without symptoms of central nervous system involvement, focal neurological signs, and encephalopathy indicate a grave prognosis. Signs of intracranial invasion, periorbital necrosis, and cavernous sinus involvement are poor prognosticating factors.

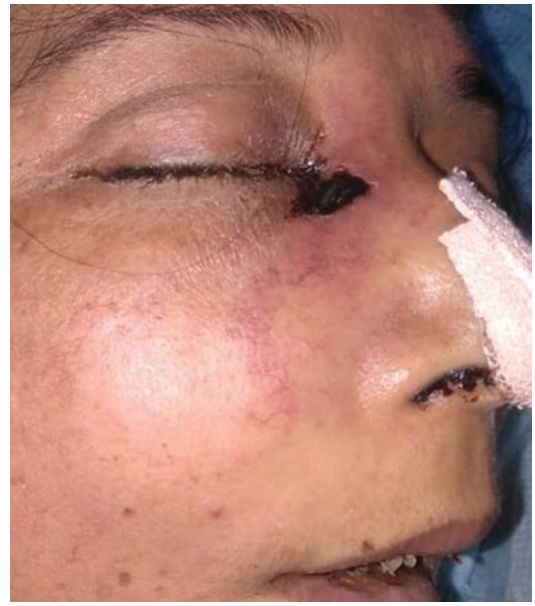

Fig. 2.16 Clinical photograph showing skin necrosis near the right medial canthus (Photo courtesy: Dr. Manisha Singh, RML Delhi)

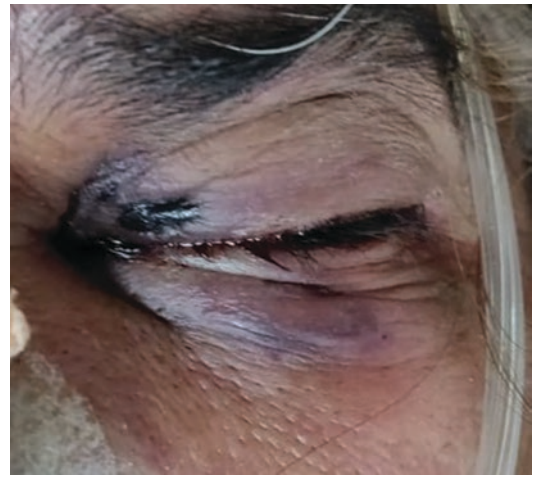

Fig. 2.17 Clinical photograph showing necrosis of the left eye-lid skin extending up to the medial canthus (Photo courtesy: Dr. Manisha Singh, RML Delhi)

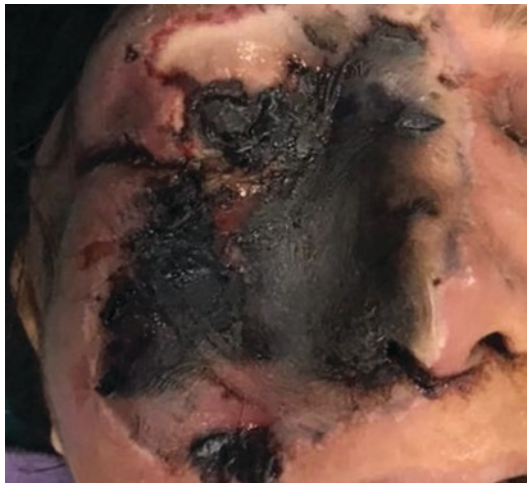

Fig. 2.18 Clinical photograph showing extensive skin necrosis (Photo Courtesy: Dr. Satish Jain Jaipur)

Fig. 2.19 Clinical photograph showing conjunctival chemosis

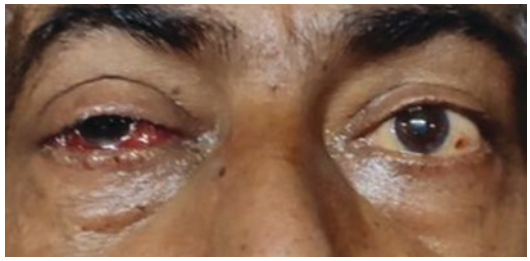

Fig. 2.20 Clinical photograph showing involvement of the anterior structures of the left eye

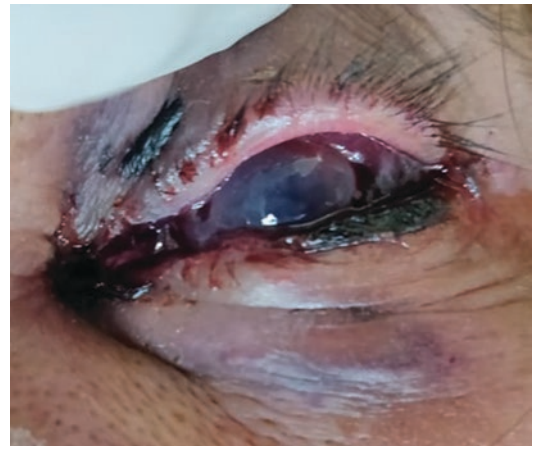

Fig. 2.21 A melting cornea with bluish discoloration of the conjunctiva (Photo courtesy: Dr. Manisha Singh, RML Delhi)

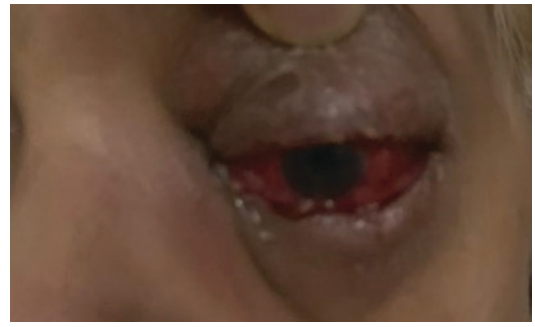

Fig. 2.22 Severe conjunctival congestion and chemosis

2.4 ROCM Pre-COVID and During COVID Pandemic

COVID-associated mucormycosis presents unique problems and can be alarming in the context of the ongoing pandemic. The COVID-Associated Mucormycosis has some distinctive features. It is more common in men, older patients, and patients who have had a complicated course of COVID-19. The latter includes the need for steroids, hypoxia, and hospitalization and new or preexisting diabetes mellitus [6].

These patients must undergo urgent diagnostic nasal endoscopy and fresh KOH preparation/ Fungal culture and biopsy, be sent from the

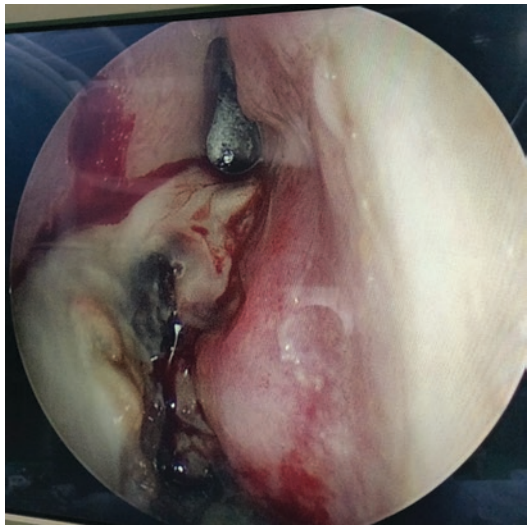

Fig. 2.23 Endoscopic view of the left nasal cavity demonstrating necrotic tissue with discharge (Photo Courtesy: Dr. Aparna, Fortis Faridabad)

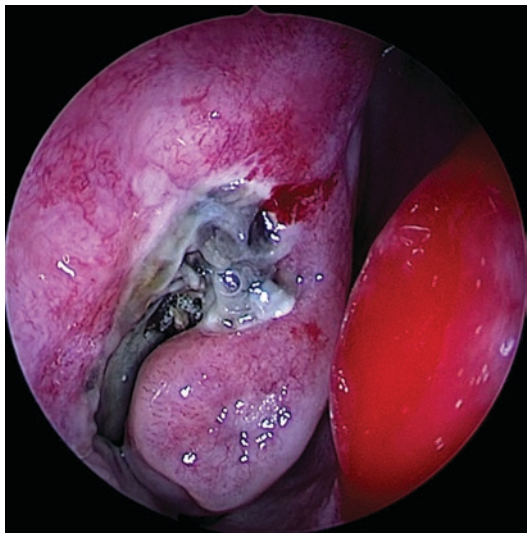

Fig. 2.24 Endoscopic view of the right nasal cavity showing characteristic eschar

affected areas involving the healthy margins adjoining the necrotic areas. Further workup of these patients in the form of radiological diagnosis has been mentioned in the subsequent chapter. The surgical debridement is planned based on disease mapping on MRI, and the steps of each procedure have been described in the chapters on surgical management of ROCM.

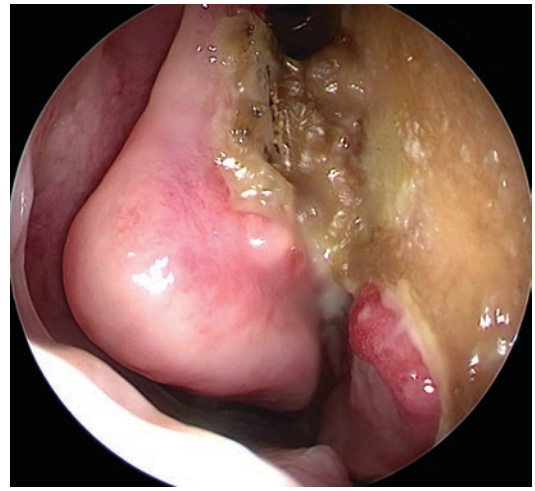

Fig. 2.25 Endoscopic view of the right nasal cavity showing necrosis of the right turbinate and septum

2.5 Conclusion

Acute ocular signs represent late presentation in COVID-associated ROCM. Despite our best efforts, the prognosis remains grim in these cases. This kind of presentation urges clinicians to keep a high degree of suspicion, educate patients about early signs and symptoms and perform a quick nasal endoscopy and imaging. Early institution of therapy leads to improved outcomes.

References

1. Ramaswami A, Sahu AK, Kumar A, Suresh S, Nair A, Gupta D, Chouhan R, Bhat R, Mathew R, Majeed JA, Aggarwal P, Nayer J, Ekka M, Thakar A, Singh G, Xess I, Wig N. COVID-19-associated mucormycosis presenting to the emergency department-an observational study of 70 patients. QJM. 2021;114(7):464–70. https://doi.org/10.1093/qjmed/hcab190.
2. Singh AK, Singh R, Joshi SR, Misra A. Mucormycosis in COVID-19: a systematic review of cases reported worldwide and in India. Diabetes Metab Syndr. 2021;15(4):102146. https://doi.org/10.1016/j.dsx.2021.05.019.
3. International Diabetes Federation Idf diabetes atlas. 2019. https://diabetesatlas.org/en/resources/.
4. Sugar AM. Mucormycosis. Clin Infect Dis. 1992;14:S126–9.

5. Peterson KL, Wang M, Canalis FR, Abemayor E. Rhinocerebral mucormycosis: evolution of the disease and treatment options. Laryngoscope. 1997;107:855–62.
6. Petrikkos G, Skiada A, Sambatakou H, Toskas A, Vaiopoulos G, Giannopoulou M, et al. Mucormycosis: ten-year experience at a tertiary-care center in Greece. Eur J Clin Microbiol Infect Dis. 2003;22:753–6.
7. Alqarihi A, Gebremariam T, Gu Y, Swidergall M, Alkhazraji S, Soliman SSM, Bruno VM, Edwards JE Jr, Filler SG, Uppuluri P, Ibrahim AS. GRP78 and integrins play different roles in host cell invasion during mucormycosis. mBio. 2020;11(3):e01087–20. https://doi.org/10.1128/mBio.01087-20.
8. Kubin CJ, McConville TH, Dietz D. Characterization of bacterial and fungal infections in hospitalized patients with COVID-19 and factors associated with healthcare-associated infections. Open Forum Infect Dis. 2021;8(6):ofab201.
9. Muthu V, Rudramurthy SM, Chakrabarti A, Agarwal R. Epidemiology and pathophysiology of COVID-19-associated mucormycosis: India versus the rest of the world. Mycopathologia. 2021 Aug;19:1–16. https://doi.org/10.1007/s11046-021-00584-8.
10. Smith HW, Kirchner JA. Cerebral mucor-mycosis: a report of 3 cases. Arch Otolaryng (Chicago). 1950;68:715–26.
11. Mukherjee B, Raichura ND, Alam MS. Fungal infections of the orbit. Indian J Ophthalmol. 2016;64(5):337–45. https://doi.org/10.4103/0301-4738.185588.

3 Imaging in Rhino-Orbito-Cerebral Mucormycosis (ROCM)

Bavaharan Rajalingam

COVID-19 has been linked to a significant rise in the incidence of rhino-orbito-cerebral mucormycosis, especially in patients with diabetes mellitus and inadvertent steroid administration. The disease carries high mortality of 50% [1]. A high index of suspicion with knowledge of various clinical and Imaging signs helps in early diagnosis and management minimizing the morbidity and mortality. Nasal endoscopy and biopsy, with microbiological and histopathological analysis, form the basis of diagnosis in ROCM.

3.1 Role of Imaging

Imaging plays a crucial role in picking up the disease early. It helps in assessing the extent of disease, planning for surgery and follow-up evaluation. Computed Tomography (CT) and Magnetic Resonance Imaging (MRI) are helpful in making a quick diagnosis of ROCM. Since MRI gives a better resolution of the soft tissue than CT scan, it provides an excellent visualization of invasion and involvement of orbital soft tissue, infratemporal fossa, intracranial structures, perineural invasion and vascular occlusion.

B. Rajalingam (✉)
Magnum Imaging and Diagnostics,
Trichy, Tamilnadu, India

3.2 Routes of Spread and Imaging Landmarks

ROCM starts from the nose and sinuses with rapid spread to the nearby areas, notably the orbit and the brain. In the nasal cavity and sinuses, mucor prefers unilateral involvement. The most common sites are middle turbinate, maxillary, ethmoid and sphenoid sinuses [2] (Figs. 3.1 and 3.2).

The fungus gets attached to the internal elastic walls of the blood vessels leading to thrombosis and occlusion resulting in, ischaemia and necrosis of tissues. The disease can erode the bones to extend into the perisinus planes or through perivascular channels, thereby being seen outside the sinuses without intervening in bone destruction. Extrasinus spread into the orbit and face may further progress to involve the infratemporal fossa, cavernous sinus, skull base and intracranial compartment [3].

In the nasal cavity, the disease causes osteonecrosis of the turbinates and erosion of the nasal septum (Table 3.1).

From the nasal cavity: It may have

- Intraorbital extension, through the nasolacrimal duct or by direct involvement of the medial orbital wall.
- Intracranial extension superiorly, through a defect in the cribriform plate [4], extending directly into the brain, leading to leptomeningitis or forming a granuloma or abscess.

N. Gupta, S. G. Honavar (eds.), *Rhino-Orbito-Cerebral Mucormycosis*,
https://doi.org/10.1007/978-981-16-9729-6_3

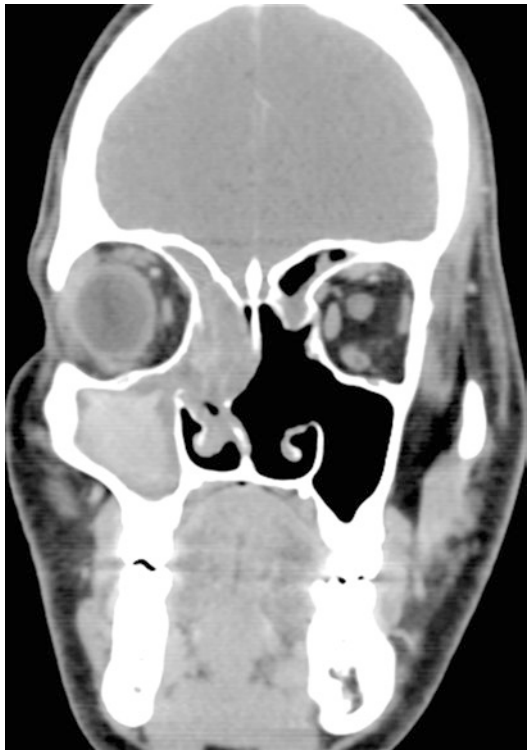

Fig. 3.1 CT scan Coronal section of paranasal sinuses and orbit showing Hyperdense areas in the maxillary and ethmoidal sinuses with osteomeatal unit obstruction

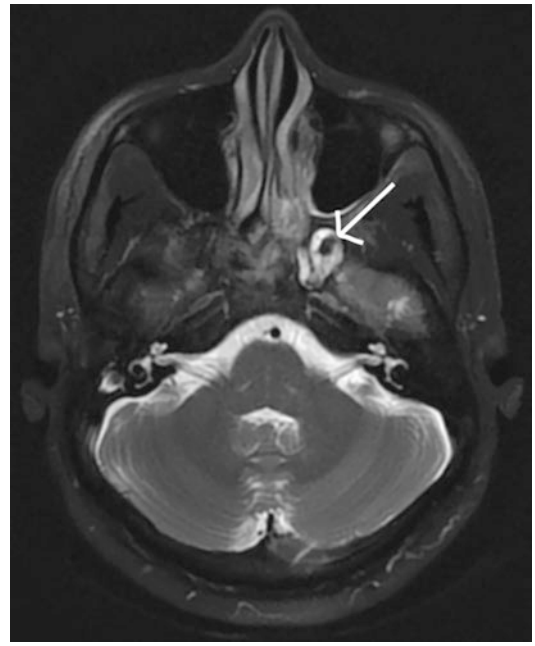

Fig. 3.2 Axial T2 Fat Suppressed (FS) section showing Hypointense area (arrow) within the left sphenoidal hyperintense mucosal thickening

Table 3.1 Anatomical regions in sinonasal neck spaces to assess in ROCM

Paranasal sinuses	Perisinus planes	Other
Mucosal thickening T2 hypointesnities on MRI in the ethmoid/maxillary/sphenoid/ frontal	Pterygopalatine fossa Infratemporal fat zygoma Masticator space parapharyngeal space Naso-pharynx and prevertebral muscles Pterygoid plates	Nasolacrimal Duct and Nasolacrimal Sac
Bony erosion		Hard palate, floor or maxillary sinus/alveolar process of maxilla, Mandible and oral cavity
		Skull base

From the maxillary sinus: The disease can extend [5]

- Anteriorly into the premaxillary space by direct erosion of the anterior wall of the maxillary sinus or through the inferior orbital foramen.
- Posteriorly, to the retro-antral space through direct erosion of the posterolateral wall of the maxillary sinus or the pterygomaxillary fissure.
- Inferiorly, it can invade the floor of the maxillary sinus to involve the alveolar surface and hard palate.
- Superiorly, it can erode the floor of the orbit with intraorbital extension.

From the sphenoid sinus: The disease can

- Erode the sphenoid sinus wall and extend into the cavernous sinus.

- Erode into the pterygoid wedge, causing osteonecrosis with soft tissue extension to the pterygoid space infiltrating the pterygoid muscles.
- May lead to erosion and osteonecrosis of the left sphenoid wing.

From the frontal sinus: The disease can extend

- Anteriorly into the prefrontal space, by eroding the anterior wall of frontal sinus.
- Posteriorly into the frontal lobe of the brain, through a defect into the posterior wall of the frontal sinus.

The orbital involvement may occur via (Table 3.2):

- The inferior meatal opening of the nasolacrimal duct.
- A defect in the lamina papyracea.
- Secondary to the involvement of the ethmoid group of cells.

Intracranial Spread [2–4] (Table 3.3): It may occur through

- The orbital apex.
- Along the vessels.
- Erosion of cribriform plate of the ethmoid bone.
- From the pterygoid space by direct erosion of the sphenoid wing or by perineural invasion through the trigeminal nerve and its branches and can extend up to the root entry zone in the pons.
- By direct erosion of the sphenoid sinus walls or frontal sinus walls.

Table 3.2 Anatomical regions in orbital and periorbital regions to assess in ROCM

Orbit and Periorbital Evaluation
• Preseptal oedema
• Extraconal fat involvement, subperiosteal abscess
• Orbital muscle cone involvement, proptosis
• Intraconal fat involvement
• Sub periosteal collection
• Orbital apex involvement, Superior and inferior orbital fissure
• Globe involvement
• Optic nerve involvement
• Superior ophthalmic vein thrombosis

Table 3.3 Anatomical regions in brain to assess in cases of ROCM

Cranial invasion of ROCM
• Skull base involvement—evaluate clivus, frontal, ethmoid, sphenoid and basi occiput
• Base of skull foramina and Perineural extension
• Meninges with contrast
• Cortical edema—focal cerebritis (frontal, anteromedial temporal lobe)
• Intracranial granulomas/abscess or Extra-axial/parenchymal collection Infarct/hemorrhage
• Cranial nerve
• Meckel's cave involvement
• Cavernous sinus involvement
• Internal carotid artery narrowing/thrombosis/pseudoaneurysm

Cerebral abscess, granuloma or ischaemia may occur either due to the direct spread of fungus or as secondary to the involvement of the internal carotid artery [4, 6–8].

Mucor can cause Cavernous sinus thrombosis by:

- Erosion of sphenoid sinus wall.
- Superior orbital fissure.
- Perineurally through the trigeminal nerve branches.

Several authors have described the staging of ROCM, proposing a four-stage system to determine the anatomical extent and severity of ROCM [9]. However, there may be a small subset of patients where the orbital involvement occurs due to the spread of infection from the pterygopalatine fossa without significant involvement of the sinuses. Therefore, staging is not much helpful in decision-making in ROCM.

3.3 Computed Tomography (CT) Technique

Plain and Contrast-enhanced CT scans of PNS and nasal cavity are performed by the instillation of non-ionic iodinated contrast at a dose of 1–1.25 mL/kg body weight, in arterial and venous phases. The coverage area is superiorly from the top of the frontal sinus, including the cavernous

sinuses, inferiorly to include jaws, anteriorly including ala of nose and Brain to be included in case of suspected involvement. Thin axial spiral sections of 1–2 mm thickness were obtained and evaluated in both soft tissue and bone windows. The axial sections of the multiplanar images thus obtained are reformatted into coronal and sagittal planes. In cases of suspected internal carotid artery occlusion, a CT angiogram is done.

3.4 Magnetic Resonance Imaging (MRI) Technique

Magnetic Resonance (MR) examination of paranasal sinuses (PNS) and nasal cavity is done in supine position with dedicated head and neck coils. Brain should always be included in the study. The Sequences are Diffusion-weighted images (DWI), T1, T2 and Short-tau inversion recovery (STIR) images in coronal and axial planes along with contrast-enhanced T1 W fat, saturated images multiple planes and in 3D sequences. 3D contrast (0.6 mm) MR images are helpful in navigation during surgery. Area of coverage should include from the top of frontal sinuses superiorly and level of the jaws inferiorly. Ensure the field of view includes cavernous sinuses and orbits. Brain assessment includes Fluid-attenuated inversion recovery (FLAIR, DWI) images and post-contrast T1. Three-dimensional (3D) post-contrast thin sections (0.6 mm) to be used at skull base level for orbital apex, cavernous sinus and cranial nerves assessment. In case of suspected perineural spread, 3D Fast Imaging Employing Steady-state Acquisition (Fiesta)/Constructive Interference in Steady State (CISS) sequences are done. MR angiography by Time-of-Flight (TOF) technique is done to assess the internal carotid artery (ICA) and its branches.

3.5 CT Scan

Mucor show varying degrees of sinus opacification, with most having a tumefactive nature [10]. Early findings include ulcerated or emphysematous nasal septum mucosa and turbinates. Inflammatory thickening of nasal mucosa and sinuses is seen, with or without fluid level [2, 11]. Fungal elements appear as hyperdense areas within the hypodense mucosal thickening in the sinus (Fig. 3.1). The same disease is seen as hypointense on MRI (Fig. 3.2) and will be explained subsequently in the MRI part. Soft tissue infiltration may extend into peri-antral fat planes, including the premaxillary and retro-antral fat plane with or without bony destruction. Erosion or infiltration around the nasolacrimal duct or sac may be seen with intra-orbital extension. Fat stranding and soft tissue enhancement can be seen in the pterygomaxillary fissure and pterygopalatine fossa, extending into the infra-temporal fat or masticator space muscles.

CT has a higher resolution in picking up the bony erosions (Fig. 3.3c, d). Nasal septal destruction, turbinate erosions, the floor of maxillary sinus erosion and reduced density of the maxillary alveolar bone around tooth sockets and hard palate due to infiltration and erosions can occur either alone or in various combinations (Figs. 3.4 and 3.5). Bony breach, orbital involvement and intracranial extension are late findings, but may appear early as the disease can spread rapidly within a short span of a few hours (Figs. 3.6 and 3.7).

Premaxillary space involvement may occur through direct erosion of the anterior wall of the maxillary sinus or the infraorbital foramen. There may be inflammatory soft tissue showing mild enhancement (Fig. 3.8). In a few cases, premaxillary space abscess formation will be seen as peripherally enhancing collection.

The CT findings of Orbital extension [11] include preseptal oedema and thickening of extraocular muscles, stranding at extraconal and intraconal orbital fat with or without enhancement, Phlegmon or inflammatory mass with or without abscess (Figs. 3.7 and 3.9), optic nerve involvement and Orbital apex disease (Fig. 3.10).

The CT findings in intracranial extension include cavernous sinus involvement, causing thrombosis and carotid artery involvement [12], with narrowing, dissection or pseudoaneurysm formation. Arterial involvement can result in mycotic aneurysms, leading to subarachnoid haemorrhage and occlusion leading to acute infarcts.

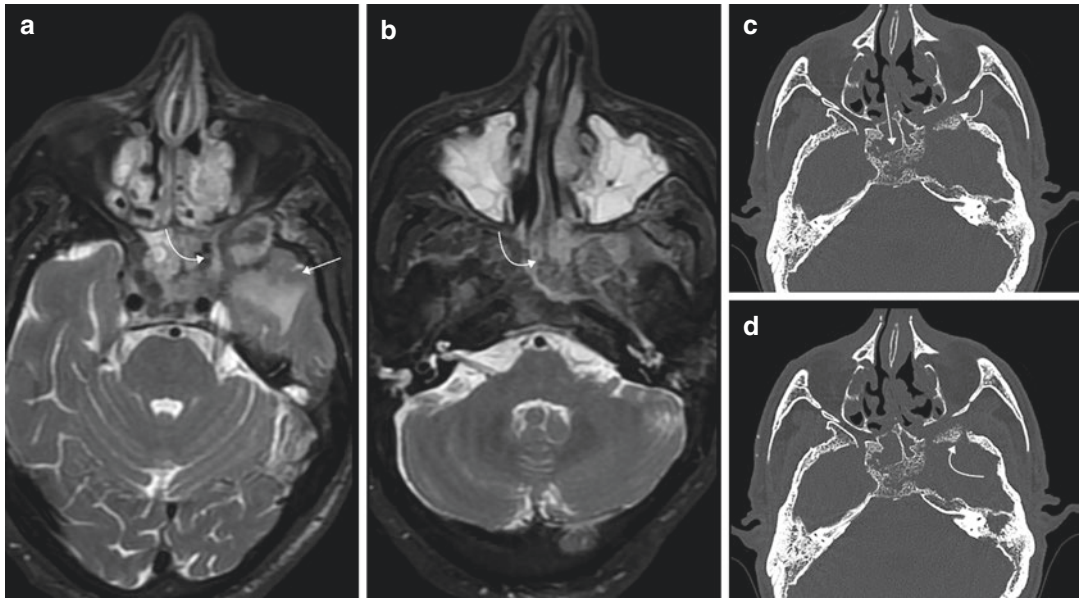

Fig. 3.3 (**a**) Axial T2FS MRI showing osteonecrosis of the clivus and left pterygoid wedge and erosion of left sphenoid wing (curved arrows) with left temporal lobe abscess formation (arrow). (**b**) Axial T2FS MRI showing osteonecrosis of the clivus and left pterygoid wedge and erosion of left sphenoid wing (curved arrows). (**c**) CT Axial images bone window showing erosion of the clivus, left pterygoid and left sphenoid wing. (**d**) CT Axial images bone window showing erosion of the clivus, left pterygoid and left sphenoid wing

Skull base erosions are visualized well on thin sections CT in bone windows (Figs. 3.3c, d and 3.4a, b). Post-contrast images can delineate abscess and their extensions.

Post-Contrast Leptomeningeal enhancement can be seen with an intracranial extension of the disease. Other manifestations are intracranial granulomas and abscess formation, with abscess showing peripheral rim enhancement and surrounding oedema.

CT has limitations in assessing intracranial disease, including cerebral cortical, meningeal, perineural and vascular invasion. Bone infiltration changes are seen later than MRI as early marrow changes can be missed. This may lead to underestimating the true extent of the disease as the enhancement pattern is also less evident on CT when compared to MRI.

3.6 Magnetic Resonance Imaging

The Early findings on MRI in mucormycosis include inflammatory mucosal thickening of nasal cavity and sinuses with or without fluid level. Soft tissue inflammation of peri-antral fat planes like premaxillary and retromaxillary fat planes is seen well on T2 fat-suppressed (FS) sequences, STIR sequences or post-contrast images. The involved areas look intermediate to hypointense on T2-weighted images (Figs. 3.2, 3.11 and 3.12) and isointense to brain on T1 images [8]. In a few cases, a hyperintense signal may also be seen.

On Post Contrast Gadolinium-enhanced imaging (T1 fat-suppressed plus contrast), lack of contrast enhancement is highly suggestive of tissue necrosis (Fig. 3.11). It is a sign of angioinvasive fungal sinusitis ("black turbinate sign") [13] (Fig. 3.13). However, homogeneous and heterogeneous patterns of enhancement may also be seen.

The soft tissue invasion can spread along the pterygomaxillary fissure or sphenopalatine foramen, replacing the retro-antral fat plane, surrounding the internal maxillary artery with soft tissue, which can infiltrate the medial and lateral Pterygoid muscles appear as hyperintense signal intensities on T2 fat-suppressed/STIR sequences.

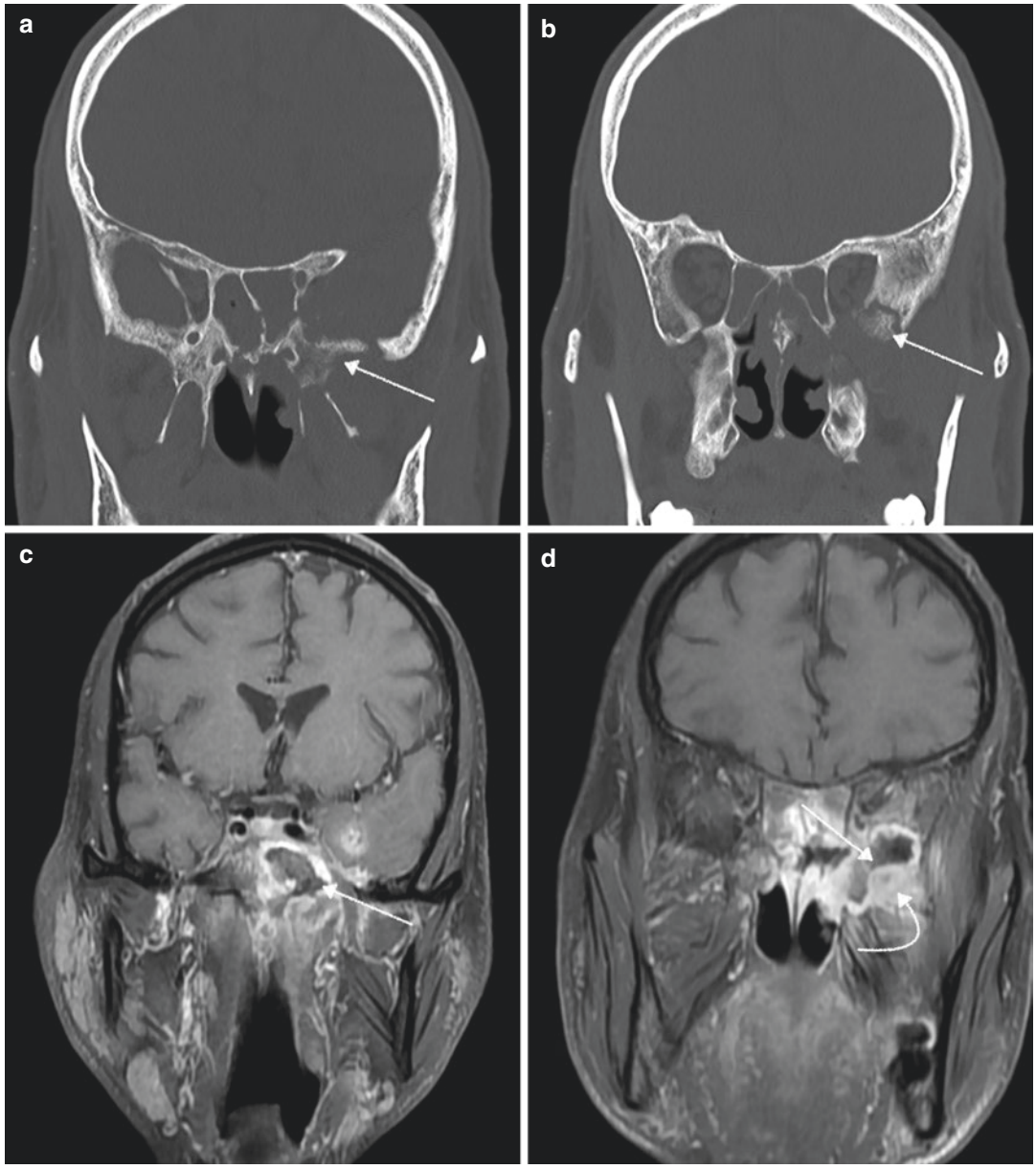

Fig. 3.4 (**a**) Coronal CT bone window shows erosion of left Pterygoid wedge and left Sphenoid wing. (**b**) Coronal CT bone window shows erosion of left Pterygoid wedge and left Sphenoid wing. (**c**) Coronal post-contrast T1 FS MRI image showing non-enhancing osteonecrosis of the left pterygoid wedge (arrow). There is also the presence of non-enhancing soft tissue in the left pterygoid space suggestive of fungal soft tissue with surrounding enhancement (curved arrow). This is suggestive of viable inflammatory tissue demarcating the zone of required surgical debridement. There is associated leptomeningeal enhancement in the left temporal lobe with early abscess formation in the left temporal lobe. (**d**) Coronal post-contrast T1 FS MRI image showing non-enhancing osteonecrosis of the left pterygoid wedge (arrow). There is the presence of non-enhancing soft tissue in the left pterygoid space suggestive of fungal soft tissue with surrounding enhancement (curved arrow). This is suggestive of viable inflammatory tissue demarcating the zone of required surgical debridement

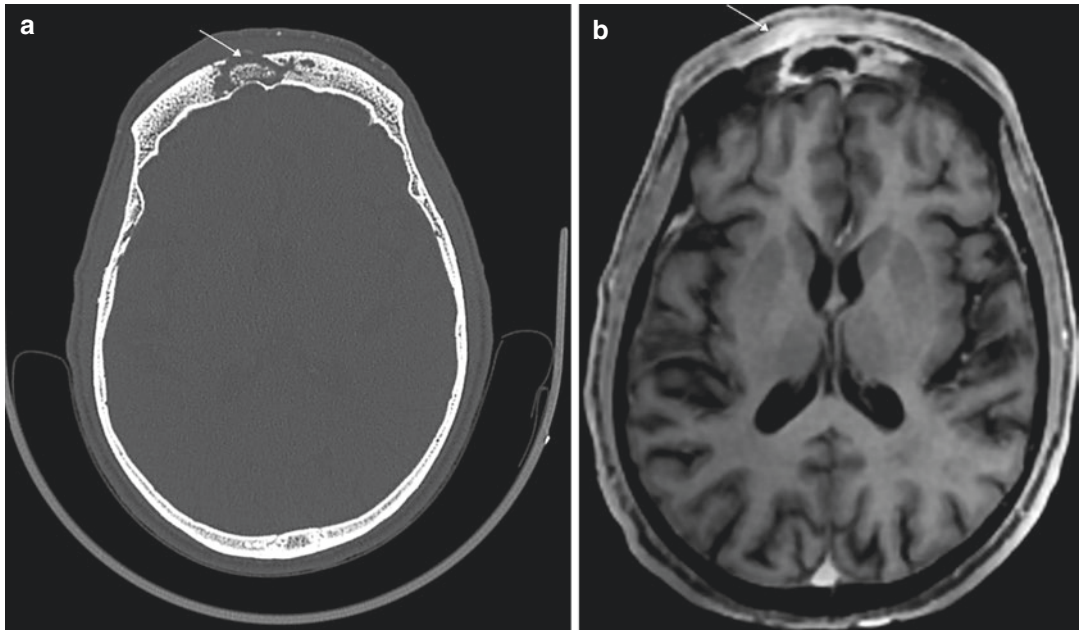

Fig. 3.5 (**a**) CT scan axial section demonstrating bone window showing erosion of the right frontal bone. (**b**) Axial section of post-contrast T1FS MRI image showing enhancing soft tissue in the prefrontal region

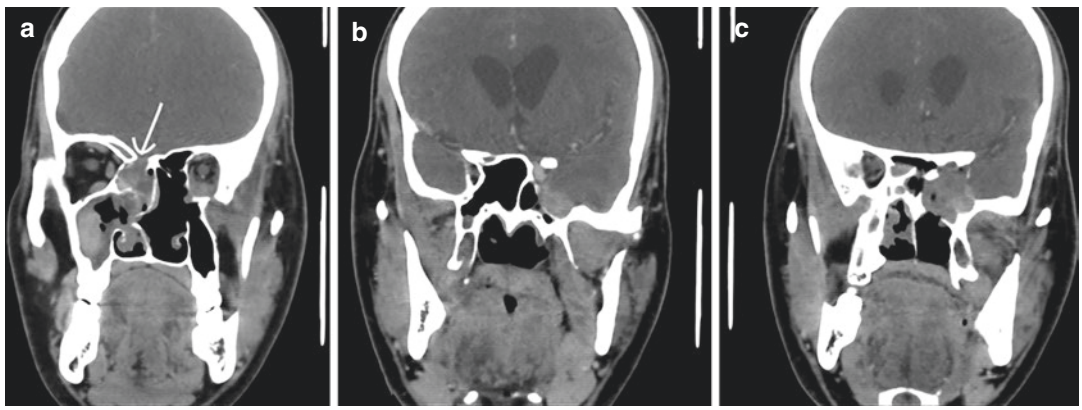

Fig. 3.6 Coronal section of contrast-enhanced CT scan showing (**a**) Erosion of roof of the ethmoid. (**b**) Erosion of left lateral sphenoid sinus wall extending into the extra-axial aspect of the left temporal lobe involving the Meckel's cave. (**c**) Soft tissue erosion into the left lateral sphenoid wall and the pterygoid wedge

The Pterygoid space can also be infiltrated by direct invasion with osteomyelitis or osteonecrosis of the pterygoid wedge (Figs. 3.14 and 3.15). On post-contrast Imaging, direct invasion and fungal soft tissue will not enhance; rather, the secondary inflammation will enhance. The margin of enhancement correlates with the plane of viable inflammatory tissue during surgical debridement (Fig. 3.4d).

In cases of Orbital extension, the preseptal thickening is seen as a high signal on T2 fat-suppressed/STIR images. Oedema and thickening of extraocular muscles are seen as high signals on T2 fat-suppressed images. On post Gadolinium enhancement with inflammatory stranding at extraconal and intraconal orbital fat. As orbital invasion commonly occurs through the lamina papyracea, the inflamed tissue or an

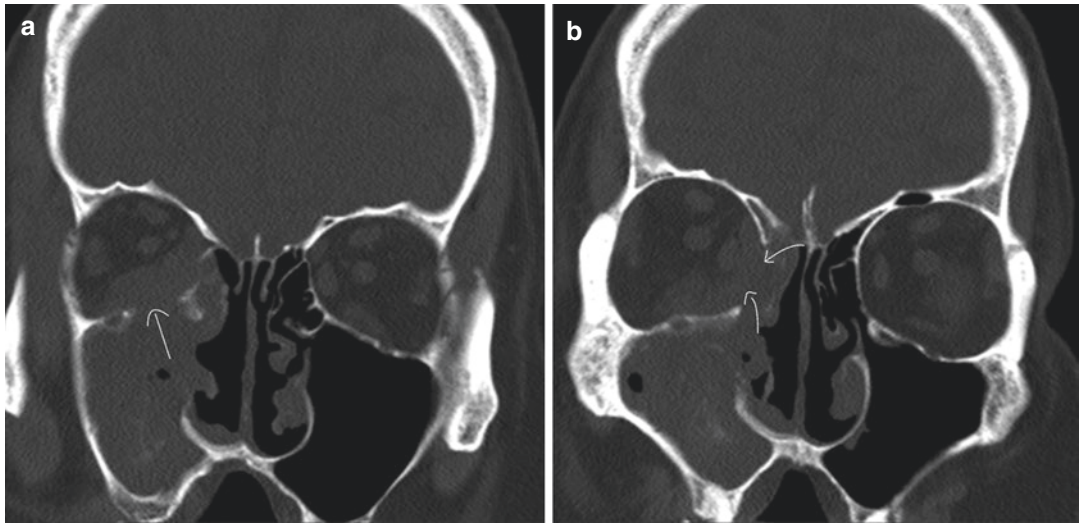

Fig. 3.7 CT scan coronal section of the bone window showing intraorbital soft tissue with an erosion of the (**a**) Floor of the right orbit (arrow). (**b**) Erosion of medial wall of the right orbit (curved arrows)

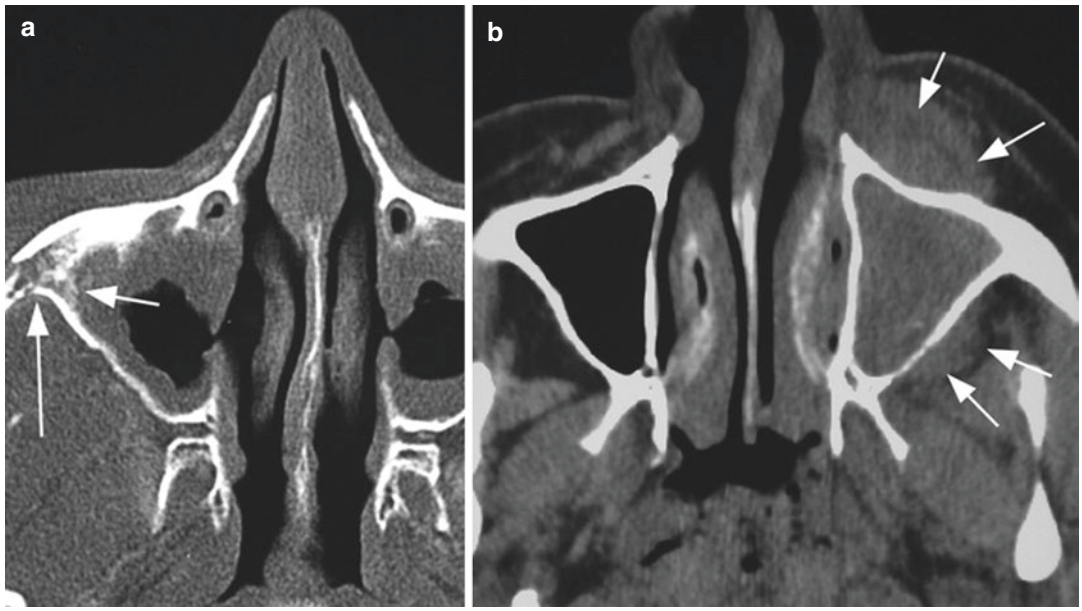

Fig. 3.8 Axial CT (**a**) Bone window showing sclerosis of the wall. (**b**) Soft tissue window showing extension of soft tissue into the left premaxillary space and the retro antral areas (arrows)

abscess formation may be seen along the medial part of the orbit with oedema and lateral displacement of the medial rectus muscle [14] (Fig. 3.11). The thickening of the extraocular muscles, fat infiltration and oedema can raise the intra-orbital pressure, leading to the globe's compression and distortion, resulting in "guitar pick sign" [15] and proptosis (Figs. 3.16 and 3.17).

In cases of optic nerve involvement, the area along the optic nerve may show enhancement along the optic nerve; Diffusion-weighted images (DWI) restriction may occur due to nerve infarction, causing blindness in these patients. Mucor can cause ophthalmic artery occlusion [16], leading to blindness, which can be picked up on MR Angiogram (Fig. 3.18).

Enhancement of the soft tissue in the area of the orbital apex and optic nerve with extension up to the superior orbital fissure may manifest with the clinical features of orbital apex syndrome. In cases of sinusitis where CT and MRI findings are associated with the presence of disease in the orbital apex area it is highly suggestive of an invasive fungal infection [17]. Intracranial spread of infection may occur from the orbital apex via the superior orbital fissure involving the cavernous sinus (Fig. 3.19). The pterygopalatine fossa and infratemporal fossa may get involved through

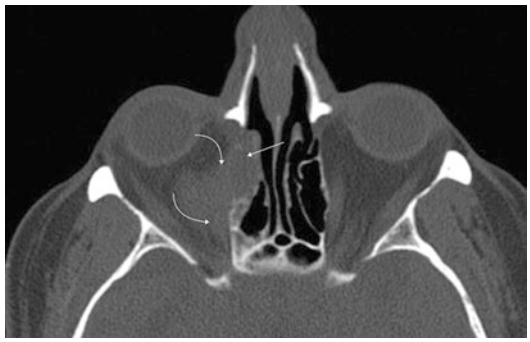

Fig. 3.9 Axial CT images showing medial orbital wall erosion (arrow) and intraorbital extension (curved arrows)

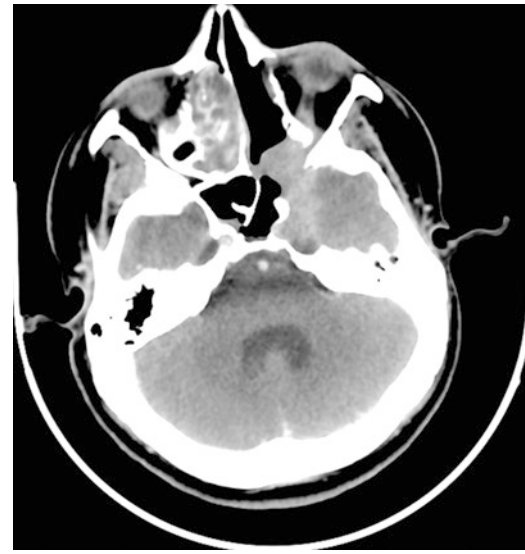

Fig. 3.10 Axial Contrast CT scan showing extension of soft tissue into the orbit

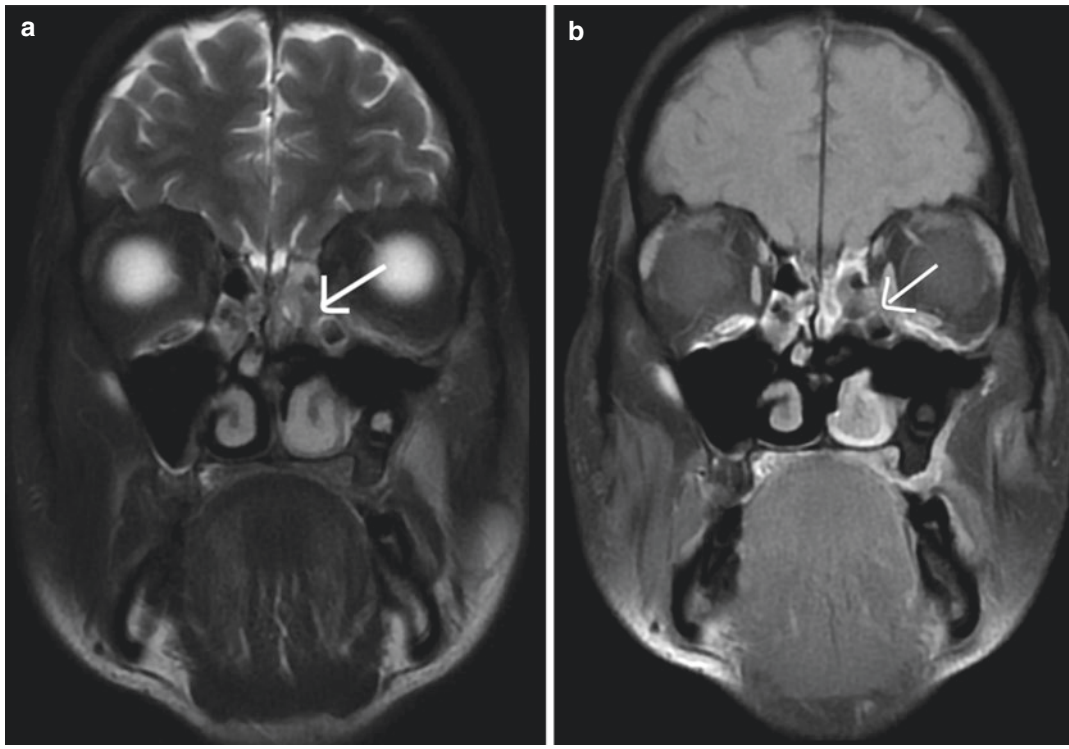

Fig. 3.11 (**a**) Coronal T2FS showing T2 hypointense areas in the left ethmoid. (**b**) Coronal T1 FS Post-contrast MRI showing non-enhancing areas left ethmoid, which appeared hypointense on T2

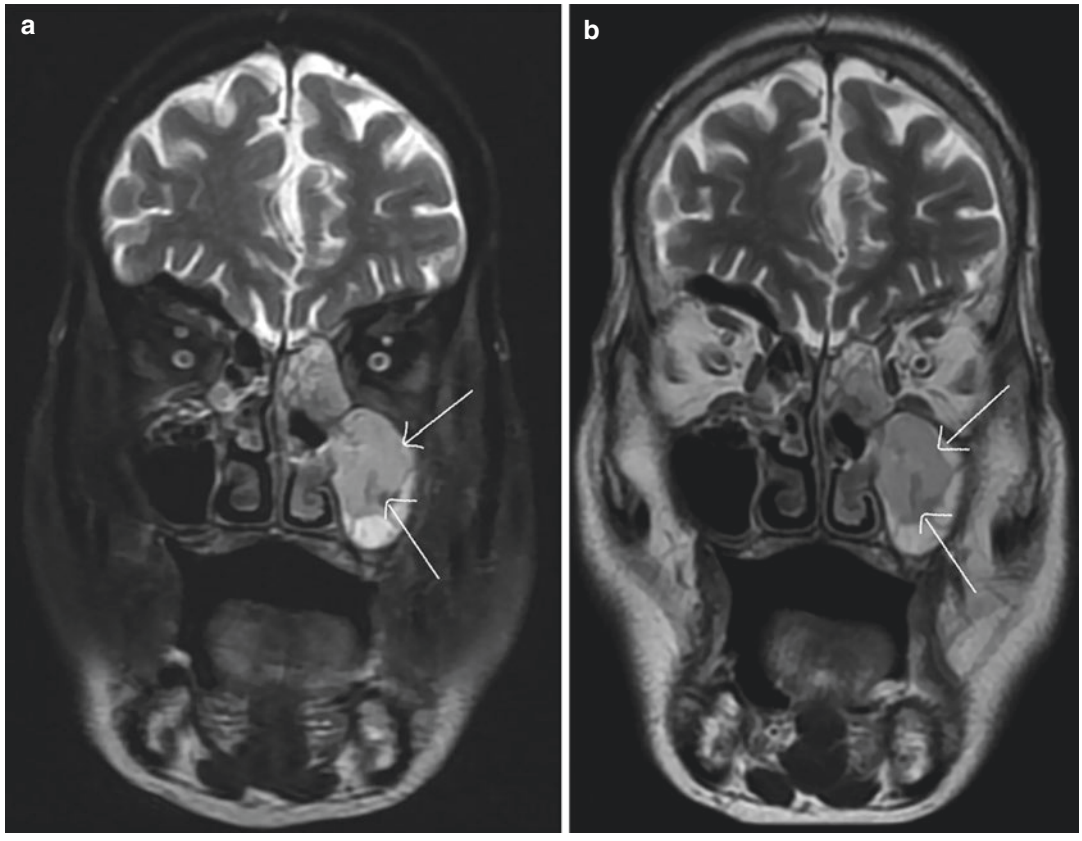

Fig. 3.12 Coronal MRI (**a**) T2 FS, (**b**) T2 showing hypointense areas within the hyperintense mucosal thickening of left maxillary and ethmoid sinuses suggestive of fungal aetiology

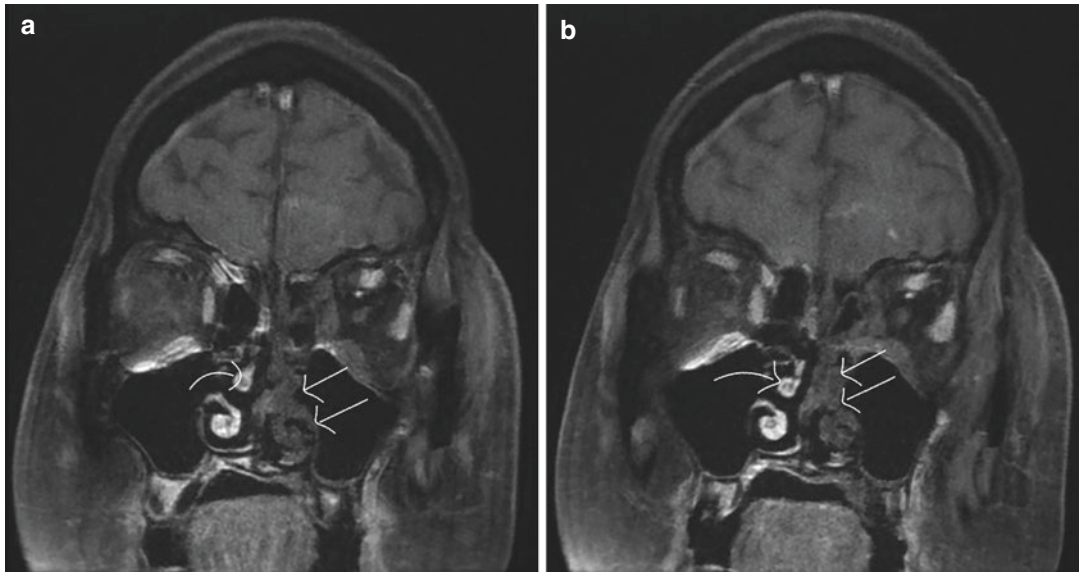

Fig. 3.13 (**a**) Coronal Post-Contrast T1 FS MRI showing non-enhancing left middle turbinate (arrows) and normally enhancing right middle turbinate (curved arrow). (**b**) Coronal Post-Contrast T1 FS MRI showing non-enhancing left middle turbinate (arrows) and normally enhancing right middle turbinate (curved arrow)

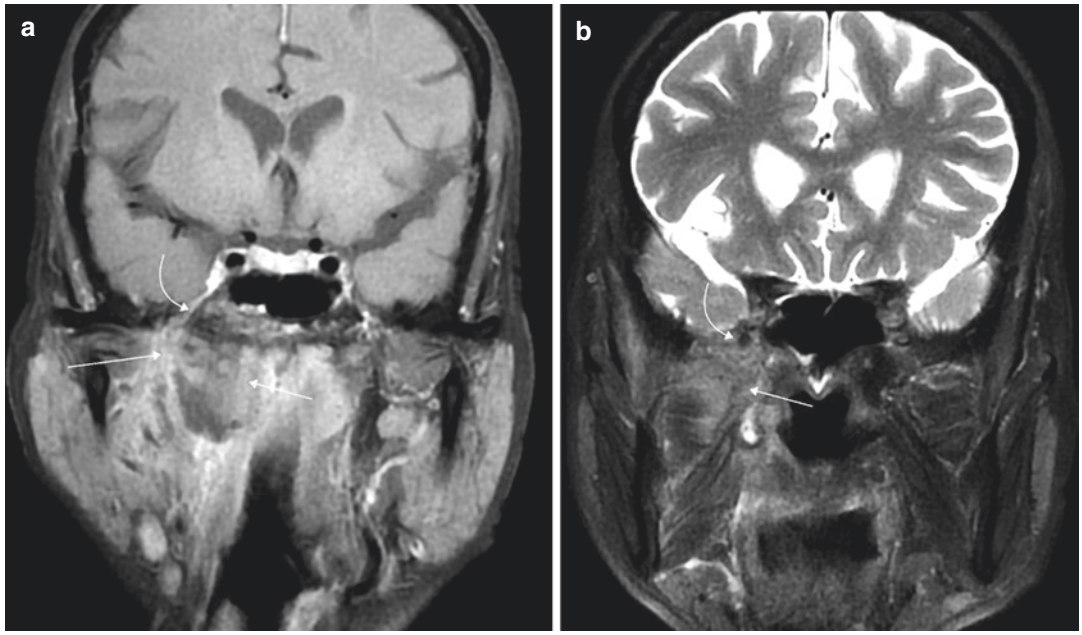

Fig. 3.14 (**a**) Post-contrast 3D T1 FS coronal MRI Showing areas of peripherally enhancing centrally non-enhancing collections (aww) in right pterygoid space. The soft tissue shows perineural extension along the right trigeminal nerve into the right cavernous sinus (curved arrow). (**b**) Coronal T2 FS MRI showing soft issue in Right pterygoid space (arrow) with infiltration of the right pterygoid wedge (curved arrow)

the inferior orbital fissure [18]. Progressive spread of ROCM along orbital apex can extend into the central nervous system. There is a partial radial occlusion of the blood vessels with a decreased speed of the blood flow in the ipsilateral internal carotid artery in the vicinity of mucor invasion [4, 6–8].

An intracranial extension may occur directly, through erosion of cribriform plate (Figs. 3.20 and 3.21), due to the erosion of the sphenoid wall, and through the orbital fissures or orbital apex. Indirect spread may occur from the infratemporal fossa through perineural extension along the trigeminal nerve (Figs. 3.23 and 3.24). Early cerebritis are seen on MRI as a high signal on FLAIR images and meningeal enhancement on Post Gadolinium-enhanced images [8]. Direct fungal invasion and Intra-cerebral fungal granulomas appear as hypointense signal intensities on T1- and T2-weighted images with minimal or no post-contrast enhancement (Figs. 3.25 and 3.26).

White matter oedema shows a high signal on FLAIR/T2W images, without diffusion restriction. Fungal abscess formation [2] seen as T2/FLAIR hyperintensities with diffusion restriction and peripheral rim enhancement with contrast (Figs. 3.21, 3.22 and 3.27). In a few cases, when there is osteonecrosis and erosion of the sphenoid wing or the roof of the orbit, extraxial or intraxial soft tissue may show mild enhancement. Leptomeningeal enhancement and thickening, seen as low signal T2 with enhancement on Post Gadolinium-enhanced images (Figs. 3.4c and 3.21d).

Mucor eroding the walls of the sphenoid sinuses cause osteomyelitis or necrosis of the clivus (Fig. 3.28) or can extend to the Meckel's cave or the cavernous sinus. Cavernous sinus extension may also occur through the superior orbital fissure or perineural invasion from the infratemporal fossa or erosion of the temporal bone. Cavernous sinus thrombosis appears as poor enhancement of cavernous sinus with convex bulging with patchy or no enhancement on post-Gadolinium-enhanced images (Fig. 3.28). Dilated Superior ophthalmic vein (>4 mm diameter) is the indirect sign of cavernous sinus involvement (Fig. 3.29). The cavernous and

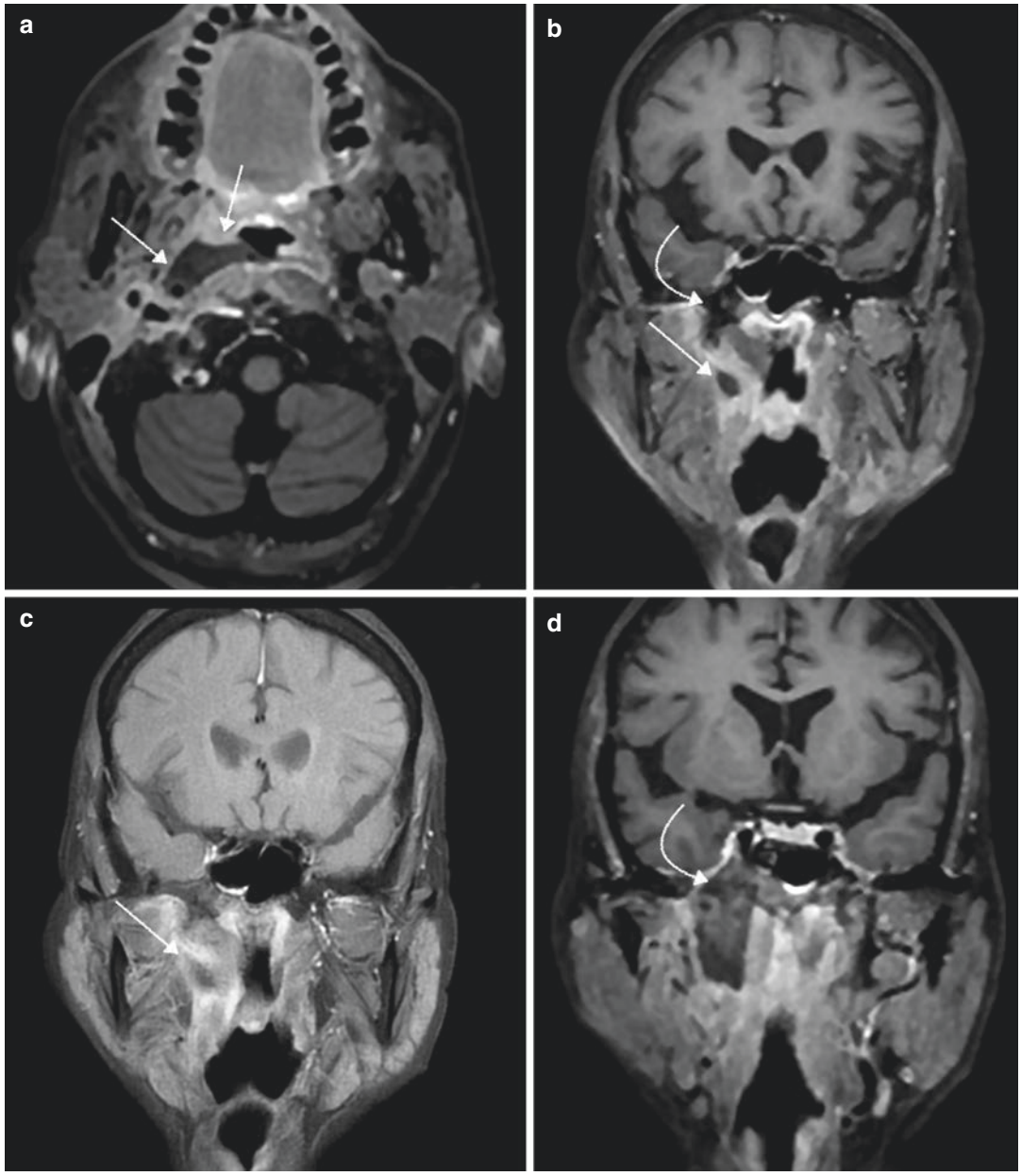

Fig. 3.15 (**a**) Post-contrast 3D T1 FS axial MRI showing nasopharyngeal abscess (arrow). (**b**) Post-contrast 3D T1 FS coronal MRI showing right nasopharyngeal fungal abscess (arrow). (**c**) Post-contrast 3D T1 FS coronal MRI showing right nasopharyngeal fungal abscess (arrow). (**d**) Post-contrast 3D T1, FS Coronal MRI showing non-enhancing right pterygoid wedge suggestive of osteonecrosis (curved arrow)

petrous segments of Internal Carotid artery may be involved. The signs of this involvement [19, 20] include wall thickening which causes narrowing, thrombosis, dissection or Pseudoaneurysm formation and are evaluated with MR non-contrast TOF (Time-of-Flight) angiogram (Figs. 3.30 and 3.31). Rupture of Mycotic aneurysm can lead to subarachnoid haemorrhage. Occlusion or stenosis of the intracranial arteries leads to acute infarcts, which are

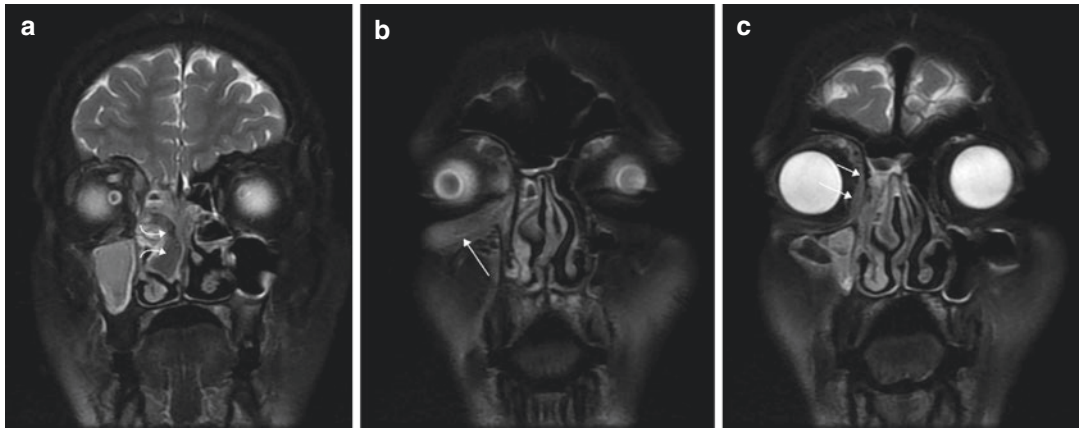

Fig. 3.16 Coronal T2 FS MRI showing (**a**) Hypointense turbinate (curved arrows), (**b**) Preseptal oedema (arrow), (**c**) Thin, soft tissue in the extraconal space of right orbit abutting the medial rectus muscle (arrows)

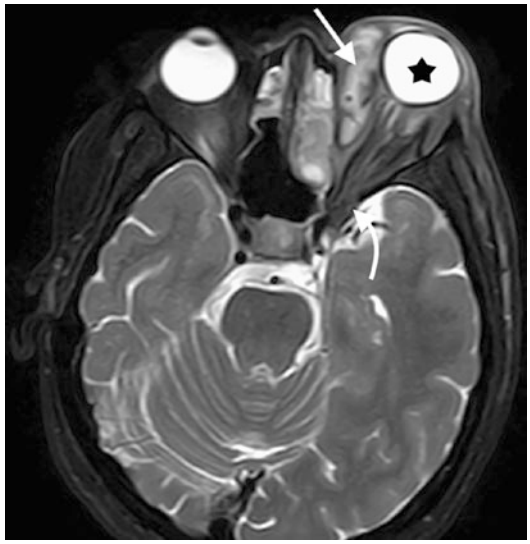

Fig. 3.17 Axial T2 FS MRI shows erosion of the medial wall of left orbit with abscess formation infiltrating the medial rectus muscle (arrows). There is increased signal intensity in the left vitreous body (*) causing severe proptosis, periorbital oedema and tenting of the posterior globe ("guitar pick" sign). There is stretching of the optic nerve (curved arrow) (Picture courtesy: Dr. Seetharaman KMCH, Coimbatore)

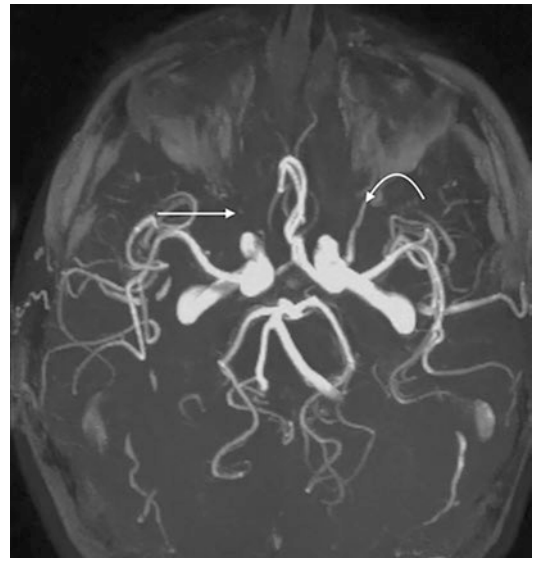

Fig. 3.18 MR Non-contrast Angiogram showing occlusion of right ophthalmic artery on the right side (arrow) and normally visualized left ophthalmic artery on left (curved arrows)

seen as diffusion-restricted lesions in the brain (Figs. 3.32 and 3.33).

Cerebral fungal infections, ischaemia of the optic nerve, tissue ischaemia and necrosis can be easily picked up by restricted diffusion on diffusion-weighted MRI [21–23]. DWI MRI sequences can also differentiate ROCM from malignancies [23].

Perineural spread or cranial nerve infiltration involving the Trigeminal nerve or its branches appears as thickening and enhancement along the nerve course up to the brain stem (Figs. 3.34 and 3.35). Fluid signal loss on T2W and mild enhancement on post-contrast images are signs of invasion of mucor (Fig. 3.24).

In long-standing, untreated cases with extensive disease, skull base osteomyelitis may occur. It is a rare complication that often occurs in the late stages of the disease [24, 25]. The disease has a preferential spread along the blood vessels due to its angioinvasive nature. It then extends to the deep soft tissues through the perivascular channels [25] (Fig. 3.3). Bone involvement occurs relatively late in the course of the disease.

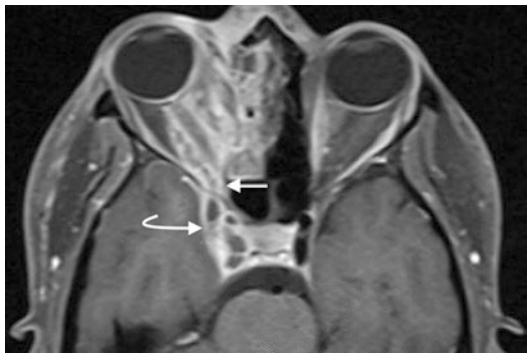

Fig. 3.19 Axial Post-contrast T1 FS axial MRI is showing right ethmoid fungal sinusitis eroding into the right orbit involving the lacrimal sac and nasolacrimal duct with extension into the right orbital apex and ipsilateral cavernous sinus

Early involvement of the bone marrow is seen as a loss of normal fat signal on T1W images. The diseased marrow appears hypointense on T1W images, hyperintense on STIR images and heterogeneously enhanced on post-contrast images [26] (Figs. 3.4c, d).

Large areas of diffused heterogenous enhancement are seen in advanced disease with bony infiltration (Fig. 3.3a, b). Adjacent normal fat planes are obliterated with T2 hyperintense areas indicating soft-tissue oedema. Perineural, and intracranial spread may also be seen. Presence of an area of fluid signal intensity with diffusion restriction in the centre and a rim enhancement in the periphery indicate an abscess formation [27] (Figs. 3.3 and 3.4).

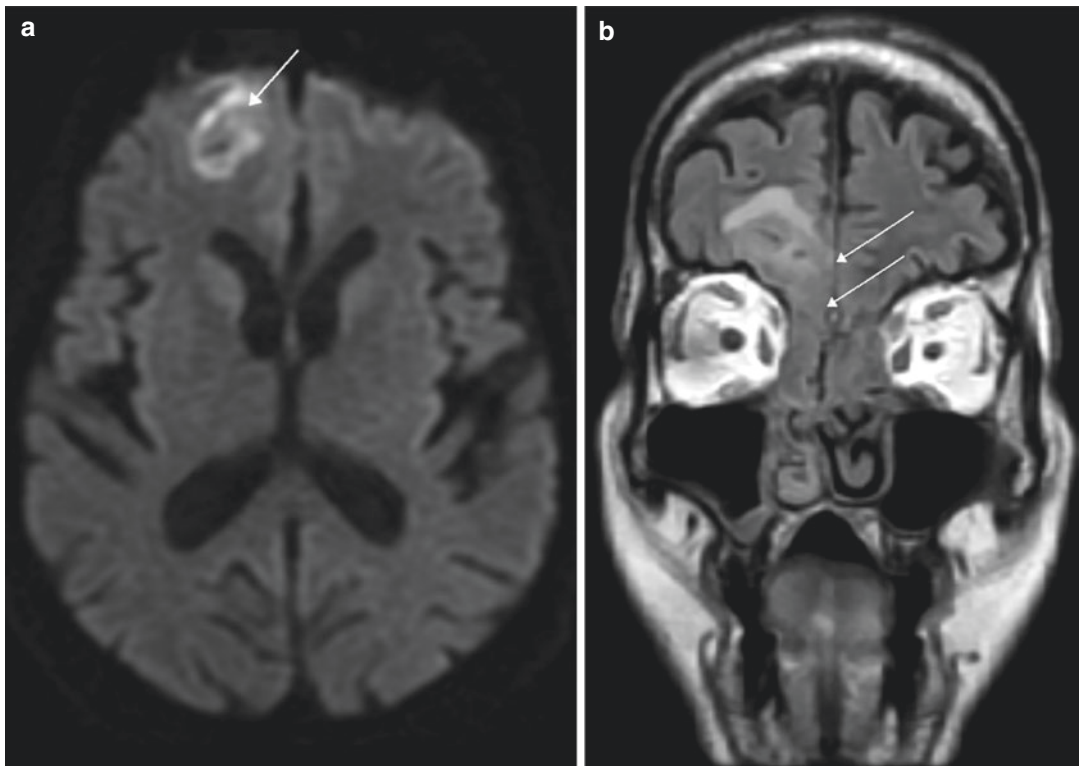

Fig. 3.20 (**a**) DWI MRI showing diffusion restriction in the right frontal lobe. (**b**) T2W coronal images showing direct extension of fungal soft tissue into the right frontal lobe from sinonasal cavity eroding the roof of the right ethmoid

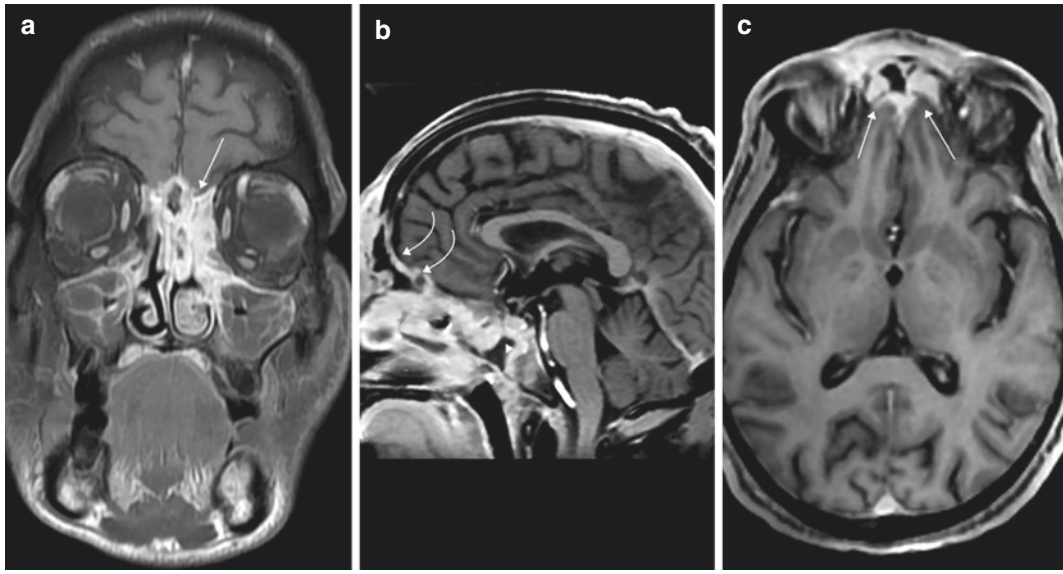

Fig. 3.21 (**a**) Coronal post-contrast T1 FS MRI showing roof of ethmoid erosion with an intracranial extradural extension of soft tissue with leptomeningeal enhancement. (**b**) Sagittal T1 Post-contrast T1FS MRI showing Frontobasal leptomeningeal enhancement (curved arrows) and clival erosion (Arrowhead). (**c**) Axial Post-Contrast T1FS MRI showing frontal sinus disease eroding intracranially with soft tissue in the interhemispheric plane (arrows)

Inferiorly, the disease can infiltrate and erode the maxillary sinus floor to involve the alveolar surface (Figs. 3.35 and 3.36). The osteonecrosis and osteomyelitis of bones are seen as hyperintense signal intensities on T2FS/STIR images with no contrast enhancement in the former. The disease can erode the hard palate with mildly enhancing soft tissue in the oral cavity (Fig. 3.37). The extent of palatal involvement must be assessed carefully to ensure complete debridement of the disease process and prevent residual disease and revision surgeries.

3.7 Follow-Up Imaging

MR imaging helps in post-operative follow-up of patients who are on medical treatment following surgery. If there is a strong suspicion of ROCM in a patient presenting with suggestive clinical features but the nasal endoscopy and initial MR imaging studies are non-conclusive, repeat imaging should be performed after 72 hours [14]. Any evidence of progression of the disease suggests fungal aetiology and the classical signs should be looked for.

MRI also helps in follow-up of patients with early disease who are either on conservative treatment, have undergone limited sinus debridement or receiving transcutaneous retrobulbar amphotericin B injections. Early pick up of disease progression facilitates a more radical approach involving orbital exenteration that helps in decreasing the disease load [14]. It is important to remember that the clinical improvement following treatment is fast but the imaging findings take time to resolve.

However, deteriorating radiological features represent disease progression [28].

3.8 Post-operative Imaging

Post-operative Imaging with plain and post-contrast MRI imaging for evaluating the residual disease and for assessing the progression is recommended:

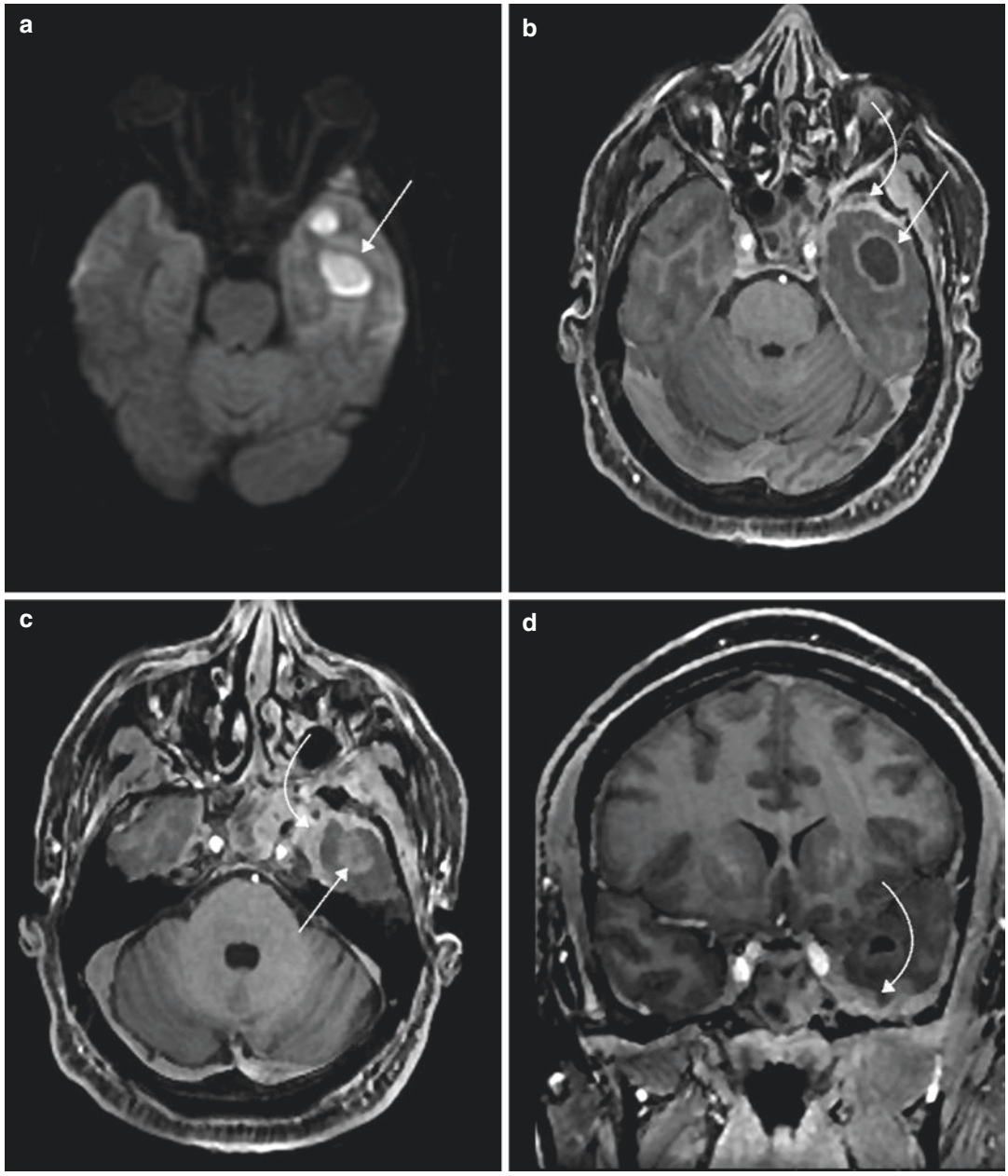

Fig. 3.22 (**a**) DWI MRI showing left temporal lobe diffusion restricted abscess. (**b**) Axial post-contrast 3D T1FS MRI images showing peripherally enhancing fungal abscess in the left temporal lobe with surrounding oedema. (**c**) Axial post-contrast 3D T1FS MRI images showing peripherally enhancing fungal abscess in the left temporal lobe with surrounding oedema. (**d**) Coronal post-contrast T1FS MRI shows enhancing left basal temporal Leptomeninges

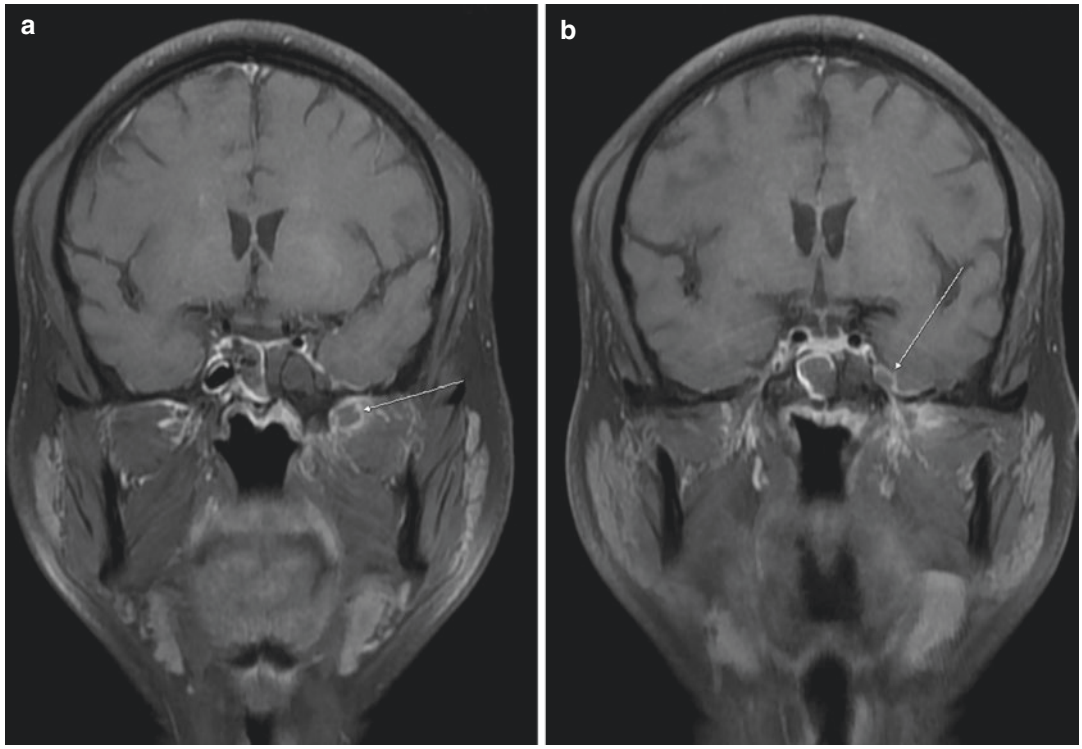

Fig. 3.23 Post-contrast T1 FS coronal MRI images showing (**a**) non-enhancing area in the left pterygoid space (arrow) and (**b**) showing perineural extension through the foramen Rotundum (arrow)

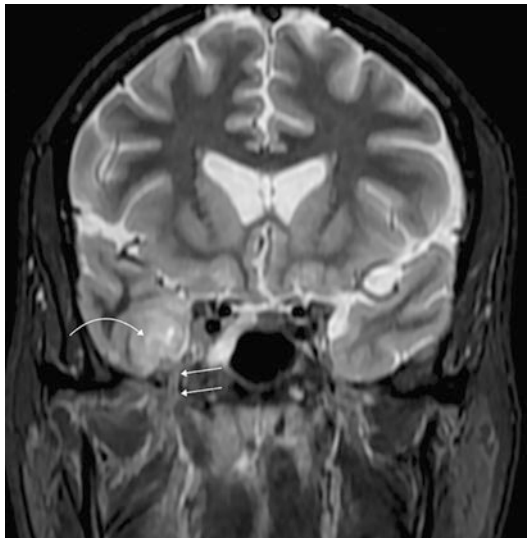

Fig. 3.24 T2 FS coronal MRI showing perineural extension (arrows) of fungal soft tissue intracranially into the right medial temporal lobe (curved arrow)

- In persistent residual or increasing pain over the face, the palate or, the maxillary region.
- Worsening symptoms with increasing visual disturbance, retroorbital pain, ophthalmoplegia, headache, seizures, hemiparesis or hemiplegia.

3.9 Pitfalls of MR Imaging

Though MRI is an extremely useful investigation in ROCM it has its own limitations. In the early phase of disease, MRI may be non-conclusive. Therefore in the event of strong suspicion of ROCM based on clinical signs and immediate endoscopic exploration, biopsy and debridement should be performed in high-risk individuals [29, 30]. Fat-saturated MR sequences may have "susceptibility artefacts", in the soft tissues around

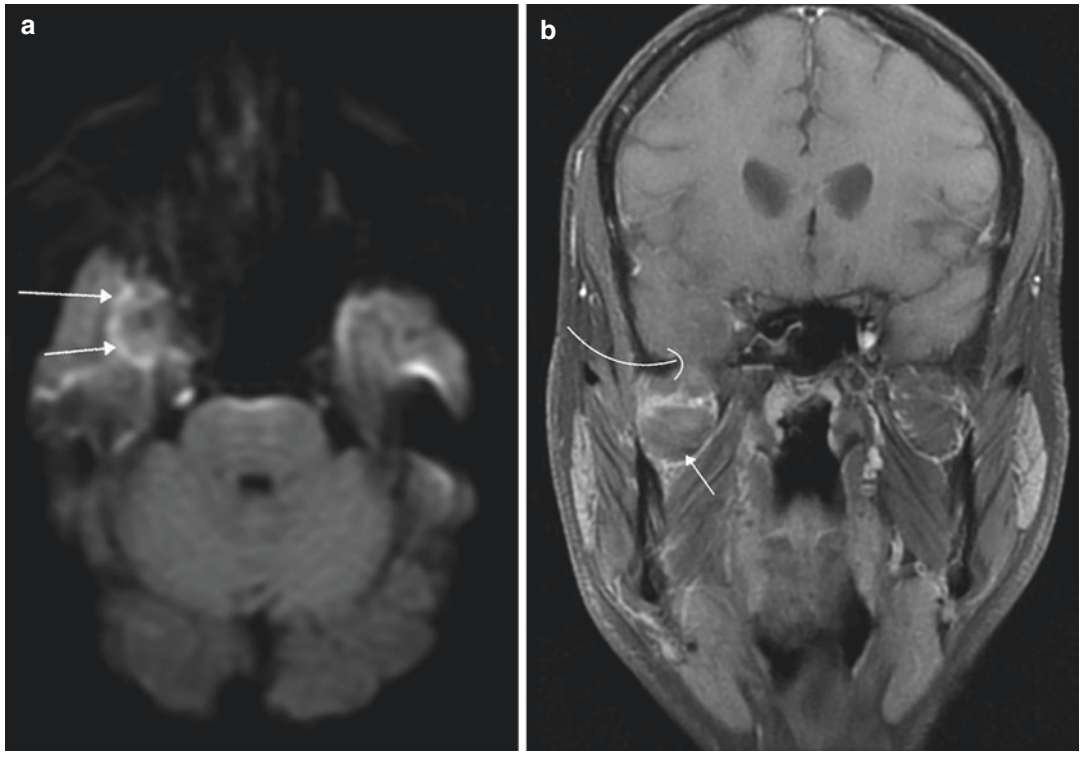

Fig. 3.25 (**a**) DWI MR scan showing subtle diffusion restricted area in the right medial temporal lobe (arrows). (**b**) Post-contrast T1 FS coronal MRI showing non-enhancing fungal soft tissue in the pterygoid space (arrows) eroding skull base (curved arrow) from and extending into the brain

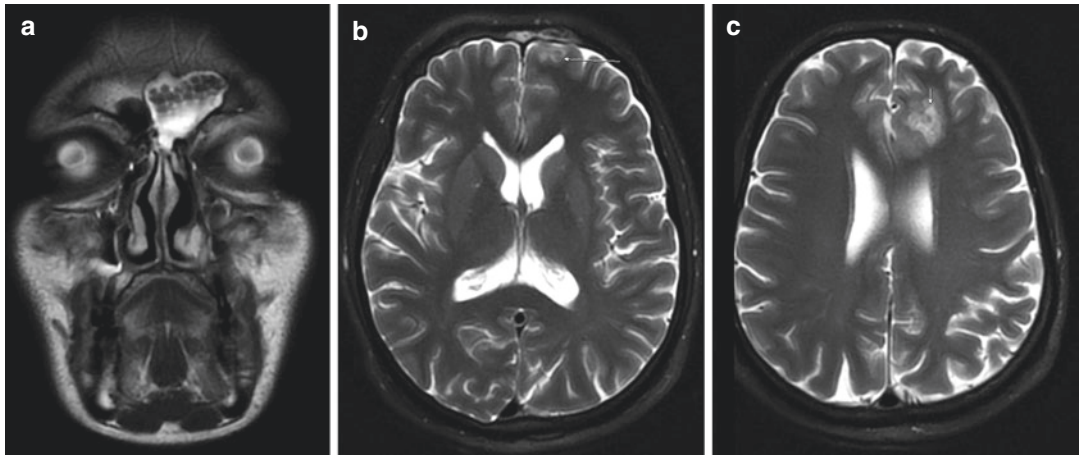

Fig. 3.26 (**a**) T2 FS MRI coronal section showing hypointensities in the left frontal sinus. (**b**) T2 FS MRI axial section showing erosion of the posterior wall of left frontal sinus with intracerebral extension (arrow). (**c**) Left frontal lobe abscess (arrow)

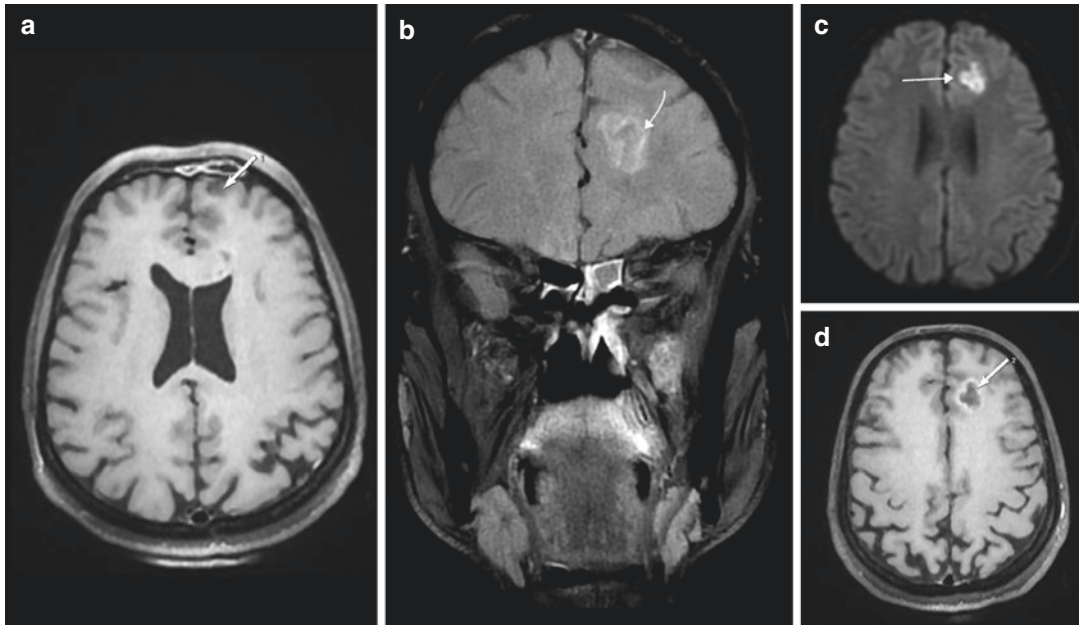

Fig. 3.27 (**a**) Post-contrast T1 Axial FS MRI scan showing peripherally enhancing fungal abscess. (**b**) Coronal post-contrast T1 images showing irregularly enhancing left frontal abscess. (**c**) DWI MRI scan showing diffusion restriction in left frontal lobe abscess. (**d**) Post-contrast T1 Axial FS MRI showing peripherally enhancing fungal abscess

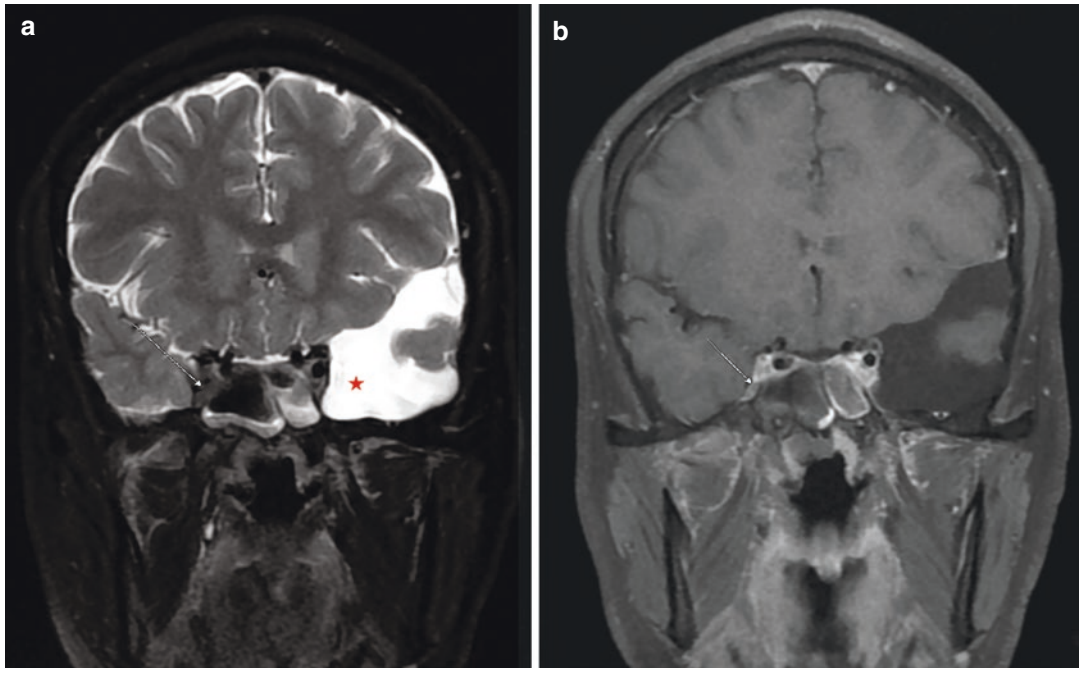

Fig. 3.28 (**a**) MRI coronal T2W scan showing hypointense soft tissue in the base of the right cavernous sinus (arrow) and incidental left temporal arachnoid cyst (red star). (**b**) Post-contrast T1 FS MRI scan showing non-enhancement of soft tissue in the base of the cavernous sinus

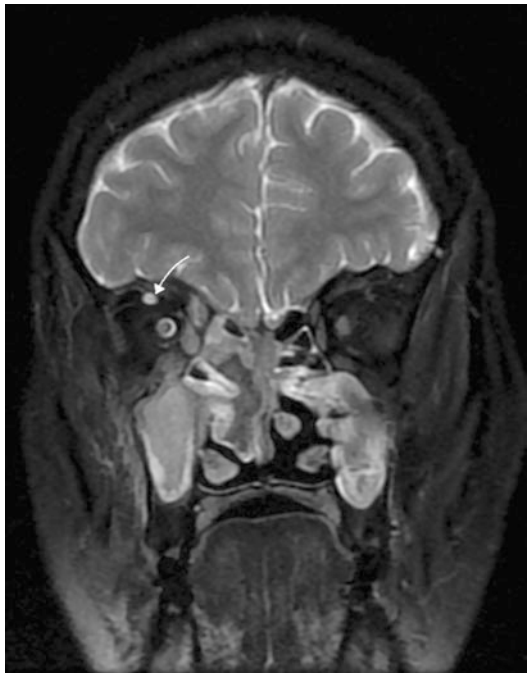

Fig. 3.29 T2W, FS coronal MRI showing dilated right superior ophthalmic vein (Curved arrow). Hypointense bilateral maxillary sinus, right ethmoid sinus and right middle turbinate

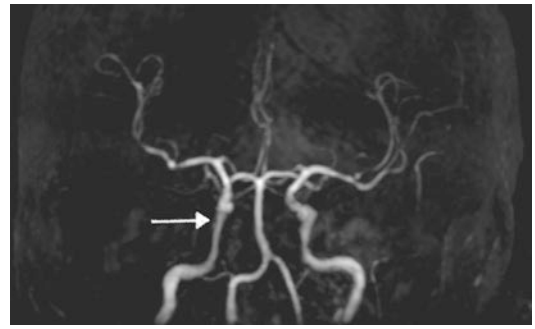

Fig. 3.30 MR non-contrast Angiogram showing diffuse right internal carotid artery narrowing (Arrow)

Fig. 3.31 MR non-contrast Angiogram showing Fusiform Aneurysm of M1 segment of right Middle Cerebral Artery (Yellow arrow 1)

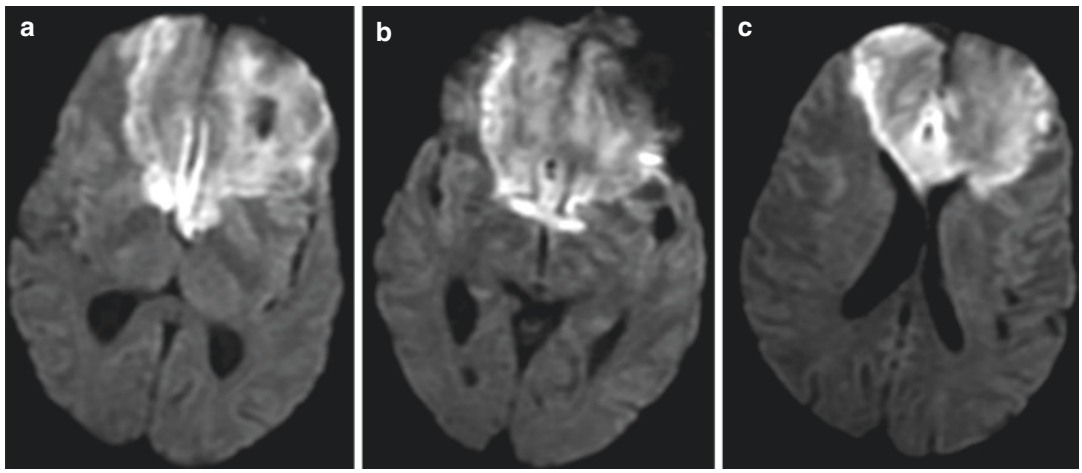

Fig. 3.32 (**a**) MR DWI MRI scan showing Invasive fungal sinusitis with bifrontal acute diffusion restricted infarcts. (**b**) MR DWI MRI scan showing Invasive fungal sinusitis with bifrontal acute diffusion restricted infarcts. (**c**) MR DWI MRI scan showing Invasive fungal sinusitis with bifrontal acute diffusion restricted infarcts

the paranasal sinuses. These artefacts appear due to the air in the sinuses and metallic dental implants that disturb the magnetic field. These artefacts are usually seen as areas of a bright signal along the floor of the orbit, at the orbital apex and in the infratemporal fossa [31].

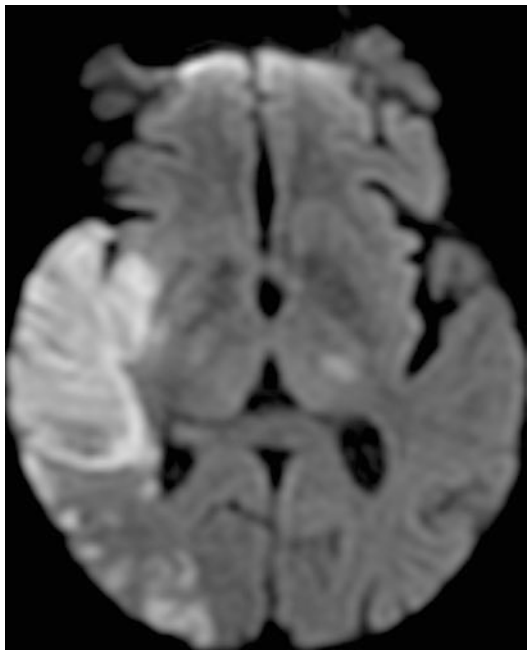

Fig. 3.33 DWI MRI showing diffusion restricted acute infarcts in right temporoparietal lobe

Non-specific findings like mucosal thickening and sinus opacification may be seen in chronic non-invasive sinusitis as well as in invasive fungal sinusitis. The loss of enhancement of the involved turbinate (black turbinate sign) has been described as an early sign of fungal aetiology. This non-enhancement of the middle turbinate extends to the contiguous structures such as fat, muscle and bone [32]. The involved regions show variable signal intensity on T2-weighted images. On contrast-enhanced MRI the posterior and mid portions of the inferior turbinate appear black with no extension into the surroundings. There is a central area of non-enhancement and a thin peripheral rim of preserved mucosal enhancement. The diseased area may be intermediate or hyperintense on T2-weighted images but never shows hypointensity. On scans done later, the non-enhancement persists in fungal sinusitis, while benign black turbinate shows progressive enhancement [33].

MRI or any imaging cannot differentiate between microbiological characteristic of any invasive fungal infection. Besides Mucorales (Mucor, Rhizopus and Absidia), *Aspergillus* species can also lead to acute invasive fungal sinus-

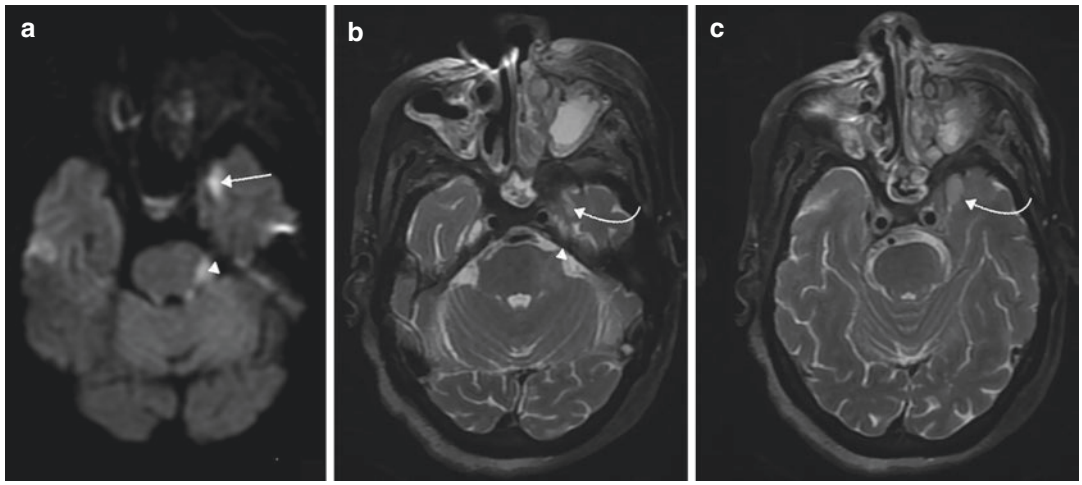

Fig. 3.34 (**a**) DWI MRI scan showing diffusion restriction along the left trigeminal nerve (Arrow) up to the root entry zone in the pons (arrowhead). (**b**) T2 axial MRI scan showing hyperintense signal along the left Trigeminal nerve (arrow) up to the pons (arrowhead). (**c**) T2 axial MRI showing hyperintense signal along the left Trigeminal nerve (arrow) up to the pons (arrowhead)

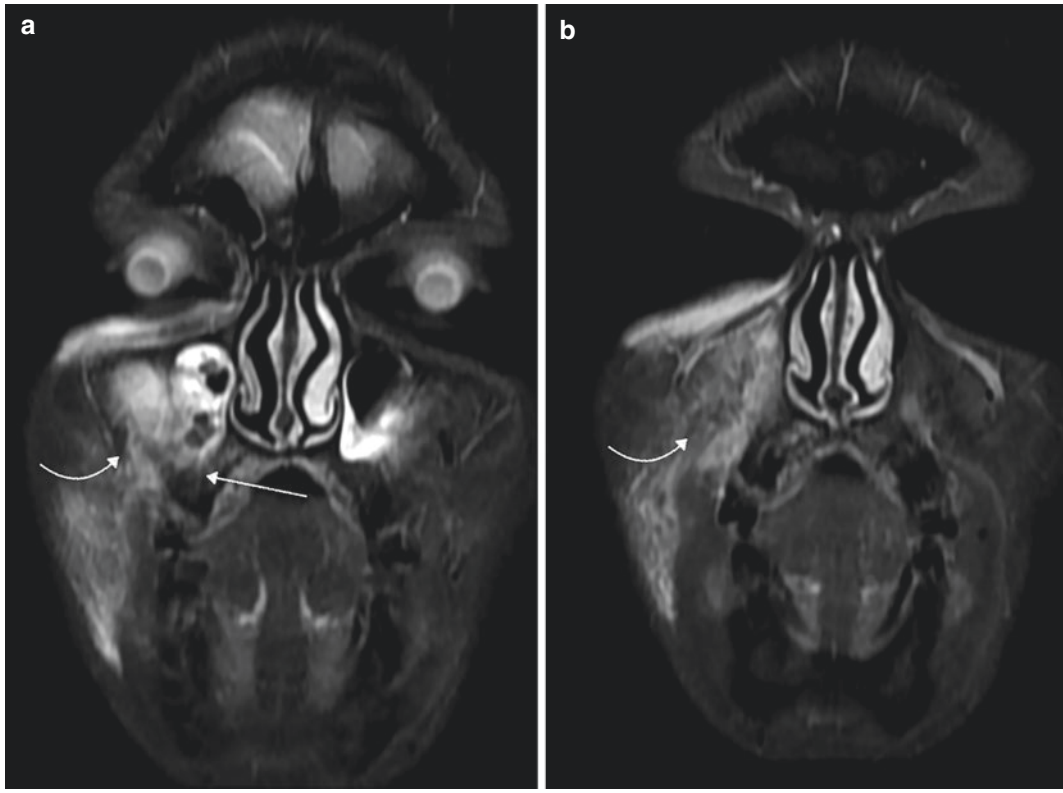

Fig. 3.35 (**a**) T2 FS coronal MRI showing right maxillary fungal sinusitis eroding the right alveolar surface of maxilla (arrows) and Premaxillary mixed-signal intense soft tissue and inflammation (Curved arrow). (**b**) T2 FS coronal MRI showing right maxillary fungal sinusitis eroding the right alveolar surface of maxilla (arrows) and Premaxillary mixed-signal intense soft tissue and inflammation (Curved arrow)

itis. Mixed invasive fungal infections are also known to occur [33]. Differentiation between these subgroups is possible only on microbiology and histopathological examination and has therapeutic and prognostic implications. It is imperative to report MRI, as possible fungal aetiology with or without invasive features and not to report as mucor.

In post-operative cases, the haemorrhage and clots may appear hypointense on T2 images, mimicking residual fungal disease. The bone oedema takes 2 weeks or more to resolve. Biochemically decreasing C-reactive protein (CRP) test values indicate the resolution of the disease. In equivocal findings, nasal endoscopic evaluation and microscopical evaluation of the scrapings from suspicious areas help reach the diagnosis.

3.10 Differential Diagnosis of ROCM

The differentiation between invasive and a non-invasive sinusitis is one is the most important information that is needed from radiology in ROCM.

Hypointense and non-enhancing soft tissues on T2W scans may point to a fungal aetiology. Similarly, involvement of the extraocular muscles without eyelid swelling or mucosal thickening in the paranasal sinus indicates fungal aetiology [32]. Other differential diagnoses of ROCM include inflammatory pathologies such as IgG4-related disease, sarcoidosis and Wegener's granulomatosis that are treated with immunosuppressive therapy. Careful clinical evaluation, nasal endoscopic examination and prompt biopsy of the lesion are important to prevent grave implications of misdiagnosis [14].

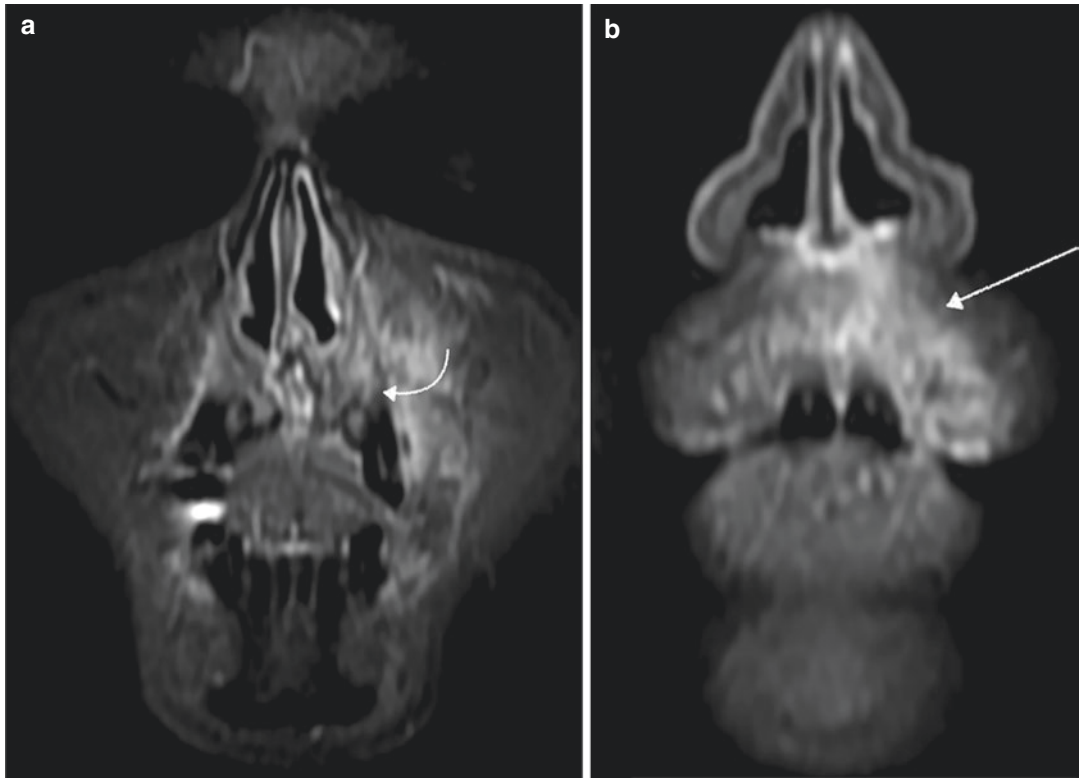

Fig. 3.36 (**a**) T2 FS coronal MRI showing invasion of the left alveolar process of the maxilla (curved arrow) and premaxillary inflammation (arrow). (**b**) T2 FS coronal MRI showing invasion of the left alveolar process of the maxilla (curved arrow) and premaxillary inflammation (arrow)

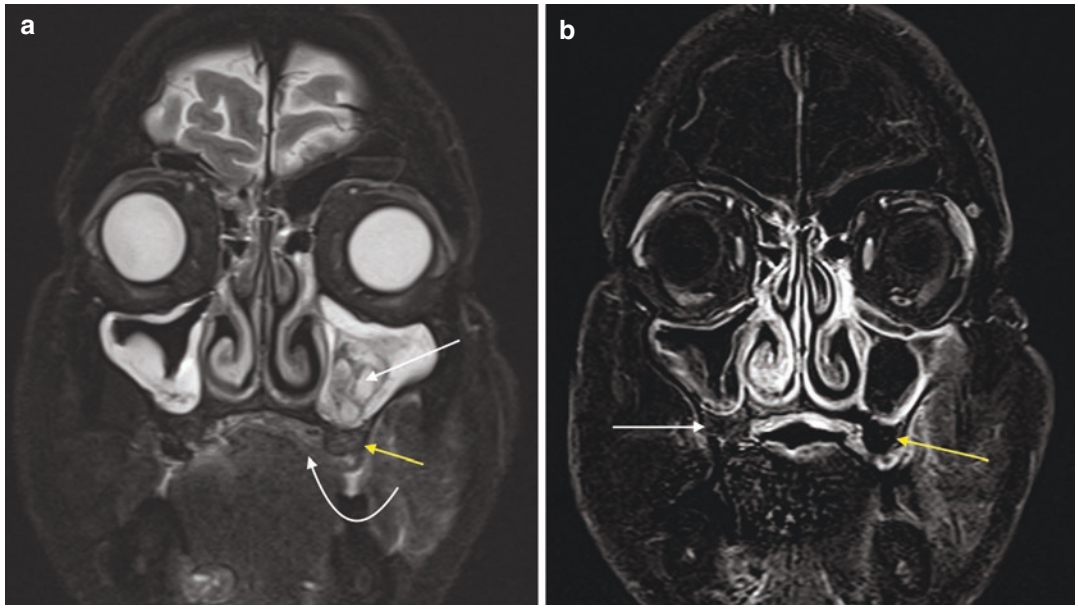

Fig. 3.37 (**a**) Coronal T2W, FS MRI shows T2 hypointense fungal sinusitis in left Maxillary sinus (arrow), with altered signal intensity in the left alveolar process of the maxilla (yellow arrow) with soft tissue in the left side of the hard palate (curved arrow). (**b**) Digitally subtracted post-contrast MRI Coronal Image, showing necrosed left the alveolar process of the maxilla (yellow arrow) compared to the viable right alveolar process of the maxilla (white arrow)

References

1. Turner JH, Soudry E, Nayak JV, et al. Survival outcomes in acute invasive fungal sinusitis: a systematic review and quantitative synthesis of published evidence. Laryngoscope. 2013;123:1112–8.
2. Gamba JL, Woodruff WW, Djang WT, Yeates AE. Craniofacial mucormycosis: assessment with CT. Radiology. 1986;160:207–12.
3. Therakathu J, Prabhu S, Irodi A, Sudhakar SV, Yadav VK, Rupa V. Imaging features of rhinocerebral mucormycosis: a study of 43 patients. Egypt J Radiol Nucl Med. 2018;49(2):447–52. https://doi.org/10.1016/j.ejrnm.2018.01.001.
4. Ochiai H, Iseda T, Miyahara S, Goya T, Wakisaka S. Rhinocerebral mucormycosis - Case report. Neurol Med Chir (Tokyo). 1993;33:373–6.
5. Hosseini SM, Borghei P. Rhinocerebral mucormycosis: pathways of spread. Eur Arch Otorhinolaryngol. 2005;262(11):932–8. https://doi.org/10.1007/s00405-005-0919-0.
6. Yousem DM, Galetta SL, Gusnard DA, Goldberg HI. MR findings in rhinocerebral mucormycosis. J Comput Assist Tomogr. 1989;13:878–82.
7. McLean FM, Ginsberg LE, Stanton CA. Perineural spread of rhinocerebral mucormycosis. AJNR Am J Neuroradiol. 1996;17:114–6.
8. Herrera DA, Dublin AB, Ormsby EL, Aminpour S, Howell LP. Imaging findings of rhinocerebral mucormycosis. Skull Base. 2009;19:117–25.
9. Honavar SG. Code mucor:guidelines for the diagnosis, staging and management of rhino-orbito-cerebral mucormycosis in the setting of COVID-19. Indian J Ophthalmol. 2021;69:1361–5.
10. Horger M, Hebart H, Schimmel H, et al. Disseminated mucormycosis in haematological patients: CT and MRI findings with pathological correlation. Br J Radiol. 2006;79(945):e88–95.
11. Centeno RS, Bentson JR, Mancuso AA. CT scanning in rhinocerebral mucormycosis and aspergillosis. Radiology. 1981;140:383–9.
12. Kilpatrick C, Tress B, King J. Computed tomography of rhinocerebral mucormycosis. Neuroradiology. 1984;26:71.
13. Safder S, Carpenter JS, Roberts TD, et al. The "black turbinate" sign: an early MR imaging finding of nasal mucormycosis. AJNR Am J Neuroradiol. 2010;31(4):771–4.
14. Sreshta K, Dave TV, Varma DR, Nair AG, Bothra N, Naik MN, Sistla SK. Magnetic resonance imaging in rhino-orbital-cerebral mucormycosis. Indian J Ophthalmol. 2021;69(7):1915–27. https://doi.org/10.4103/ijo.IJO_1439_21.
15. Theoret J, Sanz GE, Matero D, Guth T, Erickson C, Liao MM, Kendall JL. The "guitar pick" sign: a novel sign of retrobulbar haemorrhage. Can J Emerg Med. 2011;13(3):162. https://doi.org/10.2310/10.2310/8000.2011.110279.
16. Bawankar P, Lahane S, Pathak P, Gonde P, Singh A. Central retinal artery occlusion as the presenting manifestation of invasive rhino-orbital-cerebral mucormycosis. Taiwan J Ophthalmol. 2020;10(1):62–5. https://doi.org/10.4103/tjo.tjo_72_18.
17. Anders UM, Taylor EJ, Martel JR, Martel JB. Acute orbital apex syndrome and rhino-orbito-cerebral mucormycosis. Int Med Case Rep J. 2015;17(8):93–6.
18. Sotoudeh H, Shafaat O, Aboueldahab N, Vaphiades M, Sotoudeh E, Bernstock J. Superior ophthalmic vein thrombosis: what radiologist and clinician must know. Eur J Radiol Open. 2019;6:258–64.
19. Simmons JH, Zeitler PS, Fenton LZ, Abzug MJ, Fiallo-Scharer RV, Klingensmith GJ. Rhinocerebral mucormycosis complicated by internal carotid artery thrombosis in a pediatric patient with type 1 diabetes mellitus: a case report and review of the literature. Pediatr Diabetes. 2005;6(4):234–8. https://doi.org/10.1111/j.1399-543X.2005.00118.x.
20. Delbrouck C, Jacobs F, Fernandez Aguilar S, Devroede B, Choufani G, Hassid S. Carotid artery occlusion due to fulminant rhinocerebral mucormycosis. Acta Otorhinolaryngol Belg. 2004;58(2):135–40.
21. Hatipoglu HG, Gurbuz MO, Yuksel E. Restricted diffusion in the optic nerve and retina demonstrated by MRI in rhino-orbital mucormycosis. J Neuroophthalmol. 2009;29:13–5.
22. Gaviani P, Schwartz RB, Hedley-Whyte ET, Ligon KL, Robicsek A, Schaefer P, et al. Diffusion-weighted imaging of fungal cerebral infection. AJNR Am J Neuroradiol. 2005;26:1115–21.
23. Mathur S, Karimi A, Mafee MF. Acute optic nerve infarction demonstrated by diffusion-weighted imaging in a case of rhinocerebral mucormycosis. AJNR Am J Neuroradiol. 2007;28:489–90.
24. Devireddy SK, Kishore Kumar RV, Gali R. Mucormycotic skull base osteomyelitis:a case report. J Oral Maxillofacial Surg Med Pathol. 2014;26:336–9.
25. Chan LL, Singh S, Jones D, Diaz EM Jr, Ginsberg LE. Imaging of mucormycosis skull base osteomyelitis. AJNR Am J Neuroradiol. 2000;21:828–31.
26. Chapman PR, Choudhary G, Singhal A. Skull base osteomyelitis:a comprehensive imaging review. AJNR Am J Neuroradiol. 2021;42:404–13.
27. Álvarez Jáñez F, Barriga LQ, Iñigo TR, Roldán Lora F. Diagnosis of skull base osteomyelitis. Radiographics. 2021;41:156–74.
28. Sen M, Lahane S, Lahane TP, Parekh R, Honavar SG. Mucor is a viral land:a tale of two pathogens. Indian J Ophthalmol. 2021;69:244–52.
29. Rapidis AD. Orbitomaxillary mucormycosis (zygomycosis) and the surgical approach to treatment:perspectives from a maxillofacial surgeon. Clin Microbiol Infect. 2009;15(Suppl 5):98–102.

30. Groppo ER, El-Sayed IH, Aiken AH, Glastonbury CM. Computed tomography and magnetic resonance imaging characteristics of acute invasive fungal sinusitis. Arch Otolaryngol Head Neck Surg. 2011;137:1005–10.
31. Varma DR, Ponnaganti S, Dandu RV. Beware of artefacts in orbital magnetic resonance imaging. Indian J Ophthalmol. 2020;68:2516–8.
32. Han Q, Escott EJ. The black turbinate sign, a potential diagnostic pitfall:evaluation of the normal enhancement patterns of the nasal turbinates. AJNR Am J Neuroradiol. 2019;40:855–61.
33. Zayet S, Zaghdoudi A, Ammari L, Kilani B, Tiouiri Benaissa H. Cerebro-rhino-orbital mucormycosis and aspergillosis coinfection in a patient with diabetes mellitus: a case report. ID Cases. 2020;23:e01022.

4 Pathogenesis of COVID-Associated Mucormycosis

Shreya Singh, Rimjhim Kanaujia, and Shivaprakash M. Rudramurthy

4.1 Introduction

Mucormycosis is a serious fungal infection caused by ubiquitous fungi which belong to the order Mucorales. The common genera infecting humans include *Rhizopus* spp. (most commonly *R. arrhizus, R. microsporus*, and *R. homothallicus*), *Rhizomucor* spp., *Mucor* spp., *Cunninghamella* spp., *Lichtheimia* spp., and *Apophysomyces* spp. [1]. The major underlying health conditions predisposing to mucormycosis include diabetes mellitus (DM) and immunosuppression; trauma such as burns or road traffic accidents, and iron chelation therapy with deferoxamine [1–3]. An upsurge in the cases of mucormycosis has been noted over the last decade in the developed and developing world alike but has been especially concerning in Asia and specifically in India. Recently, a dramatic rise in the cases of mucormycosis infection has been observed in patients with Coronavirus-19 disease (COVID-19) or those recovering from it, as evidenced by several reports and institutional experiences [1, 3, 4]. COVID-19 is a viral inflammatory disease caused by SARS-CoV-2 characterized by an exaggerated proinflammatory response with cytokine surge, altered iron metabolism and iron overload, hemoglobinopathy, hypercoagulability state causing multisystem involvement [5–8]. Several strategies to prevent and treat mucormycosis have been used over the years, and more such strategies are urgently needed in view of its raging rise [9]. It is essential to have a clear understanding of the pathogenesis of this disease to facilitate these efforts and ensure appropriate management. Therefore, in this chapter, we will provide an overview of the pathogenesis of mucormycosis, focusing on rhino-orbital-cerebral mucormycosis (ROCM) in patients with COVID-19.

4.2 Host Risk Factors

Mucormycosis generally occurs in immunocompromised individuals with defined risk factors. Table 4.1 shows the risk factors and underlying diseases associated with mucormycosis. Diabetes mellitus is the most common underlying disease, followed by hematological malignancies and solid organ transplants [17]. Hyperglycemia is associated with defective neutrophil migration, chemotaxis, and phagocytosis [18, 19]. Other predisposing factors associated with mucormycosis are patients receiving iron chelation therapy and steroids. In India, 3–26% of mucormycosis cases were recorded from the immunocompetent host, compared to 18–19% globally and they usually present with cutaneous or isolated renal mucormycosis [17]. Trauma is the most common

S. Singh · R. Kanaujia · S. M. Rudramurthy (✉)
Department of Medical Microbiology, Postgraduate Institute of Medical Institution and Research, Chandigarh, India

N. Gupta, S. G. Honavar (eds.), *Rhino-Orbito-Cerebral Mucormycosis*,
https://doi.org/10.1007/978-981-16-9729-6_4

Table 4.1 Risk factors for mucormycosis

Predisposing condition	The predominant site of infection	Most common species	Reference
Diabetes, hyperglycemia, and ketoacidosis	ROCM	*Rhizopus* species *(R. arrhizus, R. microsporus, R. homothallicus)*	[10]
Hematological and solid organ malignancy	Pulmonary, ROCM	*Rhizopus* species, *Cunninghamella* species, *Lichtheimia* species., *Cokeromyces* species	[11]
Solid-organ transplant, HSCT	Pulmonary, ROCM	*Rhizopus* species, *Cunninghamella* species, *Lichtheimia* species	[11]
Neutropenia	Pulmonary, disseminated	*Rhizopus* species, *Lichtheimia* species. *Cunninghamella* species	[11]
Iron overload and iron chelation therapy	Pulmonary, disseminated	*Rhizopus* species, *Lichtheimia* species, *Cunninghamella* species	[1]
Corticosteroids	ROCM, pulmonary, disseminated	*Rhizopus* species, *Cunninghamella* species, *Lichtheimia* species	[1]
Malnutrition, preterm neonates, neonates with suspected necrotizing enterocolitis	Gastrointestinal	*Rhizopus* species, *Lichtheimia* species	[12]
Breach of skin (trauma due to accidents, burns, catheterization, injection site)	Cutaneous	*Apophysomyces* and *Saksenaea* species *Syncephalastrum* species	[13]
New risk factors:			
SARS-CoV-2, long term steroid use for the treatment	ROCM, pulmonary	*Rhizopus* species *(R. arrhizus, R. microsporus, R. homothallicus), Lichtheimia* species	[14]
Post pulmonary tuberculosis/ COPD	Pulmonary mucormycosis	*Rhizopus* species	[15]
Breakthrough mucormycosis after voriconazole treatment	ROCM, pulmonary	*Rhizopus* species	[16]
Immunocompetent host in the Indian subcontinent	Renal mucormycosis	*Rhizopus* and *Apophysomyces* species	[1]

ROCM Rhino-orbito-cerebral mucormycosis, *SARS-CoV-2* severe acute respiratory syndrome coronavirus 2, *COPD* chronic obstructive pulmonary disease, *HSCT* Hematopoietic Stem Cell Transplantation

risk factor associated with cutaneous mucormycosis [11]. Newer risk-factor like SARS-CoV-2 is emerging. The virus itself acts as a risk factor by decreasing immunity and irrational use of steroids for the treatment, making individuals susceptible to the infection [14].

4.3 Virulence Factors of Mucorales

Virulence factors are an essential part of Mucorales that allow these species to invade and survive within the host tissue during infection. The critical virulence traits essential to establish disease are summarized in Table 4.2.

4.4 Pathogen Entry

The agents of mucormycosis can gain entry to host tissues via various modes. The primary barriers against an invasion of any external pathogen include nasal mucosa, sinus cavities, skin, and endothelium layers. Typically, Mucorales are incapable of penetrating intact skin. Still, any breach in mucosal continuity by trauma or injury can promote fungal adherence to components of the basal epithelial cell layer such as laminin and type IV collagen [28]. Inhalation of Mucorales sporangiospores is the main entry portal. While the development of mucormycosis is not seen in immunocompetent hosts, those with risk factors can develop a progressive infection at various

Table 4.2 Virulence factors for Mucorales

Virulence traits	Function	Mechanism of virulence by Mucorales	Reference
Iron metabolism-related virulence traits *Reductase/permease systems*			
Low-affinity iron reductase	Performs in iron-rich environments and reduces iron	Patients with DKA (pH -7.3–6.88) reduce ferric ions to ferrous and facilitate *Rhizopus* spp. growth	[20]
High-affinity ferric reductase	Functions in iron-depleted environments and reduces iron	In DKA, carrier molecules bind to iron, and free iron is available only in submicromolar concentrations. The high-affinity ferric reductase facilitates the uptake of bound iron by *Rhizopus*	[20]
Other ferric reductases	Reduce iron	Allow iron uptake in iron-depleted environments and facilitates *Rhizopus* spp. growth	[21]
Copper oxidase (Cu-oxidase)	Oxidize iron	Trans cell membrane transport of iron	[20]
High-affinity iron permease (FTR1)	Helps in the transport of iron	Trans cell membrane transport of iron	[22]
Role of siderophores in Mucormycetes iron metabolism			
Siderophore permeases	Provide iron to cells by chelating iron	This siderophore supplies iron by direct transfer across the plasma membrane for *Rhizopus spp.* growth	[23]
Rhizoferrin	Siderophore that chelates iron	This siderophore supplies iron by the energy-dependent process for *Rhizopus* spp. growth	[24]
Deferoxamine	Deferoxamine extracts ferric iron from transferrin	It acts as a xenosiderophore. It attaches on the *Rhizopus* spp. and functions by transporting iron by energy-dependent reduction of iron	[25]
Role of hemin utilization in Mucormycetes iron metabolism			
Heme oxygenase	Iron uptake from heme	Obtain iron from host hemoglobin and allow angioinvasion of *Rhizopus* spp.	[22]
Others			
Proteinases • Aspartic proteinases • Subtilase protein	Protein lysis	Degrade host epithelium and contribute to the angioinvasive nature of the disease	[26]
Rhizoxin	Mycotoxin	Antimitotic metabolite that kills host cells	[27]

GRP glucose receptor protein

sites (Fig. 4.1). In patients with burns or other skin trauma/maceration, the spores can directly penetrate deeper tissues. Spores can also gain entry via application of non-sterile adhesive tapes and surgical dressings [29, 30]. Furthermore, mucormycosis spores can also gain access via contaminated tongue depressors or wooden applicators [31].

4.4.1 Spore Germination

The germination of spores and hyphal formation is critical for establishing infection in the host. In immunocompetent mice, pulmonary alveolar macrophages harvested from the lungs have been found to effectively ingest and prevent the germination of *R. arrhizus* spores both *in vitro* and after intranasal infection. In contrast, those derived from immunosuppressed mice are unable to do so [32].

4.4.2 Attachment and Invasion

The next step is attaching to extracellular protein matrices such as laminin and collagen IV. Any epithelial cell damage (e.g., due to COVID-19) can expose them for interaction with inhaled/ingested spores [28]. *Rhizopus*

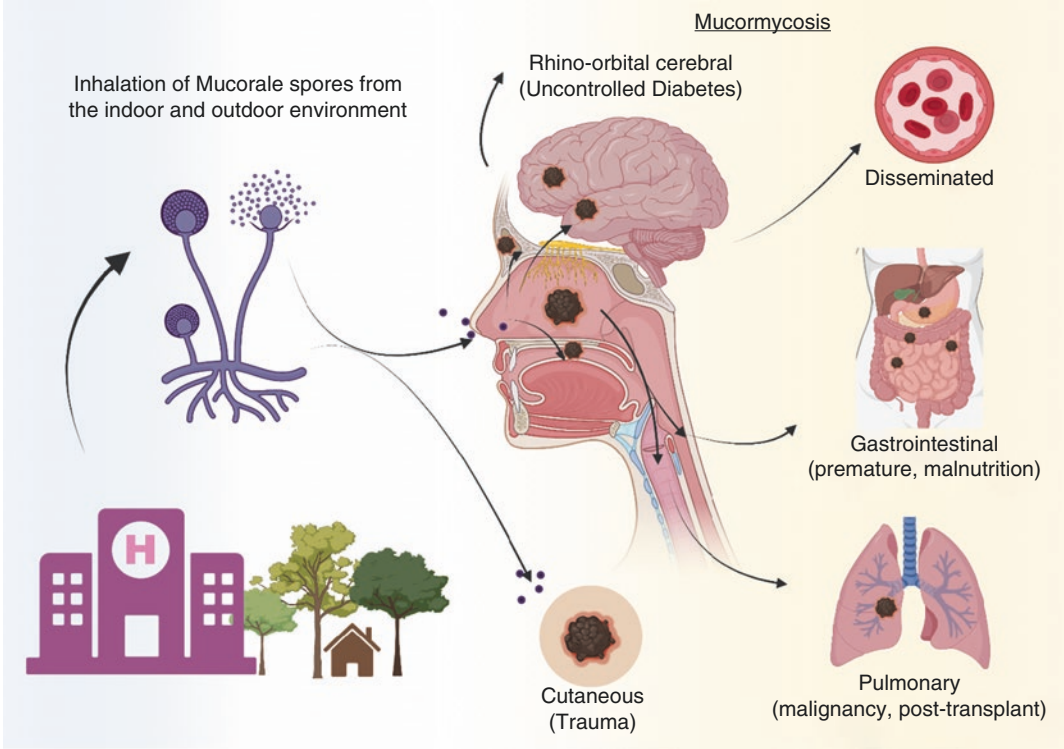

Fig. 4.1 Overview of pathogen entry and clinical presentations in mucormycosis

spp. can also attach to and invade the endothelium by recognizing a specific host receptor, the glucose-regulator protein 78 (GRP78) [33, 34]. This heat shock protein is a component of the host stress-related responses that helps in the specific binding of Mucorales germlings via the fungal ligands of the spore coat protein (CotH) family [35].

During SARS-CoV-2 infection, the endoplasmic reticulum stress is stimulated, which drives GRP78 synthesis [36]. In a recent study, nearly five times higher serum GRP78 was observed in patients with SARS-CoV-2 infection compared to the control group [37]. The GRP78 mediated attachment and internalization of the SARS-CoV-2 virus has also been reported [38]. Thus, upregulation of GRP78 enhanced by SARS-CoV-2 spike protein for its entry and by diffuse endothelial is seen in COVID-19 may also facilitate the attachment and invasion by Mucorales [39].

4.5 Immunopathogenesis

In a healthy host, the dormant/resting spores resist phagocytic killing but, swollen/germinating spores or hyphal forms are prone to degradation by immune cells. After endothelial penetration, Mucorales also encounter platelets that adhere to the spores and suppress germination, which contributes to hyphal damage, potentially hampering the fungal growth by adhering and damaging the hyphae or indirectly, by secreting inflammatory cytokines [40]. Various studies have investigated the interaction of Mucorales with host immunity (both innate and adaptive), and the details are summarized in Table 4.3.

The role of cytokines in modifying host response against the Mucorales originates from experimental studies, and its immunological interactions are depicted in Fig. 4.2.

Interleukin-1 beta (IL-1β) plays a pivotal role in response to pathogenic fungi with a significant role

Table 4.3 Interaction of the Mucorales with the immune system

Categories of the immune response with cellular type	Function	Immune evasion by Mucorales	References
Innate immune response			
Bronchial alveolar macrophages (BAM)	The first line of defense and prevents germination of Mucorale spores and has a role in iron restriction	• Inhibits phagosome maturation by cell wall melanin • Upregulation of iron acquisition genes • Upregulation of genes involved in nutrient assimilation to allow the use of alternate nutrients in a hostile macrophage environment	[32, 41–43]
Epithelial cells	The first line of defense and prevents the entrance of Mucorales spores	Mucorales damage the epithelial cells and upregulate epidermal growth factor receptor (EGFR) on the surface of epithelial cells, which promotes disease	[44, 45]
Polymorphonuclear leukocytes (PMNs) or neutrophil granulocytes	• Neutrophils produce cytokines to activate other immune cells • They can also form tight clusters around the spores containing them in structures resembling early granulomas • Neutrophil extracellular traps (NETs), reactive oxygen species and cationic peptides also damage both spore and hyphae	• Sialic acids in the cell wall protect against phagocytosis • Resting spores and the hyphae can reduce neutrophils chemotaxis	[46–48]
Natural killer (NK) cells	Natural killer (NK) cells recognize Mucorales and cause hyphal damage on activation	Mucorales hyphae have an immunosuppressive effect on dendritic cells and reduce the release of immunomodulatory molecules	[49–52]
Platelets	• Platelet recognition of Mucorales causes inhibition of spore germination and hyphal growth by secretion of various cytokines and chemokines • They also bind to and activate other immune cells	Excessive thrombosis seen in mucormycosis causes thrombocytopenia which also makes surgical interventions difficult	[40, 53]
Endothelial cells	Endothelial cells surround the innermost layer of blood vessels. It helps in hyphae recognition	The glucose-regulated protein 78 (GRP78) receptor present on endothelial cell surface facilitate angioinvasion by Mucorales	[33, 54, 55]
Dendritic cells (D.C.s)	• Dendritic cells link the innate immunity with the adaptive immunity • Production of IL23 by dendritic cells induces Th17 cells, which further promote neutrophil response	The resting (dormant) spores of Mucorales stimulate the maturation of dendritic cells	[56, 57]

(continued)

Table 4.3 (continued)

Categories of the immune response with cellular type	Function	Immune evasion by Mucorales	References
Adaptive immune response			
T cells	• Both CD4 and CD8 cells produce cytokines that mediate hyphal damage • Th17 cells produce IL 17, which promotes the antifungal defense of neutrophils • Release of interleukins (IL-4, IL-10, and IL-17) and IFNγ caused damage to hyphae		[58]

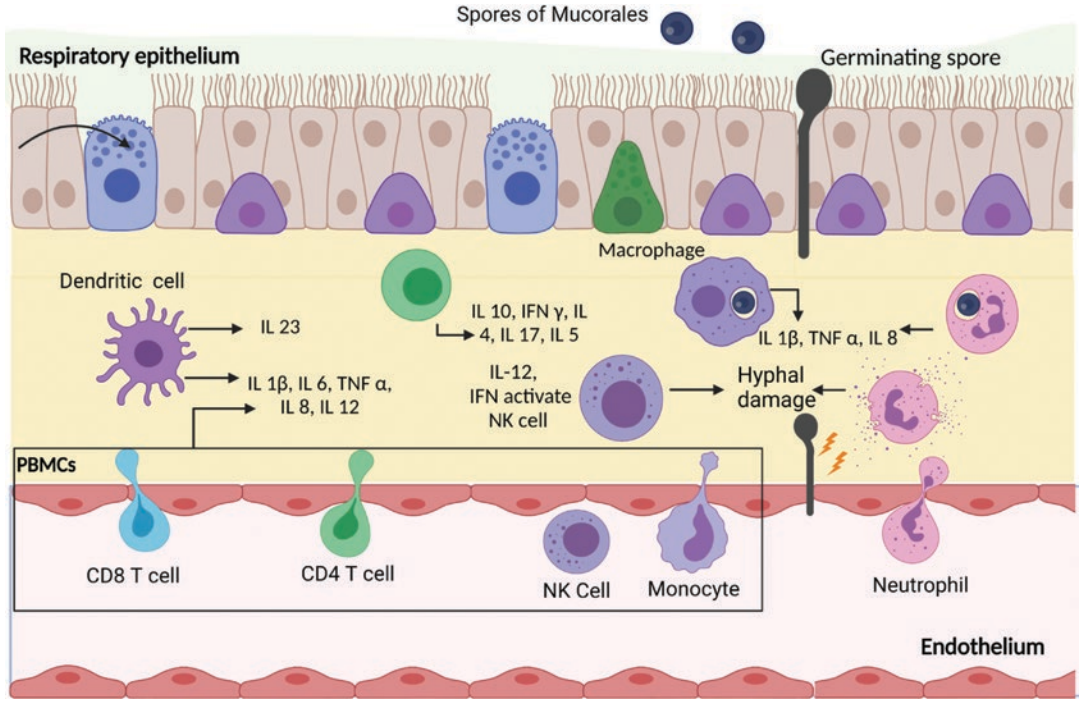

Fig. 4.2 Schematic representation of immune cells involved in the pathogenesis of mucormycosis

in the induction of other proinflammatory responses, hematopoiesis, Th17 cell differentiation, etc. [59]. Tumor necrosis factor α (TNF-α) has a dual role as an activator of inflammatory response and immunosuppression by mediating host apoptosis. At the same time, Interleukin-6 mediates leukocyte trafficking and production of acute-phase reactants while promoting T-cell proliferation and B cell responses [60]. The IL-12 promotes Th1 cell response, natural killer (N.K.) cell activation, Dendritic cell maturation, and production of interferon-γ (IFN-γ) and chemoattractant proteins like IL-8 also recruit immune cells, thereby mediating an effective immune response [60].

4.6 Factors Affecting the Pathogenesis of Mucormycosis in COVID-19

- *Hyperglycemia*: The SARS-CoV-2 impairs pancreatic beta-cell function and precipitates acute diabetic ketoacidosis (DKA) [61], and DKA has been was observed even with T2DM cases [62]. In the past, infections with SARS-CoV-1 have been seen to be associated with hyperglycemia persisting for as long as 3 years indicating long-term damage to pancreatic β-cells by these viruses [63]. Thus, SARS-CoV-2 mediated DKA could present even weeks or months after apparent recovery from the disease substantiating the late onset of CAM [14].
- *Corticosteroids*: Worsening of glycemic control can also occur secondary to the use of systemic steroids and antiviral agents in the management of COVID-19. A higher incidence of mucormycosis infections has been observed in patients who received corticosteroids during COVID-19 treatment, often in terms of inappropriate doses (≥ 6 mg/kg dexamethasone), duration (more than 10 days) or even when not indicated [14, 64]. Impaired macrophage and neutrophil function due to steroids explains suppressed antifungal immunity.
- *Iron metabolism*: Dysregulated iron metabolism is known to occur during COVID-19 [65]. The interaction between viral particles and hemoglobin perpetuates a cascade of dysfunctional hemoglobin synthesis, hemolysis, and heme accumulation with increased serum ferritin also seen in response to the inflammation [66–68]. The activation of macrophages and high IL-6 secretion also accentuates hyperferritinemia. This excessive intracellular free iron generates free radicals that cause endothelial destruction, leading to endothelitis, promoting fungal invasion [69].
- *Immune dysfunction*: The mucociliary clearance by the nasal epithelium is the primary innate immune defense against inhaled microorganisms. This clearance is delayed in COVID-19, allowing Mucorales spores to attach to the nasal epithelium [70]. Among innate immune cells, lymphopenia has been observed among COVID-19 patients, but its role in escalating the host susceptibility to mucormycosis is not clear due to insufficient data [71] (Fig. 4.3).

4.7 Common Misconceptions

The unprecedented epidemic of mucormycosis in the background of the COVID-19 pandemic has given rise to various misconceptions regarding CAM. The term “black fungus” has been used incorrectly and indiscriminately to indicate mucormycosis infection, which should be discouraged. Although the clinical presentation of mucormycosis comprises eschar and black necrotic lesions, the term “black fungus” actually denotes a completely different group of fungi that produce the pigment melanin, resulting in black hyphae, which are not seen in Mucorales. Another misconception is regarding the source of infection. The use of respirators, oxygenation during COVID-19 management, reuse of masks, etc. have been implicated as potential sources of infection, but this lacks scientific backing. There is also no evidence of human-to-human transmission, and this disease is acquired via Mucorales spores present ubiquitously in the environment, both indoors and outdoors. The prophylactic use of antifungals to prevent this infection in COVID-19 is also strongly discouraged since the incidence of infection is <10% in any COVID-19 cohort [8].

4.8 Future Perspectives

Although CAM is a new entity, various reports describing this infection have emerged over the past few months. Unfortunately, there is still a

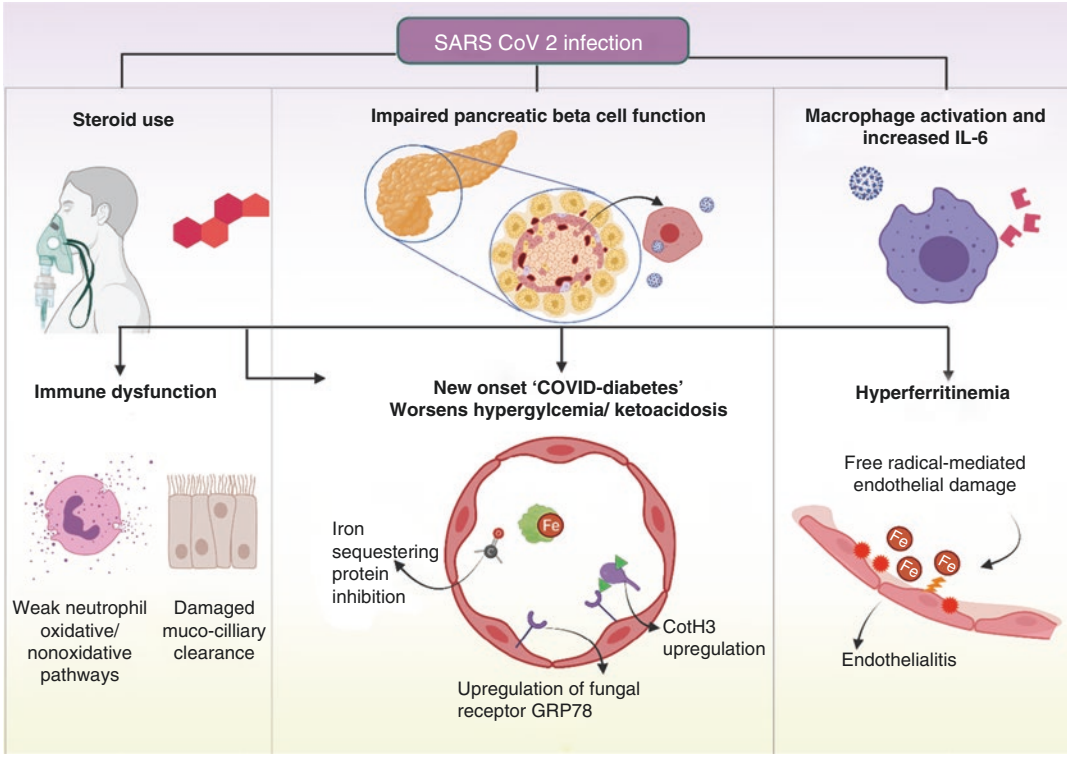

Fig. 4.3 Factors affecting pathogenesis of mucormycosis in patients with SARS CoV-2 infection

shortage of systematic prospective studies evaluating the various factors involved in disease pathogenesis and outcome, particularly in comparison to non-COVID mucormycosis cases. Studying the nature and extent of immunological dysfunction in COVID-19 and its impact on the pathogenesis of mucormycosis is a promising area of research.

4.9 Conclusion

Although host-immune response and inflammatory signalling against Mucorales have been established, the underlying molecular mechanism responsible for producing proinflammatory cytokines and activating inflammatory response against Mucorales is unknown. In the context of CAM, this field is even more unexplored. An understanding of the pathogenesis of CAM can provide new perspectives for developing novel diagnostic and treatment modalities.

References

1. Hariprasath P, Arunaloke C. Global epidemiology of mucormycosis. J Fungi. 2019;5(1). https://doi.org/10.3390/jof5010026.
2. Skiada A, Pagano L, Groll A, Zimmerli S, Dupont B, Lagrou K, et al. Zygomycosis in Europe: analysis of 230 cases accrued by the registry of the European Confederation of Medical Mycology (ECMM) Working Group on Zygomycosis between 2005 and 2007. Clin Microbiol Infect. 2011;17(12):1859–67. https://doi.org/10.1111/j.1469-0691.2010.03456.x.
3. Arunaloke C. Fungal infections in Asia: eastern frontier of mycology. ECAB Clinical update infectious Disease. 2014. Publisher: Elsevier India
4. Arunaloke C, Harsimran K, Jayanthi S, Rudramurthy Shivaprakash M, Atul P, Prakash S, et al. Epidemiology and clinical outcomes of invasive mould infections in Indian intensive care units (FISF study). J Crit Care. 2019;51:64–70. https://doi.org/10.1016/j.jcrc.2019.02.005.
5. Antonella F, Zan M, Alexander RR, Assas Bakri M. Cytokine storm and COVID-19: a chronicle of pro-inflammatory cytokines: cytokine storm: the elements of rage! Open Biol. 2020; https://doi.org/10.1098/rsob.200160.

6. Nilam M, Hunter Christopher A. Cytokine storms: understanding COVID-19. Immunity. 2020:19–25. https://doi.org/10.1016/j.immuni.2020.06.017.
7. Attilio C, Emidio T, Salvatore C. COVID-19: hemoglobin, iron, and hypoxia beyond inflammation. A narrative review. Clin Pract. 2020;10(2):24–30. https://doi.org/10.4081/CP.2020.1271.
8. Rudramurthy Shivaprakash M, Martin H, Meis Jacques F, Cornely Oliver A, Valliappan M, Pierre GJ, et al. ECMM/ISHAM recommendations for clinical management of COVID-19 associated mucormycosis in low-and middle-income countries. https://doi.org/10.1111/MYC.13335.
9. Arunaloke C, Shreya S. Management of mucormycosis. Curr Fungal Infect Rep. 2020;14(4):348–60. https://doi.org/10.1007/S12281-020-00406-2.
10. Patel A, Kaur H, Xess I, Michael JS, Savio J, Rudramurthy S, et al. A multicentre observational study on the epidemiology, risk factors, management and outcomes of mucormycosis in India. Clin Microbiol Infect. 2020;26(7):944.e9–944.e15. https://doi.org/10.1016/j.cmi.2019.11.021.
11. Jeong W, Keighley C, Wolfe R, Lee WL, Slavin MA, Kong DCM, et al. The epidemiology and clinical manifestations of mucormycosis: a systematic review and meta-analysis of case reports. Clin Microbiol Infect. 2019;25(1):26–34. https://doi.org/10.1016/j.cmi.2018.07.011.
12. Sushma P, Chirla DK, Narendar K, Mukul V, Samal SC. Unsuspected invasive neonatal gastrointestinal mucormycosis: a clinicopathological study of six cases from a tertiary care hospital. J Indian Assoc Pediatr Surg. 2012;17(4):153. https://doi.org/10.4103/0971-9261.102329.
13. Robin K. Primary cutaneous Zygomycosis in India. Indian J Surg. 2012;74(6):468–75. https://doi.org/10.1007/s12262-012-0429-4.
14. Atul P, Ritesh A, Rudramurthy Shivaprakash M, Manoj S, Immaculata X, Ratna S, et al. Multicenter epidemiologic study of coronavirus disease-associated mucormycosis, India. Emerg Infect Dis. 2021;27(9). https://doi.org/10.3201/eid2709.210934.
15. Hariprasath P, Kumar GA, Mandya RS, Pankaj S, Immaculata X, Jayanthi S, et al. A prospective multicenter study on mucormycosis in India: epidemiology, diagnosis, and treatment. Med Mycol. 2019;57(4):395–402. https://doi.org/10.1093/mmy/myy060.
16. Sushil M, Chetanya S, Sanjay T, Sreenivas V, Kabra SK, Immaculata X, et al. Oral voriconazole versus intravenous low dose amphotericin B for primary antifungal prophylaxis in pediatric acute leukemia induction. J Pediatr Hematol Oncol. 2011;33(8):e333–41. https://doi.org/10.1097/MPH.0b013e3182331bc7.
17. Hariprasath P, Arunaloke C. Epidemiology of mucormycosis in India. Microorganisms. 2021;9(3):1–12. https://doi.org/10.3390/MICROORGANISMS9030523.
18. Jagdish C, Mandeep K, Nidhi S, Punia RPS, Singhal Surinder K, Attri Ashok K, et al. Mucormycosis: battle with the deadly enemy over a five-year period in India. J Fungi (Basel, Switzerland). 2018;4(2). https://doi.org/10.3390/jof4020046.
19. Corzo-León DE, Chora-Hernández LD, Rodríguez-Zulueta AP, Walsh TJ. Diabetes mellitus as the major risk factor for mucormycosis in Mexico: epidemiology, diagnosis, and outcomes of reported cases. Med Mycol. 2018;56(1):29–43. https://doi.org/10.1093/MMY/MYX017.
20. Howard DH. Acquisition, transport, and storage of iron by pathogenic fungi. Clin Microbiol Rev. 1999;12(3):394–404. https://doi.org/10.1128/CMR.12.3.394.
21. Artis WM, Fountain JA, Delcher HK, Jones HE. A mechanism of susceptibility to mucormycosis in diabetic ketoacidosis transferrin and iron availability. Diabetes. 1982;31(12):1109–14. https://doi.org/10.2337/diacare.31.12.1109.
22. Ibrahim AS, Teclegiorgis G, Lin L, Guanpingsheng L, Husseiny Mohamed I, Skory Christopher D, et al. The high affinity iron permease is a key virulence factor required for Rhizopus oryzae pathogenesis. Mol Microbiol. 2010;77(3):587–604. https://doi.org/10.1111/j.1365-2958.2010.07234.x.
23. Ibrahim AS. Spellberg Brad, Edwards John. Iron acquisition: a novel perspective on mucormycosis pathogenesis and treatment. Curr Opin Infect Dis. 2008:620–5. https://doi.org/10.1097/QCO.0b013e3283165fd1.
24. Thieken A. Rhizoferrin: a complexone type siderophore of the mocorales and entomophthorales (zygomycetes). FEMS Microbiol Lett. 1992;94(1–2):37–41. https://doi.org/10.1016/0378-1097(92)90579-D.
25. Boelaert JR, de Locht M, Van Cutsem J, Kerrels V, Cantinieaux B, Verdonck A, et al. Mucormycosis during deferoxamine therapy is a siderophore-mediated infection. In vitro and in vivo animal studies. J Clin Invest. 1993;91(5):1979–86. https://doi.org/10.1172/JCI116419.
26. Farley PC, Sullivan PA. The Rhizopus oryzae secreted aspartic proteinase gene family: an analysis of gene expression. Microbiology. 1998;144(8):2355–66. https://doi.org/10.1099/00221287-144-8-2355.
27. White JD, Blakemore PR, Green NJ, Bryan HE, Holoboski Mark A, Keown Linda E, et al. Total synthesis of rhizoxin D, a potent antimitotic agent from the fungus Rhizopus chinensis. J Org Chem. 2002;67(22):7750–60. https://doi.org/10.1021/jo020537q.
28. Bouchara JP, Oumeziane NA, Lissitzky JC, Larcher G, Tronchin G, Chabasse D. Attachment of spores of the human pathogenic fungus Rhizopus oryzae to extracellular matrix components. Eur J Cell Biol. 1996;70(1):76–83.
29. Rammaert B, Lanternier F, Zahar JR, Dannaoui E, Bougnoux ME, Lecuit M, et al. Healthcare-associated mucormycosis. Clin Infect Dis. 2012;54(Suppl 1). https://doi.org/10.1093/CID/CIR867.
30. Alsuwaida K. Primary cutaneous mucormycosis complicating the use of adhesive tape to secure the

endotracheal tube. Can J Anaesth. 2002;49(8):880–2. https://doi.org/10.1007/BF03017426.
31. Enrique M-P, Rodríguez-Tudela JL, García DJJ, Alfonso M-L, Luis T, Jesús U, et al. Outbreak of gastric mucormycosis associated with the use of wooden tongue depressors in critically ill patients. Intensive Care Med. 2004;30(4):724–8. https://doi.org/10.1007/S00134-003-2132-1.
32. Waldorf AR, Ruderman N, Diamond RD. Specific susceptibility to mucormycosis in murine diabetes and bronchoalveolar macrophage defense against Rhizopus. J Clin Invest. 1984;74(1):150–60. https://doi.org/10.1172/JCI111395.
33. Mingfu L, Brad S, Phan QT, Yue F, Yong F, Lee AS, et al. The endothelial cell receptor GRP78 is required for mucormycosis pathogenesis in diabetic mice. J Clin Invest. 2010;120(6):1914–24. https://doi.org/10.1172/JCI42164.
34. Ibrahim Ashraf S, Brad S, Walsh Thomas J, Kontoyiannis Dimitrios P. Pathogenesis of mucormycosis. Clin Infect Dis. 2012;54(SUPPL 1). https://doi.org/10.1093/cid/cir865.
35. Teclegiorgis G, Sondus A, Soliman Sameh SM, Yiyou G, Jeon HH, Lina Z, et al. Anti-CotH3 antibodies protect mice from mucormycosis by prevention of invasion and augmenting opsonophagocytosis. Sci Adv. 2019;5(6). https://doi.org/10.1126/sciadv.aaw1327.
36. Köseler A, Sabirli R, Gören T, Türkçüer I, Kurt Ö. Endoplasmic reticulum stress markers in SARS-COV-2 infection and pneumonia: case-control study. In Vivo. 2020;34(3 Suppl):1645–50. https://doi.org/10.21873/INVIVO.11956.
37. Sabirli R, Koseler A, Goren T, Turkcuer I, Kurt O. High GRP78 levels in Covid-19 infection: a case-control study. Life Sci. 2021;265. https://doi.org/10.1016/J.LFS.2020.118781.
38. Ibrahim IM, Abdelmalek DH, Elshahat ME, Elfiky AA. COVID-19 spike-host cell receptor GRP78 binding site prediction. J Infect. 2020;80(5):554–62. https://doi.org/10.1016/J.JINF.2020.02.026.
39. Baldin C, Ibrahim AS. Molecular mechanisms of mucormycosis-the bitter and the sweet. PLoS Pathog. 2017;13(8). https://doi.org/10.1371/JOURNAL.PPAT.1006408.
40. Susanne P, Barbara K, Kehrel BE, Dierich MP, Walter N, Cornelia L-F. Potential antifungal effects of human platelets against zygomycetes in vitro. J Infect Dis. 2009;200(7):1176–9. https://doi.org/10.1086/605607.
41. Kaswara K, Hea-Reung P, Hans-Martin D, Christine S, Kerstin V, Thilo FM. Virulent strain of Lichtheimia corymbifera shows increased phagocytosis by macrophages as revealed by automated microscopy image analysis. Mycoses. 2014;57:56–66. https://doi.org/10.1111/myc.12237.
42. Andrianaki AM, Irene K, Kalliopi T, Clara B, Elias D, Soliman Sameh SM, et al. Iron restriction inside macrophages regulates pulmonary host defense against Rhizopus species. Nat Commun. 2018;9(1):3333. https://doi.org/10.1038/s41467-018-05820-2.
43. Calo S, Nicolás FE, Lee SC, Vila A, Cervantes M, Torres-Martinez S, et al. A non-canonical RNA degradation pathway suppresses RNAi-dependent epimutations in the human fungal pathogen Mucor circinelloides. PLoS Genet. 2017;13(3). https://doi.org/10.1371/JOURNAL.PGEN.1006686.
44. Ghuman H, Voelz K. Innate and adaptive immunity to mucorales. J Fungi. 2017;3(3):48. https://doi.org/10.3390/jof3030048.
45. Watkins TN, Teclegiorgis G, Marc S, Shetty AC, Graf KT, Abdullah A, et al. Inhibition of EGFR signaling protects from mucormycosis. MBio. 2018;9(4). https://doi.org/10.1128/mBio.01384-18.
46. Venizelos P. Neutrophil extracellular traps in immunity and disease. Nat Rev Immunol. 2018;18(2):134–47. https://doi.org/10.1038/nri.2017.105.
47. Chinn RY, Diamond RD. Generation of chemotactic factors by Rhizopus oryzae in the presence and absence of serum: relationship to hyphal damage mediated by human neutrophils and effects of hyperglycemia and ketoacidosis. Infect Immun. 1982;38(3):1123–9. https://doi.org/10.1128/iai.38.3.1123-1129.1982.
48. Waldorf AR, Diamond RD. Neutrophil chemotactic responses induced by fresh and swollen Rhizopus oryzae spores and Aspergillus fumigatus conidia. Infect Immun. 1985;48(2):458–63. https://doi.org/10.1128/iai.48.2.458-463.1985.
49. Eric V, Elena T, Myriam B, Thierry W, Sophie U. Functions of natural killer cells. Nat Immunol. 2008;9(5):503–10. https://doi.org/10.1038/ni1582.
50. Yokoyama WM. Natural killer cell immune responses. Immunol Res. 2005;32(1–3):317–26. https://doi.org/10.1385/IR:32:1-3:317.
51. Stanislaw S, Lars T, Susanne P, Cornelia L-F, Mitra H, Frauke R, et al. Rhizopus oryzae hyphae are damaged by human natural killer (NK) cells, but suppress NK cell mediated immunity. Immunobiology. 2013;218(7):939–44. https://doi.org/10.1016/j.imbio.2012.10.013.
52. Stanislaw S, Andreas S, Asuman D, Cornelia L-F, Thomas L. Natural killer cell-mediated damage of clinical isolates of mucormycetes. Mycoses. 2016;59(1):34–8. https://doi.org/10.1111/myc.12431.
53. Jenne CN, Paul K. Platelets in inflammation and infection. Platelets. 2015;26(4):286–92. https://doi.org/10.3109/09537104.2015.1010441.
54. Aird WC. Endothelial cell heterogeneity. Cold Spring Harb Perspect Med. 2012;2(1):a006429. https://doi.org/10.1101/cshperspect.a006429.
55. Evgenii S, Ulrike B, Christina P, Alexander M, Helmut E, Justin H, et al. In situ validation of the endothelial cell receptor GRP78 in a case of rhinocerebral mucormycosis. Antimicrob Agents Chemother. 2018;62(5). https://doi.org/10.1128/AAC.00172-18.
56. Lambrecht BN, Prins JB, Hoogsteden HC. Lung dendritic cells and host immunity to infection. Eur Respir J. 2001;18(4):692–704.
57. Sebastian W, Vanessa T, Philipp W, Paul W, Johannes E, Maria W-GA, et al. Mucorales spores induce a pro-

inflammatory cytokine response in human mononuclear phagocytes and harbor no rodlet hydrophobins. Virulence. 2017;8(8):1708–18. https://doi.org/10.1080/21505594.2017.1342920.
58. Leonardo P, Daniela V, Patrizia B, Giovanni R, Fabio F, Eleonora Z, et al. Mucorales-specific T cells emerge in the course of invasive mucormycosis and may be used as a surrogate diagnostic marker in high-risk patients. Blood. 2011;118(20):5416–9. https://doi.org/10.1182/blood-2011-07-366526.
59. Griffiths JS, Giorgio C, Kotowicz NK, Jemima H, Richardson JP, Naglik Julian R. Role for IL-1 family cytokines in fungal infections. Front Microbiol. 2021;12:633047. https://doi.org/10.3389/FMICB.2021.633047.
60. Harlene G, Kerstin V. Innate and adaptive immunity to mucorales. J Fungi. 2017;3(3):48. https://doi.org/10.3390/JOF3030048.
61. Smith SM, Boppana A, Traupman JA, Unson E, Maddock DA, Chao K, et al. Impaired glucose metabolism in patients with diabetes, prediabetes, and obesity is associated with severe COVID-19. J Med Virol. 2021;93(1):409–15. https://doi.org/10.1002/JMV.26227.
62. Pal R, Banerjee M, Yadav U, Bhattacharjee S. Clinical profile and outcomes in COVID-19 patients with diabetic ketoacidosis: a systematic review of literature. Diabetes Metab Syndr. 2020;14(6):1563–9. https://doi.org/10.1016/J.DSX.2020.08.015.
63. Yang JK, Lin SS, Ji XJ, Guo LM. Binding of SARS coronavirus to its receptor damages islets and causes acute diabetes. Acta Diabetol. 2010;47(3):193–9. https://doi.org/10.1007/S00592-009-0109-4.
64. Mrittika S, Honavar Santosh G, Rolika B, Sabyasachi S, Raksha R, Usha K, et al. Epidemiology, clinical profile, management, and outcome of COVID-19-associated rhino-orbital-cerebral mucormycosis in 2826 patients in India - collaborative OPAI-IJO study on mucormycosis in COVID-19 (COSMIC), report 1. Indian J Ophthalmol. 2021;69(7):1670–92. https://doi.org/10.4103/IJO.IJO_1565_21.
65. Anson J, Shagun S, Ajoy R, Yathin K, Saurabh A, Sunanda R. Current understanding in the pathophysiology of SARS-CoV-2-associated rhino-Orbito-cerebral mucormycosis: a comprehensive review. J Maxillofac Oral Surg. 2021;1:1–8. https://doi.org/10.1007/S12663-021-01604-2.
66. Amer M, Ashraf SM. Is hemoglobin the missing link in the pathogenesis of COVID-19? Anaesth Pain Intensive Care. 2020;24(1):9–12. https://doi.org/10.35975/APIC.V24I1.1216.
67. Carlo P, Elena B, Roberto B, Giacomo C, Maria GG, Yehuda S, et al. COVID-19 as part of the hyperferritinemic syndromes: the role of iron depletion therapy. Immunol Res. 2020;68(4):213. https://doi.org/10.1007/S12026-020-09145-5.
68. Jenifer G-P, Mitchell W, James K, Xian W, Jacob S, Palmer Andre F, et al. Hyperferritinemia in critically ill COVID-19 patients – is ferritin the product of inflammation or a pathogenic mediator? Clin Chim Acta. 2020;509:249. https://doi.org/10.1016/J.CCA.2020.06.033.
69. Vlahakos VD, Marathias KP, Nikolaos A, Vlahakos Demetrios V. Hyperferritinemia in patients with COVID-19: an opportunity for iron chelation? Artif Organs. 2021;45(2):163–7. https://doi.org/10.1111/AOR.13812.
70. Koparal M, Kurt E, Altuntas EE, Dogan F. Assessment of mucociliary clearance as an indicator of nasal function in patients with COVID-19: a cross-sectional study. Eur Arch Otorhinolaryngol. 2021;278(6):1863–8. https://doi.org/10.1007/S00405-020-06457-Y.
71. Soheil T, Taha R, Wei EX, Mohammad R. Lymphopenia during the COVID-19 infection: what it shows and what can be learned. Immunol Lett. 2020;225:31–2. https://doi.org/10.1016/j.imlet.2020.06.013.

5 Microbiological Diagnosis of Rhino-Orbito-Cerebral Mucormycosis

Harsimran Kaur, Parakriti Gupta, and Shivaprakash M. Rudramurthy

Key Points

- Rhino-orbito-cerebral mucormycosis requires a prompt diagnosis as it is a medical emergency and exhibits high mortality.
- *Mucorales* causing the disease exhibit a wide spectrum of species with the emergence of newer agents.
- Endoscopically obtained tissue samples are preferable.
- Direct microscopy (potassium hydroxide (KOH)/calcofluor white-KOH mount) quickly pinpoints broad aseptate ribbon-like hyphae of *Mucorales*.
- Culture is obtained in only 50% of cases.
- Tissue should be teased instead of grinding as *Mucorales* are very friable.
- Identification of causative agents is vital due to variation in antifungal susceptibility.
- MALDI-TOF and molecular techniques aid in the identification of agents.

5.1 Introduction

Rhino-orbito-cerebral mucormycosis (ROCM), caused by *Mucorales,* is considered a medical emergency due to its ability to cause infarction and necrosis of tissues leading to high mortality. Therefore, early diagnosis is essential for immediate management and maintaining the vitality of the unaffected tissues, thereby improving outcomes. The agents of mucormycosis belong to the phylum *Mucoromycota* subphylum *Mucoromycotina* and order *Mucorales* comprising 261 species and 55 genera (Fig. 5.1) [1]. Of 55 genera, 38 are pathogenic to humans, including commonly encountered *Rhizopus, Lichtheimia* (previously called *Absidia*), *Apophysomyces*, *Mucor*, *Rhizomucor, Saksenaea*, *Cunninghamella, Syncephalastrum, Cokeromyces, Actinomucor* and *Thamnostylum* [1].

5.2 Diagnosis

The diagnosis of ROCM is based on clinical criteria, radiological imaging, microbiological and histopathological examination. The flowchart summarizing the microbiological investigations is given in Fig. 5.2.

The detailed methods are described below.

H. Kaur · P. Gupta · S. M. Rudramurthy (✉)
Department of Medical Microbiology, Postgraduate Institute of Medical Institution and Research, Chandigarh, India

N. Gupta, S. G. Honavar (eds.), *Rhino-Orbito-Cerebral Mucormycosis*,
https://doi.org/10.1007/978-981-16-9729-6_5

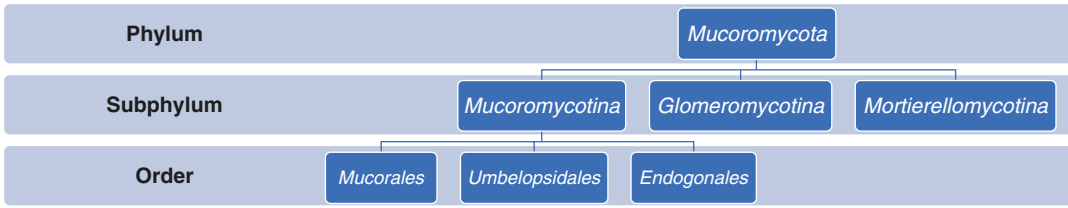

Fig. 5.1 Taxonomical classification of agents causing mucormycosis

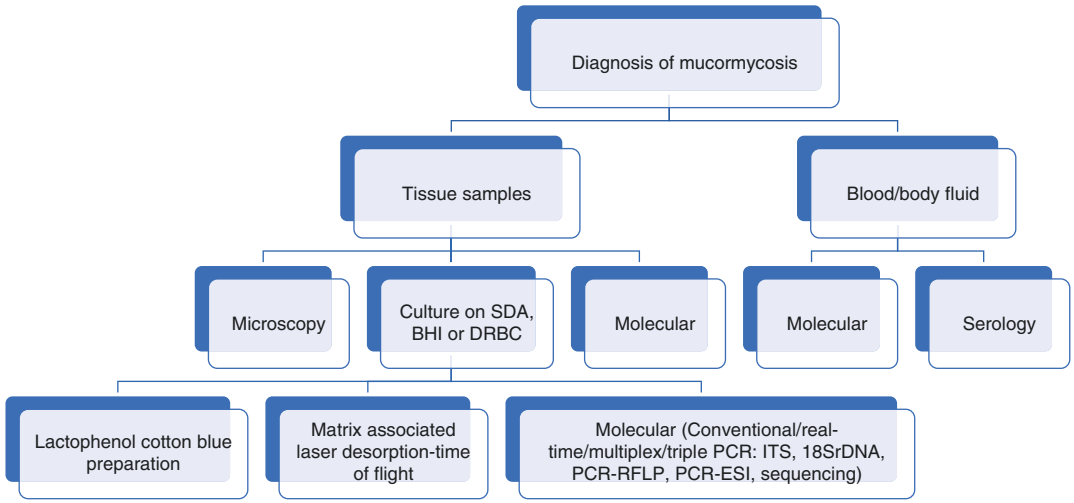

Fig. 5.2 Flowchart showing the various diagnostic modalities for diagnosis of *Mucorales* from clinical samples. *BHI* Brain–heart infusion agar, *DRBC* Dichloran rose Bengal chloramphenicol, *ITS* Internal transcribed spacer, *PCR* Polymerase chain reaction, *PCR-ESI* PCR electrospray-ionization mass spectrometry, *PCR-RFLP* PCR-restriction fragment length polymorphism, *SDA* Sabouraud dextrose agar

5.2.1 Sample Collection and Transport

Type of samples: Endoscopic or Computed Tomography (CT) guided nasal scraping/nasal biopsy, orbital tissue and brain tissue. Swabs are generally not satisfactory since they allow drying of specimens and loss of viability.

Transport: Specimens should be collected aseptically in clean, sterile and properly sealed containers, delivered to the laboratory within 2 h. If processing is to be delayed for more than several hours, it is recommended that specimens be stored under refrigeration at 4 °C.

5.2.2 Sample Processing

The specimens should be handled in a biosafety level-2 (BSL-2) laboratory facility with a Class II biosafety cabinet [2]. The sample should be processed and then inoculated to primary isolation

media within a few hours of collection. Caseous, purulent or bloody areas and necrotic parts of the sample should be selected and included for processing. The processed sample is subjected to microscopy, culture and molecular diagnosis.

5.2.2.1 Microscopy

For a quick presumptive diagnosis of ROCM, direct microscopy is a cheap, rapid and readily available technique. It forms an essential component of national and international experts' recommendations emphasizing septation, angle of branching (45–90°) and hyphal breadth (6–25 μm) [European Confederation of Medical Mycology and Mycoses Study Group Education and Research Consortium (ECMM/MSG ERC)] [3]. However, direct microscopy cannot differentiate amongst different genera or species.

1. *Potassium hydroxide (KOH) mount*: 10–20% KOH wet mount preparation of the specimen is the standard method used in direct microscopy in which characteristic broad, ribbon-like aseptate hyphae of Mucorales are characteristic broad, ribbon-like aseptate hyphae noted under microscope (Fig. 5.3a). KOH, a strong alkali, clears the cell debris and makes fungi clearly appreciable as they are resistant to digestion.
2. *KOH-Calcofluor white (CFW) solution mixture*: CFW stain binds to the cell wall of the fungi (β-1,3 and β-1,4 polysaccharides, specifically cellulose and chitin) and fluoresces bluish-white under a fluorescent microscope, thereby enhancing the visualization of the fungal element in specimens (Fig. 5.3b) [4]. Uvitex 2B and Blankophor are other alternatives. Optimal fluorescence occurs with UV excitation. Hence, the fluorescent microscope needs to have filters of UV range.

5.2.2.2 Culture

The global guidelines by ECMM/MSG ERC strongly recommend culture techniques for identification up to species level and antifungal susceptibility testing [3]. The samples suspected of mucormycosis need to be teased with sterile teasing needles instead of homogenizing due to the highly friable nature of aseptate hyphae. Routinely, the inoculation is done on two tubes of Sabouraud's dextrose agar (SDA) containing antibiotics and one tube of brain heart infusion agar (BHI). One SDA tube and BHI is incubated at 30 °C were another set of SDA at 37 °C. Compared to other moulds, *Mucorales* grow rapidly within 24–48 h. The gross morphology of the colonies classically appears cottony. The incubation at varying temperatures increases

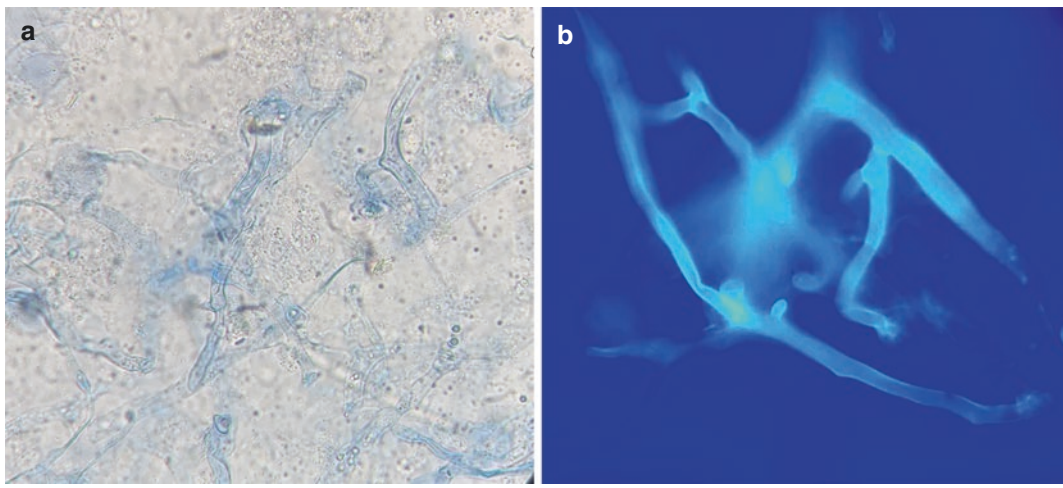

Fig. 5.3 (**a**). KOH mount of nasal scraping showing broad aseptate hyphae of *Mucorales.* (**b**) Calcofluor white (CFW)-KOH mount showing bright bluish-white broad ribbon-like aseptate hyphae of *Mucorales*

the chance of isolation and differentiates between certain members of *Mucorales*. The growth of *Mucorales* from a sterile site is considered confirmed positive, while that from a non-sterile site is judged in combination with clinical and radiological criteria. Despite the ease of sample collection from ROCM cases, culture positivity remains at 50% owing to the frangible aseptate hyphae [5, 6]. Lower culture sensitivity is particularly noted for *R. arrhizus* and *R. homothallicus* indicating their higher vulnerability to damage [7]. Recently, Vaezi et al. demonstrated higher positivity of a microculture assay from blood (28.9% vs 0%) and kidney tissue (98.8% vs 31.1%) of an immunocompetent mouse model of disseminated mucormycosis than conventional methods [8].

The identification of *Mucorales* is based on phenotypic features requiring expertise and genotypic methods. The ECMM-MSG-ERC global guidelines for mucormycosis strongly recommend the identification of *Mucorales* to the species level for epidemiological evaluation [3]. However, identification to the genus level is only marginally supported in deciding the management of patients.

Mucorales are rapidly growing and cottony in appearance, varying from white to grey to blackish colour. *Mucorales* generally produce broad non-septate or sparsely septate hyphae (10–25 μm wide), branching irregularly exhibiting asexual structures like sporangium containing spores and rhizoids apophysis, columellae and sexual structures like zygospores (Fig. 5.3). In the absence of sporulation, especially in *Apophysomyces elegans* and *Saksenaea vasiformis*, slide culture technique in nutrient-deficient media like corn meal agar, potato dextrose agar and water agar with 0.1% of yeast extract enhance the spore formation (Fig. 5.4). The phenotypic characterization is challenging due to overlapping morphological features in different species and many cryptic species [9–13]. The methods used for identification of *Mucorales* listed below include lactophenol cotton blue mount (LCB), matrix-assisted laser desorption ionization-time-of-flight mass spectrometry (MALDI-TOF MS) and PCR sequencing.

Identification of the cultures

(a) *Lactophenol cotton blue mount (LPCB)*: LPCB mount prepared from culture demonstrates microscopic morphology aiding identification of *Mucorales*. Identification features of the commonly associated *Mucorales* are described below (Fig. 5.5) [14–16].

1. *Rhizopus arrhizus*

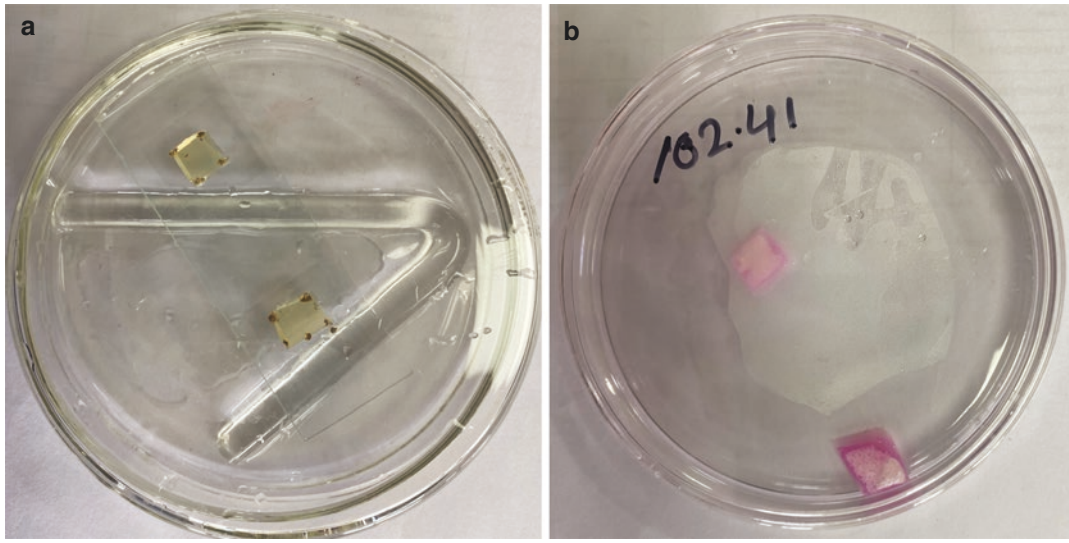

Fig. 5.4 (**a**) Slide culture technique. (**b**) Water agar technique

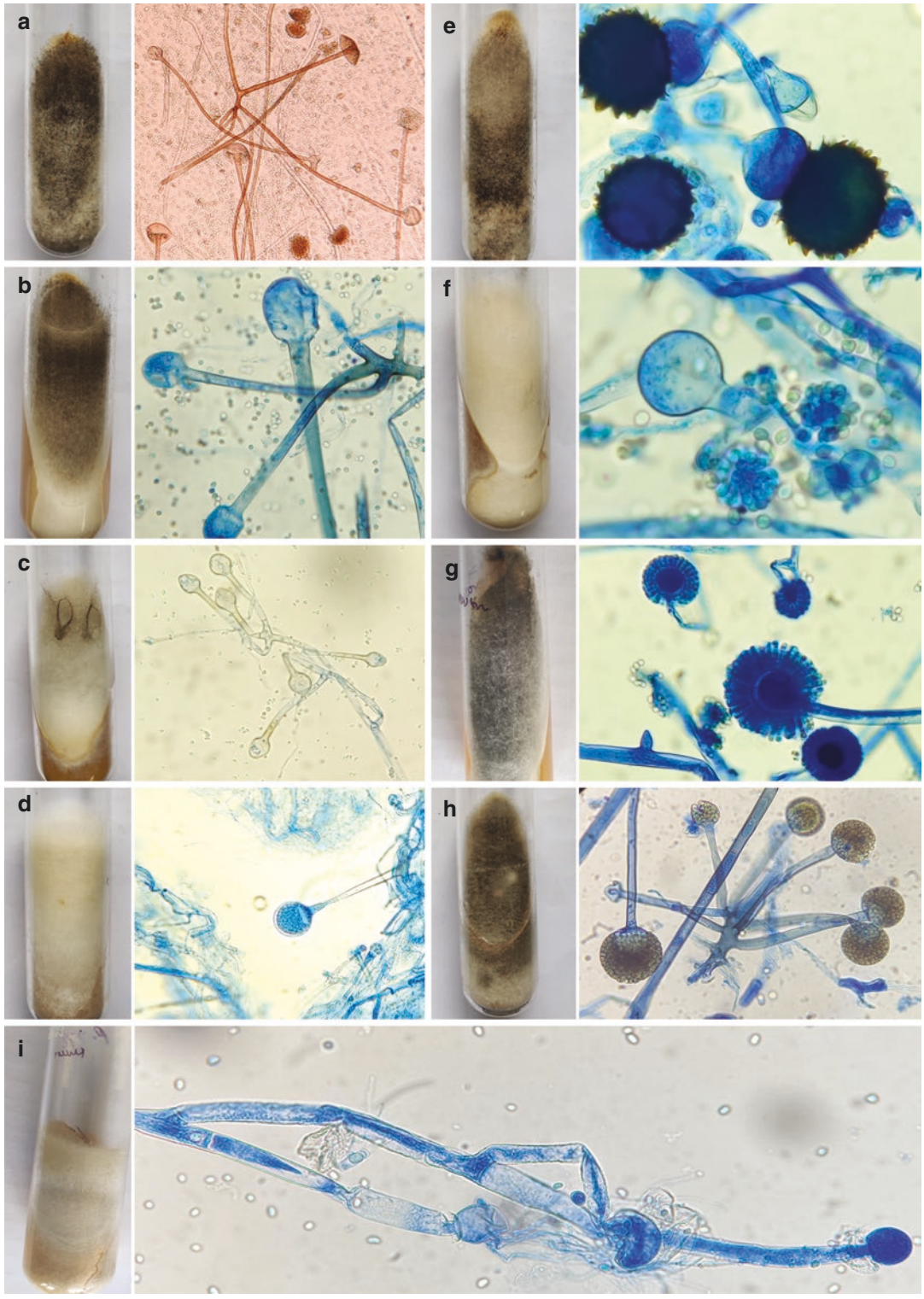

Fig. 5.5 Colony characteristics (left) and microscopic features (right) of (**A**) *R. arrhizus (x100),* (**B**) *R. microspores (x400),* (**C**) *Lichtheimia corymbifera (x100),* (**D**) *Apophysomyces variabilis (x400),* (**E**) *Rhizopus homothallicus (x400),* (**F**) *Cunninghamella bertholletiae (x400),* (**G**) *Syncephalastrum racemosum (x400),* (**H**) *Rhizomucor pusillus (x400)* and (**I**) *Mucor circinelloides (x400)*

Colony Characteristics: (SDA-25–37 °C) Rapidly growing cottony greyish white colonies. *Microscopy*: Sporangiophores are single or in groups, 1–2 mm high (18 μm wide), unbranched; sporangia spherical, brownish grey to blackish; columella covering 50–70% of sporangium; brownish rhizoids; subspherical to rhomboidal brownish sporangiospores (6–8 × 4.5–5 μm) with longitudinal striations.

2. *Rhizopus microsporus*
   Colony Characteristics: (MEA-30 °C) Cottony greyish brown colonies. *Microscopy*: Sporangiophores (8–10 μm wide) 400–500 μm high produced singly or pairs; sporangia spherical, greyish black; columella pyriform covering up to 80% of sporangium; sporangiospores (6 μm) ellipsoidal to spherical (6 and 9 μm in length), with striations.
3. *Lichtheimia corymbifera*
   Colony Characteristics: (MEA, 30 °C) Cottony greyish white rapidly growing colonies. *Microscopy*: Sporangiophores (up to 400 μm) branch repeatedly to form corymbs, sporangia pear-shaped; columella hemispherical or tapering with projections on top and a long conical apophysis; sporangiospores hyaline, smooth-walled, spherical to ellipsoidal.
4. *Apophysomyces variabilis*
   Colony Characteristics (MEA-30 °C): Rapidly growing creamy white cottony colonies turning yellowish over time. *Microscopy*: Sporangiophores (100–400 μm) unbranched, smooth-walled arising singly from a hypha; apex widening to form pyriform apophysis; sporangia pear-shaped; sporangiospores smooth-walled, hyaline to brownish and varying in shapes (cylindrical, oblong, ellipsoidal).
5. *Rhizopus homothallicus*
   Colony Characteristics: (MEA-30 °C) Rapidly growing brownish to greyish cottony colonies. *Microscopy*: Sporangiophores (5–30 μm wide) 2000 μm high; sporangia spherical, greyish black; columella subspherical; sporangiospores ellipsoidal or spherical with striations; homothallic with brownish yellow, spherical, spiny zygospores with unequal suspensors.
6. *Cunninghamella bertholletiae*
   Colony Characteristic: (MEA 37 °C) Rapidly growing greyish white colonies. *Microscopy*: Sporangiophores erect, with a whorl of short lateral branches at the apical region, ending in a swollen vesicle, single-spored sporangiola all over the vesicle attached by denticles, sporangiospores oval to spherical and smooth walled.
7. *Syncephalastrum racemosum*
   Colony Characteristics: (MEA, 25 °C) Greyish rapidly growing cottony colonies. *Microscopy*: Sporangiophores (10–25 μm wide) single or branched, arising from rhizoids, ending round vesicle, covered entirely by merosporangia, greyish cigar-shaped, containing chains of 3–18 spores; merospores smooth-walled, round to oval.
8. *Rhizomucor pusillus*
   Colony Characteristics: (MEA-30 °C) Rapidly growing cottony dark brown colonies. Being thermophilic, it grows up to 54–58 °C. *Microscopy*: Sporangiophores (11–15 μm wide) brownish, sympodially branched; rhizoids short rudimentary; sporangia spherical; columella spherical to pyriform and lacking apophysis; sporangiospores spherical, smooth-walled; homothallic or heterothallic with spherical dark brown spiny zygospores and equal suspensors.
9. *Mucor circinelloides*
   Colony Characteristics: (MEA, 24 °C) Rapidly growing brownish grey, black or yellow colonies. *Microscopy*: Sporangiophores (6 mm high, 17 μm wide) branched, elongated and shorter ones; columellae spherical to ellipsoidal; sporangiospores ellipsoidal and smooth-walled; chlamydospores absent or scanty.

(b) *Matrix-assisted laser desorption ionization-time-of-flight mass spectrometry (MALDI-TOF MS)*: MALDI-TOF MS with an upgraded database is a remarkably effective technique for identifying *Mucorales* to the tune of 100% at the genus level and 81.1% at the species level [3, 17, 18]. It is a simple, rapid, high-throughput technique for identifying *Mucorales* based on their unique main spectrum profiles (MSPs). However, the database requires continuous upgradation. The ECMM-MSG-ERC global guidelines for mucormycosis moderately support MALDI-TOF use due to its reliability on in-house databases and unavailability at many centres [3].

(c) *Other phenotypic methods*: The success of ID32C (bio Merieux, Marcy l'Étoile, France) and API 50CH (bioMerieux) kits based on carbon assimilation profiles of different *Mucorales* was described by Schwarz et al. [19].

(d) *PCR-sequencing*: The PCR sequencing targeting the internal transcribed spacer (ITS) region is the recommended molecular method for identifying *Mucorales* [3]. It is a cumbersome technique and is mainly available at reference laboratories. The concordance with phenotypic identification is reported to be >90% [20]. Other successful targets used for *Mucorales* identification include 18S rDNA, 28S rDNA, FTR1 and cytochrome b [1, 3].

5.2.2.3 Molecular Diagnosis

The need for molecular technique arises when culture does not yield growth of *Mucorales* (48–68% of direct microscopy positive) or in cases of concurrent infection due to *Aspergillus* and *Mucorales* or when the sparse fragments present in tissue make histopathological differentiation difficult [7, 21–23]. The molecular method is a quicker technique (<48 h) than culture (72–144 h) and histopathological (72–96 h) examination, although direct microscopy is the most rapid (<1 h) [7]. Molecular detection directly from fresh samples and formalin-fixed paraffin-embedded tissues is a promising technique but possesses heterogeneity in target genes (like ITS, 18S rDNA, 28S rDNA, cytochrome B, mitochondrial gene rnl or CotH genes), encompasses different methods with varying sensitivity [PCR and sequencing, semi-nested PCR, RFLP, qPCR and high-resolution melting (HRM) or electrospray ionization mass spectrometry (PCR/ESI-MS)] and lacks validation and standardization (Table 5.1) [6, 8, 24, 25]. Although histopathological examination (HPE) of tissue is an impor-

Table 5.1 Molecular diagnosis of mucormycosis

Sl no	Molecular approach	Target gene/s	Samples	Number of samples	Positivity	Remarks
1	ITS (panfungal) sequencing [38]	ITS	Fresh and FFPE tissues	$N = 8$	8 (100%)	One sample was identified as *R. pusillus* but *Absidia* by culture
2	PCR *Mucorales* specific primer sequencing [39, 40]	18S rDNA of *Mucorales*	Fresh and FFPE tissues	$N = 27$	22, of which one result was discordant with culture at species level	Semi-nested 81% sensitivity
		18S rDNA gene (Muc18S)	Blood and tissue	$N = 12$ (tissue samples) $N = 268$ (serum samples)	91% in paraffin-embedded tissue samples Serum: 100% proven/probable cases, 29% possible cases and 15% in unclassified	Probe-based *Mucorales*-specific real-time qPCR assay

(continued)

Table 5.1 (continued)

Sl no	Molecular approach	Target gene/s	Samples	Number of samples	Positivity	Remarks
3	Real-time PCR (qPCR) followed by high-resolution melt analysis (HRM) [26, 38, 41–43]	ZM1 and ZM3	Fresh and FFPE tissues	*N* = 7	100%	Semi-nested real-time PCR. Melting temperatures: *R. microsporus*, 76.46 °C; *R. oryzae*, 76.59 °C; *M. racemosus*, 76.78 °C; *M. circinelloides*, 76.98 °C; R. *pusillus*, 77.87 °C; *L. corymbifera*, 78.56 °C
		New species-specific real-time PCR assay targeting ITS2 region of ribosomal DNA	BAL	*N* = 99	9/99 (9.09%)	Sensitivity (100%) and specificity (93%); *Rhizopus* spp. (*n* = 6), *R. pusillus* (*n* = 2), and *L. corymbifera* (n = 1); results within 5 h
		Cytochrome *b* gene	Fresh tissue and paraffin-embedded tissue	*N* = 2 (fresh tissue) *N* = 62 (paraffin-embedded tissue)	–	100% sensitivity and specificity for fresh tissue 56% sensitivity and 100% specificity for paraffin-embedded tissue
		rnl gene	Tissue, blood	*N* = 21	15 (71.4% positivity)	LoD: 100 fg mucoralean DNA HRM profile in conidia-spiked blood samples: 10^4 *R. arrhizus*-conidia-spiked blood, equating *R. arrhizus* conidia/PCR reaction
		18S rDNA	Fresh tissue and FFPE	*N* = 6 (fresh tissue) *N* = 1 (FFPE)	100%	Semi nested real-time PCR
4	Multiplex real-time quantitative PCR (qPCR) [44]	Molecular beacon species-specific probes ITS1/ITS2 region with specific probes for *R. oryzae*, *R. microsporus* and *Mucor* spp.	Tissue	*N* = 12	N = 9	Two were negative as the causative agent was not included in the primer set (*R. pusillus* and *C. bertholletiae*)

Table 5.1 (continued)

Sl no	Molecular approach	Target gene/s	Samples	Number of samples	Positivity	Remarks
5	qPCR [45]	28S rDNA	Lung BAL	*N* = 98 *N* = 22	N = 97 N = 22	(99% sensitivity) (100% sensitivity)
6	PCR coupled with electrospray-ionization mass spectrometry (PCR/ESI-MS) [46]	16S-23S rRNA gene (ITS PCR) and 18S PCR	Fresh tissues	*N* = 15	Genus level: 13/15; species level: 12/15	Quantitative real-time PCR and sequencing; results within 6 h; *Cunninghamella* spp. or *Saksenaea vasiformis* misidentified
7	PCR-RFLP [7]	18S ZM1 and ZM3	Tissue	*N* = 50	100%	Identification is possible only up to genus level
8	Triple qPCRs [34, 35, 47, 48]	Acory/Muc1/ RMuc	Blood	*N* = 10	9/10	Limit of detection 3.7 to 15 fg/10 μL; positive up to 68 days before mucormycosis diagnosis; negative result in *Lichtheimia* species
			Blood	*N* = 44	36/44	Retrospective study
			BAL	*N* = 337 suspected patients	15 (5: Proven/ probable mucormycosis, 3: Probable invasive aspergillosis, 6: Invasive fungal disease, 1: No invasive fungal disease)	Sensitivity: 100% Specificity: 97%
			CSF	*N* = 1	1/1 (100%)	Single case
9	PCR-based detection of spore coat protein [27]	*CotH*	Urine	*N* = 4	4/4 (100%)	Sensitivity 90%, specificity 100% for proven mucormycosis; urine samples better than plasma or BAL in mice model
10	Genera-specific qPCR assay targeting *Cunninghamella* [49]	18S rRNA	Serum and BAL	*N* = 1	1/1 (100%)	Single case

Abbreviations: *BAL* Bronchoalveolar fluid, *CSF* Cerebrospinal fluid, *C. bertholletiae*: *Cunninghamella bertholletiae*, *DNA* Deoxyribonucleic acid, *FFPE* Formalin-fixed paraffin-embedded tissue, *ITS* Internal transcribed spacer, *LoD* Limit of detection, *L. corymbifera*: *Lichtheimia corymbifera*, *M. circinelloides*: *Mucor circinelloides*, *M. racemosus*: *Mucor racemosus*, *PCR* Polymerase chain reaction, *qPCR* Real-time PCR, *rDNA* Ribosomal DNA, *rRNA* Ribosomal ribonucleic acid, *R. arrhizus*: *Rhizopus arrhizus*, *R. microsporus*: *Rhizopus microsporus*, *R. oryzae*: *Rhizopus oryzae*, *R. pusillus*: *Rhizomucor pusillus*, *RFLP* Restriction fragment length polymorphism

tant tool for diagnosis of mucormycosis, it cannot identify the genus/species of the etiological agent. Fresh tissues (86–100% sensitivity) are generally preferred samples compared to FFPE tissues (15–90%) [3, 26–28]. Zaman et al. reported a nested PCR technique directly from fresh tissues targeting 18S rDNA with 100% results, whereas ITS sequencing could identify only 54% of the cases [7]. The lower performance of the ITS region in *Mucorales* is probably due to its longer (ITS1 region~300–350 bp) length compared to that in other fungi (~200–250 bp) [29]. Therefore, it is suggested to target the *Mucorales*-specific 18S rDNA region in a semi-nested PCR in tissues positive for aseptate hyphae than the ITS1 region, which performs better in septate fungi and yeasts [30]. The major factor hampering PCR amplification in FFPE tissues is DNA degradation due to histone cross-linking to formalin, which inversely affects the sensitivity over time [31, 32]. Another limitation of the molecular technique from FFPE is the low quality of sequence chromatograms, especially from tissues harbouring colonizing fungi interfering with amplification of target DNA [7, 29]. Jillwin et al. recorded cross-amplification in 14% of nasal/paranasal and cutaneous samples which form the majority of samples in suspected mucormycosis cases [30]. Overall, the analytical sensitivity of molecular methods in fresh tissue samples and FFPE ranges from 97% to 100% and 56% to 80%, respectively [28]. There are no commercially available methods for the same. This remains the focus of the Fungal PCR Initiative Working Group of ISHAM [33]. Apart from the tissue samples, molecular methods have been explored in blood and body fluids (BAL, CSF, urine) for early diagnosis of mucormycosis, especially pulmonary cases where deep tissue sampling is challenging (Table 5.1). Studies have shown detection of *Mucorales* DNA in serum of patients even before 3–68 days of conventional diagnosis [34, 35]. A commercially available, non-FDA-approved kit, MucorGenius (Pathonostics, Maastricht, The Netherlands), is a real-time PCR assay targeting 28S rRNA with a sensitivity of 75% and assay time of 3 h and diagnosing mucormycosis much early than the standard method [3, 24, 36]. It detects *Rhizopus* spp., *Mucor* spp., *Lichtheimia* spp., *Cunninghamella* spp. and *Rhizomucor* spp. The major drawback of these methods is lower sensitivity in patients on antifungal therapy and false-negative results in lower fungal burden [24, 35, 37]. There is still a need to standardize and validate molecular methods from clinical samples. Despite recommendations of screening high-risk patients (e.g. haematological malignancies, burns) for mucormycosis by molecular diagnosis from serum/plasma, its role in the diagnosis of ROCM may be limited.

5.2.2.4 Serological Diagnosis

There is a lack of commercially available antigen biomarkers indicating mucormycosis. The markers like galactomannan are indeed helpful in ruling out the diagnosis of mucormycosis when a high index of fungal infection is clinically suspected [3, 24]. However, one needs to be cautious of the possibility of mixed infections. The ECMM-MSG-ERC global guidelines of mucormycosis do not recommend using (1→3) ß-D-glucan (BDG) to diagnose mucormycosis. Burnham-Marusich et al. developed ELISA [using a panfungal monoclonal antibody (2DA6)] and lateral-flow immunoassay (LFIA), which could detect fucomannan present in the cell wall of numerous fungi, including *Mucorales* [50]. Detection of a serum disaccharide by mass spectrometry (MS) in mucormycosis cases has cross-reaction with other fungal pathogens. Furthermore, *Mucorales*-specific T cells (CD4+CD154+) detected by enzyme-linked immunospot (ELISpot) assay over 24 h seems to be specific for proven mucormycosis cases [51, 52]. Sato et al. identified *Rhizopus*-specific antigen (RSA) by signal sequence trapping and retrovirus-mediated expression (SST-REX) in the mouse model. They evaluated its diagnostic application by developing a monoclonal antibody-based ELISA system which demonstrated higher serum RSA levels in patients with mucormycosis as compared to invasive aspergillosis (15.1 vs 0.53 ng/mL) and negative control (0.49 ng/mL) [50, 53]. Although these tests are still in a nascent stage; their development will be

an asset to non-invasive rapid diagnostics of mucormycosis.

5.2.2.5 Metabolomics-Breath Test

Koshy et al. reported differentiation of infection caused by *R. arrhizus* var. arrhizus, *R. arrhizus* var. delemar and *R. microsporus* and from that of aspergillosis based on breath profile of volatile metabolite, sesquiterpene in mice and human cases tested by gas chromatography/tandem mass spectrometry (GC–MS) [50]. This technique seems easy, non-invasive and can be utilized for screening high-risk patients after complete validation.

5.2.2.6 Antifungal Susceptibility Testing

The ECMM-MSG-ERC global guidelines recommend performing antifungal susceptibility testing using standard methods [broth microdilution by European Committee on Antimicrobial Susceptibility Testing (EUCAST) and the CLSI] for *Mucorales* only in case of non-responders through strong recommendation exists for epidemiological investigation [5, 54, 55]. Commercial methods like E-test are, however, only marginally recommended as their results do not sometimes match with the standard methods. The major hurdle in antifungal susceptibility testing of *Mucorales* is the unavailability of clinical breakpoints, which makes interpretation difficult, although epidemiological cut-off values are available for some species. Though amphotericin B, posaconazole and isavuconazole have good activity against *Mucorales*, few *Cunninghamella* species exhibit higher MICs against amphotericin B, *Rhizopus* species against posaconazole and *Mucor circinelloides* against isavuconazole [5].

5.2.2.7 Environmental Screening

Apart from the clinical samples, *Mucorales* have also been isolated from environmental niches like air and soil. The isolation is pertinent to delineate the spore burden of *Mucorales* in environmental sources. The isolation from the air is preferably performed using DRBC with benomyl medium, which is selective for *Mucorales* [56] (Fig. 5.6). Whole-genome sequencing has also been employed to resolve the dynamics of an outbreak of mucormycosis in a burn unit in France [57].

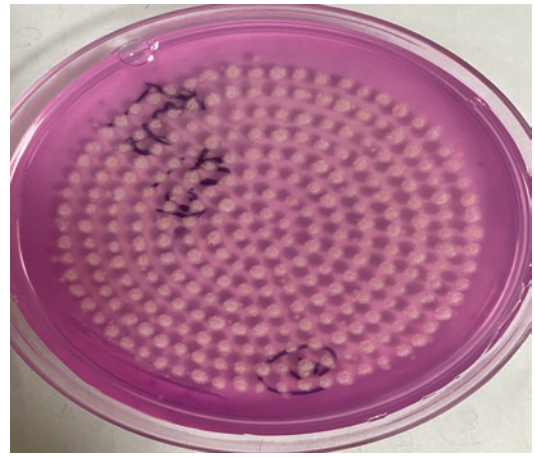

Fig. 5.6 Isolation of *Mucorales* from air on dichloran rose Bengal chloramphenicol (DRBC) with benomyl medium

5.3 Conclusion

The diagnosis of ROCM is considered as most urgent owing to progressive angioinvasion leading to a high fatality rate. High clinical suspicion and microbiological examination of endoscopic tissue biopsies is the prime requirement. Obtaining deep samples might not be possible in patients with neutropenia or thrombocytopenia. The conventional diagnostic techniques like direct microscopy and culture have low sensitivity, though optical brighteners enhance the visual field. The fragile nature of the aseptate hyphae of *Mucorales* affects the yield of culture. There is a complete void of serological markers for *Mucorales* though a negative galactomannan may decrease the likelihood of infection. The molecular techniques are emerging but are available only in reference laboratories and lack standardization.

References

1. Walther G, Wagner L, Kurzai O. Updates on the taxonomy of mucorales with an emphasis on clinically important taxa. J Fungi (Basel). 2019;5:106.

2. Meechan P, Hatcher B, Potts J, editors. Biosafety in microbiological and biomedical laboratories. 6th ed. Atlanta: HHS; 2020.
3. Cornely OA, Alastruey-Izquierdo A, Arenz D, Chen SCA, Dannaoui E, Hochhegger B, et al. Global guideline for the diagnosis and management of mucormycosis: an initiative of the European Confederation of Medical Mycology in cooperation with the Mycoses Study Group Education and Research Consortium. Lancet Infect Dis. 2019;19:e405–21.
4. Walsh TJ, Gamaletsou MN, McGinnis MR, Hayden RT, Kontoyiannis DP. Early clinical and laboratory diagnosis of invasive pulmonary, extrapulmonary, and disseminated mucormycosis (zygomycosis). Clin Infect Dis. 2012;54(SUPPL. 1):S55–60.
5. Cornely OA, Arikan-Akdagli S, Dannaoui E, Groll AH, Lagrou K, Chakrabarti A, et al. ESCMID and ECMM joint clinical guidelines for the diagnosis and management of mucormycosis 2013. Clin Microbiol Infect. 2014;20(S3):5–26.
6. Lass-Flörl C, Mayr A. Diagnosing invasive fungal diseases - limitations of microbiological diagnostic methods. Expert Opin Med Diagn. 2009;3(4):461–70.
7. Zaman K, Rudramurthy SM, Das A, Panda N, Honnavar P, Kaur H, et al. Molecular diagnosis of rhino-orbito-cerebral mucormycosis from fresh tissue samples. J Med Microbiol. 2017;66(8):1124–9.
8. Weiss ZF, Leon A, Koo S. The evolving landscape of fungal diagnostics, current and emerging microbiological approaches. J Fungi. 2021;7(2):1–27.
9. Alvarez E, Garcia-Hermoso D, Sutton DA, Cano JF, Stchigel AM, Hoinard D, et al. Molecular phylogeny and proposal of two new species of the emerging pathogenic fungus Saksenaea. J Clin Microbiol. 2010;48(12):4410–6.
10. Alastruey-Izquierdo A, Hoffmann K, de Hoog GS, Rodriguez-Tudela JL, Voigt K, Bibashi E, et al. Species recognition and clinical relevance of the zygomycetous genus Lichtheimia (syn. Absidia pro parte, Mycocladus). J Clin Microbiol. 2010;48(6):2154–70.
11. Alvarez E, Stchigel AM, Cano J, Sutton DA, Fothergill AW, Chander J, et al. Molecular phylogenetic diversity of the emerging mucoralean fungus Apophysomyces: proposal of three new species. Rev Iberoam Micol. 2010;27(2):80–9.
12. Garcia-Hermoso D, Hoinard D, Gantier J-C, Grenouillet F, Dromer F, Dannaoui E. Molecular and phenotypic evaluation of Lichtheimia corymbifera (formerly Absidia corymbifera) complex isolates associated with human mucormycosis: rehabilitation of L. ramosa. J Clin Microbiol. 2009;47(12):3862–70.
13. Walther G, Pawłowska J, Alastruey-Izquierdo A, Wrzosek M, Rodriguez-Tudela JL, Dolatabadi S, et al. DNA barcoding in Mucorales: an inventory of biodiversity. Persoonia. 2013;30:11–47.
14. de Hoog G, Guarro J, Gené J, Ahmed S, Al-Hatmi A, Figueras M, et al., editors. The atlas of clinical fungi. 4th ed. Utrecht: Centraalbureau voor Schimmelcultures; 2020.
15. Sciortino C, editor. Atlas of clinically important fungi. 1st ed. Hoboken, NJ: Wiley Blackwell; 2017.
16. Larone D, editor. Medically important fungi, a guide to identification. 5th ed. Washington, DC: ASM Press; 2011.
17. Paul S, Singh P, Rudramurthy SM, Chakrabarti A, Ghosh AK. Matrix-assisted laser desorption/ionization–time of flight mass spectrometry: protocol standardization and database expansion for rapid identification of clinically important molds. Future Microbiol. 2017;12(16):1457–66. https://doi.org/10.2217/fmb-2017-0105.
18. Shao J, Wan Z, Li R, Yu J. Species identification and delineation of pathogenic mucorales by matrix-assisted laser desorption ionization–time of flight mass spectrometry. J Clin Microbiol. 2018;56(4):e01886-17.
19. Schwarz P, Lortholary O, Dromer F, Dannaoui E. Carbon assimilation profiles as a tool for identification of zygomycetes. J Clin Microbiol. 2007;45(5):1433–9.
20. Alvarez E, Sutton DA, Cano J, Fothergill AW, Stchigel A, Rinaldi MG, et al. Spectrum of zygomycete species identified in clinically significant specimens in the United States. J Clin Microbiol. 2009;47(6):1650–6.
21. Chakrabarti A, Chatterjee SS, Das A, Panda N, Shivaprakash MR, Kaur A, et al. Invasive zygomycosis in India: experience in a tertiary care hospital. Postgrad Med J. 2009;85(1009):573–81.
22. Chakrabarti A, Das A, Sharma A, Panda N, Das S, Gupta KL, et al. Ten years' experience in zygomycosis at a Tertiary Care Centre in India. J Infect. 2001;42(4):261–6.
23. Chakrabarti A, Das A, Mandal J, Shivaprakash MR, George VK, Tarai B, et al. The rising trend of invasive zygomycosis in patients with uncontrolled diabetes mellitus. Med Mycol. 2006;44(4):335–42.
24. Skiada A, Pavleas I, Drogari-Apiranthitou M. Epidemiology and diagnosis of mucormycosis: an update. J fungi (Basel). 2020;6(4):265.
25. Skiada A, Lass-Floerl C, Klimko N, Ibrahim A, Roilides E, Petrikkos G. Challenges in the diagnosis and treatment of mucormycosis. Med Mycol. 2018;56(suppl_1):S93–101.
26. Caramalho R, Madl L, Rosam K, Rambach G, Speth C, Pallua J, et al. Evaluation of a novel mitochondrial pan-mucorales marker for the detection, identification, quantification, and growth stage determination of mucormycetes. J Fungi. 2019;5(4):98.
27. Baldin C, Soliman SSM, Jeon HH, Alkhazraji S, Gebremariam T, Gu Y, et al. PCR-based approach targeting mucorales-specific gene family for diagnosis of mucormycosis. J Clin Microbiol. 2018;56(10):e00746-18.
28. Millon L, Scherer E, Rocchi S, Bellanger A-P. Molecular strategies to diagnose mucormycosis. J Fungi. 2019;5(1):24.
29. Cabaret O, Toussain G, Abermil N, Alsamad IA, Botterel F, Costa J-M, et al. Degradation of fungal DNA in formalin-fixed paraffin-embedded sinus fun-

gal balls hampers reliable sequence-based identification of fungi. Med Mycol. 2011;49(3):329–32.
30. Jillwin J, Rudramurthy SM, Singh S, Bal A, Das A, Radotra B, et al. Molecular identification of pathogenic fungi in formalin-fixed and paraffin-embedded tissues. J Med Microbiol. 2020;70(2) https://doi.org/10.1099/jmm.0.001282.
31. Babouee Flury B, Weisser M, Prince SS, Bubendorf L, Battegay M, Frei R, et al. Performances of two different panfungal PCRs to detect mould DNA in formalin-fixed paraffin-embedded tissue: what are the limiting factors? BMC Infect Dis. 2014;14(1):692.
32. Rickerts V, Khot PD, Ko DL, Fredricks DN. Enhanced fungal DNA-extraction from formalin-fixed, paraffin-embedded tissue specimens by application of thermal energy. Med Mycol. 2012;50(6):667–72.
33. Fungal PCR Initiative (FPCRI): ISHAM.
34. Millon L, Larosa F, Lepiller Q, Legrand F, Rocchi S, Daguindau E, et al. Quantitative polymerase chain reaction detection of circulating DNA in serum for early diagnosis of mucormycosis in immunocompromised patients. Clin Infect Dis. 2013;56(10):e95–101.
35. Millon L, Herbrecht R, Grenouillet F, Morio F, Alanio A, Letscher-Bru V, et al. Early diagnosis and monitoring of mucormycosis by detection of circulating DNA in serum: retrospective analysis of 44 cases collected through the French Surveillance Network of Invasive Fungal Infections (RESSIF). Clin Microbiol Infect. 2016;22(9):810.e1–8.
36. Guegan H, Iriart X, Bougnoux M-E, Berry A, Robert-Gangneux F, Gangneux J-P. Evaluation of MucorGenius® mucorales PCR assay for the diagnosis of pulmonary mucormycosis. J Infect. 2020;81(2):311–7.
37. Caillot D, Valot S, Lafon I, Basmaciyan L, Chretien ML, Sautour M, et al. Is it time to include CT "reverse halo sign" and qPCR targeting mucorales in serum to EORTC-MSG criteria for the diagnosis of pulmonary mucormycosis in leukemia patients? Open Forum Infect Dis. 2016;3(4):ofw190.
38. Lau A, Chen S, Sorrell T, Carter D, Malik R, Martin P, et al. Development and clinical application of a panfungal PCR assay to detect and identify fungal DNA in tissue specimens. J Clin Microbiol. 2007;45(2):380–5. https://journals.asm.org/journal/jcm
39. Hammond SP, Bialek R, Milner DA, Petschnigg EM, Baden LR, et al. Molecular methods to improve diagnosis and identification of mucormycosis. J Clin Microbiol. 2011;49(6):2151–3. https://journals.asm.org/journal/jcm
40. Springer J, Lackner M, Ensinger C, Risslegger B, Morton CO, Nachbaur D, et al. Clinical evaluation of a mucorales-specific real-time PCR assay in tissue and serum samples. J Med Microbiol. 2016;65(12):1414–21.
41. Hrncirova K, Lengerova M, Kocmanova I, Racil Z, Volfova P, Palousova D, et al. Rapid detection and identification of mucormycetes from culture and tissue samples by use of high-resolution melt analysis. J Clin Microbiol. 2010;48(9):3392–4.
42. Lengerova M, Racil Z, Hrncirova K, Kocmanova I, Volfova P, Ricna D, et al. Rapid detection and identification of mucormycetes in bronchoalveolar lavage samples from immunocompromised patients with pulmonary infiltrates by use of high-resolution melt analysis. J Clin Microbiol. 2014;52(8):2824–8.
43. Hata DJ, Buckwalter SP, Pritt BS, Roberts GD, Wengenack NL. Real-time PCR method for detection of zygomycetes. J Clin Microbiol. 2008;46(7):2353–8. https://journals.asm.org/journal/jcm
44. Bernal-Martínez L, Buitrago MJ, Castelli MV, Rodriguez-Tudela JL, Cuenca-Estrella M. Development of a single tube multiplex real-time PCR to detect the most clinically relevant Mucormycetes species. Clin Microbiol Infect. 2013;19(1):E1.
45. Kasai M, Harrington SM, Francesconi A, Petraitis V, Petraitiene R, Beveridge MG, et al. Detection of a molecular biomarker for zygomycetes by quantitative PCR assays of plasma, bronchoalveolar lavage, and lung tissue in a rabbit model of experimental pulmonary zygomycosis. J Clin Microbiol. 2008;46(11):3690–702. https://journals.asm.org/journal/jcm
46. Alanio A, Garcia-Hermoso D, Mercier-Delarue S, Lanternier F, Gits-Muselli M, Menotti J, et al. Molecular identification of Mucorales in human tissues: contribution of PCR electrospray-ionization mass spectrometry. Clin Microbiol Infect. 2015;21(6):594.e1–5. https://doi.org/10.1016/j.cmi.2015.01.017.
47. Scherer E, Iriart X, Bellanger AP, Dupont D, Guitard J, Gabriel F, et al. Quantitative PCR (qPCR) detection of mucorales DNA in bronchoalveolar lavage fluid to diagnose pulmonary mucormycosis. J Clin Microbiol. 2018;56(8):1–9.
48. Shigemura T, Nakazawa Y, Matsuda K, Motobayashi M, Saito S, Koike K. Evaluation of Mucorales DNA load in cerebrospinal fluid in a patient with possible cerebral mucormycosis treated with intravenous liposomal amphotericin B. Int J Infect Dis. 2014;29:e200–2. https://doi.org/10.1016/j.ijid.2014.10.019.
49. Bellanger A-P, Berceanu A, Rocchi S, Valot B, Jean F, Chauchet A, et al. Development of a quantitative PCR detecting Cunninghamella bertholletiae to help in diagnosing this rare and aggressive mucormycosis. Bone Marrow Transplant. 2018;53:1180–3. https://doi.org/10.1038/s41409-018-0194-5.
50. Burnham-Marusich AR, Hubbard B, Kvam AJ, Gates-Hollingsworth M, Green HR, Soukup E, et al. Conservation of mannan synthesis in fungi of the zygomycota and ascomycota reveals a broad diagnostic target. mSphere. 2018;3(3):e00094-18.
51. Potenza L, Vallerini D, Barozzi P, Riva G, Gilioli A, Forghieri F, et al. Mucorales-specific T cells in patients with hematologic malignancies. PLoS One. 2016;11(2):e0149108.
52. Potenza L, Vallerini D, Barozzi P, Riva G, Forghieri F, Zanetti E, et al. Mucorales-specific T cells emerge in

the course of invasive mucormycosis and may be used as a surrogate diagnostic marker in high-risk patients. Blood. 2011;118(20):5416–9.
53. Sato K, Oinuma K-I, Niki M, Yamagoe S, Miyazaki Y, Asai K, et al. Identification of a novel rhizopus-specific antigen by screening with a signal sequence trap and evaluation as a possible diagnostic marker of mucormycosis. Med Mycol. 2017;55(7):713–9.
54. CLSI. Reference method for broth dilution antifungal susceptibility testing of filamentous fungi. CLSI standard M38. 3rd ed. Clinical and Laboratory Standards Institute; 2017.
55. Arendrup MC, Guinea J, Cuenca-Estrella M, et al. EUCAST definitive document E.DEF 9.3. Method for the determination of broth dilution minimum inhibitory concentrations of antifungal agents for conidia forming moulds. 2015.
56. Prakash H, Singh S, Rudramurthy SM, Singh P, Mehta N, Shaw D, et al. An aero mycological analysis of Mucormycetes in indoor and outdoor environments of northern India. Med Mycol. 2020;58(1):118–23.
57. Garcia-Hermoso D, Criscuolo A, Lee SC, Legrand M, Chaouat M, Denis B, et al. Outbreak of invasive wound mucormycosis in a burn unit due to multiple strains of mucor circinelloides f. circinelloides resolved by whole-genome sequencing. MBio. 2018;9(2):e00573-18.

6 Histopathological Diagnosis of Rhino-Orbito-Cerebral Mucormycosis

Aanchal Kakkar and Kavneet Kaur

6.1 Introduction

Mucormycosis is a fulminant, rapidly progressive, and opportunistic infectious disease caused by fungi of the order Mucorales, with mortality rates as high as 50% even with treatment [1]. They belong to the phylum Glomeromycota, under which there are two subphylums: Mucormycotina and Entomophthoromycotina, formerly grouped together under Zygomycetes [2]. *Rhizopus* is the most frequent genus of Mucorales, which causes human disease, accounting for up to 90% of cases, while Mucor is identified in approximately 20% of cases [3]. Other genera, viz. *Rhizomuccor*, *Lichtheimia* (formerly Absidia) are considerably rare [4]. Microbiological culture fails to grow the organism from patient specimens in approximately 50% of cases; hence, histopathology plays an important role in arriving at the correct diagnosis [5].

Infection by Mucorales is clinically classified based on the anatomical site affected, viz. Rhino-orbito-cerebral, gastrointestinal, pulmonary, cutaneous, and disseminated mucormycosis. Among these, the most common clinical manifestation is rhino-orbito-cerebral disease [5].

6.2 Pathogenesis

Mucorales have an affinity for blood vessels and nerves; hence, vascular invasion and thrombosis with resultant tissue necrosis, and neurotropism are key features of invasive mucormycosis. The endoplasmic reticulum (ER) is a vital/critical cell organelle that serves as a factory for the synthesis and assembly of secretory and membrane proteins. The normal functioning of the ER is regulated by ER chaperones. Glucose-regulated protein 78 (GRP78) is one such ER chaperone that performs various functions such as transporting polypeptides across the ER membrane, assisting in folding and assembly of protein molecules, targeting misfolded proteins for degradation, and regulating calcium levels within cellular compartments. However, its most important function is serving as a sensor of ER stress. It is considered the master regulator of ER stress through modulation of the unfolded protein response (UPR) [6]. The high availability of freely accessible iron in plasma and tissues seen in acidotic conditions like diabetes due to the displacement of protons by transferrin accentuates the expression of GRP78, further promoting angioinvasion and neurotropism. Various factors also regulate the latter in the microenvironment of the nerves [7].

A. Kakkar (✉) · K. Kaur
Department of Pathology, All India Institute of Medical Sciences, New Delhi, India
e-mail: draanchalkakkar@aiims.edu

N. Gupta, S. G. Honavar (eds.), *Rhino-Orbito-Cerebral Mucormycosis*,
https://doi.org/10.1007/978-981-16-9729-6_6

6.2.1 COVID-19 and Mucormycosis

The clinical picture of COVID-19 covers a wide spectrum, ranging from asymptomatic infection through mildly symptomatic disease to severe, fatal pneumonia. SARS CoV-2 infection, its treatment with resultant immunosuppression, and preexisting comorbidities have made patients vulnerable to secondary infections including mucormycosis. There has been a dramatic rise in the incidence of rhino-orbito-cerebral mucormycosis in 2021, accompanied by rarely seen histological features. Mucormycosis may occur concurrently with COVID-19, or may occur in patients who have recovered from the viral disease.

6.3 Histopathological Features

6.3.1 Gross Appearance

Specimens received for histopathological examination include debridements of sinonasal tissue by endoscopic surgery, soft tissue debridements, maxillectomies, and orbital exenterations. On gross examination, involved tissues appear necrotic with a blackish discoloration. Fat necrosis, if present, has a chalky white appearance.

6.3.2 Microscopic Features

6.3.2.1 Morphology of Fungal Profiles

On hematoxylin and eosin (H&E) stained sections, Mucorales are readily stained, characteristically displaying nonpigmented amphophilic hyphae that are thin-walled, imparting a pale, and translucent appearance [8] (Fig. 6.1). The hyphae are broad, varying in thickness from 6 to 50 μm, and have a ribbon-like appearance due to their nonparallel walls (Fig. 6.1d). They may reach a length of up to 200 mm [3]. They are often folded upon each other or seem crinkled and show a haphazard pattern of branching at various angles, ranging from 45° to 90° [9] (Fig. 6.1c). The fungal profiles of Mucor are often erroneously considered aseptate but indeed show occasional septae, and hence, the term pauciseptate is more apt to describe them (Fig. 6.1f). Septae should, however, be distinguished from artifacts caused by the folding of tissue on itself.

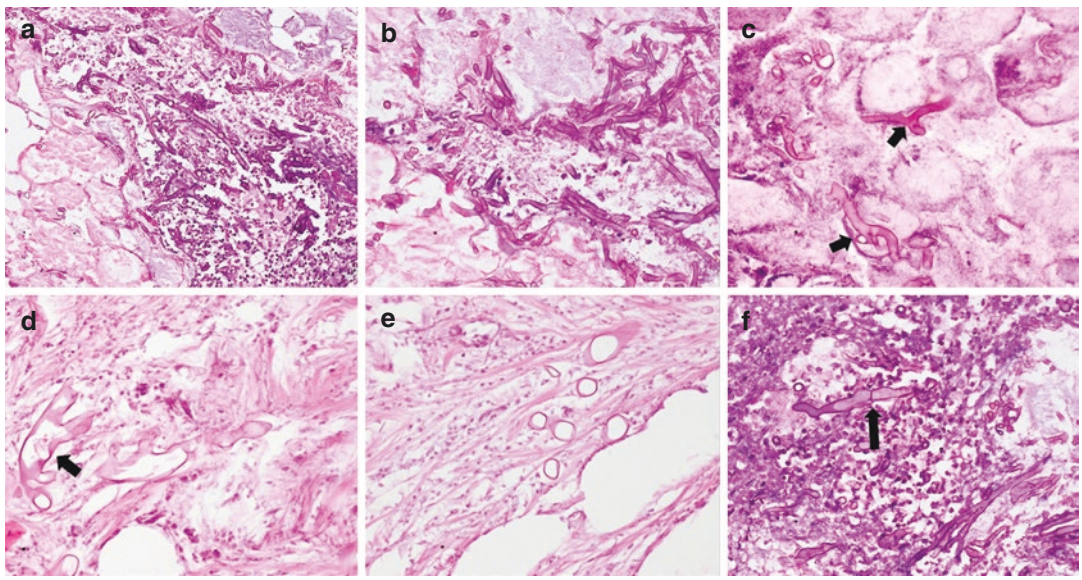

Fig. 6.1 Amphophilic hyaline fungal hyphae (**a**; ×200) with a ribbon-like appearance (**b**; ×400) and haphazard branching at variable angles (arrows) (**c**; ×400) within necrotic tissue; broad hyphae with well-delineated cell walls (**d**; ×400), and hollow transverse sections (**e**; ×400); septae (arrow) are seen in occasional hyphae (**f**; ×400)

Within any given tissue specimen, the number of fungal hyphae that are present varies considerably. When numerous, the diagnosis is relatively straightforward. However, when fungal profiles are sparse in number or only fragmented fungal hyphae are present, the above features are challenging to identify, making diagnosis onerous. Growth conditions also cause variations in morphology; in areas with high oxygen tension such as the paranasal sinuses, asexual reproduction results in the formation of sporangia, which are thick-walled sac-like structures (50–300 μm) seen at one end of a broad, elongated, relatively rigid looking, usually unbranched hypha known as a sporangiophore, which measures up to 1500 μm in length and 18 μm in diameter (Fig. 6.2). The sporangia contain spherical sporangiospores, which range from 4 to 8 μm in diameter. The sporangia, sporangiophores, and sporangiospores may be pigmented, appearing light brown in color on H&E stain (Fig. 6.2). The size and shape of sporangia and sporangiospores differ from species to species [10]. However, this distinction is difficult to make on tissue sections as sporangia are often disintegrated, with sporangiospores dispersed around them. Under polarized light, sporangiospores show a Maltese cross appearance as is seen in yeast forms of Cryptococcus and Histoplasma, and should not be mistaken for the same (Fig. 6.2d). Aggregates of fungal hyphae seen within empty spaces are known as fungal balls; they may rarely show the presence of sporangia or sporangiospores (Fig. 6.3). They are frequently present within the necrotic contents of the maxillary sinus. However, they are not identified within soft tissues and are unlikely to be seen in orbital exenteration specimens.

6.3.2.2 Host Tissue Reaction

The microscopic picture of Mucormycosis is predominated by tissue invasion, particularly angioinvasion, with resultant tissue necrosis, which has been variably described as bland or infarct-like, indicating the absence of visible cellular outlines within the necrosis. Fat necrosis (Fig. 6.4) of periocular soft tissues characteristically shows neutrophilic panniculitis with ghost adipocytes and, less frequently, finely granular basophilic calcification. Groups of necrotic adi-

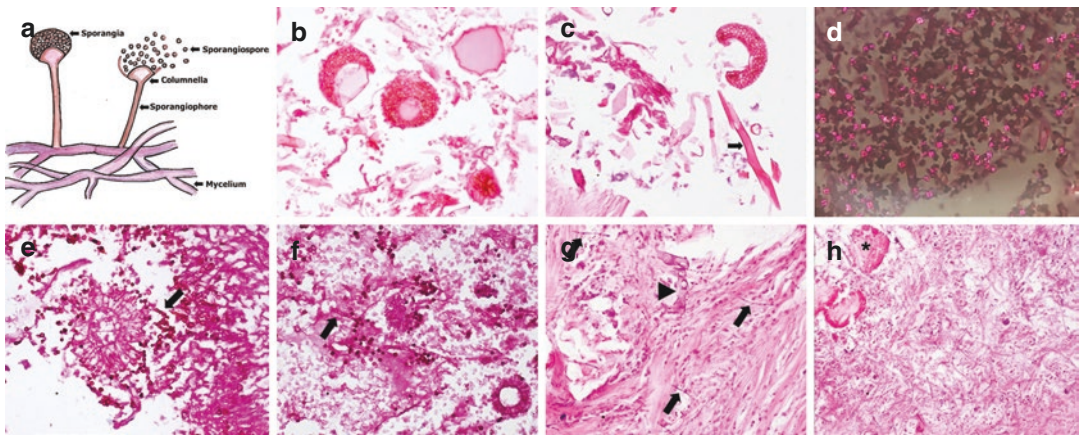

Fig. 6.2 Diagrammatic representation of structure of Mucorales (**a**); tissue sections showing sporangia containing sporangiospores, along with dispersed spores (**b**; HE, ×400); long unbranched pigmented sporangiophore (arrow) and mature sporangia packed with sporangiospores (**c**; HE, ×400); sporangiospores display Maltese cross appearance under polarized light (**d**; PAS with diastase {PAS-D}, ×200). Fruiting body of *Aspergillus* has a central vesicle with radiating phialides and chains of conidia (arrow) (**e**; HE, ×400); narrow septate hyphae (arrow) and fruiting bodies of *Aspergillus* (**f**; HE, ×400). Coinfection with Mucor (arrowhead) and pseudohyphae of invasive Candidiasis (arrows) (**g**; HE, ×400); aggregate of yeasts and pseudohyphae of *Candida* with degenerated sporangia of Mucor (asterisk) (**h**; HE, ×400)

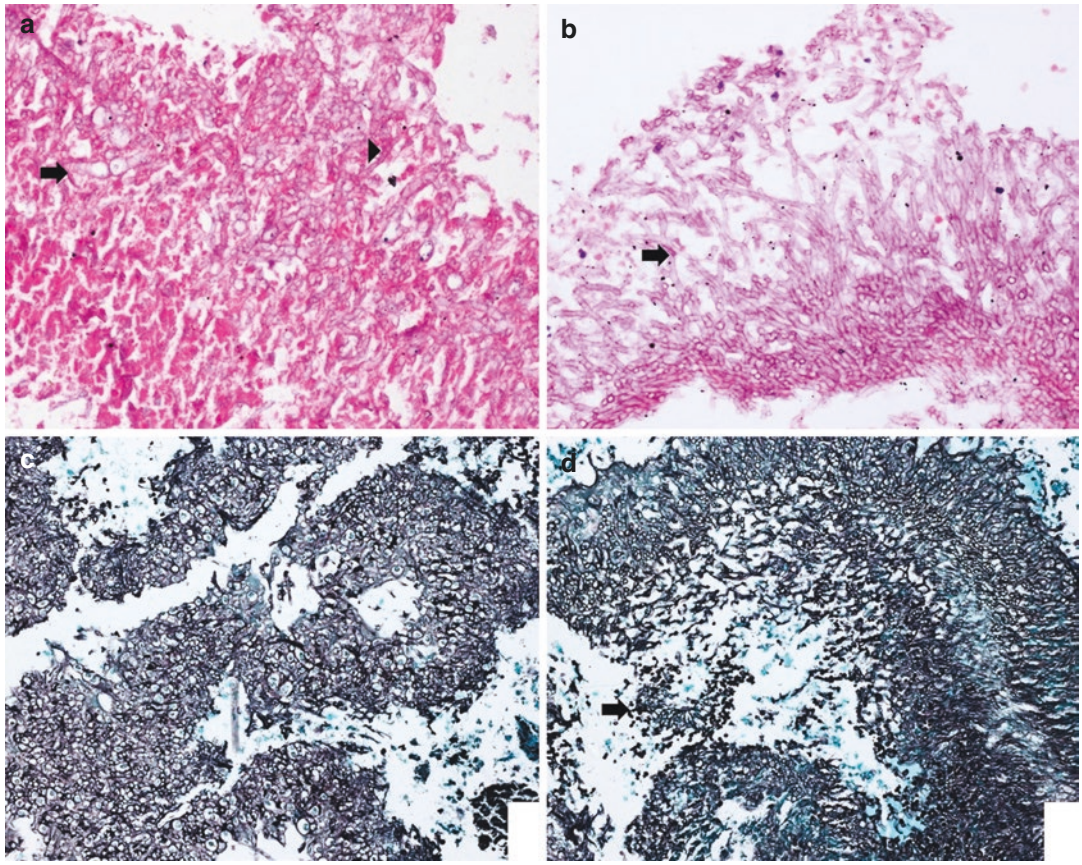

Fig. 6.3 Fungal ball of enmeshed hyphae of both Mucor (arrow) and *Aspergillus* (arrowhead) (**a**; HE, ×400); *Aspergillus* demonstrate dichotomous branching (**b**; HE, ×400). Gomori methenamine silver (GMS) stain highlighting the broad fungal hyphae of Mucorales (**c**; ×400), and slender hyphae and degenerating fruiting body (arrow) of *Aspergillus* (**d**; ×400)

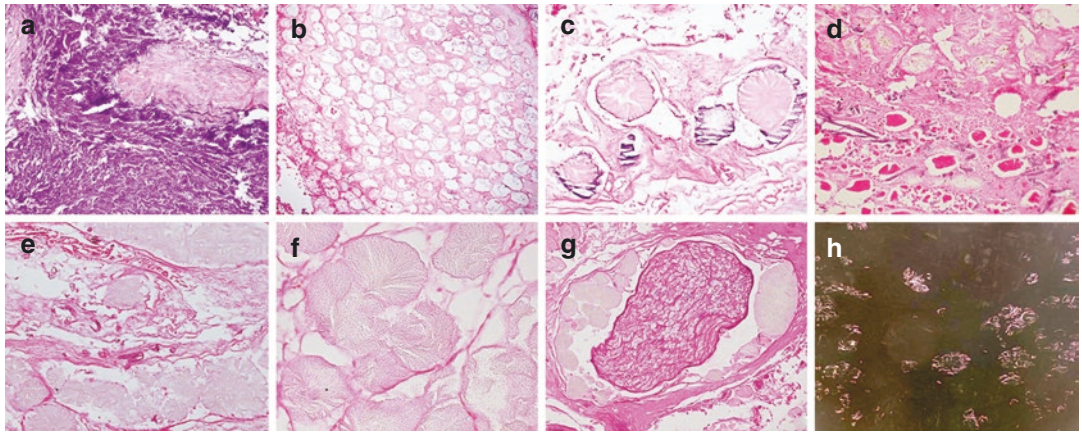

Fig. 6.4 Necrosis and acute inflammatory exudate imparting a dirty blue-gray appearance (**a**; HE, ×200); fat necrosis with ghost adipocytes (**b**; HE, ×100), non-refractile eosinophilic deposits with peripheral basophilic rim (**c**; HE, ×400), with many long fungal hyphae of Mucor (**d**; HE, ×200); refractile crystalline deposits (**e**; HE, ×200) with a pale brown color (**f**; HE, ×400) seen surrounding a nerve (**g**; HE, ×200), and showing birefringence on polarized microscopy (**h**; HE, ×200)

pocytes form round to ovoid eosinophilic deposits with a crystalline internal structure best demonstrated by lowering the microscope's condenser, upon which they appear refractile. Often, these crystalline deposits have a light brownish color on H&E staining. In many cases, the refractile crystalline deposits are present adjacent to non-refractile eosinophilic deposits of similar size and shape, indicating a progression from one to the other. Some of these have a peripheral basophilic rim due to calcium deposition. On polarized microscopy, these crystalline deposits are strongly birefringent and appear to be composed of short needle-shaped crystals that are arranged radially. This striking histological feature has been attributed to local production of lipases by mucormycetes [11].

The patterns of inflammation encountered include acute suppurative inflammation and chronic granulomatous inflammation. The acute stage is characterized by suppurative inflammation with neutrophils dominating the inflammatory infiltrate, admixed with necrotic debris, imparting a dirty blue-gray appearance on low magnification (Fig. 6.4a). Neutrophil microabscesses surrounded by lymphoplasmacytic infiltrate are also common. In chronic disease, suppurative granulomas composed of central neutrophilic micro-abscesses surrounded by palisaded or foamy histiocytes, lymphocytes, and multinucleated foreign body giant cells are often present in the periocular soft tissues (Fig. 6.5). Well-defined granulomas with epithelioid histiocytes and multinucleated foreign body giant cells may also be present (Fig. 6.5).

Angioinvasion is the hallmark of the disease (Fig. 6.6). Small, intermediate, and large-sized blood vessels show occlusion of their lumina, with fungal hyphae present in the vessel walls and enmeshed within the luminal thrombi. On occasion, a fungal ball-like aggregate of fungal hyphae may be seen lying within the vascular lumen.

Perineural spread (Fig. 6.7) is another characteristic feature of invasive mucormycosis. Fungal hyphae are often seen coursing along the entire nerves, both in necrotic and in viable tissue. The hyphae are usually concentrated within the perineurium but are also seen within the substance of the nerve. Involved nerves may show demyelination, highlighted on Luxol fast blue stain as the loss of the normal blue-staining myelin sheath

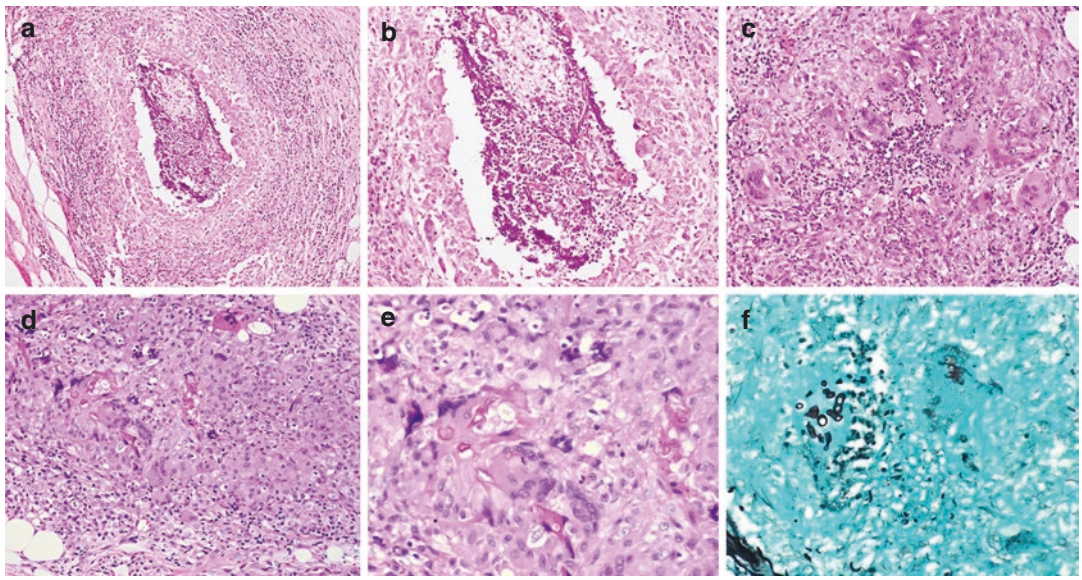

Fig. 6.5 Suppurative granuloma (**a**; HE, ×100) with central neutrophilic microabscess and fragmented fungal hyphae (**b**; HE, ×200) and foreign body giant cells (**c**; HE, ×400); epithelioid cell granuloma around fungal hyphae (**d**; HE, ×200) show hyphal fragments phagocytosed by foreign body giant cells (**e**; HE, ×400 and **f**; GMS ×400)

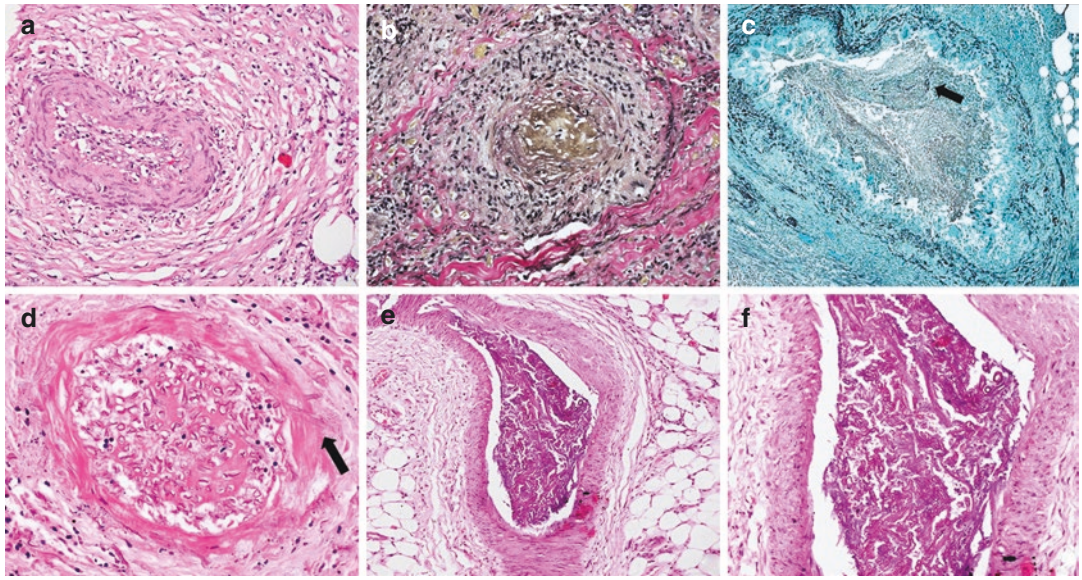

Fig. 6.6 Small muscular artery with a recanalized thrombus occluding the lumen (**a**; HE, ×200); and Verhoeff-van Gieson stain demonstrating disruption of its internal elastic lamina (**b**; ×200). GMS stain highlights fragmented fungal hyphae within the thrombi (**c**; ×40). Angioinvasion by fungal hyphae invading the vessel wall (arrow) and in the lumen (**d**; HE, ×200). Ball-like aggregate of fungal hyphae within the vascular lumen (**e**; HE, ×40 and **f**; HE, ×100)

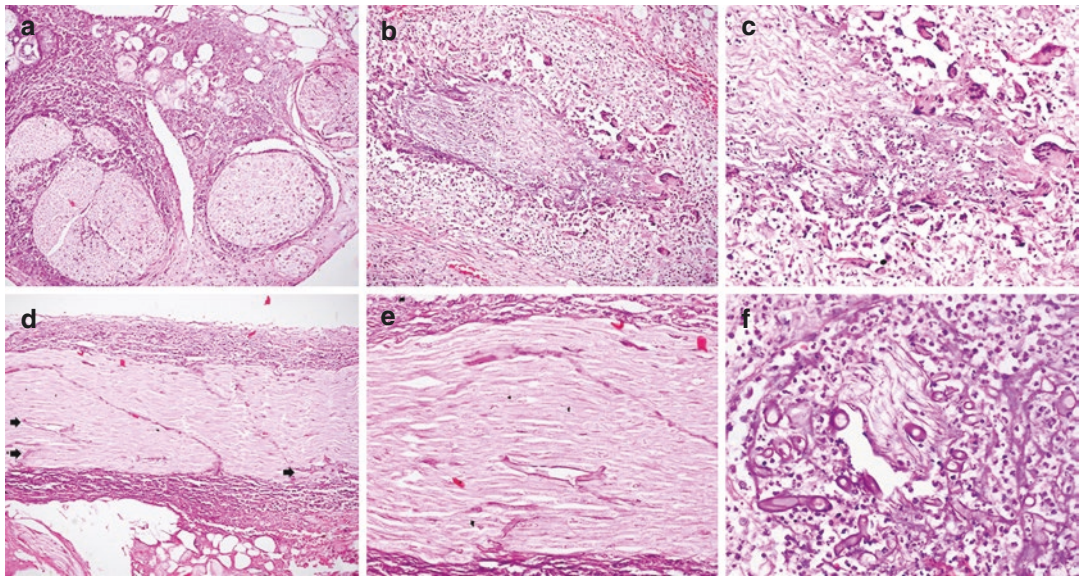

Fig. 6.7 Dense perineural acute inflammatory exudate (**a**; HE, ×100), perineural granuloma (**b**; HE, ×100) with giant cells (**c**; HE, ×200); fungal hyphae (arrows) coursing along the length of a nerve (**d**; HE, ×40 and **e**; HE, ×400); numerous fungal hyphae beneath the perineurium and in the substance of a nerve (**f**; HE, ×400)

around the red-stained axons. The perineural spread has been identified as a predictor of the advanced extent of invasion into soft tissues, including skeletal muscle and fibroadipose tissue, and extension into the central nervous system. Thus, the presence of perineural invasion in a limited specimen such as a biopsy or debridement may indicate extensively infiltrating disease, even when perineural spread is absent on magnetic resonance imaging (MRI) [12].

6.3.2.3 Extent of Inflammation

The primary site of fungal infection is often the nose and paranasal sinuses, from where the infection extends to the pterygopalatine fossa, pterygomaxillary fissure, masticator space, premaxillary soft tissues, and to the orbit and brain. Fungal balls are most commonly encountered in the maxillary sinus, followed by the sphenoid sinus.

Involvement of the orbit and its contents by mucormycosis most commonly is an endogenous infection, i.e., it occurs by spread from adjacent structures. Fungal exogenous endophthalmitis is extremely rare, usually occurring in the postoperative setting or following trauma. The infection frequently originates in the sinonasal compartment or the facial skin, causing destruction of bone and extending into the orbit (Fig. 6.8). Once the orbital soft tissue is involved, the necroinflammatory process can extend into the eyeball, with resultant scleritis (Fig. 6.9) and chorioretinitis (Fig. 6.10). Subretinal exudates and abscesses may be present (Fig. 6.10a). Endophthalmitis, i.e., inflammation of one or more coats of the eye and adjacent cavities, or panophthalmitis, i.e.,

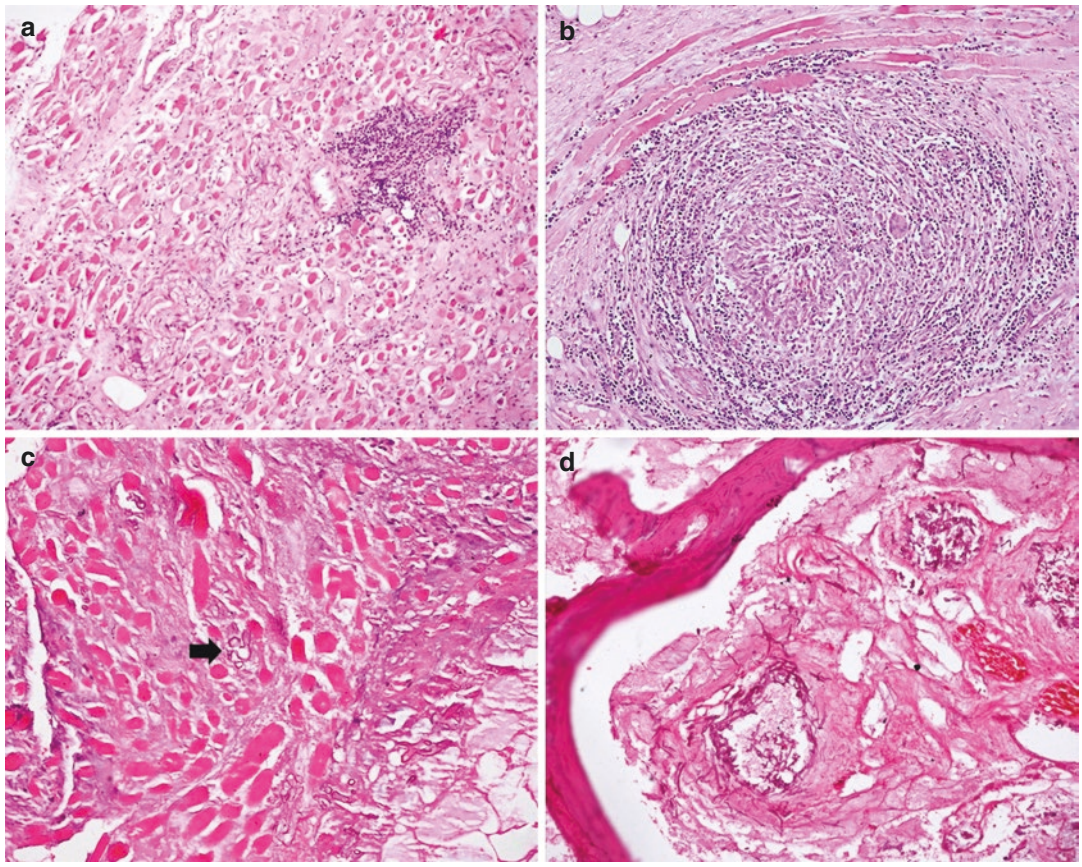

Fig. 6.8 Extraocular muscle showing chronic inflammatory cell infiltrate (**a**; HE, ×100), a granuloma (**b**; HE, ×100) and fungal hyphae (**c**; HE, ×200); bone invasion by fungal hyphae (**d**; HE, ×100)

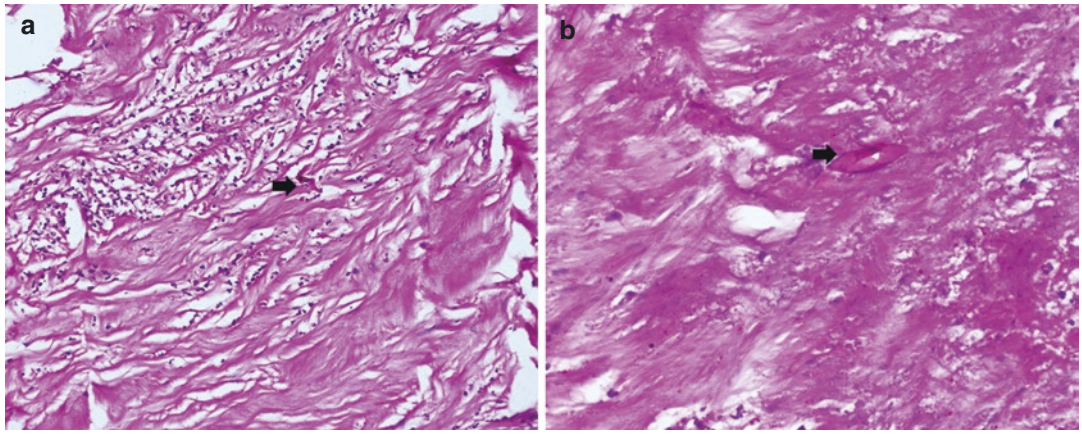

Fig. 6.9 Sclera showing neutrophilic infiltrate with fungal hyphae (**a**; PAS-D ×200 and **b**; PAS-D, ×400)

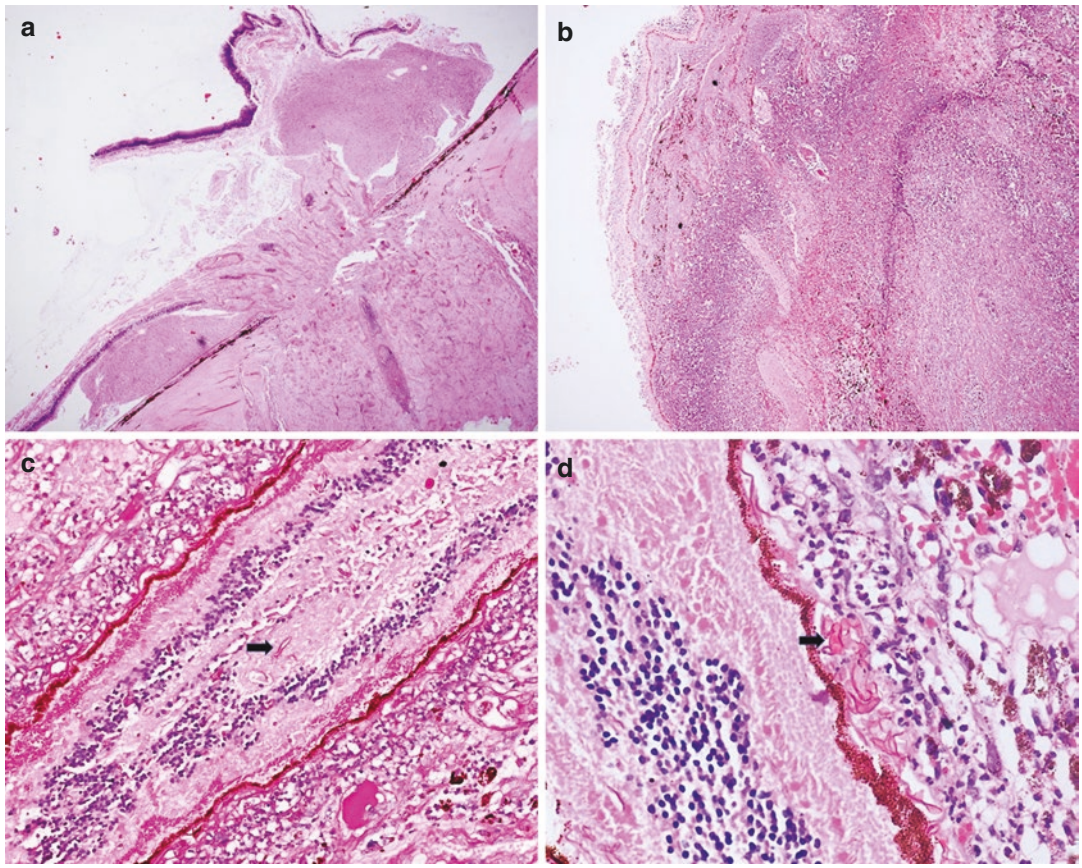

Fig. 6.10 Retina, lamina cribrosa, and optic nerve with subretinal abscesses (**a**; HE, ×20) and extensive chorioretinitis (**b**; HE, ×40). Few fungal hyphae are identified within the layers of the retina (**c**; HE, ×200) and choroid (**d**; HE, ×400)

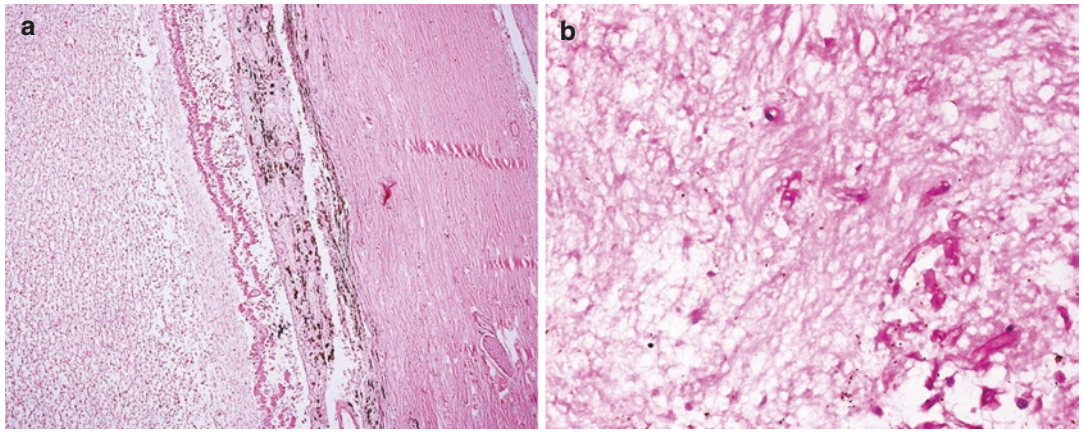

Fig. 6.11 Panophthalmitis with necrosis of all the coats of the eye (**a**; HE, ×40); fibrinous exudate in the vitreous contains occasional fungal hyphae (**b**; PAS-D, ×400)

inflammation of all three coats of the eye and adjacent cavities, may occur, with the variable presence of necrosis and neutrophilic infiltration (Fig. 6.11). Extension from the skin may lead to inflammation and ulceration of the eyelids; palpebral and bulbar conjunctiva may also show ulceration and necrosis (Fig. 6.12). Keratitis is extremely rare. The orbital inflammation can extend into the lacrimal gland resulting in dacryoadenitis and replacement fibrosis (Fig. 6.13). On H&E stained sections, fungal hyphae are difficult to identify within the ocular structures as the hyphae are sparse in number and are fragmented. The release of pigment from the necrotic uvea further hampers their identification. Histochemical staining is therefore essential to highlight the fungal profiles.

Inflammation of the optic nerve is almost always secondary to infection elsewhere due to the protective meningeal sheath around the nerve. The propensity of mucormycetes for extensive perineural invasion extends to the optic nerve as well. Neutrophilic infiltration can be seen within the nerve and the surrounding soft tissue. The presence of fungal hyphae within the optic nerve, especially at the resected end, is associated with a greater likelihood of intracranial extension. In addition to direct invasion, mucormycosis can cause infarction and necrosis of the optic nerve due to its vasoinvasive tendency [13] (Fig. 6.14).

6.3.3 Histochemical Stains

Grocott modification of Gomori methenamine silver (GMS) method and periodic acid-Schiff (PAS) with diastase are used to delineate the fungal walls (Fig. 6.15). Hyphae of Mucorales stain bright magenta with PAS. GMS stains the cell walls intensely, while the cytoplasm remains pale-staining. GMS and PAS, however, stain normal structures such as collagen in basement membranes, which may cause errors in diagnosis, particularly in the retina, where the narrow capillaries, whose basement membrane takes up the PAS or silver stains, may resemble fungal hyphae. Combined assessment of H&E features with histochemical staining results for the identification of endothelial cell nuclei and a thin rim of densely staining cytoplasm aid in distinguishing capillaries from the latter. Fontana-Masson is a histochemical stain used for the identification of melanin. As fungal walls are known to contain melanin, they may be highlighted with Fontana Masson stain on tissue sections [14, 15].

6.3.4 Differential Diagnosis

The differential diagnosis includes other fungal infections that demonstrate hyphae and spores, i.e., *Aspergillus*, and fungi characterized by pseu-

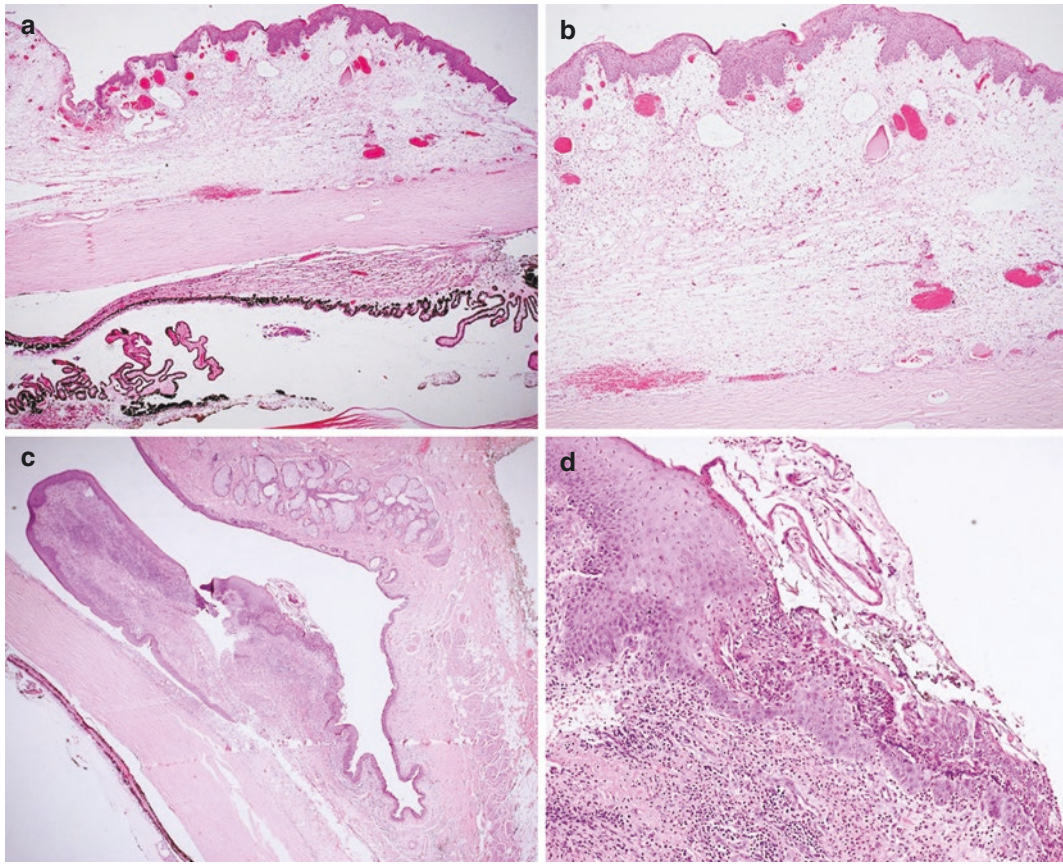

Fig. 6.12 Edema, vascular congestion, and mild chronic inflammation in the bulbar conjunctiva (**a**; HE, ×40 and **b**; HE, ×100); ulceration of the palpebral conjunctiva (**c**; HE, ×40 and **d**; HE, ×200)

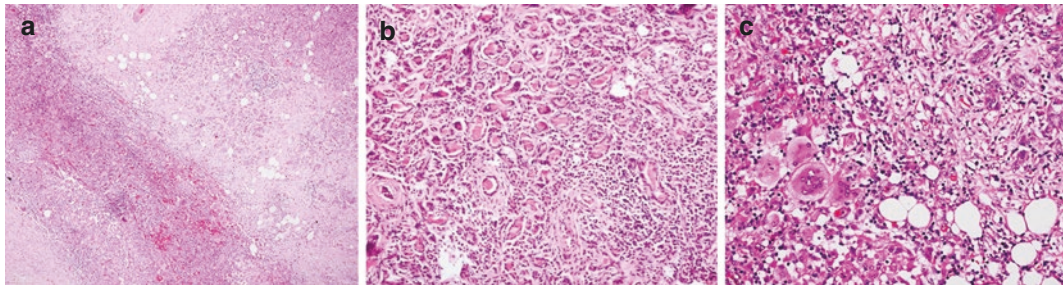

Fig. 6.13 Dacryoadenitis with fibrosis, (**a**; HE, ×20) dense chronic inflammation (**b**; HE, ×200) and foreign body giant cells (**c**; HE, ×400) around the acini

dohyphae and yeast forms, viz. *Candida*. Both *Aspergillus* and *Candida* can cause fungal keratitis and endophthalmitis in immunosuppressed patients.

Aspergillus spp. have narrow, 3–12 μm thick hyphae with prominent septae and acute-angled dichotomous branching, i.e., two equal branches forming from the division of one hyphal stem (Fig. 6.3b). However, tissue edema can result in the hyphae of *Aspergillus* appearing broader. Conidia, or fruiting bodies, of *Aspergillus*, when present, help in distinguishing invasive aspergil-

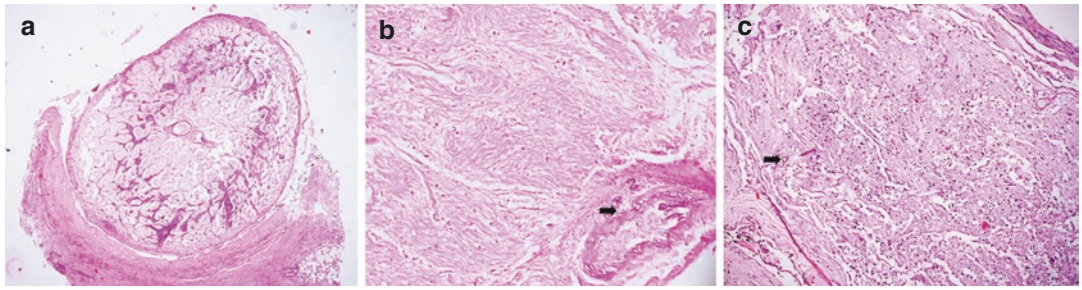

Fig. 6.14 Cross section of optic nerve with fibrin thrombi in the central retinal artery and vein (**a**; HE, ×20); necrotic optic nerve with angioinvasion (arrow) (**b**; HE, ×400); fungal hyphae (arrow) within the optic nerve (**c**; HE, ×200)

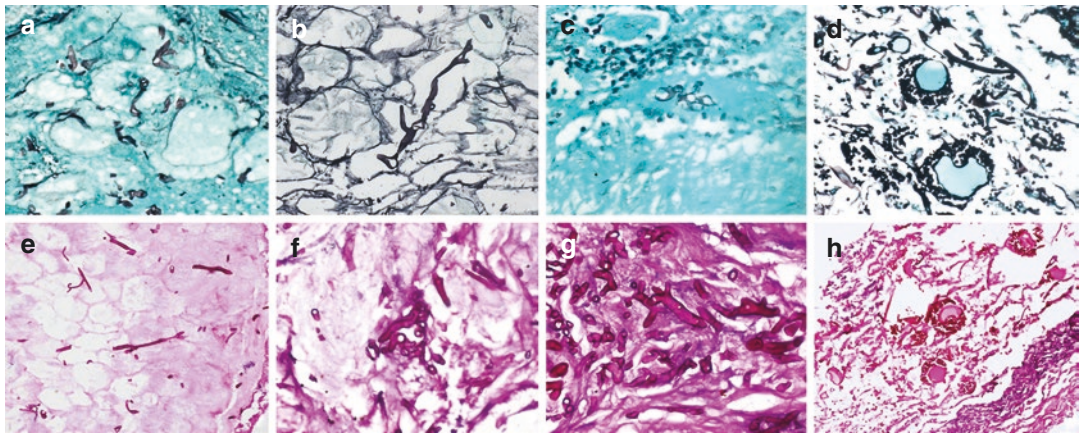

Fig. 6.15 GMS stain demonstrating Mucor with pale ribbon-like hyphae (**a**; GMS, ×200), intensely staining hyphae with nonparallel walls (**b**; GMS, ×400), and transversely sectioned broad hyphae (**c**; ×400); sporangia, sporangiophores, and sporangiospores stain black, while the columella remains unstained (**d**; GMS, ×400). PAS-D stains Mucor hyphae a bright magenta (**e**; ×100); only cell walls are highlighted, imparting a hollow appearance (**f**; PAS-D, ×400). PAS-D accentuates branching at variable angles (**g**; PAS-D, ×400) and highlights sporangia and sporangiospores (**h**; PAS-D, ×400)

losis from mucormycosis, particularly when fungal hyphae are fragmented, degenerated, or densely aggregated into a fungal ball. Each conidium is formed of a central vesicle with one or two layers of radiating phialides, to which chains of spores may be attached but are rarely seen (Fig. 6.2e, f). In culture, *A. fumigatus* shows a single row of phialides covering the upper one-third of the vesicle, while *A. niger* and *A. flavus* bear two rows of phialides around the vesicle [16]. However, this morphology is often disrupted in tissue sections. The host tissue response in invasive aspergillosis is predominated by granulomatous inflammation, with prominent fibrosis; variable necrosis and vasculitis may be present. Sinonasal debridement specimens may demonstrate allergic mucin with Curshmann spirals and Charcot-Leyden crystals.

Candidiasis is typified by the presence of narrow pseudohyphae (2–5 μm in diameter) and ovoid yeast forms that show budding. The pattern of inflammation is non-granulomatous more often than granulomatous inflammation. Pseudohyphae show constrictions at the sites of budding, where each elongated ovoid yeast form is attached to another (Fig. 6.2g, h). Candida stains intensely with PAS, while GMS staining is variable.

Sporangiospores of mucormycetes may be misinterpreted as yeast forms of Cryptococcus, espe-

cially in the absence of elongated, branching hyphae. Both mucor sporangiospores and cryptococci demonstrate a Maltese cross appearance on polarized microscopy (Fig. 6.2d). However, the latter demonstrates a mucoid capsule easily demonstrable by staining with Mucicarmine and narrow-based budding. On Alcian blue staining, the peripheral mucoid capsule stains blue while the central organism stains magenta pink. GMS, likewise, stains the yeast, but the capsule remains unstained.

When considering the differential diagnosis of invasive fungal infection by hyphal and pseudohyphal forms, a pathologist must always remain open to the possibility of the simultaneous presence of two different fungi. Coinfections of mucormycosis with *Aspergillus* and *Candida* are well documented in the literature (Fig. 6.3). In the setting of a coinfection, one fungus often outgrows the other in culture. Thus, a discrepancy between KOH mount/ microbiological culture and histological appearance may be a soft pointer toward a coinfection [17].

6.4 Intraoperative Examination

Pathologists may be called upon for intraoperative examination, i.e., frozen section examination for primary diagnosis to facilitate immediate surgical debridement and assess resection margins for fungal hyphae. A recent meta-analysis has shown that frozen section examination has high sensitivity (83%), specificity (98%), and a positive predictive value of 98% [18]. However, the sensitivity for detecting Mucorales (74%) is slightly lower than that for *Aspergillus* (81%) [18].

6.5 Ancillary Diagnostic Techniques

The low sensitivity of fungal culture methods, overlapping histomorphological features of fungi of different orders, and the frequent presence of only degenerated or swollen, fragmented fungal hyphae may hinder accurate diagnosis on histopathology specimens. Ancillary diagnostic techniques may be of value in such situations.

6.5.1 Immunohistochemistry

Immunohistochemistry (IHC) is a technique in which target protein antigens are detected in formalin-fixed paraffin-embedded tissues by utilizing an antibody that specifically binds to the target, followed by signal amplification and detection step. Studies have shown that IHC using anti-Rhizopus and anti-Aspergillus monoclonal primary antibodies has high sensitivity and specificity for differentiating between aspergillosis and mucormycosis [17, 19] and has received the support of the European Confederation of Medical Mycology in cooperation with the Mycoses Study Group Education and Research Consortium [20].

6.5.2 Molecular Diagnostic Techniques

Molecular diagnostic techniques have two benefits: they aid in detecting mucormycetes in tissue specimens for confirmation of diagnosis when histopathology is not conclusive, and they can also accurately identify the species of fungus [5]. They can be applied to fresh as well as formalin-fixed tissues; however, the former may be preferred as formalin fixation leads to DNA fragmentation to a certain extent [20]. Internal transcribed spacer (ITS) sequencing is the most useful molecular method for speciation of Mucorales. Several polymerase chain reaction (PCR) based techniques may be performed on fresh or frozen tissue samples. Matrix-assisted laser desorption ionization time-of-flight mass spectrometry (MALDI-TOF MS) is also a reliable technique, albeit not widely available. More recently, qPCR kits have become commercially available; however, they require validation in clinical settings [5].

6.5.3 Electron Microscopy

Scanning electron microscopy of fungal cultures can help differentiate between the various species of Rhizopus, based on the variations in the shape of sporangiospores, whether sub-globose to ellipsoidal, and on the pattern of ridges on their surface [21]. However, the utility of routine clinical diagnostics is limited.

6.6 Conclusion

Mucormycosis is a destructive infectious disease characterized by extensive tissue necrosis, angioinvasion, and perineural spread. Orbital mucormycosis is usually an endogenous inflammatory process secondary to local extension from the sinonasal region. Patterns of inflammation encountered vary from suppurative to granulomatous, based on the stage of the disease. Diagnosis of mucormycosis on histopathological examination is of paramount importance, as fungal culture studies are frequently negative. Aspergillosis, candidiasis, and rarely, cryptococcosis may resemble mucormycosis, causing difficulties in diagnosis. However, the eye of an experienced pathologist can discern subtle differences in fungal morphology, distinguishing the fungal profiles of mucromycetes from other fungi, enabling considerable accuracy in diagnosis.

References

1. Sen M, Honavar SG, Sharma N, Sachdev MS. COVID-19 and eye: a review of ophthalmic manifestations of COVID-19. Indian J Ophthalmol. 2021;69:488–509.
2. Jurado LF, López-Panqueva RP. Histopathology. In: Turgut M, Challa S, Akhaddar A, editors. Fungal infections of the central nervous system. Cham: Springer; 2019.
3. Shankar SK, Mahadevan A, Sundaram C, Sarkar C, Chacko G, Lanjewar DN, Santosh V, Yasha TC, Radhakrishnan VV. Pathobiology of fungal infections of the central nervous system with special reference to the Indian scenario. Neurol India. 2007;55:198–215.
4. Gomes MZ, Lewis RE, Kontoyiannis DP. Mucormycosis caused by unusual mucormycetes, non-Rhizopus, -Mucor, and -Lichtheimia species. Clin Microbiol Rev. 2011;24:411–45.
5. Skiada A, Lass-Floerl C, Klimko N, Ibrahim A, Roilides E, Petrikkos G. Challenges in the diagnosis and treatment of mucormycosis. Med Mycol. 2018;56(suppl_1):93–101.
6. Wang M, Wey S, Zhang Y, Ye R, Lee AS. Role of the unfolded protein response regulator GRP78/BiP in development, cancer, and neurological disorders. Antioxid Redox Signal. 2009;11:2307–16.
7. Morales-Franco B, Nava-Villalba M, Medina-Guerrero EO, Sánchez-Nuño YA, Davila-Villa P, Anaya-Ambriz EJ, Charles-Niño CL. Host-pathogen molecular factors contribute to the pathogenesis of Rhizopus spp. in diabetes mellitus. Curr Trop Med Rep. 2021;22:1–12.
8. Sundaram C, Mahadevan A, Laxmi V, Yasha TC, Santosh V, Murthy JM, Purohit AK, Mohandas S, Shankar SK. Cerebral zygomycosis. Mycoses. 2005;48:396–407.
9. Wenig BM. Nasal cavity and paranasal sinus. In: Wenig BM, Childers ELB, Richardson MS, Seethala RR, Thompson LDR, editors. AFIP Atlas of nontumor pathology non-neoplastic diseases of head and neck first series, fascicle. Washington: American Registry of Pathology (ARP Press); 2017. p. 1–91.
10. Branscomb R. An overview of mucormycosis. Lab medicine. 2002;33:453–5.
11. Requena L, Sitthinamsuwan P, Santonja C, Fernández-Figueras MT, Rodríguez-Peralto JL, Argenyi Z, Torrelo A, Cerroni L, Kutzner H. Cutaneous and mucosal mucormycosis mimicking pancreatic panniculitis and gouty panniculitis. J Am Acad Dermatol. 2012;66:975–84.
12. Sravani T, Uppin SG, Uppin MS, Sundaram C. Rhinocerebral mucormycosis: pathology revisited with emphasis on perineural spread. Neurol India. 2014;62:383–6.
13. Heegaard S, Grossniklaus H. Eye pathology: an illustrated guide. Berlin: Springer; 2015.
14. Kimura M, McGinnis MR. Fontana-Masson – stained tissue from culture-proven mycoses. Arch Pathol Lab Med. 1998;122:1107–11.
15. Sundaram C, Shantveer GU, Umabala P, Lakshmi V. Diagnostic utility of melanin production by fungi: study on tissue sections and culture smears with Masson-Fontana stain. Indian J Pathol Microbiol. 2014;57:217–22.
16. Anila KR, Somanathan T, Mathews A, Jayasree K. Fruiting bodies of aspergillus: an unusual finding in histopathology. Lung India. 2013;30:357–9.
17. Son HJ, Song JS, Choi S, Jung J, Kim MJ, Chong YP, Lee SO, Choi SH, Kim YS, Woo JH, Kim SH. A comparison of histomorphologic diagnosis with culture- and immunohistochemistry-based diagnosis of

invasive aspergillosis and mucormycosis. Infect Dis (Lond). 2020;52:279–83.
18. Kim DH, Kim SW, Hwang SH. Usefulness of intraoperative frozen section for diagnosing acute invasive fungal rhinosinusitis: a systematic review and meta-analysis. Int Forum Allergy Rhinol. 2021;26. Epub ahead of print
19. Verweij PE, Smedts F, Poot T, Bult P, Hoogkamp-Korstanje JA, Meis JF. Immunoperoxidase staining for identification of Aspergillus species in routinely processed tissue sections. J Clin Pathol. 1996;49:798–801.
20. Cornely OA, Alastruey-Izquierdo A, Arenz D, Chen SCA, Dannaoui E, Hochhegger B, Hoenigl M, Jensen HE, Lagrou K, Lewis RE, Mellinghoff SC, Mer M, Pana ZD, Seidel D, Sheppard DC, Wahba R, Akova M, Alanio A, Al-Hatmi AMS, Arikan-Akdagli S, Badali H, Ben-Ami R, Bonifaz A, Bretagne S, Castagnola E, Chayakulkeeree M, Colombo AL, Corzo-León DE, Drgona L, Groll AH, Guinea J, Heussel CP, Ibrahim AS, Kanj SS, Klimko N, Lackner M, Lamoth F, Lanternier F, Lass-Floerl C, Lee DG, Lehrnbecher T, Lmimouni BE, Mares M, Maschmeyer G, Meis JF, Meletiadis J, Morrissey CO, Nucci M, Oladele R, Pagano L, Pasqualotto A, Patel A, Racil Z, Richardson M, Roilides E, Ruhnke M, Seyedmousavi S, Sidharthan N, Singh N, Sinko J, Skiada A, Slavin M, Soman R, Spellberg B, Steinbach W, Tan BH, Ullmann AJ, Vehreschild JJ, Vehreschild MJGT, Walsh TJ, White PL, Wiederhold NP, Zaoutis T, Chakrabarti A, Mucormycosis ECMM MSG Global Guideline Writing Group. Global guideline for the diagnosis and management of mucormycosis: an initiative of the European Confederation of Medical Mycology in cooperation with the Mycoses Study Group Education and Research Consortium. Lancet Infect Dis. 2019;19:e405–21.
21. Nagao K, Ota T, Tanikawa A, Takae Y, Mori T, Udagawa S, Nishikawa T. Genetic identification and detection of human pathogenic Rhizopus species, a major mucormycosis agent, by multiplex PCR based on internal transcribed spacer region of rRNA gene. J Dermatol Sci. 2005;39:23–31.

7 Surgical Management of Rhino-Orbito-Cerebral Mucormycosis: Basic Endoscopic Sinus Surgery Procedures

Nishi Gupta, Poonam Singla, Nidhi Dhawan, and Sonil Jain

Surgical debridement is the mainstay of treatment for rhino-orbito-cerebral mucormycosis (ROCM). Rigorous medical therapy with liposomal amphotericin B and reversing the ketoacidosis and immunosuppressive state aid in achieving best possible results [1].

The surgical management of ROCM is complex due to the aggressiveness of the disease, multiple routes of spread, unanticipated locations that have been found to be involved and the requirement for new expertise to do extensive debridement.

Otorhinolaryngologists, ophthalmologists, neurosurgeons and faciomaxillary surgeons, as well as the diagnostic and medical management teams will benefit from this book. As a result, the surgical management of ROCM is divided into four chapters, including basic endoscopic sinus surgery procedures, approach to pterygopalatine fossa (PPF), and infratemporal fossa (ITF) pterygoid process, advanced drilling beyond sinuses, and globe sparing orbital exenteration.

Detailed steps of functional endoscopic sinus surgery are beyond the preview of this book. This chapter provides a pictorial representation of basic steps. This brief summary will assist non-rhinologists in performing these steps and progressing to the advanced endoscopic procedures. Since most of the landmarks are destroyed in advanced cases of rhino-orbito-cerebral mucormycosis (ROCM), all the basic steps may not be needed in strict sequence. However, it is essential to open up all the sinuses widely where ever needed, before proceeding to advanced debridement beyond sinuses.

The endoscopic anatomy of the nose must be understood before planning a ROCM debridement.

It is possible to understand it in three steps or passes as described earlier [2].

First Pass The standard 4 mm 0^0 endoscope and image 1S camera (Karl Storz, Tuttlingen Germany) were used. The inferior turbinate, septum, nasopharynx, taurus tubarius, inferior meatus and nasolacrimal duct entrance are all examined during the first pass (Figs. 7.1, 7.2, 7.3, and 7.4).

Second Pass The endoscope is negotiated between the septum and the middle turbinate in the second pass to inspect the sphenoethmoid recess. A distinct opening of the sphenoid sinus can be noticed on occasion. The superior turbinate and sphenoid ostium can be seen (Figs. 7.5 and 7.6).

Third Pass The middle meatus is visualized in the third pass, along with its contents which include the uncinate process, bulla ethmoidal, hiatus semilunaris, and infundibular area (Fig. 7.7).

N. Gupta (✉) · P. Singla · N. Dhawan · S. Jain
Dr Shroff's Charity Eye Hospital, New Delhi, India

N. Gupta, S. G. Honavar (eds.), *Rhino-Orbito-Cerebral Mucormycosis*,
https://doi.org/10.1007/978-981-16-9729-6_7

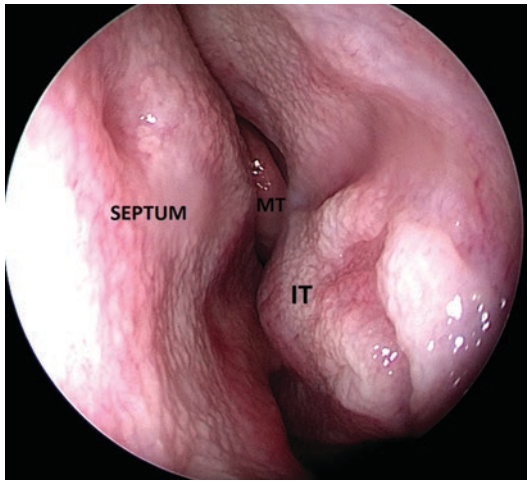

Fig. 7.1 Endoscopic view of the First pass showing inferior turbinate (IT) and septum. MT; Middle turbinate

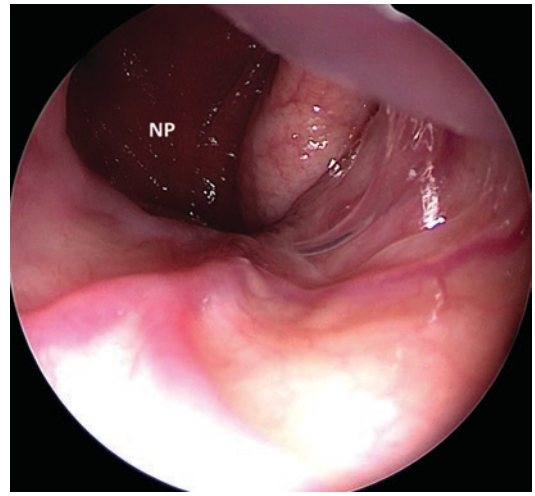

Fig. 7.3 View of nasopharynx (NP) showing taurus tubarius

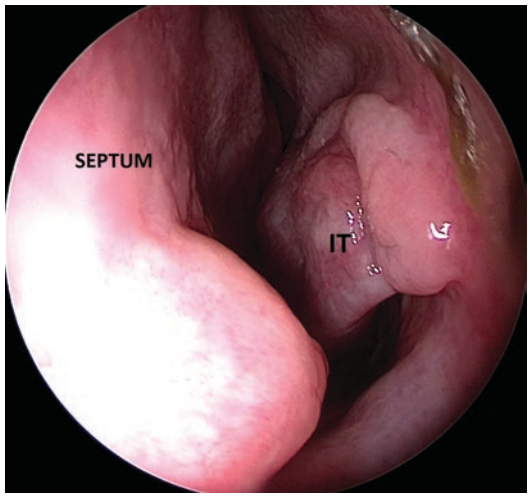

Fig. 7.2 Endoscope is negotiated along the floor of the nose. IT; Inferior turbinate

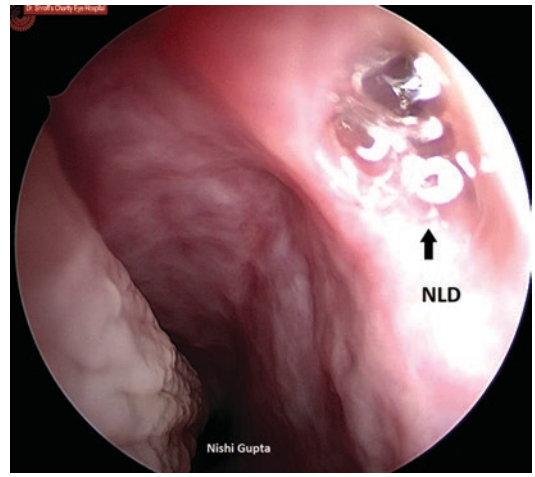

Fig. 7.4 Inferior meatus showing distal nasolacrimal duct opening. Source: Author's own figure (Endoscopic Dacryocystorhinostomy, with permission from Springer)

The several passes described above aid in a preliminary assessment of all the nasal cavity structures. However as discussed below, relevant structures, must be investigated in greater depth.

1. **Agger nasi**

Agger nasi is an ethmoidal air cell and it lies anterior and superior to the junction of the anterior end of the middle turbinate with the lateral wall (Fig. 7.8).

Agger nasi is related anteriorly to the frontal process of maxilla, posteriorly to the ethmoid infundibulum, superiorly to the frontal recess, inferiorly and medially to the uncinate process [1].

2. **Uncinate process**

The uncinate process is a thin bony structure, shaped like a sickle and lies on the lateral wall of the nose. It has two borders, a convex border attached to the lateral nasal wall and a free

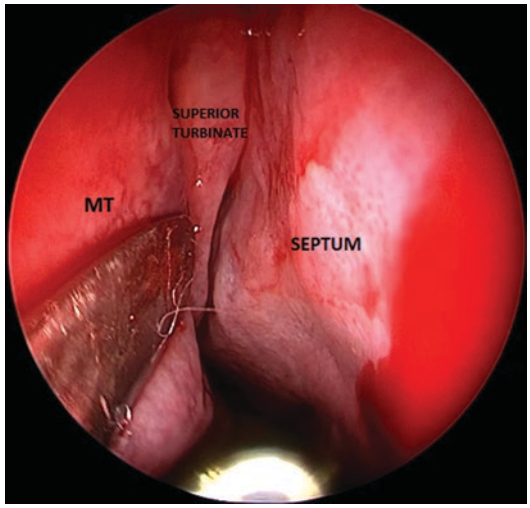

Fig. 7.5 Second pass showing superior turbinate. MT; Middle turbinate

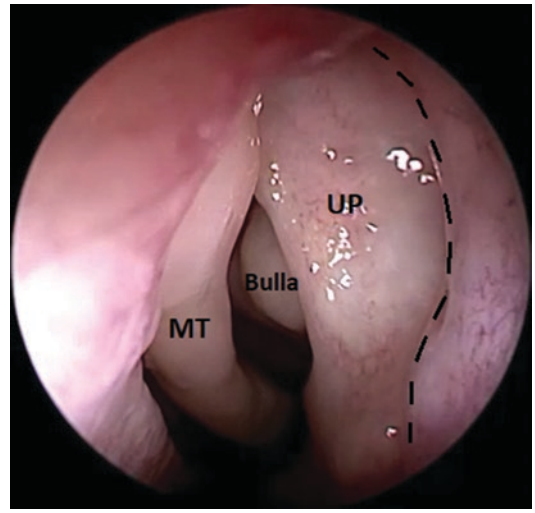

Fig. 7.7 The third pass demonstrating the important structures, including uncinate process (UP), bulla and premaxillary line (black dotted line)

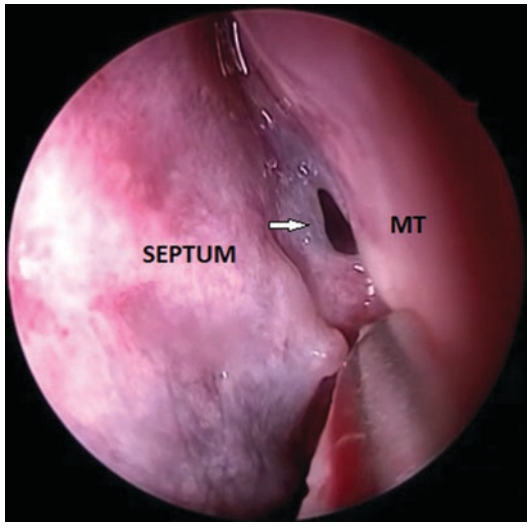

Fig. 7.6 Natural opening of the sphenoid sinus is seen during the second pass

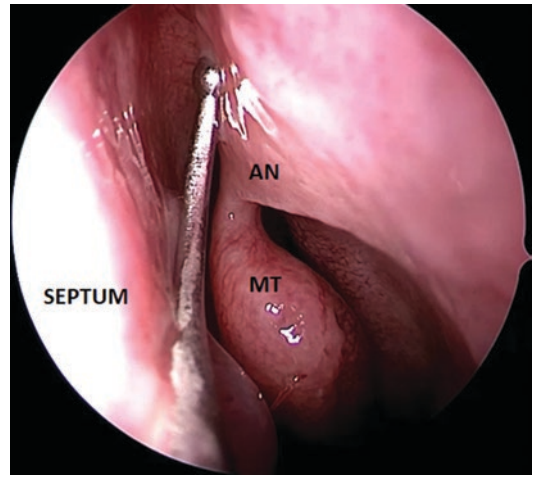

Fig. 7.8 Agger nasi (AN), and middle turbinate in view (MT)

border that is concave (Fig. 7.7). The lower and posterior part of uncinate process curves posteriorly to get attached to the perpendicular plate of ethmoid.

Superiorly the uncinate process may get attached to the lateral nasal wall, lamina papyracea or the middle turbinate and determines the drainage path of the frontal sinus.

Bulla ethmoidalis

Bulla is the anterior ethmoid air cells and lies posterior to the uncinate process [3–6] (Fig. 7.7). Bulla is bounded laterally by lamina papyracea, superiorly to the suprasellar recess that separates bulla from the fovea ethmoidal, posteriorly to the retrobulbar recess that separates it from the basal lamella of the

middle turbinate and medially to the hiatus semilunaris superioris [7, 8].

The dissection should be performed by keeping the instrument tip medial during an ethmoidectomy to prevent injury to the lamina papyracea and orbit via a breach in the lamina papyracea.

3. **Hiatus semilunaris**

Hiatus semilunaris is divided into hiatus semilunaris superioris and hiatus semilunaris inferioris [1]. Hiatus semilunaris superioris (HSLS) is a cleft between ethmoid bulla and middle turbinate, and it leads superiorly into the frontal recess (Fig. 7.9). Hiatus semilunaris inferioris (HSLI) lies between the bulla and the free concave margin of the uncinate process. It is a two-dimensional structure and leads into an infundibulum lateral to the bulla.

4. **Middle turbinate**

The middle turbinate is the most reliable and constant landmark for endoscopic sinus surgery [3]. It has three parts; the first part lies in the sagittal plane and is attached to the skull base. The second part lies in the coronal plane and is attached to the lamina papyracea; the middle turbinate is called basal lamella. The third part of the middle turbinate lies in an axial plane and is attached to the perpendicular plate of palatine bone [1] (Fig. 7.10).

A pneumatized middle turbinate is called concha bullosa and needs to be addressed during endoscopic sinus surgery.

5. **Paranasal sinuses**

Paranasal sinuses are grouped into the anterior and posterior groups. The anterior group comprises the frontal sinus, maxillary sinus, and anterior ethmoid sinuses. The posterior group of sinuses include posterior ethmoids and the sphenoid sinuses [3].

6. **Meatuses**

The middle meatus lies deep to the middle turbinate, and the inferior meatus is the space between the inferior turbinate and lateral wall of nose. The nasolacrimal duct opens into this inferior meatus.

7.1 Steps of Surgery

7.1.1 Uncinectomy and Maxillary Sinus Clearance

The first step during endoscopic sinus surgery is the removal of the uncinate process. The uncinate

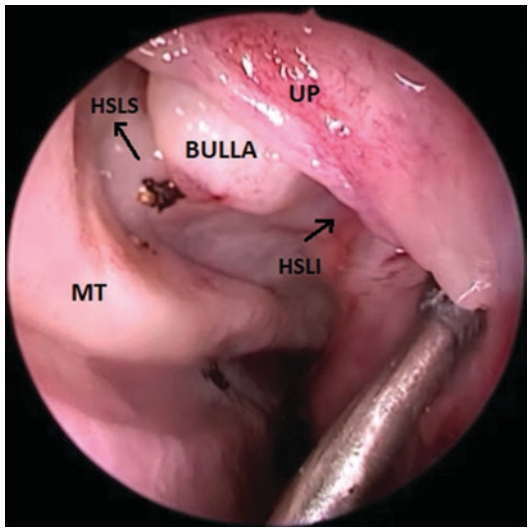

Fig. 7.9 Hiatus semilunaris superioris (HSLS) and hiatus semilunaris inferioris (HSLI), UP; Uncinate process, MT; Middle turbinate

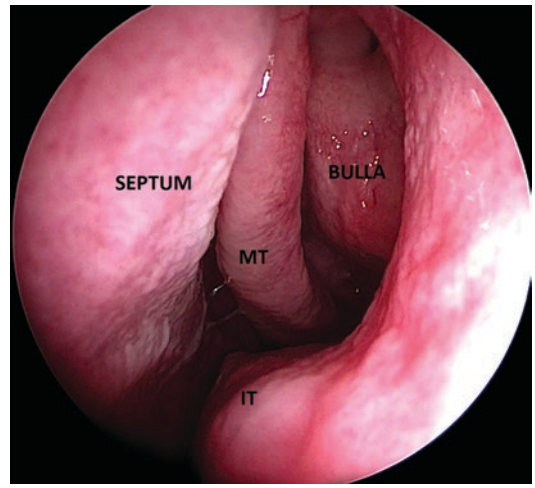

Fig. 7.10 Middle turbinate (MT) showing its first and third part

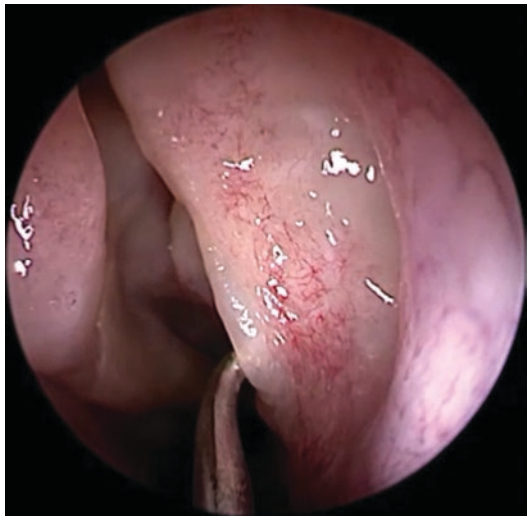

Fig. 7.11 A ball pointer is used to evert the free edge of uncinate process away from the lateral wall. This aids in moving the uncinate away from the lateral wall and protect the orbit during uncinectomy

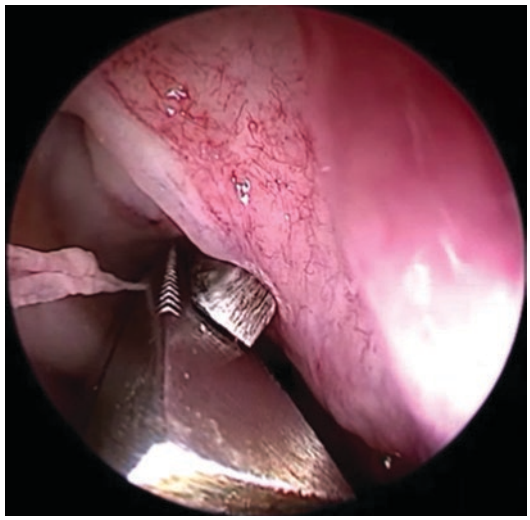

Fig. 7.12 Backbiting forceps is used to resect lower end of the uncinate process

process is gently everted using a ball pointer (Fig. 7.11). A backbiting forceps is passed into the hiatus semiluaris to engage it under the free edge if uncinate process (Fig. 7.12). It is then stabilized, and jaws are closed to punch out the inferior part of the uncinate process. Uncinectomy at the level is performed by keeping the backbiting forceps in

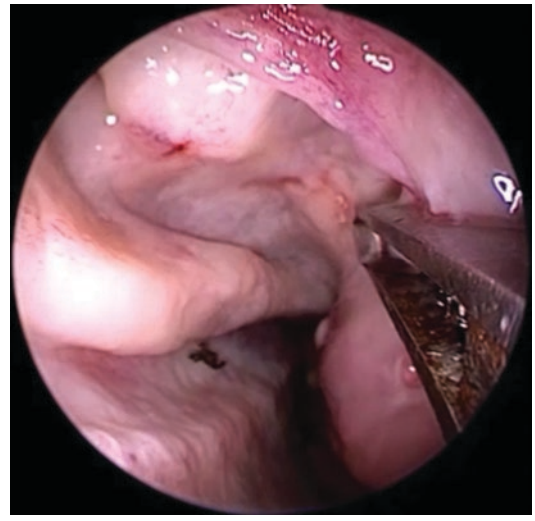

Fig. 7.13 Backbiting forceps is directed inferiorly and posteriorly to avoid injury to the nasolacrimal duct

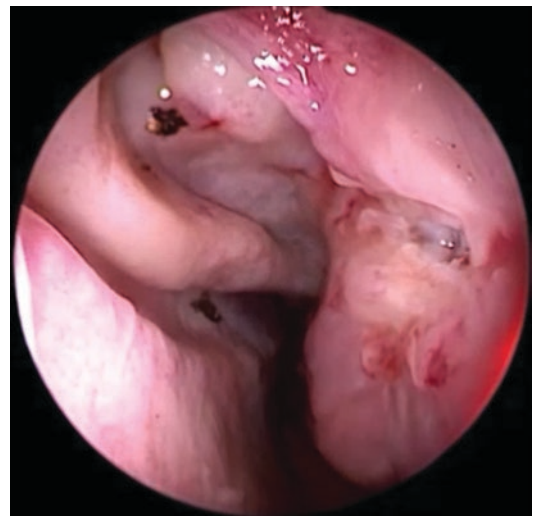

Fig. 7.14 Maxillary sinus ostium can be seen

the posteroinferior direction to avoid injury to the lacrimal drainage system [9] (Fig. 7.13).

It takes two- to three bites for the maxillary sinus ostium to become apparent (Fig. 7.14). The maxillary sinus is then entered with a curved suction. The remaining horizontal part of the uncinate process is then fractured medially using the curved suction (Fig. 7.15). Once mobilized, this part is removed using forceps or microdebrider.

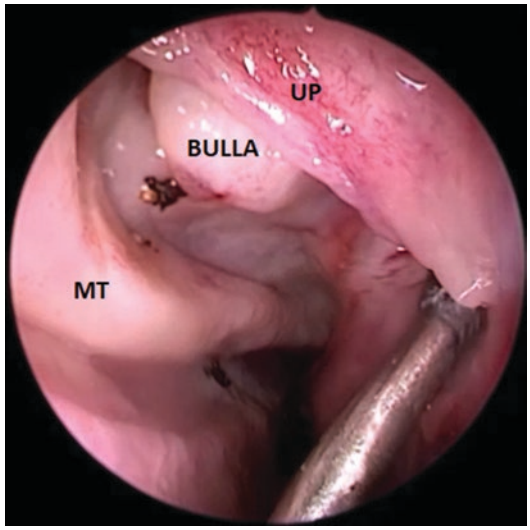

Fig. 7.15 Maxillary sinus ostium is widened

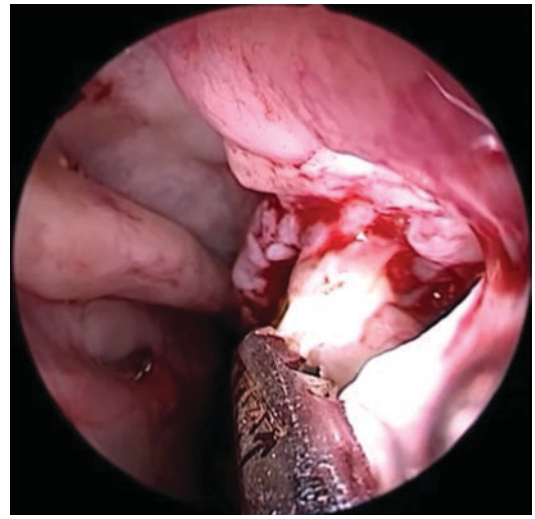

Fig. 7.17 Inflamed tissue filling the maxillary antrum is removed with a microdebrider

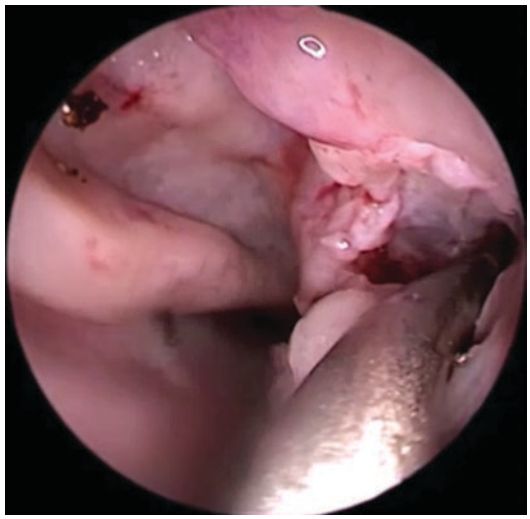

Fig. 7.16 A curved suction tip is placed into the maxillary sinus ostium, and the horizontal portion of the uncinate process is fractured inferiorly and medially

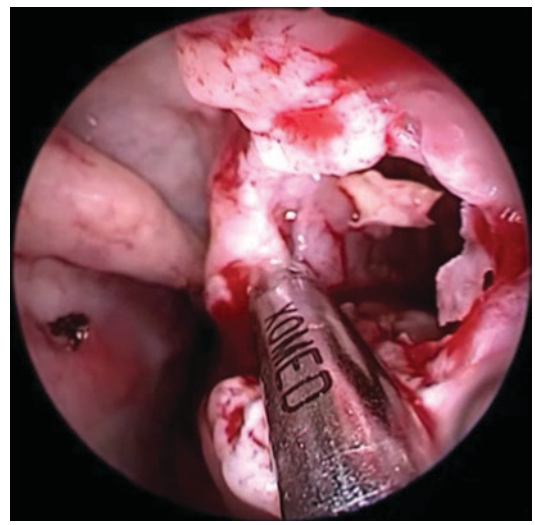

Fig. 7.18 Maxillary antrostomy is further widened by debriding the inflammed tissue

Any opening of antrum visible without doing an uncinectomy is the accessory ostium. The natural ostium of the maxillary sinus cannot be visualized unless the uncinate process is removed as the uncinate process acts as a lid covering the maxillary sinus ostium. If an accessory ostium is present, it is joined with the natural ostium of the maxillary antrum.

The maxillary sinus ostium is widened, and the antrum's inflammatory tissue is cleared using a microdebrider (Figs. 7.16, 7.17, and 7.18). A wide antrostomy is created, and a widely opened sinus can be visualized (Fig. 7.19).

The next step involves completing the uncinectomy. There are multiple ways an uncinate process can be removed. A blunt dissector, a sickle knife with its tip pointing medially, a microdebrider or an upturned through cut forceps can all be used. The goal is to remove the thin bone and mucosa carefully while avoiding any breach in the lamina papyracea.

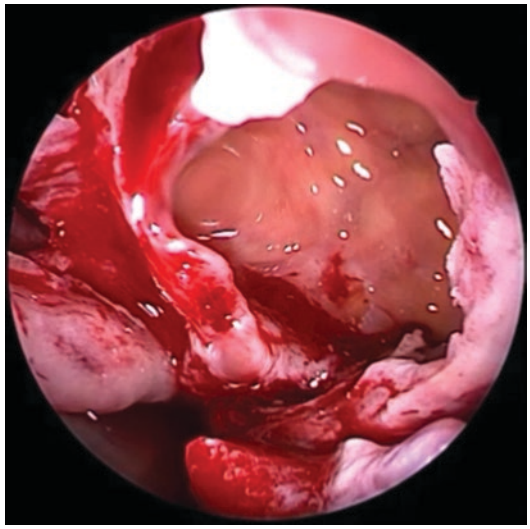

Fig. 7.19 A maxillary sinus is visible through a wide ostium

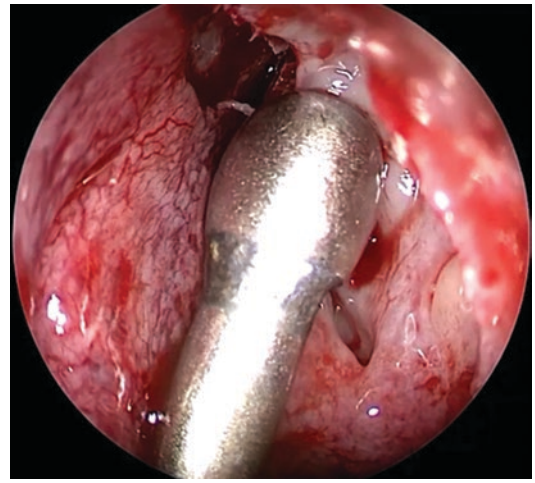

Fig. 7.21 Agger nasi is an important landmark for the frontal process; the area is palpated with a blunt suction tip and cleared

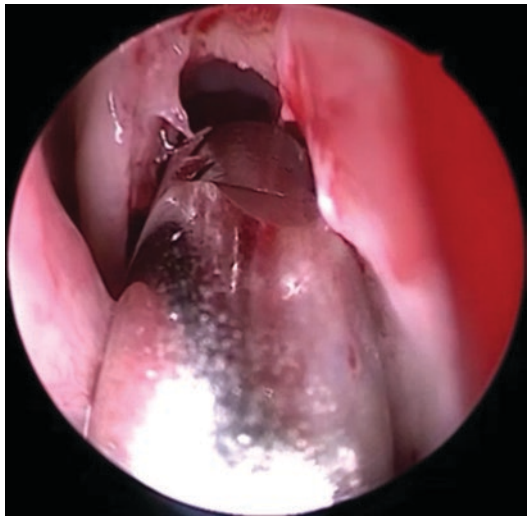

Fig. 7.20 Residual uncinate in the superior part is debrided to reach the frontal sinus

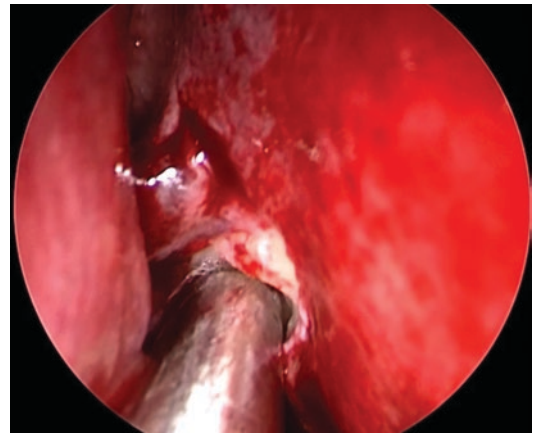

Fig. 7.22 A 70-degree endoscope is used, and a curved suction is placed into the frontal sinus

7.1.2 Frontal Sinus

Superior remnant of the uncinate process is removed to approach the frontal sinus (Fig. 7.20). Agger nasi is a vital landmark to reach the frontal beak. The medial wall of the agger nasi is marked by the uncinate process and the frontal process of the maxilla (Fig. 7.21). Frontal beak is identified, a 70-degree endoscope and a curved suction are used to clear inflammatory tissue and mucopurulent discharge from the frontal sinuses (Figs. 7.22, 7.23, 7.24, and 7.25). A clear view of the huge frontal sinus is obtained (Figs. 7.26 and 7.27).

7.1.3 Ethmoidectomy

By passing a ball pointer posterior to Bulla, it is fractured anteriorly (Fig. 7.28). The thin bony walls can be easily removed revealing the intra cell septa (Figs. 7.29, 7.30, and 7.31). Medial and lateral bony attachments of the

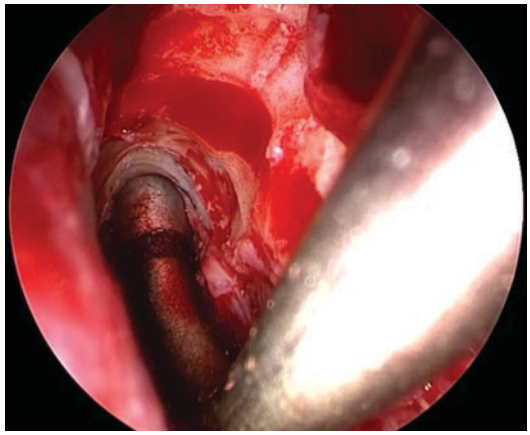

Fig. 7.23 The frontal beak has been drilled and a curved suction is passed into the sinus

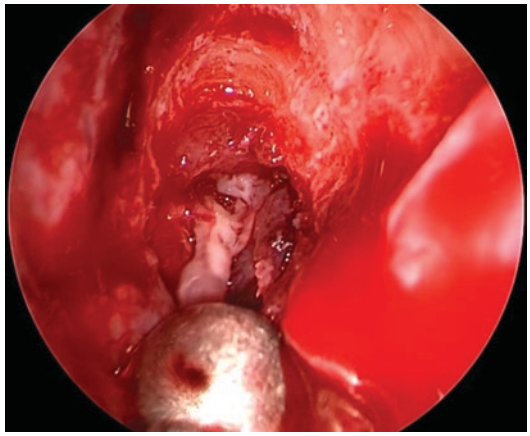

Fig. 7.24 Mucopurulent discharge with inflamed tissue can be seen prolapsing out of the frontal sinus

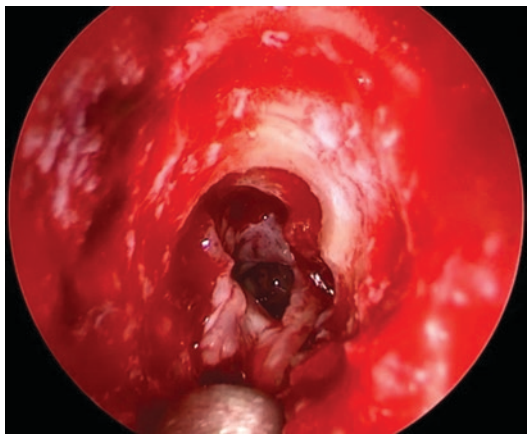

Fig. 7.25 Frontal sinus ostium starts coming in view

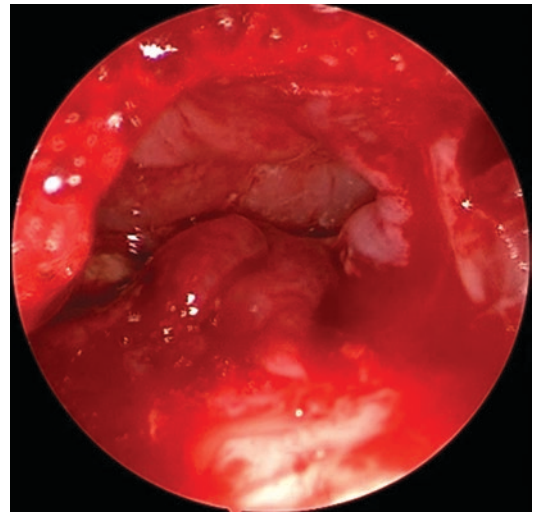

Fig. 7.26 A good view of frontal sinus is obtained

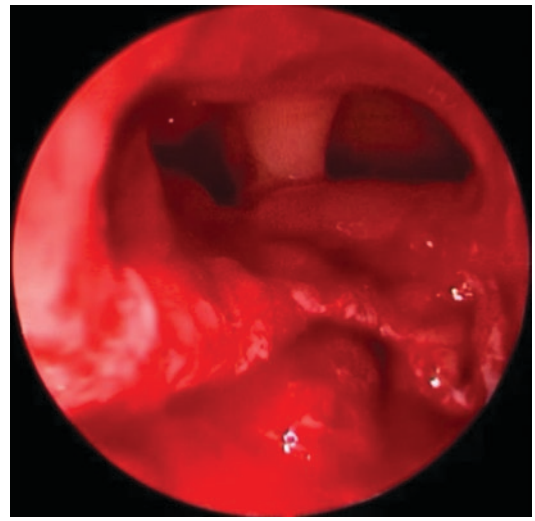

Fig. 7.27 A wide and clear frontal sinus is seen

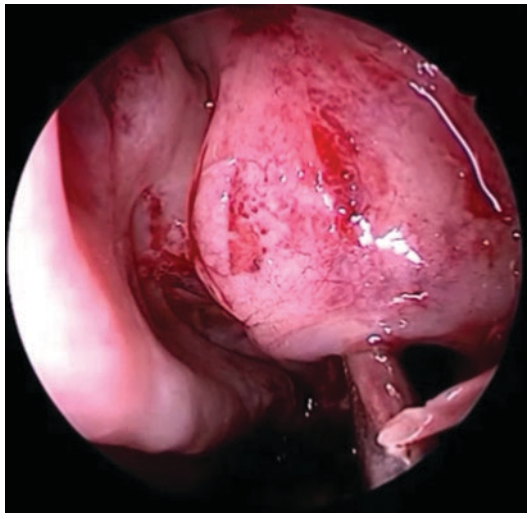

Fig. 7.28 Ethmoids are cleared next, and a ball pointer is passed posterior to the bulla

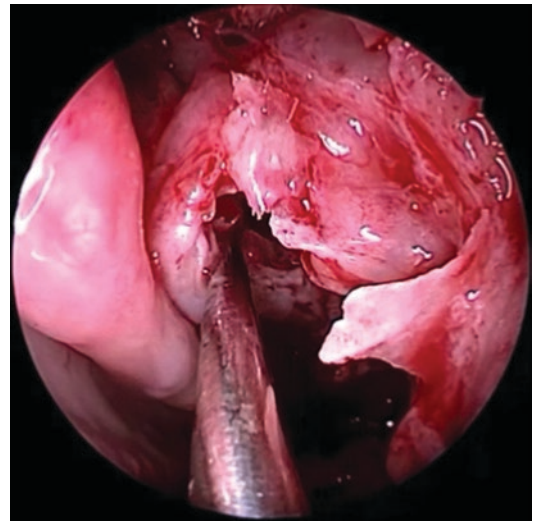

Fig. 7.30 Bony walls of the bulla are removed

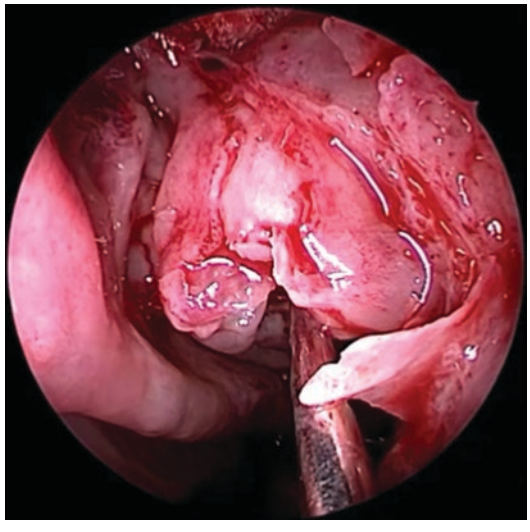

Fig. 7.29 The bulla is fractured to enter into the anterior ethmoid cells

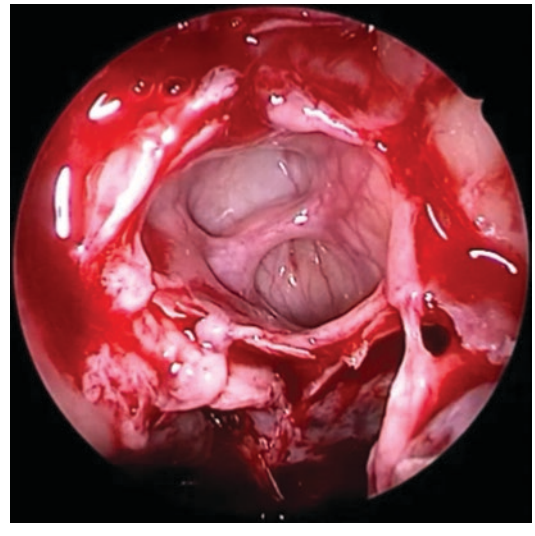

Fig. 7.31 The intracell partitions are visible

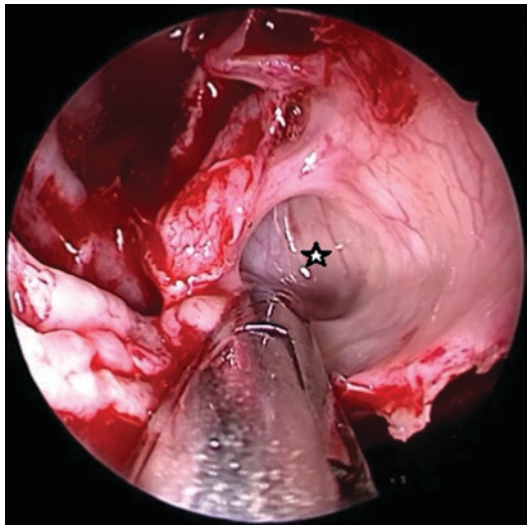

Fig. 7.32 The remnants of the bulla walls (star) are removed

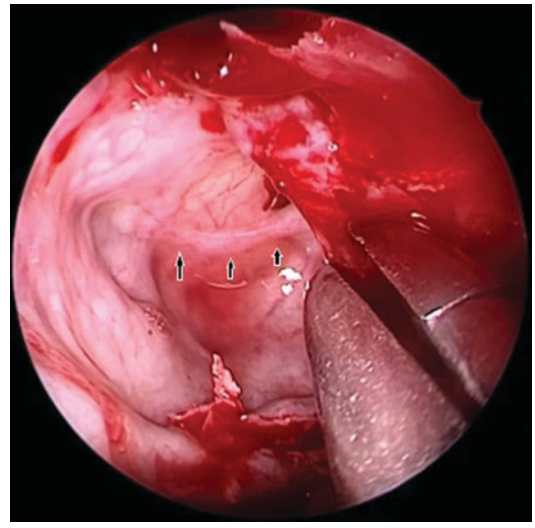

Fig. 7.34 Close up view of anterior ethmoidal artery (arrows)

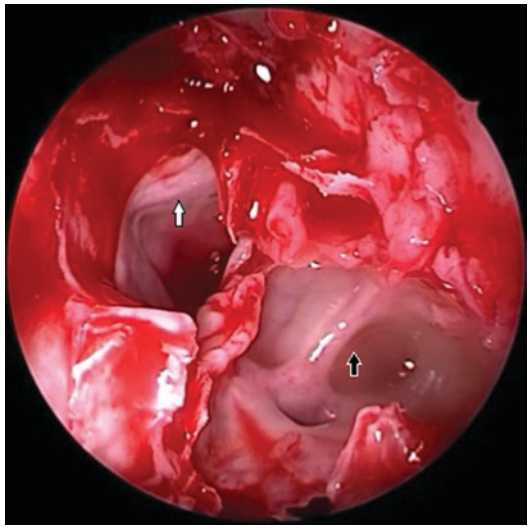

Fig. 7.33 The intrabullar partition (black arrow), and anterior ethmoidal artery (white arrow) are seen

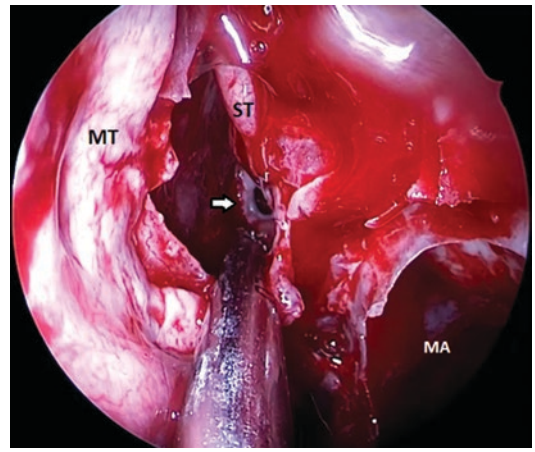

Fig. 7.35 The natural opening of the sphenoid sinus (arrow) is visible after removing the inferior part of the superior turbinate (ST), MA; maxillary antrum

bulla are removed (Fig. 7.32). The superior thin bone is removed and the anterior ethmoidal artery can be seen running in the base of skull (Figs. 7.33 and 7.34). Posterior ethmoid sinuses can be approached by palpating and gently perforating the ground lamella using a blunt dissector. Opening up of the posterior ethmoid exposes the anterior wall of the sphenoid sinus.

7.1.4 Sphenoid Sinus

After a wide maxillary antrostomy and ethmoidectomy, superior turbinate is identified (Fig. 7.35). The lower half of the superior turbi-

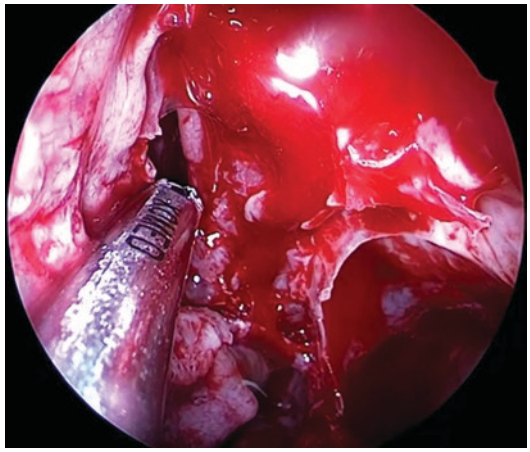

Fig. 7.36 Tissue around the sphenoid ostium is debrided

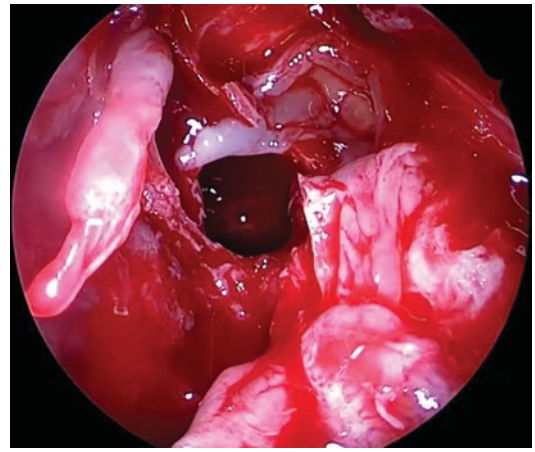

Fig. 7.38 A view of the lumen of the sphenoid sinus is obtained

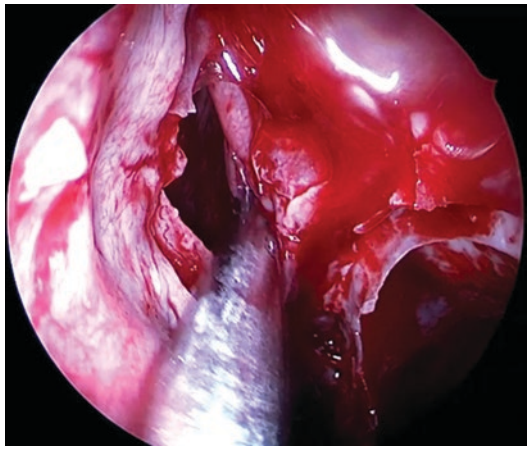

Fig. 7.37 The sphenoid sinus opening is widened

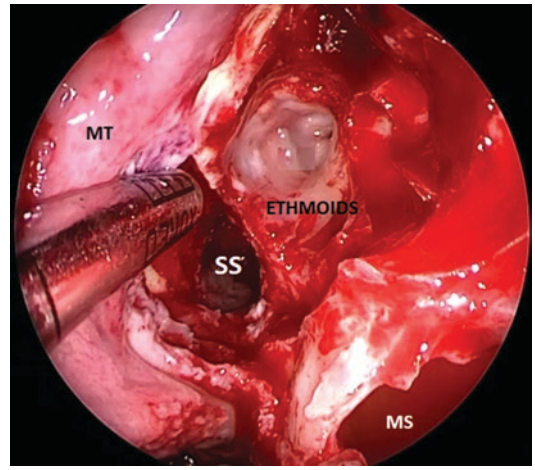

Fig. 7.39 Sphenoid sinus (SS), ethmoids, and maxillary antrum (MA) are seen along with middle turbinate (MT)

nate is resected, and the sphenoid sinus's natural ostium comes in view [10] (Figs. 7.36 and 7.37).

If the sphenoid sinus ostium is not easily located, it is important to stay below the maxillary sinus's roof to prevent injury to the skull base. Draw an imaginary line from the superior border of the maxillary sinus ostium to the septum. Sphenoid sinus ostium lies inferior to this line. Once identified, the sphenoid sinus opening is widened (Figs. 7.38 and 7.39) and any inflammatory tissue in the sphenoid sinuses is cleared. Aggressive cases of ROCM may involve the bone of the sphenoid sinus and can be easily detected on MRI. For better results this bone must be drilled, as discussed in the following chapters.

7.2 Basic Procedures in Cases with Limited Disease

7.2.1 Case 1: Involvement of Turbinates and Sphenoid Sinuses

The turbinates, maxillary sinus, and sphenoid sinus were all affected in this example, however the middle meatus was normal (Fig. 7.40). The maxillary sinus was opened using backbiting forceps; the opening was enlarged and cleared

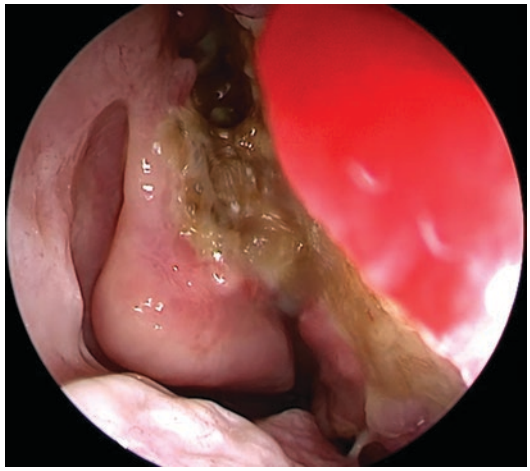

Fig. 7.40 Mucormycosis involving the turbinate and the sphenoid sinus

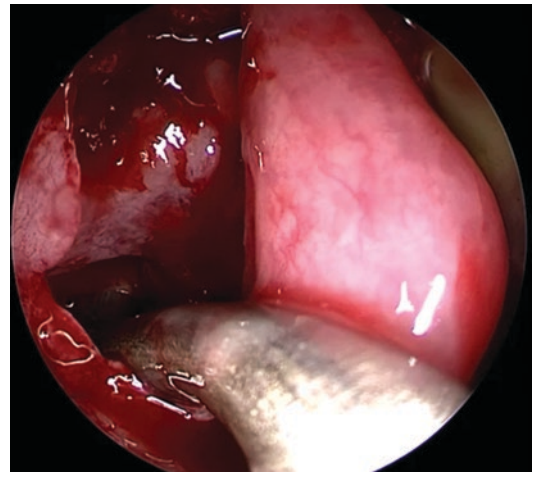

Fig. 7.42 Maxillary sinus is opened

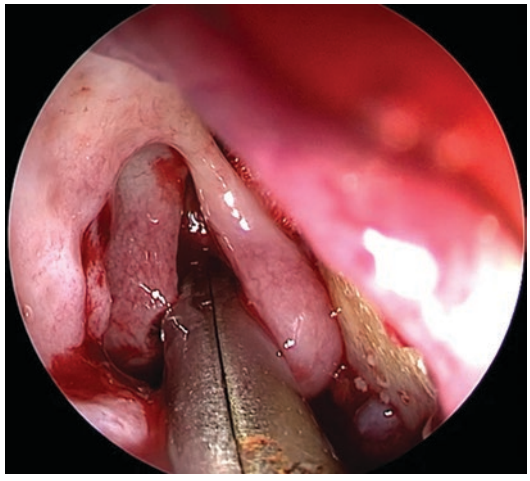

Fig. 7.41 Uncinectomy is in process

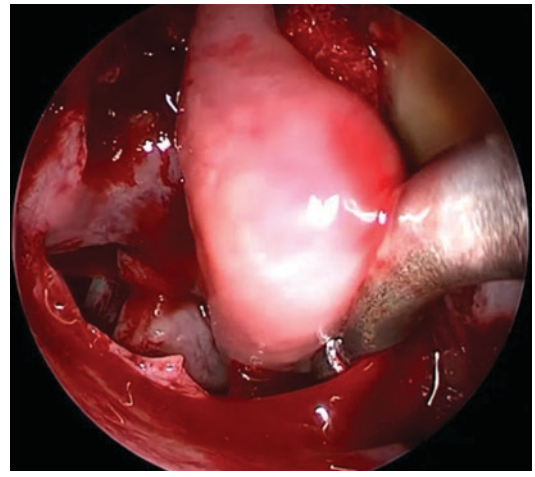

Fig. 7.43 Mucopurulent discharge is cleared from the maxillary sinus

(Figs. 7.41, 7.42, and 7.43). Basal lamella is perforated with the help of a suction dissector in the inferomedial part (Figs. 7.44, 7.45, and 7.46). The Sphenoid sinus is then exposed and was found to be full of dirty yellow inspissated discharge. It was widened and cleared (Figs. 7.47, 7.48, 7.49, and 7.50). Posterior ethmoids are cleared.

7.2.2 Case 2: Middle Meatus Involvement

Middle turbinate, uncinate process, ethmoids, and maxillary antrum are implicated in this case (Fig. 7.51). Some material is obtained for biopsy before debridement (Figs. 7.52 and 7.53). The maxillary antrum is cleared using suction.

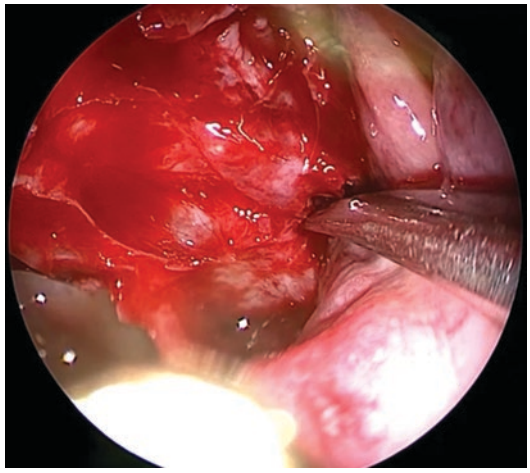

Fig. 7.44 Ground lamella is perforated at the inferomedial end

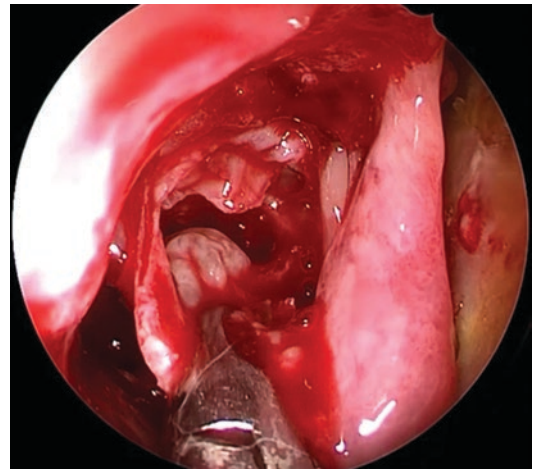

Fig. 7.46 Disease from ethmoid and sphenoid is cleared

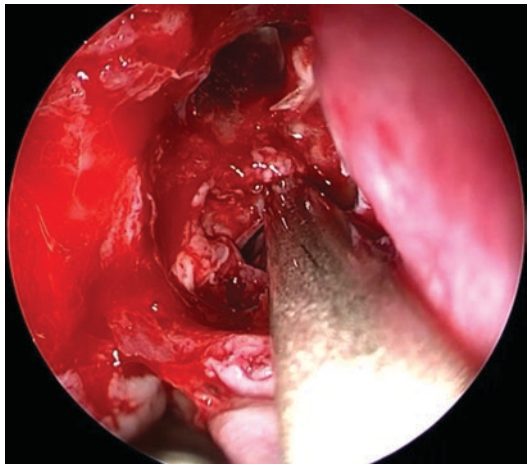

Fig. 7.45 Posterior ethmoid and sphenoid sinuses are opened

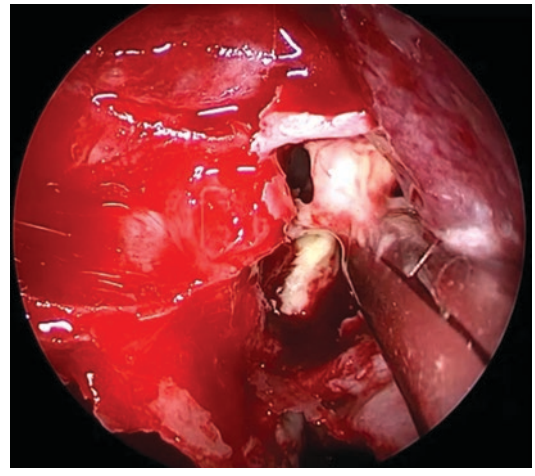

Fig. 7.47 Fungus and discharge can be seen filling the sphenoid sinus

Diseased tissue is removed from the maxillary antrum and anterior ethmoids (Figs. 7.54 and 7.55). Sphenoid sinus was free of disease, and a large clear maxillary antrum can also be seen (Fig. 7.56). This chapter is for all specialties, including cross-specialty surgeons, who want to learn the fundamentals of endoscopic sinus surgery. As a result they will be able to handle cases of limited disease on their own. It will also assist with preoperative endoscopic disease assessment and postoperative follow-up. Basic steps will also benefit those who want to take it a step further and perform advanced endoscopic procedures.

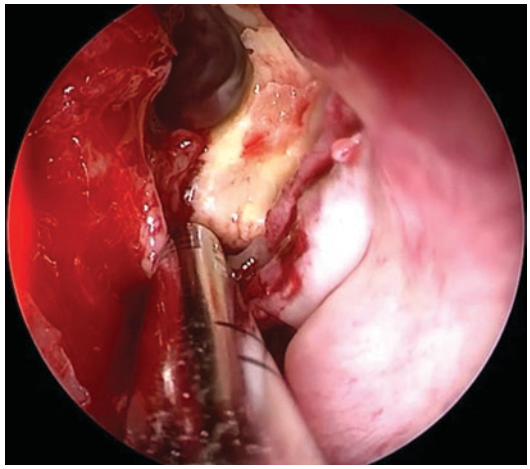

Fig. 7.48 Mucopurulent discharge is cleared from the sphenoid sinus

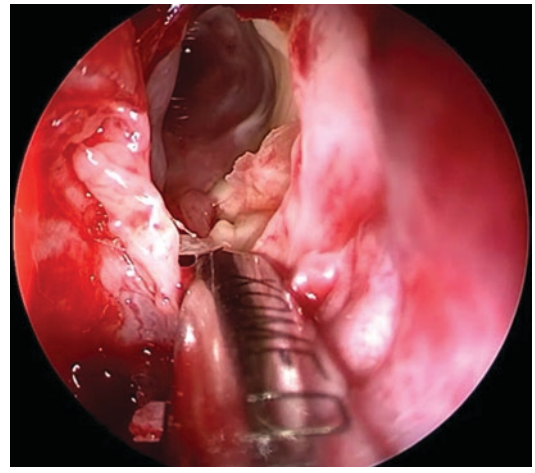

Fig. 7.50 Mucosal tags around the sphenoid sinus ostium are debrided

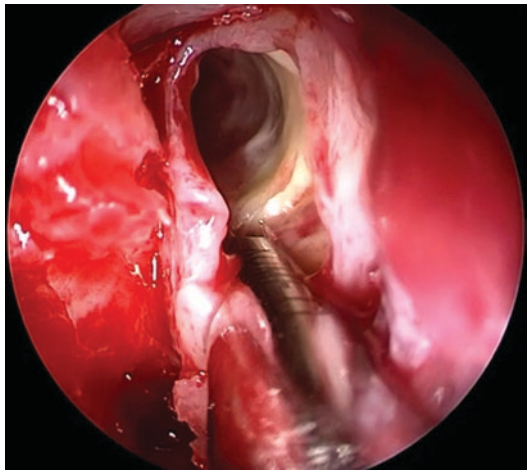

Fig. 7.49 A wide-open sphenoid can be seen

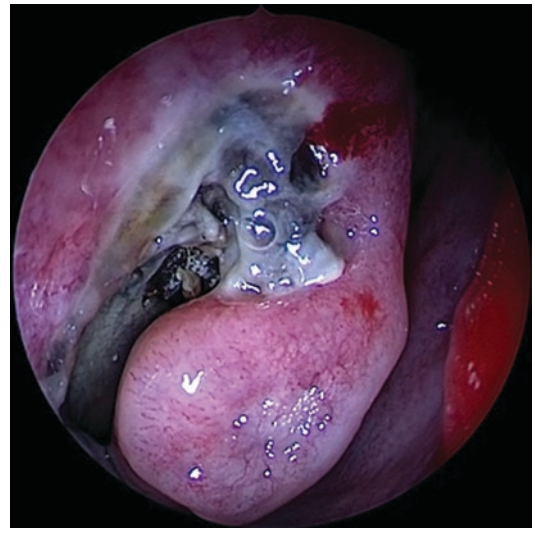

Fig. 7.51 Mucormycosis involving the middle meatus including the turbinate

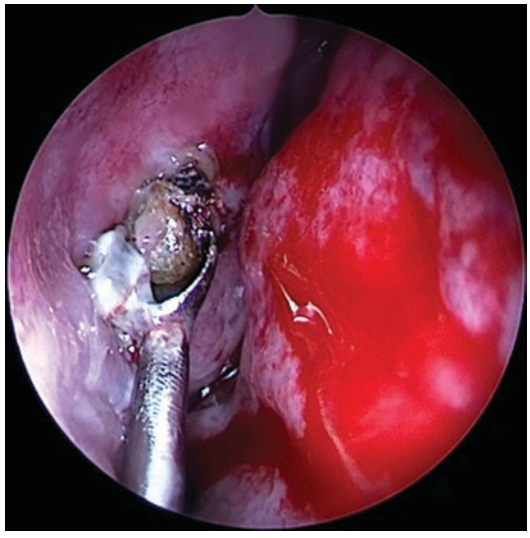

Fig. 7.52 A curette is used to obtain a sample for testing

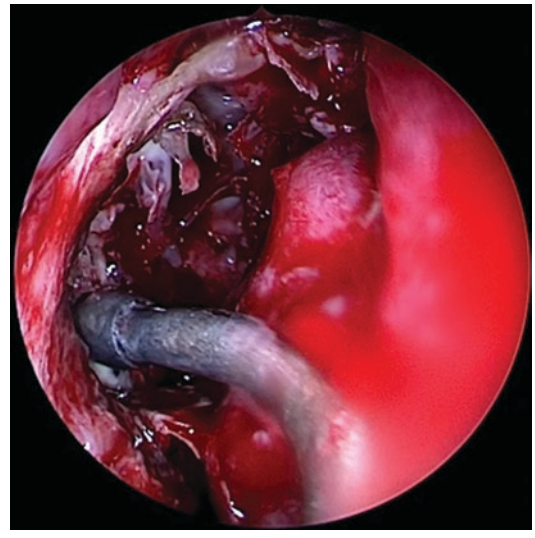

Fig. 7.54 A curved suction is used to clear the disease

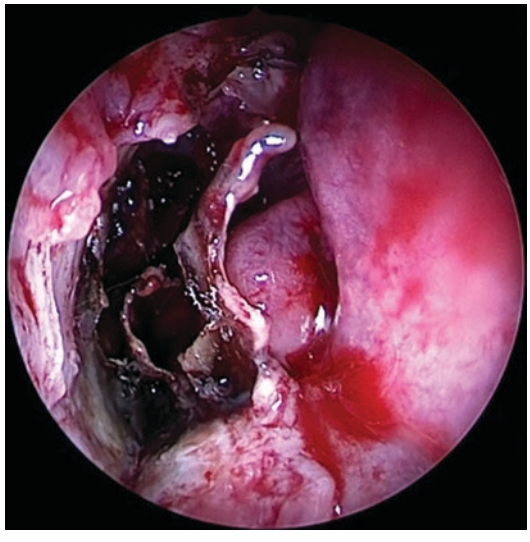

Fig. 7.53 Uncinectomy is done

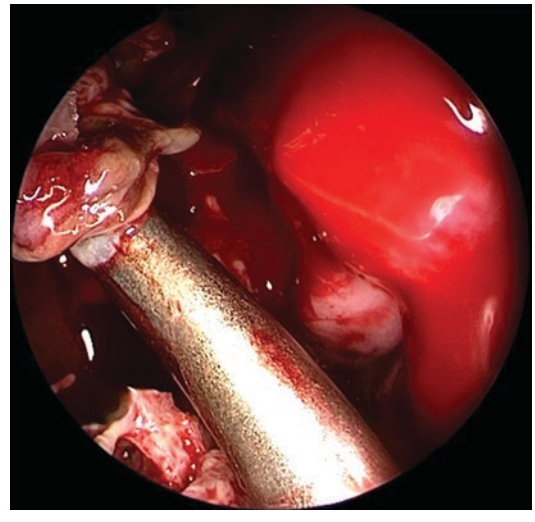

Fig. 7.55 Mucopurulent discharge and inflamed tissue are cleared

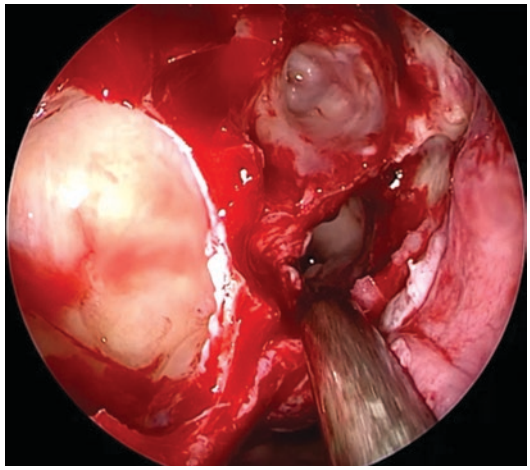

Fig. 7.56 A large maxillary antrum and a disease-free sphenoid sinus is done

References

1. Nithyanandam S, Jacob MS, Battu RR, Thomas RK, Correa MA, D'Souza O. Rhino-orbitocerebral mucormycosis. A retrospective analysis of clinical features and treatment outcomes. Indian J Ophthalmol. 2003;51(3):231–6.
2. Gupta N. Endoscopic anatomy of the lacrimal drainage system. Endoscopic dacryocystorhinostomy. Springer; 2020. p. 23–34.
3. Singh AP. Functional endoscopic sinus surgery. Atlas and comprehensive review of basic, clinical and surgical considerations. Aditya Medical Publisher; 2002. p. 17–37.
4. Rice DH, Schaefer SD. Endoscopic paranasal sinus surgery. 2nd ed. New York: Raven Press; 1992.
5. Schaefer JP. The nose, paranasal sinuses, nasolacrimal passageways and olfactory organ in man. Philadelphia: Blakiston; 1920. p. 125–9.
6. Schaefer IP. The genesis development and adult anatomy of nasofrontal region in man. Am J Anat. 1916;20:125.
7. Shaik KV, Haripriya. Management of nasolacrimal-cutaneous fistula – a maxillofacial review and sharing experience. Ann Int Med Dental Res. 2016;2(6).
8. Mauriello JA, Rosen A. Surgical anatomy of the lacrimal drainage system. In: Mauriello JA, editor. Unfavorable results of eyelid and lacrimal surgery. Prevention and management. Boston: Butterworth Heinemann; 2000. p. 361–80.
9. Unlu HH, Goktan C, Aslan A, Tarhan S. Injury to the lacrimal apparatus after endoscopic sinus surgery: surgical implications from active transport dacryocystography. Otolaryngol Head Neck Surg. 2001;124(3):308–12. https://doi.org/10.1067/mhn.2001.112433.
10. Youssef TA. Endoscopic approaches to the sphenoid: how I do it? Egypt J Otolaryngol. 2013;29:284–9. https://doi.org/10.7123/01.EJO.0000434902.23128.3c.

8 Surgical Management of Rhino-Orbito-Cerebral Mucormycosis (ROCM); Approach to Pterygopalatine Fossa, Pterygoid Process, Infratemporal Fossa, and Orbit

Nishi Gupta

Surgical management of Rhino-Orbito-Cerebral Mucormycosis (ROCM) is often challenging. Most otorhinolaryngologists are well versed in endoscopic sinus surgery procedures and can use the same approach for advanced debridement as needed using a multidisciplinary approach the preceding chapter, on Surgical Management of Rhino Orbito Cerebral Mucormycosis; Basic Endoscopic Sinus Surgery Procedures, provides a summary and graphic demonstration of the essential procedures for the other specialties.

However, rather than the technology, it is the decision making in ROCM that needs attention.

This chapter examines locations that are often overlooked but contain hidden diseases and hence must be addressed during surgical care of ROCM. The pterygopalatine fossa is one such region that serves as a conduit for the infection to reach the orbit. It also acts as a disease reservoir, and is thus one of major reasons of recurrent/residual mucor in ROCM.

Orbital spread of disease through lamina papyracea was uncommon in our series, and another route was found to be responsible for the disease's orbital transmission. In most of ROCM cases the lamina papyracea was found to be intact, as previously reported [1]. It was noted that the disease does not always follow the typical route of spread from nose and sinuses to orbit and intracranial structures. In the chapter on debates in ROCM; classification dilemma, it is described in further detail [2–6].

Improved outcomes can be obtained by planning the first debridement as the most aggressive one based on the disease mapping on CT and MRI. Learnings from detailed analysis during revision debridement helped us refine the strategy of dealing with ROCM cases, and that is how some of the best practises emerged.

8.1 Pterygopalatine Fossa

The pathway of extension from the nasal cavity to the orbit and intracranial cavity has already been described [7–14]. The pterygopalatine fossa (PPF) is the principal reservoir for mucor that serves as a conduit for the infection to move to other sites [1]. The PPF is bounded anteriorly by the posterior wall of the maxillary sinus, posteriorly by pterygoid processes and medially by the perpendicular plate of palatine bone (Fig. 8.1). The infraorbital fissure(IOF) connects PPF to the retrobulbar space while the pterygomaxillary fissure (PMF) connects it to the infratemporal fossa (Figs. 8.1, 8.2, 8.3, and 8.4). The spread of disease may occur across all these boundaries of PPF [1].

N. Gupta (✉)
Dr Shroff's Charity Eye Hospital, New Delhi, India

N. Gupta, S. G. Honavar (eds.), *Rhino-Orbito-Cerebral Mucormycosis*,
https://doi.org/10.1007/978-981-16-9729-6_8

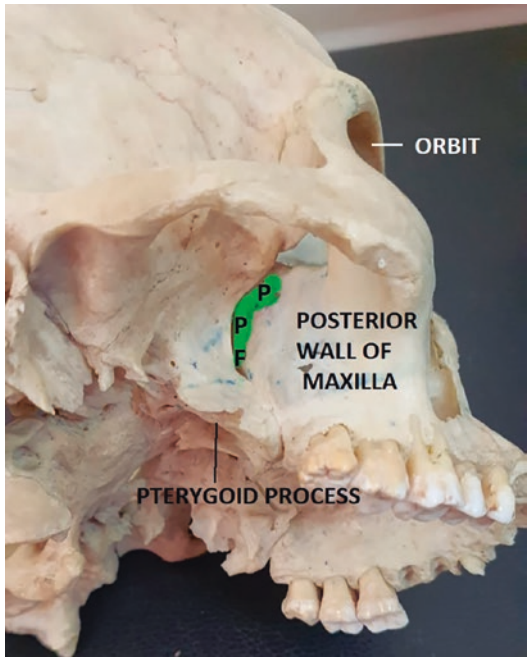

Fig. 8.1 A Skull photograph depicting the boundaries of pterygopalatine fossa

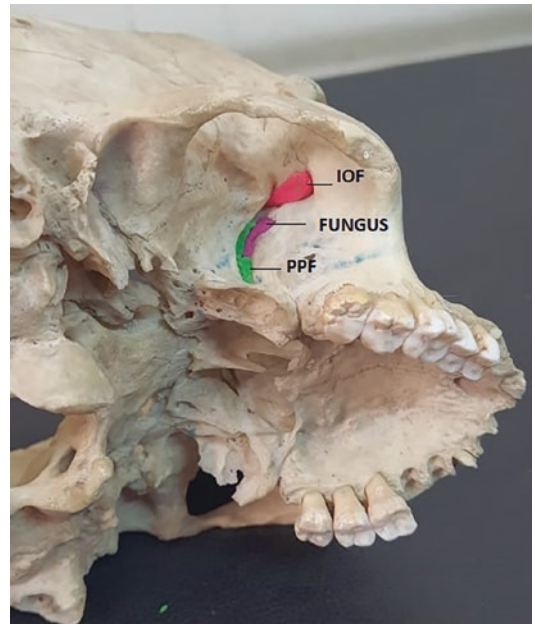

Fig. 8.3 The infraorbital fissure (IOF) connects the PPF to the retrobulbar space. Disease (purple) can be seen occupying the PPF

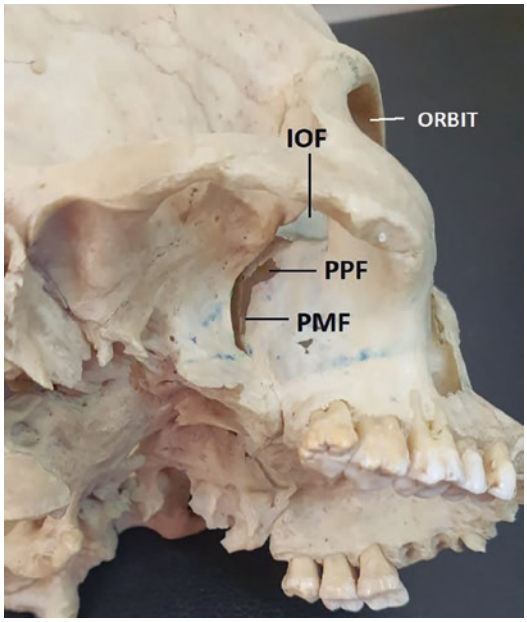

Fig. 8.2 A skull photograph depicting an infraorbital fissure (IOF) connecting pterygopalatine fossa (PPF) to the orbit. (PMF; Pterygomaxillary fissure)

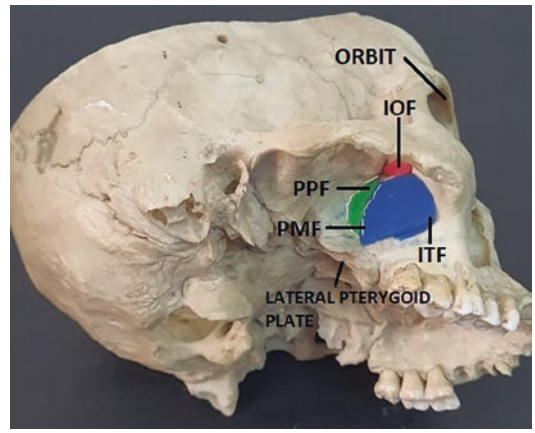

Fig. 8.4 The infraorbital fissure (IOF), pink connects the PPF, green to retrobulbar region while the pterygomaxillary fissure (PMF), white connects it to the infratemporal fossa (ITF), blue

The mucor can extend from the PPF to the infratemporal fossa via the pterygomaxillary fissure [1, 15] (Figs. 8.4 and 8.5). Orbital involvement can occur due to the spread of disease from PPF to orbit through IOF (Figs. 8.3, 8.4, and 8.5). The condition may affect superior orbital fissure, orbital apex, cavernous sinus, and intracranial structures through the orbit (Figs. 8.6 and 8.7). Direct spread of disease through lamina papyracea

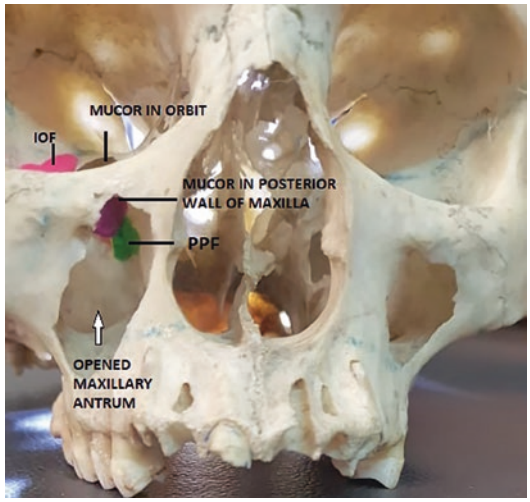

Fig. 8.5 The anterior wall of the maxilla is removed, revealing the pterygopalatine fossa, seen through it (green) with the spread channel (purple)

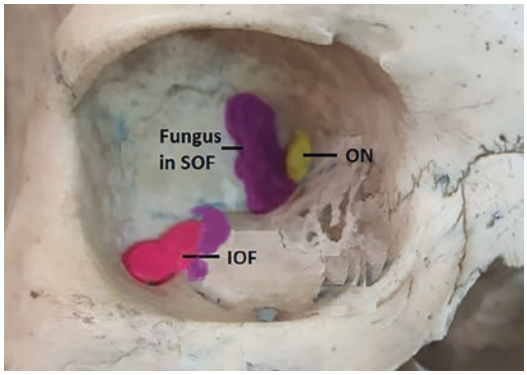

Fig. 8.6 Disease can be seen in both the inferior and superior orbital fissure (purple). The disease can spread to the orbital apex, cavernous sinus, and intracranial structures via the superior orbital fissure (SOF). ON; Optic nerve

to the orbit is rare [1]. Similarly, the posterior wall of the maxillary antrum is often intact with no defect for the disease manifestation into PPF. The involvement of PPF may occur along the sphenopalatine foramen [1]. PPF involvement is indicated by orbital invasion, swelling, and numbness over the face, facial palsy, and palate erosion.

New symptoms of face swelling, numbness, dental pain, and exacerbated ocular symptoms were found in revision cases in our practise. These new symptoms appear due to the thrombosis of the sphenopalatine vessels in the pterygopalatine fossa with or without the involvement of anterior ethmoid vessels in the orbit [1]. All these patients were found to be to have extensive disease in the pterygopalatine fossa.

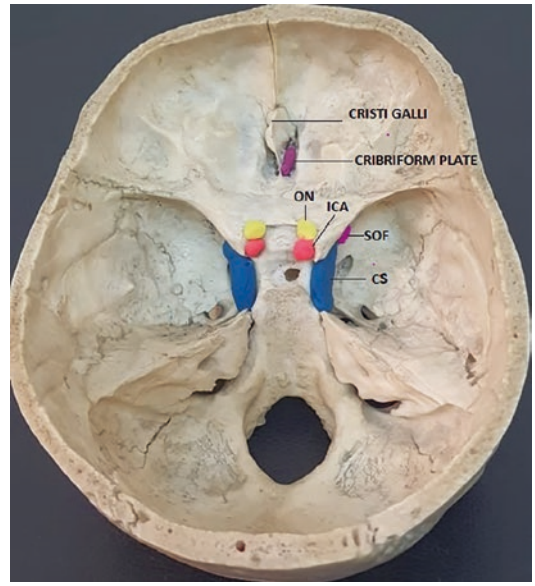

Fig. 8.7 Spread of disease (purple) to the intracranial structures may occur through the cribriform plate and the superior orbital fissure

8.1.1 Steps of Surgery for PPF

Denker's modified medial maxillectomy is the first most important surgical procedure to approach PPF. Alfred Denker originally described the anteromedial maxillectomy in 1906. It was further modified into the endonasal technique by Sturmann and Canfield to evolve into the current endoscopic technique [16–19].

Steps

- The surgery is carried out using 4 mm, 0-degree endoscopes connected to a high-definition camera and monitor unit (Karl Storz Endoscopy, Tuttlingen, Germany)
- A perfect access into the maxilla entails drilling a window into the anterolateral wall of the maxilla. A 15° curved burr on a microdebrider handle or an MR-8 Stylus drill (Medtronic Inc. USA) can be used for drilling as can a coarse diamond burr on a microdebrider han-

dle (4.0 mm; 1,884,004; Medtronic Inc., USA).

- The nose is examined, and the edge of the piriform aperture is palpated. The area anterior to the intersection of the inferior turbinate head with the lateral wall serves as a landmark for locating the pyriform aperture (Fig. 8.8).
- The mucosa across the lateral nasal wall is coblated as the initial step after identification (Fig. 8.9). Though little bleeding is expected in mucor cases, bleeding may occur in situations where intervening areas are disease free, lengthening the surgical time.
- The inferior turbinate is excised with scissors, or ablated with a coblator if it bleeds owing to non-involvement (Figs. 8.10, 8.11, and 8.12). After the inferior turbinate is removed the pyriform aperture comes in view. The piriform aperture is palpated with the dissector (Fig. 8.13, arrow), and a sharp incision is made (Figs. 8.14 and 8.15). After the coblation, the incision can be given with the perios-

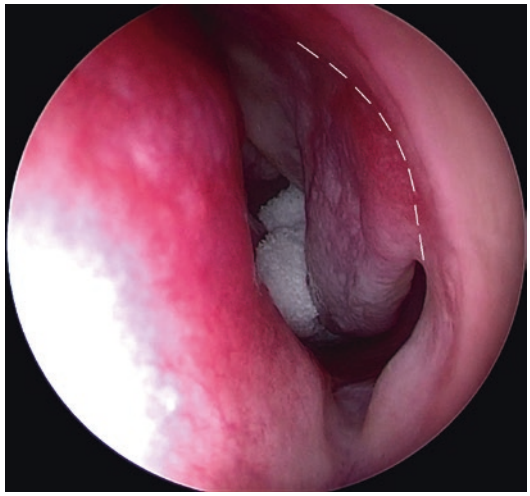

Fig. 8.8 The area anterior to the intersection of the head of the inferior turbinate with the lateral wall serves as a landmark for locating the pyriform aperture (white dotted line)

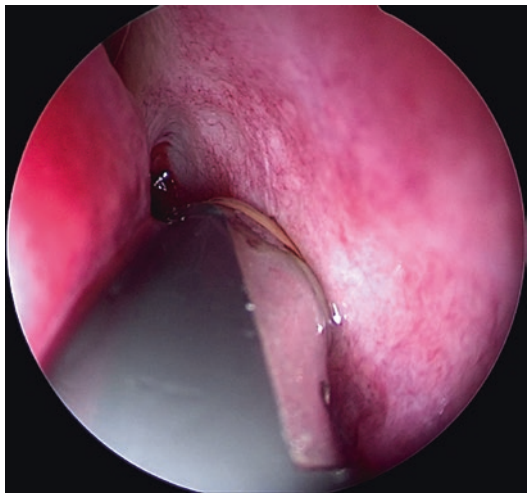

Fig. 8.9 Mucosal coblation over the lateral nasal wall

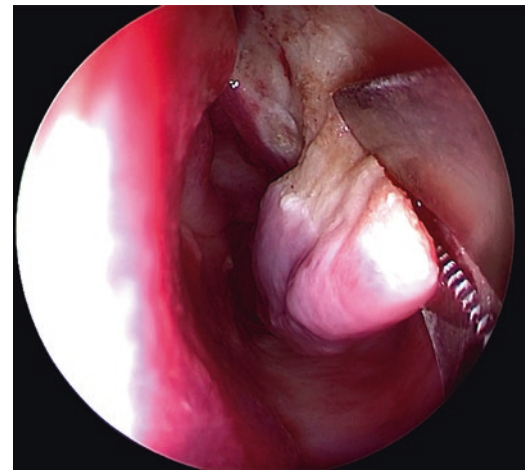

Fig. 8.10 Scissors are used in conjunction with the inferior turbinate's lateral attachment

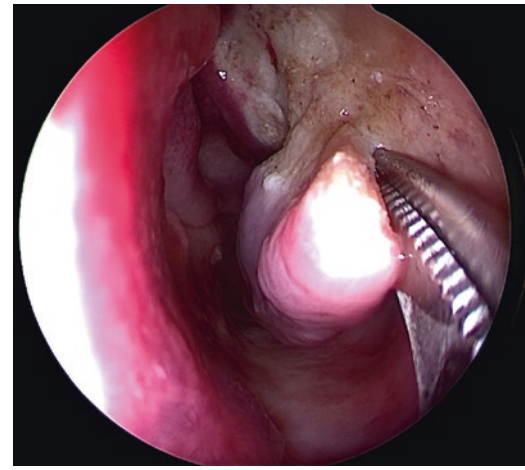

Fig. 8.11 Incision over the junction of inferior turbinate with the lateral wall

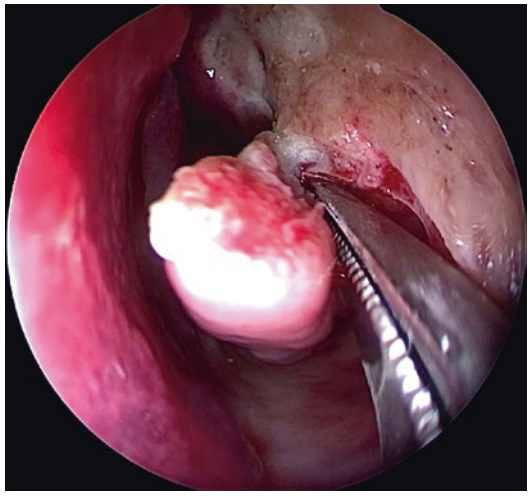

Fig. 8.12 Removal of inferior turbinate using scissors

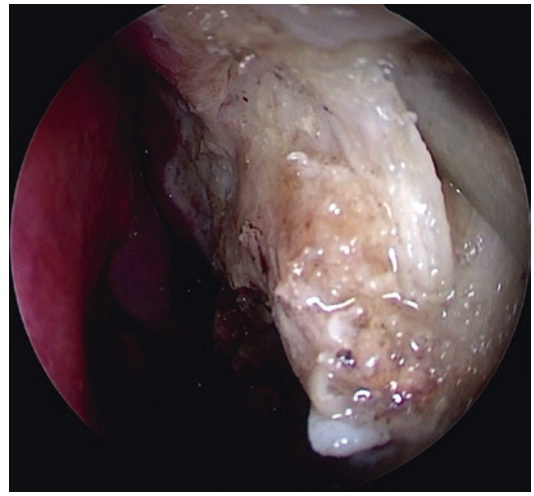

Fig. 8.14 A blunt dissector is used to lift up the muco-periosteal flaps

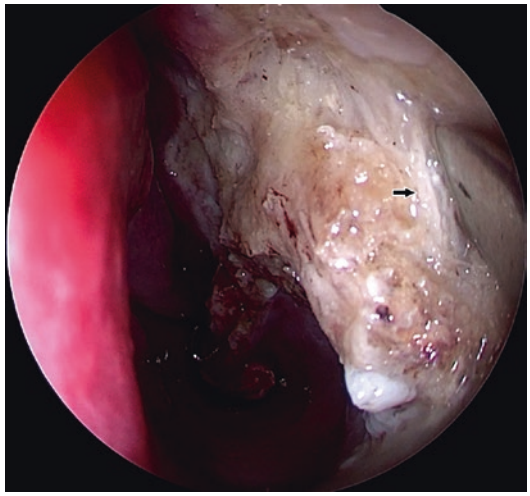

Fig. 8.13 Pyriform aperture is identified and palpated with the blunt dissector (arrow)

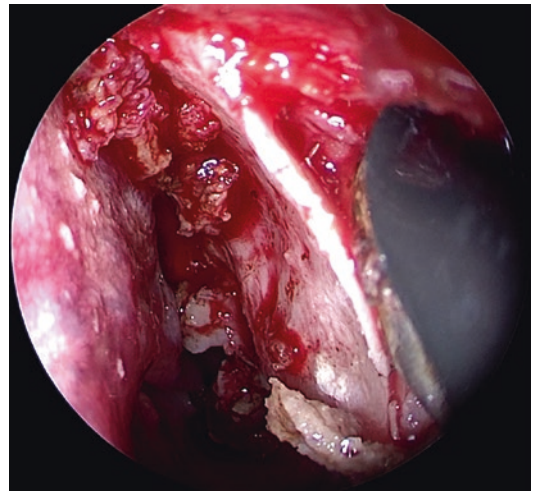

Fig. 8.15 The lateral flap is lifted using a coblator to achieve excellent haemostasis

teal elevator. The mucosa is split vertically, and the mucoperiosteal flaps are lifted (Fig. 8.16).

- Subperiosteal dissection of the pyriform aperture continues till the anterior wall of the maxilla is reached. Both the anterosuperior alveolar nerve and the infraorbital nerves are preserved by lifting the flap (Figs. 8.17 and 8.18). The anterior superior alveolar nerve is a branch of the infraorbital nerve, which is a branch of the maxillary nerve (V_2). The anterior superior alveolar nerve arises from the infraorbital nerve within the infraorbital canal before the infraorbital nerve exits through the infraorbital foramen [16]. It is important to stay on the bone while dissecting as entry into soft tissue anterior to the pyriform border may cause injury to the alar cartilage. The lateral limit of exposure depends on the severity of disease.
- The anterolateral wall of the maxilla is drilled to create a window in the anterior wall of the maxilla inferior to the infraorbital foramen

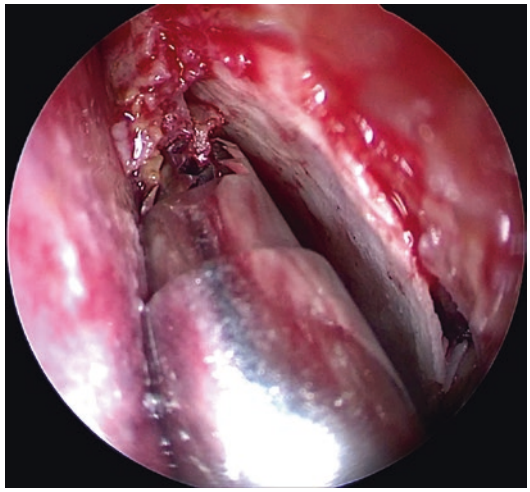

Fig. 8.16 The coblator is used to lift mucoperiosteal flaps on the medial side

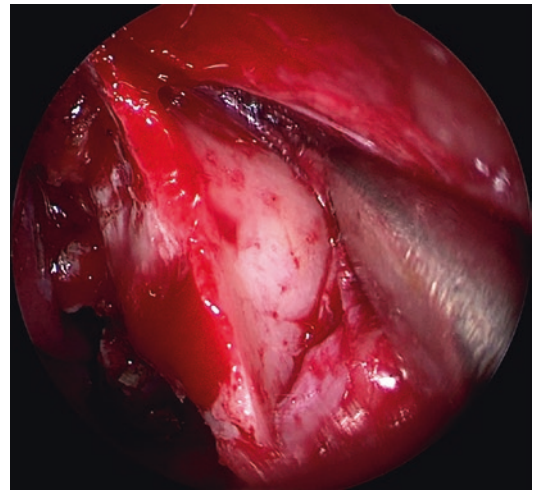

Fig. 8.18 Infraorbital nerve can be taken as the lateral limit of the flap elevation unless the dissection needs to be done more laterally based on the extent of disease

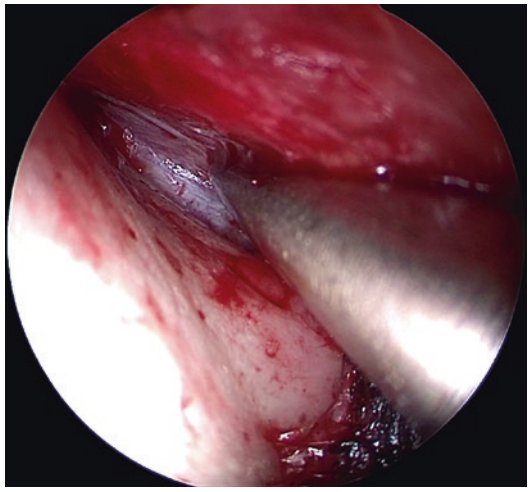

Fig. 8.17 The flap is lifted, preserving both the anterosuperior alveolar nerve and the infraorbital nerves

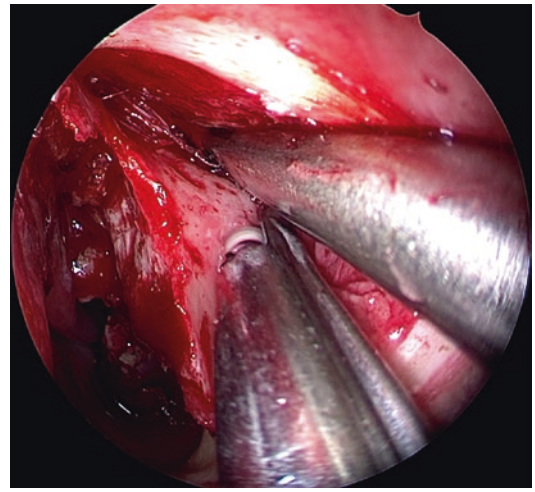

Fig. 8.19 Anterolateral wall of the maxilla is identified for drilling

(Figs. 8.19 and 8.20). This landmark protects the infraorbital and anterosuperior alveolar nerves from injury as well as preventing entry into the orbit.

- Drilling the anterolateral wall allowed examination of the diseased tissue filled maxillary sinus in this case (Fig. 8.21). Drilling a window also aids in preservation of the orbital floor and allows us to easily access the posterior wall of the maxilla along the orbital floor. Anterior border of the thin bone of the pyriform border can be removed using Luc's forceps, carefully preserving the nasolacrimal duct (NLD) that looks inflamed in this case (Figs. 8.22 and 8.23).
- To prevent NLD from hanging into the nasal cavity the bone covering the proximal end of NLD is drilled, and the NLD is incised flush with the orbital floor. The incision is given obliquely to create a broader lumen that helps in preventing epiphora (Figs. 8.24 and 8.25).

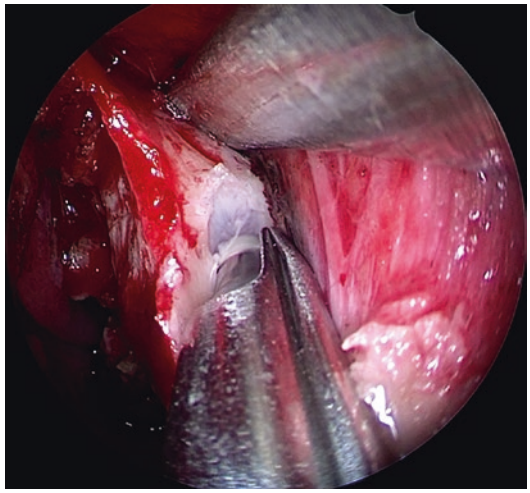

Fig. 8.20 Anterolateral wall of the maxilla is drilled to create a window in the anterior wall of the maxilla inferior to the infraorbital foramen

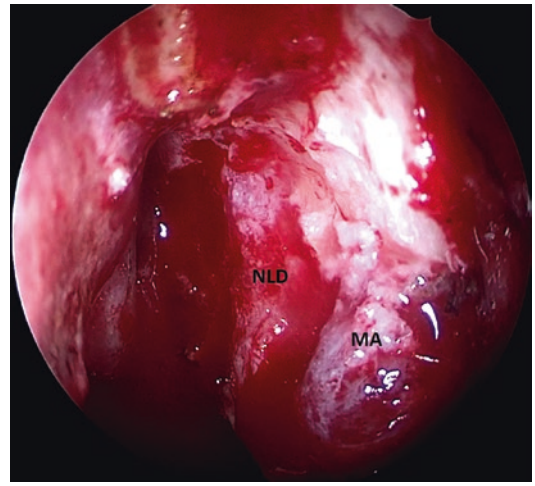

Fig. 8.22 Maxillary sinuses can be seen filled with fungal mass

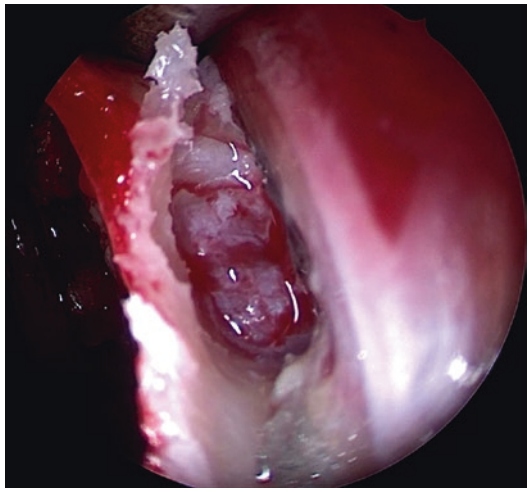

Fig. 8.21 Drilling the anterolateral wall allows examination of the maxillary sinus

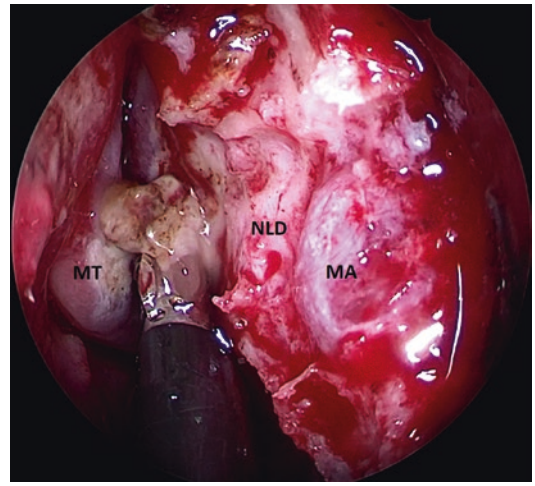

Fig. 8.23 Inflamed nasolacrimal duct is seen along with the disease in the maxillary antrum

- The maxillary sinus is cleared of the necrotic material and infected secretions. The inferior ledge of the bone is drilled flush with the nasal cavity's floor (Fig. 8.26).
- Sphenopalatine artery exit is evaluated (Fig. 8.27), and the bone of the anterior wall of the sphenopalatine foramen is removed with Kerrison's rongeur to expose the pterygopalatine fossa. Bone removal is continued inferiorly and laterally up to the inferior orbital fissure. After the disease is cleared completely, the posterior wall of the maxilla is palpated.
- The posterior wall looks intact but once removed, the pterygopalatine fossa is found to be involved with the disease (Fig. 8.28). The maxillary artery is located and exposed, and Karl Storz Liga clips are applied over the artery's most lateral part (Fig. 8.29). Pterygopalatine fossa is examined, and any unhealthy tissue is removed.

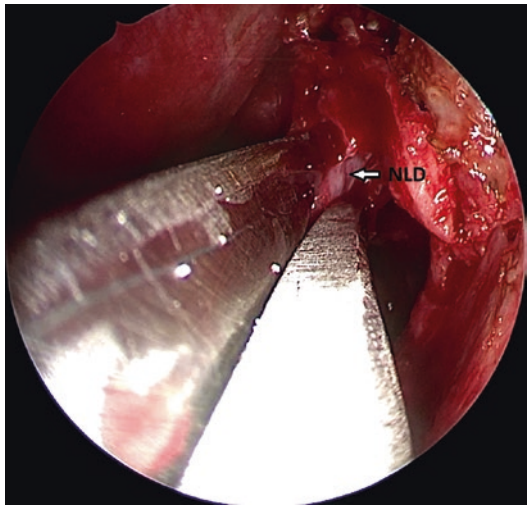

Fig. 8.24 The NLD is incised close to the orbital floor

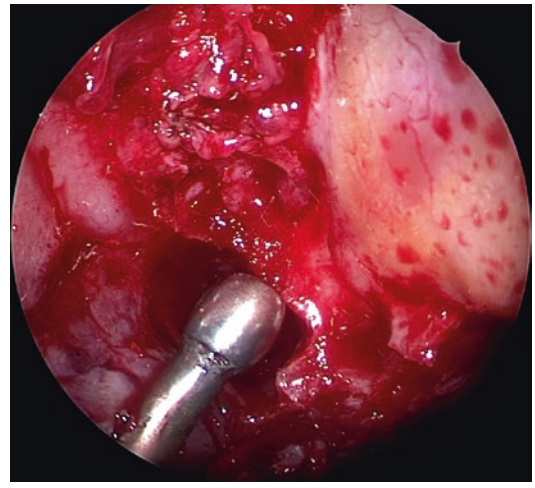

Fig. 8.26 A clear view of the posterior wall of the maxillary sinus is obtained

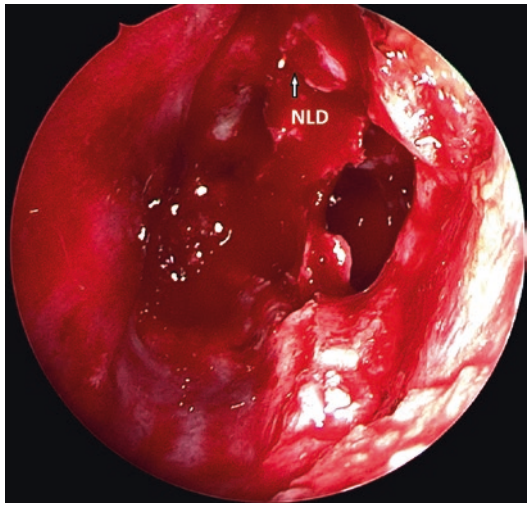

Fig. 8.25 Incised end of NLD is seen

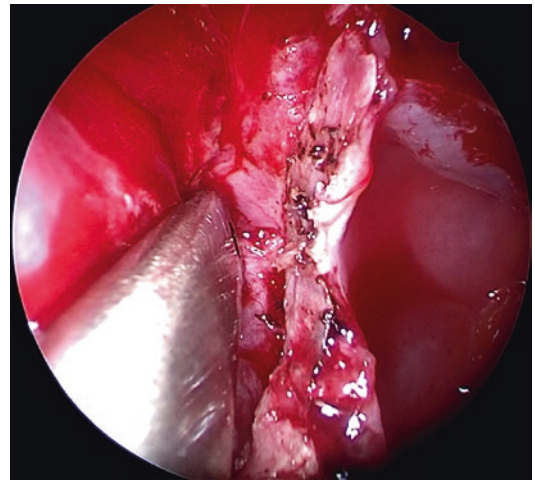

Fig. 8.27 Tissue around the sphenopalatine foramen is debrided and coagulated to facilitate removal of the posterior bony wall

It is important to remember that even a minor infection in the form of blackish discolouration of nasal mucosa does not always suggest the inoculation of disease at this site; it could be the result of vascular necrosis. These limited signs in the nasal cavity and sinuses may be the only evidence of isolated involvement of the pterygopalatine fossa [1]. Limited resection in this situation, will result in progression of residual disease, highlighting the importance of PPF debridement particularly, in cases involving the orbit.

Pterygopalatine fossa debridement must be performed in ROCM to limit the risk of residual/recurrent mucor and to prevent the spread of disease to orbit.

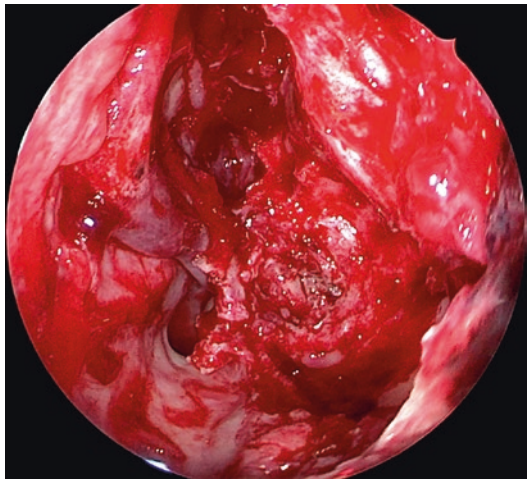

Fig. 8.28 Posterior wall of the maxillary sinus is removed

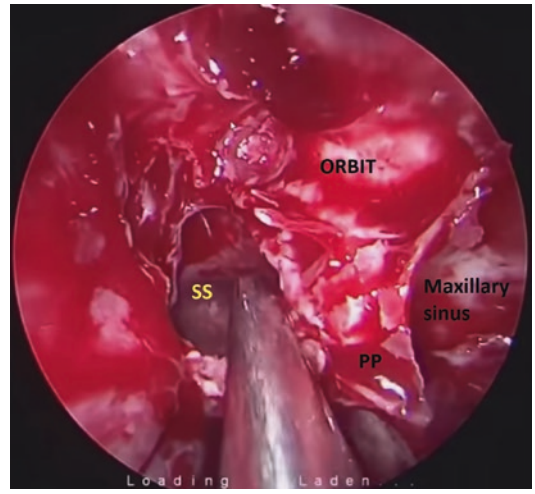

Fig. 8.30 Sphenoid sinus ostium is widened (Fig courtesy Dr. Satish Jain)

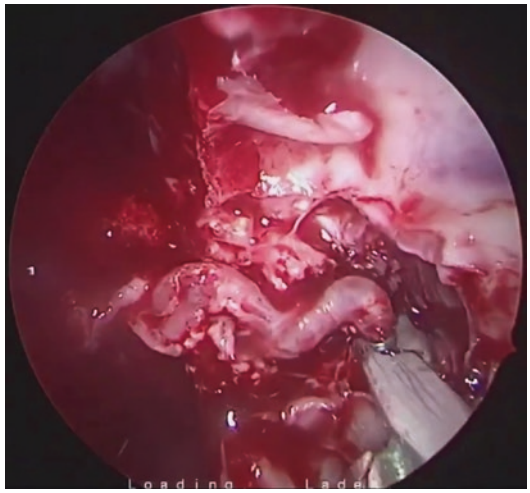

Fig. 8.29 Maxillary artery is identified, and Ligur clips are applied (Fig courtesy Dr. Satish Jain)

8.2 Approach to Pterygoid Process and Infratemporal Fossa

The infratemporal fossa is located behind the posterior wall of the maxilla, below the middle cranial fossa floor, medial to the ramus of the mandible. Its roof is formed by the infratemporal surface of the greater wing of the sphenoid, and its medial wall is formed of the lateral pterygoid plate. Temporalis muscle forms its lateral boundary. Medially, the infratemporal fossa communicates with the pterygopalatine fossa via the pterygomaxillary fissure [20–24].

The landmarks for identifying the infratemporal fossa are the infraorbital nerve at a point where it arises from the maxillary nerve near the foramen rotundum, before entering the infraorbital canal. This part of the infraorbital nerve defines the border between the infratemporal fossa and pterygopalatine fossa [8].

Infratemporal fossa can be exposed by removing the posterior wall of the maxilla from its floor till the roof. The sphenoid sinus ostium is widened laterally, and the lateral recess of the sphenoid sinus is opened [7] (Fig. 8.30). The internal maxillary artery is divided, and the pterygoid process is exposed to gain entry into the infratemporal fossa. The pterygoid process is drilled (Fig. 8.31), the marrow bone of the pterygoid is exposed, and the necrotic tissue is debrided [20]. The infratemporal fossa can be accessed to remove the necrotic tissue (Fig. 8.32). Pterygoid drilling is discussed in more detail in the subsequent chapter on drilling beyond sinuses, where drilling of the sphenoid and bony canal of the maxillary (V2) nerve have also been described.

If the disease has spread to the infratemporal fossa, more lateral dissection is needed to expose the bone that forms the floor of the middle cranial fossa, which is the superior boundary of the

infratemporal fossa. The lateral limit is reached when the vertically-oriented temporalis muscle can be visualized in a vertical plane [21].

It is important to preserve the area showing enhancement and only debride the necrotic part. The infratemporal fossa contains important structures like the pterygoid muscles, the mandibular nerve (V3), the internal maxillary artery, the carotid sheath, internal jugular vein, and cranial nerves [8–11].

Removal of too much tissue from the infratemporal fossa will lead to significant morbidity.

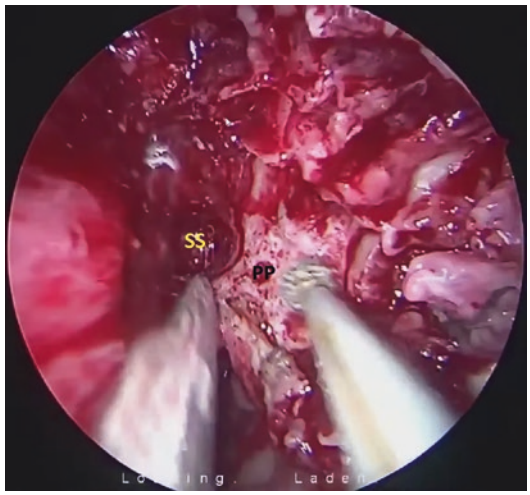

Fig. 8.31 Drilling of the pterygoid process (Fig courtesy Dr. Satish Jain)

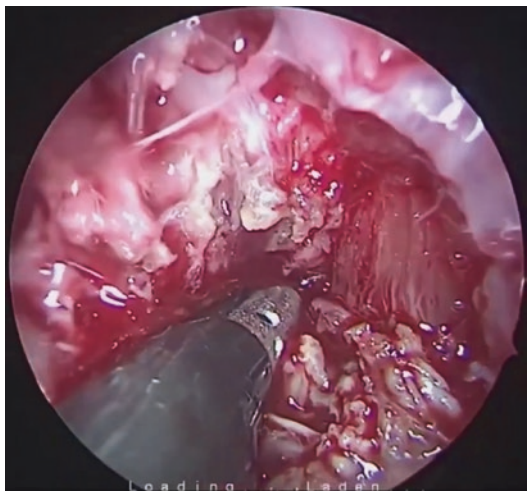

Fig. 8.32 Exposure of the infratemporal fossa (Fig courtesy Dr. Satish Jain)

Therefore, the area showing enhancement is treated with intravenous amphotericin B.

8.3 Orbital Clearance

A modified medial maxillectomy and debridement of the pterygopalatine fossa is a prerequisite for orbital clearance. The next step is a complete ethmoidectomy, opening and enlarging the sphenoid sinus ostium to obtain better exposure.

The first step in orbital clearance is to remove the lamina papyracea and expose the periorbita (Figs. 8.33 and 8.34). In cases of extensive disease, fat can be seen prolapsing as soon as the lamina papyracea is removed (Fig. 8.35). The orbit may even appear soft with thinned out periorbita, making it easy to debride the necrotic tissue as detailed in the chapter on transnasal endoscopic globe sparing orbital exenteration. In cases where the periorbita is thick, an incision is given over it to evaluate the orbital content. However, this step is performed only if there is evidence of orbital infiltration on MRI.

The periorbital incision is gradually deepened to allow fat to prolapse into the nasal cavity. The fat is subsequently teased and the periorbita is removed as well. The diseased fat is debrided while the muscle is not

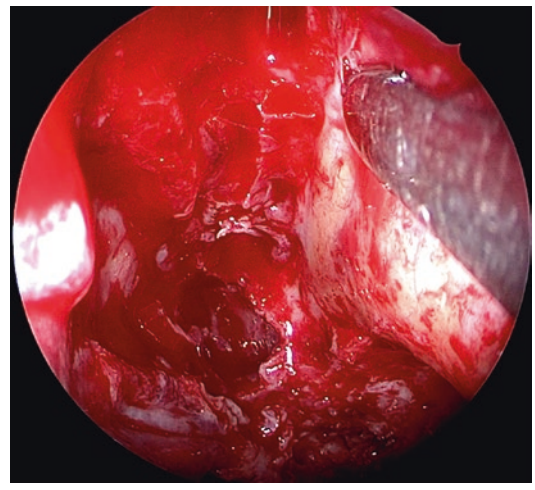

Fig. 8.33 A good view of the orbit is obtained by doing a median maxillectomy and sphenoid sinus widening

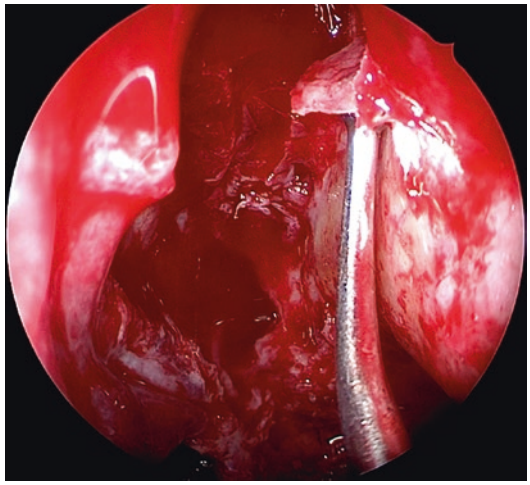

Fig. 8.34 Lamina papyracea is removed using ball pointer

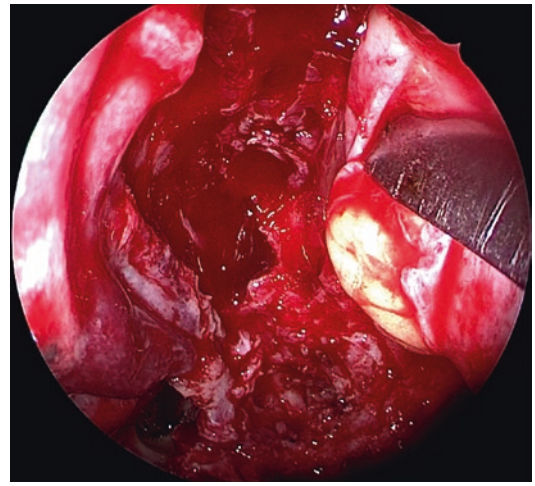

Fig. 8.36 The fat is teased gently to identify the diseased area

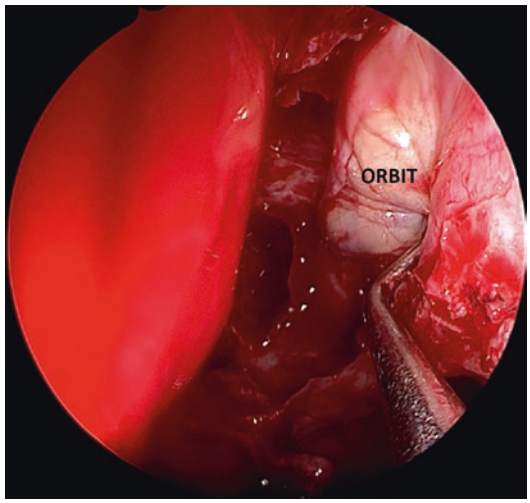

Fig. 8.35 The orbital fat is allowed to prolapse into the field

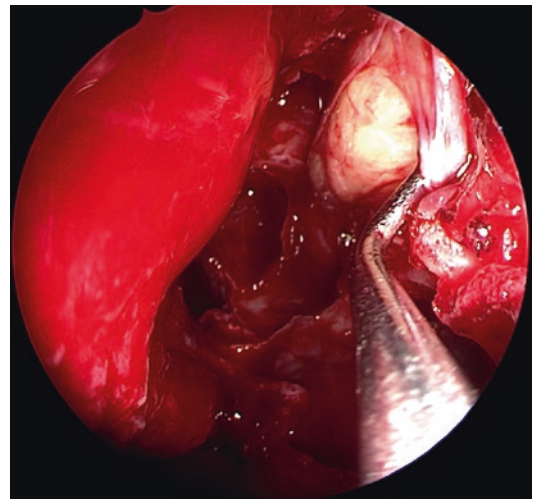

Fig. 8.37 Exposure is improved by removing any remnant of periorbita

(Figs. 8.35, 8.36, 8.37, 8.38, and 8.39). The muscles are usually last to get involved, so they are not disturbed. An Onodi cell condition is present in optic nerve. When substantial disease is present in the sphenoid sinus and orbit, the removal of the disease reveals a bare optic nerve (Fig. 8.40), which is followed by an excellent postoperative cosmetic appearance of the eye (Fig. 8.41).

Performing a modified Denker's maxillectomy is a useful procedure for gaining access to the maxillary sinus and its adjacent locations. The PPF is a major reservoir for mucor and serves as a conduit for the infection to travel to other parts. In our experience in most of the revision cases, the pterygopalatine fossa was left unopened during a previous surgery. Debriding the disease from PPF helped in achieving better outcomes. Although disease in the PPF can be detected with the use of numerous MRI sequences, imaging or clinical evaluation may fail to detect disease in PPF at times.

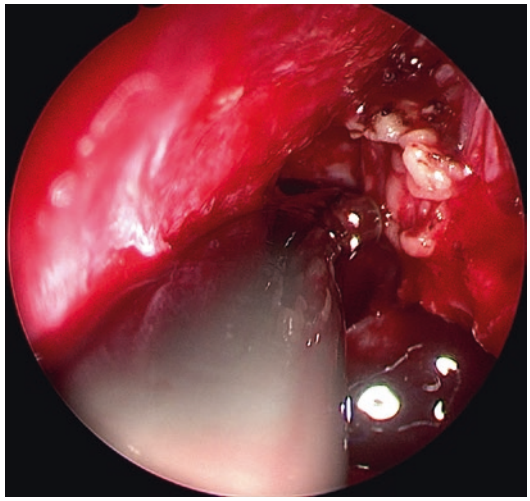

Fig. 8.38 The diseased fat is identified and removed

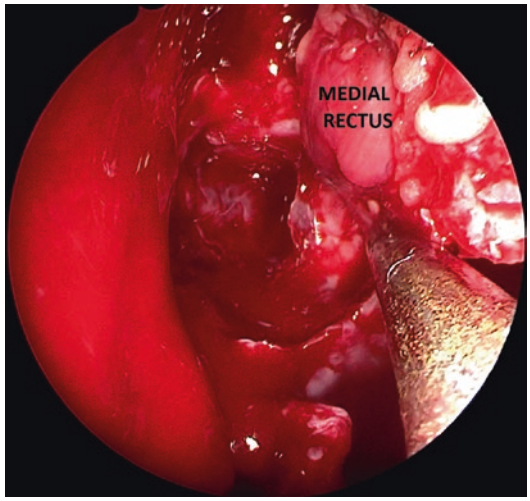

Fig. 8.39 Medial rectus muscle is identified

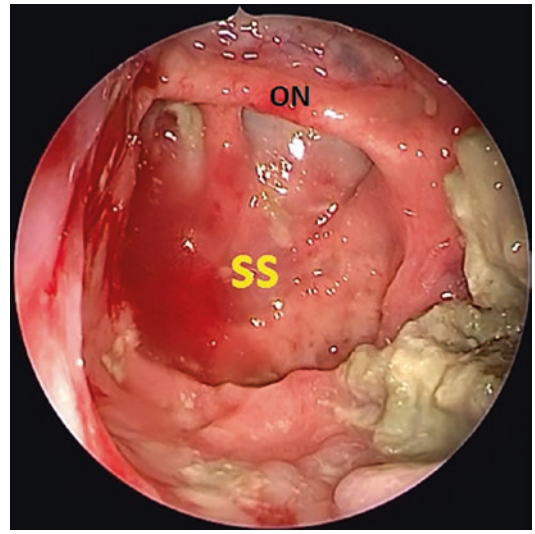

Fig. 8.40 Optic nerve (ON) is seen in the sphenoid sinus (SS)

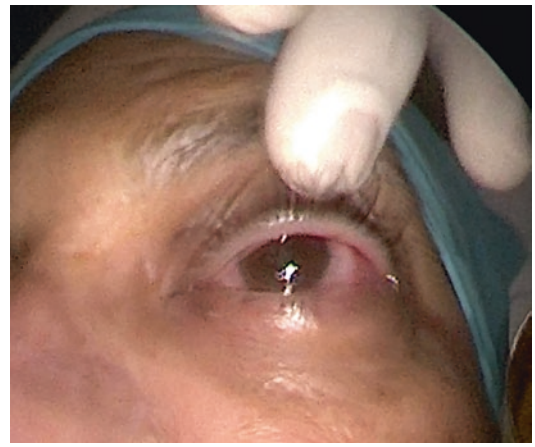

Fig. 8.41 Postoperative clinical photograph of the patient after endoscopic orbital debridement

There are, however, some clear indicatiors that PPF should be opened

1. Facial pain and numbness.
2. Any ocular symptom such as ptosis, proptosis, ophthalmoplegia, diplopia, and partial loss of vision, etc.
3. Intracranial involvement regardless of the spread path.
4. Massive disease involving the cheek.
5. During orbital exenteration as an adjuvant (endoscopic or external).

Advantages of Denker's medial maxillectomy

- It is required to reach the PPF fossa, and in extensive disease, infratemporal fossa can be cleared as well.
- It also allows for more access which makes clearing of orbital or intracranial disease easier.
- It was thus the mainstay of mucor management in most of the cases during mucor endemic in India. Most of the patients pre-

sented with aggressive disease and orbital manifestation were the first sign in 60% of our cases. Therefore, it became mandatory to perform Denkers in all these cases.

- Only those instances on multiple MRI sequences that showed no signs of dissemination beyond sinuses were excluded. However, due to the disease's aggressive nature during the second wave of the Covid pandemic in India such cases were extremely rare.

References

1. Hosseini SMS, Borghei P. Rhinocerebral mucormycosis: pathways of spread. Eur Arch Otorhinolaryngol. 2005;262:932–8. https://doi.org/10.1007/s00405-005-0919-0.
2. Honavar SG. Code mucor: guidelines for the diagnosis, staging and management of rhino-orbito-cerebral mucormycosis in the setting of COVID-19. Indian J Ophthalmol. 2021;69(6):1361–5. https://doi.org/10.4103/ijo.IJO_1165_21.
3. Naik MN, Rath S. The ROC staging system for COVID-related rhino-orbital-cerebral Mucormycosis. Semin Ophthalmol. 2021; https://doi.org/10.1080/08820538.2021.1946094.
4. Shah K, Dave V, Bradoo R, Shinde C, Prathibha M. Orbital exenteration in rhino-orbito-cerebral Mucormycosis: a prospective analytical study with scoring system. Indian J Otolaryngol Head Neck Surg. 2019;71(2):259–65. https://doi.org/10.1007/s12070-018-1293-8.
5. Talmi YP, Goldschmied-Reouven A, Bakon M, Barshack I, Wolf M, Horowitz Z, Berkowicz M, Keller N, Kronenberg J. Rhino-orbital and rhino-orbito-cerebral mucormycosis. Otolaryngol Head Neck Surg. 2002;127(1):22–31. https://doi.org/10.1067/mhn.2002.126587.
6. Wali U, Balkhair A, Al-Mujaini A. Cerebro-rhino orbital mucormycosis: an update. J Infect Public Health. 2012;5(2):116–26., ISSN 1876-0341. https://doi.org/10.1016/j.jiph.2012.01.003.
7. Hendrickson RG, Olshaker J, Duckett O. Rhinocerebral mucormycosis: a case of a rare but deadly disease. J Emerg Med. 1999;17:641–5. times has been challenged by others 10
8. Prabhu RM, Patel R. Mucormycosis and entomophthoramycosis: a review of the clinical manifestations, diagnosis and treatment. Clin Microbiol Infect. 2004;10:31–47.
9. Hussain S, Salahuddin N, Ahmad I, Salahudin I, Jooma R. Rhinocerebral invasive mycosis: occurrence in immunocompetent individuals. Eur J Radiol. 1995;20:151–5.
10. Pelton RW, Peterson EA, Patel BC, Davis K. Successful treatment of rhino-orbital mucormycosis without exenteration: the use of multiple treatment modalities. Ophthal Plast Reconstr Surg. 2001;17:62–6.
11. Raj P, Vella EJ, Bickerton RC. Successful treatment of rhinocerebral mucormycosis by a combination of aggressive surgical debridement and the use of systemic liposomal amphotericin B and local therapy with nebulized amphotericin – a case report. J Laryngol Otol. 1998;112:367–70.
12. Alleyne CH Jr, Vishteh AG, Spetzler RF, Detwiler PW. Long-term survival of a patient with invasive cranial base rhinocerebral mucormycosis treated with combined endovascular, surgical, and medical therapies: case report. Neurosurgery. 1999;45:1461–4.
13. Sponsler TA, Sassani JW, Johnson LN, Towfighi J. Ocular invasion in mucormycosis. Surv Ophthalmol. 1992;36:345–50.
14. Weprin BE, Hall WA, Goodman J, Adams GL. Longterm survival in rhinocerebral mucormycosis. Case report. J Neurosurg. 1998;88:570–5.
15. Neri G, Ciardo MG, Croce A. Rhinocerebral mucormycosis: report of a rare case in the head, neck and chest area. Acta Otorhinolaryngol Ital. 2002;22:28–33.
16. Upadhyay S, Dolci RL, Buohliqah L, Prevedello DM, Otto BA, Carrau RL. Endoscopic endonasal anterior maxillotomy. Laryngoscope. 2015;125(12):2668–71. https://doi.org/10.1002/lary.25205. Epub 2015 Feb 17
17. Denker A. Ein neuer Wegfur die operation der Malignen Nasentumoren. Munch Med Wochenschr. 1906;20:953–6.
18. Sturmann D. Die Intranasale Eroffnung der Kieferhohle. Berliner klinische Wochenschrift. 1908;45:1273–4.
19. Canfield RB. The submucous resection of the lateral nasal wall in chronic empyema of the antrum, ethmoid and sphenoid. JAMA. 1908;14:1136–41.
20. Kasemsiri P, Prevedello DM, Otto BA, Old M, Ditzel Filho L, Kassam AB, Carrau RL. Endoscopic endonasal technique: treatment of paranasal and anterior skull base malignancies. Braz J Otorhinolaryngol. 2013;79(6):760–79. English, Portuguese. https://doi.org/10.5935/1808-8694.20130138.
21. Youssef A, Carrau RL, Tantawy A, Ibrahim AA. Endoscopic approach to the infratemporal fossa. Alexandria J Med. 2014;50(2):127–30. https://doi.org/10.1016/j.ajme.2013.12.001.
22. Carrau R, Kassam A, Arriaga M. Anterior and subtemporal approaches to the infratemporal fossa. Otologic surgery. 3rd ed. Brackmann Shelton Arriaga Saunders Elsevier, Philadelphia. 2010. [Crossref], [Google Scholar]
23. Hitotsumatsu T, Rhoton AL Jr. Unilateral upper and lower subtotal maxillectomy approaches to the cranial base: microsurgical anatomy. Neurosurgery. 2001;46:4161452 [Crossref], [Web of Science®], [Google Scholar]
24. Isolan GR, Rowe R, Al-Mefty O. Microanatomy and surgical approaches to the infratemporal fossa: an anaglyphic three dimensional stereoscopic printing study. Skull Base. 2007;17:285302 [Crossref], [Google Scholar]

9 Surgical Management of Rhino-Orbito-Cerebral Mucormycosis; Drilling Beyond Sinuses in Rhino-Orbito-Cerebral Mucormycosis

Satish Jain and Nishi Gupta

Meticulous debridement and thorough cleaning of the involved area are essential in managing rhino-orbito-cerebral mucormycosis (ROCM). Because there is no penetration of drugs in the bone and necrotic tissue; therefore, all this dead tissue must be debrided. After seeing every type of ROCM and close follow-up of cases, we have been able to refine our technique in a way that is sure to enhance survival in ROCM cases. During the Indian mucormycosis outbreak, the front line teams did an excellent job of addressing the critical areas of in ROCM.

Various aspects of surgical management in ROCM have been described as separate chapters, including basic endoscopic sinus surgery procedures, approach to the pterygopalatine fossa, pterygoid process, infratemporal fossa, orbit, globe sparing orbital exenteration and craniocerebral mucormycosis.

However, there are some preferential areas involved in ROCM, like the pterygoid process, greater wing of the sphenoid, floor of the sphenoid sinus and clivus. During endoscopic debridement of sinuses, sometimes the sphenoid sinus lumen looks healthy after the disease is cleared, but the sphenoid floor might be involved. A preoperative MRI scan of this area may be beneficial, and if it is implicated it must be drilled. Drilling in these places is dangerous due to the vital structures in the vicinity. However, a good knowledge of anatomy helps in the thorough debridement of these areas.

The steps and necessity of cleaning the Pterygoid bone, Sphenoid Bone, Clivus, the frontal sinus, and the ethmoidal roof are highlighted in this chapter.

9.1 Pterygoid Bone

Since the pterygopalatine fossa (PPF) acts as the reservoir of disease [1], Denkers modified median maxillectomy is done in all cases except those with limited disease [2, 3]. It helps in clearing the PPF and infratemporal fossa and provides a better view of the orbit.

The authors found a significantly higher possibility of residual/recurrent disease where the pterygoid wedge acted as a hidden area and was not addressed in the first surgery. Mucormycosis simillar to juvenile nasopharyngeal angiofibroma infiltrates the Haversian canal of pterygoid bone. As a result pterygoid wedge drilling reduces the risk of residual disease [4, 5].

S. Jain
Jain ENT Hospital, Jaipur, India

N. Gupta (✉)
Department of Otorhinolaryngology, Dr Shroff's Charity Eye Hospital, New Delhi, India

N. Gupta, S. G. Honavar (eds.), *Rhino-Orbito-Cerebral Mucormycosis*,
https://doi.org/10.1007/978-981-16-9729-6_9

Drilling the pterygoid, on the other hand, necessitates a high level of competence as well as a thorough understanding of anatomy. This chapter depicts the many steps needed in the clearing pterygoid bone and drilling beyond the pterygoids using illustrations.

Steps

- After Denker's medial maxillectomy, a complete sphenoethmoidectomy, and orbital clearance, the posterior wall of the maxilla and the pterygoid process are evaluated, and the weak bone is removed with Luc's forceps (Figs. 9.1 and 9.2).
- After drilling the the pterygoid wedge and clearance of PPF, a clear view of structures such as Maxillary nerve (V2) and Vidian nerve can be seen (Fig. 9.3).
- The bone around V2 and Vidian nerve appears to be diseased and weak and it can be easily removed with forceps (Fig. 9.4). Because bone removal exposes the underlying disease;

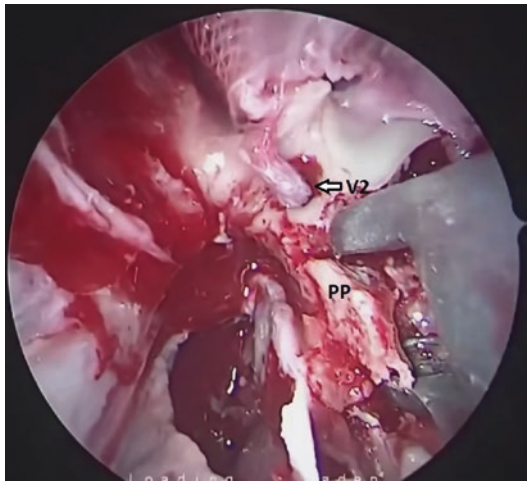

Fig. 9.1 Endoscopic view of the left nasal cavity after Denker's median maxillectomy and pterygoid process (PP) clearing

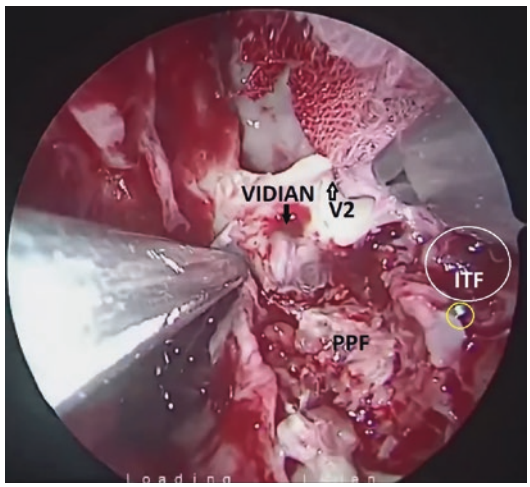

Fig. 9.2 A clear view of foramen rotundum with V2 laterally and Vidian at sphenoid's floor as well as pterygopalatine fossa (PPF), ITF; Infratemporal fossa

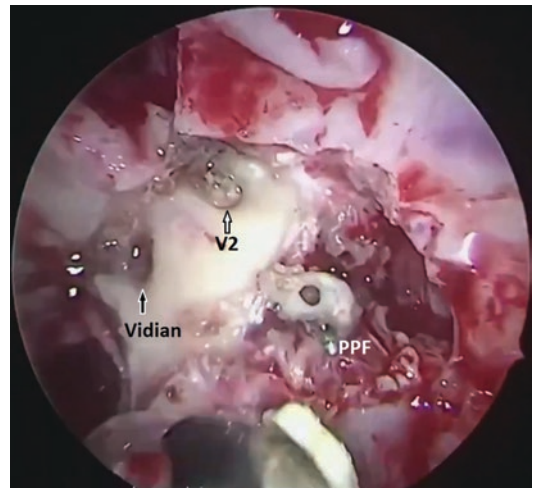

Fig. 9.3 A close-up of V2, the Vidian nerve reveals the diseased bone that surrounds it

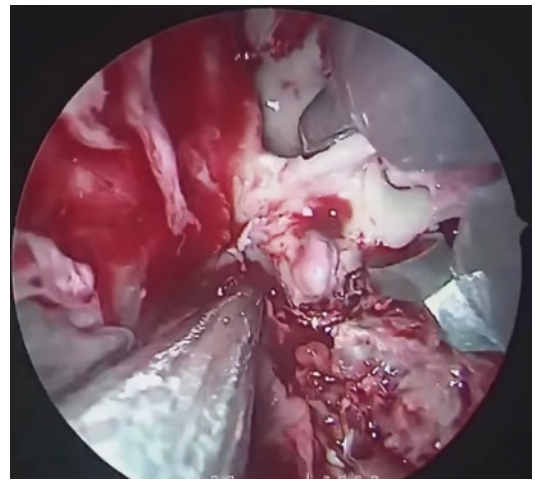

Fig. 9.4 Luc's forceps were used to remove the osteomyelitic bone from around foramen rotundum

more bone is removed (Fig. 9.5). Deep skull infiltration with mucormycosis can be seen (Fig. 9.6).

- The infected area is suctioned clean and heavy strands of discharge are removed (Fig. 9.7).

9.2 Sphenoid Bone

The bone that surround the Vidian canal is removed (Fig. 9.8). The steps of clearing sphenoid bone are demonstrated in (Figs. 9.9, 9.10, 9.11, 9.12, 9.13, 9.14, 9.15, and 9.16). Drilling takes place around the Vidian nerve (Figs. 9.17 and 9.18). The Vidian nerve serves as an important landmark for the carotid artery (CA) (Fig. 9.19). The carotid artery is safe as long as the drilling is done below the Vidian nerve.

The next step is the removal of the thin bone from the face of the sphenoid to get a head-on view of the sphenoid sinus. This bone removal is done using a chisel and hammer, and the sphenoid sinus is cleared (Figs. 9.20 and 9.21).

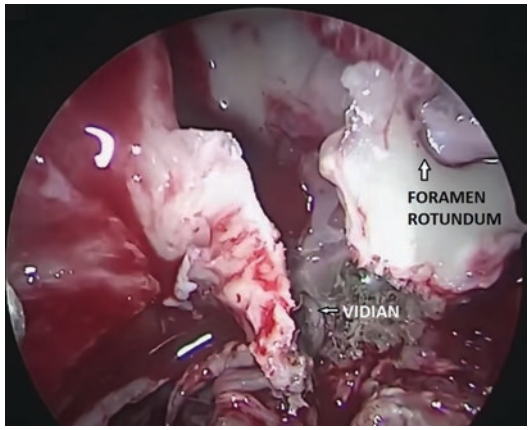

Fig. 9.5 After removing bone the hidden disease becomes evident

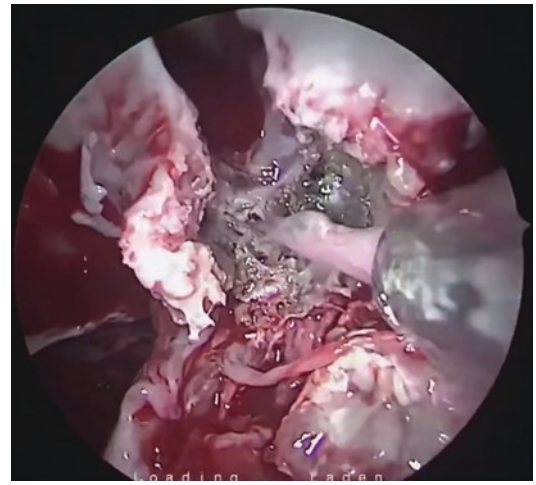

Fig. 9.7 Mucoid secretions strands with the necrotic material over the greater wing of the sphenoid

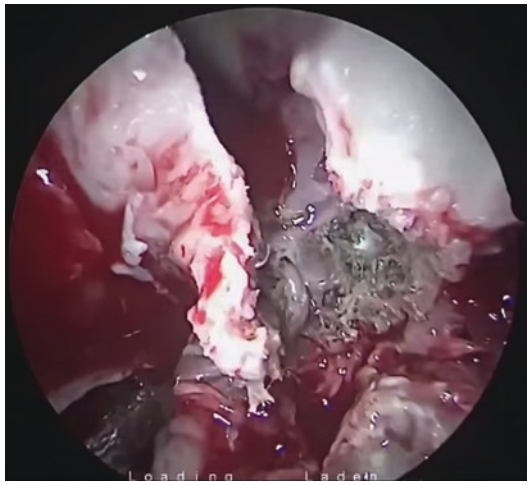

Fig. 9.6 The sphenoid bone has been infiltrated

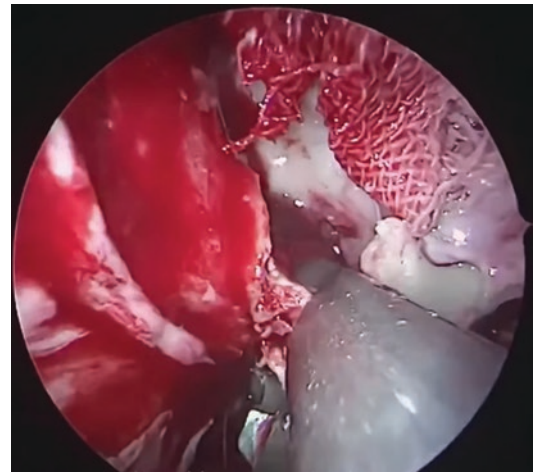

Fig. 9.8 Luc's forceps are used to remove more bone around Vidian nerve

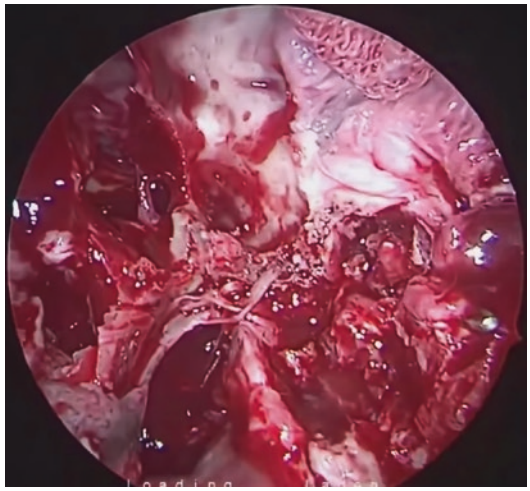

Fig. 9.9 Greater wing of sphenoid infiltrated with the disease

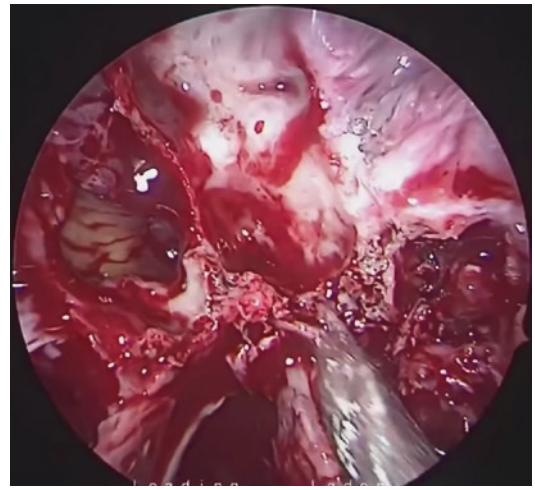

Fig. 9.11 The sphenoid sinus lumen is clean while the greater wing of the sphenoid is infiltrated

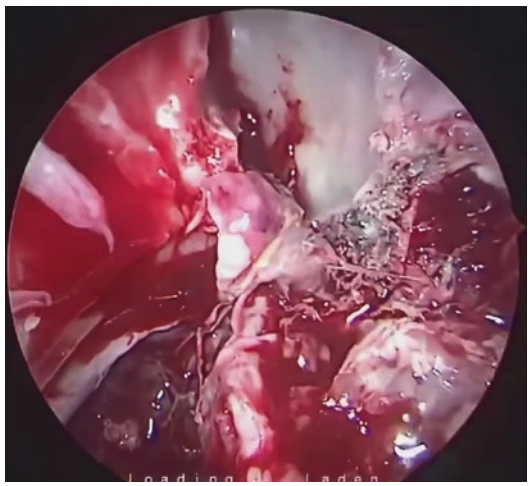

Fig. 9.10 Infiltration of deep skull base

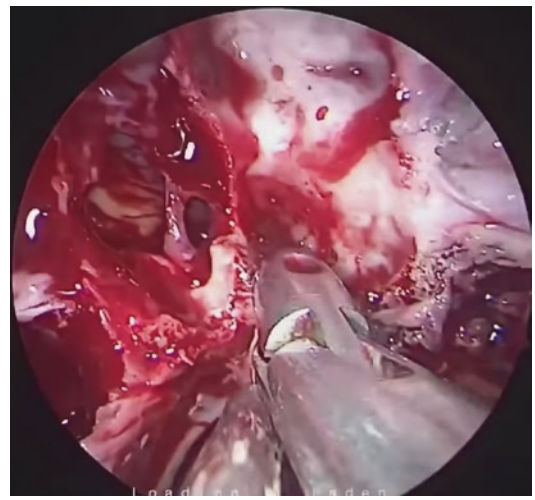

Fig. 9.12 Clearing the disease from the sphenoid bone

9.3 Clivus Drilling

- The clivus drilling starts from the inferior aspect of the sphenoid sinuses. The bone along the floor of the sphenoid sinus is removed using forceps (Figs. 9.22, 9.23, 9.24, and 9.25).
- A clear view of the lumen of the sphenoid sinus is obtained with sella turcica, clival recess and orbit in view (Fig. 9.25).
- A coblator is used to elevate the nasopharyngeal periosteum, and the eustachian tube area is also coagulated (Figs. 9.26 and 9.27).
- Clivus drilling begins after a decent exposure (Fig. 9.28). Clivus handling creates a lot of bleeding in normal circumstances, making it difficult to work in the clival region. In mucor indued osteomyelitis there is no bleeding during the drilling of clivus due to the loss of blood supply (Figs. 9.29, 9.30, 9.31, and 9.32). The bone is porous, blackish and fragile. Drilling is carried out untill healthy bone is seen.

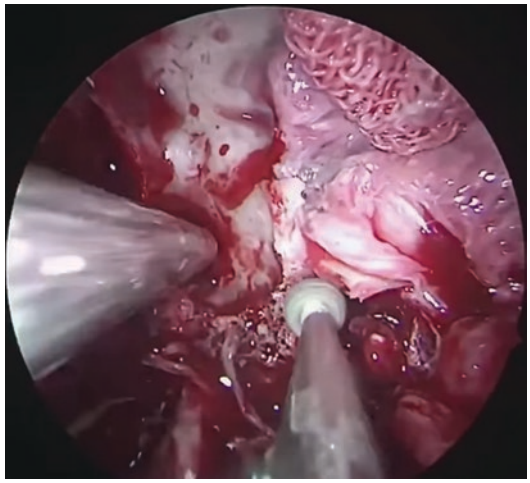

Fig. 9.13 Drilling the bone over the greater wing of the sphenoid

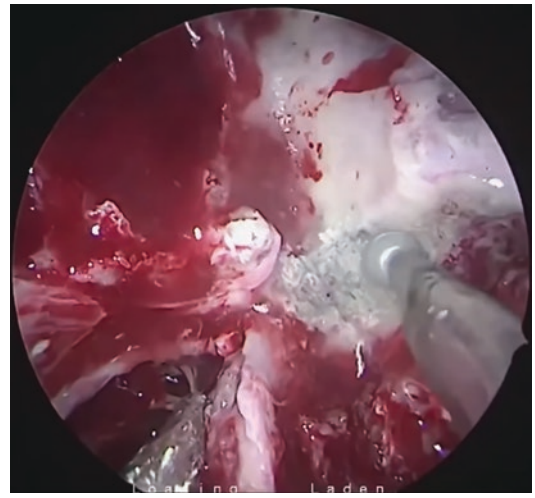

Fig. 9.15 Drilling continues untill the bone is no longer unhealthy

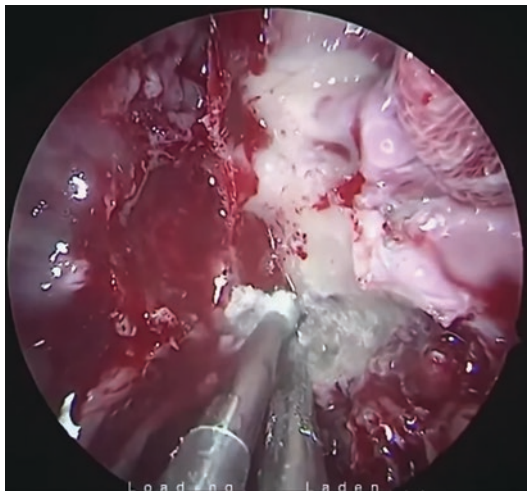

Fig. 9.14 Drilling reveals a necrotic bone

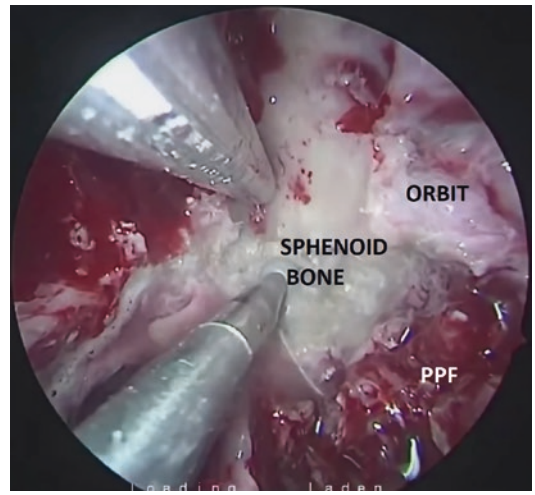

Fig. 9.16 Healthy bone start appearing after drilling the damaged bone

9.4 Frontal Sinus (Figs. 9.33, 9.34, and 9.35)

Although the frontal sinus is not often involved in ROCM, it must be debrided if it is. In this case, disease from the adjacent cribriform area was also cleaned. Careful identification and debridement of the affected areas led to better outcomes.

This chapter focuses on the locations that may have hidden disease. These are tough to access and demand a high level of expertise. The procedure for clearing these regions via endoscopic means is discussed. This will aid readers in not only focusing on these regions on preoperative imaging, but also in performing an effective surgical clearance. Debridement with care yields great results.

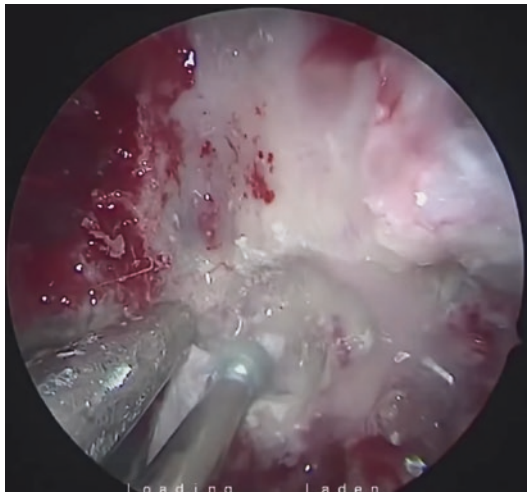

Fig. 9.17 Drilling around the Vidian is done to thin out the affected bone even more

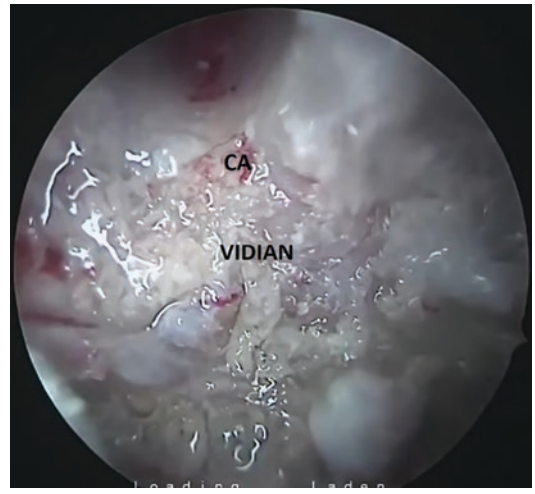

Fig. 9.19 Underneath the thinned-out bone, a glimpse of the carotid can be seen

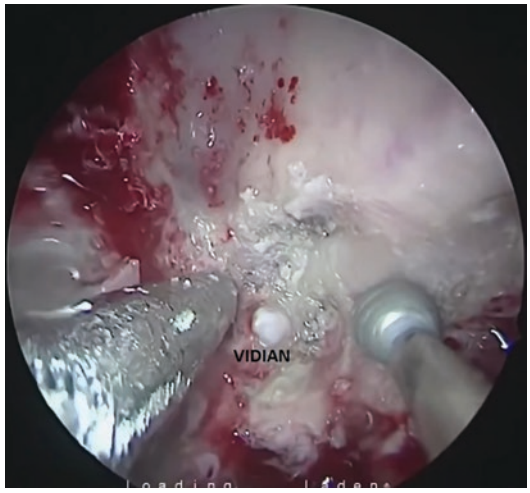

Fig. 9.18 The healthy plate of bone begins to appear

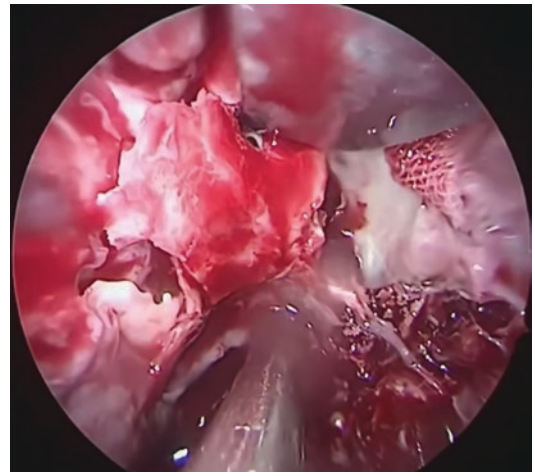

Fig. 9.20 Removal of the thin bone covering the face of the sphenoid sinus using a chisel and hammer

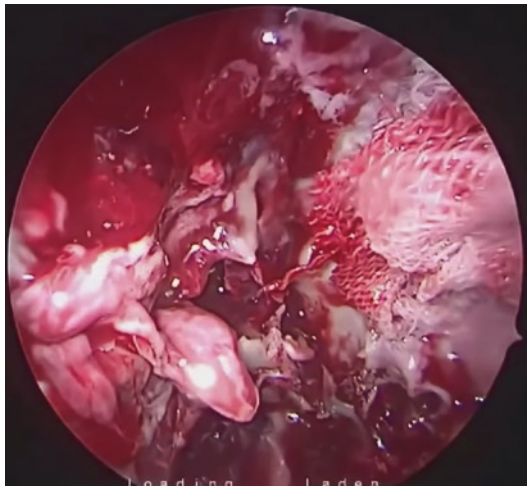

Fig. 9.21 The sphenoid sinus, as well as the septum next to it, is infected

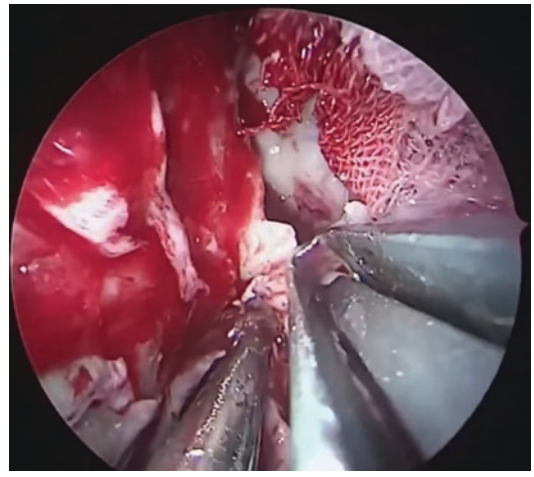

Fig. 9.23 Bone is removed from the sphenoid sinus's floor

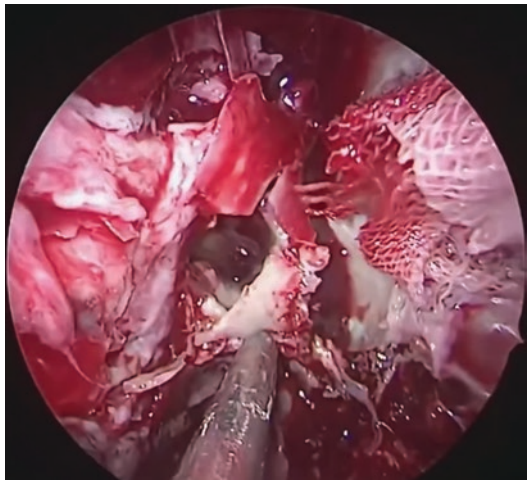

Fig. 9.22 Clearance of the disease from Sphenoid sinus disease with a clear view of sinus's lumen

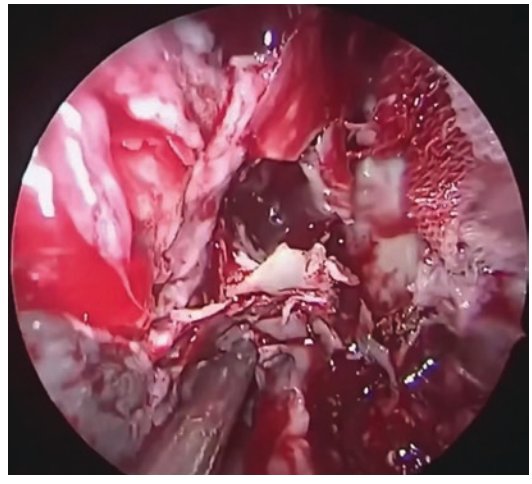

Fig. 9.24 The sphenoid sinus is clearly visible

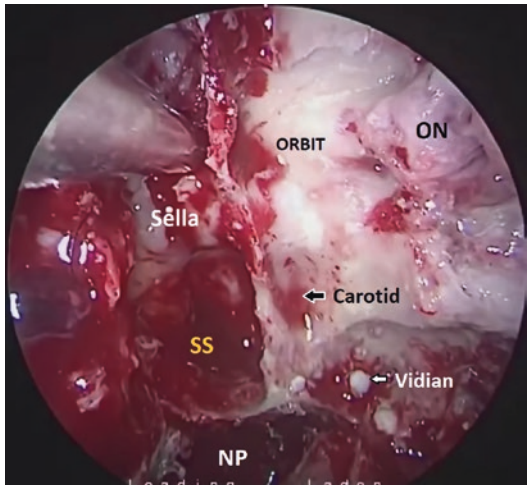

Fig. 9.25 A close-up of the anatomy including the sphenoid sinus (SS), sella turcica, clival recess and nasopharynx

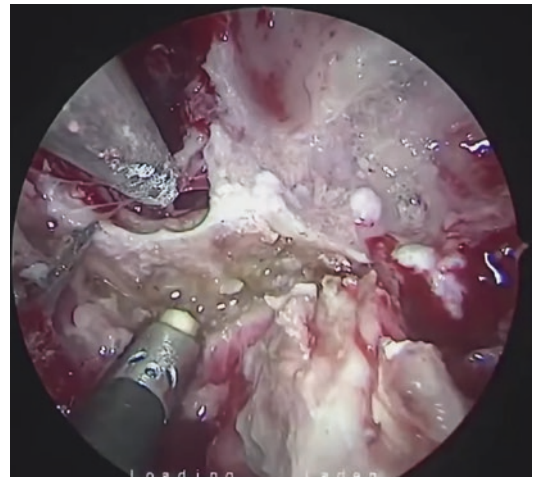

Fig. 9.27 The periosteum of the nasopharynx is lifted

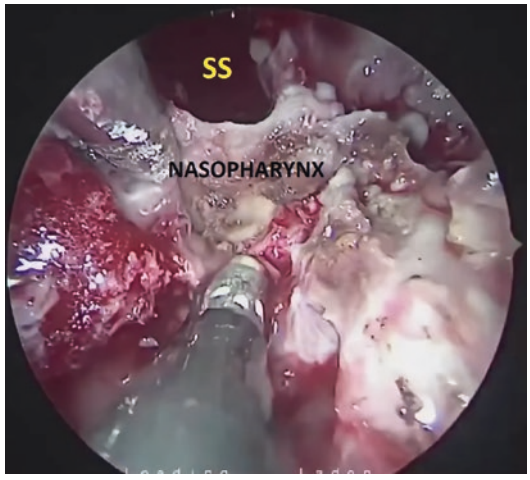

Fig. 9.26 The nasopharyngeal periosteal flap is lifted with a coblator. SS stands for Sphenoid sinus

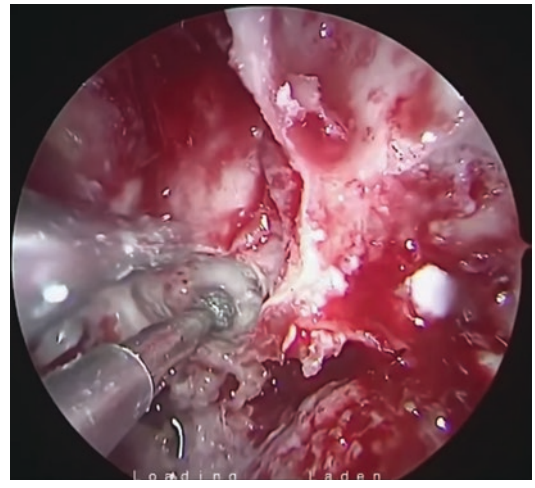

Fig. 9.28 Drilling of unhealthy Clivus bone to clear the disease

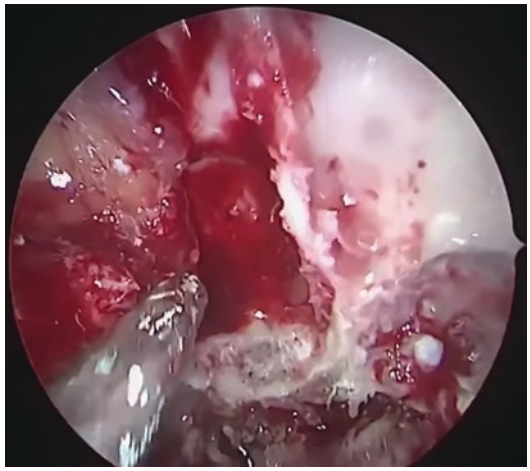

Fig. 9.29 The Clivus bone is periodically examined and is found to be necrotic with minimal bleeding during drilling, unlike in other skull base procedures

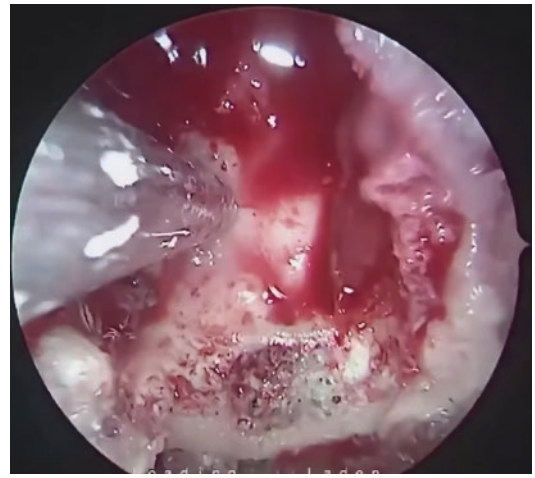

Fig. 9.31 In the clival region an unhealthy porous bone is seen with a blackish discolouration

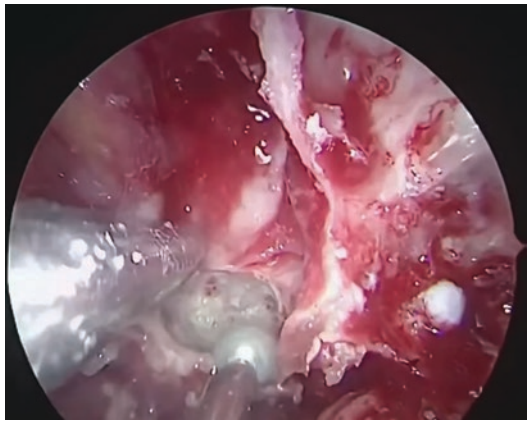

Fig. 9.30 Drilling is continued in clival area untill healthy bone is found

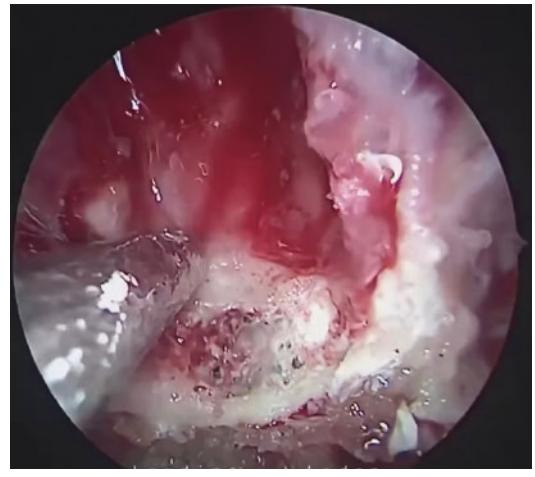

Fig. 9.32 This unhealthy porous blackish clivus bone is further drilled

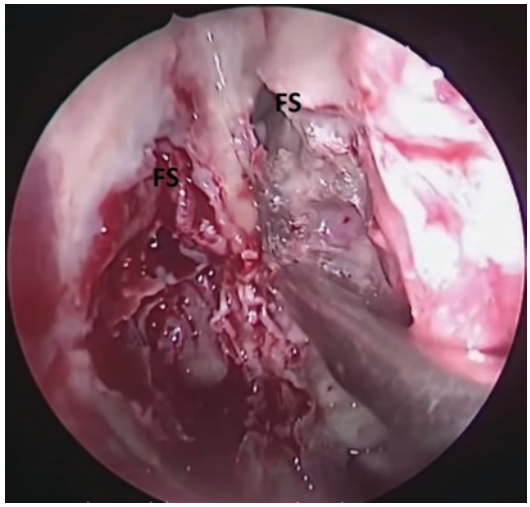

Fig. 9.33 The ethmoid roof has been free of disease with frontal sinuses of both sides in view. FS; Frontal sinus

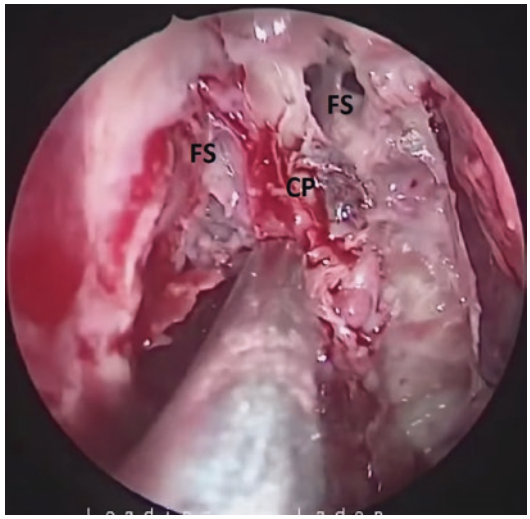

Fig. 9.34 The area around the Cribriform plate (CP) is free of disease

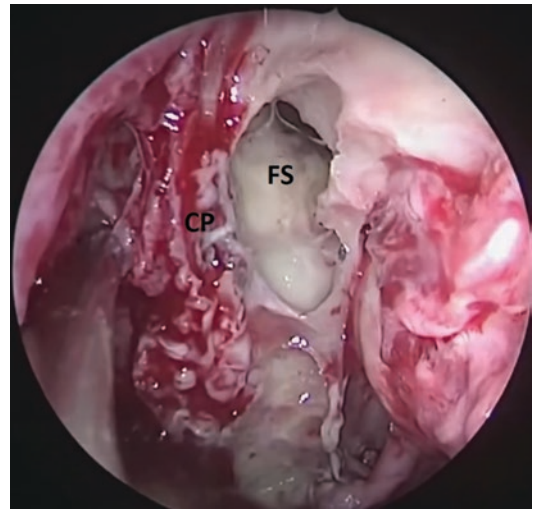

Fig. 9.35 The frontal sinuses on both sides are opened

References

1. Upadhyay S, Dolci RL, Buohliqah L, Prevedello DM, Otto BA, Carrau RL. Endoscopic endonasal anterior maxillotomy. Laryngoscope. 2015;125(12):2668–71. https://doi.org/10.1002/lary.25205. Epub 2015 Feb 17
2. Denker A. Ein neuer Wegfur die Operation der Malignen Nasentumoren. Munch Med Wochenschr. 1906;20:953–6.
3. Janakiram TN, Sharma SB, Kasper E, Deshmukh O, Cherian I. Comprehensive preoperative staging system for endoscopic single and multicorridor approaches to juvenile nasal angiofibromas. Surg Neurol Int. 2017;8:55. https://doi.org/10.4103/sni.sni_295_16.
4. Janakiram TN, Sharma SB, Samavedam UC, Deshmukh O, Rajalingam B. Imaging in Juvenile nasopharyngeal angiofibroma: clinical significance of ramharan and chopstick sign. Indian J Otolaryngol Head Neck Surg. 2017;69(1):81–7. https://doi.org/10.1007/s12070-016-1039-4. Epub 2016 Dec 23
5. Hosseini SMS, Borghei P. Rhinocerebral mucormycosis: pathways of spread. Eur Arch Otorhinolaryngol. 2005;262:932–8. https://doi.org/10.1007/s00405-005-0919-0.

10 Globe Sparing Transnasal Endoscopic Orbital Exenteration in Rhino-Orbito-Cerebral Mucormycosis

Satish Jain and Nishi Gupta

Catalano et al. coined the phrase globe sparing orbital exenteration [1]. They performed globe sparing orbital exenteration in malignant tumours of the sinuses, infratemporal fossa, orbital adnexa, cavernous sinus, and clival area that involved the posterior part of the orbit. Malignant tumours of the lacrimal gland, eyelids, conjunctiva, and medial or lateral canthal areas were all excluded. They also ruled out tumours that had come in contact with the Tenon's capsule [1].

Orbital exenteration is defined as the removal of the entire contents of the orbit, including the periorbita, appendages and eyelids with or without the surrounding skin [2]. Total orbital exenteration involving the globe, periorbita, and retrobulbar structures has long been the surgical standard of care for rhino-orbital-cerebral mucormycosis (ROCM) [3]. From time to time different authors have proposed various modifications in the extent of resection during orbital exenteration [4, 5]. Orbital exenteration is cosmetically disfiguring and causes functional, aesthetic, and psychological consequences.

Some studies have shown that orbital exenteration may not be required in all cases of rhino-orbio-cerebral mucormycosis but there is no clear consensus whether orbital preservation is safe [6–11].

During the Covid pandemic, a novel method of globe sparing orbital exenteration was developed for the treatment of orbital mucormycosis. The damaged orbital tissue was debrided using a transnasal endoscopic method, avoiding the loss of globe and the optic nerve.

This chapter describes the surgical steps of endoscopic globe sparing orbital exenteration approach for controlling the orbital portion of rhino-orbito-cerebral mucormycosis (ROCM). Depending on the severity of the disease, it entails radical endoscopic debridement of the orbital content. Globe sparing orbital exenteration is a novel approach that has shown encouraging results. The method gained popularity when an extended series of globe preserving orbital exenterations were performed during a mucormycosis outbreak in India.

The initial few cases admitted for this procedure had extensive orbital disease with signs of total ophthalmoplegia and vision loss. The anterior contents of the orbit, including eyelids, conjunctiva, cornea, and lens, were all intact in these cases. An aggressive transnasal endoscopic orbital clearance of all the retroorbital diseased tissue was performed, sparing the globe, optic nerve, and the conjunctiva. The cosmetic appearance of the eye was preserved due to the rich blood supply and collaterals in the anterior part.

S. Jain
Jain ENT Hospital, Jaipur, India

N. Gupta (✉)
Department of Otorhinolaryngology, Dr Shroff's Charity Eye Hospital, New Delhi, India

N. Gupta, S. G. Honavar (eds.), *Rhino-Orbito-Cerebral Mucormycosis*,
https://doi.org/10.1007/978-981-16-9729-6_10

Encouraged by the outcomes, we began doing endoscopic orbital debridement in all cases of orbital mucormycosis, including those with limited disease and normal vision. Postoperatively good mucosalization of the orbital cavity took place, and surgeons were able to retain the ashtetic look of the eye in the majority of the patients. Those with the advanced disease showed changes in the shape and occasional fistula which were treated subsequently. Patients, on the other hand, preferred this preserved globe over complete exenteration.

10.1 Blood Supply

Orbit gets its vascular supply from the ophthalmic artery (a branch of internal carotid artery) and vein, central retinal artery (the first branch from an ophthalmic artery) and vein, facial artery and vein and anterior and posterior ethmoidal vessels, supratrochlear artery, medial palpebral arteries, and supraorbital arteries. Vessels make extensive collateral around the anterior part of the orbit including eyelids, conjunctiva, cornea, medial and lateral canthal tendon, and Tenon's capsule [1].

This arterial and venous arcade via branches of the external carotid and jugular venous systems, respectively, keeps the globe vascularized after the globe sparing extensive retrobulbar radical debridement [1]. The viability of the anterior structures is unaffected by any interruption of the blood supply of the posterior content.

10.2 Indications of Globe Sparing Orbital Exenteration

- All cases of limited or extensive orbital disease with the intact anterior part of the eye including cornea, conjunctiva, lids, etc., are good candidates for globe sparing orbital exenteration.

10.3 Contraindications of Globe Sparing Orbital Exenteration

- It is contraindicated in the disease invading the globe, medial and lateral canthal tendon, conjunctiva, or Tenon's capsule.
- Extensive disease involving the skin of the eyelids and cheek.
- Involvement of palate with massive orbital disease involving anterior orbital contents.

10.4 Role of MRI in Decision Making

Multiple sequences of MRI, including T2W, T2W fat-suppressed, T1W, and T1W with contrast, should be done in all cases. In cases of impending vision loss or the presence of bilateral disease on preoperative MRI, diffusion-weighted MRI and MR angiography should also be done. Various sequences are ordered and studied in collaboration with the radiologist for the disease mapping. Diffusion-weighted MRI and MRI angiography help in prognostication and counselling of the patient. From a medicolegal point of view, it is essential that the patient is made well aware of all these complications before any intervention. Surgeons must obtain written informed consent from the patient about the possibility of postoperative vision loss due to impending damage based on the presence of thrombus in the optic nerve on DW MRI. The decision regarding the extent of debridement is based on the detailed mapping of the disease on MRI. Various sequences of MRI are put together to differentiate between inflammation, secretions, and the disease. Anything that enhances on fat-suppressed MRI is the disease, while enhancement on a routine MRI is normal. In contrast-enhanced MRI, the diseased portion will not be enhanced. An excellent intraoperative correlation of MRI findings results in adequate disease clearance.

Case 1

MRI

Figure 10.1 shows a comparison of 3 MRI sequences to evaluate the extent of orbital disease. The first image is fat-suppressed (Fig. 10.1a), the second is non-fat suppressed (Fig. 10.1b), and the third is contrast-enhanced (Fig. 10.1c). In the first fat-suppressed image, disease in the maxillary antrum is hyperintense, and the enhancing areas in the orbit represent disease (Fig. 10.1a). In the second image, the inflammation is seen with high intensity in the maxilla, ethmoid, and orbit. As the fat is suppressed, it is easy to map the disease in orbit (Fig. 10.1b). In the third contrast-enhanced image, there is no enhancement in the maxillary ethmoid and orbital areas, confirming the presence of disease (Fig. 10.1c).

Steps of Surgery

1. The first step is modified Denkers approach (as described in the chapter on Surgical management of Rhino-Orbito-Cerebral Mucormycosis (ROCM); approach to Pterygopalatine fossa, Pterygoid process, Infratemporal fossa, and orbit) followed by the ethmoidal and sphenoid sinus clearance to achieve a complete exposure before entering orbit. In endoscopic orbital debridement, decompression, or globe sparing orbital exenteration, the orbit is always entered from the medial side.
2. The lamina papyracea may be intact or may have a preexisting breach in cases of extensive disease. The lamina is removed to expose the periorbita, and all the thin bony chips covering the periorbita are removed (Fig. 10.2). Periorbita is incised and, the extent of the disease is examined.
3. Once inside the orbit, it is better to shift to a 70-degree endoscope and a Medtronic microdebrider Rad 60 blade (Medtronic Xomed Inc). The unhealthy orbital fat can be differentiated from the normal fat as the unhealthy fat is flaky and looks dirty. (Figs. 10.3 and 10.4). The orbit is retracted laterally by the assistant while the diseased portion is debrided. After the debridement is complete, a clear view of the entry site into the orbit is obtained (Fig. 10.5). At the end of the procedure, no necrotic area was seen inside the orbit (Fig. 10.6).

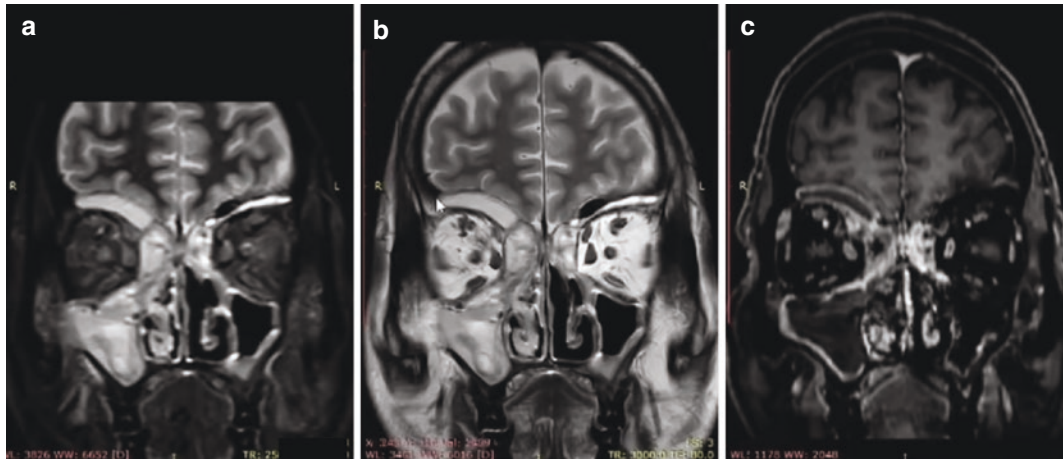

Fig. 10.1 Case 1 demonstrating a comparison of 3 MRI sequences in a case of orbital involvement in ROCM. (**a**) Fat-suppressed T2W image showing hyperintense areas in right maxillary antrum with enhancing areas in right orbit indicating limited disease. (**b**) Non-fat suppressed T2W image showing inflammation as high intensity in the right maxilla, ethmoid, and orbit. (**c**) On the contrast-enhanced image, there is loss of enhancement in the maxillary ethmoid and orbital areas, confirming the presence of disease

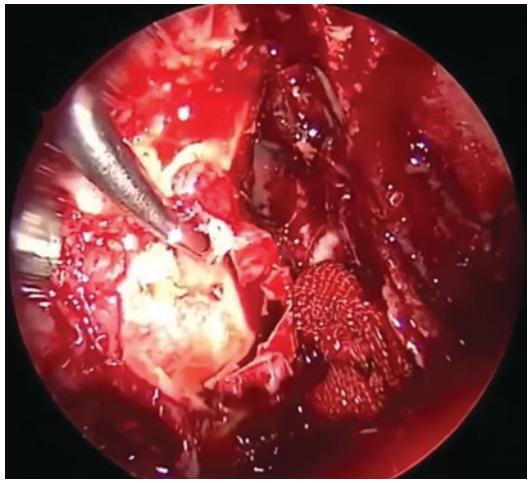

Fig. 10.2 Endoscopic view of the right nasal cavity showing removal of lamina papyracea to expose the right periorbita

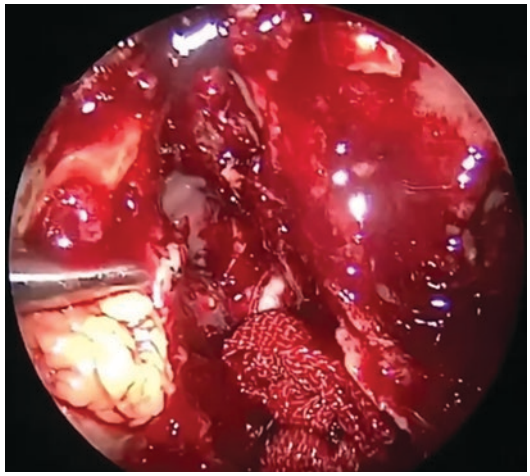

Fig. 10.3 Diseased fat from the superior part of the orbit is debrided

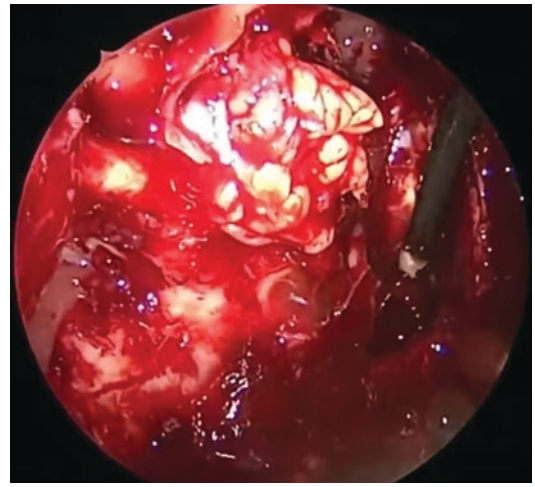

Fig. 10.4 Healthy orbital fat is seen after removing the diseased part from right orbit

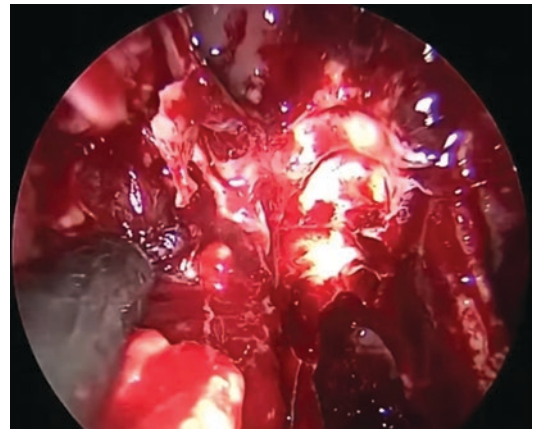

Fig. 10.5 To remove the disease from the inferior part of the orbit, the healthy fat is retracted up

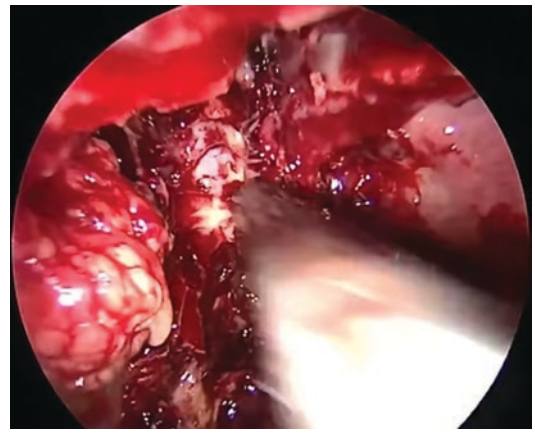

Fig. 10.6 No necrotic area is seen inside the right orbit at the end of the procedure

Case 2

MRI

Two sections of MRI can be seen in one frame, a fat-suppressed T2W MRI scan showing severe disease in the left orbit (Fig. 10.7a) and a normal T2W image showing enhancement in the left maxilla and with hypertrophy of all the recti muscles (Fig. 10.7b). The left eye has proptosis with the disease in the maxillary antrum with peri-antral spread. There is an invasion of the orbital floor and involvement of bilateral turbinates and the left orbital apex (Figs. 10.8 and 10.9).

On sagittal and coronal sections, extensive disease in the left orbit can be seen, involving the carotid artery and the cavernous sinus. The sella is enhanced but, there is a loss of contrast in the left cavernous sinus and left carotid artery, unlike the right side. On the right hand side, the carotid artery and cavernous sinus show regular enhancement (Fig. 10.10a, b). In the sagittal section, there is disease encasing the left carotid artery, extending to the cavernous sinus.

Steps of Surgery

1. The first four steps are the same as in case 1 (Figs. 10.11 and 10.12).
2. In case of extensive disease, a left modified Denker's median maxillectomy is done and, the orbital floor is examined. On removal of the lamina, the orbital contents start bulging into the nose (Fig. 10.13), and the unhealthy fat can be easily identified and debrided.
3. The unhealthy tissue looks dirty, friable, and darker than the usual yellow fat and is debrided using a 60-degree blade on a microdebrider (Figs. 10.14 and 10.15).
4. The disease has eroded the orbital apex, and all the structures, including the optic nerve, carotid artery, foramen rotundum with thrombosed maxillary nerve, and Vidian nerve, are visible. The orbital apex is approached by tracing the optic nerve and is cleaned meticulously. (Figs. 10.16 and 10.17a–c). The disease from the superior orbital fissure area is cleared (Figs. 10.18 and 10.19). Disease lateral to the nerve is cleared by gently retracting the optic nerve. (Figs. 10.20, 10.21, and 10.22).
5. The optic nerve is pushed inferiorly, and the diseased tissue in the retrobulbar area of the orbit is cleared (Figs. 10.23, 10.24, 10.25, 10.26, and 10.27).
6. The posterior neurovascular bundles come into view with the surrounding healthy area (Fig. 10.28). The globe is now reasonably mobile and is lifted gently to go lateral to clear the disease.
7. At the end of the procedure, the globe and intact optic nerve can be seen (Figs. 10.29 and 10.30a, b).
8. The intranasal endoscopic approach to the orbit provides excellent visualization, unlike external exenteration, where the posterior fat dissection is blind.
9. After the complete debridement of the disease, the operated area is irrigated with amphotericin B solution.

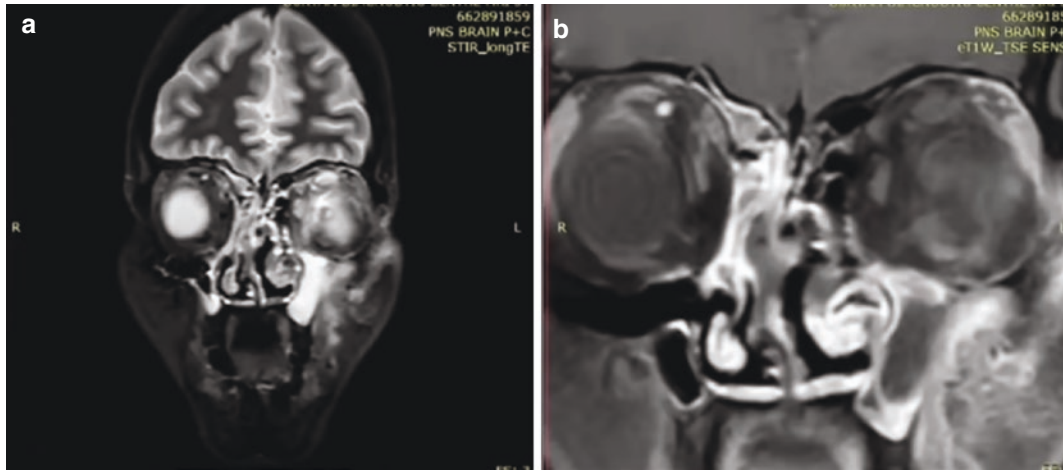

Fig. 10.7 (**a**) Case 2, Fat-suppressed T2W MRI demonstrating extensive disease in the left orbit. (**b**) A standard T2W image demonstrating enhancement in the left maxilla and hypertrophy of all recti muscles

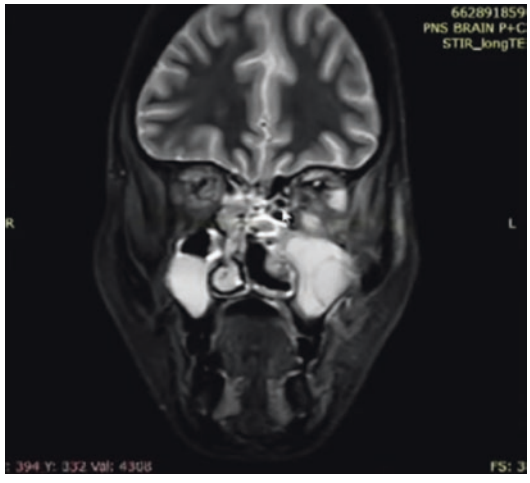

Fig. 10.8 The left eye has proptosis, and the disease is seen in the maxillary antrum with peri-antral spread

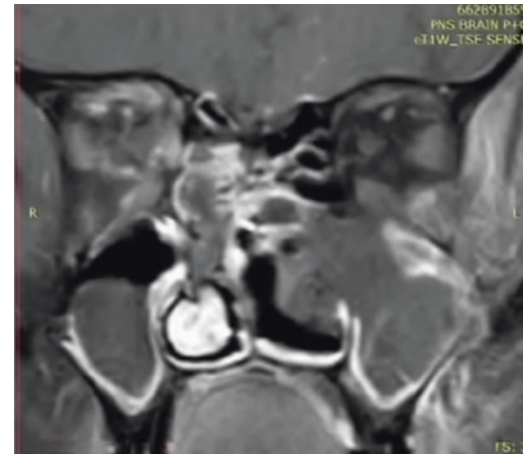

Fig. 10.9 There is an invasion of the orbital floor and the involvement of turbinates of both sides with the involvement of the orbital apex on the left

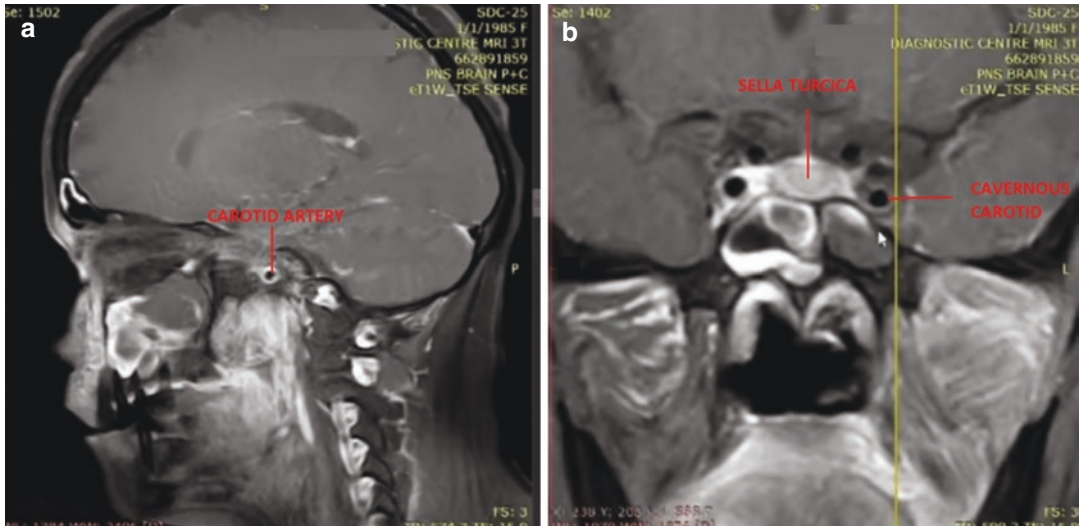

Fig. 10.10 (**a**) Sagittal section demonstrating the left carotid artery surrounded by the disease extending to the cavernous sinus. (**b**) The extensive disease is seen in the left orbit, involving the carotid artery and cavernous sinus in coronal sections. Sella can be seen enhancing in the middle, but there is a loss of contrast in the left cavernous sinus and left carotid artery, unlike the right side. On the right hand side, the carotid artery and cavernous sinus show regular enhancement

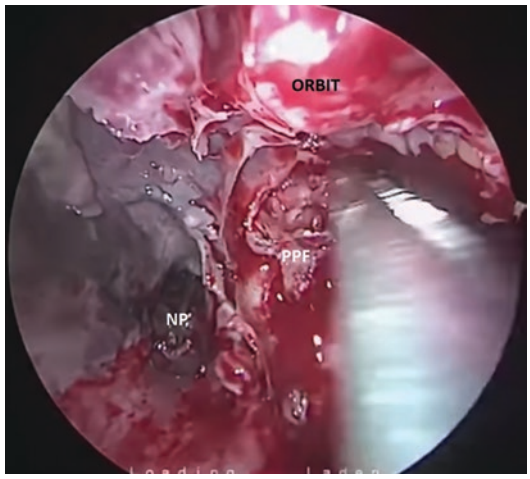

Fig. 10.11 Complete Denker's modified medial maxillectomy has been done with a view of the pterygopalatine fossa (PPF) and orbit. *NP* Nasopharynx

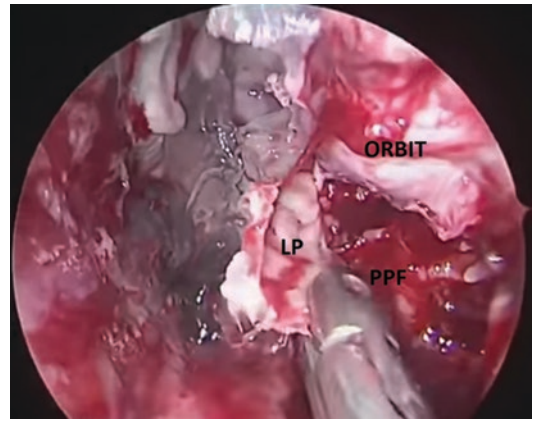

Fig. 10.12 The bony chips of lamina papyracea (LP) covering the periorbita are removed, PPF; Pterygopalatine fossa

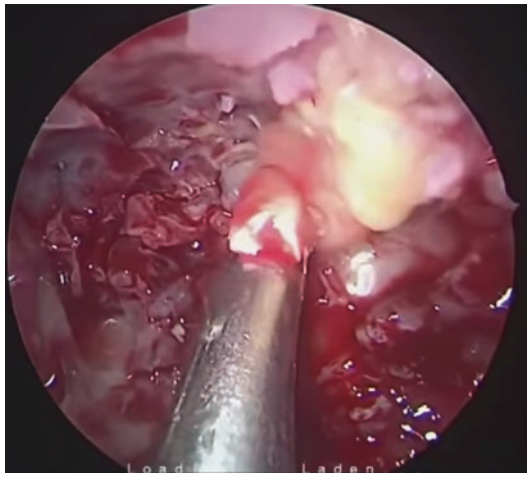

Fig. 10.13 Unhealthy fat is removed using a microdebrider

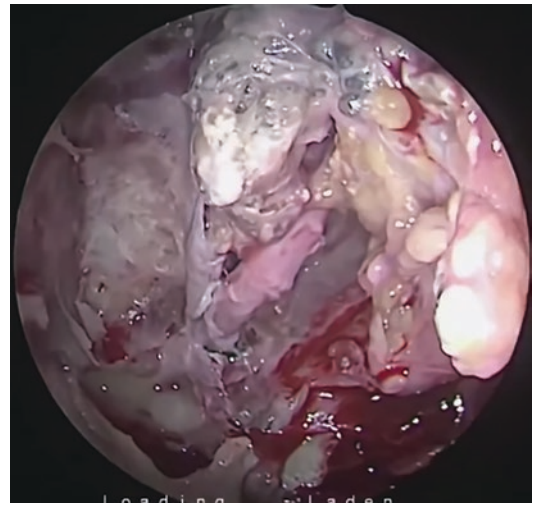

Fig. 10.15 Optic nerve can be seen in the centre with the diseased tissue all around it

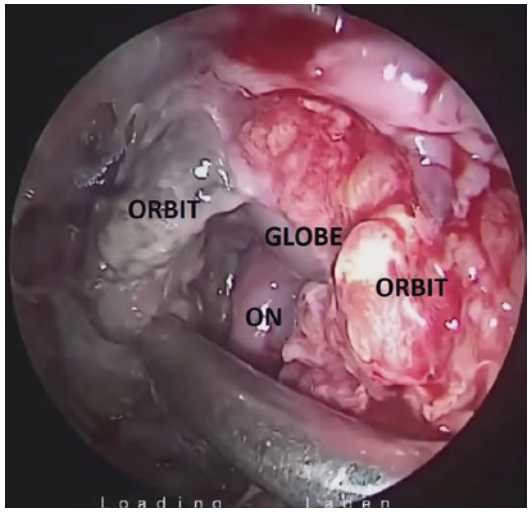

Fig. 10.14 Extensive disease can be seen filling the superior and inferior parts of the left orbit. In the central part, the globe and the optic nerve can be visualized after disease clearance. ON; Optic nerve

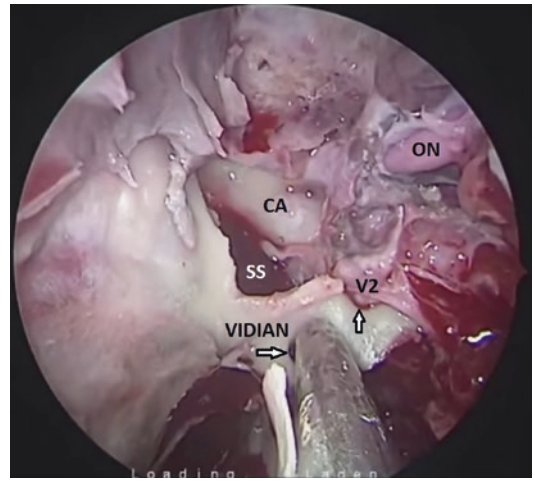

Fig. 10.16 Area of the left orbital apex (OA) is seen with the carotid artery (CA), optic nerve (ON), maxillary nerve (V2), and Vidian canal, SS; Sphenoid sinus

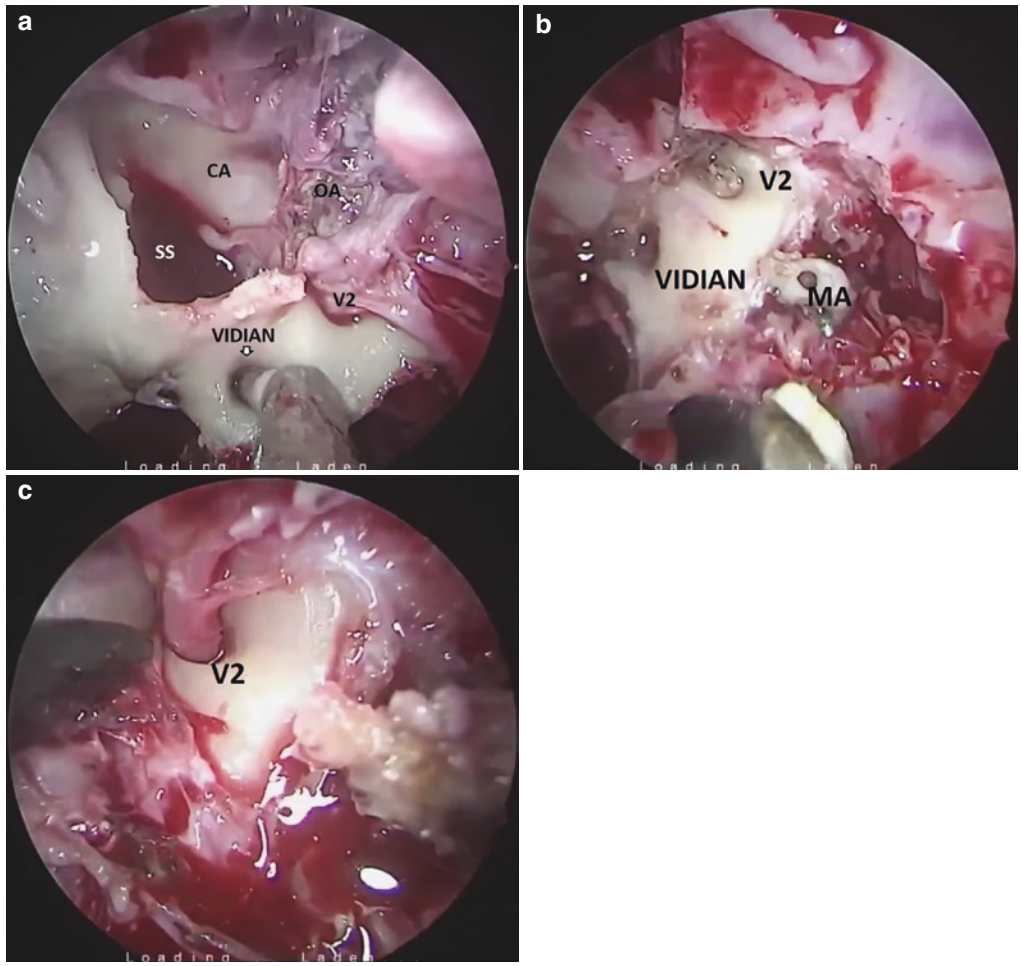

Fig. 10.17 A close-up view of the structures at the left orbital apex. (**a**) Maxillary nerve (V2) and Vidian canal can be seen. (**b**) V2, Vidian nerve and maxillary artery (MA) in view. (**c**) Thrombosed V2. CA; Carotid artery, OA; Orbital apex, MA; Maxillary artery

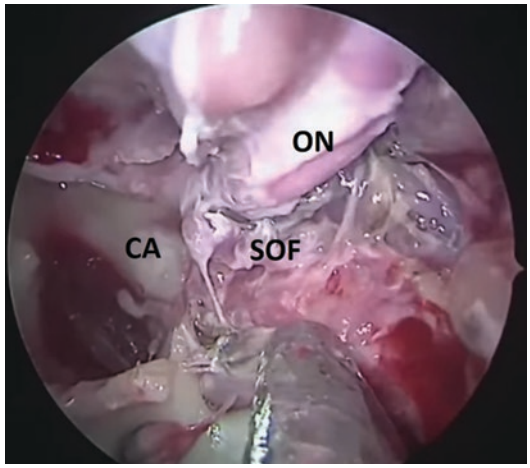

Fig. 10.18 Clearing the disease from the superior orbital fissure, SOF; superior orbital fissure, CA; Carotid artery, ON; Optic nerve

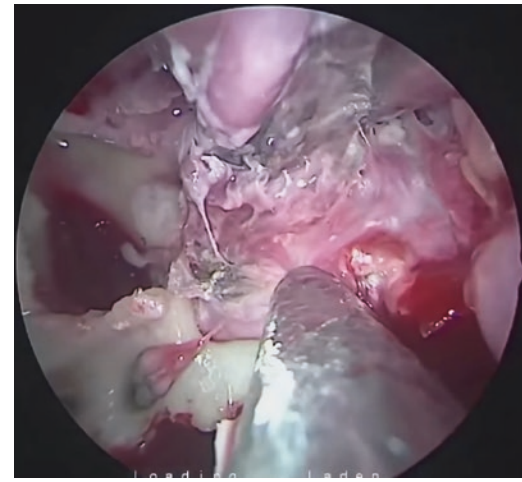

Fig. 10.19 Diseased tissue lateral to the optic nerve is debrided

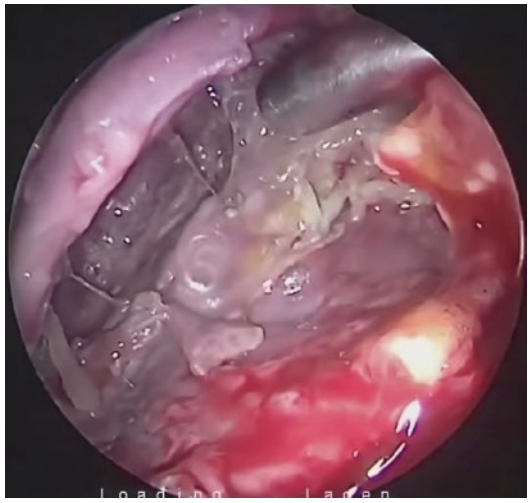

Fig. 10.20 Optic nerve is pushed up, and the retrobulbar area is cleared

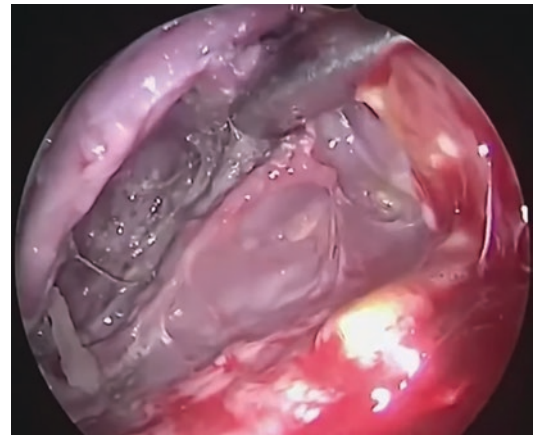

Fig. 10.22 The optic nerve is gently pushed up to clear the disease lateral to it

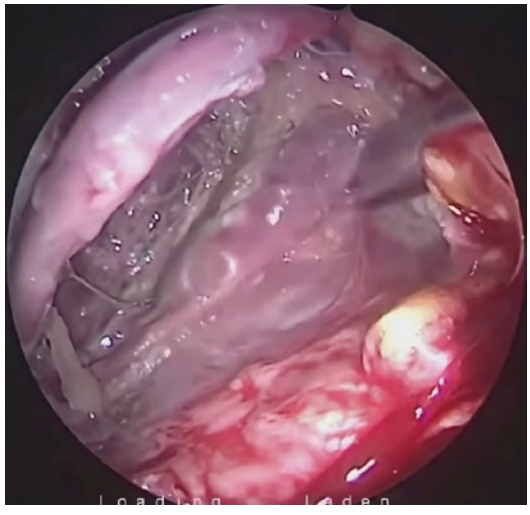

Fig. 10.21 Clearance of the disease posteriorly is continued

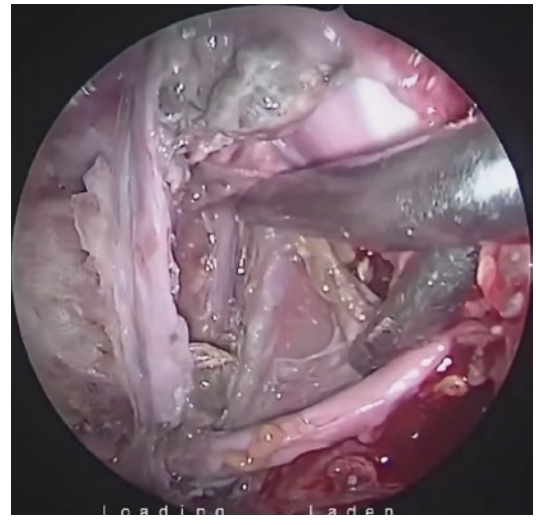

Fig. 10.23 The optic nerve is now pushed inferiorly to clear the disease from the superolateral part of the orbit

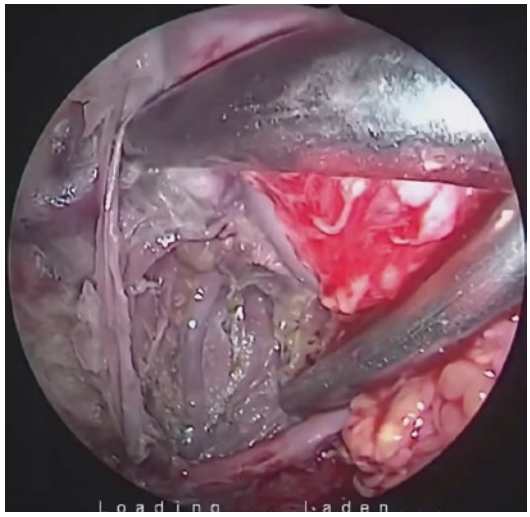

Fig. 10.24 Clearance of disease continues superiorly while the optic nerve is gently retracted and stabilized inferiorly

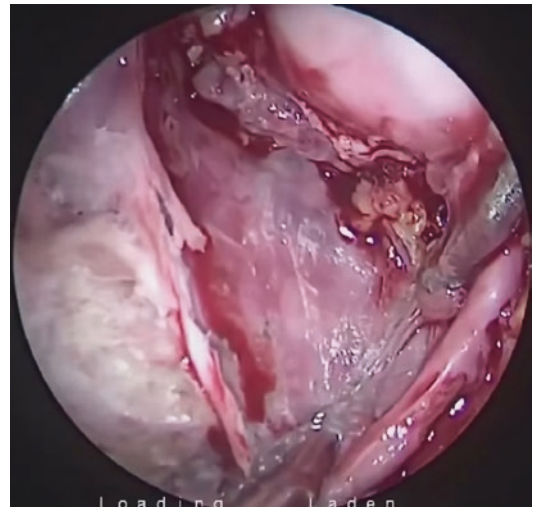

Fig. 10.26 Intraorbital area appears clean after disease removal

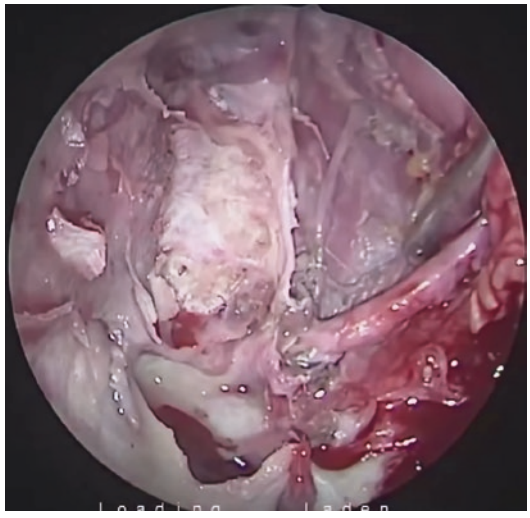

Fig. 10.25 Area near the globe is cleared while the optic nerve is gently pushed down

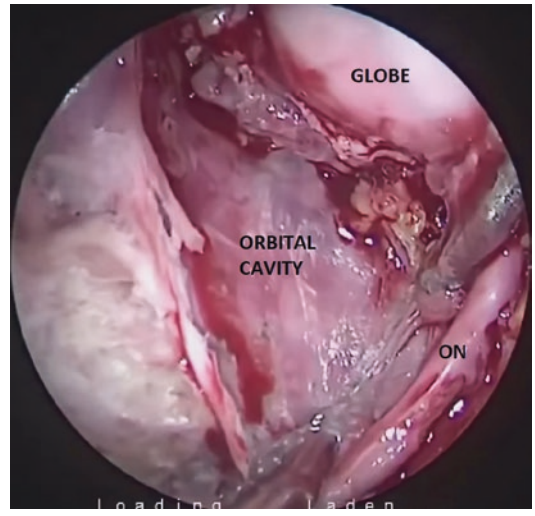

Fig. 10.27 A close look inside the orbit shows a better view of the globe and optic nerve

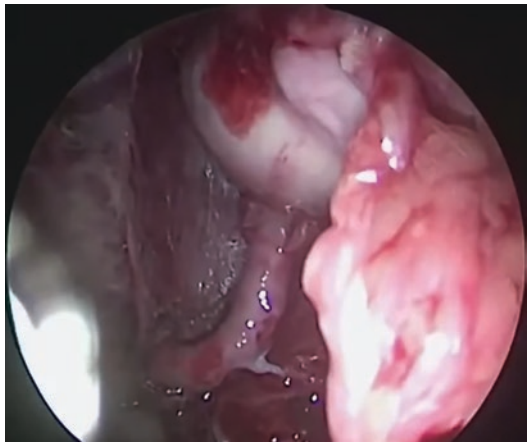

Fig. 10.28 Healthy fat can be seen prolapsing inferior to the globe

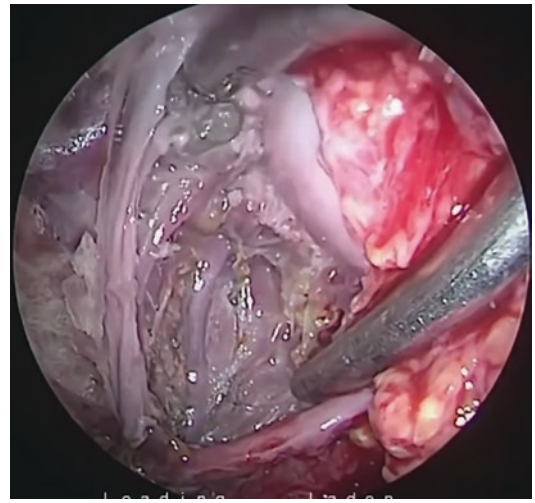

Fig. 10.29 The optic nerve is gently pushed down, and the disease posterior to it is cleared

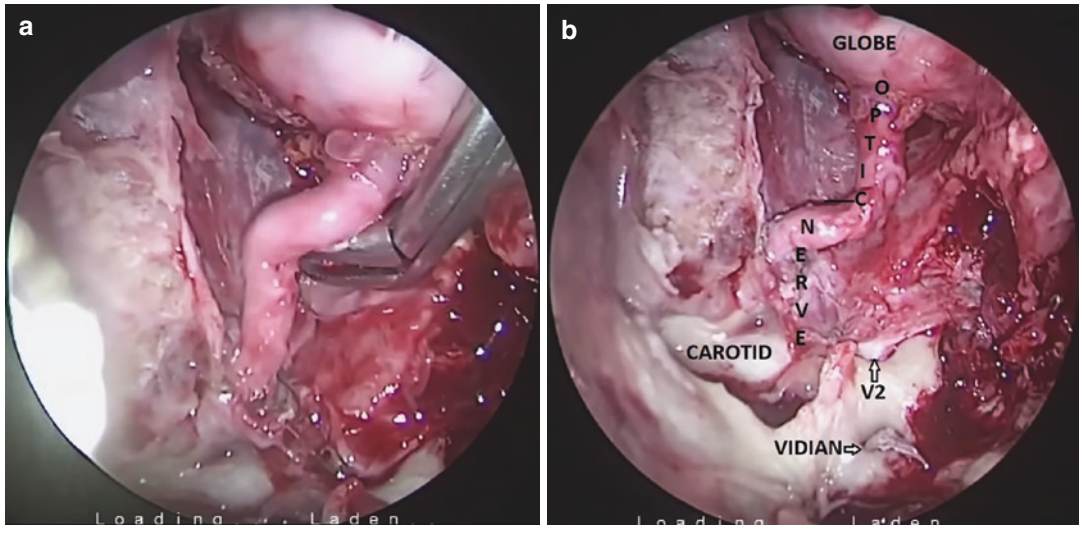

Fig. 10.30 (**a**) Globe and optic nerve in a disease-free intraorbital space. (**b**) Complete disease clearance from the orbital apex is seen with the optic nerve, globe, V2, Vidian, and cavernous carotid

Case 3

MRI

T1W MRI shows the area of enhancement in the right orbit (Fig. 10.31a). On the parallel T2W image, the same area in the right orbit is enhanced (Fig. 10.31b) in a previously operated case where the orbital disease was not addressed.

The best way to differentiate inflammation from disease is to compare the T1W contrast-enhanced MRI scan (Fig. 10.32a) with a fat-suppressed T2W image (Fig. 10.32b). The disease is a non-enhanced area in the right orbit in Fig. 10.32a, and the same area shows enhancement on a fat-suppressed T2W image in Fig. 10.32b.

Surgical Steps

Surgical steps are the same, including clearance of the sphenoid sinus (Fig. 10.33), improving exposure by clearing the field, removing the diseased part of the nasal septum, and opening up the sphenoids. Orbital clearance of the disease is the next step (Figs. 10.34, 10.35, 10.36, and 10.37).

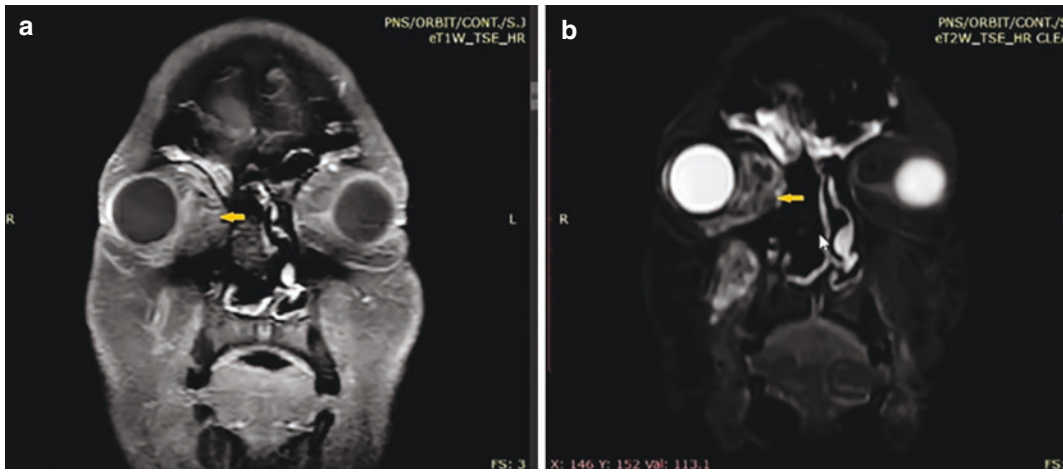

Fig. 10.31 (**a**) T1W MRI of case 3 showing the area of enhancement in the right orbit (arrow). (**b**) An enhanced T2W image of the same area in the right orbit can be seen in previously operated cases in which orbital disease was not addressed (arrow)

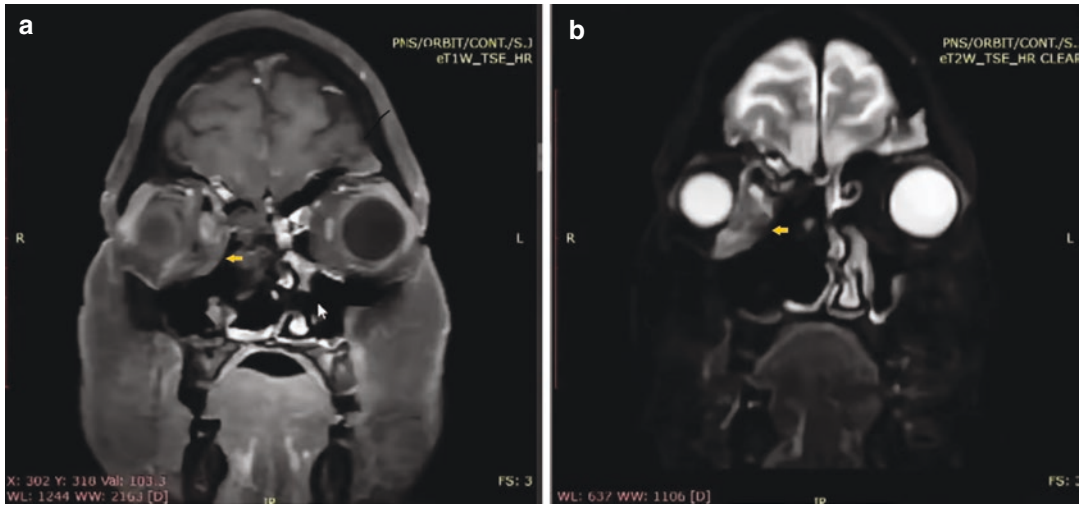

Fig. 10.32 (**a**) T1W contrast-enhanced MRI scan shows the non-enhanced area of disease in the right orbit (arrow). (**b**) Fat-suppressed T2W image showing the enhancement indicating the presence of disease in right orbit (arrow)

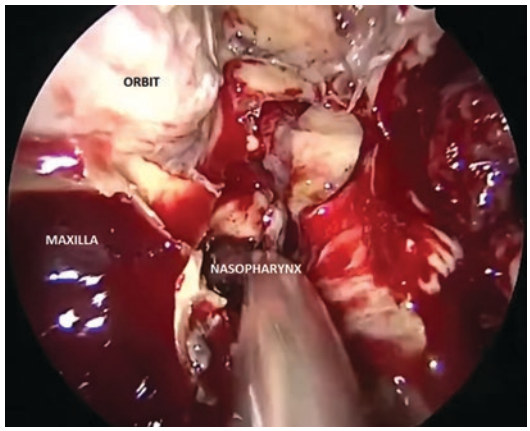

Fig. 10.33 Clearance of disease from sinuses on the right side

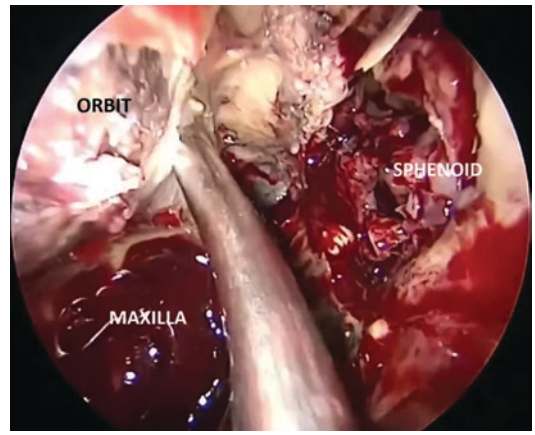

Fig. 10.35 Entry into the orbit is made, and the necrotic tissue is debrided

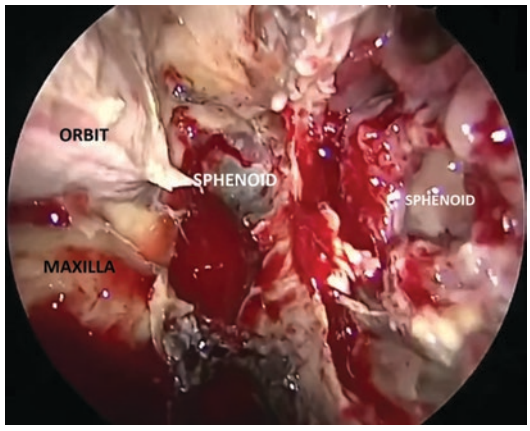

Fig. 10.34 Improving exposure by clearing the field where the diseased part of the nasal septum has been removed and both sides sphenoid sinuses can be seen

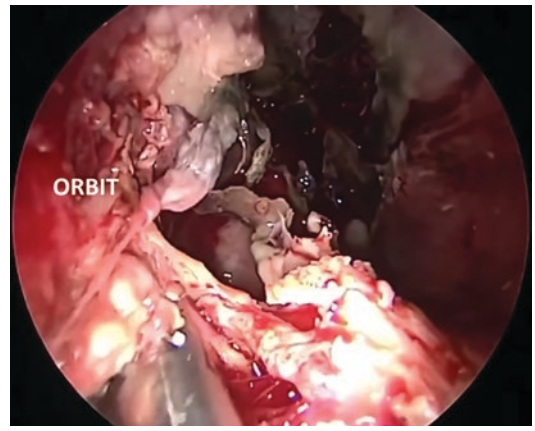

Fig. 10.36 Intraorbital clearance of disease is carried out

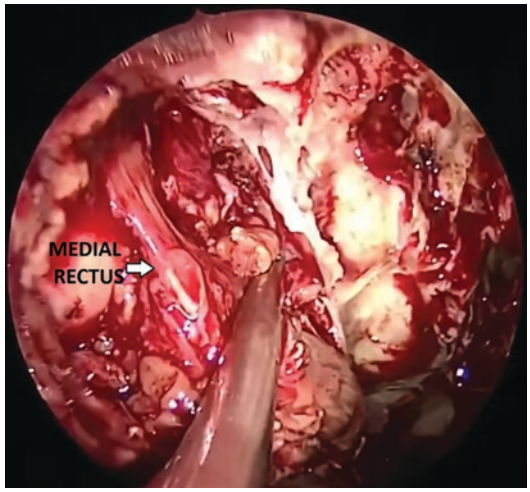

Fig. 10.37 Medial rectus muscle is identified and preserved as muscles are generally not involved

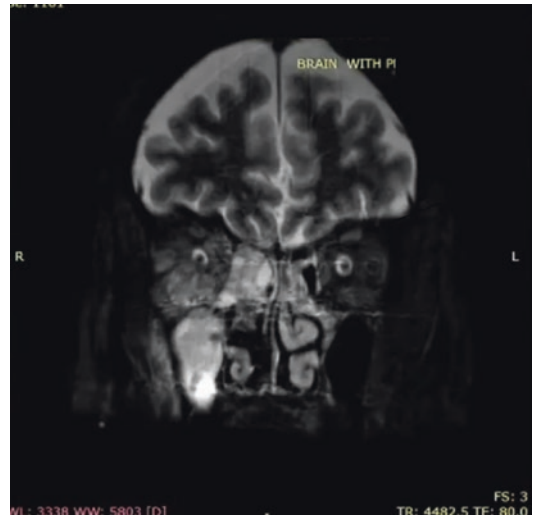

Fig. 10.38 Case 4, T2W fat-suppressed MRI showing disease in the right orbit

Case 4

MRI

T2W fat-suppressed MRI showing disease in the right orbit (Fig. 10.38).

Steps of Surgery

Standard surgical steps of orbital debridement were carried out (Figs. 10.39, 10.40, 10.41, 10.42, and 10.43).

Postoperatively, good mucosalization of the cavity was noted in most of the cases. Some patients had altered shapes and size of their eyes, with occasional fistula formation (Figs. 10.44, 10.45, and 10.46). Cosmetically, however, it remained superior to the total exenteration. Patients were very receptive and preferred a slight deformity over the total exenteration.

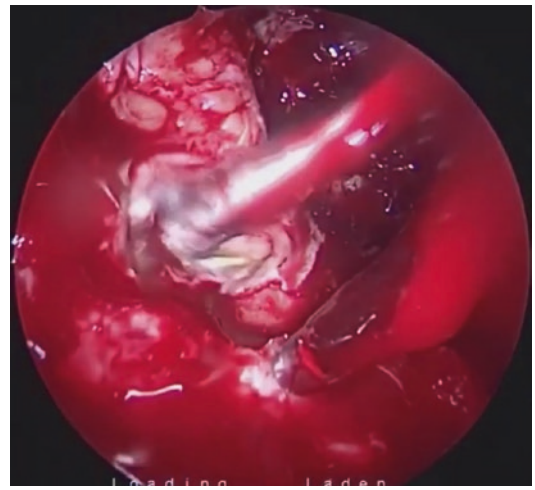

Fig. 10.39 Endoscopic orbital debridement of the case 3 showing healthy fat superiorly with necrotic tissue being debrided inferiorly

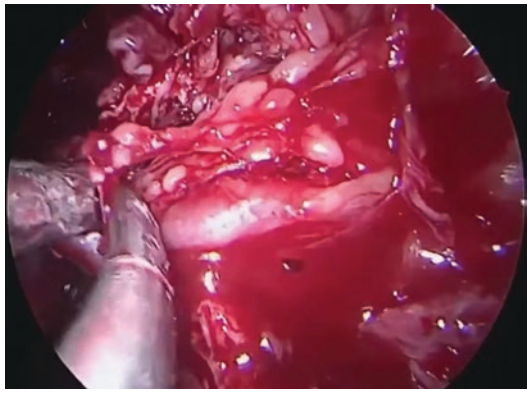

Fig. 10.40 Intraorbital debridement of the diseased part is carried out

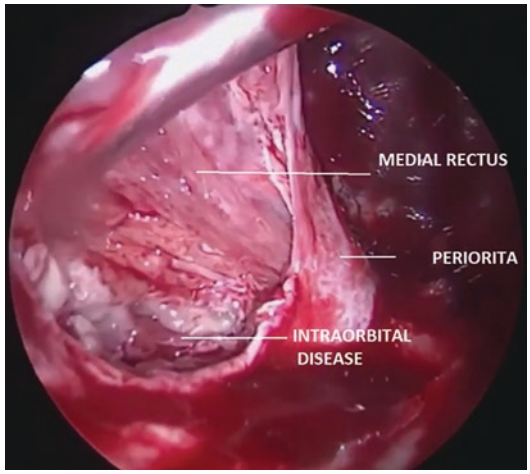

Fig. 10.41 The periorbita is incised, and the disease can be seen in the inferior part while the medial rectus is normal

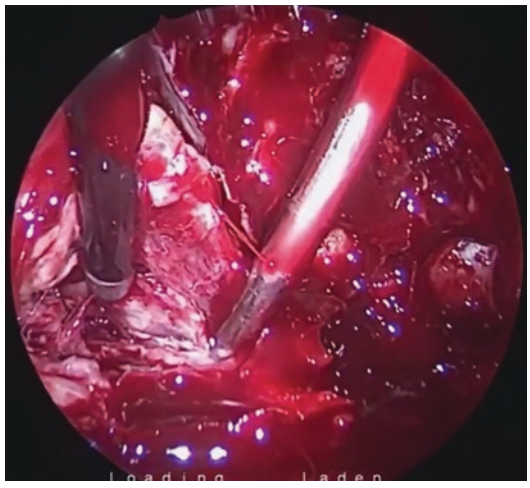

Fig. 10.42 Medial rectus is retracted to clear the disease lateral to it

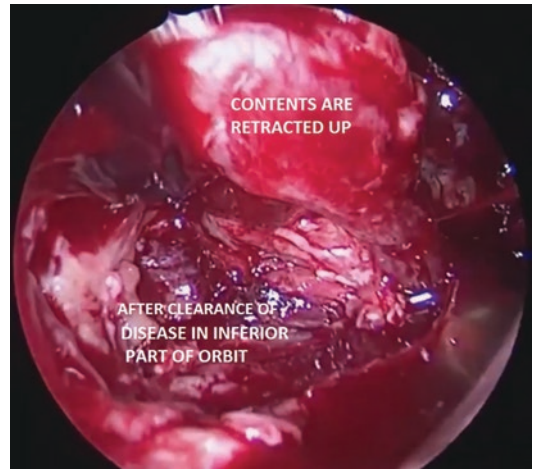

Fig. 10.43 Interior part of the orbit is visible after disease clearance

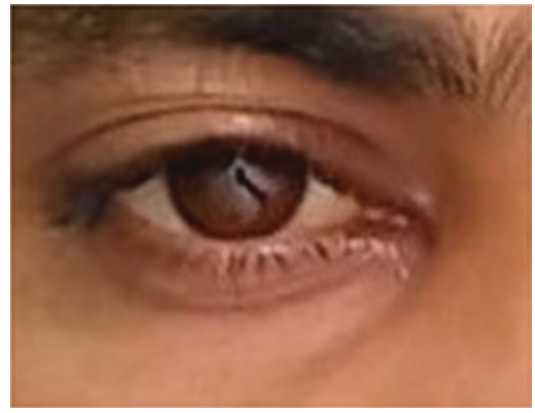

Fig. 10.44 Right eye after surgery

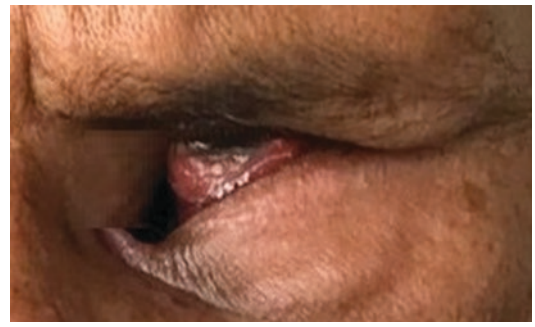

Fig. 10.45 Left eye after surgey

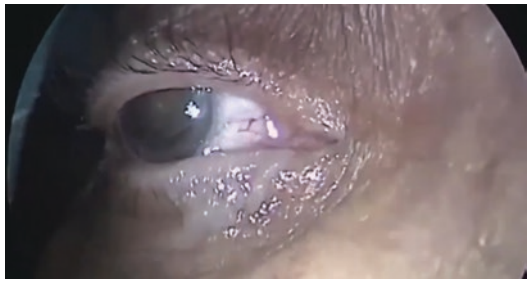

Fig. 10.46 Right eye after surgery

10.5 Advantages of Globe Sparing Orbital Exenteration

Endoscopic globe sparing orbital exenteration is an excellent surgery that saves the patient from devastating aesthetic and psychological losses. It prevents morbidity and, therefore, obviates the need for further complex rehabilitative surgery.

10.6 Postoperative Management

Regular check endoscopies are needed in the postoperative period. Due to good exposure during surgery, a nasal endoscopic inspection of all these areas is possible during postoperative follow-up. Endoscopic visualization obviates the need for repeated MRI in an otherwise asymptomatic patient. Endoscopic monitoring of the operated site and trend analysis of the level of inflammatory markers help regulate medical management. Aggressive treatment with antifungal drugs leads to a good mucosalization of the orbital cavity with excellent recovery.

10.7 Need of Developing Globe Sparing Technique for Orbital Disease

Convincing the patient of the need for orbital exenteration during a mucormycosis outbreak has been a difficult task. Orbital exenteration is associated with a high rate of morbidity, and the decision to do it is even more challenging in patients having normal eyesight [12].

There have been doubts, misperceptions, and uncertainties concerning orbital exenteration. Hargrove et al. felt that there is a lack of unanimity among treating physicians when it comes to exenteration [11]. Furthermore, although generating severe morbidity, orbital exenteration, may not enhance overall survival [12].

Various authors have attempted successful treatment of orbital mucormycosis without orbital exenteration in the past [1, 2, 10–12]. Catalano et al. stressed the necessity, for globe sparing orbital exenteration in malignant tumours of orbit and adjacent regions, as well as case selection and satisfactory outcomes [1].

In the administartion of ROCM, we accomplished a globe sparing orbital exenteration based on the same notion. Various MRI sequences serve as a road map for intraorbital tracing and disease clearance. It also allows us to focus on the hidden areas that are debrided during orbital clearing. The pterygopalatine fossa is a vital location from which the infection can quickly migrate into the orbit via infraorbital fissure. In a study by Ergun et al., pterygopalatine fossa involvement was noted in 81.8% of patients [12]. Thus, pterygopalatine fossa should be cleared in all the cases undergoing endoscopic globe sparing orbital exenteration. In general globe sparing orbital clearance in ROCM appears to be a promising technique.

10.8 Conclusion

The surgical therapy of ocular mucormycosis has undergone a paradigm change with the globe sparing endoscopic orbital exenteration. A better understanding of the orbital disease is possible because of excellent disease mapping on multiple MRI sequences. This is supported by high-definition endoscope and camera units that provide superb visibility, as well as development of minimally invasive techniques.

References

1. Catalano PJ, Laidlaw D, Sen C. Globe sparing orbital exenteration. Otolaryngol Head Neck Surg. 2001;125(4):379–84. https://doi.org/10.1067/mhn.2001.118247.
2. Croce A, Moretti A, D'Agostino L, Zingariello P. Orbital exenteration in elderly patients: personal experience. Acta Otorhinolaryngol Ital. 2008;28(4):193–9.
3. Songu M, Unlu HH, Gunhan K, Ilker SS, Nese N. Orbital exenteration: a dilemma in mucormycosis presented with orbital apex syndrome. Am J Rhinol. 2008;22(1):98–103. https://doi.org/10.2500/ajr.2008.22.3121.
4. Radici M, Bicciolo G, Palma O, Bozza F. Il massiccio facciale. In: De Campora E, Marzetti F, editors. La chirurgia oncologica della testa e del collo. Pisa: Pacini Editore; 1996. p. 345–81.
5. Zaoli G, Motta G. La chirurgia ricostruttiva nel cancro della testa e del collo. Padova: Piccin Editore; 1978.
6. Blitzer A, Lawson W, Meyers BR, Biller HF. Patient survival factors in paranasal sinus mucormycosis. Laryngoscope. 1980;90:635–48.
7. Dooley DP, Holsten DA, Grimes SR, et al. Indolent orbital apex syndrome caused by occult mucormycosis. J Clin Neuroophthalmol. 1992;12:245–9.
8. Kohn R, Hepler R. Management of limited rhino-orbital mucormycosis without exenteration. Ophthalmology. 1985;92:1440–4.
9. Peterson KL, Wang M, Canalis RF, Abemayor E. Rhinocerebral mucormycosis: evolution of the disease and treatment options. Laryngoscope. 1997;107:855–62.
10. Pelton RW, Peterson EA, Patel BC, et al. Successful treatment of rhino-orbital mucormycosis without exenteration: the use of multiple treatment modalities. Ophthal Plast Reconstr Surg. 2001;17:62–6.
11. Hargrove RN, Wesley RE, Klippenstein KA, et al. Indications for orbital exenteration in mucormycosis. Ophthal Plast Reconstr Surg. 2006;22:286–91.
12. Ergun O, Tahir E, Kuscu CO, Ozgen B, Yilmaz T. Acute invasive fungal rhinosinusitis: presentation of 19 cases, review of the literature and a new classification system. J Oral Maxillofac Surg. 2016; https://doi.org/10.1016/j.joms.2016.11.004.

11 Open Surgery in Rhino-Orbito-Cerebral Mucormycosis

Hitesh Verma and Kapil Sikka

The corona virus disease 2019 (COVID-19) infection is caused by the unique severe acute respiratory syndrome coronavirus 2 [1]. COVID-19 infection is associated with a wide spectrum of bacterial and fungal infections. Currently, Indian subcontinent has noticed a surge in mucormycosis. COVID-19-associated mucormycosis (CAM) may be induced by its mutant strain [2], its impact on innate immunity, generated cytokines, and increased risk of diabetes by selective damage of insulin-producing cells in the pancreas [2, 3]. Irrational use of steroids and other COVID-associated treatment has come up as a major risk for CAM.

The progression of CAM is variable amongst the patients. The progression pattern of disease depends on the patient's immune status and the status of comorbidities. Rapidly progressive course mandates aggressive medical and surgical treatment mandatory. Control of underlying immune-compromising condition is initiated as emergency. This chapter will focus on rhino-orbito-cerebral mucormycosis (ROCM). Endoscopic approach has emerged as standard of care for excision of fungal debris, necrotic soft tissues and bone, and also for taking biopsy from suspicious areas. Acute form of invasive fungus has tendency to extend beyond the confines of sinonasal region via natural foramina and perivascular channels and by erosion of surrounding bones making the access difficult with endoscopes, especially in narrow corridors. Involvement of the anterior wall of the maxillary sinus is quite frequently encountered in our practice, which is not accessible with standard endoscopic procedures.

The extended endoscopic approaches (Denker's [4], medial orbital wall removal and extended skull base approach) allow removal of lateral nasal wall, a major part of the anterior wall of the maxillary sinus, medial orbital wall and tissue, skull base and beyond. The procedure, however, requires expertise, good assistance and specialized instruments. The angle of surgical instrumentation via the nostrils in Denker's approach narrows down the working area during the removal of lateral part of anterior wall of maxilla and soft tissues of cheek. The exposure of the superior part of the anterior wall of maxilla, zygomatic arch, and anterior orbital contents is difficult even with experienced surgeons [5, 6]. The simultaneous presence of skin discoloration/blackening of the anterior face is a contraindication for endoscopic approach. The surgical volumes of ROCM cases encountered during CAM epidemic also created feasibility challenges. Operating in multiple unfriendly suites, COVID-positive and medically unstable patients mandated procedures to be completed fast and

H. Verma (✉) · K. Sikka
Department of Otorhinolaryngology, Head and Neck Surgery, All India Institute of Medical Sciences, New Delhi, India

N. Gupta, S. G. Honavar (eds.), *Rhino-Orbito-Cerebral Mucormycosis*,
https://doi.org/10.1007/978-981-16-9729-6_11

efficient. All these scenarios mandated open surgical procedures (OSP) in the management of ROCM.

Most of the cases of ROCM can be managed with endoscopic approach. However, endoscopic procedures take much longer, are equipment intensive and need assistants. In a tertiary hospital like ours that happened to be one of the largest COVID facility also, there was an acute shortage of manpower, and everyone was expected to act fast. There was a heavy load of ROCM patients needing immediate attention. Therefore, patients were managed with OSP. OSP allows excellent visualization of all those sinonasal areas that may be hidden in the endoscopic approaches. The surgical procedures have a short learning curve and can be performed with a limited number of instruments. A proper tissue handling limits the visibility of surgical scar.

Patients of ROCM with the following symptoms were managed using OSP:

1. Numbness of cheek, medial canthus and supraorbital region.
2. Significant facial fullness indicating anterior cheek spread (Fig. 11.1a).
3. Facial discoloration/blackening and involvement of subcutaneous tissue (Fig. 11.1b).
4. Palatal discoloration, palatal perforation, and palatal perforation and loosening of teeth (Fig. 11.1c).

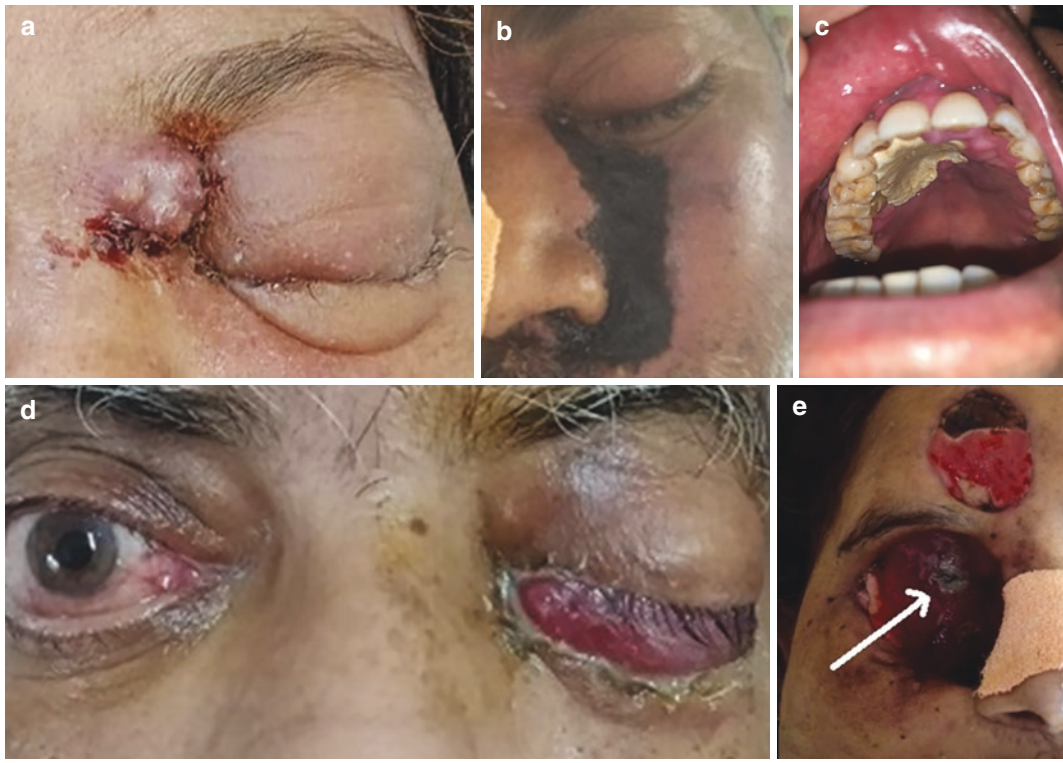

Fig. 11.1 (**a**) Clinical photograph showing extension of disease to the lacrimal drainage system with cutaneous invasion and facial fullness. (**b**) Clinical photograph showing facial discoloration indicating gross bone invasion by the disease leading to the fungal involvement of the skin after erosion of anterior wall of maxilla. (**c**) Bogginess of the palate and ulceration and loosening of teeth. (**d**) Ptosis, proptosis and conjunctival chemosis on the left. (**e**) A case of post orbital exenteration showing intracranial progression of residual/impending disease in ROCM

5. Proptosis/discoloration of orbital contents with loss of vision (Fig. 11.1b).
6. Failed extended endoscopic procedure.
7. Intracranial extension of disease (Fig. 11.1e).

11.1 Role of Radiology in Surgical Planning

Contrast CT and MRI [1] are the advised radiological investigations. In view of sudden surge in ROCM cases needing immediate surgical debridement and imitations of MRI facilities across all surgical units of the hospital, contrast-enhanced computed tomography (CECT) was taken as the acceptable preoperative radiological investigation. CECT is easy to perform, cost effective and quicker and provides details of bony anatomy. CECT also provides worthwhile anatomical information of orbital and cranial tissue involvement. Contrast-enhanced MRI was reserved for cases with orbital involvement and suspected intracranial spread and for follow-up assessment. MR angiography was used to assess superior ophthalmic artery and central retinal artery in selected cases. The radiological indications for OSP are:

1. Obliteration of pre-antral fat plan (Fig. 11.2a).
2. Simultaneous obliteration of pre-antral and retro-antral fat plans (Fig. 11.2a, b).
3. Collection of fluid anterior to the anterior wall of the maxilla.
4. Erosion/destruction of anterior/inferior wall of maxilla.
5. Residual disease in anterior wall/inferior wall of maxilla after extended endoscopic procedures (Fig. 11.2b).
6. Gross intra-orbital disease (Fig. 11.2c).
7. Lateral orbital wall erosion.
8. Central retinal artery occlusion.
9. Intracranial extension of disease (Fig. 11.2d). Though minimal intracranial extension can be accessed endoscopically, large abscesses and necrosis mandates neurosurgical assistance and craniotomy.

11.2 Diagnosis

The diagnosis is established by a specific clinical profile of the patient. The risk factors in the current surge are the history of COVID-19 infection, uncontrolled diabetes, uncontrolled kidney disease, transplanted severely immunocompromised patients, prolonged use of immunity-lowering drugs (steroids, chemotherapy, etc.). A good clinical assessment (discoloration and crusting of sinonasal region) is required to confirm the diagnosis. Nasal endoscopic assessment is performed to obtain certain information like tissue appearance and disease extent. Tissue biopsy is done for fungal smear and culture, and histopathology. Simultaneous assessment of blood and serum parameters is done to prepare the patient for surgery, to control the comorbidities and to obtain effectiveness of antifungal therapy.

11.3 Surgical Procedures

11.3.1 Sublabial Approach [4, 5, 7, 8]

The indications for sublabial approach are infrastructural maxillectomy, removal of subcutaneous tissue and anterior wall of maxilla, and combined removal of anterior and medial wall of the maxilla (Denker's procedure). The approach allows good exposure of the anterior wall of the maxilla. The incision is made 3–5 mm above the upper gingivo-buccal sulcus (Fig. 11.3a). The incision is deepened till the anterior wall of the maxilla. The periosteum elevator is used to elevate the tissue from the anterior wall of the maxilla. Often pus can be found collecting subperiosteally via infraorbital foramina [2, 3]. Canine fossa is used to enter the maxillary sinus in Caldwell Luc approach by chisel, osteotome or drill. The widening of the anterior wall window is done in all directions with Kerrison rongeur, bone nibbler or drill. The procedure allows simultaneous removal of unhealthy subcutaneous tissue, medial, superior and posterior wall of maxilla. The wound is closed with 3-0 vicryl suture in layers.

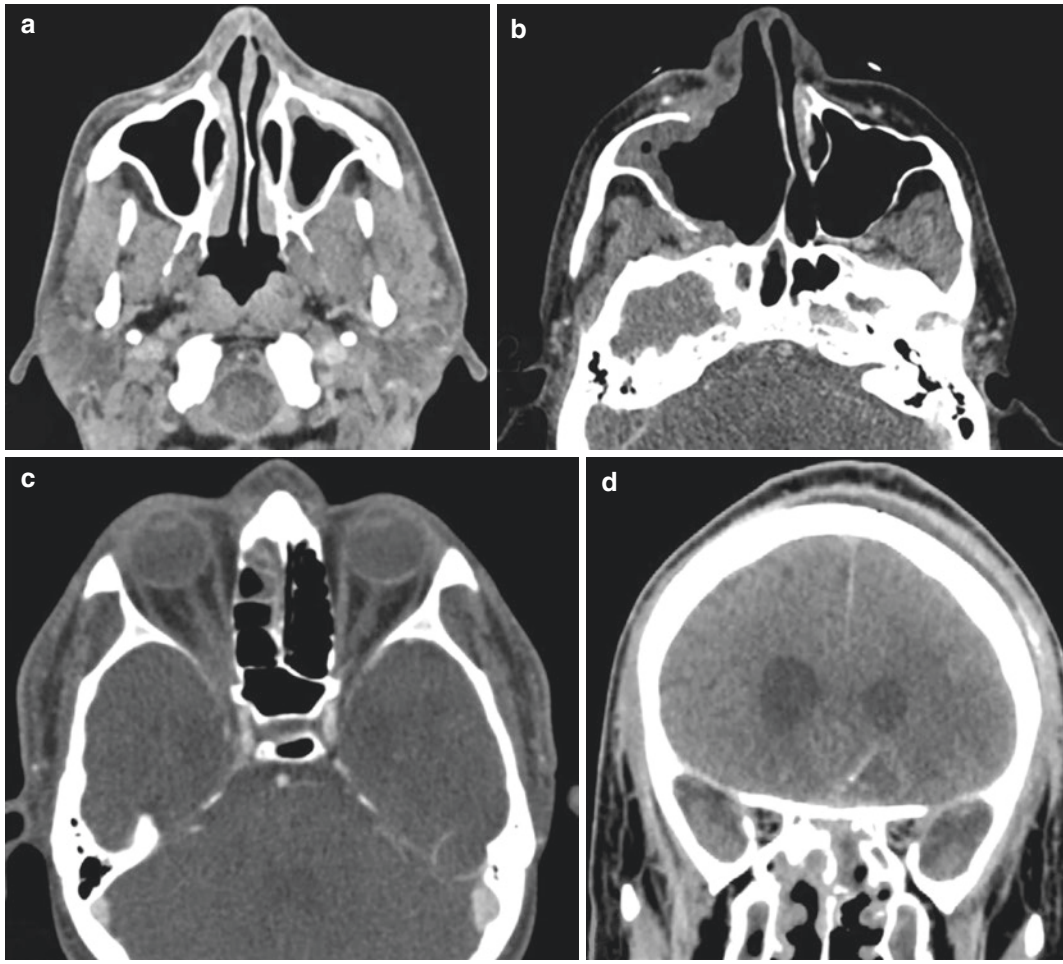

Fig. 11.2 (**a**) Radiological findings in cases treated with open approaches showing obliteration of pre-antral fat on left. Simultaneous obliteration of pre-antral and retro-antral fat plans. (**b**) Obliteration & infilteration of anterior wall of maxillary in post endoscopic maxillectomy case. (**c**) Gross intra-orbital disease. (**d**) Left anterior cranial cavity showing rim enhancement with hypointense mass

Infrastructural maxillectomy is done by incising the palatal mucosa medial and posterior to the diseased tissue with adequate margin (Fig. 11.3b). The osteotomy is made below the inferior orbital fissure from pyriform aperture till the posterior limit of the anterior wall of the maxilla. Curved osteotome is used to separate the posterior maxilla from the pterygoid plates. The heavy scissors are used to cut soft tissue around specimen. Internal maxillary artery bleed is secured after removal of the anterior specimen. Involved pterygoid plates, pterygoid muscles, involved infratemporal fossa contents and involved nasopharyngeal tissue can be removed after the removal of the anterior specimen. Pterygoid plexus ooze is managed by cautery, digital pressure and surgery. The conventional pack is placed after creating a bed with suture. The artificial palate can be applied in the same sitting if available. The pack removal is generally done after 2–3 days. Ryles tube feeding can be given in non-rehabilitated patients till rehabilitation with artificial palate.

The limitations for sublabial approach are the exposure of the supero-lateral part of anterior wall of maxilla, superior part of the ethmoid

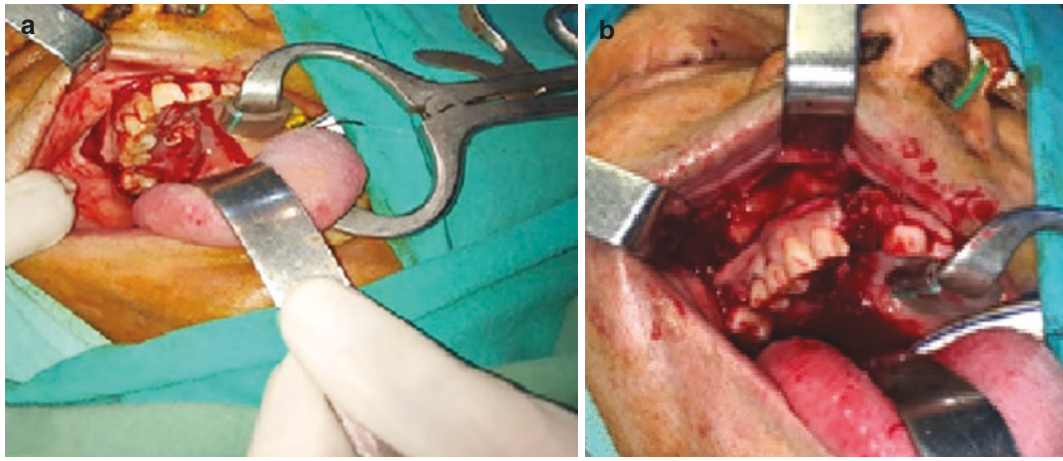

Fig. 11.3 (**a**) Intraoperative photographs showing palatal excision by sublabial approach. (**b**) Palatal incision and separation of right inferior maxilla from the rest of the maxilla

sinus, frontal sinus, sphenoid sinus and anterior-superior orbital tissue. Certain limitations of procedure can be overcome by using endoscopic assistance.

11.3.2 Lateral Rhinotomy Approach [5, 9, 10]

It is the best open approach to deal with the sino-nasal pathology. The procedure allows exposure of complete maxilla, anterior maxillary contents, retro-maxillary space (infratemporal fossa, pterygomaxillary fossa), nasal cavity, and ethmoid and sphenoid sinus. The incision is made along the naso-facial groove from medial canthus. The incision is curved around the nasal ala (Fig. 11.4). The incision is deepened till the frontal process of maxilla and pyriform aperture. The nasal cavity is being entered along the pyriform aperture. The medial flap is secured with stay suture anteriorly for easy handling of nasal tissue. The lacrimal sac is being lifted from the lacrimal fossa. The nasolacrimal duct is cut with a sharp instrument. The flap is elevated subperiosteally to expose the anterior wall of the maxilla.

After lip splitting incision the lateral flap is reflected laterally. This facilitates easy manoeuvring of the soft tissue contents present anterior, lateral, inferior and posterior to maxillary bone. Hence the lateral rhinotomy incision can be combined with lip splitting incision to deal with these para-maxillary areas if required (Fig. 11.5). The debridement of tissue is performed till clinical necrosis is found. The presence of bleeding margin is suggestive of healthy tissue.

For total maxillectomy, the osteotomy is made at the level of the frontal process of the maxilla, zygomatic arch, hard palate and retro-maxillary areas to separate the maxillary bone from surrounding tissues [5].

Combining Lynch Howarth incision with lateral rhinotomy incision allows clearance of disease from frontal sinus, medial orbit and anterior skull base (Fig. 11.6). The flap is raised by elevating the periorbita from lamina papyracea. Lamina papyracea with ethmoid air cells is removed to access the nasal cavity. The upper limit of lamina papyracea removal is the fronto-ethmoid suture line. Kerrison rongeur is used to remove the frontal sinus anterior wall for access in the frontal sinus. The skull base is identified at the ethmoid roof and followed posteriorly to clear the disease along the skull base and sphenoid sinus. Involved medial orbital fat, periorbita and medial muscles can be removed by the same approach. The posterior septum can be removed to access the contralateral side of the nasal cavity if required. Endoscopic assistance provides superior quality view when disease extends close to vital

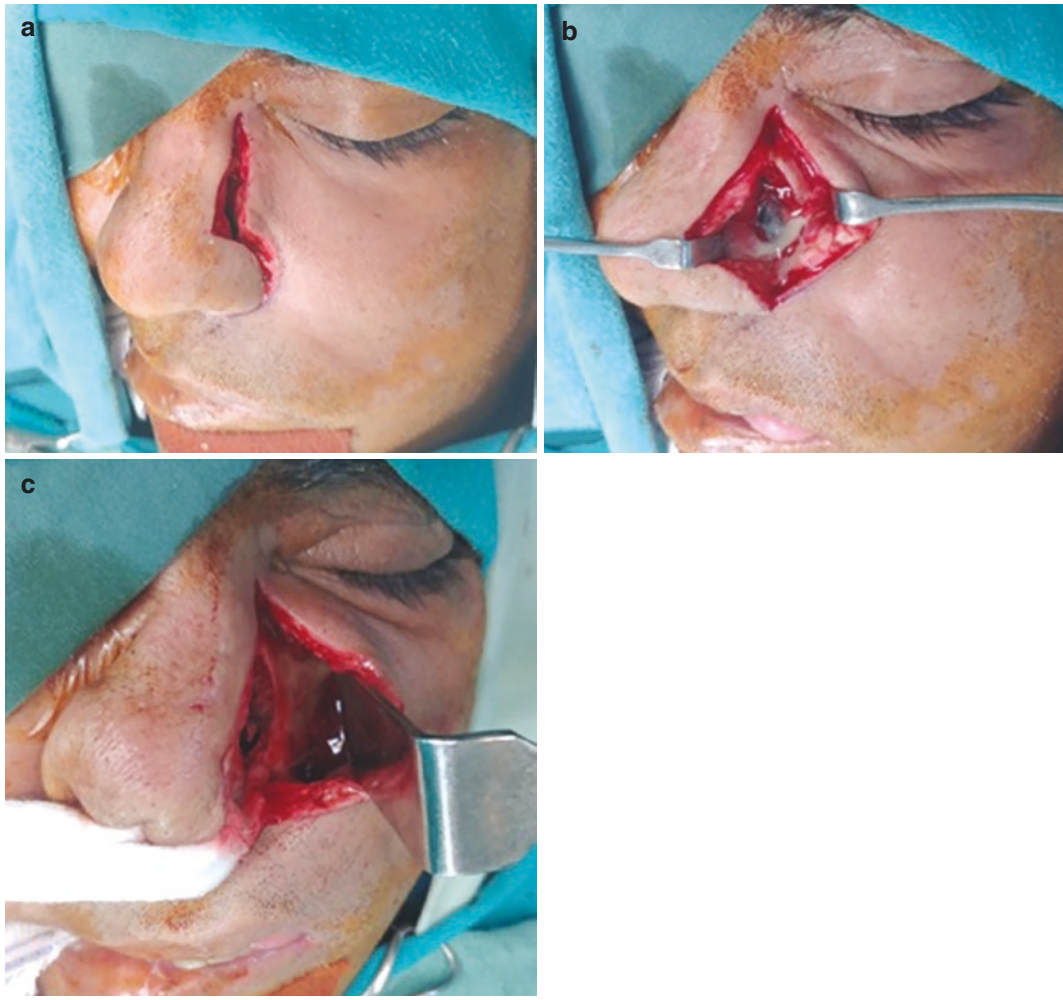

Fig. 11.4 (**a**) Lateral rhinotomy incision. (**b**) Mucopurulent discharge can be seen pouring out as soon as the flap is raised. (**c**) Exposure of anterior wall of maxilla and the nasal cavity

structures like skull base and orbital tissue. The procedure has certain limitations in dealing with lateral orbital contents, zygomatic bone and temporal fossa, and in the case of need of simultaneous orbital exenteration.

11.3.3 Weber Ferguson Approach [5]

It allows complete exposure of maxillary bone, para-maxillary spaces, orbital tissue, infratemporal fossa, zygomatic bone, lateral orbital wall and temporal fossa (Fig. 11.7). It can be combined with bi-coronal incision to handle the anterior skull-base contents. Orbital exenteration is mostly done with this incision. Sub-ciliary incision is combined with lateral rhinotomy incision. Lateral extension of incision is based on the lateral limit of the disease. Sub-ciliary incision runs 3–5 mm inferior to the inferior lid margin. Sub-ciliary incision is combined with supra-ciliary incision to remove lid edges. The flaps are raised as mentioned in the lateral rhinotomy approach. The orbital tissue is released from the anterior orbital rim by incising periorbita. Medial and lateral canthal ligaments are

incised. The plane is created subperiosteally around the orbital contents till the orbital apex. The curved artery clap is applied at the level of the orbital apex. Heavy scissor is used to cut the tissue from the orbital apex anterior to clamp. Further slicing of orbital apex tissue can be done after removal of the anterior orbital contents. The left-out orbital apex tissue is sutured or cauterized to limit the chances of ophthalmic artery bleeding. The cut edges of lids are sutured to prevent contamination from external environment. The cavity is filled with medicated packs. The dental rehabilitation is done with palatal prosthesis by placing it intraoperatively or in an early postoperative period.

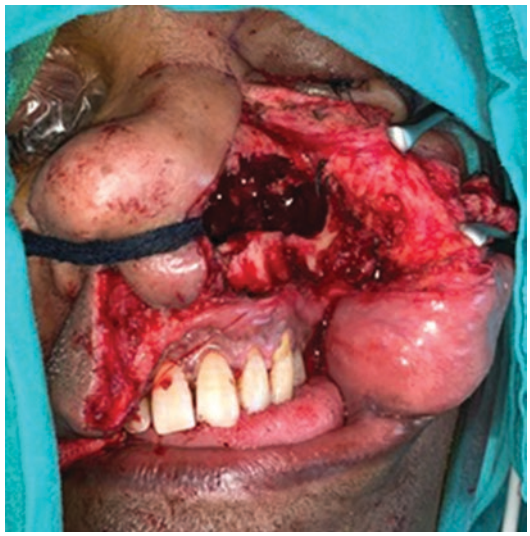

Fig. 11.5 Lip splitting incision allows easy lateral access

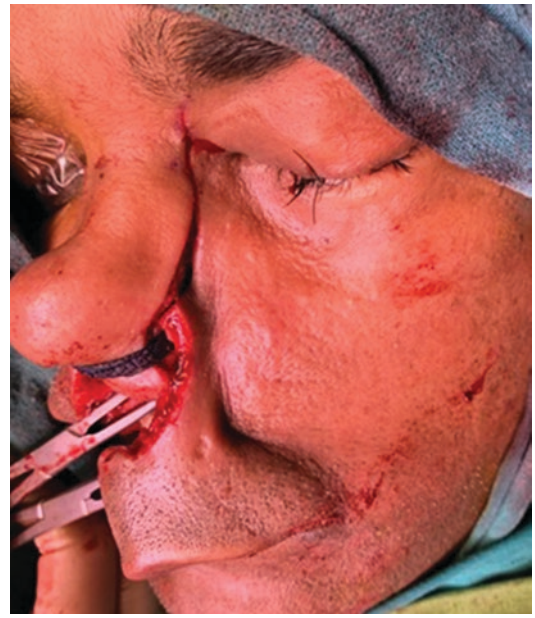

Fig. 11.6 Combination of lateral rhinotomy with Lynch Howarth incision

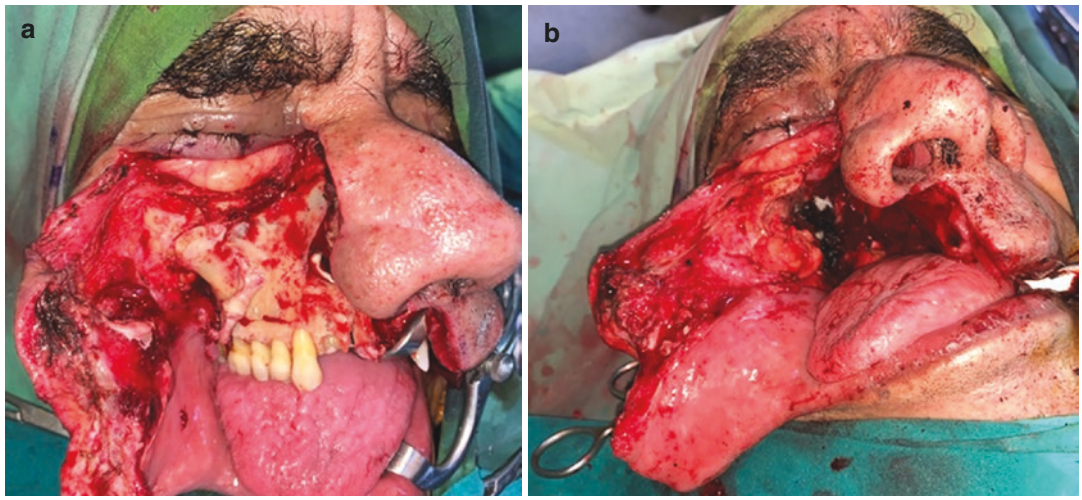

Fig. 11.7 (**a**) Weber Ferguson approach allows complete exposure of maxillary bone and peri-antral tissue. (**b**) Surgicel is visible after maxillectomy in intra-temporal fossa

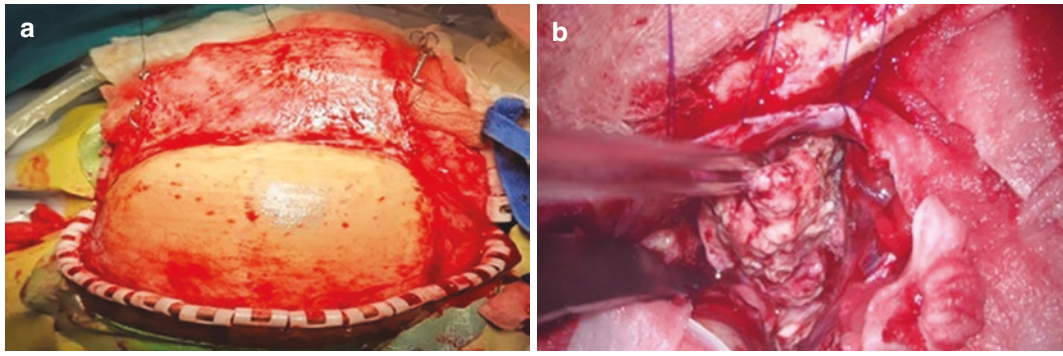

Fig. 11.8 (**a**) Bi-coronal incision and flap. (**b**) Microscopic picture of fungal mass

11.3.4 Transcranial Approach [5–13]

Anterior and middle cranial fossa is mostly invaded by the CAM. The routes of extension are cribriform plate, orbital apex, roof and sphenoid body. The cerebral involvement is considered life threatening as surgical excision is difficult and amphotericin has limitations in crossing blood brain barrier. The surgical excision may have survival advantage in the early stage of cerebral extension. Bi-coronal approach or extended endoscopic approach is the most preferred approach as it allows exposure of the entire anterior skull base.

Bi-coronal incision is made a few centimetres behind the hairline (Fig. 11.8a). The flap is elevated over pericranium till the orbital rim. The wide pericranial flap is made for the postoperative skull base reconstruction. The osteotomy is made, and brain tissue is elevated from the skull base. The diseased tissue is removed (Fig. 11.8b).

11.4 Postoperative Management

Surgical cavity pack is removed on the 2–3 postoperative days. The nasal douche is advised after pack removal to prevent mucosal dryness. The cavity cleaning is done regularly for early epithelialization. Facial suture removal is done between seventh and tenth postoperative days. Palatal prosthesis is placed intraoperatively or after a certain interval from surgery for oral rehabilitation. Ryle's tube feeding is removed after placement of prosthesis. Dressing is applied over orbital exenteration sites to prevent crusting. The open surgical cavity can be obliterated by flaps or free tissue transfer after a certain interval from complete treatment. The patient can wear dark goggles for cosmetic issues till an artificial eye is applied.

References

1. Mohamadian M, Chiti H, Shoghli A, Biglari S, Parsamanesh N, Esmaeilzadeh A. COVID-19: Virology, biology and novel laboratory diagnosis. J Gene Med. 2021;23(2):e3303. https://doi.org/10.1002/jgm.3303.
2. Pal R, Singh B, Bhadada SK, Banerjee M, Bhogal RS, Hage N, Kumar A. COVID-19-associated mucormycosis: an updated systematic review of literature. Mycoses. 2021;64(12):1452–9. https://doi.org/10.1111/myc.13338.
3. Song G, Liang G, Liu W. Fungal co-infections associated with global COVID-19 pandemic: a clinical and diagnostic perspective from China. Mycopathologia. 2020;185(4):599–606. https://doi.org/10.1007/s11046-020-00462-9.
4. Ashman A, Psaltis AJ, Wormald PJ, Tan NC. Extended endoscopic approaches to the maxillary sinus. J Laryngol Otol. 2020;134(6):473–80. https://doi.org/10.1017/S0022215120000882.
5. Mittal P, Verma H, Kesari A, et al. Extended procedures. In: Verma H, Thakar A, editors. Essentials of rhinology. Singapore: Springer; 2021. https://doi.org/10.1007/978-981-33-6284-0_7.
6. Singh G, et al. Diagnostic method and instrumentation in rhinology. In: Verma H, Thakar A, editors. Essentials of rhinology. Singapore: Springer; 2021. https://doi.org/10.1007/978-981-33-6284-0_5.
7. Lee DH, Lim HR, Lee JK, Lim SC. Infrastructure maxillectomy for maxillary sinus and hard palate neo-

plasms. Mol Clin Oncol. 2021;15(3):180. https://doi.org/10.3892/mco.2021.2342.
8. Omura K, Nomura K, Aoki S, Otori N, Tanaka Y. Direct approach to the anterior and lateral part of the maxillary sinus with an endoscope. Auris Nasus Larynx. 2019;46(6):871–5. https://doi.org/10.1016/j.anl.2019.03.006.
9. Weisman R. Lateral rhinotomy and medial maxillectomy. Otolaryngol Clin N Am. 1995;28(6):1145–56.
10. Das S, Banerjee P, Das A, Sinha R. Lateral rhinotomy – revisited. Indian J Otolaryngol Head Neck Surg. 2007;59(3):215–20. https://doi.org/10.1007/s12070-007-0064-8.
11. Davraj K, et al. Nasal physiology and sinusitis. In: Verma H, Thakar A, editors. Essentials of rhinology. Singapore: Springer; 2021. https://doi.org/10.1007/978-981-33-6284-0_3.
12. Kanodia A, Verma H, Jain A, et al. Prevention and management of complications. In: Verma H, Thakar A, editors. Essentials of rhinology. Singapore: Springer; 2021. https://doi.org/10.1007/978-981-33-6284-0_8.
13. Ozlen F, Abuzayed B, Dashti R, Isler C, Tanriover N, Sanus GZ. Low-profile 1-piece bifrontal craniotomy for anterior skull base approach and reconstruction. J Craniofac Surg. 2010;21(1):233–8. https://doi.org/10.1097/SCS.0b013e3181c5a217.

Cranio-Cerebral Mucormycosis

12

Ravisankar Manogaran, Arulalan Mathialagan, Amit Keshri, Govind Bhuskute, Ashutosh Kumar, Arun Srivastava, Rungmei S. K. Marak, and Sanjay Behari

12.1 Introduction

Mucormycosis is an opportunistic invasive fungal infection that occurs commonly in an immunocompromised host. The patients who develop these fulminant infections are those on immunosuppressants, like post-organ transplant patients, patients with chronic immunological disorders, haematological malignancies, and uncontrolled diabetes mellites with or without diabetic ketoacidosis [1]. The second wave of COVID-19, the altered nasal immunity and the pre-diabetic and diabetic states caused by the use of high-dose steroids, and the irregular high antibiotic use, has possibly made the incidence of mucormycosis rise rapidly [2, 3]. The involvement of the nasal cavity, paranasal sinus (PNS), and orbit has been commonly seen. Even though rhino-orbital-cerebral-mucormycosis is the most common form, it can rarely be present as pulmonary, cutaneous, gastrointestinal, or disseminated forms. The paranasal sinuses and orbits, like the nasal cavity, are closely associated with the skull base; thus, skull base involvement, and eventually intracranial compartment involvement, is inevitable if not treated by radical surgical debridement of the nasal and PNS followed by high doses of intravenous antifungal medication. Mucormycosis is prone to causing tissue invasion and angioinvasion [4]. Thus, spread of fungus to the intracranial cavity can occur by direct skull base invasion as well as through haematogenous spread. Intracranial involvement is an indicator of poor survival rates.

12.2 Pathophysiology

Mucormycosis is caused by Mucorales fungi, a ubiquitous, saprophytic fungus that morphologically has broad aseptate or sparsely septate ribbon-like hyphae. Around 27 species of *Mucorales* cause human infection; the common species are *rhizopus*, *rhizomuco*, and *lichtheimia.* Infection is caused by inhalation of sporangiospores or rarely by traumatic inoculation. In an immunocompetent individual, mucor spores may even be present in the nasal mucosa. However, in immunocompromised states, these spores germinate and invade the local tissue and vessels. In COVID-associated mucormycosis, several clusters of risk factors act together to suppress immunity and potentiate the spread of

R. Manogaran · A. Mathialagan · A. Keshri
G. Bhuskute · A. Kumar · A. Srivastava
S. Behari (✉)
Department of Neurosurgery, Sanjay Gandhi Postgraduate Institute of Medical Sciences, Lucknow, Uttar Pradesh, India

R. S. K. Marak
Department of Microbiology, Sanjay Gandhi Postgraduate Institute of Medical Sciences, Lucknow, Uttar Pradesh, India

N. Gupta, S. G. Honavar (eds.), *Rhino-Orbito-Cerebral Mucormycosis*,
https://doi.org/10.1007/978-981-16-9729-6_12

infection. Most of the patients with COVID-associated mucormycosis (CAM) have diabetes mellitus. COVID-19 viral infection is known to cause overexpression of inflammatory cytokines and impair cell-mediated immunity. Endothelial cell dysfunction caused by inflammatory mediators is one of the characteristic features of COVID-19 infection. This endothelial damage and increased expression of endothelial receptors facilitate the tissue and angioinvasion of mucormycosis [4]. There is also a role for iron in the pathogenesis of this disease. In the setting of uncontrolled diabetes mellitus and sepsis, there is acidosis, which impairs the iron homeostasis and increases the serum ferritin, free iron, and free oxygen radicals. This causes further damage to the normal cells and potentiates the growth of mucorales as it incorporates iron into its cells [5, 6]. Once angioinvasion occurs, fungi spread into the peri-sinus structures and the skull base by various routes. As it breaches the dura and enters the brain parenchyma, there is angioinvasion with vascular occlusion and thrombosis, which causes cerebral infarction and tissue hypoxia. Fungal invasion of glial cells causes further inflammatory reactions and abscess formation. The resultant phagocytosis of dead cells causes more damage to the normal brain tissue.

12.3 Anatomical Considerations

The route of entry of the fungal spores is via the nasal route. The nose and paranasal sinus mucosa become the primary sites of colonization and growth of saprophytic fungi. As they germinate, they cause tissue invasion and angioinvasion, leading to a rapid spread. The nasal cavity, paranasal sinuses, and the orbit form the close anatomical contiguous structures, which are the primary areas of mucor infection. The entire ventral skull base forms the roof of the nasal cavity, the paranasal sinus, and the orbit. Thus, the involvement of the skull base occurs if the fungal growth is not detected early in the disease and if the host immunity is very poor. Mucormycosis of the frontal sinus, ethmoidal sinus, and orbital roof spreads to the anterior skull base. Fungal growth involving the sphenoid sinus, orbital apex, and maxillary sinus spreads to the middle cranial fossa. In most patients, the disease spreads to the middle cranial fossa via the cavernous sinus and pterygoids. Fungi can gain access into the posterior cranial fossa by extensively destroying the clivus. The cranial nerve and its foramina are the potential entry pathways into the cranium; intracranial involvement rarely occurs via a haematogenous route. The standard central nervous system occurrences are a cerebral abscess (frontal abscess), cavernous sinus thrombosis, and internal carotid occlusion.

In Fig. 12.1, the possible ways in which the disease can enter the intracranial compartment are demonstrated.

12.4 Clinical Presentation

Rhinological	Orbital	Intracranial	General
Nasal obstruction	Diminution of vision to complete loss of vision	Seizures	Fever
Facial swelling	Orbital swelling	Hemiplegia	Generalized weakness
Headache	Restricted eye movements	Altered sensorium	
Facial pain	Ptosis		
Facial numbness	chemosis		
Blood-stained nasal discharge			

12.5 Investigations

The diagnosis of mucormycosis is usually based on the clinical presentation that reveals a fulminant course of the disease. Still, various other diagnostic tools help confirm the diagnosis and provide information regarding decision-making in its management. A diagnostic nasal endoscopy can demonstrate a well-established disease's

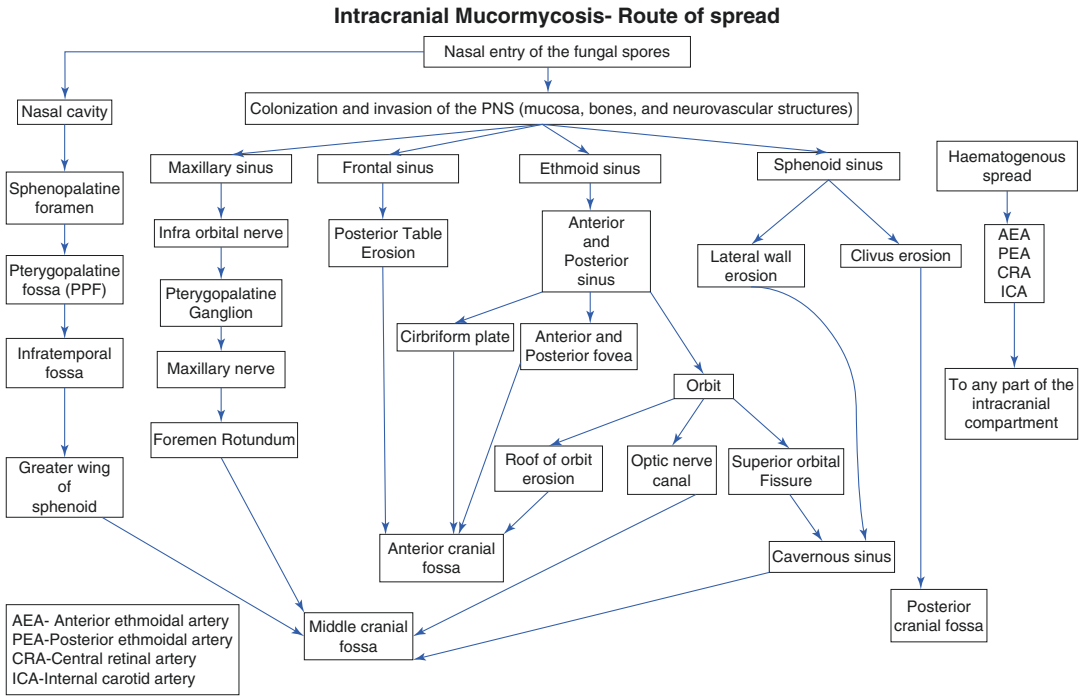

Fig. 12.1 The possible ways in which the disease can enter the intracranial compartment are demonstrated

blackening of the turbinates and nasal mucosa (Fig. 12.1). However, a routine nasal endoscopy cannot rule out the presence of the disease if there is strong clinical suspicion. Imaging modalities like computed tomography (CT) and contrast-enhanced magnetic resonance imaging (MRI) can help diagnose the disease and make decisions. Although CT findings are not specific enough to diagnose mucormycosis, they do provide valuable information about the extent of bony involvement. MRI will give more precise details about the extent of intracranial and intraorbital involvement than CT scan images. An oedematous sinus mucosa, cellulitis, cerebral ischaemia, and inflammation will appear hypointense on T1-weighted MRI images and hyperintense on T2-weighted images. On T1- and T2-weighted images; the sinus and intracranial lesions may be hypointense this is possible due to the accumulation of haemorrhagic products and paramagnetic materials such as iron, magnesium, and manganese. As the fungus causes angioinvasion, the involved tissues might show the classical contrast cut-off sign. The definitive diagnosis can be made by demonstrating the fungal hyphae on a wet mount from the specimen collected from the nasal cavity or the paranasal sinus (Fig. 12.2). The culture of the sample can also provide a definitive diagnosis. On the specimen, histopathological demonstration of tissue invasion, angioinvasion, fungal spores, and hyphae can be done. Other investigations that need to be done are procalcitonin and serum ferritin levels; both of these are seen to be very high in mucormycosis.

12.6 Case Scenarios

12.6.1 Anterior Cranial Fossa Involvement: Frontal Lobe Abscess

(a) Through anterior and posterior ethmoid sinus (Figs. 12.3 and 12.4a).
(b) Through the supraorbital part of the ethmoidal system (Fig. 12.4b).
(c) Though the posterior table of the frontal sinus.

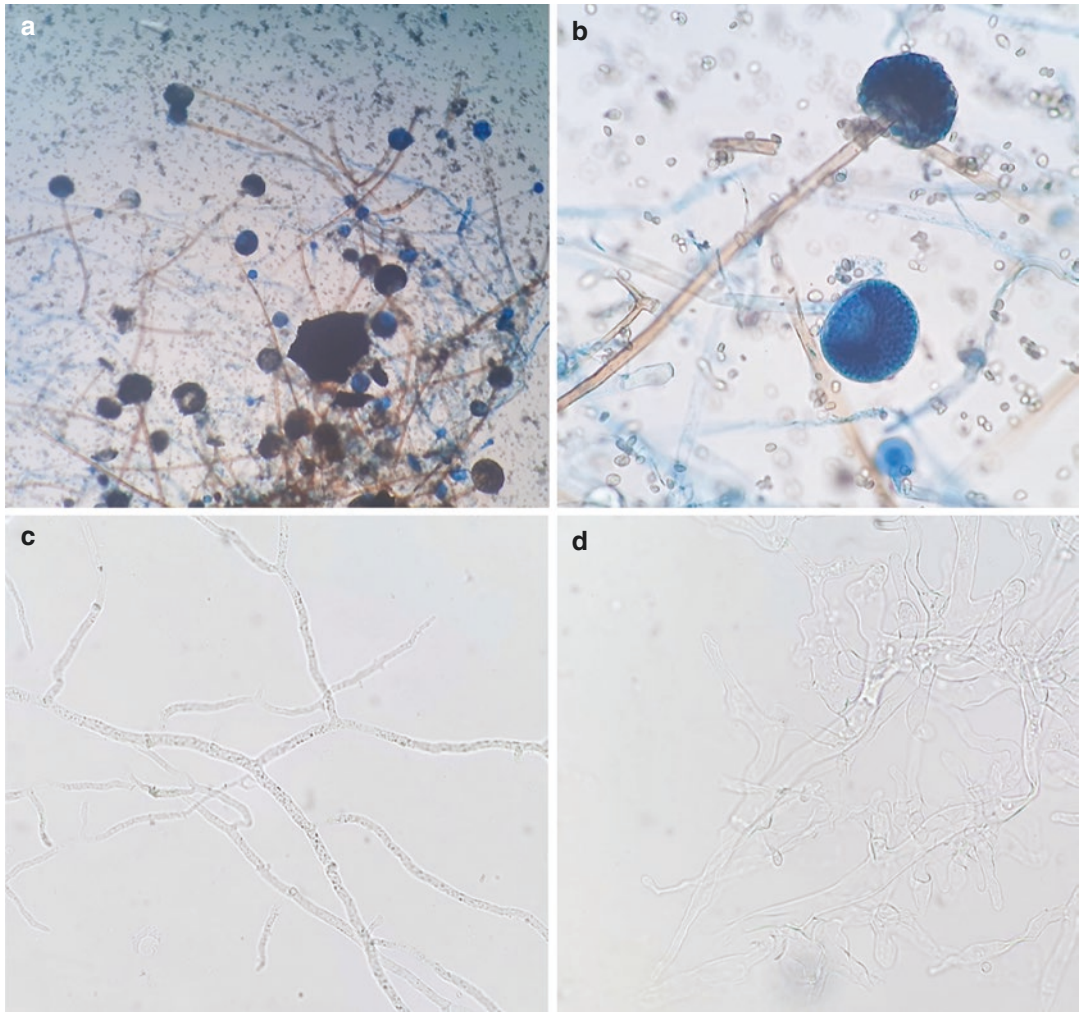

Fig. 12.2 (**a**, **b**) Lactophenol cotton blue mount of culture shows colonies of mucormycetes, with sporangiophores arising directly opposite to the rhizoids and sporangium containing plenty of sporangiospores (40×). The agent was phenotypically identified as *Rhizopus arrhizus*. (**c**, **d**) Direct 10% KOH wet mount of a tissue specimen shows broad aseptate right-angled branching fungal hyphae of mucormycetes (40×). Image courtesy: Microbiology Department, SGPGIMS, Lucknow

12.6.2 Middle Cranial Fossa: Temporal Lobe Abscess (Figs. 12.5 and 12.6)

(a) The disease involves the infraorbital nerve from the maxillary sinus, from there to the pterygopalatine ganglion, from the pterygopalatine fossa (PPF) to the greater wing of the sphenoid, and eventually to the middle cranial fossa (MCF).

(b) From the nasal cavity, the fungus invades the sphenopalatine foramen, the pterygoid body, the greater wing of the sphenoid, and eventually the middle cranial fossa.

(c) The posterior wall of the maxillary sinus erosion leads to the involvement of the infratemporal fossa (ITF). The greater wing of the sphenoid forms the roof of the ITF; its erosion leads to MCF involvement.

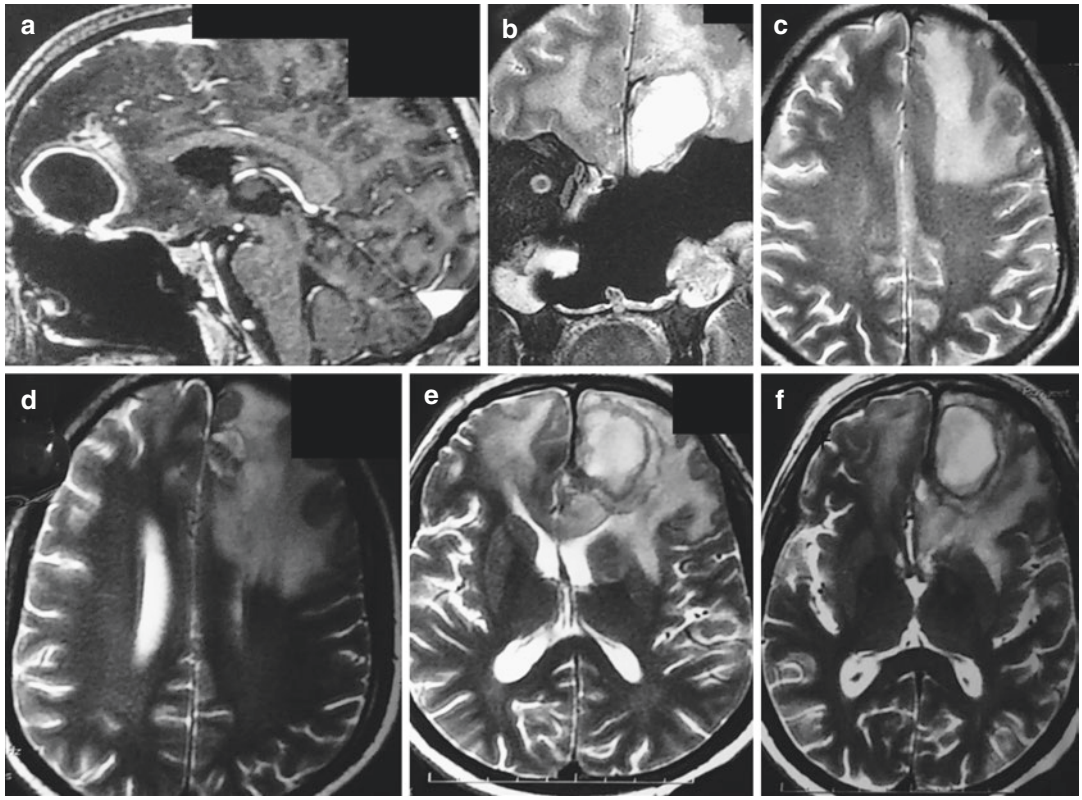

Fig. 12.3 Recurrent frontal abscess after left orbital eventration. (**a**) T1W contrast MRI showing a large abscess in the left basi-frontal lobe, with an enhancing abscess wall; (**b**) T2W MRI, coronal section, showing a large left frontal abscess; (**c**–**f**) T2W axial section showing gross oedema in bilateral frontal lobes

(d) Sphenoid sinus involvement leads to lateral wall erosion, leading to cavernous sinus involvement, and from there to the MCF.

Pterygoid and cavernous sinus are the primary sites from where the fungal infection can spread into the middle cranial fossa.

Cavernous Sinus Involvement

The disease can spread to the cavernous sinus from:

(a) Superior orbital fissure of the orbit
(b) Sphenoid sinus lateral wall (Fig. 12.7)
(c) Optic nerve and its canal (Fig. 12.8)
(d) Maxillary nerve and pterygopalatine ganglion (Fig. 12.9)
(e) Directly from the pterygoid body

12.6.3 Posterior Fossa: Cerebellar Abscess

Through the haematogenous spread, mucormycosis can form a fungal abscess (Fig. 12.10).

12.6.4 Internal Carotid Artery Thrombosis (Fig. 12.11)

The angioinvasive nature of the fungus is the primary reason for extensive tissue destruction. Mucormycosis can also cause complete occlusion of the cavernous internal carotid artery (ICA). Patients can develop a stroke due to this ICA occlusion.

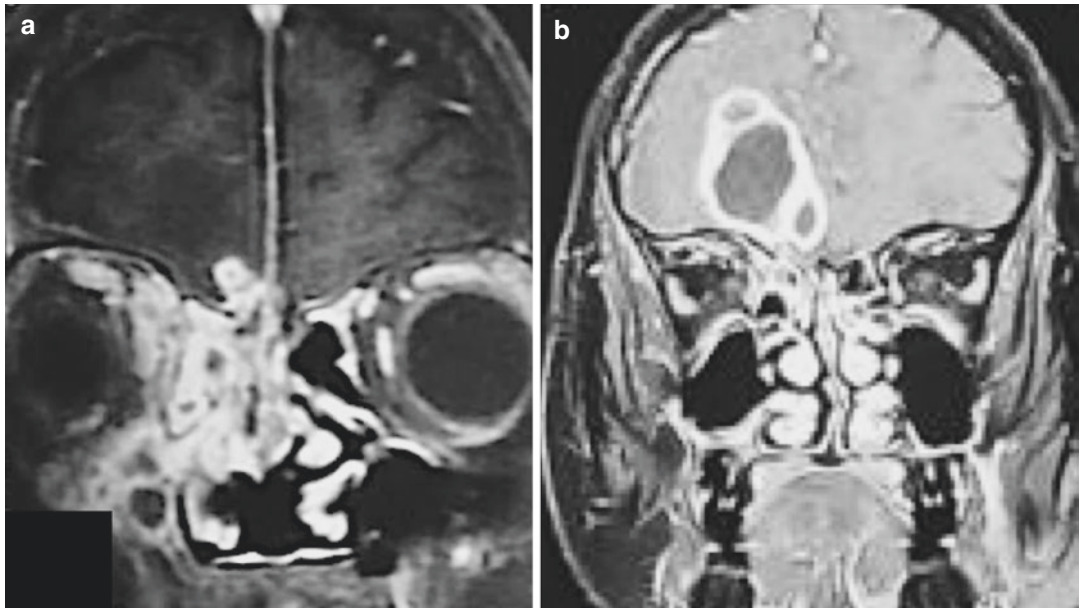

Fig. 12.4 Frontal lobe involvement through the anterior skull base involvement. (**a**) Right frontal lobe abscess due to extension from the cribriform plate and anterior ethmoid fovea area. The patient developed cerebritis, and (**b**) right frontal abscess from the roof of the supraorbital cells

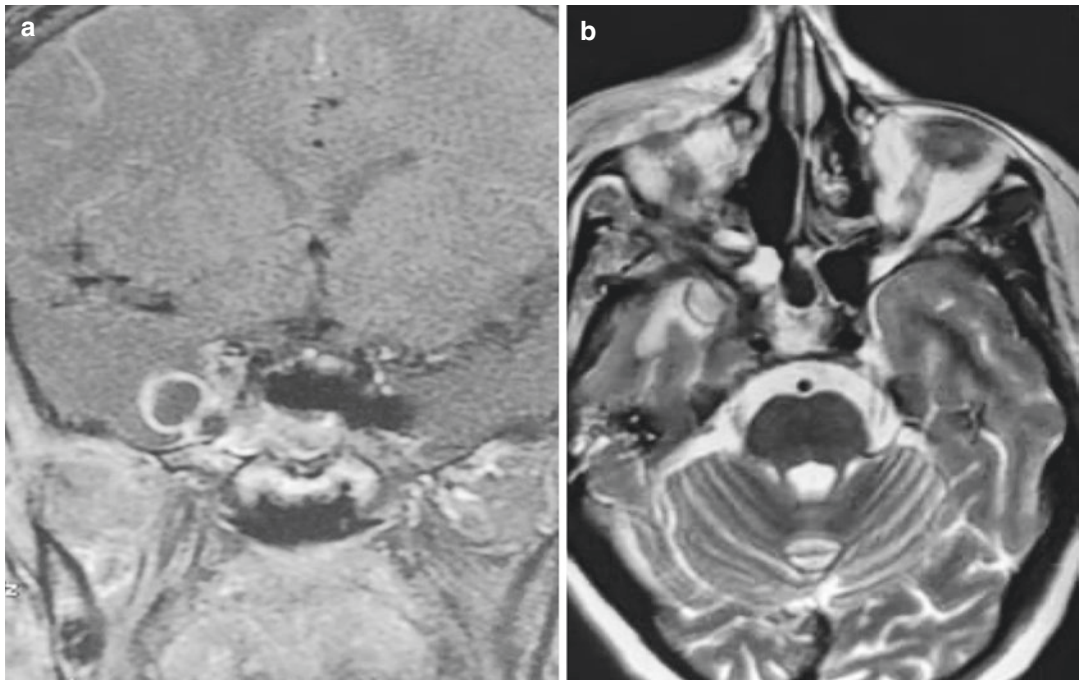

Fig. 12.5 Temporal abscess developed from cavernous sinus involvement. (**a**) T1W contrast MRI showing abscess cavity in the medial temporal lobe on the right side, and (**b**) T2W MRI showing abscess with gross peri-abscess oedema

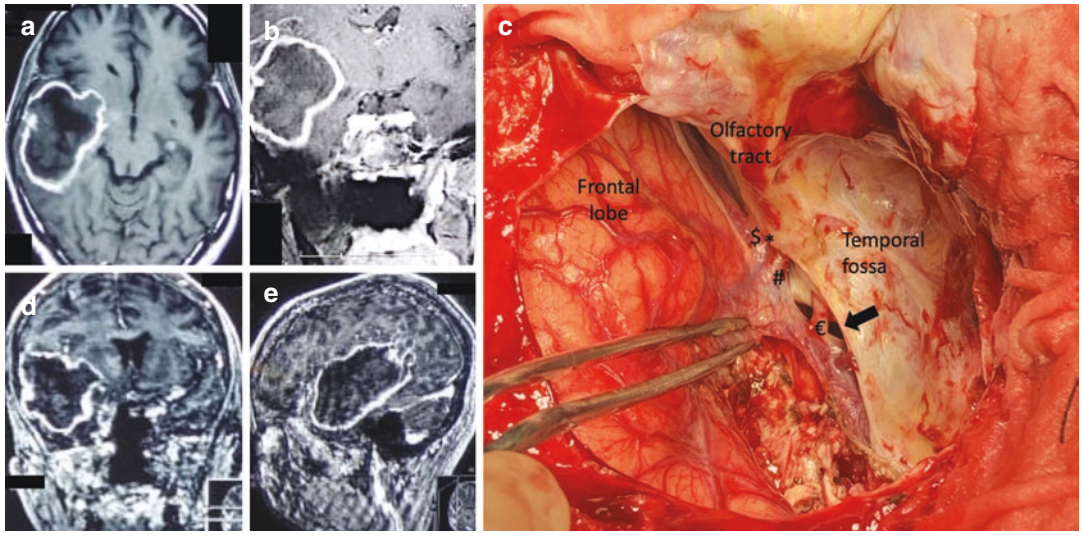

Fig. 12.6 Large temporal lobe abscess. (**a**–**d**) Contrast-enhanced MRI showing a large temporal lobe abscess; (**e**) the temporal lobe was completely involved, requiring complete temporal lobectomy. [$ = optic nerve, * = clinoid process, # = right internal carotid artery, € = third nerve, arrow = tentorial margin]

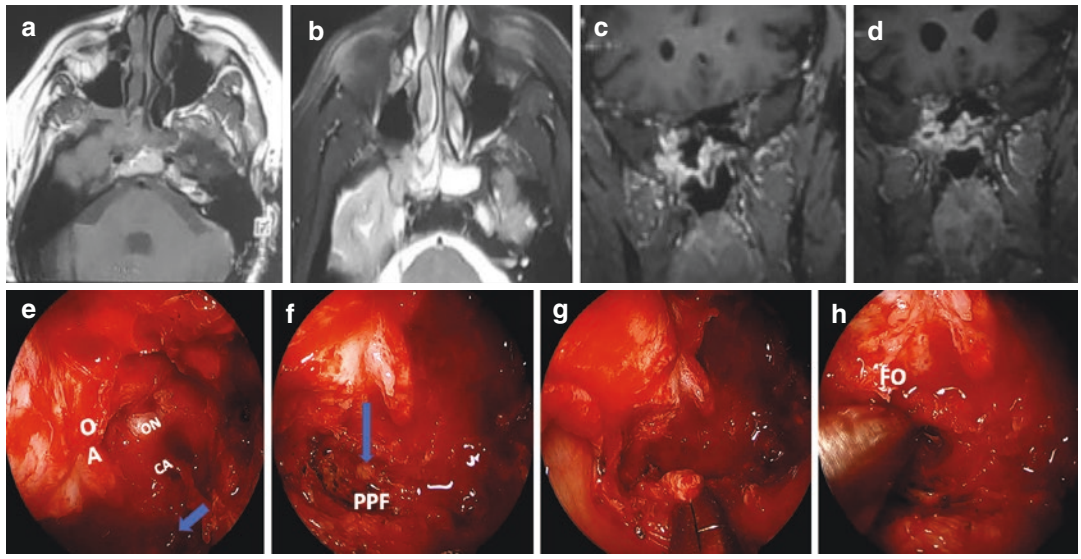

Fig. 12.7 (**a**) T1W MRI showing an isointense lesion in bilateral sphenoid sinuses with a missing plane between the right sphenoid sinus and the cavernous sinus; (**b**) T2W MRI showing the collection in bilateral sphenoid sinuses and the disease extension from the right lateral wall and pterygopalatine fossa (PPF) region into the right cavernous sinus; (**c**) and (**d**) T1W contrast coronal section shows a hypointense abscess cavity (arrow) extending from the PPF to the right cavernous sinus; (**e**) exposure of right lateral wall of sphenoid; (**f**) exposure of the PPF and the necrosed tissue in the PPF (arrow); (**g**) removal of the necrosed tissue; (**h**) communication between the PPT and cavernous sinus visualized due to erosion of greater wing of sphenoid by the disease process. ON, optic nerve; A, internal carotid artery; PPF, pterygopalatine foramen; FO, floor of orbital apex

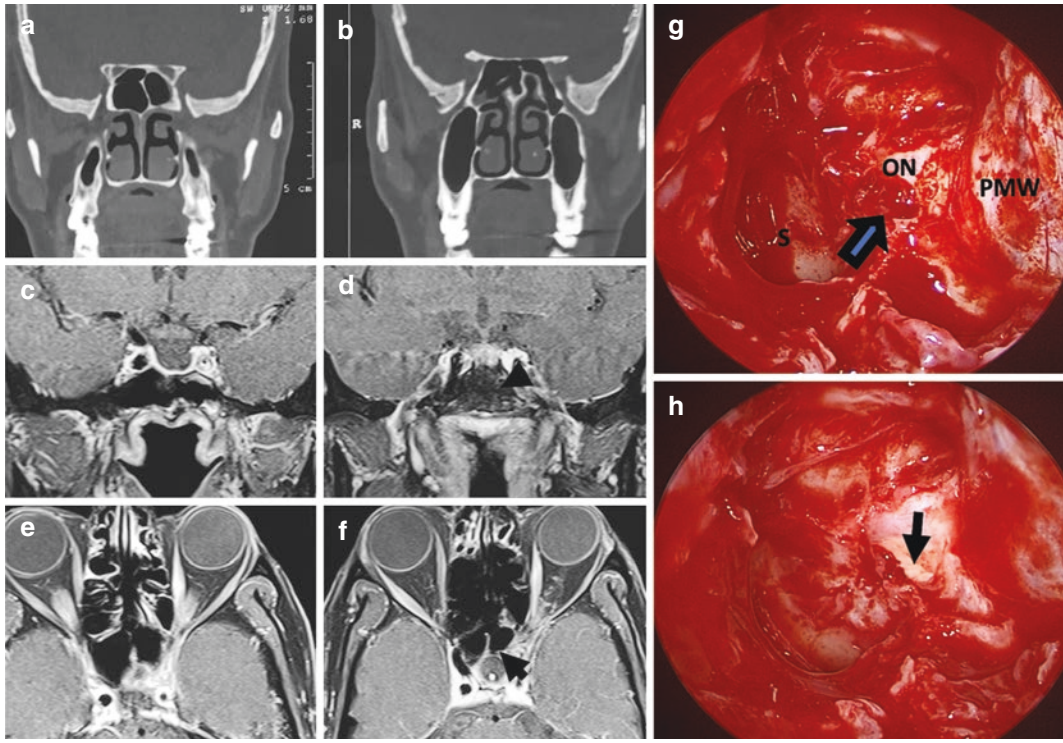

Fig. 12.8 Orbital apex lesion extending into the cavernous sinus. (**a**) and (**b**) No evidence of gross pathology on a non-contrast CT scan; (**c**) left cavernous ICA narrowing on a T1W contrast MRI scan; (**d**) abscess inside the left cavernous sinus (arrow); (**e**) and (**f**) T1W contrast MRI scan, axial section showing the extension of infection from the left orbital apex to the cavernous sinus; (**g**) and (**h**) intraoperative endoscopic image showing the optic nerve (ON), periorbita covering the medial wall of the orbit (PWMS), granulation at the orbital apex (blue arrow), the involved optic nerve sheath (black arrow)

12.7 Management

The mainstream modality of managing rhinocerebral mucormycosis is radical surgical debridement followed by intravenous amphotericin B and the reversal of the immunocompromised state [7, 8].

12.7.1 Surgical Debridement

Radical debridement of the sino-nasal and orbital involvement has to be done to reduce the fungal load. As the fungus causes angioinvasion, the involved tissues and margins do not have patent blood vessels. As a result, the antifungal medication cannot reach these areas. The surgery aims to remove all the devitalized, avascular, necrosed tissue till the normal bleeding mucosa is reached. This aids in the removal of the disease load and helps the intravenous antifungal drug reach the affected sites [9, 10].

As far as the intracranial disease is concerned, the abscess has to be managed by

(a) Burr hole and aspiration of the abscess, in the case of a small abscess.
(b) Craniotomy and excision of the abscess cavity.
(c) Endoscopic transnasal drainage of the abscess.
(d) High-dose intravenous antifungal therapy alone instilled in a small abscess cavity.

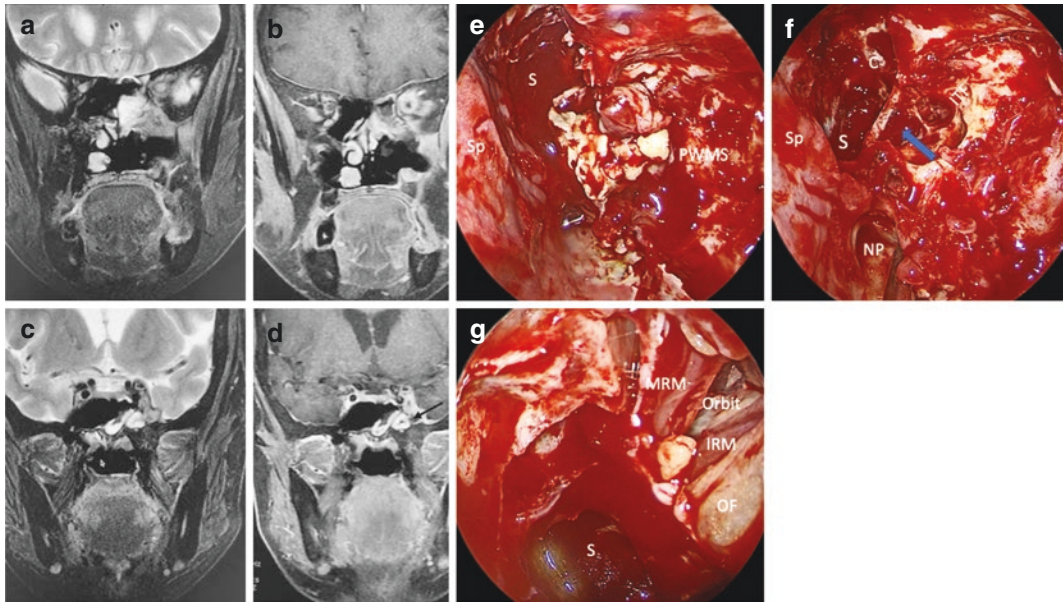

Fig. 12.9 Lateral recess fungal infection spreading into the cavernous sinus and localized supraorbital abscess. (**a**) T2W MRI showing a hypointense lesion in the superior-medial part of the orbit and the pterygopalatine fossa (PPF) involvement; (**b**) T1W contrast MRI showing a non-enhancing area in the PPF and a small non-enhancing part in the orbital area (arrow); (**c**) and (**d**) T2 and T1 contrast MRI scan shows the spread of infection from the left sphenoid lateral recess to the cavernous sinus; (**e**) necrosed tissue in the pterygopalatine fossa (PPF); (**f**) tract (blue arrow) communicating the lateral recess with the cavernous sinus; (**g**) orbital abscess drained between the medial and superior rectus muscle (*Sp* nasal septum, *S* sphenoid sinus, *PPF* pterygopalatine foramen, *C* cavernous sinus, *ITF* infratemporal fossa, *NP* nasopharynx, *PF* pterygoid fossa, *MRM* medial rectus muscle, *IRM* inferior rectus muscle, *OF* orbital fat)

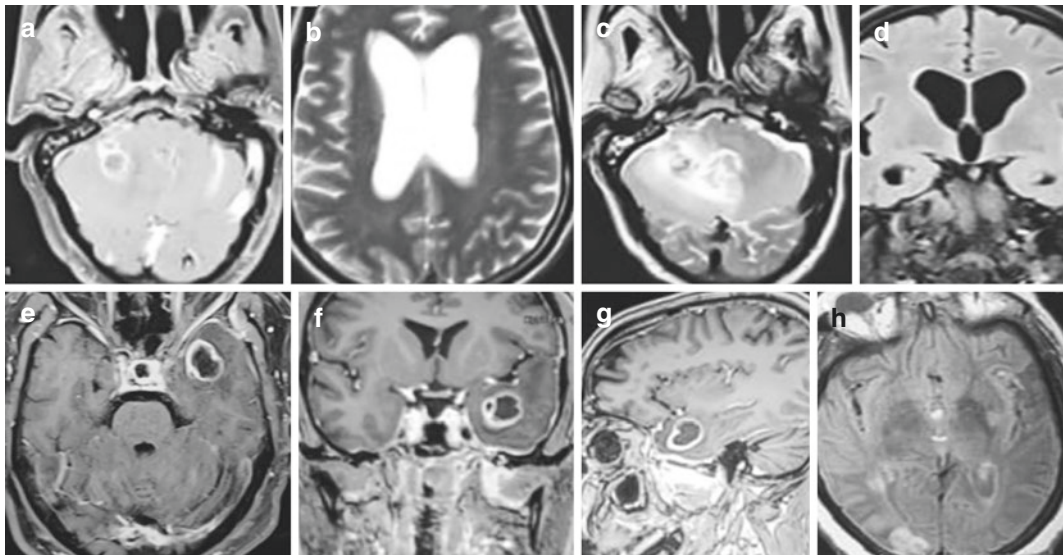

Fig. 12.10 Haematogenous spread. (**a**–**d**) Abscess formation in the right cerebellar hemisphere (posterior cranial fossa) with upstream hydrocephalus; (**e**–**g**) abscess formation in the temporal lobe (middle cranial fossa); (**h**) parieto-occipital abscess; and (**i**) and (**j**) parietal abscess

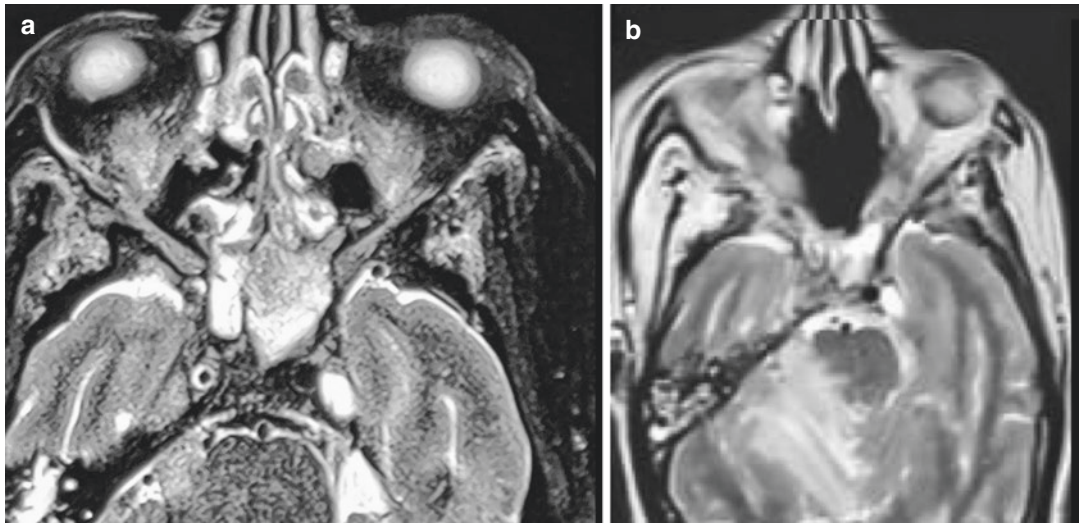

Fig. 12.11 ICA thrombosis. (**a**) Inflammation in the walls of cavernous ICA with circumferential narrowing (arrow); and (**b**) complete narrowing of the right cavernous ICA (arrow)

12.7.2 Medical Treatment

12.7.2.1 Antifungal Therapy

Intravenous antifungal therapy is the mainstay in the management of mucormycosis. The use of amphotericin B has been shown to contain the disease progression in the majority of patients. The use of other second-line drugs has increased mainly due to the toxic nature of amphotericin B. Adjuvant therapy is also available but with less efficacy than intravenous drugs.

Amphotericin B

1. Conventional amphotericin B (amphotericin B deoxycholate)
2. Amphotericin B lipid complex
3. Liposomal amphotericin B
4. Amphotericin B cholesteryl sulphate complex

Mechanism of Action

- It binds to ergosterol in the cell membrane of the fungi. After binding with ergosterol, it causes the formation of ion channels, leading to the loss of protons and monovalent cations, which results in depolarization and concentration-dependent cell killing.
- It produces free radicals, which cause oxidative damage to the cells.
- It potentiates the action of phagocytic cells.

Dosage

1. The conventional amphotericin B dosage is 1–1.5 mg/kg/day over 5–6 h. Premedication with injections of pheniramine maleate and paracetamol is required to prevent chills, rigours and fever. Pre-drug intravenous hydration should be ensured, preferably with normal saline. The cumulative dose for conventional preparation is up to 5 g. The infusion bottle should be covered to prevent the degradation of the drug from light exposure.
2. Amphotericin B lipid complex

The amphotericin B molecule is packed into a ribbon-like fat globule, allowing its penetration into the cell membrane. This preparation is better tolerated and less nephrotoxic than the conventional variant. The maximum dose for administration should not exceed 5 mg/kg/day and should be given as an infusion over 3–4 h with prior premedication.

3. Liposomal amphotericin B

It is similar the lipid complex, but the globules are more uniform and smaller in size it is well tolerated and has the least nephrotoxicity and reactivity. It can be administered at, up to 8–10 mg/kg/day as an infusion over 2–3 hours. Premedication is to be given before administration. There is no absolute limit for the cumulative dose. It must be decided based on

the extent of disease, the response to the medication, and the patient's tolerance.

Note: All amphotericin B drug formulations are to be administered in 5% dextrose infusion neutralized appropriately

Once the infusion is started, temperature, pulse, blood pressure recording, and input/output monitoring are required at least 8-hourly. Monitoring involves conducting baseline renal function tests, liver function tests, electrolytes, and a complete blood count. Everyday monitoring and charting of electrolytes and serum creatinine are mandatory. If there are signs of hypokalaemia, an electrocardiogram (ECG) must be done.

Adverse Effects

The medication can cause multi-organ dysfunction, acute kidney injury, liver failure, bone marrow failure, dyselectrolytaemia (most common hypokalaemia), chills, rash, fever, hypotension, pleural effusion.

Posaconazole

It is a triazole antifungal active against candida, aspergillus, and mucor species of fungi.

Mechanism of Action

It inhibits the fungal enzyme lanosterol, which decreases fungal cell wall ergosterol synthesis, vital for forming fungal cell walls. Cell wall abnormalities result in either cell death or blunted cell growth.

Dosage

Loading dose of 300 mg twice a day should be given on the first day, followed by 300 mg once daily. Duration of treatment can be for up to 3–6 months, depending on the extent of the disease.

Formulations

(a) Injectable Posaconazole must be judiciously given to patients with chronic kidney disease.
(b) Oral gastro-resistant tablets have a better bioavailability than the syrup form and have minor gastrointestinal side effects.
(c) The syrup form has low bioavailability and must be taken with fatty meals to improve absorption. The syrup dose is 5 mL twice a day with 1 mL of drug having 40 mg of Posaconazole.

Adverse Effects

Hepatotoxicity, liver failure, nausea, vomiting, loss of appetite, acute and chronic kidney disease, deep vein thrombosis, neutropenia are all possible side effects.

Isavuconazole

It is an extended-spectrum triazole with activity against yeasts, moulds, and dimorphic fungi.

Mechanism of Action

It inhibits cytochrome P450-dependent 14α-lanosterol demethylation, essential for fungal cell membrane ergosterol synthesis. Thus, it helps compromise fungal cell wall integrity.

Dosage

It is available as an intravenous and an oral formulation. The dose for both forms is 200 mg thrice a day for 1 day, followed by 200 mg once daily. The duration of treatment can be adjusted depending on the response and disease extension. Intravenous formulations are known to cause thrombophlebitis and cross-reactivity. Hence, it should be administered as an infusion over 1 h.

The adverse effects include hypersensitivity, nausea, vomiting, diarrhoea, headache, rash, and pedal oedema. It should not be given to patients along with rifampicin.

Other modalities of management include

1. Hyperbaric oxygen therapy
2. Iron chelation agents
3. Immune-argumentation strategies

12.8 Sequel of Rhinocerebral Mucormycosis

Following the occurrence of rhinocerebral mucormycosis, the survival rate ranges between 18 and 87%. This occurs due to metabolic or immunologic imbalance; surgical debridement in critical areas such as the cavernous sinus, internal carotid artery, cavernous sinus, and temporal lobe; adverse effects of diabetes mellitus and ketoacidosis. The *rhizopus* species have an active ketone-reductase system. They thrive in an acid pH and a glucose-rich medium in an environment of decreased phagocytic activity of polymorphonuclear leucocytes as there is a decreased local-

ized inflammatory response in ketoacidosis patients. The deferoxamine influences the pathogenicity of the organism in rhinocerebral mucormycosis. It is routinely used for iron and aluminium overload, especially in haemodialysis patients, as there is increased virus virulence, alters immune cell function by inhibiting the production of free radicals by iron-catalysed peroxidase, and inhibits the fungistatic activity of transferrin and other iron-binding proteins [11]. The intracranial sequel of rhinocerebral mucormycosis can be categorized into three groups: (a) due to direct venous invasion and necrosis, such as meningitis, brain abscess, and multiple cranial nerve palsies; (b) due to vascular invasions such as cavernous sinus thrombosis, internal carotid artery thrombosis or aneurysm formation, carotico-cavernous fistula or ischaemic infarct formation, and the development of subdural or intracerebral haemorrhage; and (c) due to space-occupying lesions resulting in obstructive hydrocephalus and behavioural changes [11].

12.9 Summary of Management of Some of the Sequel

12.9.1 Proptosis

Proptosis may occur either due to infiltration of the orbit by the fungal skull base mass or due to ophthalmic vein dilatation as a result of cavernous sinus venous hypertension. Excision of the mass under the cover of antifungal agents in the case of a significant mass and necrotic tissue in orbit helps combat this entity. Proptosis may result in mechanical diplopia due to the restriction of globe movements or corneal ulceration and visual loss, even occasionally leading to complete loss of vision or phthisis bulbi.

12.9.2 Cavernous Sinus Thrombosis

This may result in a congested erythematous nasal mucosa, conjunctival erythema and oedema, purulent nasal discharge, and contrast-enhanced CT or MR scan showing dilated ophthalmic veins as well as enhancement and dilation of the cavernous sinuses. The maxillary, ethmoid, and sphenoid sinuses show mucosal thickening and retention of purulent material. A unilateral thrombosis may extend to the other side due to the involvement of the intercavernous sinuses. An endoscopic paranasal sinus debridement, antibiotics, and antifungals are to be given for prolonged periods. Unfractionated heparin and low-molecular-weight heparin may be initially used to combat cavernous sinus thrombosis. Patients may also require long-term anticoagulation with an oral anticoagulant, such as warfarin, with a targeted international normalized ratio of 2.5 [12].

12.9.3 Internal Carotid Artery Occlusion or Aneurysm Formation

For a patient with an intracranial fungal infection who develops a sudden-onset focal neurologic deficit, an immediate CT scan to rule out an infarction or haemorrhage and an angiographic investigation to detect a possible internal carotid artery (ICA) occlusion or aneurysm formation are warranted. Infection can invade the adventitia of adjacent blood vessels, including the retinal artery, ophthalmic artery, and ICA, causing intracranial infection, systemic embolism, intracerebral haemorrhage, subarachnoid haemorrhage, and cerebral infarction. Sporadic cases have shown ICA occlusion and secondary abscess formation. Leptomeningeal collateral circulation from cortical branches may sustain the circulation in some cases. The treatment consists of early radical debridement, drainage, early decision of ocular exenteration (especially for those with visual loss), appropriate parenteral and local amphotericin B treatment, management of underlying medical conditions, and hyperbaric oxygen therapy [13]. A decompressive craniectomy with or without resection of the infarcted area or the endoscopic or open drainage of the haemorrhagic clot may be in the case of mass effect brought about by hemispheric infarction or haemorrhage considered [14]. A peripheral mycotic aneurysm may require repeated observations under the cover of antifun-

gal medication. Endovascular coiling or stent may be required for a proximal aneurysm arising from a large or middle-sized artery.

12.9.4 Meningitis, Cerebritis, and Abscess Formation

Patients with fungal meningitis may present with fever, headache, stiff neck, nausea, vomiting, photophobia (eyes being more sensitive to light), and altered mental status (confusion). Samples of cerebrospinal fluid may show fungal organisms and a positive culture. High-dose intravenous antifungal medications and long-term antifungal medications orally may be required. The total length of treatment depends on the patient's immune system and the type of fungus causing the infection. Arachnoidal and pial breaches by the fungal infection may result in cortical end-artery thrombosis, cerebritis, and brain abscess formation. The abscess may be drained or excised under the cover of antibiotics and antifungal management. Multiple pyaemic abscesses in an immunocompromised patient usually occur due to haematogenous spread and require anti-oedema measures like mannitol with intravenous antifungal management.

12.9.5 Cerebral Fungal Granuloma

Fungal granulomas may spread through the haematogenous spread in immunocompromised patients with intracranial lesions and diabetic patients with intracranial and rhinocerebral mass lesions. A large solitary granuloma in a non-eloquent area may require surgical excision to combat raised intracranial pressure. Long-term antifungal medication may be required.

12.10 Management Nuances

A cerebral abscess (Fig. 12.12):

The initial therapy should be commenced with broad-spectrum antibiotics and antifungal agents, that can cross the blood-brain barrier in adequate concentration. On aspiration of the pus, antibiotic sensitivity reports become available. Then, specific antifungal and bactericidal agents for the organism cultured should be administered. Corticosteroids may be used perioperatively to reduce intracranial pressure to avoid brain herniation. Seizures occur in up to 25%–43% of cases of brain abscess. The duration of antiepileptic treatment may be at least 3 months if no more seizures have occurred. Discontinuation of antiepileptic drugs should only be considered when the patient is seizure-free for at least 2 years after surgery and electroencephalogram (EEG) shows no epileptic activity [14].

The "Infection in Neurosurgery Working Party of the British Society for Antimicrobial Chemotherapy" recommends surgical drainage or excision: to reduce raised intracranial pressure by aspiration of the cavity, to confirm the diagnosis, to obtain pus for microbiological diagnosis, to enhance the efficacy of antibiotic therapy, and to avoid the iatrogenic spread of infection into the ventricles [15].

Emergent drainage is indicated both therapeutically and to establish the causative offending pathogen. Surgical excision may be the choice if the pus is thick; the abscess is multiloculated; a subdural empyema, a cerebellar abscess, or a brain stem abscess is present. Multiple abscesses may require aspiration of the largest one for diagnosis and others if they are causing mass effects. A peripherally placed abscess that fails to respond to aspiration may require a craniotomy and excision [14].

Stereotactic biopsy/aspiration may be mandated in the case of a deep-seated (e.g. ganglionic, brain stem, thalamus) fungal abscess or granuloma, the location of this lesion in an eloquent brain region, or when the masses are multiple. Ommaya reservoirs may be placed stereotactically into the abscess cavity, and amphotericin B can be injected directly into the cavity [16].

An open craniotomy is performed for suspected intracranial fungal mass lesions in relatively accessible regions of the brain and when perceived to be safe.

Hydrocephalus may require a cerebrospinal fluid diversion procedure such as external ventricular drainage, a third ventriculostomy, or the placement of a ventriculoperitoneal (VP) shunt. A fungal aneurysm may require surgical clipping

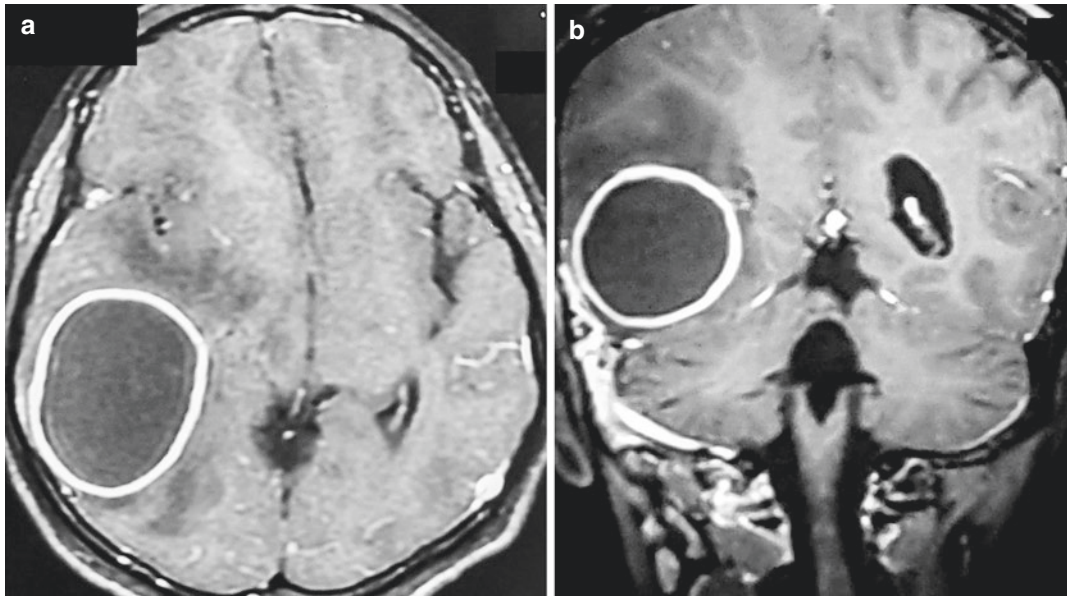

Fig. 12.12 (**a**) Contrast-enhanced T1-weighted axial view showing a well-loculated abscess in the temporal lobe with associated perifocal oedema. (**b**) Contrast-enhanced T1-weighted coronal view showing the temporal abscess with granulation tissue along the transverse sigmoid junction and the temporal base. Using temporal craniotomy, this abscess was aspirated and then excised

or endovascular coiling or stenting. The paranasal sinus disease may be treated with functional endoscopic sinus surgery to remove the paranasal sinus mass and facilitate aeration that prevents regrowth of the fungal organisms [16].

12.11 Transcranial Approaches to Excision of Fungal Abscess/Granuloma or Skull Base Extensive Lesion

Intracranial lesions: A fungal abscess or granuloma of the petrous bone or an otogenic fungal abscess are likely to form an intracranial lesion in the temporal lobe or the cerebellar hemisphere. A temporal lesion will require a temporal craniotomy, and a cerebellar lesion will require a retromastoid suboccipital craniotomy for excision. A lesion extending along the frontal base from the paranasal sinus may be accessed using a frontal craniotomy or a minimally invasive supraorbital craniotomy.

A surfacing abscess or granuloma at the grey-white matter junction in the frontal, parietal, or occipital lobe is usually due to haematogenous dissemination. It may be removed using a corresponding frontal, parietal, or occipital craniotomy, respectively.

A frontotemporal trans-sylvian approach may be required for a lesion in the sellar-suprasellar region with or without a parasellar, cavernous, or retrosellar extension. Four corridors may be used to access the lesion: interoptic, optico-carotid, lamina terminalis, or carotico-oculomotor.

A lateral rhinotomy may also be used for a sellar-suprasellar lesion with or without sphenoid sinus extension.

An intradural (trans-sylvian and subtemporal) approach may be used for a sellar-suprasellar lesion with or without a predominantly middle fossa base/cavernous sinus and or retrosellar extension.

An anterior or posterior interhemispheric approach may be used for a lesion situated in the anterior or posterior interhemispheric fissure, respectively.

A frontal parasagittal transcortical or transcallosal approach may be used for accessing intraventricular granulomas or abscesses.

Extracranial extensive lesions at the skull base require extradural approaches:

- *The frontal skull base approaches:* Minimally invasive endoscopic or microscopic trans-sphenoidal approaches may be used for lesions with sellar-suprasellar and sphenoid sinus lesions predominantly occupying the midline. An extended trans-sphenoidal approach may be used for a lesion spreading along the anterior skull base to the tuberculum sellae, planum sphenoidal, or the cribriform plate up to the frontal sinuses or the medial portion of the orbit [17].
  An extended frontobasal approach may be utilized for an extensive skull base lesion extending from the anterior paranasal sinuses and nasopharynx right up to the clival region.
- *Lateral skull base approaches* (Figs. 12.13, 12.14, and 12.15)*:* a transzygomatic frontotemporal craniotomy with interdural dissection of the temporal dura from the cavernous sinus dura helps access cavernous sinus and the extradural skull base from the lateral aspect. A subtemporal approach and an anterior petrosectomy help in accessing the lesion located at the petrous apex.

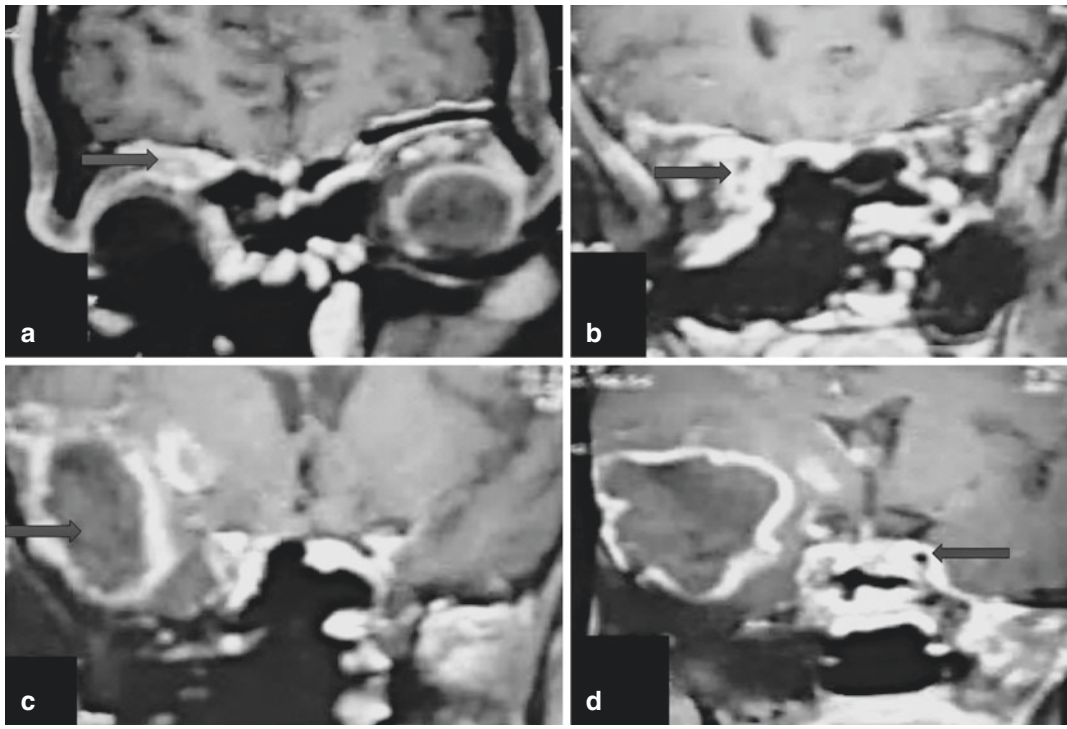

Fig. 12.13 (**a**) Mucormycosis granulation tissue along the frontal base and orbital roof bilaterally (arrow) causing mild orbital proptosis; (**b**) granulation tissue in the cavernous sinus (arrow); (**c**) a temporal abscess with satellite lesions along the Sylvian fissure (arrow); (**d**) granulation tissue in the sella and bilateral cavernous sinuses encasing the internal carotid artery (arrow)

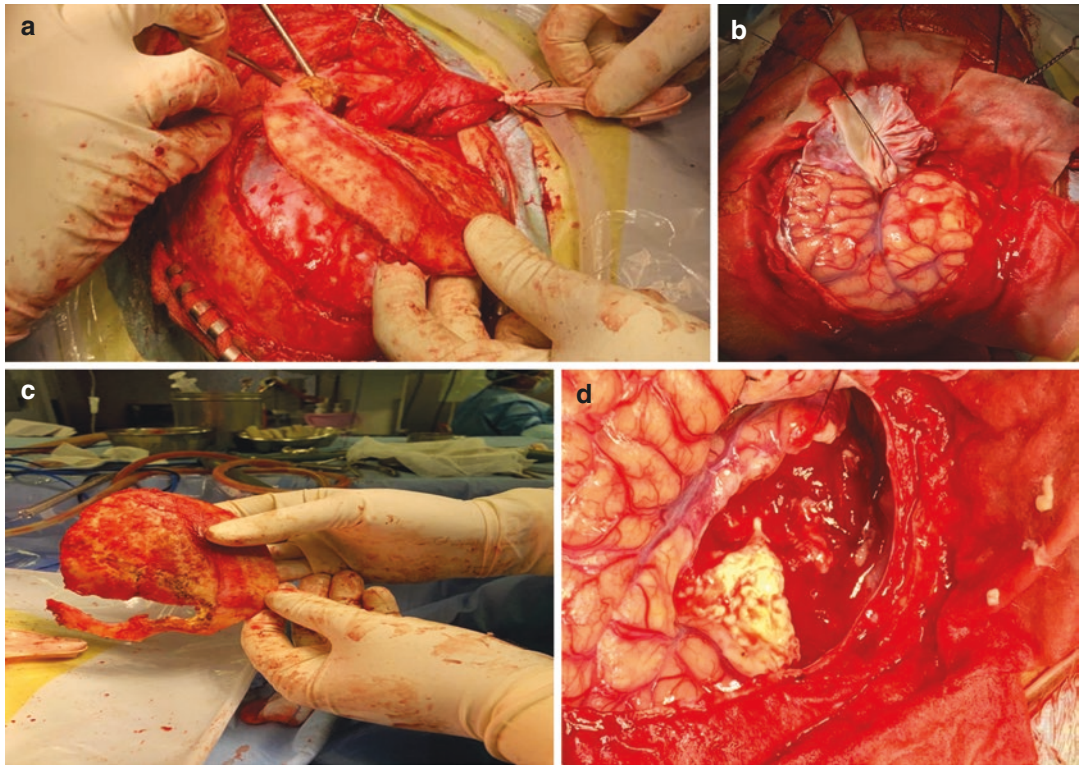

Fig. 12.14 (**a**) A frontotemporal craniotomy with orbitozygomatic osteotomy with the reflection of the temporalis muscle exposes the frontotemporal dura; (**b**) opening the dura exposes the frontal and temporal lobes and the interposed Sylvian fissure. The temporal lobe appears bulged; (**c**) the elevated bone flap is demonstrated; (**d**) the temporal lobectomy with excision of the temporal abscess exposes the granulation tissue of mucormycosis at the temporal base

Finally, posterior petrosectomy helps access an extensive fungal invasive lesion of the mastoid and posterior petrosal region.

12.12 Causes of Prolonged Morbidity and Mortality

Raised intracranial pressure due to the presence of multiple or extensive fungal lesions with or without perifocal oedema may cause obtundation due to subfalcine, transtentorial, or tonsillar herniation. An extensive meningoencephalitis or ventriculitis due to a fungal infection may result in a significant morbidity. The development of acute hydrocephalus may also result in sudden neurological deterioration.

Vascular invasion with the formation of a pseudo-aneurysm with subsequent haemorrhage, arterial occlusion or dissection with the development of infarction, and cortical venous or venous sinus infiltration and occlusion resulting in venous thrombosis may result in prolonged and persistent morbidity.

Fungal sepsis, particularly in immunocompromised individuals, may also result in encephalitis.

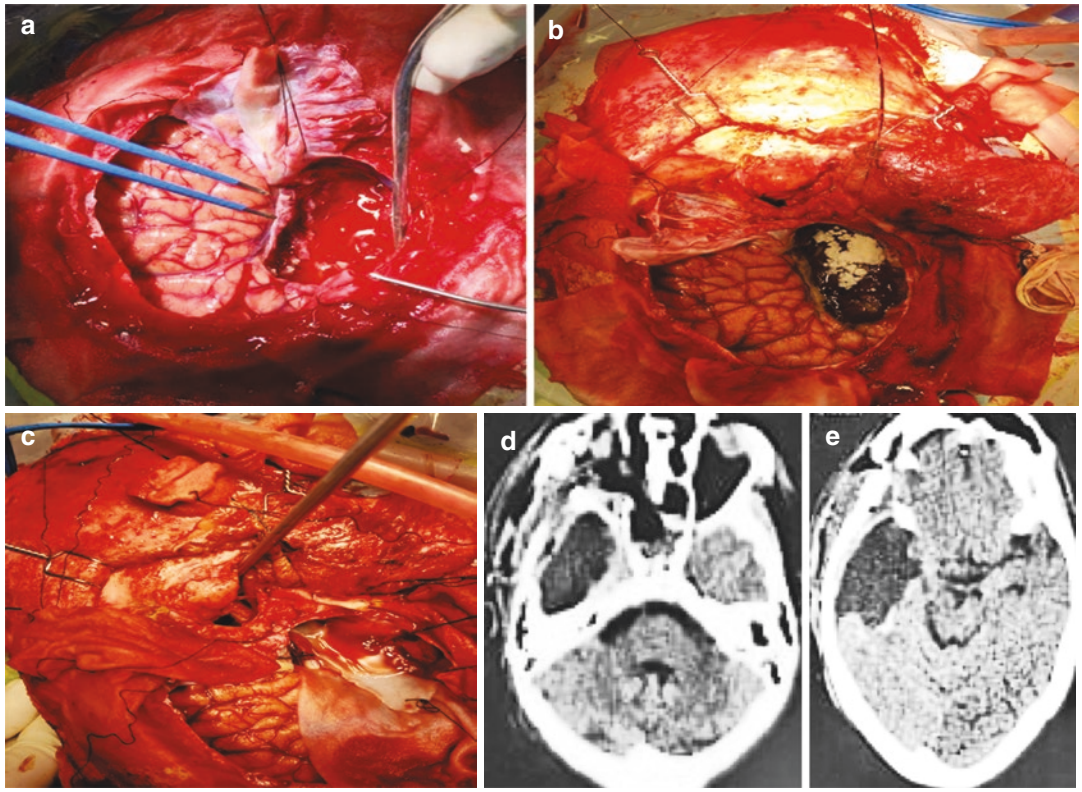

Fig. 12.15 (**a**) The excision of the mucormycosis granulation tissue at the temporal base exposes the temporal dura until the tentorium cerebelli; (**b**) the black granulation tissue of mucormycosis is seen at the temporal base; (**c**) the fungal tissue is also removed from the orbital apex; (**d**) and (**e**) postoperative contrast axial CT scan image showing the gross total excision of the fungal lesion. The midline shift has significantly decreased

12.13 Conclusion

Rhinocerebral mucormycosis requires an early diagnosis, surgical decompression, and a complete course of antifungal therapy. Multispeciality care is usually required to combat the infection as well as its sequelae.

References

1. Prakash H, Chakrabarti A. Global epidemiology of mucormycosis. J Fungi (Basel). 2019;5(1):26. https://doi.org/10.3390/jof5010026.
2. Tay MZ, Poh CM, Rénia L, MacAry PA, Ng LFP. The trinity of COVID-19: immunity, inflammation and intervention. Nat Rev Immunol. 2020;20:363–74. https://doi.org/10.1038/s41577-020-0311-8.
3. John TM, Jacob CN, Kontoyiannis DP. When uncontrolled diabetes mellitus and severe covid-19 converge: the perfect storm for mucormycosis. J Fungi (Basel). 2021;7:298. https://doi.org/10.3390/jof7040298.
4. Bonaventura A, Vecchié A, Dagna L, Martinod K, Dixon DL, Van Tassell BW, Dentali F, Montecucco F, Massberg S, Levi M, Abbate A. Endothelial dysfunction and immunothrombosis as key pathogenic mechanisms in COVID-19. Nat Rev Immunol. 2021;21:319–29. https://doi.org/10.1038/s41577-021-00536-9.
5. Lax C, Pérez-Arques C, Navarro-Mendoza MI, Cánovas-Márquez JT, Tahiri G, Pérez-Ruiz JA, Osorio-Concepción M, Murcia-Flores L, Navarro E, Garre V, Nicolás FE. Genes, pathways, and mechanisms involved in the virulence of mucorales. Genes (Basel). 2020;11:317. https://doi.org/10.3390/genes11030317.
6. Stanford FA, Matthies N, Cseresnyés Z, Figge MT, Hassan MIA, Voigt K. Expression patterns in reduc-

tive iron assimilation and functional consequences during phagocytosis of *lichtheimia corymbifera*, an emerging cause of mucormycosis. J Fungi (Basel). 2021;7:272. https://doi.org/10.3390/jof7040272.
7. Sipsas NV, Gamaletsou MN, Anastasopoulou A, Kontoyiannis DP. Therapy of mucormycosis. J Fungi (Basel). 2018;4:90. https://doi.org/10.3390/jof4030090.
8. Prakash H, Skiada A, Paul RA, Chakrabarti A, Rudramurthy SM. Connecting the dots: interplay of pathogenic mechanisms between COVID-19 disease and mucormycosis. J Fungi (Basel). 2021;7:616. https://doi.org/10.3390/jof7080616.
9. Soare AY, Watkins TN, Bruno VM. Understanding mucormycoses in the age of "omics". Front Genet. 2020;11:699. https://doi.org/10.3389/fgene.2020.00699.
10. Ahmadikia K, Hashemi SJ, Khodavaisy S, Getso MI, Alijani N, Badali H, Mirhendi H, Salehi M, Tabari A, Mohammadi Ardehali M, Kord M, Roilides E, Rezaie S. The double-edged sword of systemic corticosteroid therapy in viral pneumonia: A case report and comparative review of influenza-associated mucormycosis versus COVID-19 associated mucormycosis. Mycoses. 2021;64:798–808. https://doi.org/10.1111/myc.13256.
11. Anand VK, Alemar G, Grisworld JA. Intracranial complications of mucormycosis: an experimental model and clinical review. Laryngoscope. 1992;102:656–62.
12. Komatsu H, Matsumoto F, Kasai M, Kurano K, Sasaki D, Ikeda K. Cavernous sinus thrombosis caused by contralateral sphenoid sinusitis: a case report. Head Face Med. 2013;9:9. https://doi.org/10.1186/1746-160X-9-9.
13. Kim JP, Park BJ, Lee MS, Lim YJ. Occlusion of the internal carotid artery due to intracranial fungal infection. J Korean Neurosurg Soc. 2011;49:186–9.
14. Mishra A, Prabhuraj AR, Shukla DP, Nandeesh BN, Chandrashekar N, Ramalingaiah A, Arivazhagan A, Bhat DI, Somanna S, Devi BI. Intracranial fungal granuloma: a single-institute study of 90 cases over 18 years. Neurosurg Focus. 2019;47(2):E14.
15. Alvis Miranda H, Castellar-Leones SM, Elzain MA, Moscote-Salazar LR. Brain abscess: current management. J Neurosci Rural Pract. 2013;4(Suppl 1):S67–81.
16. Infection in Neurosurgery Working Party of the British Society for Antimicrobial Chemotherapy. The rational use of antibiotics in the treatment of brain abscess. Br J Neurosurg. 2000;14:525–30.
17. Nayak S, Dabadghao P, Dixit P, Dwivedi V, Srivastava AK, Behari S. Cushing's disease in children: a review. Neurol India. 2020;68:52–65.

13 Palatal Disease in Rhino-Orbito-Cerebral Mucormycosis

Aditya Moorthy and Tulasi Nayak

13.1 Introduction

Mucormycosis was a rare but devastatingly disfiguring disease caused by a group of mucormycetes mould with a very high mortality rate (>50%) [1, 2]. Early diagnosis and aggressive treatment are vital. In spite of it, survivors are left with complex craniofacial defects affecting both form and function.

With mucormycosis primarily originating in the paranasal sinuses, bony involvement is common [3]. The basic pathology is the avascular necrosis secondary to transmural fungal invasion of both the small and medium blood vessels [4]. The extent of angioinvasion and the involved blood vessels determines the degree of avascular necrosis. Aggressive surgical management of palatal disease is vital to preserve adjacent uninvolved bone, halt disease progression and prevent disease resurgence [5, 6].

The aim of surgical resection in invasive fungal infection is the reduction of disease (fungal) burden and excision of all devascularized tissue to enable effective antifungal therapy [6]. The philosophy is similar to limb salvage surgery where an infected part is removed to save the rest of the limb. Since disease eradication isn't the surgical objective, enbloc resection isn't always necessary or possible. Bone removal follows the surgical philosophy of osteomyelitis management rather than oncological principles.

13.2 Anatomy of Palatal Spread of Mucormycosis

There are three probable routes of fungal spread to the infrastructure of the maxilla, pterygopalatine fossa (Fig. 13.1a) and palatal alveolus. The first and most common is contiguous spread of antral disease. The second is angioinvasion of blood vessels, commonly the descending palatine, greater palatine and the infraorbital vessels. Lastly, infection could spread via the socket of a fresh extraction socket (Fig. 13.1a). Once bony invasion occurs, it results in rapid spread along the medul-

A. Moorthy (✉)
Department of Oral and Maxillofacial Surgery, Rangadore Memorial Hospital, Bangalore, India

Department of Oral and Maxillofacial Surgery, Trustwell Hospitals, Bangalore, India

Department of Oral and Maxillofacial Surgery, Apollo Hospitals, Bangalore, India

T. Nayak
Department of Oral and Maxillofacial Surgery, Rangadore Memorial Hospital, Bangalore, India

Department of Oral and Maxillofacial Surgery, Trustwell Hospitals, Bangalore, India

N. Gupta, S. G. Honavar (eds.), *Rhino-Orbito-Cerebral Mucormycosis*,
https://doi.org/10.1007/978-981-16-9729-6_13

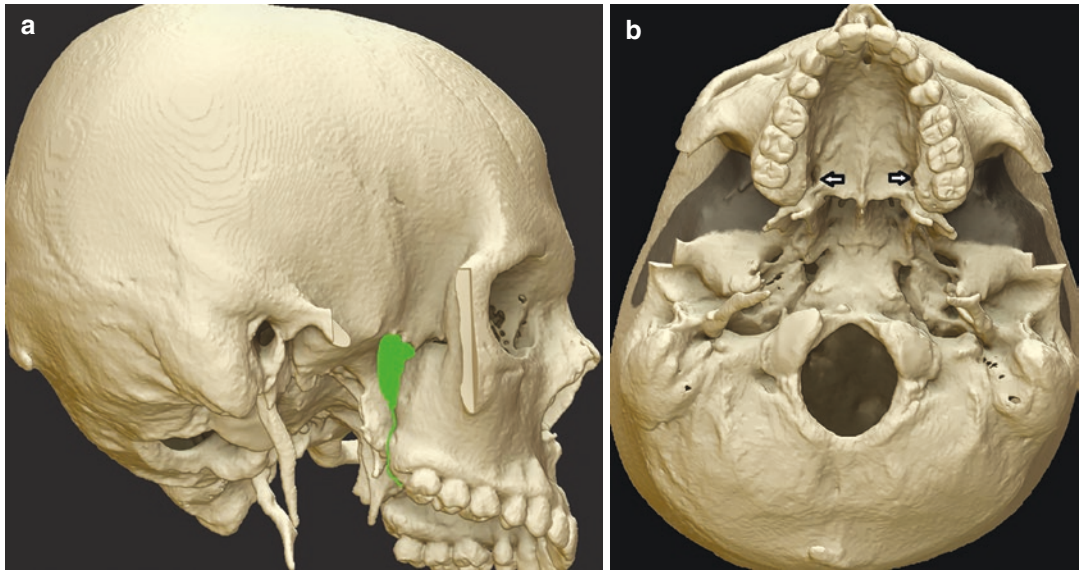

Fig. 13.1 (**a**) Pterygopalatine fossa. (**b**) Bilateral greater palatine foraminae

lary spaces resulting in avascular necrosis with or without supervening bacterial infection.

If the palate (infrastructure maxilla) is involved primarily, it is prudent to address it surgically in an aggressive manner as contiguous involvement of the retromaxillary area and pterygopalatine fissure are precursors to orbital involvement and spread of infection to the skull base.

13.3 Clinical Presentation

History taking is of critical importance in determining current or impending involvement of the infrastructure of the maxilla. A referral made by a dentist to the ENT/maxillofacial surgeon should raise the index of suspicion of bony involvement. Likewise, sudden mobility of hitherto firm teeth, acute-onset periodontal disease and recent dental extractions in the background of a possible diagnosis of CAM should be considered strong indicators of palatal involvement.

With the fungi having different portals of entry available into the bony maxilla, the clinical presentation doesn't follow a set pattern, and consequently, the signs and symptoms do not necessarily follow one another and do not reflect an increasing severity of involvement.

13.4 Signs of Palatal Involvement

- Bogginess of the palatal mucosa (Fig. 13.2)
- Obliteration of palatal rugae (Fig. 13.2a)
- Duskiness of palatal mucosa that is often clearly delineated (Figs. 13.2 and 13.3)
- Mucopurulent discharge and sinus formation (Fig. 13.4)
- Exposed palatal bone and soft tissue necrosis (Fig. 13.5)
- Discharging sinuses in the labial alveolus (Fig. 13.6)
- Obvious avascular necrosis with maxillary mobility (Fig. 13.7)

13.5 Symptoms of Palatal Involvement

- Odd taste in the mouth
- Mobility of teeth
- Mobility of the entire palate (elicited by gripping the front teeth between thumb and forefinger and tugging gently)
- Spontaneous exfoliation of teeth.
- Nasal regurgitation.
- Primary palatal pain is surprisingly uncommon.

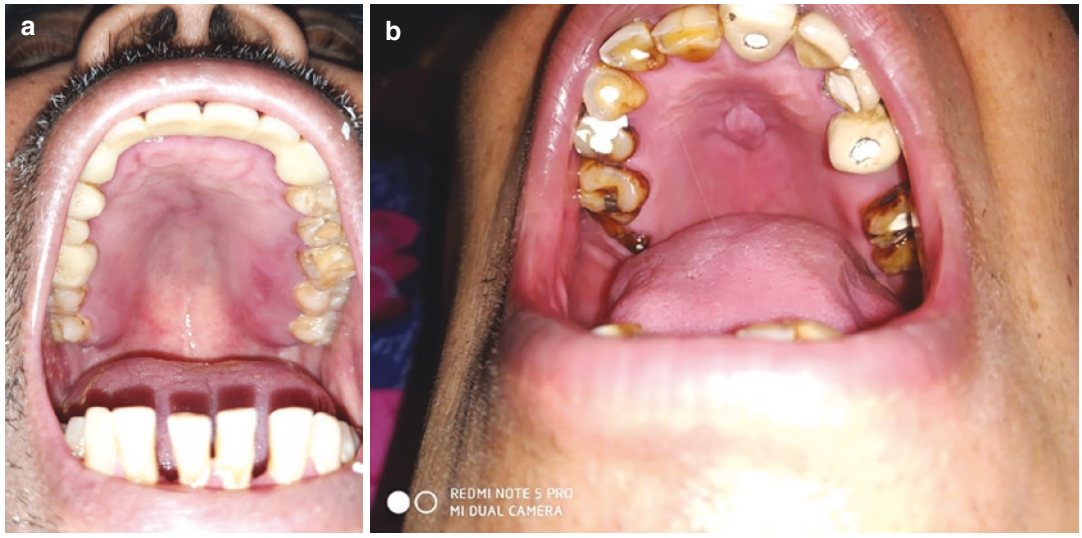

Fig. 13.2 (**a**) Dusky hue of the palate with blunting of palatine rugae. (**b**) Midpalatal boggy tissue and sinus

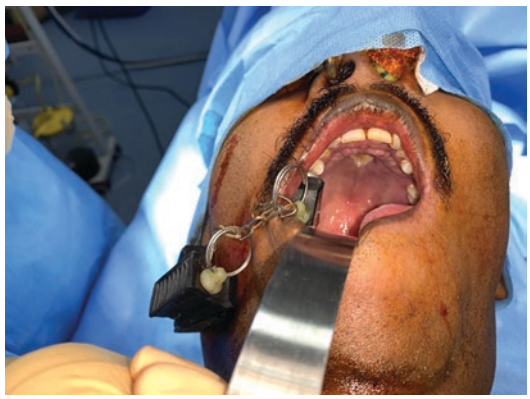

Fig. 13.3 Early palatal erosion with surrounding mucosal duskiness

Early palatal involvement presents with subtle clinical signs like duskiness of the palate and early mobility of teeth. The fear of overtreating the patient surgically creates a vexing dilemma. A close watch on these patients is warranted to ensure early re-intervention. Late disease progression to involve the palate occasionally occurs, and recurrent or progressive involvement isn't rare. Treatment planning, especially reconstruction, should account for these possibilities.

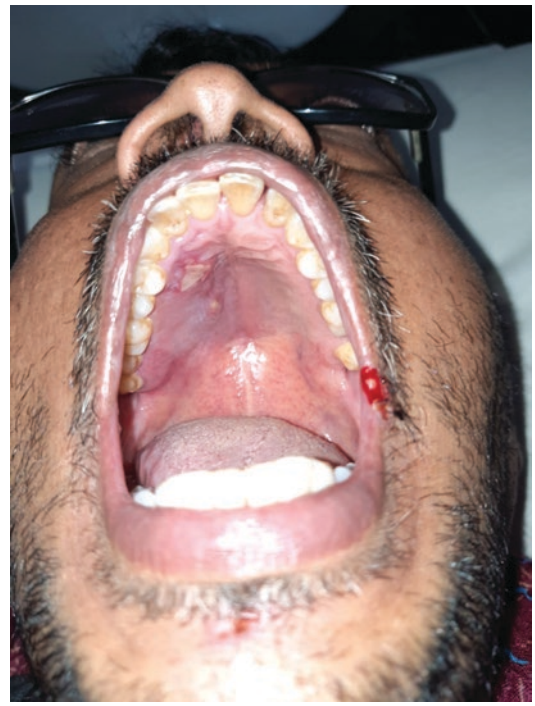

Fig. 13.4 Palatal mucosal erosion with discharging sinus

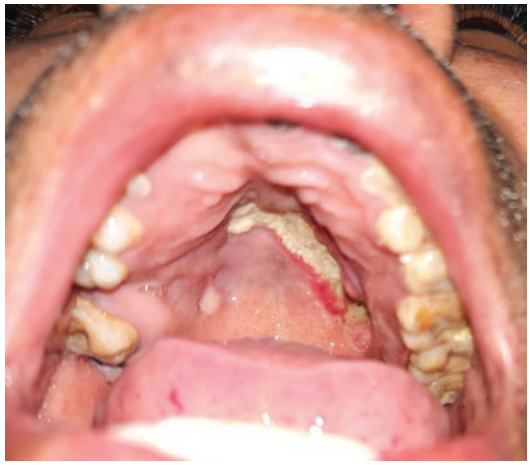

Fig. 13.5 Exposed palatal bone with mucosal necrosis

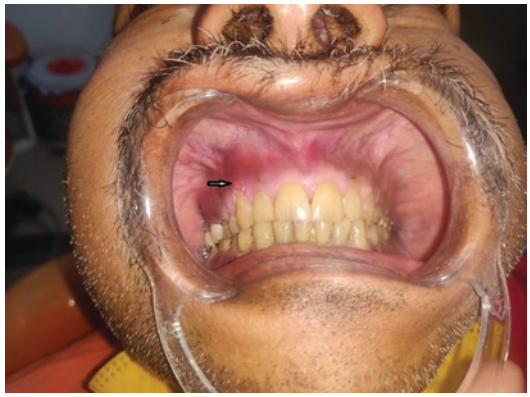

Fig. 13.6 Discharging sinus in buccal alveolus

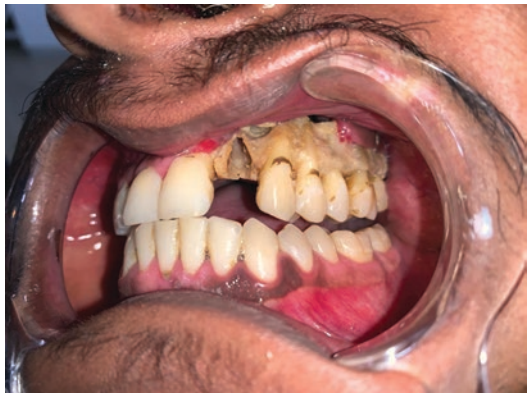

Fig. 13.7 Avascular necrosis of maxilla

13.6 Diagnostic Imaging

Imaging plays two vital roles in the management of mucormycosis [2, 3, 7]. One, the diagnosis of clinically ambivalent disease and two, providing details of the spread and extent of bony involvement for subsequent reconstruction and rehabilitation [3]. The complexity of the infected environment with a mix of soft tissue and bony disease requires multiple imaging modalities for accurate diagnosis.

Conventional (plain) radiography is of limited value to assess this composite hard and soft tissue infection. The mainstay for imaging the bony maxilla remains the CT scan, and contrast-enhanced CT is highly recommended for accurate definition of infected bone. This remains the ideal scan for established bony disease [3] (Figs. 13.8, 13.9, and 13.10).

However, with CAM assuming epidemic proportions, the medical community developed a high index of suspicion and CAM was diagnosed early in the clinical course of the disease. CT images only capture disease with gross bony disease, and early scans with little changes can lull the surgeon into the false sense of confidence that the disease is limited to the paranasal sinuses. In such situations, MRI scans provide information that both supplements and complements the CT scans [8]. Three-dimensional reconstructions are

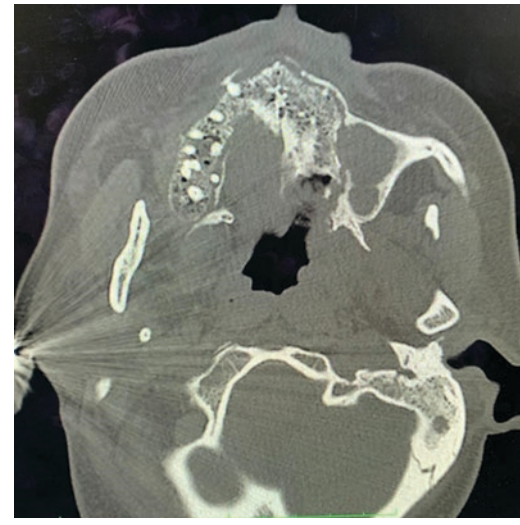

Fig. 13.8 Axial section showing erosions on the palate and maxillary alveolus

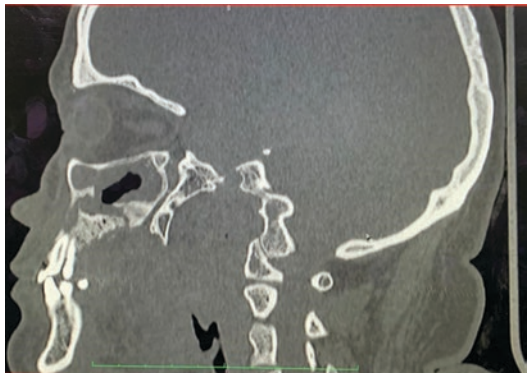

Fig. 13.9 Sagittal section showing maxillary erosion

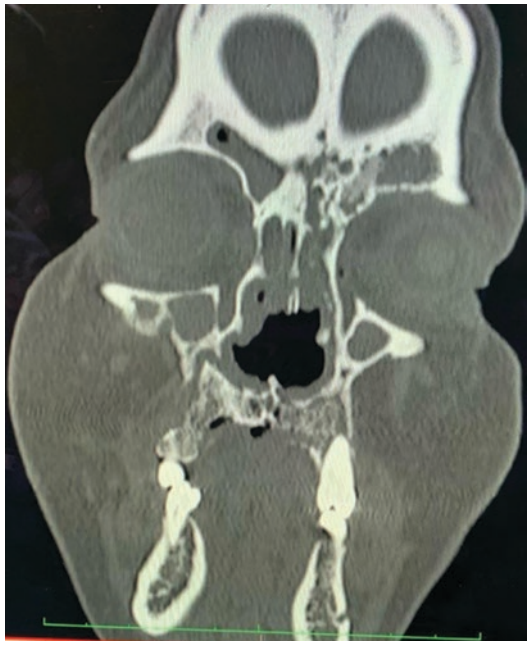

Fig. 13.10 Coronal section showing erosions in the maxilla and frontal bone

useful in both surgical planning and patient education (Figs. 13.12, 13.13, and 13.14).

Early changes seen in MRI scans (especially contrast enhanced ones) include marrow oedema and subperiosteal erosions. Subperiosteal abscess tend to appear bright on T2-weighted images. Fat-suppressed images are required to ensure adipose tissue doesn't muddle the margins. T1-weighted images, especially in well-established diseases, display the characteristic loss of enhancement (LOE) (Fig. 13.11).

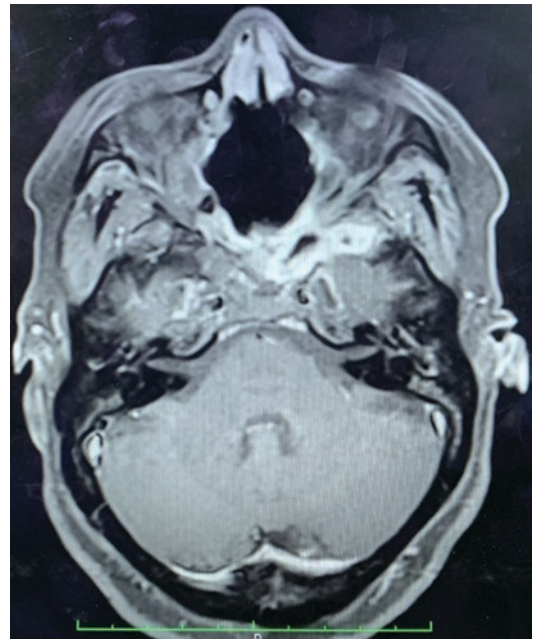

Fig. 13.11 T2W and T2W IRFSE sequences showing edematous fat stranding and inhomogeneously enhancing soft tissue thickening in the retromaxillary region extending into the pterygopalatine fossa medially

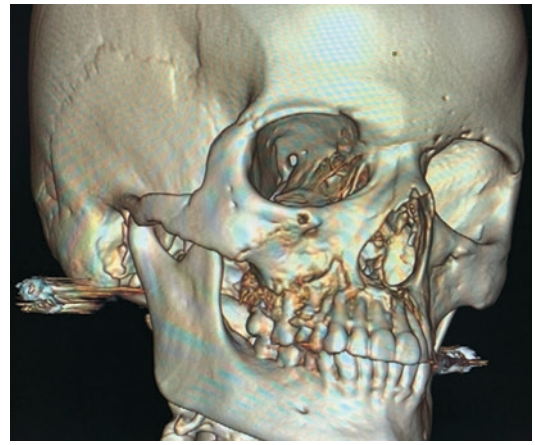

Fig. 13.12 Three-dimensional reconstruction of bony erosions on maxilla and alveolus

13.7 Treatment Planning and Decision Making in Palatal Surgery

Asymptomatic and radiologically uninvolved palates in mucormycosis involving the maxilla do not need specific intervention. However,

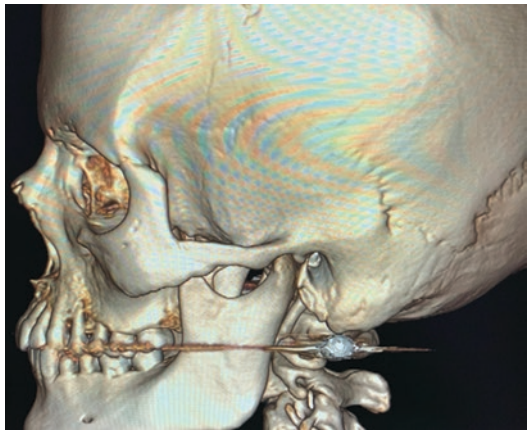

Fig. 13.13 Three-dimensional reconstruction of bony erosions on the alveolus

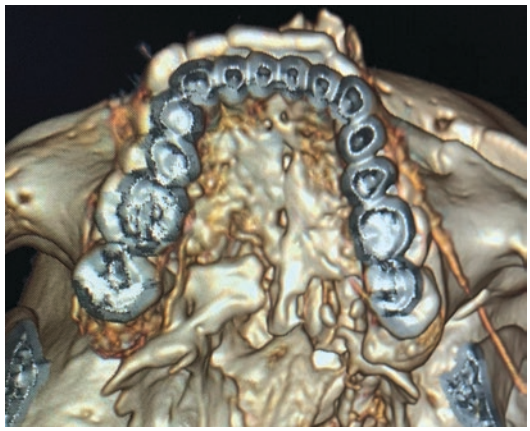

Fig. 13.14 Three-dimensional reconstruction of bony erosions on palate

extreme attention to detail is necessary to rule out palatal involvement. Thorough historical, clinical and radiological assessment might provide clues towards involvement of the palate. Subtle signs like duskiness of the palatal mucosa, acute onset of periodontal inflammation and mobility of teeth may indicate early palatal involvement and warrant close follow-up. Gross signs and symptoms like tissue necrosis, bony exposure, sequestration and alveolar mobility will require aggressive resection/debridement till necrotic tissue is removed and healthy bleeding bone is encountered [9].

When partial/subtotal palatectomy is performed and when the surgeon can be sure that some amount of the alveolus can be preserved, it is very useful to obtain dental impressions and fabricate an immediate palatal obturator/healing plate if time permits. However, the patient will need to be counselled that he/she may require nasogastric feed in the short term in spite of the prosthesis.

While enbloc resection isn't a requirement, in gross maxillary bony disease, well-delineated bone may allow for expeditious removal of the involved palate. In cases where doubt exists regarding the involved bone, incremental removal of bone with a rongeur will allow us to achieve clearance of diseased bone without loss of normal tissue. Segmental avascular necrosis is noted mostly along the distribution of involved blood vessels. This is commonly seen in the hemi maxilla when the descending palatine artery is involved, and the premaxilla with the involvement of the infraorbital neurovascular bundle. With significantly destructive pan-sinus disease, the entire infrastructure of the maxilla can undergo avascular necrosis secondary to the involvement of bilateral descending/greater palatine disease. Bony necrosis often precedes soft tissue necrosis [10], and in several instances, the mucoperiosteum of the palate can be predicably preserved because of its collateral blood supply from the twigs of the ascending pharyngeal vessels via the soft palate. It also follows that soft tissue breakdown and bone exposure are pathognomonic of necrosis of underlying bone.

13.8 Surgical Treatment Objectives

As discussed earlier, enbloc resection of the necrotic palate is a procedure of convenience rather than necessity. As a consequence, most of the maxillectomies including the ones involving the orbital floor can be performed transorally with a gingival crevicular incision entirely obviating the need of a Weber Ferguson incision and avoiding a

facial scar. Even total (bilateral) maxillectomies can be performed and the specimen can be delivered transorally by the simple expedient of sectioning it into two or more pieces. Also, unlike osteomyelitis secondary to bacterial infection, it is not adequate to just rid the maxilla and the palate of devascularized bone and its attendant involucra and sequestrae [11]. Owing to the angioinvasive nature of the disease, it is vital to excise the entire neurovascular bundles when encountered to prevent further anterograde and retrograde spread of the disease whenever possible.

Furthermore, great care should be taken in preserving every bit of vital mucosa to prevent unnecessary oroantral/oronasal communication and minimize their size if they were to occur. It is extremely helpful to preserve as much dentition as possible but not at the cost of leaving visible disease and obvious necrotic tissue behind.

13.9 Surgical Technique: (Figs. 13.15, 13.16, 13.17, 13.18, 13.19, and 13.20)

Palatal surgery is often performed in conjunction with endoscopic sinus debridement precluding the possibility of naso-tracheal intubation. While a tube change can be performed following endoscopic surgery, it is often cumbersome and unnecessary. A submental intubation or tracheostomy can be considered to free the oral cavity of the endotracheal tube but is rarely necessary. A tracheostomy should be considered in the event of postoperative or other general consider-

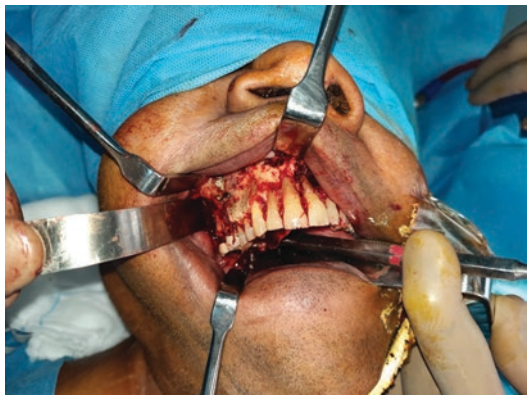

Fig. 13.15 Intraoral crevicular incision and exposure of necrotic bone

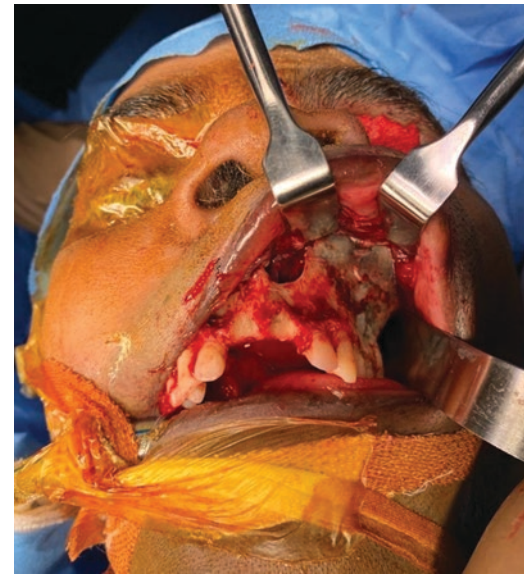

Fig. 13.16 Extent of disease in necrotic bone

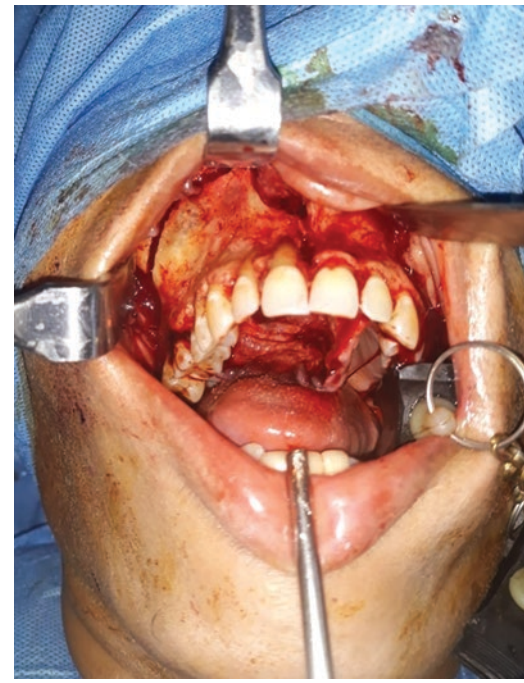

Fig. 13.17 Palatal exposure and bony cuts

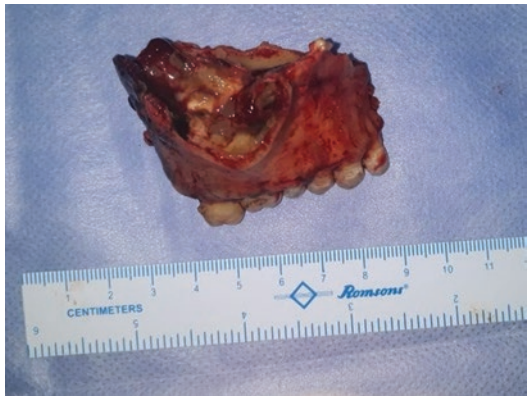

Fig. 13.18 Necrotic bone and maxillary sinus tissue

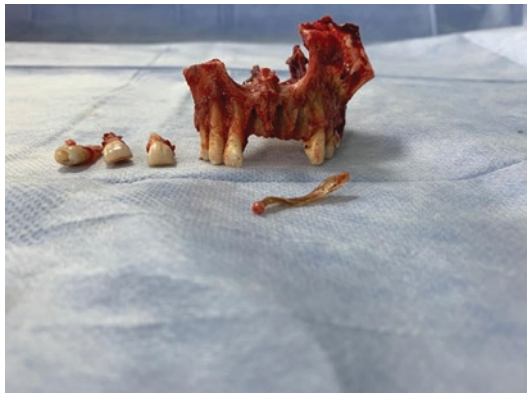

Fig. 13.19 Near total maxillectomy removed in toto

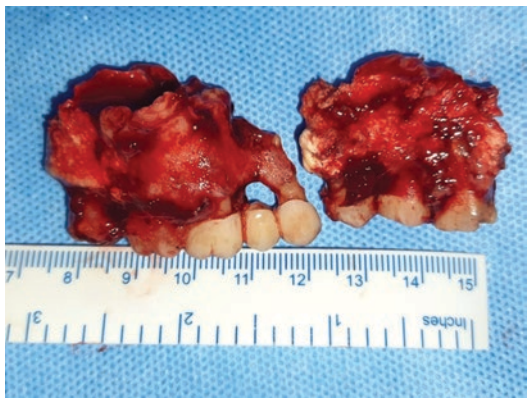

Fig. 13.20 Piecemeal excision of necrotic palate

ations. Unless the tissue is frankly necrotic an incision is placed with a no 15 Bard Parker Knife into the gingival crevice extending across the labial aspect of the maxilla. This incision can be extended along the maxillary tuberosity if required. The procedure is repeated on the palatal aspect, and the tissue is reflected off the underlying bone beginning from around the neck of the teeth (Figs. 13.15 and 13.16). The dissection is maintained on a subperiosteal plane along its entirety where mucoperiosteal elevation can be performed with ease. If needed the nasopalatine neurovascular bundle can be coagulated with diathermy and sectioned. The labial reflection of mucosa is carried on till healthy bone is visualized. The procedure is repeated on the palatal aspect exposing the palatal shelf and vault to the required extent. When necessary, the greater palatine artery on one side can be safely coagulated and divided with little risk of further necrosis.

On occasion, the avascular necrosis is advanced, and a mobile maxilla can be eased out with gentle digital pressure following division of the soft tissue attachments. More often it is ideal to use a reciprocating saw from the tuberosity to the nasal aperture protecting the nasal mucosa. Following removal of the palate/infrastructure maxilla, the area of the thrombosed greater palatine artery is inspected to ensure that there is no risk of bleeding and the artery is clipped if in doubt. It is prudent to place the primary osteotomy cut a millimetre or so within the necrotic bone (Fig. 13.17). The remanent necrotic bone can be incrementally removed either by hand or by rotary instrument (Figs. 13.18, 13.19, and 13.20).

We recommend a ribbon gauze soaked in BIPP (Bismuth Iodoform Paraffin Paste) to be placed in the wound bed with the end brought out through the nose or the oral cavity. Closure is achieved placing interrupted mattress sutures using a resorbable suture material (Fig. 13.21).

13.10 Postoperative Course

13.10.1 Wound Care

The BIPP pack remains in situ for the first 7 days as it doesn't necessarily require any change [12]. In cases where no oroantral com-

munication exists, the BIPP pack is removed and is not replaced. In case of loss of palatal mucoperiosteum and/or oroantral or oronasal communication, the BIPP pack is replaced weekly till an interim dental obturator can be fabricated at the end of 3 weeks. Oral care consists of mouth washes four to six times a day and gentle brushing of remaining teeth on the unoperated side and the mandible. The patient remains on nasogastric tube feed till primary healing is complete. In cases where the palatal mucosa is mostly untouched, the final healing is extremely satisfactory and oral feeds can commence as early as 10 days postoperatively (Fig. 13.22).

In spite of the significant morbidity and impact on the quality of life, reconstruction is deferred in most cases due to the aggressive nature of the disease and the need for frequent wound bed inspection.

13.10.2 Complications

Postoperative bleeding can be expected either in the immediate 48 h or following primary pack change in occasional cases. Late bleeding can also occur as a part of disease progression and vascular erosion [13].

In cases where significant palatal mucosa has been removed, micro-aspiration is a possibility. Oronasal/oroantral communication causes nasal regurgitation, and nasal air escape can cause significant speech disturbance and subsequent difficulty in communication. Gross weight loss and nutritional deficiencies can occur owing to the disruption of both masticatory function and deglutition.

The loss of dentition, especially anterior teeth and anterior nasal spine will lead to significant cosmetic deformity due to the collapse of the lower midface (Figs. 13.23a, b).

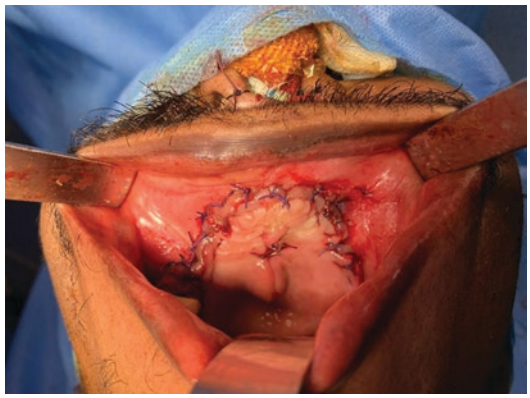

Fig. 13.21 Closure

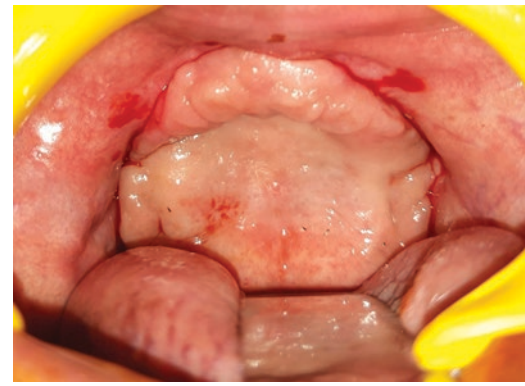

Fig. 13.22 Late postoperative view of oral mucosa sparing maxillectomy

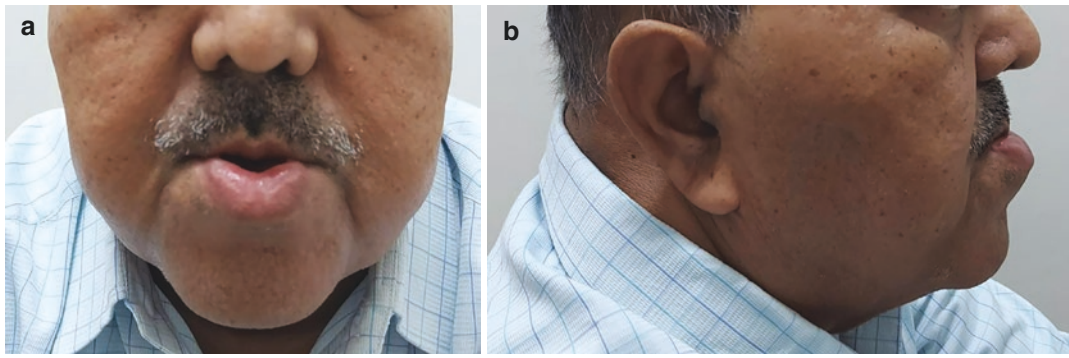

Fig. 13.23 (**a**) Midface deficiency following total maxillectomy; frontal view. (**b**) Midface deficiency following total maxillectomy; lateral view

13.11 Postoperative Rehabilitation

13.11.1 Objectives of Immediate Rehabilitation

- Separation of oral and sino-nasal cavities
- Restoration of deglutition
- Restoration of speech
- Restoration of appearance

In the immediate postoperative period, the patient needs to be provided a semblance of normalcy. In cases of oncological resection or osteomyelitis (bacterial resection), immediate reconstruction with a loco regional flap (FAMM/temporalis flaps) or microvascular free tissue transfer achieves most of the objectives and provides a foundation for long-term rehabilitation [14]. However, immediate reconstruction is precluded in cases of aggressive and rapidly progressing mucormycosis as medical treatment follows for several months and there is a distinct possibility that the patient will require further intervention. Moreover, any procedure that plugs the surgical cavity as a part of reconstruction also renders that the area is unavailable for visual inspection. For these reasons, reconstruction is delayed by several months. When possible, the immediate obturator serves to separate the oral from the sino-nasal cavities and facilitates speech and swallowing [15]. In most cases, when only one side of the maxilla is involved, an interim obturator can contain teeth to make up for the cosmetic deficit. As healing progresses, the interim obturator may be modified several times and a final obturator is planned when the patient is considered disease free.

13.11.2 Reconstruction of the Maxilla

Unilateral maxillary defects are best managed with a maxillofacial tooth-bearing prosthesis. Loco regional reconstruction can be achieved by a temporalis flap, and larger defects of the maxilla would require free tissue transfer. While the rectus abdominus and anterolateral thigh flaps have been used, they tend to be bulky and not receptive to further dental rehabilitation [16]. A microvascular free fibula flap would provide a bony base for final dental rehabilitation with osseointegrated dental implants.

With the advent of zygomatic implants, patients with a disease-free zygomatic complex can receive complete dental rehabilitation based on these implants alone [17]. This is especially true when the entire palatal mucosa has been preserved and the patient's rehabilitation requirement is purely one of dentition. With these many options, it is evident that the decision of reconstruction is highly individualized and is made on a case-to-case basis. The results are both functionally and aesthetically satisfying.

Three-dimensional printing technology has simplified complex craniofacial implant-based reconstruction to a great extent, ensuring predictable and reproducible results [18]. Computer generated programs, combined with accurate preoperative assessment of bone quality ensure the placement of implants accurately. Implant placement guides can be fabricated virtually, and implants can be placed with precision, eliminating the need to 'eyeball' the position of these implants (Figs. 13.24, 13.25, 13.26, and 13.27). With this, immediate fabrication and loading of the dental prosthesis is possible—significantly reducing the downtime of the entire process. This advance in technology and material science has ensured that implant-based reconstruction is a viable alternative to traditional techniques (Figs. 13.28, 13.29, 13.30, 13.31, 13.32, 13.33, 13.34, 13.35, 13.36, 13.37, and 13.38).

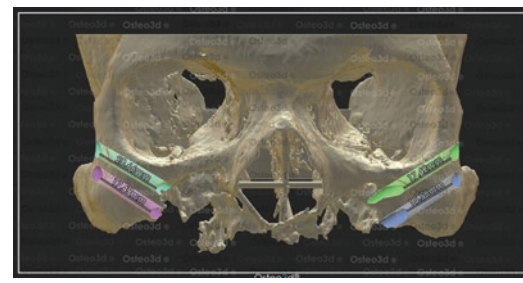

Fig. 13.24 Virtual planning for zygomatic implants

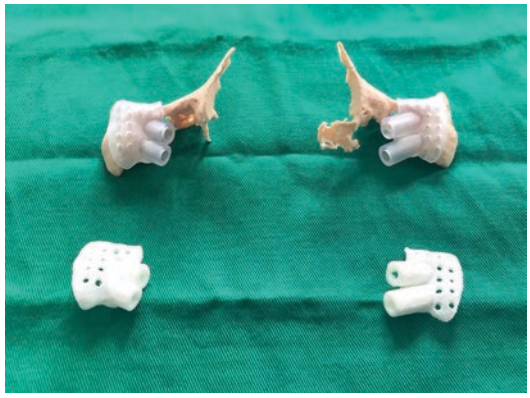

Fig. 13.25 Three-dimensional printed drill guides—to assist accurate placement of zygoma implants

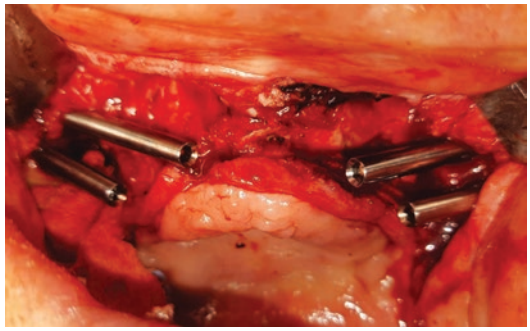

Fig. 13.26 Implant placement

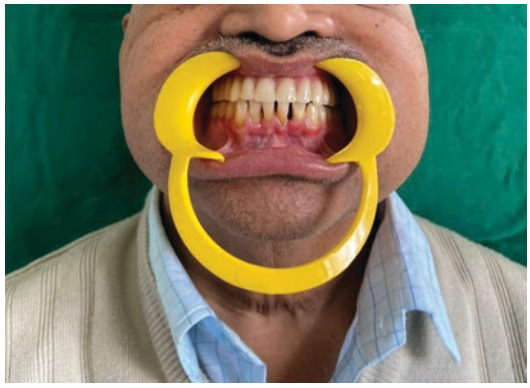

Fig. 13.27 Final prosthesis in situ

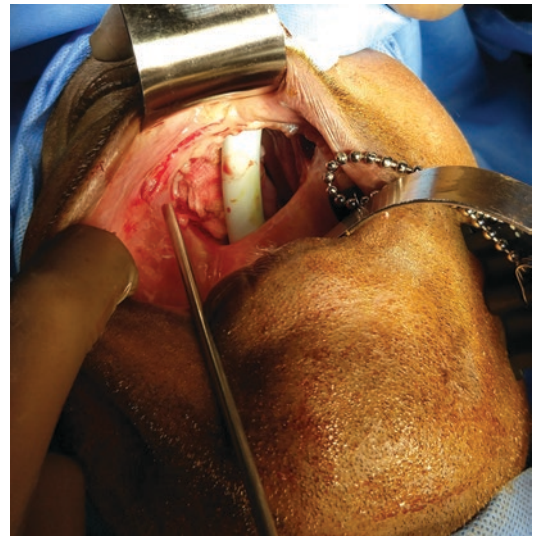

Fig. 13.28 Unilateral palatal defect

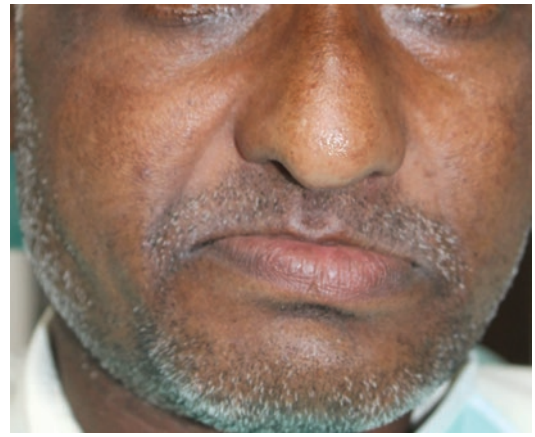

Fig. 13.29 Midface deficiency frontal view

Fig. 13.30 Midface deficiency lateral view

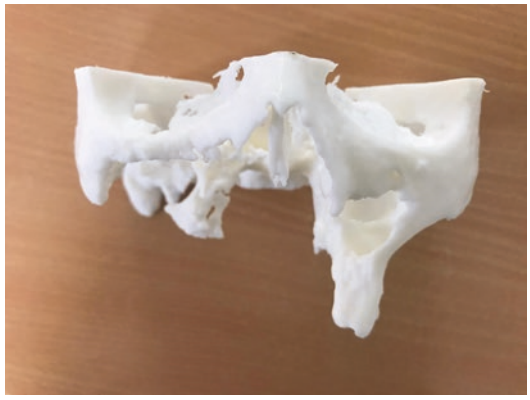

Fig. 13.31 Three-dimensional printed planning model

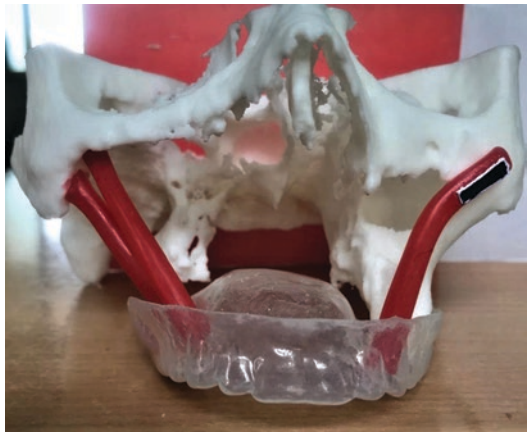

Fig. 13.32 Mock-up of implant position

Fig. 13.33 Post-implant placement

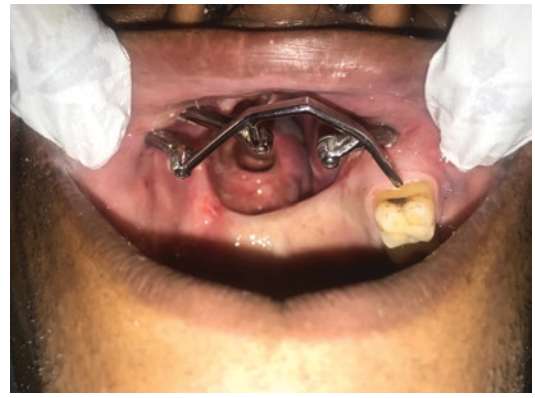

Fig. 13.34 Implant with prosthetic framework

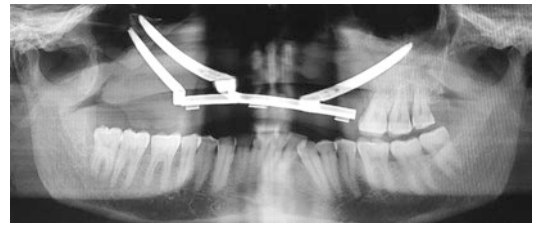

Fig. 13.35 Postop Orthopantomogram

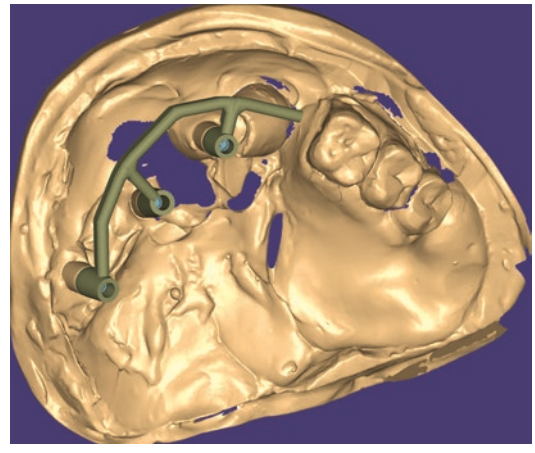

Fig. 13.36 Dental model with prosthetic framework

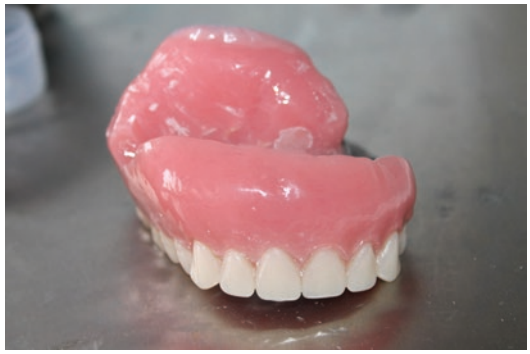

Fig. 13.37 Palatal obturator prosthesis with dentition

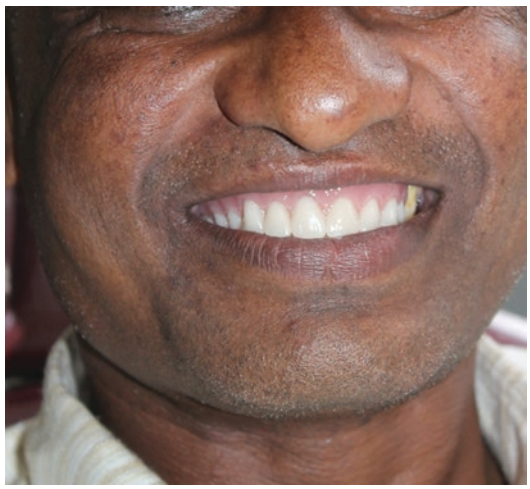

Fig. 13.38 Final prosthesis in situ

13.11.3 Long-Term Rehabilitation

Following reconstruction, it is imperative that the patient is treated holistically. Most patients will require further speech therapy despite excellent reconstructive effort. Final dental rehabilitation may take as long as 3 months following the secondary reconstruction.

13.12 Conclusion

Mucormycosis is a long-drawn disease with far-reaching implications. The patients feel the after-effects of medical and surgical therapy for months, and perhaps years after the disease. It has an immense impact on the social, financial and emotional well-being of the patient, and it is incumbent on the treating doctors to understand and empathize.

References

1. Prakash H, Chakrabarti A. Epidemiology of mucormycosis in India. Microorganisms. 2021;9(3):523. https://doi.org/10.3390/microorganisms9030523.
2. Spellberg B, Kontoyiannis DP, Fredricks D, Morris MI, Perfect JR, Chin-Hong PV, Ibrahim AS, Brass EP. Risk factors for mortality in patients with mucormycosis. Med Mycol. 2012;50(6):611–8. https://doi.org/10.3109/13693786.2012.669502.
3. Yasmin F, Najeeb H, Naeem A, Dapke K, Phadke R, Asghar MS, et al. COVID-19 associated mucormycosis: a systematic review from diagnostic challenges to management. Diseases. 2021;9(4):65.
4. Ben-Ami R, Luna M, Lewis RE, Walsh TJ, Kontoyiannis DP. A clinicopathological study of pulmonary mucormycosis in cancer patients: extensive angioinvasion but limited inflammatory response. J Infect. 2009;59(2):134–8.
5. Pandilwar P, Khan K, Shah K, Sanap M, Anoop Unnikrishnan KS, Nerurkar S. Mucormycosis: a rare entity with rising clinical presentation in immunocompromised hosts. Int J Surg Case Rep. 2020;77:57–61.
6. Patel A, Agarwal R, Rudramurthy SM, et al. Multicenter epidemiologic study of coronavirus disease-associated mucormycosis, India. Emerg Infect Dis. 2021;27(9):2349–59. https://doi.org/10.3201/eid2709.210934.
7. Herrera DA, Dublin AB, Ormsby EL, Aminpour S, Howell LP. Imaging findings of rhinocerebral mucormycosis. Skull Base. 2009;19(02):117–25.
8. Terk MR, Underwood DJ, Zee CS, Colletti PM. MR imaging in rhinocerebral and intracranial mucormycosis with CT and pathologic correlation. Magn Reson Imaging. 1992;10(1):81–7.
9. Moorthy A, Gaikwad R, Krishna S, Hegde R, Tripathi KK, Kale PG, Rao PS, Haldipur D, Bonanthaya K. SARS-CoV-2, uncontrolled diabetes and corticosteroids—an unholy trinity in invasive fungal infections of the maxillofacial region? A retrospective, multi-centric analysis. J Maxillofac Oral Surg. 2021;20:418–25.
10. Fourie J, Boy SC. Oral mucosal ulceration – a clinician's guide to diagnosis and treatment. S Afr Dent J. 2016;71(10):500–8.
11. Zahoor BA, Piercey JE, Wall DR, Tetsworth KD. A surgical approach in the management of mucormycosis in a trauma patient. Ann R Coll Surg Engl. 2016;98(8):e173–7.
12. Morawala A, Shirol D, Chunawala Y, Kanchan N, Kale M. Bismuth subnitrate iodoform parafin paste used in the management of inflammatory follicular cyst–Report of two cases. J Indian Soc Pedod Prevent Dent. 2017;35(3):269.

13. Aljanabi KSK, Almaqbali T, Alkilidar AAH, Salim YARM. Case report: parapharyngeal mucormycosis rare presentation with literature review. Indian J Otolaryngol Head Neck Surg. 2020; https://doi.org/10.1007/s12070-020-02263-4.
14. Sarukawa S, Sakuraba M, Asano T, Yano T, Kimata Y, Hayashi R, Ebihara S. Immediate maxillary reconstruction after malignant tumor extirpation. Eur J Surg Oncol. 2007;33(4):518–23. https://doi.org/10.1016/j.ejso.2006.10.027.
15. Smith DE. Interim dentures and treatment dentures. Dent Clin N Am. 1984;28(2):253–71.
16. Eitezaz FA, Rashid M, Yousaf S, Rehman IU, Fatima S, Masud M, Sanober A, Khan AH, Rashid HU. Can the anterolateral thigh flap replace the rectus abdominis free flap in the reconstruction of complex maxillary defects? J Ayub Med Coll Abbottabad. 2018;30(1):74–7.
17. Aparicio C, Manresa C, Francisco K, Claros P, Alández J, González-Martín O, Albrektsson T. Zygomatic implants: indications, techniques and outcomes, and the zygomatic success code. Periodontology 2000. 2014;66(1):41–58. https://doi.org/10.1111/prd.12038.
18. Wang Y, Qu X, Jiang J, Sun J, Zhang C, He Y. Aesthetical and accuracy outcomes of reconstruction of maxillary defect by 3D virtual surgical planning. Front Oncol. 2021;11:718946. https://doi.org/10.3389/fonc.2021.718946.

14 Lacrimal Drainage System in Rhino-Orbito-Cerebral Mucormycosis

Nishi Gupta, Rafal Nowak, and Shreya Aggarwal

A unique chapter on lacrimal drainage system (LDS) in rhino-orbito-cerebral mucormycosis (ROCM) is included to highlight the various changes in LDS (especially the lacrimal sac and nasolacrimal duct) seen during surgical management of ROCM in covid pandemic. Never before have such a large number of sac and nasolacrimal ducts been investigated for the amount of their involvement in mucormycosis as well as their microbiological and histological features.

Endoscopic Cleaning of pterygopalatine fossa (PPF) needs endoscopic median maxillectomy for surgical care of ROCM. In all the cases where medial wall of maxilla is removed, the nasolacrimal duct (NLD) is exposed. The clinical presentation of mucormycosis involving LDS, imaging, diagnostic confirmation, surgical methods involving the handling of LDS, and LDS involvement in aspergillosis in comparison to mucormycosis are all discussed in this chapter.

N. Gupta (✉)
Dr Shroff's Charity Eye Hospital, New Delhi, India

R. Nowak
Department of Ophthalmology, Military Institute of Medicine, Warsaw, Poland

S. Aggarwal
All India Institute of Medical Sciences, New Delhi, India

14.1 Various Appearances of the sac and NLD

The steps for exposing the sac and NLD are the same as those outlined in the chapter on surgical management of ROCM. All of the cases underwent drilling of the bone covering the sac and NLD after a control hole was drilled in anterolateral wall of maxilla during Denker's modified medial maxillectomy. In cases with disease limited to the pterygopalatine fossa, the NLD wall may not be impacted (Figs. 14.1, 14.2, and 14.3). NLD is traced upto the lacrimal sac and the lower part of the sac is also examined. For the complete clearance of disease from pterygopalatine fossa, NLD needs to be severed. In an oblique fashion, it is sliced flush with the orbital floor. The sac is left in place, and the oblique cut creates a larger lumen in the sac, allowing for tear drainage. The resected NLD is examined (Figs. 14.4, 14.5, and 14.6) and while resecting no part of NLD should be left hanging in the nasal cavity. Any remaining NLD left hanging into the nose undergoes fibrosis, closure and causes epiphora.

In the case of inflammatory tissue and mucopurulent discharge filling the antrum, the NLD wall was involved with bluish discolouration and thick wall (Fig. 14.7). After removing the inferior turbinate (yellow arrow) the distal end of NLD was examined using a probe in situ (black arrow) (Fig. 14.8). The NLD was split vertically, and the inspissated purulent discharge and inflammatory

N. Gupta, S. G. Honavar (eds.), *Rhino-Orbito-Cerebral Mucormycosis*,
https://doi.org/10.1007/978-981-16-9729-6_14

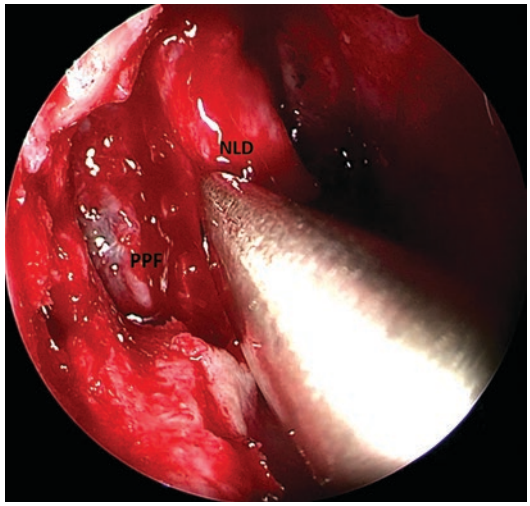

Fig. 14.1 Endoscopic view of the right nasal cavity demonstrating a thin-walled nasolacrimal duct (NLD) with the disease in the right maxillary antrum. (*PPF* Pterygopalatine fossa)

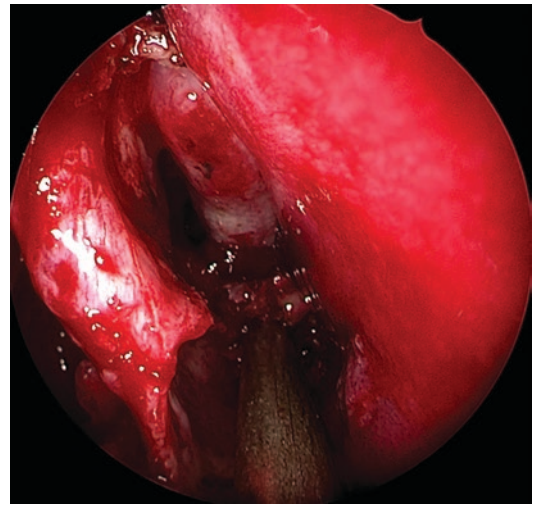

Fig. 14.3 A view of the lower part of the right sac and NLD from a close distance

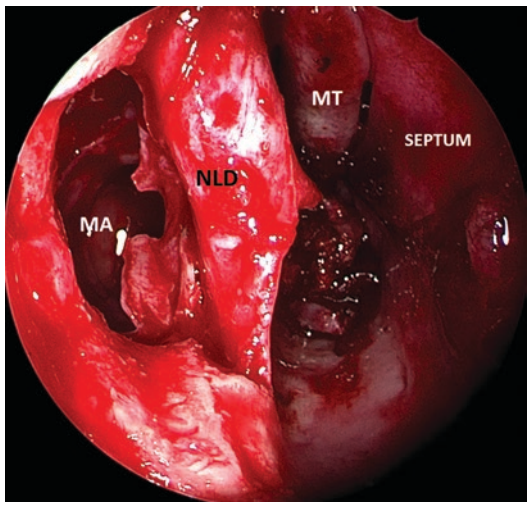

Fig. 14.2 A pinkish lower part of the sac and NLD with normal walls in a case of limited disease. (*MA* Maxillary antrum, *MT* Middle turbinate)

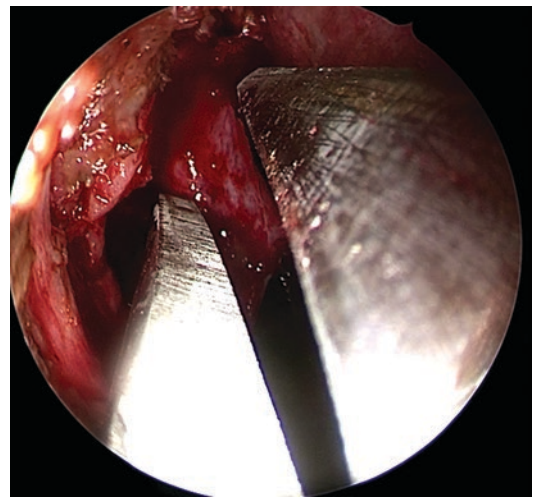

Fig. 14.4 A pair of scissors is inserted at the sac duct junction

tissue were removed from the antrum (Figs. 14.9 and 14.10). The NLD lumen was found to be patent with only the inflammatory alterations in the wall (Fig. 14.11). The NLD was cut out and analysed (Fig. 14.12).

In cases of extensive disease filling the nose, maxillary sinus, pterygopalatine fossa, the NLD was thickened, pale and thrombotic (Fig. 14.13). In such cases, the frontal process of maxilla is drilled higher up until the orbital floor so that no bone is left over the sac duct junction (Fig. 14.14). It allows NLD severance more proximal with no postoperative epiphora (Fig. 14.15).

In cases where the lower part of the sac is seen on proximal drilling of the bone that looks healthy (Fig. 14.16), it can be marsupialized at

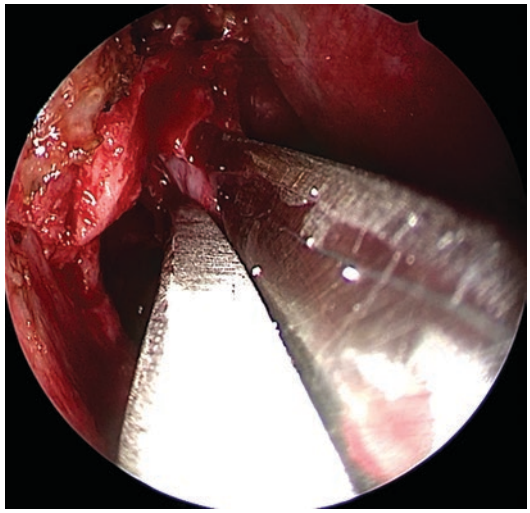

Fig. 14.5 The NLD is incised at sac duct junction and flushed to the orbital floor so that it does not hang into the nose

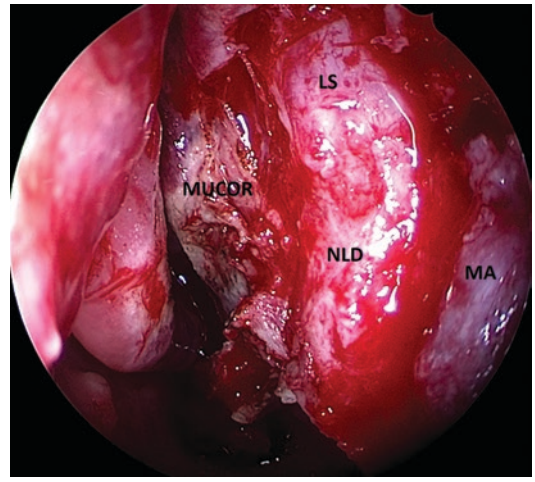

Fig. 14.7 An oedematous bluish and inflamed lacrimal sac and NLD appears to be surrounded by disease filled maxillary. (*MA* Maxillary antrum, *Ls* Lacrimal sac, *NLD* Nasolacrimal duct)

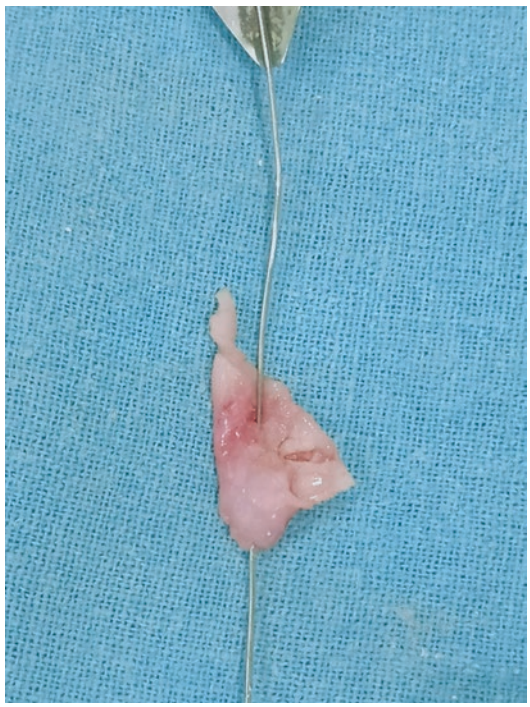

Fig. 14.6 The removed NLD is pinkish in colour and appears to be free of inflammation

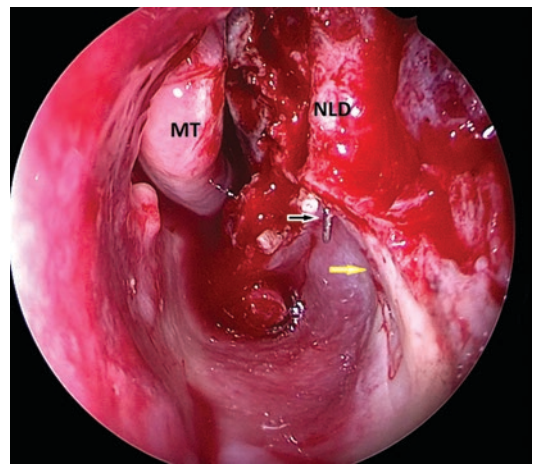

Fig. 14.8 The inferior meatus (yellow arrow) with a probe in situ (white arrow) in the distal opening of NLD. (*MT* Middle turbinate)

this level. In other cases, the bone of the frontal process of the maxilla may look unhealthy. The underlying sac and NLD are often thrombosed and may need a more superior resection (Figs. 14.17 and 14.18).

The full NLD appearance in cases of significant orbital disease may vary from a damaged friable and inflamed NLD to a whitish necrotic rope-like structure (Figs. 14.19 and 14.20). In a widespread disease a completely melted NLD remnant may be visible (Fig. 14.21).

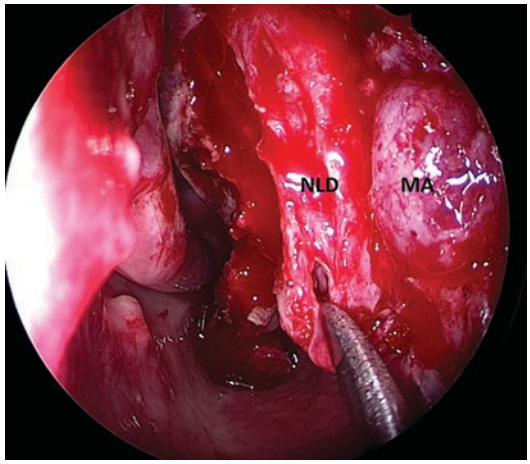

Fig. 14.9 The NLD is split open vertically (*MA* Maxillary antrum)

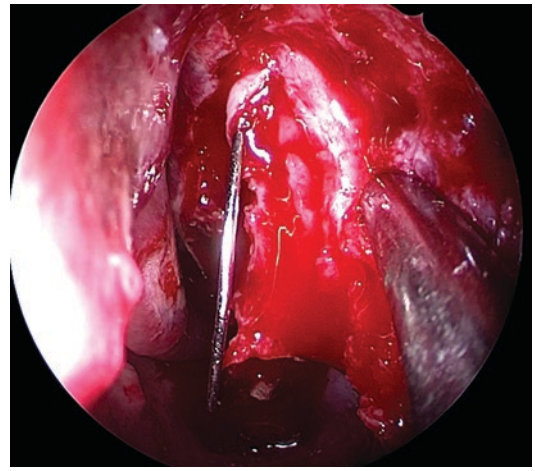

Fig. 14.11 Antrum is cleared, and the probe is rotated in all the directions to examine the NLD lumen

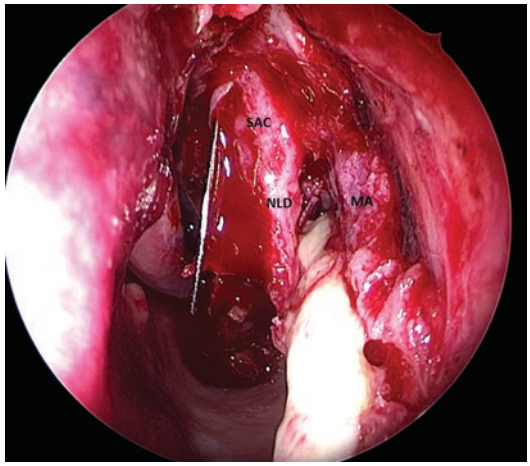

Fig. 14.10 The lumen of NLD seems clean, but the purulent discharge can be observed flowing out of the maxillary antrum (*MA* Maxillary antrum)

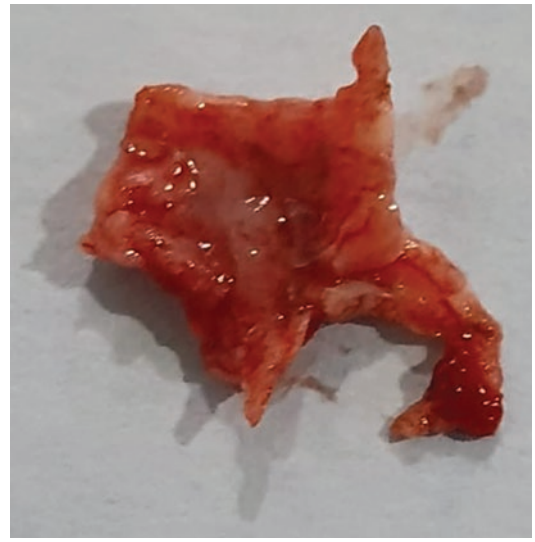

Fig. 14.12 Excised NLD looks inflamed and oedematous

14.2 Clinical Presentation of Mucormycosis Involving LDS

Patients with LDS involvement in ROCM presented with a variety of clinical symptoms, which varied depending on the severity of the cases. Epiphora, necrosis of the skin around the medial canthal (Fig. 14.22), and a large fistula involving the punta and canaliculi were among the symptoms.

14.3 Imaging

CT scans and MRI revealed involvement of the LDS as a component of other sinonasal structures. LDS lesions were seen as a hypodense mass with evidence of soft tissue density lesion on coronal CT section in the left lacrimal sac area with distorted bony NLD, compared to a normal

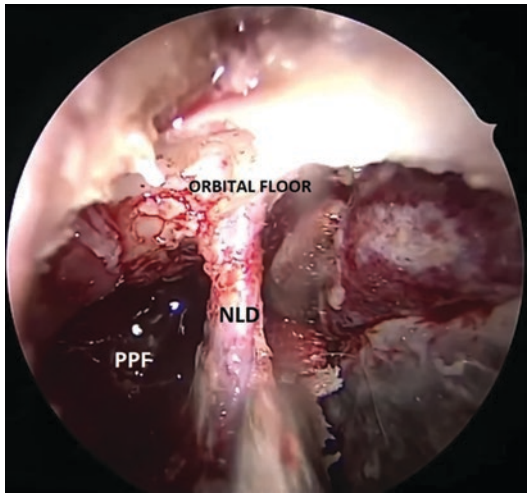

Fig. 14.13 In a case of disease filling the antrum, the NLD looks pale and unhealthy. (*PPF* Pterygopalatine fossa) (Photo courtesy: Dr Satish Jain Jaipur)

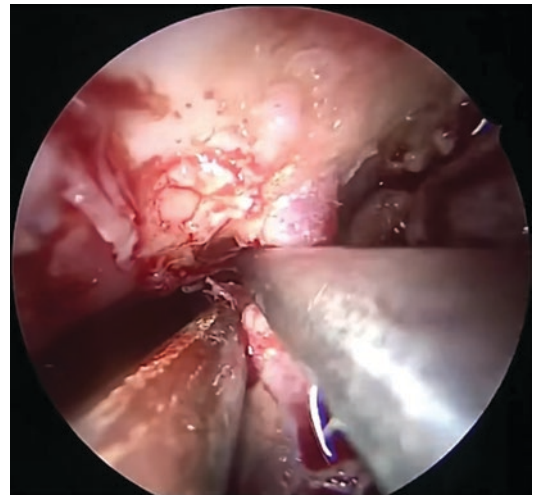

Fig. 14.15 The NLD is cut flush with the orbital floor (Photo courtesy: Dr Satish Jain Jaipur)

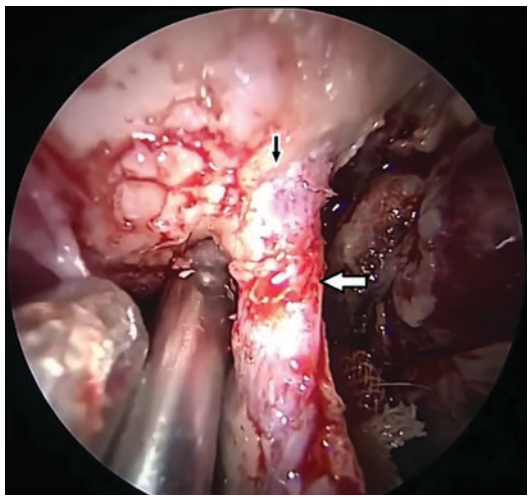

Fig. 14.14 The overlying bone is drilled all the way to the sac duct junction (white arrow), and then the bone is drilled till the orbital floor (white arrow) (Photo courtesy: Dr Satish Jain Jaipur)

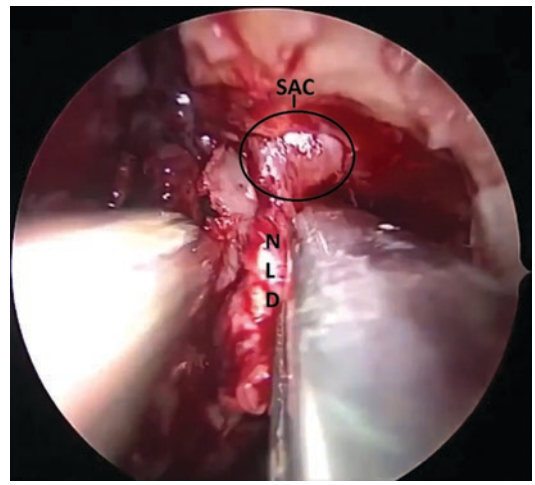

Fig. 14.16 The level of a marsupialization of the lacrimal drainage system is determined by the sac's state. The lower section of the sac is exposed in this case the sac, and it appears to be healthy (black circle). A sharp incision is given to cut the NLD obliquely (Photo courtesy: Dr Satish Jain Jaipur)

nasolacrimal system on the right side (Figs. 14.23 and 14.24). On axial sections, the disease was seen in the left maxillary antrum reaching up to the NLD and lamina papyracea (Fig. 14.25). On gadolinium-enhanced MRI, different zones of enhancement and non-enhancement were detected in the lacrimal sac and surrounding ethmoid cells in an extensive case of ROCM (Fig. 14.26).

14.4 Diagnostic Confirmation

14.4.1 Microscopy

The material is inoculated on Sabouraud dextrose agar and brain heart infusion agar [1] (Fig. 14.27).

Direct microscopy allows for a rapid diagnosis based on septation, angle of branching and

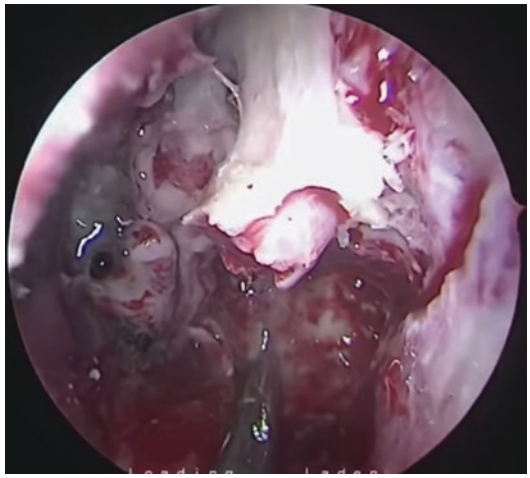

Fig. 14.17 In cases of extensive disease filling the pterygopalatine fossa, the frontal process of the maxilla is generally unhealthy. On drilling it, a totally thrombosed NLD can be noticed (Photo courtesy: Dr Satish Jain Jaipur)

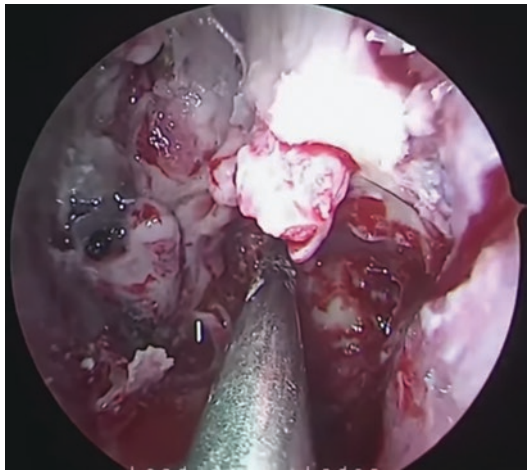

Fig. 14.18 When probing the cut end no lumen could be found

width of the hyphae. Potassium hydroxide (KOH) mount in 10–20% KOH preparation reveals characteristic broad, ribbon-like aseptate hyphae of Mucorales on direct microscopy. Under a fluorescent microscope KOH-Calcofluor white solution enhances the visualization of the fungal element in specimens.

14.4.2 Histopathology

Histopathology revealed fungal hyphae with a ribbon-like appearance with random branching at various angles (Fig. 14.28).

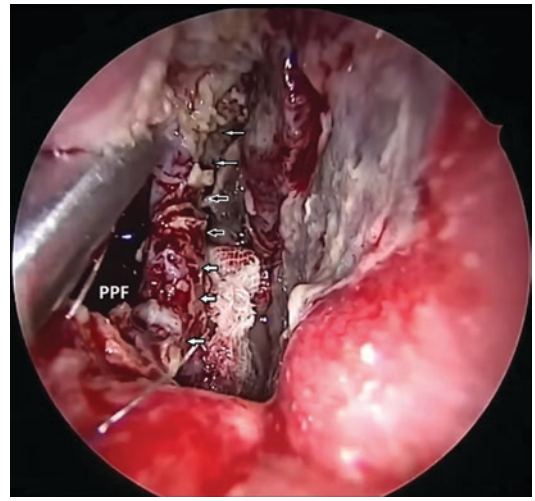

Fig. 14.19 In an instance of significant disease a friable necrotic and sloughed-out right NLD was seen (arrows) (*PPF* Pterygopalatine fossa) (Photo courtesy: Dr Satish Jain Jaipur)

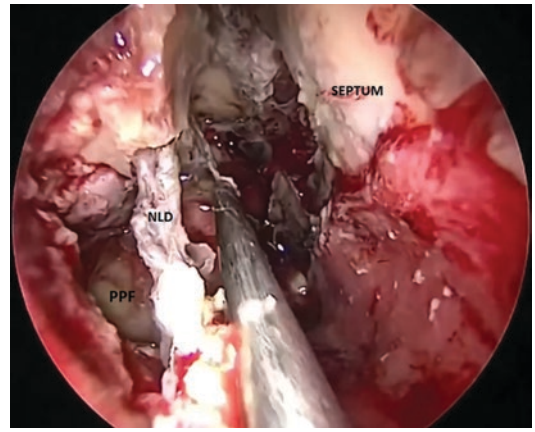

Fig. 14.20 A completely necrotic thinned-out rope-like NLD with slough and blackish discolouration (*PPF* Pterygopalatine fossa) (Photo courtesy: Dr Satish Jain Jaipur)

14.5 NLD as a Possible Disease Spread Route to the Orbit

NLD has been mentioned by several publications as a probable route of spread of disease transmission from the nose to orbit [2–7].

According to them, the orbital involvement is caused by nasolacrimal duct invasion which then spreads to the orbit via the thin medial orbital wall [2]. However, there was no specific evidence for us to prove that. The inferior

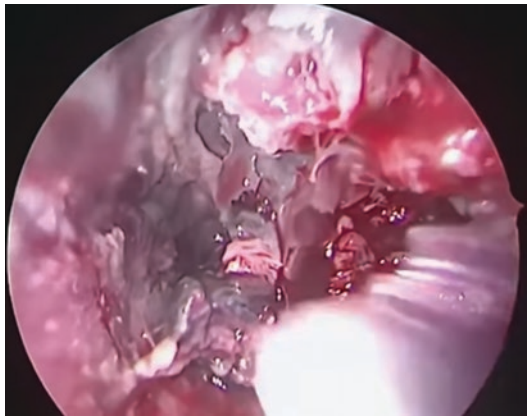

Fig. 14.21 A melted and damaged NLD (Photo courtesy: Dr Satish Jain Jaipur)

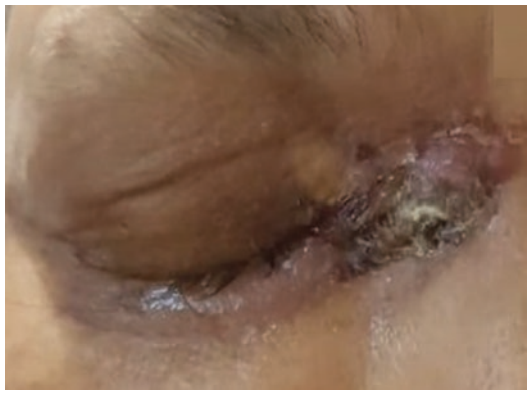

Fig. 14.22 External photograph of a patient with mucormycosis of the lacrimal drainage system (LDS), showing the diffuse involvement of the puncta and canaliculi secondary to the involvement of sinuses

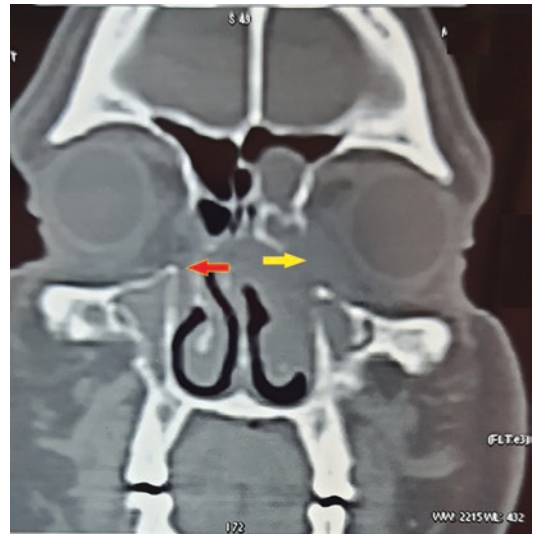

Fig. 14.23 Computed tomographic scan of the patient demonstrating soft tissue density in the left maxillary antrum and ethmoid cells along with the involvement of left LDS (yellow arrow) and a normal LDS on the right (red arrow)

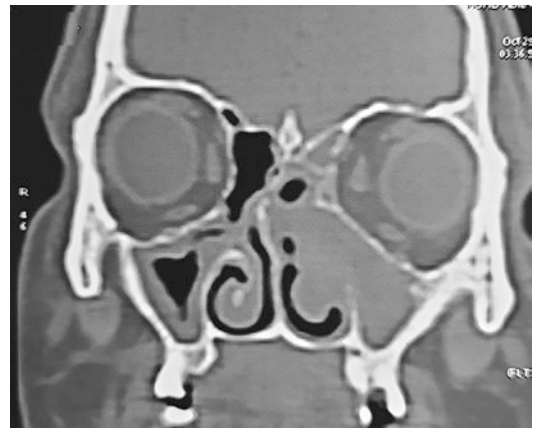

Fig. 14.24 Computed tomographic scan coronal section showing soft tissue density filling the left-sided sinuses with involvement of the lacrimal drainage system

meatus was normal, and in the cases where NLD was patent, the medial canthal area was pressed, and the discharge could be seen accumulating at the distal end of NLD, indicating a patent NLD (Fig. 14.29). A sample from this location was sent to the lab for fungal culture (Fig. 14.30), which was found to be mucor free. Patients, however, did have orbital disease indicating a different route of dissemination.

In cases of widespread disease, NLD itself was engulfed and eroded by the disease that surrounded it from all sides. In advanced cases, the orbital disease was massive, pterygopalatine fossa was filled with the disease and NLD had secondary involvement. It suggests that the disease did not spread to the orbit through NLD. There was no instance in which NLD involvement and infiltration with the mucormycosis was greater than the surrounding disease, and vice versa. It appears that NLD involvement was secondary in all of these cases.

There has never been a comprehensive examination of the extent and kind of LDS involvement as well as emergence and therapy in invasive fungal infections.

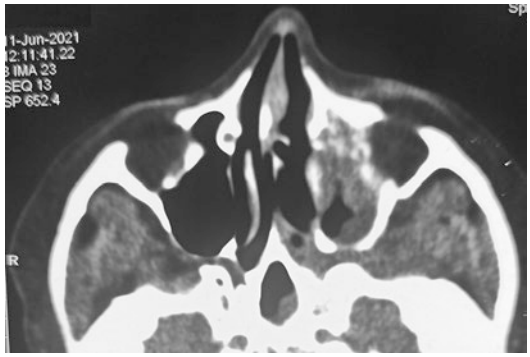

Fig. 14.25 Erosion of the left bony NLD with opacified maxillary antrum

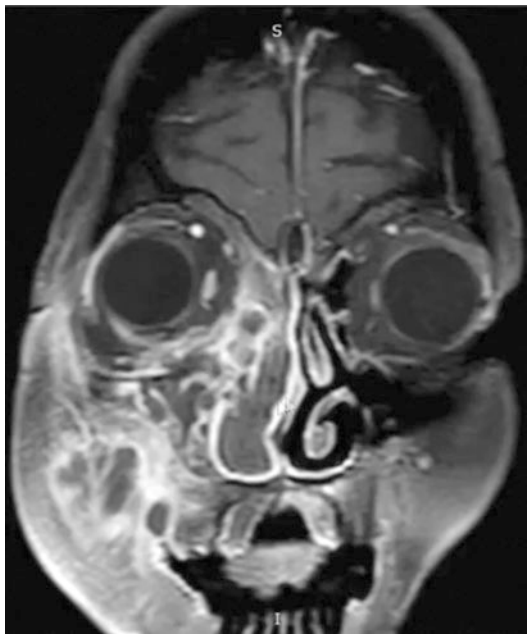

Fig. 14.26 MRI showing diverse areas of enhancement and non-enhancement in the right lacrimal sac is in a case with widespread disease

14.6 Surgical Procedures Involving LDS

LDS is a vital structure that we come across during the management of various sinonasal conditions like inverted papilloma, juvenile nasopharyngeal angiofibroma, sinonasal tumours and invasive fungal disorders of the sino-orbital areas. The approaches involving LDS are Denker's modified medial maxillectomy in which

Fig. 14.27 Fungal growth was seen on Sabouraud agar and brain heart infusion agar

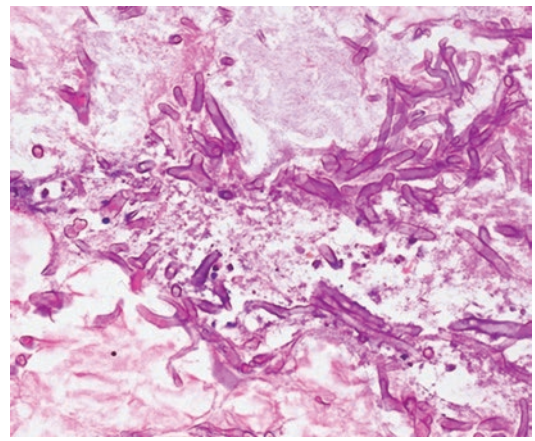

Fig. 14.28 Fungal hyphae with a ribbon-like appearance with random branching at variable angles (Photo courtesy; Dr Aanchal Kakkar, AIIMS Delhi)

a window is created first and then distal half of the sac and the nasolacrimal duct are exposed

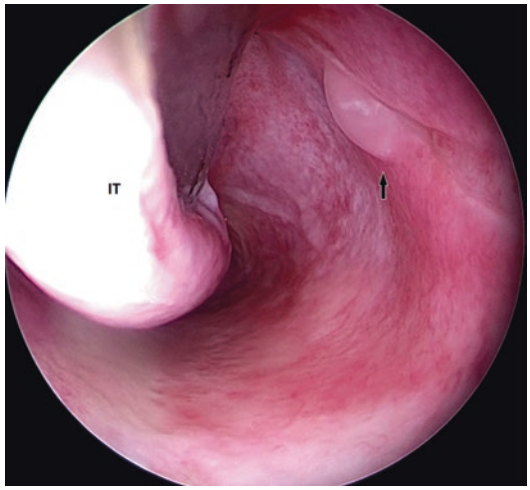

Fig. 14.29 Discharge can be seen flowing into the nose through the NLD opening into the inferior meatus (arrow), on pressing over the medial canthus. IT; Inferior turbinate

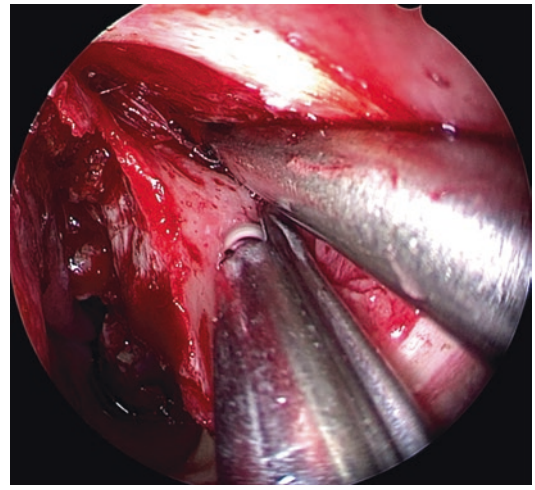

Fig. 14.31 Drilling a hole into the anterolateral wall of the maxilla for the inspection of disease inside the antrum during Denker's medial maxillectomy

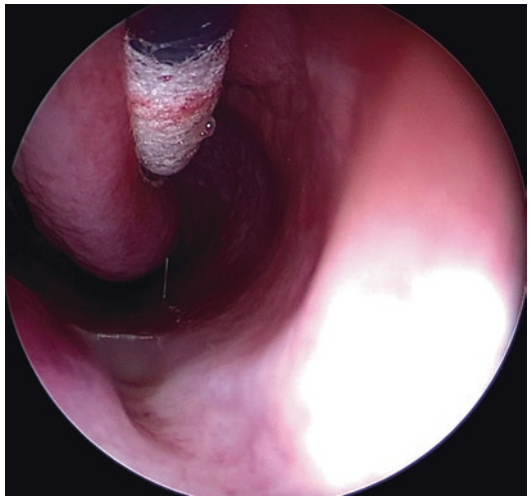

Fig. 14.30 A swab from the inferior meatus is obtained and sent for culture

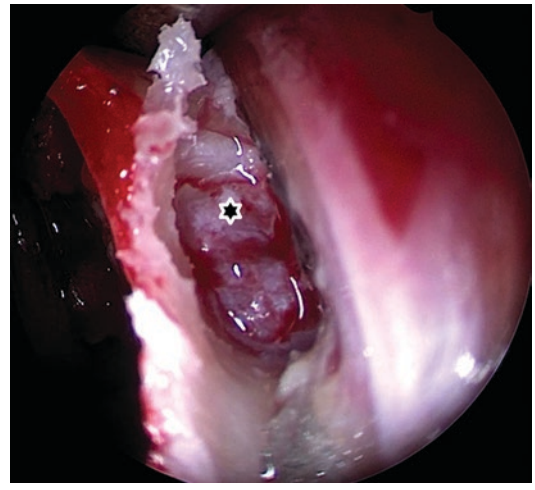

Fig. 14.32 Maxillary antrum has been opened up and can be seen filled with the disease (star). The medial wall of the maxilla overlying the NLD is still intact

(Figs. 14.31, 14.32, and 14.33). In Denker's NLD is severed to access the disease in the pterygopalatine fossa while in prelacrimal approach NLD may be preserved.

Denker's modified medial maxillectomy approach is the most popular approach for accessing the disease in the maxillary sinus, pterygopalatine fossa and infratemporal fossa [8–11]. The classic medial maxillectomy involves the resection of the whole medial maxillary sinus wall, including the inferior turbinate and the nasolacrimal duct [12–14].

The prelacrimal approach is used to gain improved access by resecting a part of the piriform aperture and the anterior wall of the maxillary sinus. In this approach, inferior turbinate is temporarily displaced to gain access and then repositioned to reduce morbidity. This procedure provides excellent visualization of the ante-

rior wall of the maxillary sinus and the prelacrimal recess. It allows the inferior turbinate and the nasolacrimal duct to be preserved [15–28].

14.6.1 Medical Management

Liposomal amphotericin B is the medication of choice for mucormycosis. The chapter on antifungal treatment has more information on the doses and types of amphotericin B that are available.

There are only a few cases of primary mucormycosis of the lacrimal sac in the literature. One of them is of a 72-year-old woman with several dacryoliths and mucormycosis on histopathology [29]. Another patient was a known case of diabetic ketoacidosis who was operated for lacrimal sac infection, and on histopathology revealed mucormycosis [30].

Let us look at the other type of invasive fungal infection of the lacrimal sac, aspergillosis, which was seen during the Covid epidemic.

14.7 Aspergillosis of the LDS

Aspergillosis is a slower-progressing lesion of the LDS as compared to mucormycosis and is also less deadly. Owing to slow progression, sometimes patients present with lacrimal sac abscesses, and the biopsy reveals aspergillosis. A case of aspergillosis masquerading as lacrimal sac abscess has been reported [31].

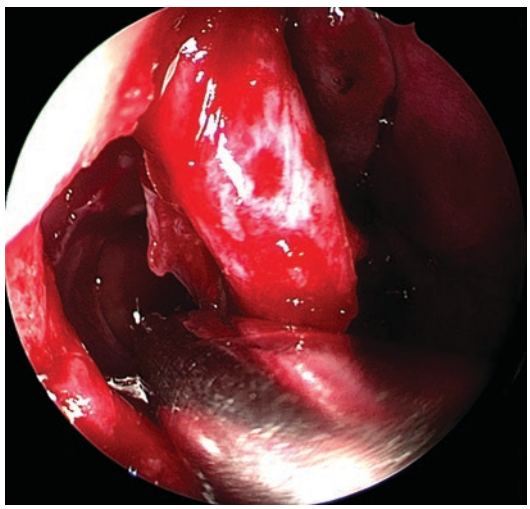

Fig. 14.33 Premaxillary approach: the NLD (right side in this case) can be kept intact depending on the indication

14.7.1 Clinical Presentation

The presenting symptom in invasive aspergillosis of LDS is epiphora with medial canthal swelling. However, as previously mentioned, it can present as a lacrimal sac abscess, which can cause confusion for the surgeon, and if a biopsy is not performed during surgery, the diagnosis may be missed.

Epiphora is generally the first sign followed by swelling that develops after a long gap. It shows that NLD is the earliest site of aspergillosis inoculation, as its narrow lumen causes it to get clogged early. Further disease progression develops a mass lesion in the lacrimal sac, which starts distending and manifests as a swelling in the medial canthal region.

14.7.2 Examination

External examination shows a mass in the medial canthal area extending laterally along the inferior lid margin (Fig. 14.34). Nasal endoscopy shows a bulge over the lateral wall encroaching the premaxillary line with prominent blood vessels across it (Fig. 14.35).

14.7.3 Imaging in Aspergillo

A significant soft tissue mass in the right lacrimal fossa, a breach in the lacrimal bone and

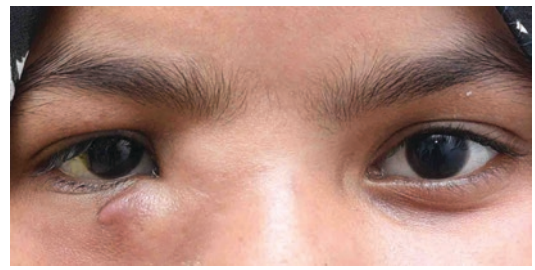

Fig. 14.34 External photograph of a patient with invasive aspergillosis of the right lacrimal drainage system

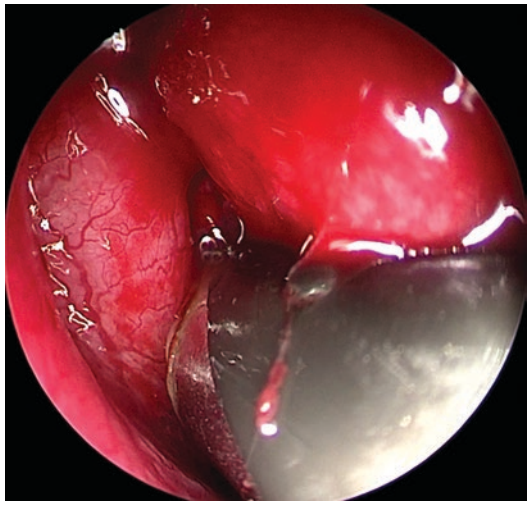

Fig. 14.35 An endoscopic view of the right nasal cavity with a protrusion in the nasolacrimal area

lamina papyracea with soft tissue extension into the ethmoid sinuses can be seen on computed tomography (CT) scan coronal (Fig. 14.36), axial (Fig. 14.37) and sagittal sections (Fig. 14.38) in aspergillosis of the lacrimal sac. An extension of the soft tissue oedema into the inferior meatus is seen.

14.7.4 Management of Aspergillosis of the Lacrimal Sac

In aspergillosis, unlike LDS mucormycosis, the whole sac and NLD are filled with a solid mass. Coblation of the prominent vessels over the bulging lateral wall is one of the measures in treating LDS aspergillosis (Fig. 14.39). After that a blunt periosteal elevator is used to make an incision. The frontal process of maxilla is seen after the dissected portion is lifted and removed (Fig. 14.40).

The bone of the frontal process of the maxilla is removed using a Kerrison punch (Fig. 14.41). The lacrimal sac is opened, and the mass is examined. Aspergillus is a firm mass and has rubber-like consistency (Fig. 14.42). It is often peeled off from the underlying structures and is debrided. The superior part of the sac is palpated (Fig. 14.43). The lumen of the sac is examined,

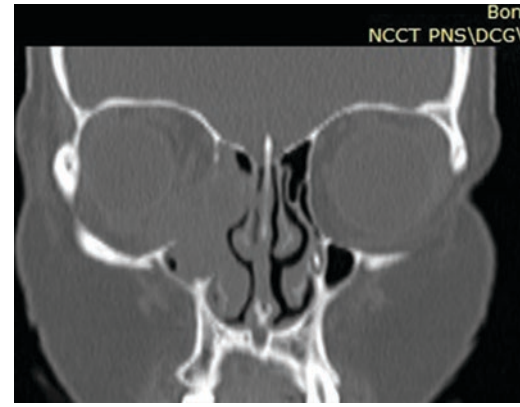

Fig. 14.36 Non-contrast computed tomography (NCCT) of sinuses and orbit, coronal section demonstrating soft tissue mass occupying the right lacrimal sac, NLD and ethmoids

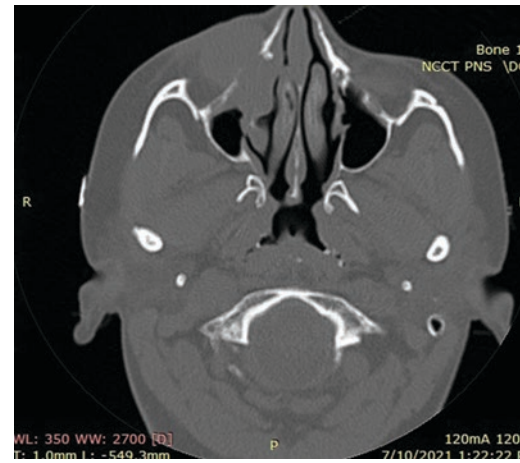

Fig. 14.37 NCCT of sinuses and orbit axial section demonstrating soft tissue mass occupying the right lacrimal sac, NLD and ethmoids

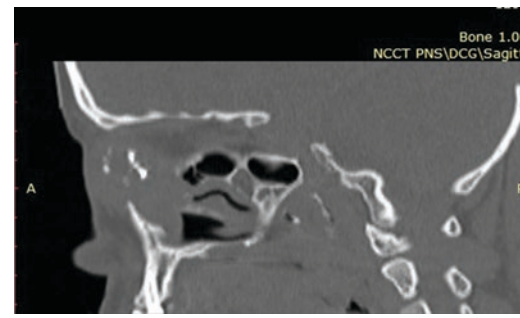

Fig. 14.38 Sagittal section on CT DCG showing a mass filling the lacrimal sac, NLD and the surrounding area

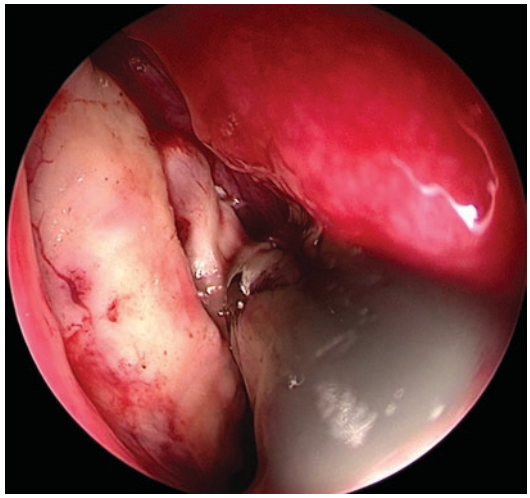

Fig. 14.39 The lateral wall bulge is coblated to minimize bleeding

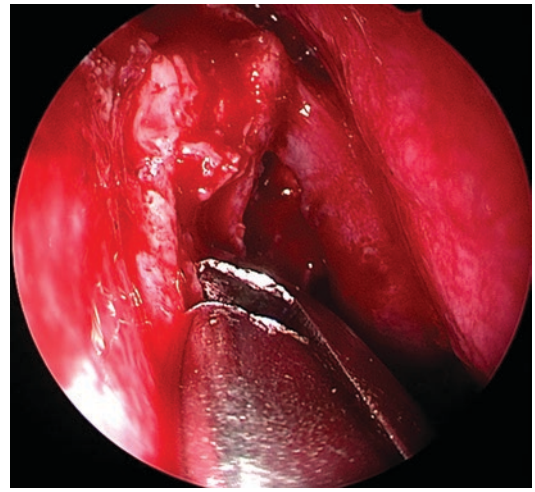

Fig. 14.41 Kerrison punch is used to remove the bone of the frontal process of the maxilla

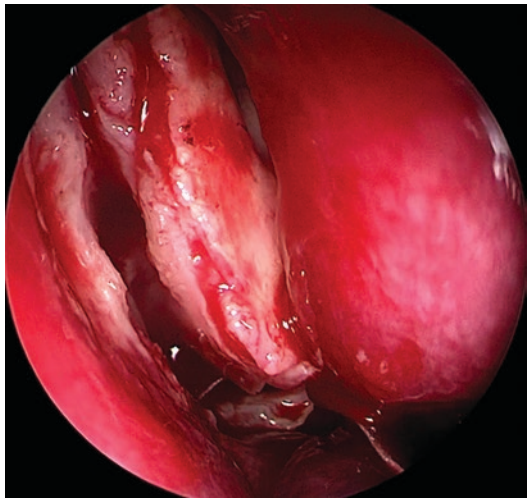

Fig. 14.40 The hypertrophied tissue on the lateral wall is lifted off in continuation with the uncinate process

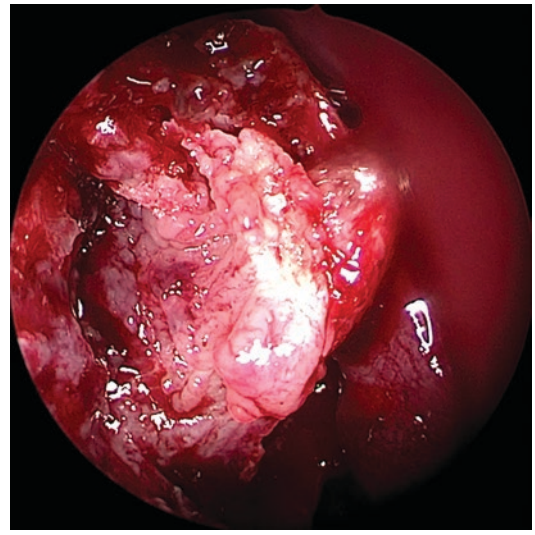

Fig. 14.42 The rubber-like mass is seen filling the sac, occluding its lumen. The tissue filling the sac is teased out and debrided

and the probe can be seen in situ (Figs. 14.44 and 14.45). After clearing the fungal mass, the sac and NLD are then dissected off the fossa, a dacryocystectomy is carried out, and the specimen is sent to the lab.

14.7.5 Microbiology and Histopathology

KOH mount showed bright green septate hyphae of *aspergillosis* under *a* fluorescence microscope (Fig. 14.46). Microphotograph shows PAS-stained giant cells along with septate hyphae in the granulomatous area (Fig. 14.47).

14.7.6 Antifungals and Prognosis

Aspergillosis responds to voriconazole that is available in intravenous as well as oral formulations and is well tolerated. We found only a

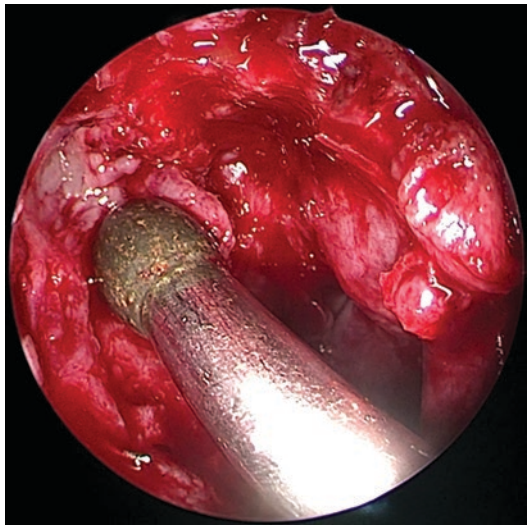

Fig. 14.43 The superior part of the sac is checked with a curved blunt suction tip, and any residual disease is debrided

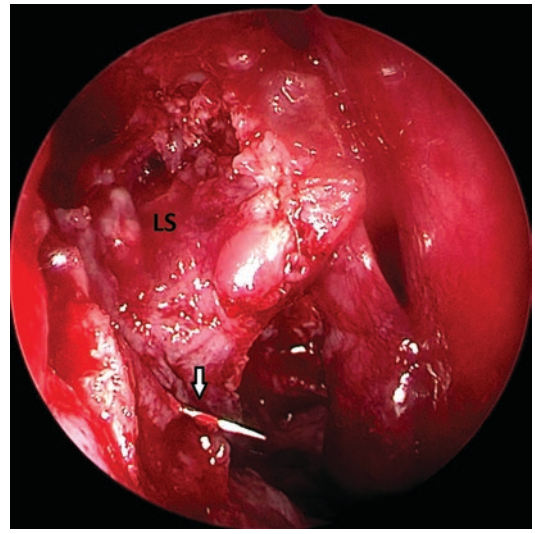

Fig. 14.45 Probe can be seen in situ (arrow). (*LS* lacrimal sac)

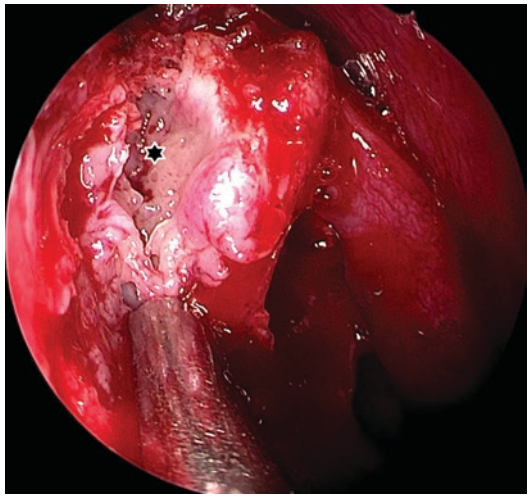

Fig. 14.44 Sac lumen is visible after disease clearance (star). The soft tissue mass seen all around the lumen is debrided

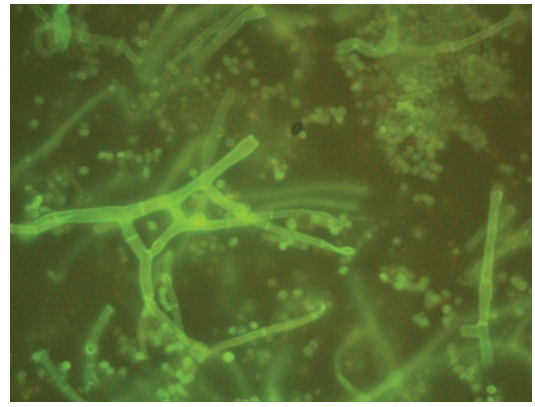

Fig. 14.46 KOH mount showing bright green septate hyphae of aspergillosis under fluorescence microscope (Photo courtesy: Dr Arpan Gandhi, SCEH, Delhi)

few cases of isolated lacrimal sac aspergillosis in literature [31, 32]. The cases were successfully treated with surgery and antifungal medication.

Invasive fungal infections of the isolated lacrimal drainage system are rare. Very few cases of invasive mucormycosis and aspergillosis of the lacrimal drainage system (LDS) have been reported in the literature [29–32]. The second wave of Covid pandemic in India resulted in an unexpected increase in invasive fungal infections of LDS. Although incidences of LDS mucormycosis were discovered during an endemic of rhino-orbito-cerebral (ROC) mucormycosis, occurrences of LDS aspergillosis were also on the rise.

14.8 Comparison of LDS Aspergillosis and LDS Mucormycosis

The features of various invasive fungal infections of the lacrimal drainage system are compared in Table 14.1.

Prognosis of invasive fungal infection of LDS is good with surgery, antifungal drugs and the management of underlying medical conditions. To summarise, in aspergillosis, ROCM surgical debridement entails sacrificing the NLD which is cut flush to the floor of the orbit, and performing a dacryocystectomy with complete sac and NLD removal.

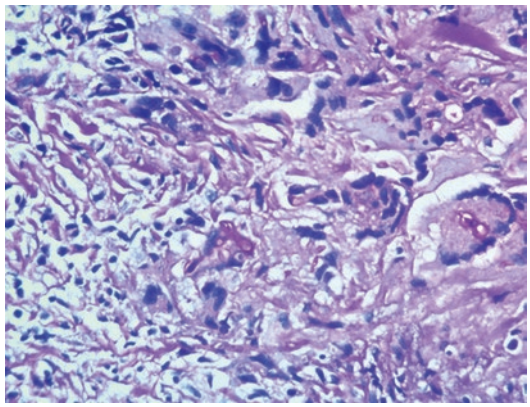

Fig. 14.47 Microphotograph showing PAS-stained giant cells along with septate hyphae in the granulomatous area—20× (Photo courtesy: Dr Arpan Gandhi, SCEH, Delhi)

References

1. Walther G, Wagner L, Kurzai O. Updates on the taxonomy of mucorales with an emphasis on clinically important taxa. J Fungi (Basel). 2019;5(4):106.
2. Herrera DA, Dublin AB, Ormsby EL, Aminpour S, Howell LP. Imaging findings of rhinocerebral mucormycosis. Skull Base. 2009;19(2):117–25. https://doi.org/10.1055/s-0028-1096209.
3. Kohn R, Helper R. Management of limited rhino-orbital mucormycosis without exenteration. Ophthalmology. 1985;92:1440–3.
4. Abramson E, Wilson D, Arky RA. Rhinocerbral phycomycosis in association with diabetic ketoacidosis. Ann Intern Med. 1967;66(742):735.
5. Vaughan C, Bartolo A, Vallabh N, Leong SC. A meta-analysis of survival factors in rhino-orbital-cerebral mucormycosis-has anything changed in the past 20 years? Clin Otolaryngol. 2018;43(6):1454–64. https://doi.org/10.1111/coa.13175.
6. Gupta S, Goyal R, Kaore NM. Rhino-orbital-cerebral mucormycosis: battle with the deadly enemy. Indian J Otolaryngol Head Neck Surg. 2020;72(1):104–11. https://doi.org/10.1007/s12070-019-01774-z.
7. Jolie KH. Guevara. Isolated orbital mucormycosis in an immunocompetent adolescent. MSRJ. 2014;03(Spring):55–9. www.msrj.org
8. Upadhyay S, Dolci RL, Buohliqah L, Prevedello DM, Otto BA, Carrau RL. Endoscopic endonasal anterior maxillotomy. Laryngoscope. 2015;125(12):2668–71. https://doi.org/10.1002/lary.25205.
9. Denker A. Ein neuer Wegfur die Operation der Malignen Nasentumoren. Munchener Medizinische Wochenschrift. 1906;20:953–6.
10. Sturmann D. Die Intranasale Eroffnung der Kieferhohle. Berliner klinische Wochenschrift. 1908;45:1273–4.
11. Canfield RB. The submucous resection of the lateral nasal wall in chronic empyema of the antrum, ethmoid and sphenoid. JAMA. 1908;14:1136–41.
12. Hildenbrand T, Weber R, Mertens J, Stuck BA, Hoch S, Giotakis E. Surgery of inverted papilloma of the maxillary sinus via translacrimal

Table 14.1 Invasive fungal infection of the lacrimal drainage system: comparison of aspergillosis and mucormycosis

SN	Clinical features	Aspergillosis	Mucormycosis
1	Swelling in the medial canthal area	Present	May or may not be present
2	Onset	Slow, may get detected only after secondary infection sets in	Incidental finding [1, 2] or seen in association with the sinonasal disease with rapid progression during Covid
3	Isolated LDS involvement	Has been seen [3, 8]	Not seen in our cases, though reported earlier [1, 2]
4	Management	Surgery and voriconazole	Surgery and amphotericin B
5	Intraoperative	Consistency is rubber like and difficult to debride	Soft and easy to debride
6	Histopathology	Septate hyphae	Aseptate hyphae

approach—long-term outcome and literature review. J Clin Med. 2019;8(11):1873. https://doi.org/10.3390/jcm8111873.
13. Wormald PJ, Ooi E, van Hasselt CA, Nair S. Endoscopic removal of sinonasal inverted papilloma including endoscopic medial maxillectomy. Laryngoscope. 2003;113:867–73.
14. Simmen DJN. Manual of endoscopic sinus and skull base surgery. 2nd ed. Stuttgart: Thieme; 2013.
15. Wang C, Han D, Zhang L. Modified endoscopic maxillary medial sinusotomy for sinonasal inverted papilloma with attachment to the anterior medial wall of maxillary sinus. ORL J Otorhinolaryngol Relat Spec. 2012;74:97–101.
16. Tomenzoli D, Castelnuovo P, Pagella F, Berlucchi M, Pianta L, Delu G, Maroldi R, Nicolai P. Different endoscopic surgical strategies in the management of inverted papilloma of the sinonasal tract: experience with 47 patients. Laryngoscope. 2004;114:193–200.
17. Erbek SS, Koycu A, Buyuklu F. Endoscopic modified medial maxillectomy for treatment of inverted papilloma originating from the maxillary sinus. J Craniofac Surg. 2015;26:e244–6.
18. Weber RK, Werner JA, Hildenbrand T. Endonasal endoscopic medial maxillectomy with preservation of the inferior turbinate. Am J Rhinol Allergy. 2010;24:132–5.
19. Zhou B, Han DM, Cui SJ, Huang Q, Wang CS. Intranasal endoscopic prelacrimal recess approach to maxillary sinus. Chin Med J (Engl). 2013;126:1276–80.
20. Zhou B, Han DM, Cui SJ, Huang Q, Wei YX, Liu HC, Liu M. Endoscopic nasal lateral wall dissection approach to maxillary sinus. Zhonghua Er Bi Yan Hou Tou Jing Wai Ke Za Zhi. 2007;42:743–8.
21. Suzuki M, Nakamura Y, Nakayama M, Inagaki A, Murakami S, Takemura K, Yokota M. Modified transnasal endoscopic medial maxillectomy with medial shift of preserved inferior turbinate and nasolacrimal duct. Laryngoscope. 2011;121:2399–401.
22. Suzuki M, Nakamura Y, Yokota M, Ozaki S, Murakami S. Modified transnasal endoscopic medial maxillectomy through prelacrimal duct approach. Laryngoscope. 2017;127:2205–9.
23. Rutherford KD, Brown SM. Endoscopic resection of maxillary sinus inverted papillomas with inferior turbinate preservation. Otolaryngol Head Neck Surg. 2010;142:760–2.
24. Nakayama T, Asaka D, Okushi T, Yoshikawa M, Moriyama H, Otori N. Endoscopic medial maxillectomy with preservation of inferior turbinate and nasolacrimal duct. Am J Rhinol Allergy. 2012;26:405–8.
25. Nakamaru Y, Furuta Y, Takagi D, Oridate N, Fukuda S. Preservation of the nasolacrimal duct during endoscopic medial maxillectomy for sinonasal inverted papilloma. Rhinology. 2010;48:452–6.
26. Pagella F, Pusateri A, Matti E, Avato I, Zaccari D, Emanuelli E, Volo T, Cazzador D, Citraro L, Ricci G, et al. "TuNa-saving" endoscopic medial maxillectomy: a surgical technique for maxillary inverted papilloma. Eur Arch Otorhinolaryngol. 2017;274:2785–91.
27. Morrissey DK, Wormald PJ, Psaltis AJ. Prelacrimal approach to the maxillary sinus. Int Forum Allergy Rhinol. 2016;6:214–8.
28. Gras-Cabrerizo JR, Massegur-Solench H, Pujol-Olmo A, Montserrat-Gili JR, Adema-Alcover JM, Zarraonandia-Andraca I. Endoscopic medial maxillectomy with preservation of inferior turbinate: how do we do it? Eur Arch Otorhinolaryngol. 2011;268:389–92.
29. Kapur R, Aakalu VK, August CZ, Weiss RA. Mucormycosis infection of the lacrimal sac. Ophthalmic Plast Reconstr Surg. 2009;25(6):494–6. https://doi.org/10.1097/IOP.0b013e3181b80e81.
30. Halawa A, Yacoub G, Al Hassan M, Byrd RP Jr, Roy TM. Dacryocystitis: an unusual form of Mucorales infection. J Ky Med Assoc. 2008;106(11):520–4.
31. Hirabayashi KEMD, Kalin-Hajdu EMD, Vagefi MRMD, Kersten RCMD. Invasive aspergillosis masquerading as a lacrimal sac abscess. Ophthal Plastic Reconstr Surg. 2018;34(3):e104. https://doi.org/10.1097/IOP.0000000000000895.
32. Gupta N, Singla P, Gandhi A, Kumari N, Das S. Endoscopic features of lacrimal sac in invasive aspergillosis. ORBIT. https://doi.org/10.1080/01676830.2021.1987479.

15 Antifungal Therapy in Rhino-Orbito-Cerebral Mucormycosis (ROCM)

Rajeev Soman and Sujata Rege

COVID-19-associated Mucormycosis has taken not just the infectious diseases physician but almost all specialities in the hospital by storm [1]. As everyone scrambles to get his/her act together, an in-depth understanding of the pathogen, the drugs used for treatment and other aspects of management has become necessary.

Successful management of mucormycosis requires the following steps [2]:

1. Early suspicion and establishing the diagnosis.
2. Risk stratification, staging the disease, and assessing its tempo of progression.
3. Prompt effective antifungal therapy.
4. Aggressive and often repeated surgical debridement.
5. Adjuvant therapy.
6. Reversal of underlying predisposing risk factors.
7. Involvement of a multidisciplinary team.

R. Soman (✉)
Jupiter Hospital, Pune, India

Deenanath Mangeshkar Hospital, Pune, India

S. Rege
Bharati Hospital and Research Centre, Pune, India

15.1 Antifungal Therapy

The cornerstone of antifungal therapy has been an Amphotericin B product.

15.1.1 Polyenes

Amphotericin B has been grandfathered into the treatment of mucormycosis over the past 60 years, with all subsequent drugs being compared to it as the gold standard [3].

> Although Amphotericin B deoxycholate was initially used, lipid formulations have several advantages and are increasingly used when affordable. Slow escalation of dose over several days is no longer recommended [4].

Mechanism of action involves AmB binds to ergosterol in the fungal cell membrane, leading to increased membrane permeability which causes leakage of intracellular contents.

(a) *Formulations*: Table 15.1
- Amphotericin B deoxycholate (ABD)
- Amphotericin B lipid complex (ABLC)
- Liposomal Amphotericin B (LAMB)
- Amphotericin B Lipid emulsion

(b) *Dosage and administration*:
- Dose for Amphotericin B deoxycholate is 0.7–1 mg/kg/day.
- Amphotericin B lipid complex and Amphotericin B Lipid emulsions 5 mg/kg/day.

N. Gupta, S. G. Honavar (eds.), *Rhino-Orbito-Cerebral Mucormycosis*,
https://doi.org/10.1007/978-981-16-9729-6_15

Table 15.1 Comparison between various types of Amphotericin B formulations

	Amphotericin B deoxycholate	Amphotericin B lipid emulsion	Amphotericin B lipid complex	Liposomal amphotericin B
Structure	Micelles	Colloidal discs	Ribbon-like complexes	Unilamellar liposomes
Size (nm)	25	100	4500	80
Release			Release from complexes by macrophages	LAMB fits snugly into the liposome and is released only into fungal cells
Volume of distribution	2.4			0.42
COVID-19 associated Mucormycosis	1.7			14.4
Area under the dose response curve	17	36	14	555
Dose	0.7–1 mg/kg/day	3–4 mg/kg/day	5 mg/kg/day	5–10 mg/kg/day

- LAMB is 5–10 mg/kg/day. Dose for intracranial involvement is 10 mg/kg/day.

(c) *Administration*:
- Test dose: 1 mg Liposomal Amphotericin B in 100 mL 5% dextrose over 1 h and to watch for reactions like shaking chills and fever.
- Premedication: This may include all of the following:
  – 500 mL 0.9% normal saline is given over 30–60 min.
  – Tablet Paracetamol 500 mg.
  – Tablet Pheniramine maleate (25 mg).
  – Intravenous Hydrocortisone 25 mg.
- Infusion:
  – Intravenous (IV)AMB as per dose in 500 mL of 5% Dextrose to be infused over 4–6 h.
  – AMB infusion is followed by 500 mL 0.9% normal saline (NS) to ensure adequate hydration. These steps help to avoid both infusional toxicity and nephrotoxicity.

(d) *Pharmacokinetic/Pharmacodynamic (PK/PD) considerations* [5]:
- Amphotericin B deoxycholate is 95% protein-bound and is stored in tissues, and re-enters circulation slowly. The route of elimination is unknown, but a small amount is eliminated in the faeces. Hence blood levels of Amphotericin B deoxycholate are unaffected by hepatic, renal failure, or dialysis, except in patients with lipaemic plasma wherein the drug adheres to the dialysis membrane.
- Amphotericin B deoxycholate penetrates poorly into cerebrospinal fluid, saliva, bronchial secretions, brain, muscle, and bone, whereas it concentrates in kidneys.
- Lipid formulations of AMB produce tissue concentrations ranging from 10 to 500% of those seen with Amphotericin B deoxycholate with an 80–90% reduction in nephrotoxicity. The higher but equipotent doses are better tolerated, have lower rates of infusion-related reactions and chronic nephrotoxicity.
- Liposomal Amphotericin B has the advantage of intracranial penetration and immunomodulatory properties, whereas ABLC accumulates better in the reticuloendothelial system.

(e) *ROCM*/MIC (Maximum concentration after a single dose of antimicrobial/Minimum inhibitory concentration of antimicrobial).

It has been found that the pharmacodynamic index most is predictive of efficacy for Amphotericin B. However, free drug level does not increase even with rapid infusion due to its highly protein-bound nature. On the other hand, a rapid infusion leads to

increased infusional toxicity, thus favouring slow administration over 4–6 h.

(f) Resistance and Breakthrough infections [6]:

As there are no Clinical breakpoints (CBP) for Mucorales and antifungal agents, Epidemiological cut-offs (ECVs) are proposed. Certain Mucorales like Apophysomyces and Cunninghamella exhibit high MICs to Amphotericin B, leading to treatment failure. About 10% of mucormycosis cases have co-infection of *Aspergillus*, especially *A. flavus*, which has intrinsic resistance to Amphotericin B, leading to therapeutic failure.

(g) *Adverse drug reactions*:

- *Acute infusion-related reactions*:

  These reactions can be alleviated by premedication using paracetamol, hydrocortisone and administering the infusion slowly. These reactions are not considered a contraindication for further infusions.
- *Nephrotoxicity*:

  Amphotericin B deoxycholate produces a dose-dependent decrease in Glomerular filtration rate (GFR) due to vasoconstrictive effect on afferent renal arterioles. Other side effects are potassium, magnesium and bicarbonate wasting and decreased erythropoietin production. Monitoring renal function tests and Serum electrolytes are required while on amphotericin B. Correction of electrolyte imbalances and cessation of therapy if Serum Creatinine doubles from baseline is necessary. Saline loading before infusion reduced nephrotoxicity.
- *Rare Adverse drug reactions*: Bone marrow suppression, hepatotoxicity, arrhythmias, seizures, haemolysis, haemorrhagic enteritis, tinnitus may occur.

15.1.2 Azoles

Mechanism of action: Azoles inhibit C-14α demethylation of lanosterol in fungi by binding to one of the cytochrome P-450 enzymes, leading to accumulation of C-14α methyl sterols and reduced concentrations of ergosterol, essential for fungal cytoplasmic membrane.

15.1.2.1 Posaconazole

Posaconazole is an extended-spectrum triazole with action against *Candida*, *Aspergillus* and Zygomycetes.

(a) Formulations:
- Suspension: 40 mg/mL
- Tablet (Delayed release/ Gastro-resistant): 100 mg
- Intravenous: 300 mg/vial.

(b) Dosage:
- Suspension: 200 mg QID/ 400 mg BD.
- Tablet and Intravenous: Loading dose—300 mg BD followed by 300 mg daily.
- Slow escalation of doses is not recommended, instead, a full daily dose should be given from the first day.

(c) Administration:
- Suspension: Should be taken 20 min following a full meal or with an acidic carbonated beverage.
- Tablet: Should be swallowed whole without crushing/dissolving. It should be administered with food.
- Intravenous: Should be infused with 100 mL 0.9% NS administered over 90 min via a central line with a 0.2-micron filter.

(d) Pharmacokinetic/Pharmacodynamic considerations [7]:

Posaconazole is lipophilic, >98% protein-bound and has a greater volume of distribution than water, thus leading to an extensive distribution and tissue penetration. AUC/MIC (Area under the curve, i.e. Total exposure of an antimicrobial to an organism divided by the minimum concentration of antimicrobial to inhibit the organism's growth) has been found to be the pharmacodynamic index most predictive of therapeutic efficacy of posaconazole.

Due to its potent dose-dependent cidal action, using a loading dose helps to achieve therapeutic levels faster. Posaconazole accu-

mulates in peripheral tissues, especially in lungs, kidneys, liver and heart, but has inconsistent cerebrospinal fluid and brain parenchyma distribution. There is no data about its bone penetration. An AUC0–24/MIC ratio of >100 proved to be the target associated with the half-maximal effect of lung fungal burden based on a neutropenic murine model of pulmonary mucormycosis infected with *R. arrhizus*, but human data are lacking [8].

It is cleared primarily by faecal excretion and minority by renal clearance. Renal adjustment is hence not necessary, nor is it removed by haemodialysis. Posaconazole is not metabolized by CYP450 enzymes but by hepatic glucuronidation (UGT1A4). It is a substrate for P-glycoprotein and inhibits hepatic CYP3A4 enzyme, leading to drug interactions.

The oral suspension has an erratic absorption profile influenced by food, acidic pH of gastric content, often leading to suboptimal plasma Posaconazole levels. Administration with a high-fatty meal or an acidic carbonated beverage is necessary for enhancing bioavailability. The delayed release tablet and intravenous formulation have better systemic bioavailability and are hence preferred. Achieving therapeutic levels is difficult in obese individuals with BMI > 30 or weight > 90 kg. Mucositis, diarrhoea and administration of crushed tablets through a feeding tube lead to reduction of absorption. Avoiding antacids (H2 blockers, PPIs) and prokinetic motility agents has to be stressed while using posaconazole.

Therapeutic drug monitoring (TDM) is necessary to ensure adequate exposure and ensure compliance for posaconazole. Target trough levels of >0.7 mg/l for prophylaxis and > 1.2 for treatment are advised [9]. TDM is checked after a week of initiating posaconazole, repeated if dose adjustment is needed to ensure adequate trough level, and in case of clinical worsening on therapy (ineffectiveness, compliance or toxicity). Using intravenous formulation upfront followed by switching to an oral formulation helps achieve therapeutic levels faster [10].

(e) Resistance:

Posaconazole has variable in vitro activity against Mucorales, which is species dependent. While Mucor spp. are most responsive to posaconazole, Rhizopus spp. is less susceptible [11].

(f) Adverse drug reactions:

Posaconazole is generally well tolerated, with headache and gastrointestinal symptoms being most commonly reported. Serious adverse events include hepatotoxicity (cholestasis, elevation of transaminases), Qt prolongation (especially when used with other Qt prolonging drugs), hypokalaemia and adrenal insufficiency. Coadministration with CYP3A4 substrates can increase the exposure of these drugs leading to toxicity. Monitoring liver function tests, ECG, serum electrolytes should be done while on therapy.

(g) Role in Mucormycosis therapy:

Posaconazole has been approved only in prophylaxis for invasive mould infections in the stem cell transplant population. There is limited data from the MoveOn trial [12] wherein oral gastro-resistant formulation was used and found to be an effective treatment in mucormycosis. Though it has low serum levels, tissue levels are approximately 40 times more, making it an attractive option for the treatment of mucormycosis.

15.1.2.2 Isavuconazole

Isavuconazonium sulphate is a water-soluble prodrug of isavuconazole, a broad spectrum, second-generation triazole.

(a) Formulations

Oral: 200 mg

Intravenous: 200 mg

(b) Dosage:

Oral: 200 mg 8 hourly for 2 days followed by 200 mg once daily.

Intravenous (IV): 200 mg 8 hourly for six doses (2 days) followed by 200 mg daily.

(c) Administration

Oral: Can be administered with or without food. Capsule should be ideally swallowed

whole, but a small PK study on IV and crushed capsules through NG tube administration showed bioequivalence.

Nasogastric (NG): Should be administered within an hour of reconstitution. After a dose, NG tube should be flushed with 5 mL water thrice.

Intravenous to be infused over an hour through the infusion set with a 0.2-micron filter. Iv line should be flushed with NS or 5% dextrose before and after the infusion.

(d) PK/PD considerations [13]:

Isavuconazole is administered as its prodrug isavuconazonium sulphate, which is hydrolyzed by plasma esterases to isavuconazole and an inactive cleavage product. Plasma protein binding is >99%, and total exposure of prodrug is <1% of that of isavuconazole.

It exhibits dose-proportional pharmacokinetics and bioavailability of 98%, thereby enabling the interchange of intravenous to oral preparations. Isavuconazole has a high volume of distribution leading to excellent tissue distribution. Animal data have shown that it exhibits hysteresis, i.e. it persists in tissues long after plasma concentration levels fall below detectable limits. Isavuconazole is widely distributed to most tissues, including the brain, liver, lung and bone. However, in neutropenic patients, the ultimate therapeutic effect heavily depends on recovery from neutropenia.

AUC/MIC ratio is the important PD index for isavuconazole efficacy.

It is metabolized via CYP3A4 and CYP3A5 followed by biotransformation involving UGT, making it prone to drug interactions. Less than 1% is excreted really. Hence it does not require renal dosing. No dosage adjustments are required in patients with mild to moderate hepatic impairment.

Since only minimal variability has been found in subjects receiving isavuconazole, TDM levels are not available or recommended at this time but would be helpful in situations where there is coadministration with interacting drugs, diarrhoea, GI graft versus host disease and CNS infection where the assurance of an adequate exposure is needed.

(e) Resistance:

Mucor circinelloides and *Rhizopus oryzae* exhibit high MICs; hence species identification and susceptibility testing are recommended [14, 15]. However, due to excellent pharmacokinetic properties, an adequate level is usually achieved at the top of the dose-exposure-response relationship.

(f) Adverse drug reactions:

Gastrointestinal side effects are most commonly reported. Hepatotoxicity can occur but to a lesser extent than with other azoles. Contrary to other azoles, it causes shortening of QTc interval.

(g) Role in Therapy:

Isavuconazole has a labelled indication as initial treatment of mucormycosis based on VITAL [16] and SECURE [17] trials.

15.1.3 Adjunctive Treatments

(a) Deferasirox:

Deferasirox is an iron chelator without xenosiderophore activity. Mucor, especially Rhizopus cannot synthesize hydroxamate siderophores hence relies on free iron which is taken up by Rhizoferrin from which iron permeases release iron. Haemeoxygenase enhances the angioinvasive potential of this fungus. Deferasirox chelates iron, thereby starving the fungus of iron which is critical for its growth and pathogenicity [18]. It has been used as salvage therapy in cases of mucormycosis with some success [19]. It has independent fungicidal activity against *Rhizopus* species ut less for Mucor species and Cunninghamella.

(b) Caspofungin:

Although echinocandins have no in vitro activity against *Mucorales*, *Rhizopus oryzae* expresses the FKS gene for target enzyme (1,3 B-d-glucan (BG) synthase) for echinocandin, justifying its use as salvage therapy [20]. Caspofungin may disrupt BG, thereby enhancing polyene penetration, increase the

action of polymorphonuclear leukocytes, stunt filamentation, altering cell wall content, reducing virulence, and enhancing host responses. It has been found to be beneficial for Rhino-orbital involvement by Rhizopus in non-neutropenic patients [21].

(c) Hyperbaric oxygen [22]:

Hyperbaric oxygen therapy has been found to be a beneficial adjunctive therapy for mucormycosis, particularly in diabetic patients with ROCM. The increased partial pressure of oxygen achieved with hyperbaric therapy improves antifungal effect, neutrophil activity, tissue healing and oxidative killing by amphotericin B. Additionally, high concentrations of oxygen can inhibit the growth of Mucorales in vitro and improve the rate of wound healing by increasing the release of tissue growth factors. It is most effective for post-traumatic mucormycosis.

(d) Statins:

Statins have shown in vitro and in vivo activity against *Rhizopus* spp. for reducing virulence [23]. Additionally, they have modulated signal transduction, cytokine transcription, inflammatory cascade and produce fungal apoptosis by inhibiting protein prenylation [24]. Drug interaction with azoles should be considered while using statins.

(e) Aspirin:

Acetylsalicylic acid is an anti-inflammatory and antimitochondrial drug which additionally targets sporangium development of *Mucor circinelloides* [25]. It is used as an adjuvant therapy in mucormycosis. It may also benefit in reducing the thrombotic effects of fungal vascular invasion.

15.1.4 Step-Down or Step-Up Treatment

Patients who have improved or are stable on amphotericin B may transition to oral treatment with Azoles, or those who have not may undergo salvage treatment with Azoles. This creates uncertainty about the exact role of the Azoles as step-down or step-up treatment. It is also unknown when this switch may be done in an individual patient and only clinical judgment can be used considering other factors like the adequacy of surgical debridement and resolution of the underlying cause. Adverse effects, cost of treatment and patient preference also force some of these decisions. The unfortunate reality in India is that about a third of patients cannot continue treatment due to the anticipated expenses, risks of surgery, morbidity and mortality. Post-COVID-19 Mucormycosis is a particular but somewhat avoidable misfortune to an already devastated patient and family. In this context, an oral antifungal medication offers some promise.

15.1.5 Role of Combination Therapy

There is no definitive data to recommend antifungal combination therapy but has been increasingly used to enhance early antifungal effect, especially to benefit those at highest risk of poor outcome and in those who may have a relatively resistant Mucorales or have a co-infection with *Aspergillus*. While there may be antagonism between Azoles and AMB, the role of the Azole may be viewed as that of a supporting drug due to likely interruptions in AMB treatment owing to toxicity and erratic supplies.

15.2 Duration of Therapy [26]

The duration of therapy necessary to treat mucormycosis is unknown. It requires weeks to months of therapy. In general, therapy should be continued until resolution of signs and symptoms of infection, substantial radiological improvement, normal findings on repeated examination by an ear-nose-throat specialist and ophthalmologist, microbiologic and histologic assessment. Treatment duration should be personalized, wherein adequacy of surgical debridement and resolution of the underlying causes is assured. Patients who show relapse after treatment withdrawal or remain severely immunocompromised need re-treatment or secondary prophylaxis, respectively.

15.3 Concluding Remarks

The COVID-19 waves have generated an avalanche of cases of COVID-19-associated Mucormycosis. This has been an opportunity to study various aspects of the management of this disease. There is a paucity of controlled trial data and only expert opinion based on anecdotal experience and single centre studies is available. The clinical outcome, however, is a composite of many drugs, processes and host factors. For all these reasons, the management of Mucormycosis appears to be a challenging frontier of medical mycology.

References

1. Patel A, Agarwal R, Rudramurthy SM, Shevkani M, Xess I, Sharma R, et al. Multicenter epidemiologic study of coronavirus disease-associated mucormycosis, India. Emerg Infect Dis. 2021;27(9):2349–59.
2. Soman R, Sunavala A. Post COVID-19 mucormycosis-from the frying pan into the fire. J Assoc Physicians India. 2021;69(1):13–4.
3. Soman R, Sunavala A. Post COVID-19 mucormycosis in the second wave-realities, uncertainties and myths. J Assoc Physicians India. 2021;69(7):11–2.
4. Rex JH, Stevens DA. Drugs active against fungi, pneumocystis, and microsporidia. In: Mandell, Douglas, and Bennett's principles and practice of infectious diseases. WB Saunders; 2015. p. 479–94.
5. Cavassin FB, Baú-Carneiro JL, Vilas-Boas RR, et al. Sixty years of amphotericin B: an overview of the main antifungal agent used to treat invasive fungal infections. Infect Dis Ther. 2021;10:115–47.
6. Espinel-Ingroff A, Chakrabarti A, Chowdhary A, Cordoba S, Dannaoui E, Dufresne P, et al. Multicenter evaluation of MIC distributions for epidemiologic cutoff value definition to detect amphotericin B, posaconazole, and itraconazole resistance among the most clinically relevant species of Mucorales. Antimicrob Agents Chemother. 2015;59(3):1745–50.
7. Lepak AJ, Andes DR. Antifungal pharmacokinetics and pharmacodynamics. Cold Spring Harb Perspect Med. 2014;5(5):a019653.
8. Lewis RE, Albert ND, Kontoyiannis DP. Comparative pharmacodynamics of posaconazole in neutropenic murine models of invasive pulmonary aspergillosis and mucormycosis. Antimicrob Agents Chemother. 2014;58(11):6767–72.
9. Ashbee HR, Barnes RA, Johnson EM, Richardson MD, Gorton R, Hope WW. Therapeutic drug monitoring (TDM) of antifungal agents: guidelines from the British Society for Medical Mycology. J Antimicrob Chemother. 2014;69(5):1162–76.
10. Soman R. How soon are therapeutic posaconazole trough levels achieved after i.v. administration in the treatment of mucormycosis? Paper presented at ECCMID, Amsterdam; 2019.
11. Sipsas NV, Gamaletsou MN, Anastasopoulou A, Kontoyiannis DP. Therapy of mucormycosis. J Fungi. 2018;4(3):90.
12. Salmanton-García J, Seidel D, Koehler P, Mellinghoff SC, Herbrecht R, Klimko N, et al. FungiScope® ECMM/ISHAM Working Group. Matched-paired analysis of patients treated for invasive mucormycosis: standard treatment versus posaconazole new formulations (MoveOn). J Antimicrob Chemother. 2019;74(11):3315–27.
13. Ellsworth M, Ostrosky-Zeichner L. Isavuconazole: mechanism of action, clinical efficacy, and resistance. J Fungi. 2020;6(4):324.
14. Arendrup MC, Jensen RH, Meletiadis J. In vitro activity of isavuconazole and comparators against clinical isolates of the mucorales order. Antimicrob Agents Chemother. 2015;59(12):7735–42.
15. Jørgensen KM, Astvad KM, Hare RK, Arendrup MC. EUCAST susceptibility testing of isavuconazole: MIC data for contemporary clinical mold and yeast isolates. Antimicrob Agents Chemother. 2019;63(6):e00073–19.
16. Marty FM, Ostrosky-Zeichner L, Cornely OA, Mullane KM, Perfect JR, Thompson GR 3rd, et al. VITAL and fungiscope mucormycosis investigators. isavuconazole treatment for mucormycosis: a single-arm open-label trial and case-control analysis. Lancet Infect Dis. 2016;16(7):828–37.
17. Maertens JA, Raad II, Marr KA, Patterson TF, Kontoyiannis DP, Cornely OA, et al. Isavuconazole versus voriconazole for primary treatment of invasive mould disease caused by Aspergillus and other filamentous fungi (SECURE): a phase 3, randomised-controlled, non-inferiority trial. Lancet. 2016;387(10020):760–9.
18. Spellberg B, Ibrahim AS, Chin-Hong PV, Kontoyiannis DP, Morris MI, Perfect JR, et al. The deferasirox–ambisome therapy for mucormycosis (DEFEAT Mucor) study: a randomized, double-blinded, placebo-controlled trial. J Antimicrob Chem. 2012;67(3):715–22.
19. Soman R, Gupta N, Shetty A, Rodrigues C. Deferasirox in mucormycosis: hopefully, not defeated. J Antimicrob Chem. 2012;67(3):783–4.
20. Ibrahim AS, Bowman JC, Avanessian V, Brown K, Spellberg B, Edwards JE Jr, Douglas CM. Caspofungin inhibits Rhizopus oryzae 1,3-beta-D-glucan synthase, lowers burden in brain measured by quantitative PCR, and improves survival at a low but not a high dose during murine disseminated zygomycosis. Antimicrob Agents Chemother. 2005;49(2):721–7.
21. Reed C, Bryant R, Ibrahim AS, Edwards J Jr, Filler SG, Goldberg R, Spellberg B. Combination polyene-caspofungin treatment of rhino-orbital-cerebral mucormycosis. Clin Infect Dis. 2008;47(3):364–71.

22. John BV, Chamilos G, Kontoyiannis DP. Hyperbaric oxygen as an adjunctive treatment for zygomycosis. Clin Microbiol Infect. 2005;11(7):515–7.
23. Bellanger AP, Tatara AM, Shirazi F, Gebremariam T, Albert ND, Lewis RE, et al. Statin concentrations below the minimum inhibitory concentration attenuate the virulence of Rhizopus oryzae. J Infect Dis. 2016;214(1):114–21.
24. Terblanche M, Almog Y, Rosenson RS, Smith TS, Hackam DG. Statins and sepsis: multiple modifications at multiple levels. Lancet Infect Dis. 2007;7(5):358–68.
25. Leeuw NJ, Swart CW, Ncango DM, Kriel WM, Pohl CH, van Wyk PW, Kock JL. Anti-inflammatory drugs selectively target sporangium development in Mucor. Can J Microbiol. 2009;55(12):1392–6.
26. Cornely OA, Alastruey-Izquierdo A, Arenz D, Chen SC, Dannaoui E, Hochhegger B, et al. Global guideline for the diagnosis and management of mucormycosis: an initiative of the European Confederation of Medical Mycology in cooperation with the Mycoses Study Group Education and Research Consortium. Lancet Infect Dis. 2019;19(12):e405–21.

16 Medical Management of Patients with Rhino-Orbito-Cerebral Mucormycosis

Bhushan S. Bansal

In the year 2019 world encountered COVID-19 pandemic. The first wave hit the world in 2019, the second one being more lethal hit India in 2021. In the second wave, a large number of individuals were affected and required critical care too. Soon we were facing an unprecedented tsunami of mucormycosis. We were familiar with a deadly fungal disease in the past, but this time's magnitude and extent threw new challenges in patient care. There are a variety of factors that make COVID-19 patients more susceptible to mucormycosis. Management of mucormycosis involves a multidisciplinary team approach. This chapter describes the role of a physician in the evaluation and management of this devastating disease.

16.1 Evaluation of the Patient

16.1.1 Initial Workup

All the patients admitted to the hospital are thoroughly investigated in the first 24 h to know the extent of the disease. KOH staining, fungal and bacterial cultures from the areas affected, and rapid molecular tests should be sent. Computed tomography and magnetic resonance imaging are ordered to ascertain the stage of the disease. Patients with extensive involvement of sinuses, orbit and brain need to be managed more aggressively as mucor gives very little time to save the life.

16.1.2 Treatment of COVID

16.1.2.1 The Exact Date of Onset of Infection

It is necessary to know the exact date of onset of illness as the likelihood of developing cytokine storms decreases as time elapses.

16.1.2.2 Hospital-Based Treatment (ICU/HDU/Ward) or Home Isolation

The previous history of hospitalization for COVID helps us know the nature and extent of COVID pneumonia, oxygen requirement and other organ involvement. Previously hospitalized patients are more prone to have hospital-acquired bacterial infections. So it helps us in deciding the empirical selection of antibiotics till we have the culture reports.

16.1.2.3 Use of Steroids

The history of steroid usage has an important implication. We should make a note of the dose and duration of the steroid. The indications of

B. S. Bansal (✉)
Jindal Institute of Medical Sciences,
Hisar, Haryana, India

N. Gupta, S. G. Honavar (eds.), *Rhino-Orbito-Cerebral Mucormycosis*,
https://doi.org/10.1007/978-981-16-9729-6_16

steroid usage during COVID treatment should also be documented.

16.1.2.4 Use of Immunosuppressants

Severe COVID pneumonia has put us in place to use immunosuppressants to manage the dysregulated host immune response. Many patients with severe COVID-19 do not respond to steroids and other adjuvant therapies. The magnitude of cytokine storm compels the healthcare provider to use immunosuppressants to save human life in limited cases. There are a plethora of immunosuppressants used in this pandemic like tocilizumab, bevacizumab, tofacitinib and baricitinib. These drugs helped us save a few patients but put the patients at risk of opportunistic infections by lowering the host immunity. So knowledge of their usage helps us to tailor the treatment.

16.1.2.5 Respiratory Evaluation

A careful evaluation of the respiratory system should be done as the patient's oxygen requirement seriously affects the treatment protocols. Those patients still suffering from severe COVID pneumonia requiring high-flow oxygen or ventilator support will be the most difficult to manage. Many of these patients will not be medically fit for any surgery or debridement for mucormycosis. High-resolution computed tomographic scan of the chest should be done in all such patients to know the CT severity index of COVID pneumonia. The severity of previously underlying chronic lung diseases like asthma, chronic obstructive pulmonary airway disease and interstitial lung disease should be accommodated in the treatment protocols.

16.2 Pulmonary Mucormycosis

Pulmonary mucormycosis is a rare opportunistic infection caused by this fungus and generally affects the hosts with poor immunity. This infection has a high mortality (40–76%) [1–3] and is a source of serious morbidity as the fungus causes extensive tissue destruction rapidly. It presents with fever, cough, haemoptysis and rapidly deteriorating lung functions causing life-threatening hypoxia. Radiologically it presents with multiple cavitary lesions in lungs especially in those individuals who have poorly controlled diabetes and are immunocompromised due to associated comorbidities. Fibreoptic bronchoscopy in expert hands can be used to obtain biopsy from the suspected lung lesions. A combined approach of surgical resection and amphotericin B therapy is the best possible treatment option in such scenario right now. Future studies are needed to evaluate treatment protocol and outcomes in patients suffering from this disease.

With the involvement of lungs, although rare, we have seen cases of fungal pneumonia in this pandemic. A few patients, on rare occasions, can have disseminated mucor infection in the lungs too. The presence of fungal pneumonia will pose a further challenge in the treatment of these patients. Serial chest X-ray and arterial blood gas analysis should be carried out. Patients with mucormycosis who are stable and not on oxygen support should be subjected to pulmonary function testing and 6-min walk test for the evaluation and fitness of surgery if required.

16.3 Blood Tests

All patients suffering from mucormycosis should undergo routine blood investigations like complete blood count, kidney function tests, liver function tests, thyroid function tests, glycosylated haemoglobin, C-reactive protein quantitative and D-Dimer. Procalcitonin, blood culture, urine culture and galactomannan assay should also be done in seriously ill patients.

16.3.1 Evaluation of Diabetes

Extensive diabetic and stress hyperglycaemia evaluation should be carried out in all the patients. Hyperglycaemia in mucormycosis patients further propagates the disease and hampers recovery. Random blood sugar levels more than 200, fasting blood sugar levels more than 124 and HbA1c levels more than 6.4 are diagnostic of diabetes mellitus [4, 5]. Some of the patients do not

fit into these criteria on admission but develop random blood sugar levels more than 200 later in the course of disease due to stress hormones or the use of steroids. So it is necessary to check the blood sugar levels regularly, even in non-diabetic patients. Such patients should also be managed like a diabetic patient till their blood sugar levels are normal.

16.3.2 Evaluation of Comorbidities

Extensive evaluation of all the patients of COVID-19 and mucormycosis should be done for the underlying comorbidities like coronary artery disease, chronic liver disease (CLD), chronic obstructive airway disease (COAD), chronic kidney disease (CKD), hypertension, stroke, post organ transplant, post chemotherapy. Patients already on antiplatelets should be offered anticoagulants in lower doses than necessary. Patients with CLD and CKD have alrered baseline coagulation profile, so PT and aPTT should be tested before beginning anticoagulants and should be monitored later on. The advice of concerned subspeciality should be sought as all these are immunocompromised states, and any new organ failure will further jeopardize patients' complete care and prognosis.

16.4 Management

16.4.1 Management of Mucor

Mucormycosis is a devastating disease and spreads very rapidly. This fungus is angio-invasive and leads to infarction of tissue. If not treated appropriately, it can prove fatal. Patients should be first categorized based on the severity. Those aged 60 years and above, with ocular and neural involvement, immunosuppressed, uncontrolled diabetes, and severe COVID pneumonia requiring high flow oxygen or ventilator support should be treated more aggressively. Antifungal therapy and surgery remain the mainstay of treatment. For those patients who are unfit for surgery, medical management continues until they become fit for surgery. Surgery should be planned as early as the conditions permit.

16.4.2 Treatment of COVID Pneumonia

Treatment of COVID pneumonia includes anticoagulation, oxygen, and ventilator support to all patients suffering from active COVID pneumonia.

Steroids should be avoided as far as possible if the patient is not on supplemental oxygen or ventilator therapy. Patients requiring supplemental oxygen and ventilator therapy, steroids can be considered in minimal possible doses, i.e. 0.5 mg/kg of methylprednisolone. The dose and duration should be tailored according to the clinical scenario and tapered off quickly.

Immunosuppressants like tocilizumab and baricitinib should be avoided in the management of such patients as it will risk the flare-up of mucormycosis.

Antibiotics: Routine and prolonged use of broad-spectrum antibiotics should be discouraged. Broad-spectrum antibiotics can be considered empirically in seriously ill patients till the report of bacterial culture is awaited. Afterwards, the de-escalation of the antibiotic regime according to the culture report should be instituted.

16.4.3 Management of Diabetes

The prevalence of diabetes in India is 11.8% [6]. The high prevalence and absence of routine health checkups have put a large number of asymptomatic, previously undiagnosed, uncontrolled diabetic patients at risk of severe COVID infection and, later on, mucormycosis. Steroid usage is recommended and life-saving for severe COVID-19 pneumonia, but their indiscriminate overuse also poses a challenge for the control of diabetes. High blood sugar levels, steroids, malnutrition, immunosuppression and COVID-19 infection per se set the stage for mucormycosis. So it is imperative to control blood sugar levels tightly to prevent the onset of mucormycosis and

prevent its complications. Basic principles for the control of diabetes in such patients are as follows.

1. Insulin infusion is the mainstay of therapy for seriously ill patients requiring vasopressors and ventilator support and a very high blood sugar more than 400 [7, 8].
2. The basal bolus regimen is ideal for all stable patients taking regular meals or on RT feeding.
3. Oral hypoglycaemic agents can be adjuvants in stable patients with previously controlled diabetes or requiring large doses of insulin therapy. Long-acting insulin secretagogues and SGLT2 inhibitors should be avoided [9]. DPP4 inhibitors and metformin can help manage diabetes in such patients [9].

The target glucose levels are 140–180 irrespective of the meal [9]. Insulin infusion should be considered in seriously ill patients admitted to intensive care units with very high blood sugar levels.

16.4.3.1 . Insulin Infusion

Insulin infusion can be prepared by mixing 50 units insulin regular in 49 CC of normal saline and should be administered with the help of an infusion pump [10, 11]. The initial rate of infusion should be blood glucose divided by 100. The rate of infusion should be titrated every hour to maintain blood glucose between 140 and 180. Once the patient gets stabilized, transition to subcutaneous insulin should be planned. The basal insulin (degludec, glargine and detemir) should be added first. The starting dose of basal insulin can be 20–30% of the total daily requirements [10, 11]. The basal insulin dose should be less in patients with underlying comorbidities like chronic liver disease, chronic kidney disease and heart failure.

16.4.3.2 Sliding-Scale Insulin Regimen

Sliding-scale insulin regimen is not a good regimen for inpatient diabetes management. It does not provide a stable control of blood glucose levels but can be used in limited settings where oral intake is deficient and blood sugar levels are not so high. It can be used in patients whose blood sugar levels are <250, but it provides a roller-coaster kind of control with excursions sometimes and low sugar levels at other times so it should be better avoided.

16.4.3.3 Oral Hypoglycaemic Agents

Oral hypoglycaemic agents can be used in the limited settings of hospitalized patients like stable patients taking regular meals, those who have high insulin requirements, high insulin resistance, and patients with no underlying chronic kidney disease or chronic liver disease. Currently, metformin can be used in non-critically ill patients with preserved renal and hepatic functions. It primarily acts on the liver and prevents gluconeogenesis, and it increases insulin sensitivity, so it helps in the control of fasting blood glucose. The initial dose of metformin should be 500 mg per day, and it can be titrated up to 2000 mg per day depending on the tolerability of the patient. DPP4 inhibitors like sitagliptin, vildagliptin, alogliptin, saxagliptin and linagliptin can be used in stable patients [9–12]. They should be avoided in patients with past history of pancreatitis. Dose modification will be required in hepatic and renal impairment. They mainly affect postprandial blood glucose levels.

Patients with uncontrolled blood glucose levels at the time of admission should be discharged on insulin and oral hypoglycaemic agents. As insulin is an anabolic hormone, it helps in the recovery of the patients and it should be continued at least 4–6 weeks after the patient's discharge from the hospital.

16.4.4 Anticoagulation in COVID

COVID-19 leads to thrombosis in microvasulature of lungs and other internal organs leading to ischaemic changes. These ischaemic changes can manifest as pulmonary thromboembolism, deep-vein thrombosis, myocardial infarction, ischaemic stroke and renal artery thrombosis in rare cases. The incidence of thrombotic disease in

individuals affected by COVID-19 is reported as high as 31% [13, 14]. So it is imperative to use anticoagulants to prevent these complications in high-risk individuals as well as to treat these complications.

Those patients who are taking anticoagulant or antiplatelet therapies for their medical disorders should continue these drugs if they get COVID-19 infection.

Hospitalized adults with COVID-19 should receive prophylactic dose anticoagulation.

There is currently insufficient evidence to recommend either for or against the use of thrombolytics or higher than the prophylactic dose of anticoagulation for VTE prophylaxis in hospitalized COVID-19 patients [14, 15].

Patients with COVID-19 who experience thromboembolic event (deep-vein thrombosis or pulmonary embolism, cavernous sinus thrombosis, renal or splenic artery thrombosis, ischaemic stroke) or who are highly suspected of having thromboembolic disease should be managed with therapeutic doses of anticoagulant therapy.

Low-molecular-weight heparin is the preferred agent for anticoagulation. The therapeutic dose is 1 mg/kg/dose twice daily. Unfractionated heparin can be used in patients with altered kidney functions with serial monitoring of aPTT. aPTT should be kept around twice the normal upper limit.

16.4.5 Amphotericin B-induced Nephrotoxicity

Amphotericin B can cause nephrotoxicity in the form of acute renal failure and hypokalaemia. So it is necessary to measure kidney functions and electrolytes on a daily basis to evaluate for such damage. Patient's hydration should be well maintained, and any other nephrotoxic drug should be avoided. On discontinuation of antifungal therapy the renal functions are gradually regained. New preparations of the drug, such as liposomal amphotericin B, are very less nephrotoxic.

In a nutshell, mucor and COVID are a deadly combination. The addition of other comorbidities further complicates the clinical scenario and hampers the adequate management of patients. So it is of utmost importance to evaluate and treat the patient in toto to achieve the desired outcome. Further prospective randomized controlled studies are needed for a better understanding of treatment options and their adequate duration.

References

1. Roden MM, Zaoutis TE, Buchanan WL, Knudsen TA, Sarkisova TA, Schaufele RL, et al. Epidemiology and outcome of zygomycosis: a review of 929 reported cases. Clin Infect Dis. 2005;41(5):634–53.
2. Lee FY, Mossad SB, Adal KA. Pulmonary mucormycosis: the last 30 years. Arch Intern Med. 1999;159(12):1301–9.
3. Smith JA, Kauffman CA. Pulmonary fungal infections. Respirology. 2012;17(6):913–26.
4. International Expert Committee. International Expert Committee report on the role of the A1C assay in the diagnosis of diabetes. Diabetes Care. 2009;32:1327–34.
5. American Diabetes Association. Diagnosis and classification of diabetes mellitus. Diabetes Care. 2014;37(Suppl. 1):S81–90.
6. National Diabetes and Diabetic Retinopathy Survey report 2019.
7. Umpierrez G, Hellman R, Korytkowski MT, et al. Management of hyperglycemia in hospitalized patients in non-critical care setting: an endocrine society clinical practice guideline. J Clin Endocrinol Metab. 2012;97(1):16–38.
8. Moghissi ES, Korytkowski MT, Dinardo MM, et al. American Association of Clinical Endocrinologists and American Diabetes Association consensus statement on inpatient glycemic control. Diabetes Care. 2009;32(6):1119–31.
9. Government of India Ministry of Health & Family Welfare. Clinical guidance on diagnosis and management of diabetes at COVID-19 patient management facility version 2.0.
10. Rayman G, Lumb A, Kennon B, et al. New guidance on managing inpatient hyperglycaemia during the COVID-19 pandemic. Diabet Med. 2020;37(7):1210–3. https://doi.org/10.1111/dme.14327.
11. Kelly JL. Continuous insulin infusion: when, where, and how? Diabetes Spectr. 2014;27(3):218–23.
12. Gupta Y, Goyal A, Kubihal S, Golla KK, Tandon N. A guidance on diagnosis and management of hyperglycemia at COVID care facilities in India. Diabetes Metab Syndr. 2021;15(1):407–13.
13. Tang N, Li D, Wang X, Sun Z. Abnormal coagulation parameters are associated with poor prognosis in patients with novel coronavirus pneumonia [published

online ahead of print March 13 2020]. J Thromb Haemost. 2020;18(4):844–7. https://doi.org/10.1111/jth.14768.

14. Bikdeli B, Madhavan MV, Jimenez D, Chuich T, Dreyfus I, Driggin E, et al. COVID-19 and thrombotic or thromboembolic disease: implications for prevention, antithrombotic therapy, and follow-up. J Am Coll Cardiol. 2020; https://doi.org/10.1016/j.jacc.2020.04.031.
15. Cui S, Chen S, Li X, et al. Prevalence of venous thromboembolism in patients with severe novel coronavirus pneumonia. [Published online ahead of print April 9 20202]. J Thromb Haemost. 2020; https://doi.org/10.1111/jth.14830.

17 Clinical Profile and Management of a Series of Rhino-Orbital-Cerebral Mucormycosis Cases at Otorhinolaryngology Department of a Tertiary Hospital

Madhuri Mehta, Priyanka Chhabra, and Akanksha Jain

The years from 2020 until July 2021 were a nightmare to the human race due to the pandemic caused by COVID-19, which gripped the whole world, not once but twice. No living person could have ever comprehended the damage caused to the human race by this tiny, invisible enemy called 'the coronavirus'. The health system worldwide has gone topsy-turvy since the first human case was detected in December 2019.

The first wave in 2020 caused many causalities but gave doctors and the health care system worldwide insight into developing and practising protocol-based treatment for COVID-19. In 2021, the second wave hit the world with more force, speed, and vengeance. This time, the virus was more virulent and associated with numerous complications that were not part of the first wave. These complications were attributed to the side effects of overzealous treatment of COVID-19 infection.

During the first wave, the complications were mainly related to the lungs and the central and peripheral nervous systems. The second wave was accompanied by an altogether different complication called 'mucormycosis' which is though, a systemic disease, but this time, it was explicitly 'rhino-orbito-cerebral mucormycosis (ROCM)'.

17.1 Background

Severe Acute Respiratory Syndrome Coronavirus 2 (SARS-CoV-2) has been proven to be the causative organism of the novel coronavirus disease (COVID-19).

COVID-19 is known to cause respiratory system complications, primarily pneumonia (mild to severe), with superadded bacterial and fungal co-infections.

The second wave of the COVID-19 pandemic in India created grounds for fungus (mucormycosis) to grow and infect the human race with grave severity. ROCM, which was found to be associated with COVID-19, is the most common form of mucormycosis and a life-threatening opportunistic fungal infection characterized by rapidly progressive invasion of the nose, paranasal sinuses, orbit, hard palate, and brain. In the past, this angioinvasive fungal infection, which was noticed very rarely, suddenly saw an acute spurt in post-COVID patients during the second wave.

M. Mehta (✉)
Department of Otorhinolaryngology and Head and Neck, Jindal Institute of Medical Sciences, Hisar, India

P. Chhabra
Department of Radiology, Jindal Institute of Medical Sciences, Hisar, India

A. Jain
Fellowship under Dr. Madhuri Mehta, Jindal Institute of Medical Sciences, Hisar, India

N. Gupta, S. G. Honavar (eds.), *Rhino-Orbito-Cerebral Mucormycosis*,
https://doi.org/10.1007/978-981-16-9729-6_17

17.2 Spread

The fungi that cause ROCM are ubiquitous in the environment, and human beings are constantly exposed to them. In immunocompromised patients, the airborne fungal spores attach to the nasal and oral mucosae and start proliferating and germinating into hyphae. From the nasal, oral, and nasopharyngeal mucosae, the spores/hyphae invade the paranasal sinuses. The further spread of this infection can be classified into different stages.

17.3 Classification of ROCM

Depending upon the anatomical spread and severity:

1. Sino Nasal Mucormycosis
   (a) Disease can be limited to nasal mucosa, middle turbinate, inferior turbinate and the ostium of nasolacrimal duct (NLD).
   (b) Disease can extend to paranasal sinuses and involve mostly a single sinus or more than one sinuses mucosa and bony walls, as well as the opposite-sided sinuses, which hold a grave prognosis.
2. Extra Sinus Extra Cranial Mucormycosis
   (a) It includes the involvement of palate, maxilla/facial tissue/retro antral spaces like pterygopalatine fossa, infratemporal fossa and masticator space.
   (b) Involvement of the orbit
   Orbital spread via NLD/medial orbital wall (thin lamina papyracea/congenital dehiscence/along perivascular spaces)/ Infarorbital foramen.
3. Intracranial Mucormycosis

Intracranial spread can be through three potential pathways: Shreshtha

1. *Direct extension*: From sinonasal cavities through osteolytic defects in the base of skull-like cribriform plate (CP). Infection from Sphenoid sinus (SS) can extend into cavernous sinus (CS), or invade internal carotid artery (ICA) and from there embolize the frontal and parietal lobes.
2. *Perivascular and perineural invasion*: Perivascular spread can occur through spaces around vessels in CP of ethmoid bones to frontal lobe or through spaces around emissary veins in lamina papyracea (LP) into orbit, superior orbital fissure/orbital apex to cavernous sinus and ICA. Posterior fossa involvement can occur through perineural spread from the cavernous sinus along the trigeminal nerve.
3. *Haematogenous Spread*: From invasion of arterial wall due to its occlusion, leading to ischemia, infarct and/or abscess formation.

17.4 The Important Areas Involved During Spread of ROCM Are

17.4.1 The Pterygopalatine Fossa

The pterygopalatine fossa plays a very important role in spreading the fungal hyphae to areas beyond the paranasal sinuses. It actually acts as a reservoir from where the spread of infection takes place to areas like the orbit, soft tissues, in the pre and post maxillary areas, the palate, infratemporal fossa, and cavernous sinus. Infection reaches the pterygopalatine fossa through either the posterior maxillary wall or the sphenopalatine foramen and from here spreads in different directions. Debridement of diseased tissue with complete clearance of mucor from the pterygopalatine fossa becomes mandatory to prevent further spread of disease.

17.4.2 Palate

The palate can be directly eroded by the spread of fungus from nose and paranasal sinuses. Painful, reddish to dark-brown ulceration, well-defined irregular raised border, variegated necrotic surface, and fast progression are the main features of these lesions. The other areas around palate which get infected by mucor are the gingiva, cheek mucosa and pharyngeal surface [2].

17.4.3 Orbital Involvement [1]

The Orbital invasion is usually through the path of least resistance which is the medial wall. It includes thin lamina papyracea, nasolacrimal duct, congenital dehiscence and perivascular spaces in lamina papyracea. At times, aggressive disease from the maxillary sinus can spread to orbit through the infraorbital foramen along the infraorbital nerve. The other pathway for infection is through pterygopalatine fossa and inferior orbital fissure to the retro global space of the orbit. Orbital involvement can be categorized into:

1. In the Early stages, the disease can be involving nasolacrimal system or can infiltrate the periorbital soft tissue leading to inflammation and oedema in the retroorbital fat around the extraocular muscles. This inflammation can further cause abscess formation along the medial aspect of the orbit leading to inflammation of the medial rectus muscle and may cause its lateral displacement. Vision remains unaffected in this situation.
2. Diffuse orbital involvement in the form of infection reaching contents of both extra and intraconal compartments leading to diffused proptosis.
3. Occlusion of Central retinal artery or ophthalmic artery or thrombosis of superior ophthalmic vein leads to superior orbital fissure or orbital apex syndrome. The loss of vision is associated in this situation due to the optic nerve infarct.

17.4.4 Orbital Apex Involvement

The infection travels from the ethmoid sinus through the thin lamina papyracea into the orbit and its contents. This creates a pathway for the organism to extend posteriorly up to the orbital apex, leading to orbital apex syndrome. At this stage, there may be vision loss due to affection of the optic nerve. The progression of the infection may be very rapid because of the aggressive invasive nature of the organism.

The disease can also progress posteriorly from orbital apex, through the inferior orbital fissure across the pterygopalatine fossa into the infratemporal fossa. In some cases, it can spread to the superior orbital fissure causing diplopia, ophthalmoplegia and sensory loss to the corresponding areas of the cornea and face because of the involvement of cranial nerves III, IV and VI, and branches of V1 and V2 [3]. As it spreads more posteriorly it infects cavernous sinus and then the brain parenchyma underlying cause being vascular thrombosis and infarction.

17.4.5 Optic Nerve Involvement

The pathogenesis behind optic nerve involvement is invasion of the organism directly into either the optic nerve fibres or the walls of central retinal or ophthalmic artery causing occlusion or thrombosis of the vessels. Diffusion-weighted sequences of MRI are the right diagnostic tool for picking up optic nerve ischaemia earliest even when other MR sequences appear normal. Sudden infarction of the optic nerve leading to sudden onset blindness is a very grave situation and demands urgent treatment.

17.4.6 Cavernous Sinus and Internal Carotid Artery

The spread to cavernous sinus can happen due to the posterior extension of disease from the superior orbital fissure or fossa. Further invasion and occlusion of the cavernous part of the internal carotid artery, becomes the cause of brain infarcts.

17.5 Presentation

The presenting symptoms of patient are that of acute sinusitis with fever, nasal congestion, purulent nasal discharge, headache and facial pain. Although it can involve all paranasal sinuses, there is a propensity for maxillary sinus followed by ethmoids, sphenoid and frontal sinus. The disease is usually seen involving unilateral sinus or sinuses, but rarely bilateral involvement can be seen, which is of grave severity. The spread to the

surrounding structures, such as premaxillary space, palate, orbit and brain, is relatively rapid within a very short period.

During this growth phase, through angioinvasion, tissue necrosis occurs due to endarteritis resulting in characteristic black eschar formation in the nasal mucosa, palate, or skin around nose and orbit gives it the title 'Black fungus'. The necrosis can involve nasal septum, soft tissue and bones of turbinates, paranasal sinuses and palate. At times, the facial skin's swelling, erythema and cyanosis overlying the involved sinuses and or orbit can be seen. In COVID-associated mucormycosis, the spread of disease was so rapid that pus and osteomyelitis were seen more than the pathognomonic 'Eshcar' formation in the affected parts of the nose paranasal sinuses. Signs of orbital involvement depend upon the extent of involvement of orbit and beyond. It includes periorbital oedema, proptosis, ptosis, diplopia and diminution of vision to complete blindness. On examination, there can be conjunctival chemosis, restricted ocular mobility, ptosis, proptosis, Infraorbital nerve and V1, V2 nerve anaesthesia, CN III, IV and VI palsy indicates orbital apex/Superior Orbital fissure/cavernous sinus involvement and complete loss of vision.

Further extension into the internal carotid artery and brain can result in paralysis, altered sensorium, focal seizures etc.

17.6 Evaluation and Assessment of ROCM

17.6.1 Primary Assessment

- Nasal endoscopy
- Craniofacial computed tomography (CT scan)
- Contrast-enhanced Magnetic Resonance Imaging (MRI)

CT scan and MRI are reviewed together by an otorhinolaryngologist, ophthalmologist and a neuroradiologist and graded according to the extent of the disease. The final correlation is done with the clinical features of the patient.

17.6.2 Confirmation of Diagnosis

The aggressive presentation of ROCM can make the diagnosis easy, but the final diagnosis depends on demonstration of fungal tissue on the KOH mount and tissue cultures.

- KOH wet mount is a primary screening tool to identify the fungal elements present in the specimen. In suspected fungal rhinosinusitis cases, nasal discharge or crusting can be sent as a sample (a. 17.1).
- *Biopsy for HPE*: Necrotic tissue from the involved site (nose, orbital) is sent for histopathological examination. The stains used are H & E (haematoxylin & Eosin), specialized fungal stains like Grocott methenamine-silver (GMS) or periodic acid-Schiff (PAS). It shows pathognomonic broad, irregular, ribbon-like, aseptate or sparsely septate hyphae with irregular acute angle branching.
- The culture of biopsy samples is done to determine species of Mucorales. Crushing or grinding of the specimen should be avoided as it leads to the destruction of fungal elements. Lactophenol cotton blue (LCB) stain demonstrates specific hyphae and spores of mucor organisms (Fig. 17.2).

17.7 Imaging

17.7.1 Craniofacial Computed Tomography (CT)

Although CT scan is not a very specific investigation to differentiate between chronic sinusitis and invasive fungal sinusitis, it serves as a valuable tool for easy identification of bony invasion, if there is any. It also helps in planning surgical approach in a case of mucormycosis.

The specific CT sequences needed in ROCM are routine and contrast-enhanced CT-Scan of paranasal sinuses, orbit and hard palate and brain, if the clinical picture suggests intracranial extension of the disease. One to three millimetre

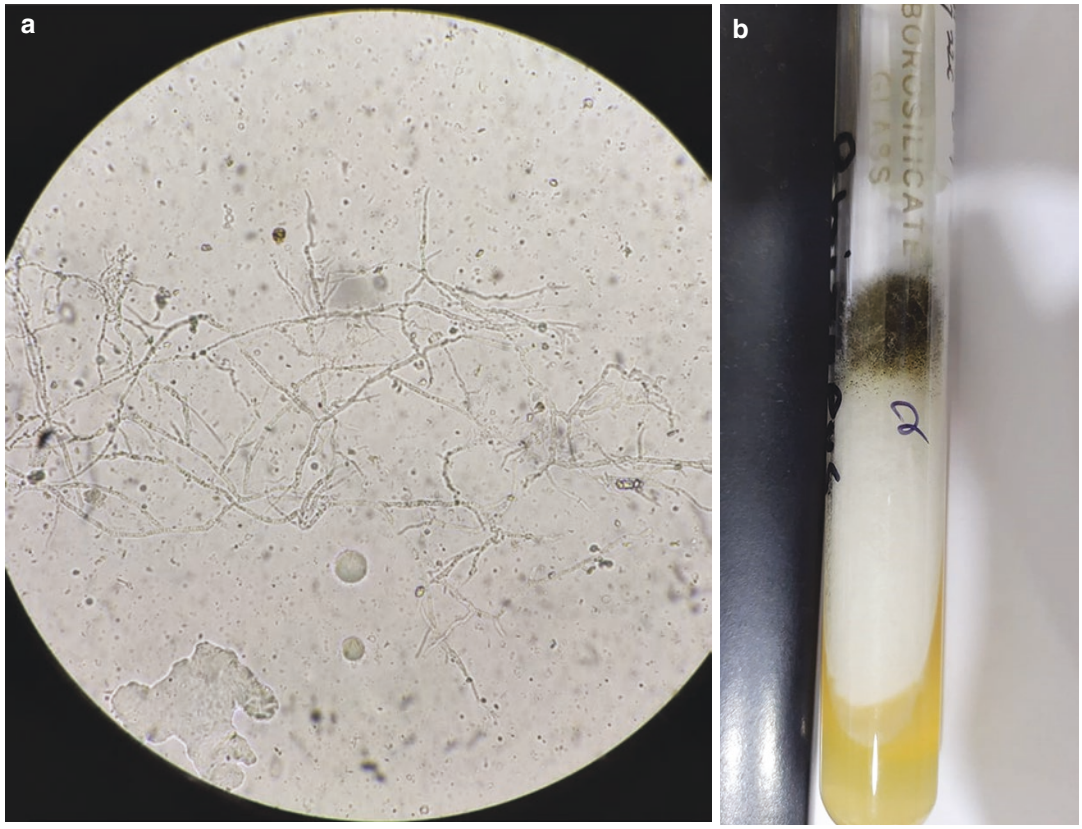

Fig. 17.1 (**a**) KOH stain showing broad, aseptate ribbon-like fungal hyphae. (**b**) Culture tube showing growth of blackish-grey colonies of mucor (Courtesy—Dr. Satish Kumar, MD pathology, Department of Pathology, Jindal institute of medical sciences, Haryana)

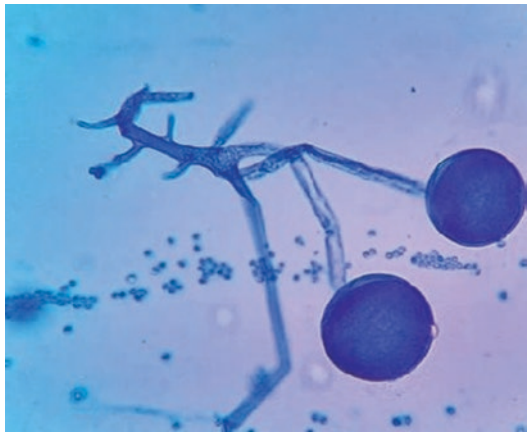

Fig. 17.2 Lactophenol cotton blue (LCB) stain showing fungal hyphae and conidiophore-specific mucor organisms (Courtesy—Dr. Satish Kumar, MD pathology, Department of Pathology, Jindal institute of medical sciences, Haryana)

sections are taken in the axial plane with reformations in coronal and sagittal planes. These are evaluated in soft tissue and bone window by a team of neuroradiologist, otorhinolaryngologist, neurosurgeon and ophthalmologist. Evaluation and grading are done for mucosal thickening in nose and paranasal sinuses and extent of inflammation and disease are evaluated in the following anatomical sites: anterior and posterior peri antral fat, sphenopalatine foramen, pterygopalatine foramen, nasolacrimal duct, medial and inferior orbital fat, facial soft tissue and the masticator space. Mucosal thickening of more than 3 mm in the nasal cavity and paranasal sinuses is recorded as present. Bony dehiscence in the sinonasal area or hard palate is recorded as present or absent.

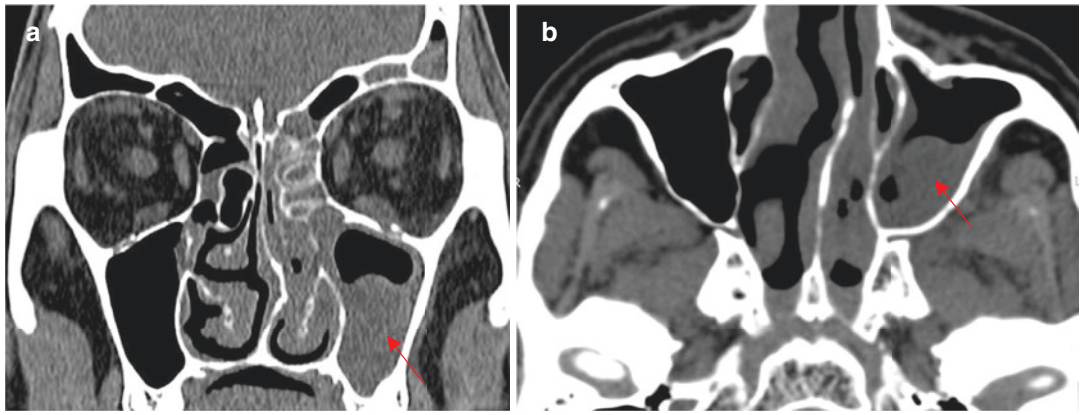

Fig. 17.3 Non-contrast CT PNS images in coronal (**a**) and axial (**b**) planes show nodular mucosal thickening in the left maxillary sinus (red arrow). Mucosal thickening was also seen in the left nasal cavity and ethmoid air cells

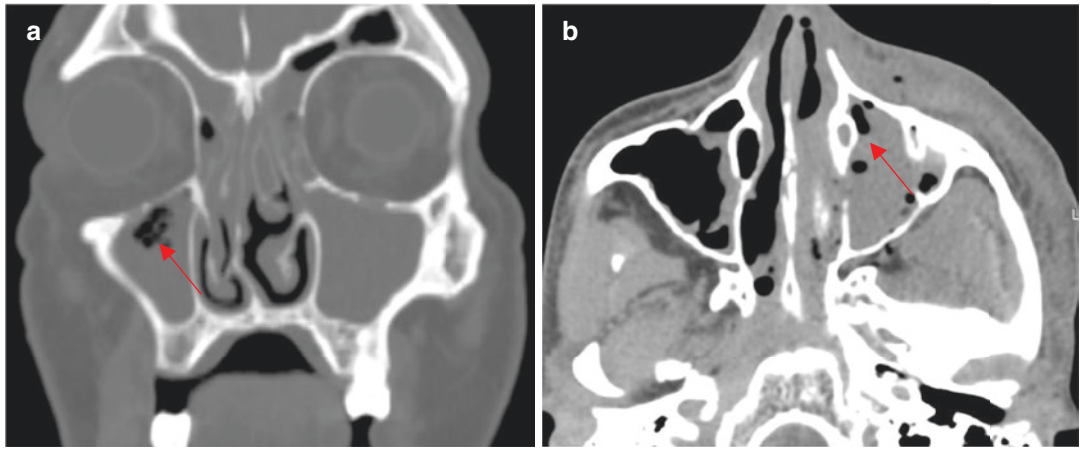

Fig. 17.4 Non-contrast CT PNS images in the coronal (**a**) and axial (**b**) planes show mucosal thickening in both maxillary sinuses, causing almost complete opacification. Air fluid levels are seen as bubble-like lucencies within soft tissue density (red arrow)

17.7.1.1 CT Findings in Early Stage of Mucormycosis

- *Nose and Paranasal sinuses (PNS)*: Mucoperiosteal inflammation presents as nodular mucosal thickening. Sinonasal mucosal thickening >3 mm recorded as present (Fig. 17.3).
- Air/fluid levels can also be seen in sinuses along with soft tissue density due to mucosal hypertrophy leading to partial to complete sinus opacification (Fig. 17.4).
- Soft tissue opacification of the sinuses with areas of increased density with well-defined, markedly hyperdense foci within inflammatory reaction: due to dense matted fungal hyphae and calcium phosphate and sulphate deposits in necrotic areas of mycetoma (Fig. 17.5).
- *Soft-tissue infiltration of peri-antral fat planes.* Infiltration can extend up to premaxillary area (peri-antral) or post-maxillary area (retro antral), sphenopalatine foramen, pterygopalatine fossa characterized by obliteration of the normal fat planes in these areas. Soft tissue infiltration can also involve nasolacrimal duct, medial and inferior orbital fat and facial soft tissue (Fig. 17.6).

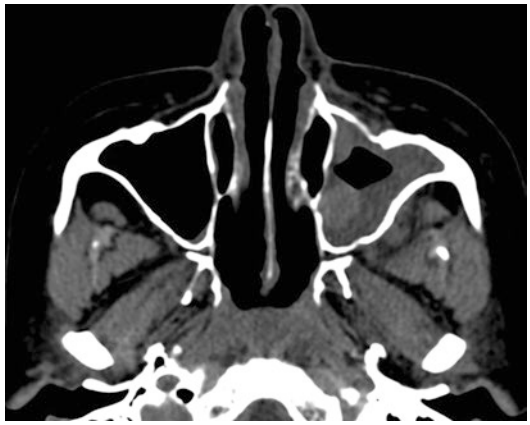

Fig. 17.5 Non-contrast CT PNS image in axial plane shows nodular mucosal thickening in left maxillary sinus with hyperdense material in sinus cavity suggesting chronic inspissated secretions or fungal ball

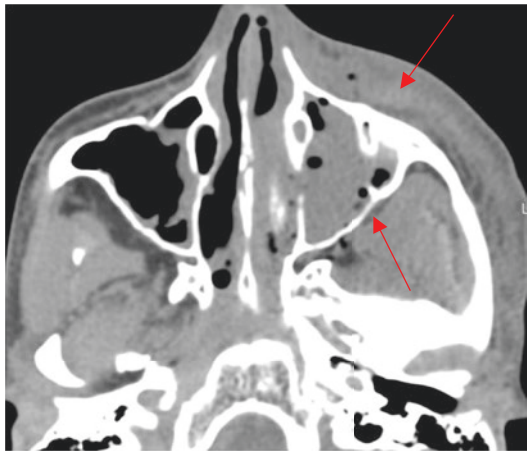

Fig. 17.6 Non-Contrast CT PNS images in axial plane show left maxillary sinus opacification with soft tissue density and air foci. There is the involvement of left middle turbinate and thickening of left premaxillary soft tissue and retroantral soft tissue (red arrow). Air fluid levels are seen as bubble-like lucencies within soft tissue density in the left maxillary sinus

17.7.1.2 CT Findings in Advanced Stage of Mucormycosis

CT scan shows bone involvement in the form of bone rarefaction, erosions and permeative destruction. Bony dehiscence in lamina papyracea (leading to orbital invasion), posterior and superior wall of the maxillary sinus, cribriform plate (leading to intracranial extension), palatine bone (leading to palate invasion) (Fig. 17.7) are recorded as present or absent. In most cases, the extra sinus involvement occurred with intact bones, indicating the perineural/perivascular invasion of the fungus without destroying bone. In such cases, retroantral, facial and orbital fat stranding without involving bone indicate the aggressive nature and advanced stage of the disease.

17.8 Magnetic Resonance Imaging

Magnetic resonance imaging is the most informative investigation in both early and late stages of mucormycosis involving the paranasal sinuses, peri antral soft tissue, orbital soft tissue, perineural spread, skull base infiltration, intracranial complications and vascular obstruction involving cavernous sinuses and internal carotid artery. It can pick up the earliest changes in soft tissue beyond paranasal sinuses, when bone involvement has not happened which is better appreciated on CT scan. The sequences of MRI most suitable to pick these early signs are fat-suppressed T2W and fat-suppressed postcontrast T1W images. The images can show enhancement of the premaxillary and retroantral fat suggesting a further extension of disease or inflammation into these regions. Further extension in the form of enhancement involving the muscles of mastication suggests extension into the infratemporal fossa (Fig. 17.4). The involvement of pterygopalatine fossa can be appreciated by the presence of enhancing soft tissue obliterating the normal fat signals surrounding the maxillary sinus posterior wall supplied by posterior branches of the internal maxillary artery.

In mucormycosis, the affected sinuses appear iso to hypointense on T1-weighted images. While on T2-weighted sequences, tissues involved have a variable enhancement pattern. The extent of necrosis determines the T2W signal intensity (causing hyperintensity) and the presence of paramagnetic elements such as calcium concretions, iron and manganese within the fungal hyphae (causing hypointensity).

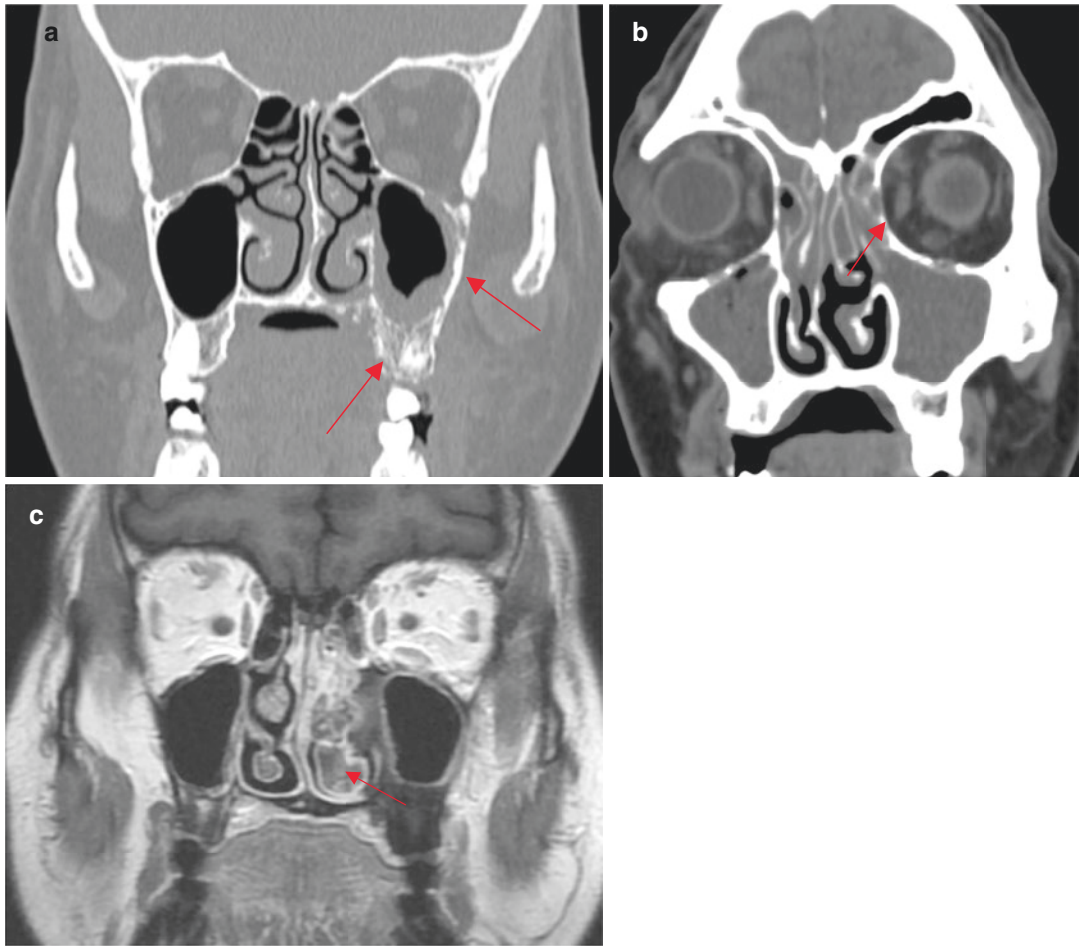

Fig. 17.7 (**a**) Non-contrast CT PNS images in the coronal plane show nodular mucosal thickening in the left maxillary sinus with bony walls erosions. Erosions are well visualized in the left half of the hard palate and the bony walls of left nasal cavity (red arrow). (**b**) Non-contrast CT PNS images in the coronal plane show almost complete bilateral maxillary opacification and visualized ethmoid sinuses. Bony erosions are seen in the left lamina papyracea. (**c**) Black turbinate sign left inferior turbinate (red arrow)

Hence not a reliable marker for mucormycosis alone.

On postcontrast (gadolinium) scans, the contents of the sinuses can show intense homogenous enhancement or variable enhancing and non-enhancing areas or complete central non-enhancing areas with or without a thin irregular rim of peripheral enhancement. An important finding in mucor although not pathognomonic, is the absence of enhancement in areas that usually do enhance. This feature is mainly because of the angioinvasion by the fungus, leading to microthrombosis and tissue necrosis in the affected regions. This appearance, if seen in turbinate bone, is termed as the 'Black Turbinate sign'[4] (Fig. 17.7c). This MRI representation of disease can be correlated to the endoscopic appearance of the necrosis and eschar seen involving the turbinate. Identification of this sign helps in the early and timely treatment of mucor.

Another important finding which is picked up on MRI is the earliest extra sinus involvement seen as fat stranding in the premaxillary or retro maxillary fat, orbital fat or altered fat signals in pterygopalatine fossa, infratemporal fossa or masticator space. This finding is suggestive of the diagnosis of invasive fungal infection in the appropriate clinical setting.

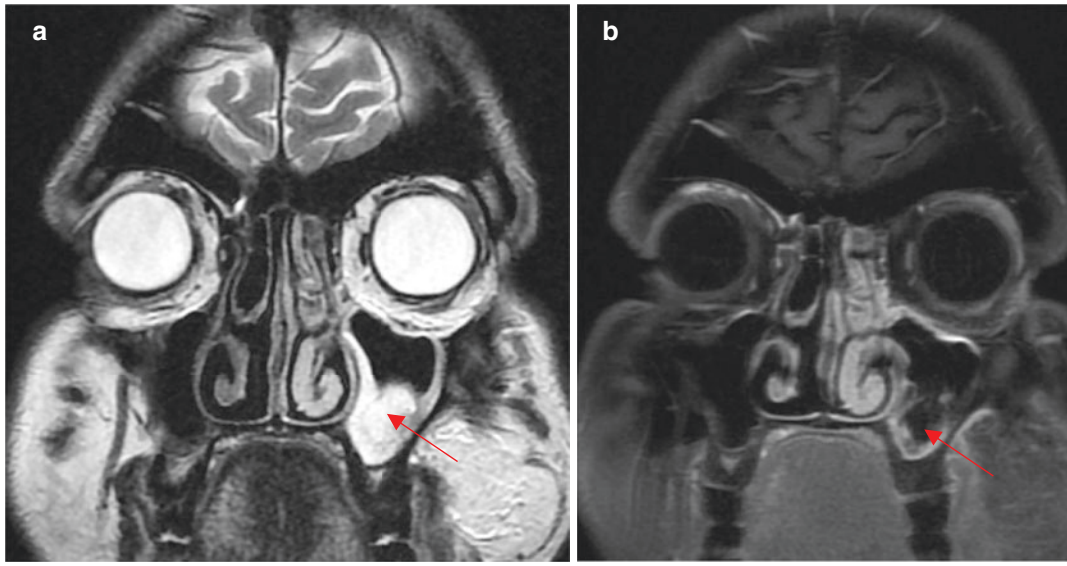

Fig. 17.8 (**a**) Non-contrast T2W image of MRI PNS in coronal plane shows hyperintense nodular mucosal thickening in the left maxillary sinus. (**b**) Contrast-enhanced fat-suppressed T1W image of MRI PNS in coronal plane shows enhancing thin mucosal lining in the left maxillary sinus and focal non-enhancing lesion in sinus cavity possibly a fungal ball or chronic inspissated secretions

Specific sequences like STIR and FLAIR can show inflammatory changes or oedema as a bright signal in involved soft tissues.

Diffusion-weighted sequences are used to evaluate areas of cerebral and optic nerve infarctions. They demonstrate optic nerve infarction (bright signal) when regular MR sequences show normal optic nerves (Fig. 17.11a).

17.8.1 MR Findings

- Non-contrast T2W MRI PNS shows sinusitis as hyperintense nodular mucosal thickening without air-fluid levels (Fig. 17.8a).
- In the same patient, contrast-enhanced T1W images of MRI PNS show mucosal enhancement in involved sinuses and focal non-enhancing areas in nasal/sinus cavities or walls, suggesting the possibility of angioinvasive fungal infection or chronic inspissated secretions (Figs. 17.8 and 17.9).
- Infiltration of the periantral fat planes with a rim of soft tissue attenuation of variable thickness along the walls of the involved sinuses is the earliest MRI finding of extra sinus extension in ROCM (Fig. 17.9). Soft tissue infiltration of premaxillary area or post-maxillary area (characterized by obliteration of the normal fat planes in the infratemporal fossa, pterygopalatine fossa and pterygomaxillary fissure) may be noted (Fig. 17.9).

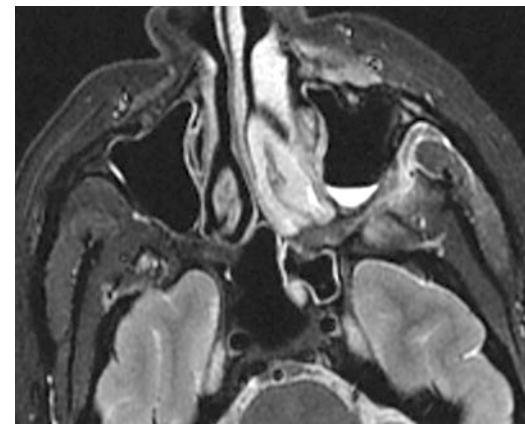

Fig. 17.9 STIR image of MRI PNS in axial plane shows hyperintense infiltration in thickened premaxillary soft tissues on the left side. Air fluid levels seen in the left maxillary sinus and hyperintensity in retro antral fat are quite specific for fungal infection

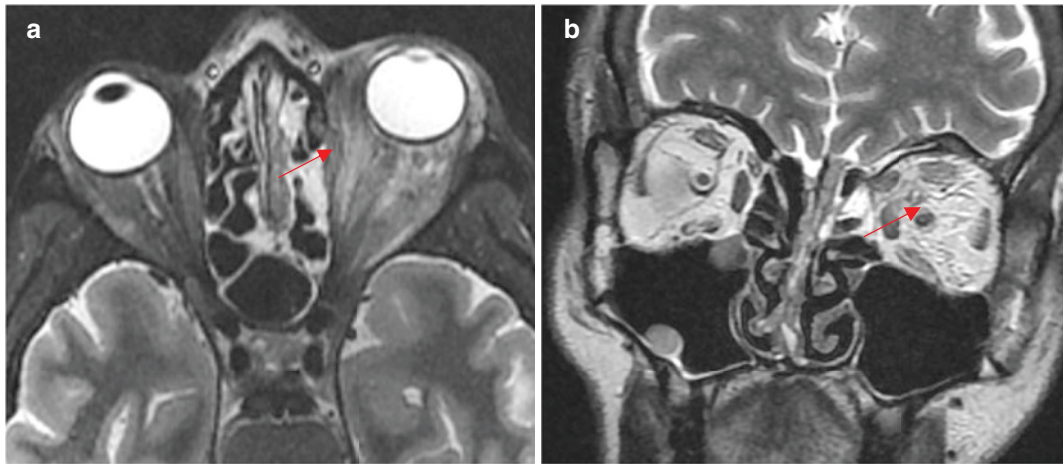

Fig. 17.10 (**a**) MRI PNS STIR image in the axial plane and (**b**) T2W image in coronal plane shows infiltration of left orbital fat, bulky and hyperintense ocular muscles suggesting orbital cellulitis (red arrow)

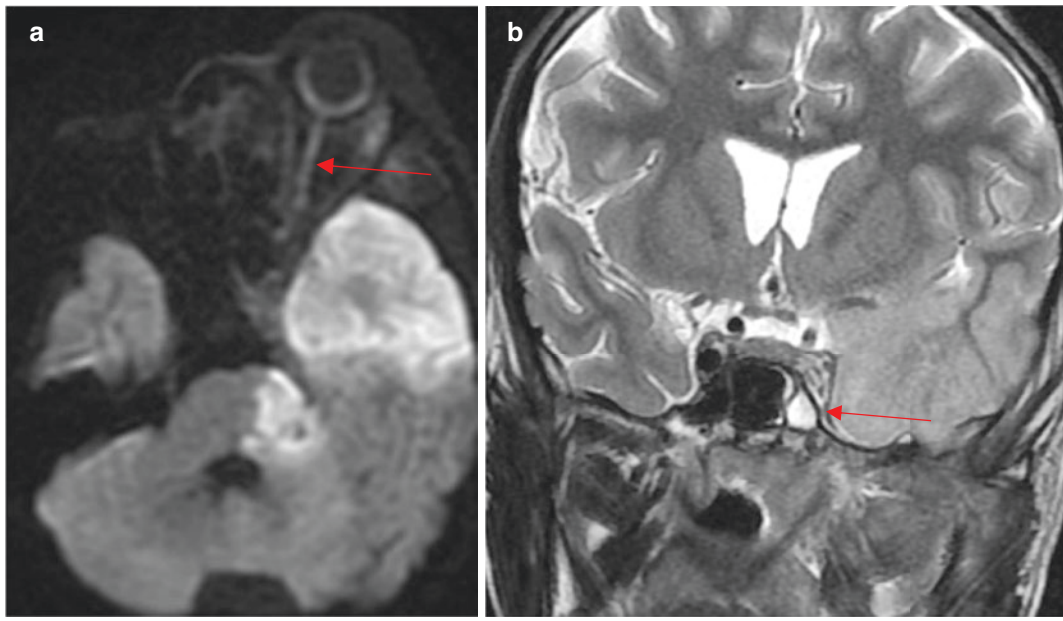

Fig. 17.11 (**a**) DW image of MRI brain shows ischaemic areas in the left temporal lobe and left pons. The bright signal is also noted in optic nerve suggestive of optic nerve infarct (red arrow). (**b**) T2W image of MRI brain of same patient shows left cavernous sinus thrombosis and occluded left ICA

Orbital invasion is seen as hyperintensity in region of retroorbital fat around the extraocular muscles suggests soft tissue infiltration and oedema. The medial rectus muscle in early stages can be seen thickened and laterally displaced (Fig. 17.10a, b). Further orbital involvement can vary in severity from cellulitis, subperiosteal abscess, an orbital abscess to central retinal artery or ophthalmic artery occlusion leading to optic nerve infarction, or there can be direct infiltration of the optic nerve (Fig. 17.11a). Patient presenting with severe proptosis and tenting of the globe suggests diffuse orbital invasion.

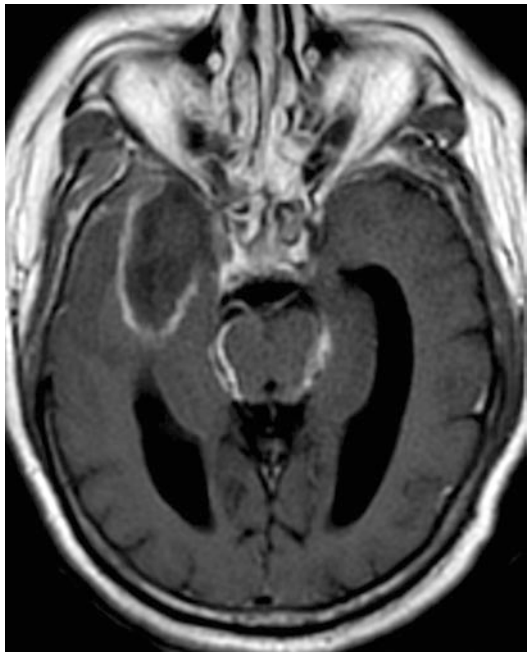

Fig. 17.12 Contrast-enhanced T1W images of MRI BRAIN in the axial plane show well-defined Intra-axial peripherally enhancing hypointense lesion in the right temporal lobe suggestive of the abscess

- Intracranial findings include infarcts due to vascular thrombosis or mycotic emboli leading to the formation of frontal/temporal lobe abscesses, epidural and subdural abscesses and central venous thrombosis (Figs. 17.11 and 17.12).
- Lack of enhancement of major vessels like the internal carotid artery, superior ophthalmic vein or ophthalmic artery is suggestive of thrombus formation due to angioinvasive nature of the fungus.

17.8.2 Management

- Early clinical diagnosis and a high index of suspicion is the key to reducing patient morbidity and mortality.
- Nasal endoscopy is performed at the earliest, and a sample from suspicious tissue or discharge is taken and sent for KOH mount. Empirical antifungal therapy is initiated in suspected cases, even when the report of KOH staining is awaited.
- Stringent control of hyperglycaemia and Ketoacidosis is achieved. In case D-dimer is raised due to associated COVID-19 infection, anticoagulant therapy is also continued. The physician's role is vital in achieving control of hyperglycaemia and post-COVID complications other than mucormycosis.
- Surgery includes an endoscopic approach in case disease is limited to sinuses, endoscopic medial maxillectomy if the disease is located in the deeper posterolateral part of maxillary sinuses or involving the pterygopalatine fossa. In case of orbital involvement, removing lamina papyracea and clearing diseased tissue and intraorbital irrigation with amphotericin B (extra and intraconal depending on the extent of disease) is performed. Once the extra sinus spread involves palate, open approach surgery in the form of subtotal, total maxillectomy (Weber Ferguson approach) with or without orbital exenteration (in case of diffuse orbital involvement with complete ophthalmoplegia) is performed.
- Early and aggressive debridement of the eschar and necrotic tissue is a must to decrease the fungal load, reduce the complications (e.g. vascular thrombosis) and also for maximum delivery of antifungal medications to remaining viable tissue. The debridement is continued and followed till its last extent, and all necrotic tissue, pus and eschar are removed till normal well-perfused bleeding tissue appears.
- Antifungal therapy (parenteral amphotericin B or *Isavuconazole*) is started at the earliest. Based on safety and efficacy data Liposomal Amphotericin B remains the drug of choice. Renal functions are monitored essentially to detect the amphotericin B-induced nephrotoxicity at the earliest.
- The recommended dose of Amphotericin is: Injection Liposomal Amphotericin B, 3–5 mg/kg/day to a total of up to 5.6 g. The drug is continued for weeks together, and once the disease is controlled, the dose is decreased to a maintenance dose of 1 mg/kg/day, followed by a step-down therapy with the antifungal

drug Posaconazole. The response to treatment is evaluated by clinical improvement, endoscopic clearance and repeated KOH staining and culture and radiological studies.

- Topical Amphotericin is also used for irrigation of the involved orbit and paranasal sinuses after surgery and in the post-operative period at regular intervals with excellent results. In cases of orbital involvement, delivery of topical amphotericin B volume 15 mL (0.5–1 mg/mL) to the infected site once or twice daily can achieve excellent results. Intraconal injection of amphotericin B (1 mg/mL) for at least a week along with intravenous amphotericin B is used in cases of extensive orbital involvement.
- Recommended dosage and schedule of the antifungal medication, Isavuconazole in case Amphotericin molecule is toxic, is a loading dose of 200 mg intravenous or oral Isavuconazole eight hourly for 48 h followed by 100 mg capsules two capsules once a day for 7 days
- Once the disease and other patient parameters are under control, maintenance therapy with oral Posaconazole 300 mg twice a day is to be given for 1 month, followed by 300 mg once a day until the patient is completely disease free.
- The patient is to be assessed clinically, regularly, with endoscopic clearance of disease and necrotic tissue every 48 h until the disease is completely cleared or eradicated.

17.9 Surgical Management

17.9.1 Case 1: Involvement of the Anterior Part of the Nasal Septum

A patient presented to us with a history of breathlessness, nasal obstruction, blood-stained nasal discharge and facial pain. He tested positive for COVID 20 days before presenting to us. He was suffering from Diabetes Mellitus, and others had systemic features of COVID at the time of presentation.

17.9.1.1 Clinical and Haematological Evaluation

At the time of admission patient was found afebrile, breathless and hypoxic. He underwent a complete systemic and laboratory evaluation. Relevant baseline investigations revealed a haemoglobin value of 10.40 g/dL (normal 13–17 g/dL), mild lymphopenia (9.60%; normal 20–40%) and elevated serum creatinine (1.57 mg/dL; normal 0.70–1.20). C-reactive protein (CRP) was 29.53 mg/l (normal <5.0), procalcitonin (PCT) was 0.34 ng/mL (normal <0.5), with a D-dimer assay of 1547 ng/mL (normal 0–243) and an IL6 level of 3439 micrograms/mL (normal 0–7.0), suggestive of a severe cytokine storm.

Other blood tests were also performed like complete blood count (CBC), kidney function test (KFT), liver function test (LFT), thyroid-stimulating hormone (TSH), glycosylated haemoglobin (HBAIC), random blood sugar (RBS), C-reactive protein quantitative, D-Dimer and serum ferritin. HBAIC, RBS, CRP and D-Dimer were found to be raised while the total leucocyte count was within the normal limit.

Twice daily evaluation of other parameters was carried out as per mucor checklist for further progression of disease.

The patient underwent a thorough assessment by a multidisciplinary team of otorhinolaryngologist, physician, pulmonologist, neurosurgeon and ophthalmologist. A diagnosis of post-COVID mucormycosis with bilateral pneumonitis and diabetes mellitus was made.

17.9.1.2 Imaging

Imaging included computed tomographic scans and magnetic resonance imaging of paranasal sinuses (PNS), orbit and brain. Chest status was also assessed by X-ray Chest PA view followed by HRCT thorax. Both X-ray and CT thorax showed central and peripheral areas of ground glass opacities. There was an interstitial septal thickening more in bilateral lower lobes and the CT severity scoring was 22/25. The radiological diagnosis was bilateral post-COVID pneumonitis with fungal infection involving anterior part of the nasal septum.

17.9.1.3 Confirmation of Diagnosis

Confirmation of diagnosis was done by collecting smear/biopsy from the lesion with appropriate precautions and sent for KOH staining. The KOH stain showed aseptate hyphae suggesting mucormycosis. Histopathological evaluation (HPE) of the nasal discharge revealed broad aseptate ribbon-like fungal hyphae on KOH wet mount. A nasal swab did not have significant findings but a nasal biopsy from the middle turbinate revealed broad aseptate filamentous fungal hyphae suggestive of mucormycosis and Sabouraud dextrose agar (SDA) media grew mucormycosis.

17.9.1.4 Treatment of COVID

The exact date of onset of COVID is noted and the treatment is started by the physician. Use of steroids and immunosuppressant drugs like tocilizumab is avoided.

1. *Evaluation and management of Diabetes*

As hyperglycaemia in mucormycosis leads to the flaring up of the disease, it needs to be treated rigorously using a strategical approach. Since the patient had a Random blood sugar of more than 200 mg/dL, fasting blood sugar more than 124 mg/dL % and HBAIC more than 6.4% diagnosis of diabetes mellitus was confirmed. Antidiabetic treatment was started immediately in the form of insulin infusion followed by oral hypoglycaemic agents and his blood glucose levels were kept well under control. All those patients who never had diabetes before covid but showed a high level of sugar owing to the steroid intake were also treated as cases of diabetes mellitus.

2. *Treatment for respiratory system*

The status of the respiratory system was assessed on HRCT chest. There was no fungal dissemination to the lungs but as HRCT chest showed severe COVID-associated pneumonia. Patient was put on supplemental high flow oxygen support, antifibrotic drugs like Nintedanib tablet formulations and anticoagulants. Steroids and immunosuppressants are avoided in these patients as they may lead to further exacerbation of mucormycosis. Broad-spectrum antibiotics were also avoided and only culture-specific antibiotics were given. Once the patient's lung condition improved, he was subjected to pulmonary function tests and 6 min walk test and finally could be weaned off the oxygen support on the 25th day of admission. Doses of anticoagulants and antifibrotic drugs were also tailored according to requirement of patient and finally tapered off after 1 month.

17.9.1.5 Treatment of Mucormycosis

1. *Medical management:*

Patient was treated with injection liposomal amphotericin B in the dose of 0.5 mg/kg/day. He was also given intravenous meropenem (1 g thrice daily) and vancomycin (1 gram twice daily) with the addition of amphotericin B.

2. *Surgical management:*

After the improvement in patient's general condition, endoscopic debridement was carried out. Since this case had limited disease involving only the anterior part of the nasal septum, the lesion was debrided and sent for histopathology and culture.

Lactophenol cotton blue (LPCB) stain after culture on Sabouraud dextrose agar (SDA) showed broad aseptate ribbon-like hyphae branching at right angles (black arrow) with sporangium.

Post-operative nasal endoscopy and cleaning were performed every 48 h and the crusts were sent for KOH till they became negative for mucormycosis (Figs. 17.13, 17.14, 17.15, 17.16, and 17.17).

17.9.2 Case 2: Involvement of the Posterosuperior Part of the Nasal Septum and Bilateral Sinuses

17.9.2.1 Imaging (Figs. 17.18 and 17.19)

The CT scan of paranasal sinuses showed pansinusitis involving all the sinuses on both sides. A post-gadolinium-enhanced MRI, however, showed mucor involving only the nasal septum in its posterosuperior part.

Fig. 17.13 Patient on high flow oxygen support as a patient suffering from post-COVID pneumonia

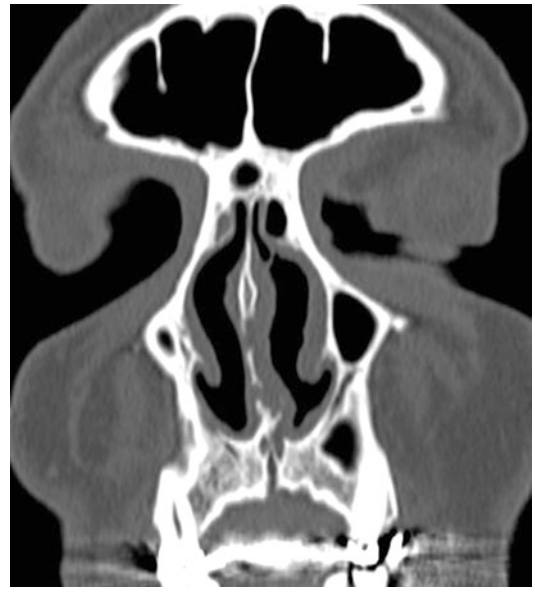

Fig. 17.14 Non-contrast CT PNS image in coronal plane shows irregular mucosal thickening with bony erosions in anteroinferior nasal septum on the left side

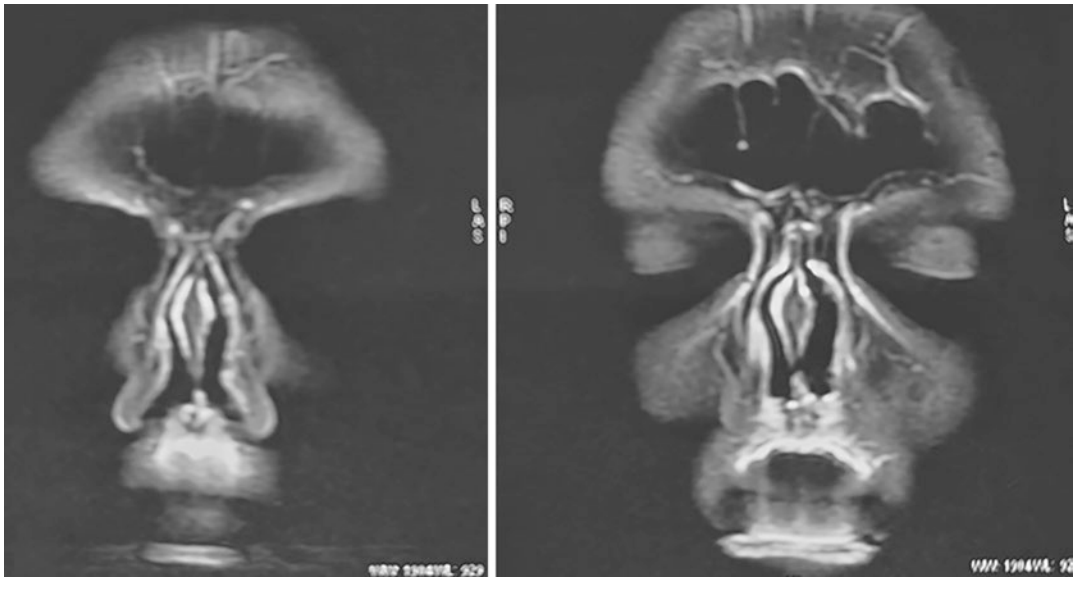

Fig. 17.15 (**a**, **b**) Contrast-enhanced MRI PNS fat-suppressed T1W images in coronal plane show mucosal irregularity and non-enhancing areas in nasal septum anteriorly

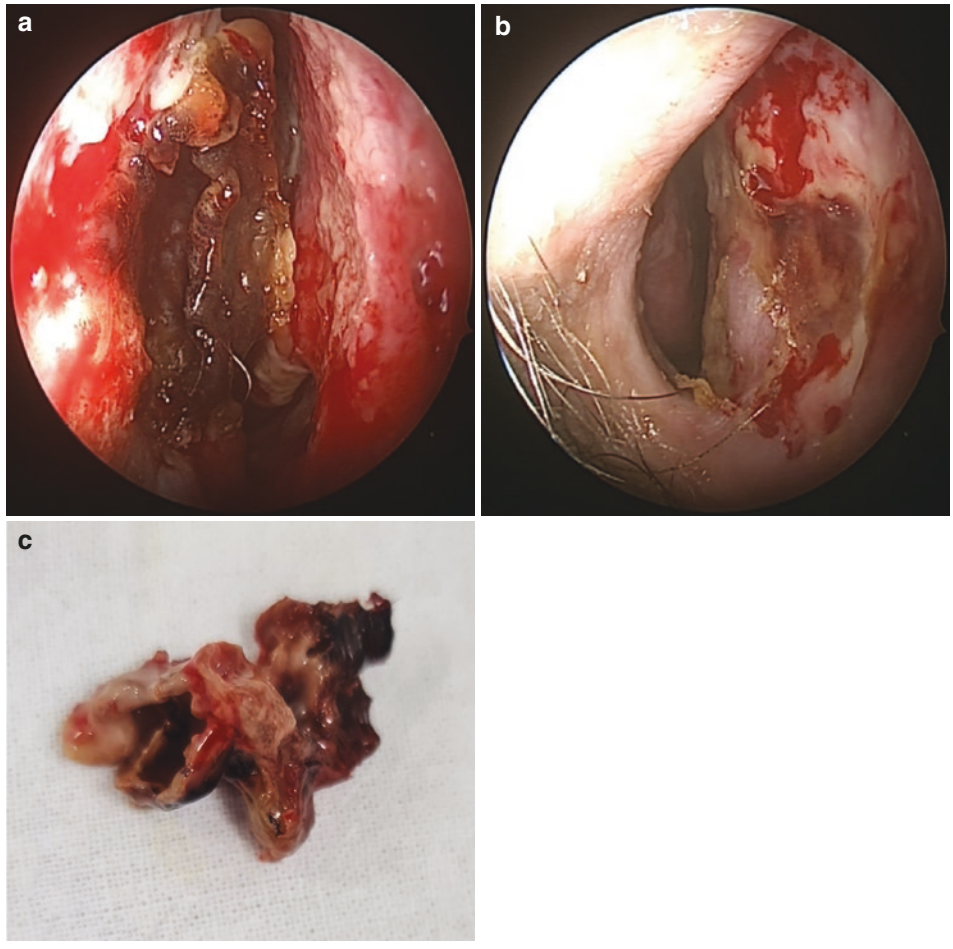

Fig. 17.16 (**a**) Eschar formation and mucor involving anterior part of the nasal septum on left and (**b**) On the right side. (**c**) Excised necrotic tissue with eschar to be sent for KOH staining and culture sensitivity

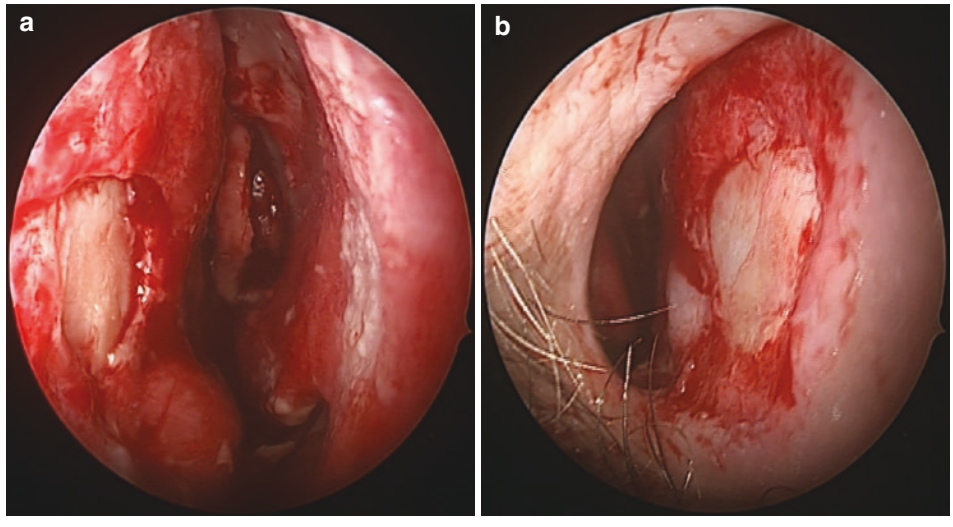

Fig. 17.17 (**a**) Clearance of disease on the left side. (**b**) Clearance of disease on the right side

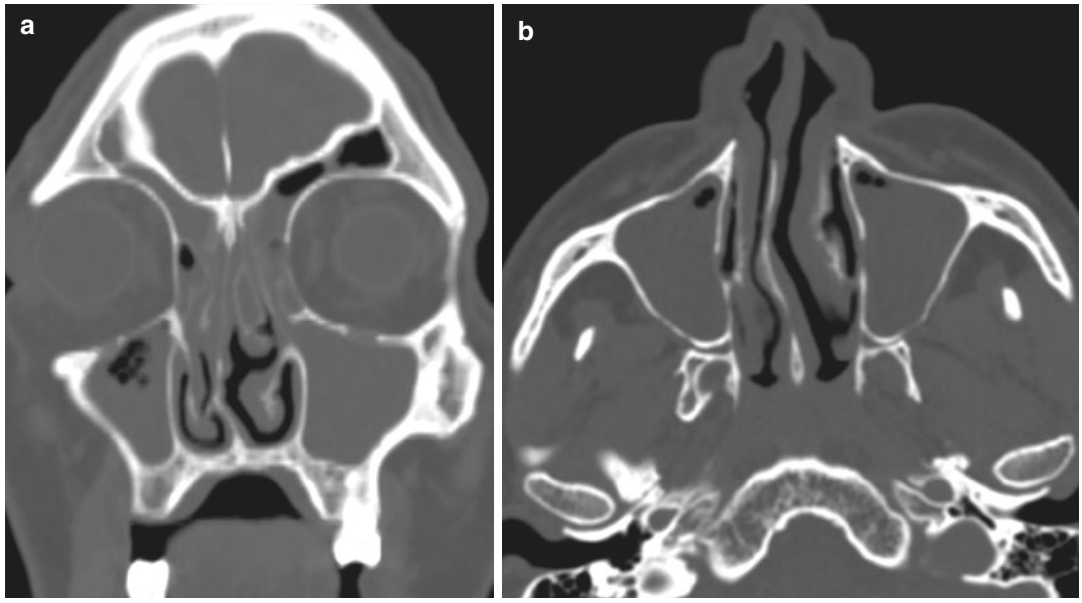

Fig. 17.18 Non-contrast CT PNS images in coronal (**a**) and axial (**b**) planes show almost complete opacification of bilateral frontal, maxillary and ethmoid sinuses. Soft tissue density is also seen in fronto-ethmoid recesses

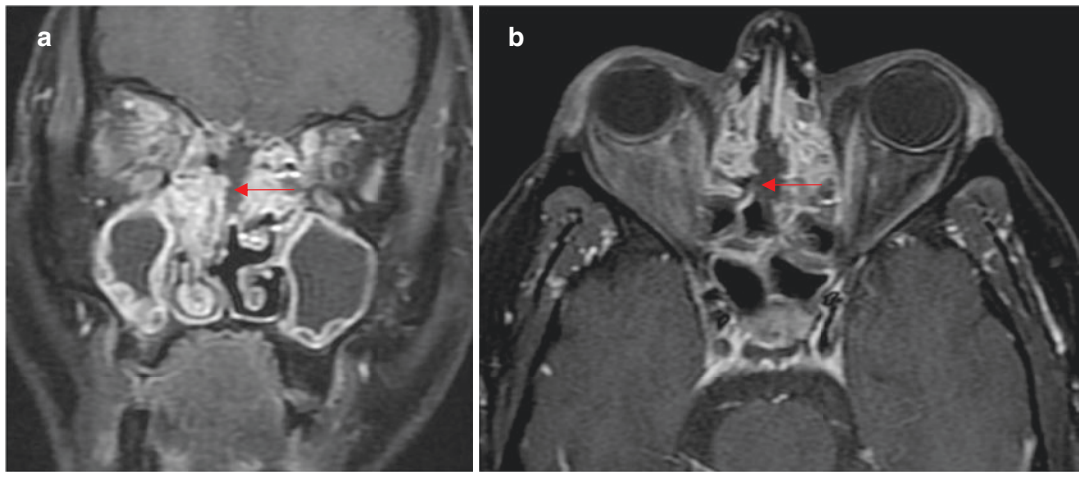

Fig. 17.19 MRI PNS Contrast-enhanced fat-suppressed T1W images in axial (**a**) and coronal (**b**) planes show enhancement of mucosal lining in bilateral maxillary and ethmoid sinuses. Non-enhancing areas are seen in sinus cavities suggesting thick secretions/pus. Focal non-enhancing area seen in the superior part of nasal septum suggests fungal infestation (red arrow)

17.9.2.2 **Surgical Findings** (Figs. 17.20 and 17.21)

On endoscopic surgical management, the sinuses were found to be filled with pus and fungal infection found to be involving only the posterosuperior part of nasal septum with involvement of both bone and cartilage. All sinuses were cleared, and the mucor infested nasal septum was excised till normal healthy septal margins were reached in all directions.

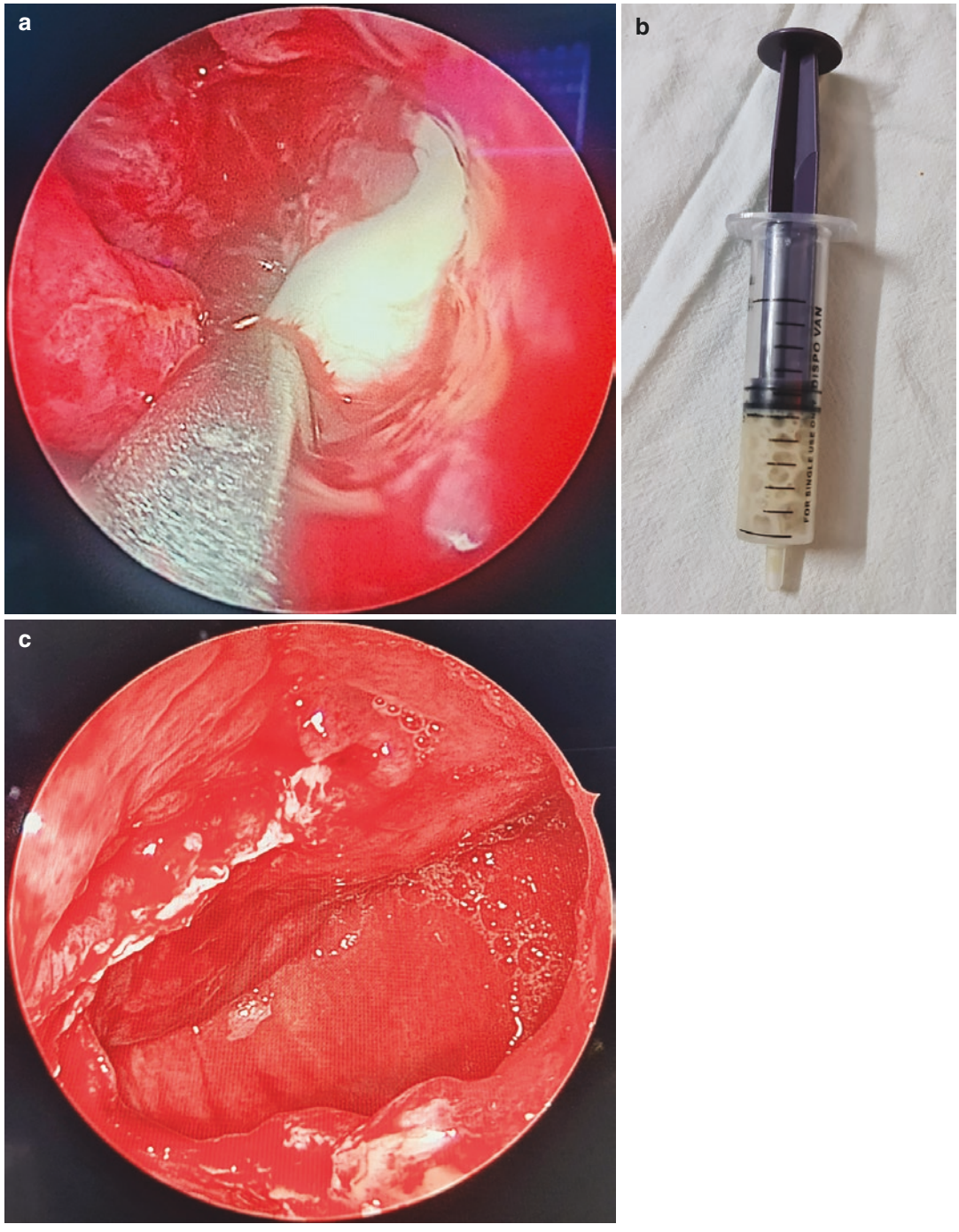

Fig. 17.20 (**a**) Left nostril: after uncinectomy, pus filling left maxillary sinus aspirated and sinus cleared of disease. (**b**) Aspirated pus. (**c**) The left maxillary sinus shows no trace of mucor

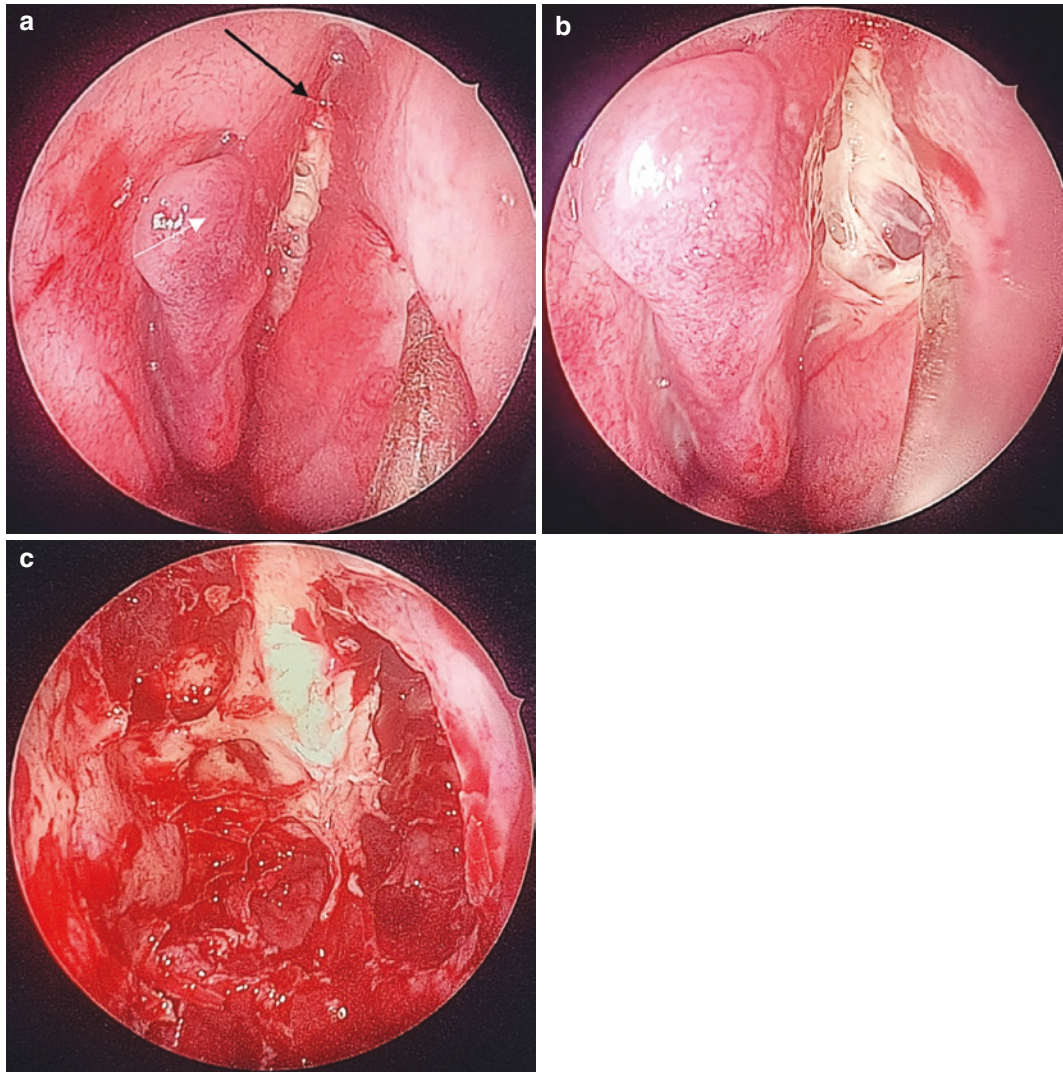

Fig. 17.21 (**a**) Right nasal cavity with healthy middle turbinate (white arrow) and involvement of posterosuperior part of septum by mucormycosis (black arrow) proved on KOH staining. (**b**) mucor involving posterosuperior part of septum. (**c**) Final picture, after clearance of disease from all paranasal sinuses on both sides and excision of diseased septum till normal septum reached in all directions

17.9.3 Case 3: Involvement of the Left Maxillary Sinus and its Lateral Wall

17.9.3.1 Radiological Findings (Figs. 17.22, 17.23, 17.24, and 17.25)

The CT scan showed polypoidal mucosal thickening involving left maxillary sinus in its medial and inferior part. The MRI T2W images showed hyperintense mucosal thickening with few hypointense areas within it, involving the medial and inferior part of the left maxillary sinus.

17.9.3.2 Surgical Management (Fig. 17.26)

Endoscopic surgery in the form of uncinectomy and middle meatal antrostomy was performed via

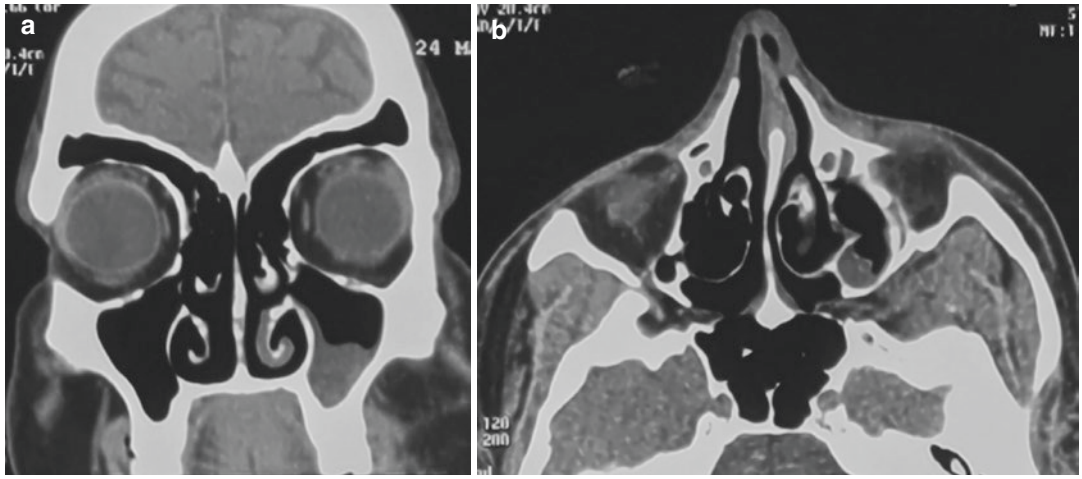

Fig. 17.22 (**a**, **b**) Non-contrast CT PNS images in coronal and axial planes show polypoidal mucosal thickening in left maxillary sinus in its inferior and medial part

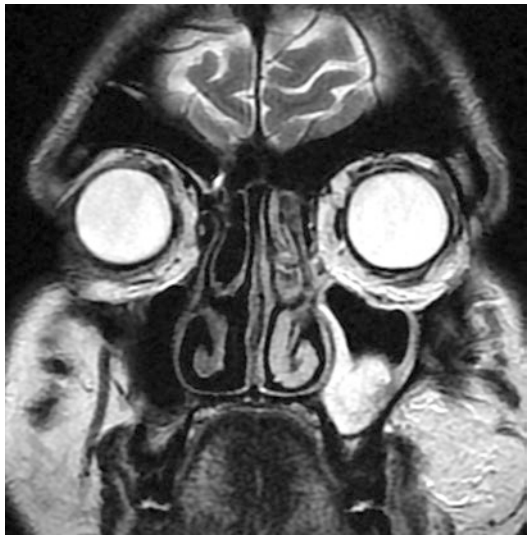

Fig. 17.23 T2W MRI PNS images in coronal plane show hyperintense mucosal thickening in left maxillary sinus with few hypointense areas within it

left nostril. Complete clearance of the disease was achieved and the necrotic tissue excised was sent for KOH mount. On receiving positive report for nucor, the patient was put on medical treatment which included Injection of Liposomal Amphotericin B. Patient became disease free within 3 weeks.

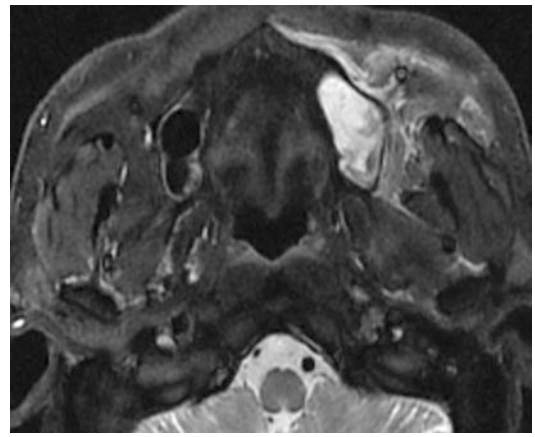

Fig. 17.24 STIR images of MRI PNS in axial plane show left maxillary sinusitis with inflammation/oedema in left premaxillary as well as periantral soft tissues

17.9.4 Case 4: Involvement of the Lateral Wall of the Maxilla

17.9.4.1 Radiological Findings (Figs. 17.27 and 17.28)

CT scan and MRI showed disease localized to maxillary sinus left side involving its lateral most part.

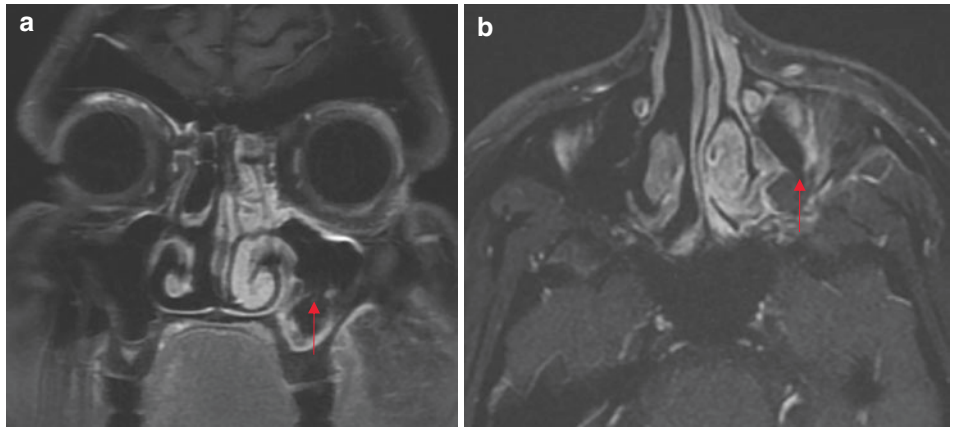

Fig. 17.25 Contrast-enhanced fat-suppressed T1W images in coronal (**a**) and axial (**b**) planes showing non-enhancing lesion involving inferior and medial quadrant of left maxillary sinus (red arrow)

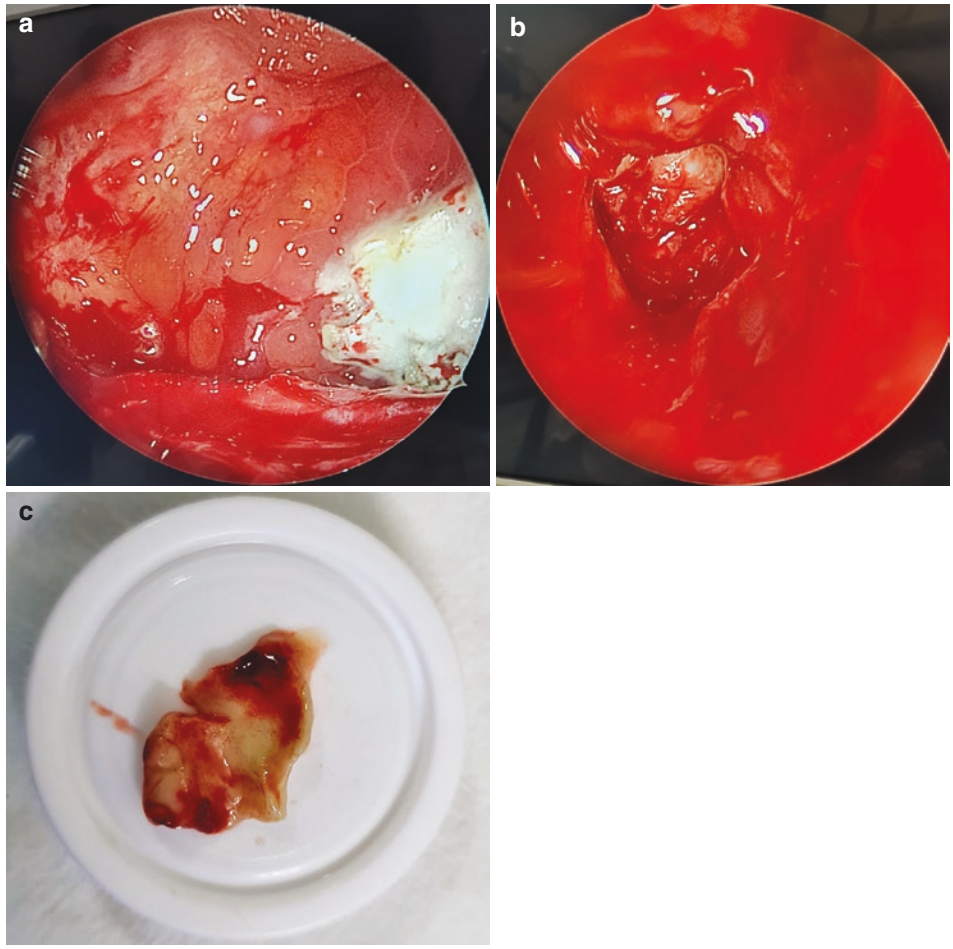

Fig. 17.26 (**a**) Uncinectomy and middle meatal antrostomy performed on left side. Per operative findings showing fungal involvement of inferior and medial part of left maxillary sinus. (**b**) After clearance of disease, the healthy though hypertrophic mucosa of maxillary sinus visible. (**c**) The mucor infested necrotic tissue

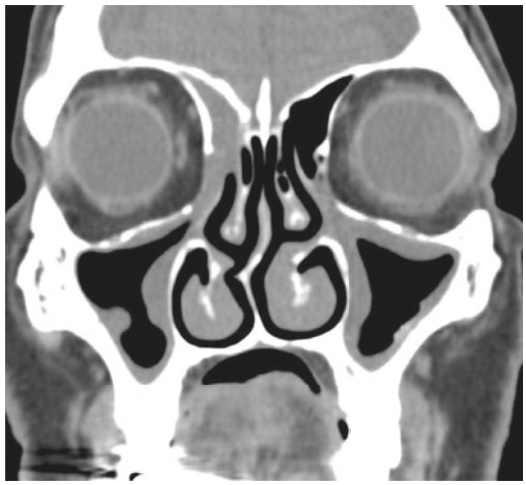

Fig. 17.27 CT PNS images in the coronal plane show nodular mucosal thickening in bilateral maxillary sinuses

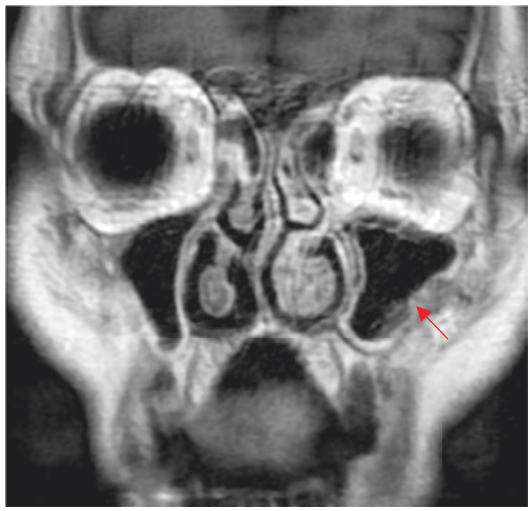

Fig. 17.28 Contrast-enhanced T1W image in coronal plane shows non-enhancing sinus mucosa in left maxillary sinus (red arrow)

17.9.4.2 Surgical Steps and Findings (Figs. 17.29 and 17.30)

Endoscopic sinus surgery: Uncinectomy with middle meatal antrostomy could not expose the area infested with mucormycosis. Endoscopic medial maxillectomy was performed to reach the lateral most part of sinus and complete clearance of disease was achieved. Medical treatment started after confirmation of aseptate broad hyphae on KOH mount.

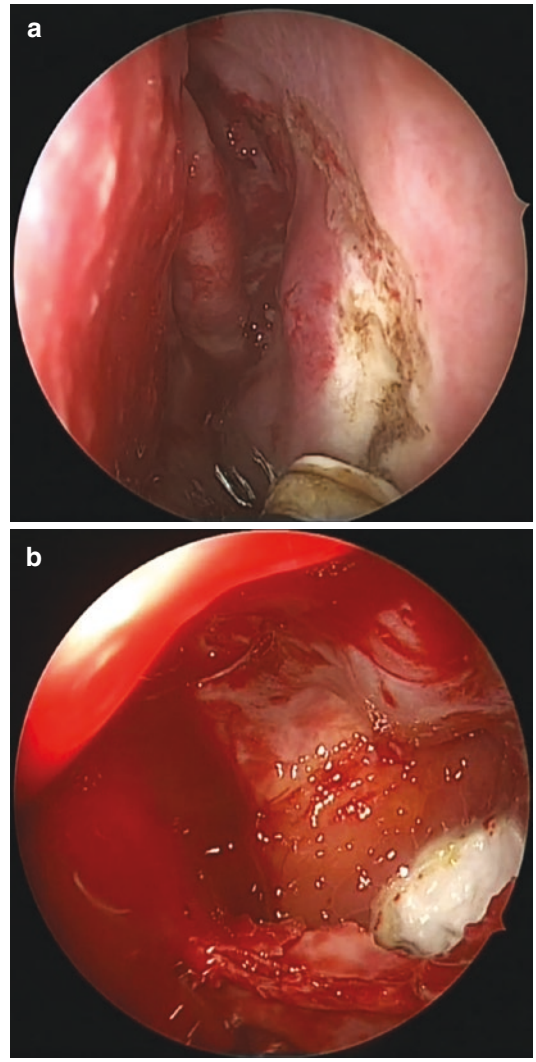

Fig. 17.29 (**a**) Left nostril: A showing medial maxillectomy in progress. (**b**) Location of disease far more laterally in maxillary sinus

The two cases described above, show how the treatment is to be customized according to the location and extent of disease.

17.9.5 Case 5: Involvement of the Sinuses, Pterygopalatine Fossa and Orbit

A Thirty-eight year-old male came to emergency department on tenth day of COVID illness with complaints of left-sided facial pain, pain over left

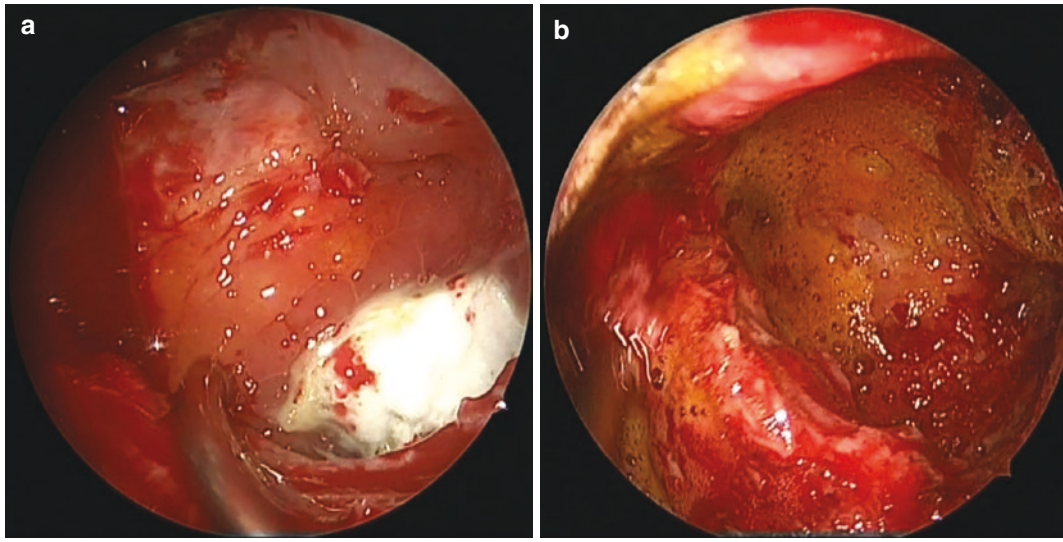

Fig. 17.30 (**a**) After medial maxillectomy the complete extent of disease is visualized. (**b**) Complete clearance of disease

upper jaw, fever and breathlessness. The patient was a known case of poliomyelitis.

17.9.5.1 Clinical Features

Patient presented with a history of drooping of the left upper eyelid and facial swelling. On examination he was afebrile, but had proptosis left eye with oedema over the left side of the face. He underwent a complete systemic and laboratory evaluation.

A multidisciplinary team including otorhinolaryngologist, radiologist, physician, neurosurgeon and ophthalmologist carried out a comprehensive evaluation of the patient and a diagnosis of COVID-associated mucormycosis was made.

17.9.5.2 Investigations

The investigation performed were CT PNS, orbit and brain (Fig. 17.31), MRI PNS with contrast (Figs. 17.31 and 17.32) and X-ray Chest PA view followed by HRCT chest.

The baseline blood investigations showed raised blood sugar levels and patient was found to be suffering from undetected diabetes mellitus.

Nasal crusting was sent for KOH wet mount examination and revealed broad aseptate acute angle branching hyphae suggestive of mucormycosis.

17.9.5.3 Blood Screening

The team sent routine blood investigations, including complete blood count, kidney function test, liver function test, random blood sugar, glycosylated haemoglobin and arterial blood gas analysis. All the levels were deranged, including a high total leukocyte count that kept rising for 5–6 days. Twice daily evaluation was performed, as per mucor checklist for further disease progression and following treatment started.

17.9.5.4 Treatment for COVID

The exact onset date was noted, and the physician started the treatment taking care to avoid the use of steroids and immunosuppressant drugs like tocilizumab as the patient was already immunocompromised. He was started on low-molecular weight heparin in the dose of 0.4 unit subcutaneous once a day, as his D-dimer levels were raised.

17.9.5.5 Evaluation and Management of Hyperglycaemia

He was a case of undetected diabetes, so his blood sugar levels were monitored every 4 h and the physician started subcutaneous insulin. Later he switched the patient on oral hypoglycaemic agents.

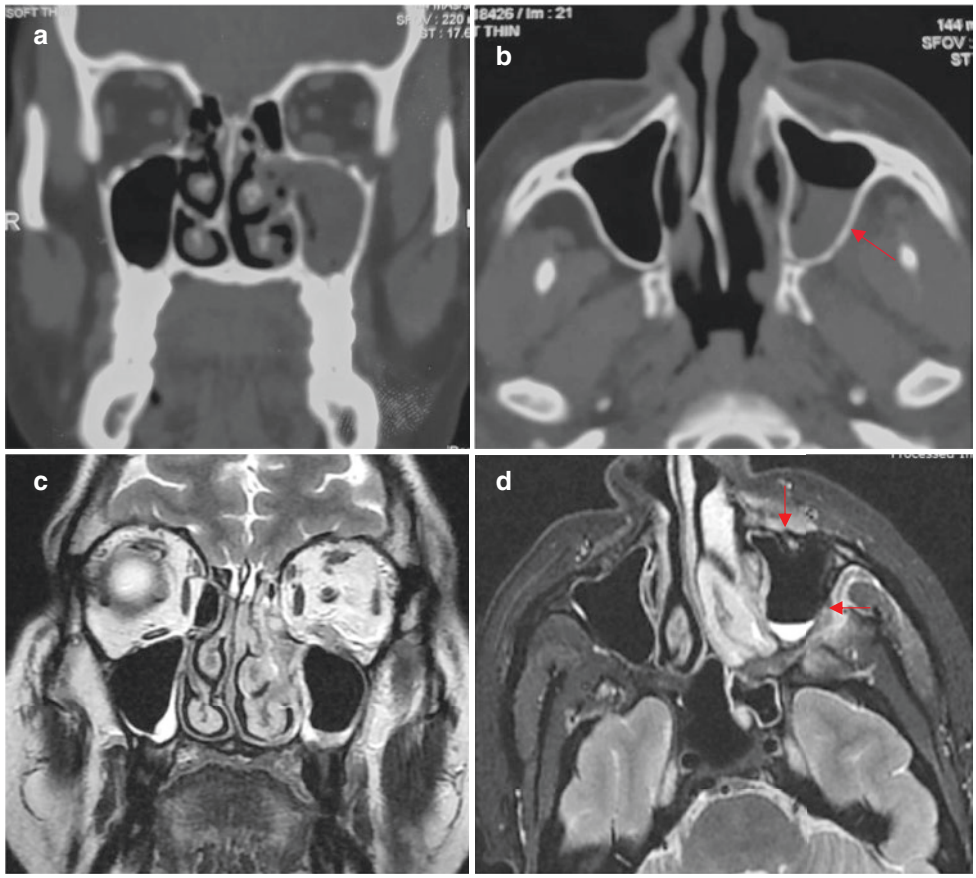

Fig. 17.31 (**a**) CT PNS showing opacification of left maxillary sinus. (**b**) Left maxillary sinus opacification with soft tissue density and thickening of left retroantral soft tissue (red arrow). (**c**, **d**) T2W image of MRI PNS in coronal and axial plane shows mucosal hypertrophy of left middle and inferior turbinates with soft tissue infiltration of preantral and retroantral area suggesting involvement of pterygopalatine area (red arrows)

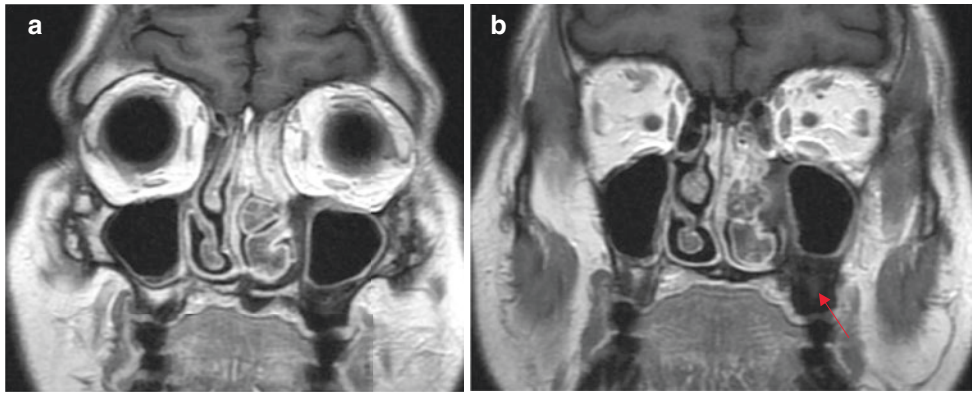

Fig. 17.32 Contrast-enhanced T1W images of MRI PNS in coronal plane (**a**) and (**b**) show non-enhancing areas in left middle and inferior nasal turbinates and also in lateral and inferior wall of left nasal cavity (red arrow)

17.9.5.6 Treatment of Respiratory System

The physician reviewed HRCT chest, and as the patient was maintaining SpO_2 on room air, no active management was needed for his respiratory system.

17.9.5.7 Treatment of Mucormycosis

Once the KOH was suggestive of mucormycosis first-line antifungal treatment with Inj. Liposomal amphotericin-B was started (5 mg/kg/day, the total being 300 mg single dose i/v). Supportive therapy with intravenous injection cefoperazone with sulbactam (1.5 g BD) was also started.

17.9.5.8 Surgical Treatment

As the contrast-enhanced T1W image of MRI PNS in axial plane showed involvement of left pterygopalatine fossa, though the posterior wall of left maxillary sinus was intact, endoscopic surgical debridement in the form of left medial maxillectomy along with excision of necrotic part of middle turbinate was performed to clear disease from maxillary sinus and pterygopalatine fossa. Posterior bony wall of maxillary sinus was removed and the necrotic diseased tissue was excised from pterygopalatine fossa after clipping the sphenopalatine artery.

Debridement and regular cleaning were performed every 48 h for 14 days along with injectable antifungal in the form of liposomal amphotericin B for 10 days which then was followed by tab Posaconazole 300 mg BD for 3 weeks further followed by maintenance therapy of posaconazole 300 mg once a day for 15 days. Patient became disease free after 2 months.

The fungal culture reported from HPE sample was *Rhizopus Microsporum*.

Three months after surgery and antifungal treatment, complete clearance of disease achieved (Fig. 17.33).

17.9.6 Case 6: Mucor Involving Lateral Wall and Floor of the Right Maxillary Sinus and Hard Palate

17.9.6.1 Radiological Findings

Figures 17.34 and 17.35.

17.9.6.2 Surgical Steps and Findings

As the mucor was invading the bone in the inferior and lateral wall of the right maxillary sinus along with involvement of right-sided hard palate, subtotal (infrastructure) maxillectomy was planned.

Pre-operatively following are discussed with patients and relatives about facial incisions, potential injury to the infraorbital nerve, reconstructive options and the loss of dentition with the need to wear dentures or have dental implants and are also included in the consent.

Intraoperatively necrotic tissue was found in the right maxillary sinus and inferior and lateral bony maxillary walls were eroded.

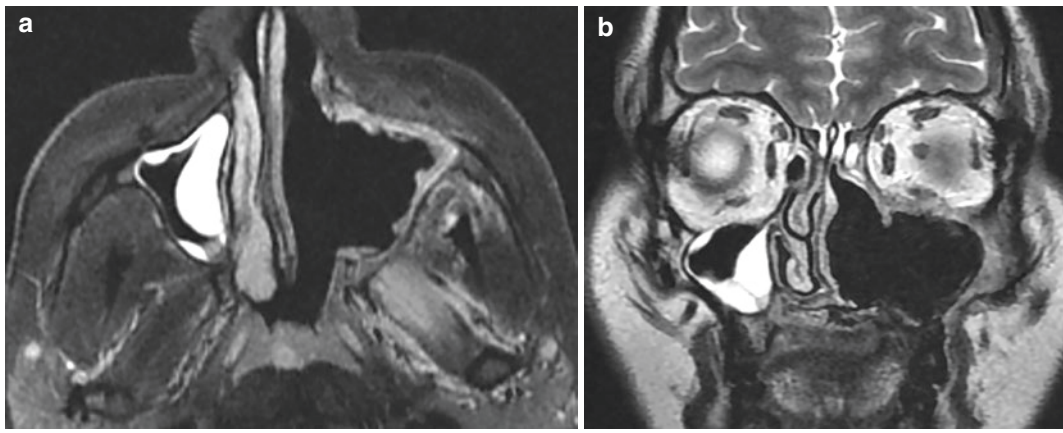

Fig. 17.33 (**a**) STIR axial and (**b**) T2W coronal images show post-operative defects in left nasal cavity and left maxillary sinus with complete clearance of disease

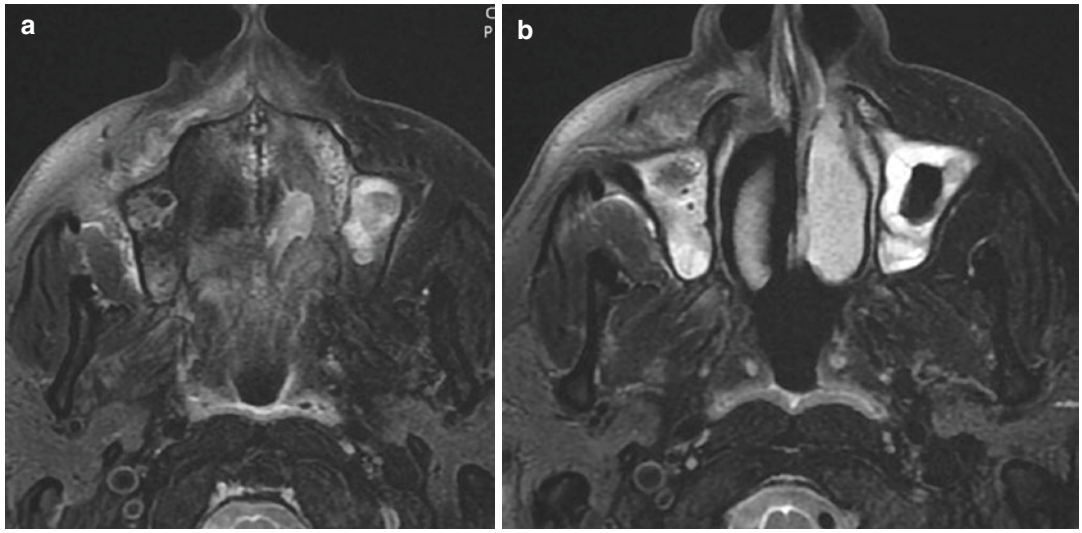

Fig. 17.34 (**a**) Axial STIR images show bilateral maxillary sinusitis along with involvement of palate. (**b**) Inflammation is seen in the right premaxillary and retroantral space

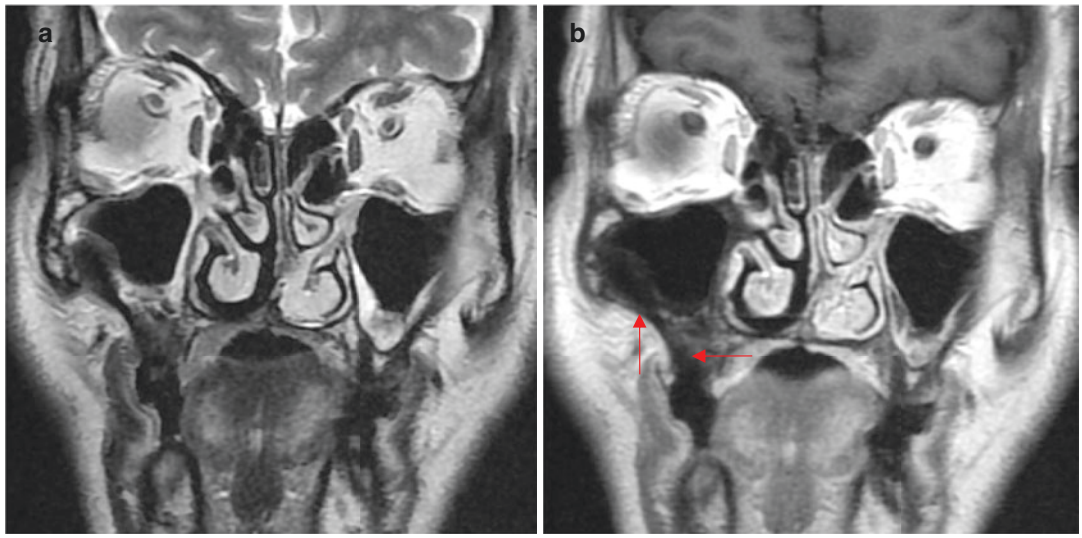

Fig. 17.35 (**a**) T2W and (**b**) contrast-enhanced T1W images in coronal plane show non-enhancement of lateral and inferior walls of right maxillary sinus and hard palate (red arrow)

Subtotal (Infrastructure) maxillectomy is performed in three stages:

1. Soft tissue dissection and bone exposure
2. Bone resection
3. Closure and reconstruction

In subtotal (infra structure) maxillectomy, the upper one-third consisting of the orbital floor formed by the roof of the maxillary sinus and the zygomatic arch is disconnected from lower two-thirds, including the hard palate and alveolar ridge. This is done by an osteotomy just beneath the infraorbital foramen.

Classical Weber Ferguson sub-ciliary incision was given and skin and subcutaneous flap elevated off the surface of maxilla. Next, a full-thickness incision was given on upper lip and divided up to the gingivolabial sulcus. The upper cheek flap was elevated completely by taking an

incision in upper gingivobuccal sulcus remaining close to the gingiva and extended up to the maxillary tuberosity. The key to elevating cheek flap completely is to remain right over the periosteum of the maxilla until its posterolateral aspect is exposed. While elevating this flap we encounter the infraorbital nerve exiting from the infraorbital foramen and entering into soft tissue of cheek. The nerve was preserved in this case. Then the soft tissue along the ala of the nose was divided and through the mucosa of lateral wall of the nasal cavity entry was made into the nasal cavity.

Osteotomies were performed in the following sequence:

Lateral wall of the maxillary sinus.

Anterior wall up to nasal vestibule.

Parallel to the orbital floor. Markings for bony cuts were made in a way that a rim of bone around the infraorbital foramen was preserved.

Posteriorly pterygoid plates are made free from the maxillary tuberosity.

The hard palate osteotomy began with a vertical cut in between the central and lateral incisors on the alveolar ridge, then continued backward in a parasagittal plane on the ipsilateral side of the nasal septum, parallel to the intermaxillary and interpalatine sutures to reach the posterior edge of the hard palate. The hard palate was then separated from soft palate.

To complete the osteotomy a horizontal cut was made through the lateral maxillary wall and a vertical cut extending across the front of the posterior maxillary wall and through the retromolar region, reaching the medial maxillary wall and the perpendicular plate of the palatine bone, which is wedged into the lateral nasal wall between the maxilla and the sphenoid pterygoid process. The next bone cut is continued done keeping in mind, if possible to leave a ledge of the posterior maxillary wall attached to the pterygoid process. This cut is made through the inferior or middle nasal meatus to the pyriform aperture. Initially, all bone cuts are made using a power saw or drill, then sharp osteotome is used to connect the cuts or holes made by drill, and the surgical specimen is removed by clearing all soft tissue connections using electrocautery (Figs. 17.36, 17.37, 17.38, and 17.39).

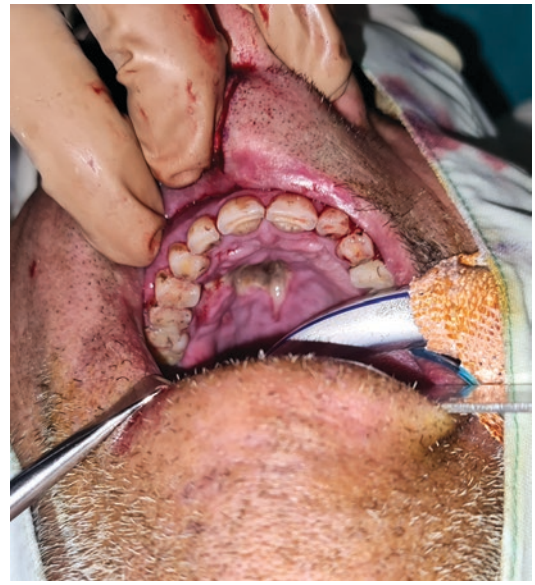

Fig. 17.36 Erosion of right-sided palate (bone and mucosa) by the disease

Fig. 17.37 Weber-Ferguson incision left side

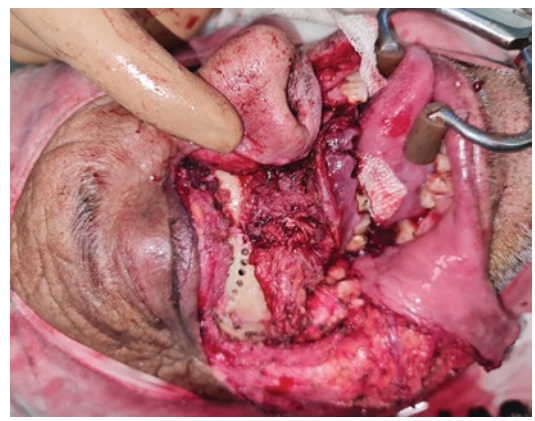

Fig. 17.38 After lifting the skin flap, the soft tissues of the face are elevated off the face of the maxilla. Markings on maxilla for bone cuts are visible

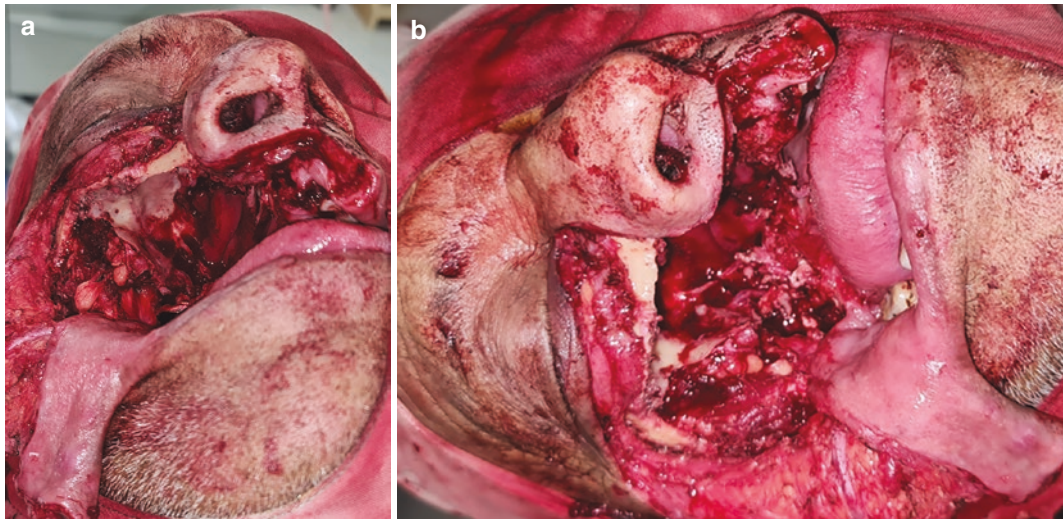

Fig. 17.39 Excision of the hard palate, lateral and medial wall along with floor of right maxilla, and teeth performed

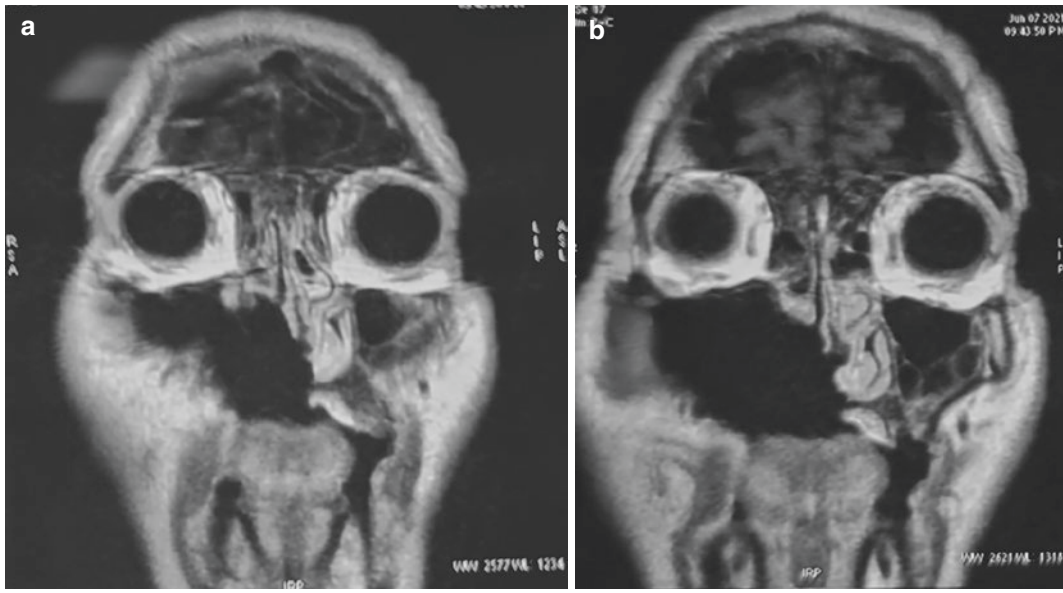

Fig. 17.40 (**a**, **b**) Post-surgical findings at the surgical site after two months showing complete clearance of disease with healthy mucosa covering all the raw areas

- *Post-surgery radiological findings* (Fig. 17.40).
- Two months after surgery and complete course of anti fungal medication, complete clearance of disease could be achieved with healthy mucosa covering all the raw areas (Fig. 17.41).
- For reconstruction of palatal defect, pedicled temporalis muscle flap surgery was performed in second stage after 3 months of primary surgery, once all the laboratory and radiological parameters showed complete clearance of disease (Figs. 17.42, 17.43, 17.44, and 17.45).

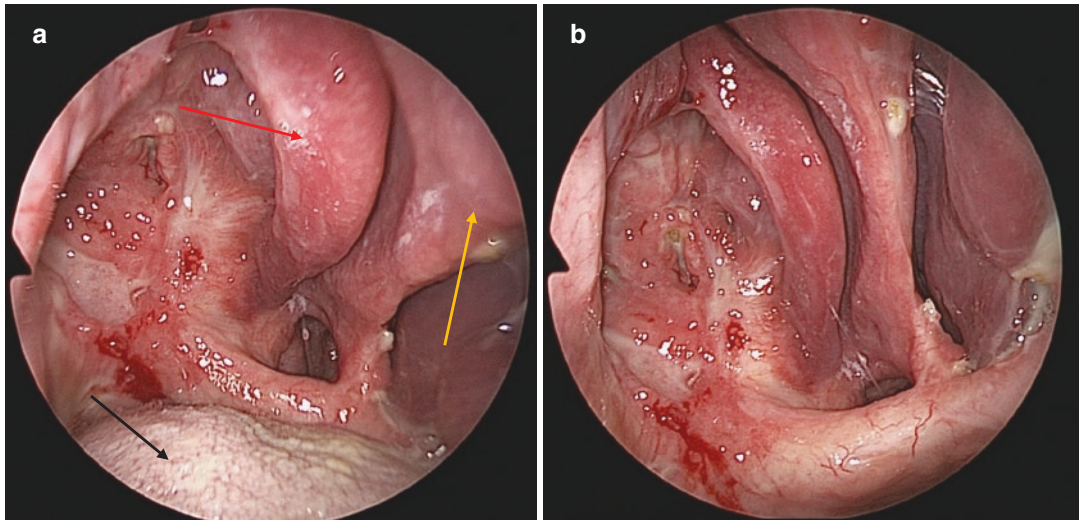

Fig. 17.41 (**a**, **b**) Post-subtotal maxillectomy right side showing complete clearance of disease with healthy mucosa covering all the raw areas. Tongue black arrow, middle turbinate red arrow, septum yellow arrow

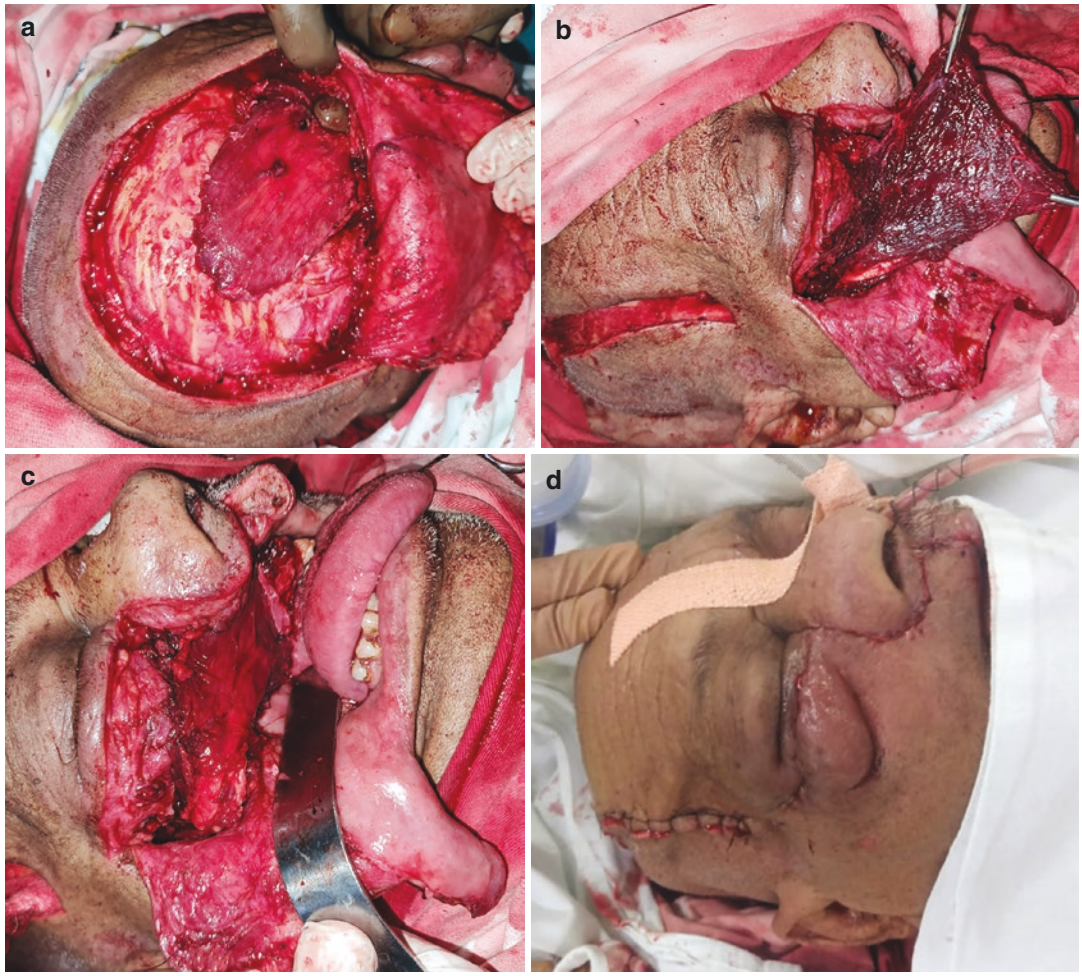

Fig. 17.42 (**a**) Temporalis muscle harvested. (**b**) Temporalis muscle transferred to face from beneath zygomatic bone. (**c**) Temporalis muscle flap sutured to surrounding soft tissue. (**d**) Final suturing of incision line

17.9.7 Cases of Orbital Involvement

17.9.7.1 Case Number 7a

17.9.7.2 Case Number 7b

17.9.7.3 Case Number 7c

17.9.7.4 Case Number 7d

A 47-year-old male presented with a history of pain in the right upper jaw, watering from his right eye, swelling around the right eye and breathlessness. He developed these symptoms a month after the COVID. He had a history of coronary artery disease and was a known case of diabetes mellitus, hypertension and hypothyroidism.

Evaluation

On admission, he was afebrile, tachypnoeic and hypoxic. He underwent a complete systemic and laboratory evaluation. A multidisciplinary team evaluated the patient as per protocol. Nasal discharge was sent for KOH wet mount that revealed broad aseptate hyphae.

Imaging

CT scan of paranasal sinuses and orbit, various sequences of MRI along with HRCT chest performed. Contrast-enhanced T1W MRI revealed a non-enhancing focus in the right inferior turbinate and right maxillary sinus with mucosal thickening in the right ethmoidal and frontal sinuses. HRCT Chest revealed multiple patchy ground glass opacities in bilateral lower lobes CT severity score 15/25.

Blood Screening

After admission, the various blood tests performed were CBC, KFT, LFT, TSH, HBA1C, RBS, CRP QUANTITATIVE, D-Dimer and S. Ferritin.

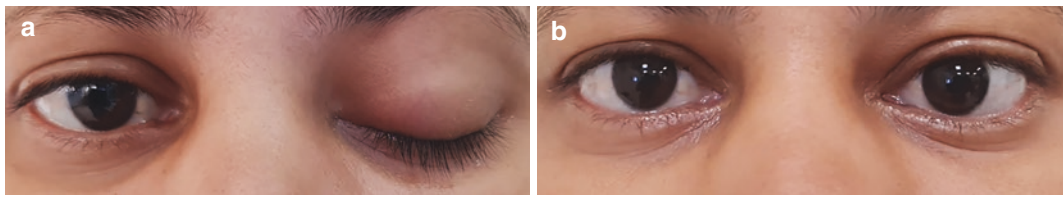

Fig. 17.43 (**a**) Left eye ptosis on the day of admission. (**b**) 30 days after surgery ptosis is resolved

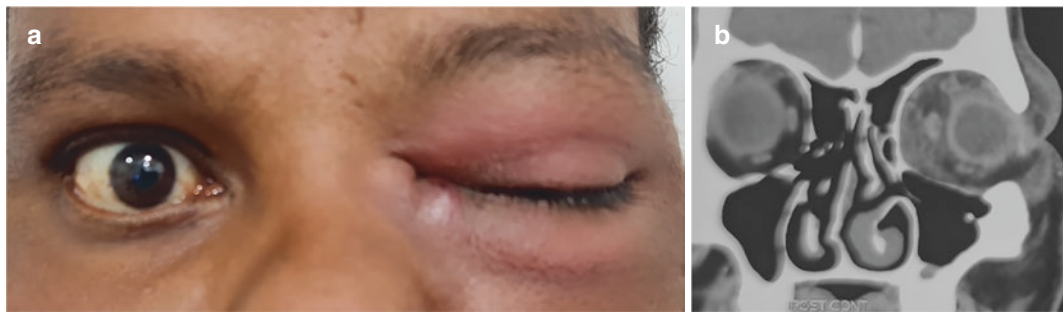

Fig. 17.44 (**a**) Patient with left periorbital swelling, ptosis. (**b**) Coronal CT-PNS of the same patient showing fat stranding in medial and superior extra conal compartment of left orbit. Medial rectus muscle is bulky

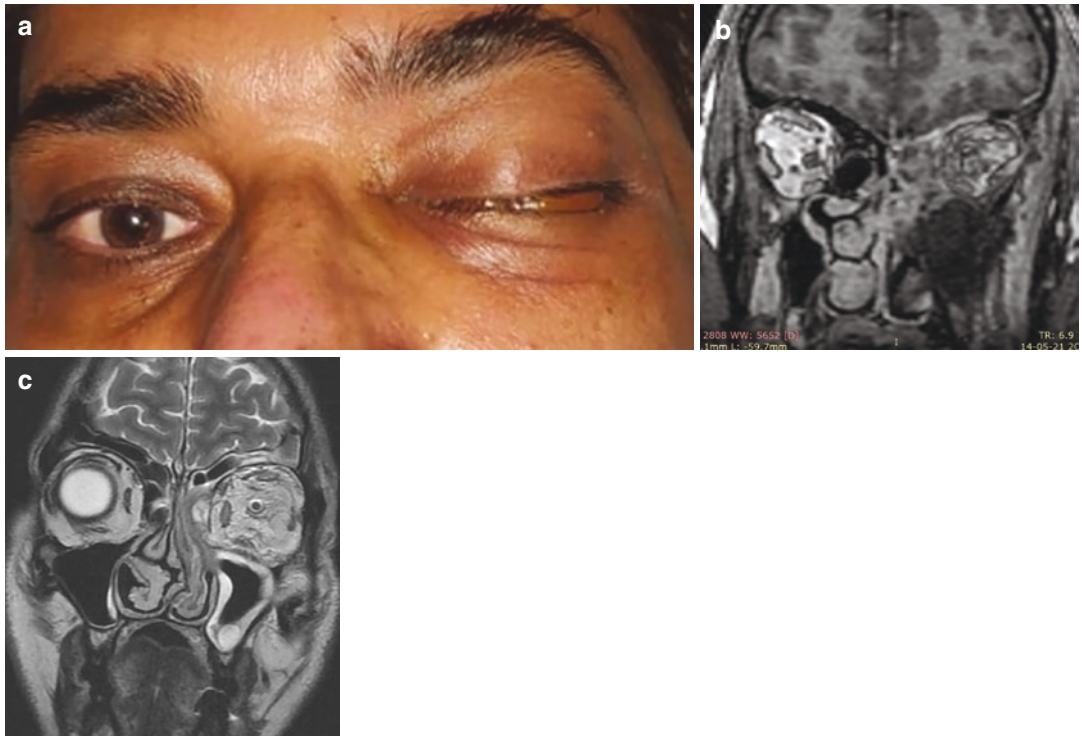

Fig. 17.45 (**a**) Left eye proptosis and ptosis, (**b**) MRI PNS contrast-enhanced T1W coronal images—hypointense and non-enhancing left inferior turbinate, part of middle turbinate, posterior part of maxillary sinus, floor of orbit and bulky extraocular muscles. (**c**) T2W coronal images show nodular mucosal thickening in left maxillary sinus and T2 hypointense areas in left middle and inferior nasal turbinates. Fat stranding is seen in left orbital space

Treatment

Evaluation and management of Diabetes Mellitus and Coronary artery disease were carried out. Since the patient was an old case of diabetes mellitus and had undergone coronary artery bypass grafting 5 years ago, a cardiologist's opinion was taken.

Simultaneous management under the intensivist and pulmonologist was continued. The patient was hypoxic, and the HRCT chest revealed signs of atypical pneumonitis. The patient was put on oxygen supplementation intermittently for a week and was then weaned off the oxygen successfully. He has continued on intravenous meropenem 1 g thrice daily along with IV moxifloxacin 100 mL twice a day.

As KOH wet mount revealed broad aseptate hyphae, he was also given an injection of Liposomal amphotericin-B (5 mg/kg/day). Regular monitoring of renal function tests was done with the period of drug holiday as and when the serum creatinine level doubled the baseline. Potassium supplementation was also given to tackle hypokalaemia.

Surgical Management

The patient was taken up for Endoscopic surgical debridement with ICU backup. Medial maxillectomy with excision of inferior and middle turbinate with clearance of necrotic fungal debris from the maxillary sinus and pterygopalatine fossa performed and tissue sent for HPE and fungal culture. Clinically patient had orbital symptoms which were correlated with per operative findings, so orbital decompression was performed, infected lamina papyracea and infected extraconal fat strands were cleared.

1. After a few days, the patient was relieved of his orbital swelling and watery discharge from the eye. Endoscopic suction and cleaning were done every 48 h. The patient was contin-

ued on Inj. Liposomal amphotericin-B for 14 days and then shifted to Tab Posaconazole 300 mg BD for 21 days followed by tab posaconazole 300 mg once a day for 1 month.

The patient is under regular follow-up and MRI 45 days after surgery confirmed clearance of disease.

- Pre-operative radiological finding (Fig. 17.46).
- Post-surgery (45 days) (Fig. 17.47): Clinical picture showing the disappearance of periorbital oedema and radiological images showing complete clearance of disease.

17.9.8 Case 8: Extensive Orbital Involvement

A 50-year-old male presented to the emergency department on the fifth day of his COVID illness with complaints of fever, left-sided facial pain, pain over the left upper jaw and ptosis, proptosis, diplopia and loss of vision in the left eye.

17.9.8.1 Examination

The patient was febrile, had conjunctival chemosis, restricted left extraocular movements, ptosis and proptosis. He was admitted, and a complete systemic and laboratory evaluation was done by a multidisciplinary team of otorhinolaryngologists, radiologists, ophthalmologists and a physician.

17.9.8.2 Investigations

All routine biochemical investigations were done, including complete blood count, random blood sugar, kidney function tests, liver function test, glycosylated haemoglobin, C-reactive protein (quantitative), Serum Ferritin and D-dimer were done.

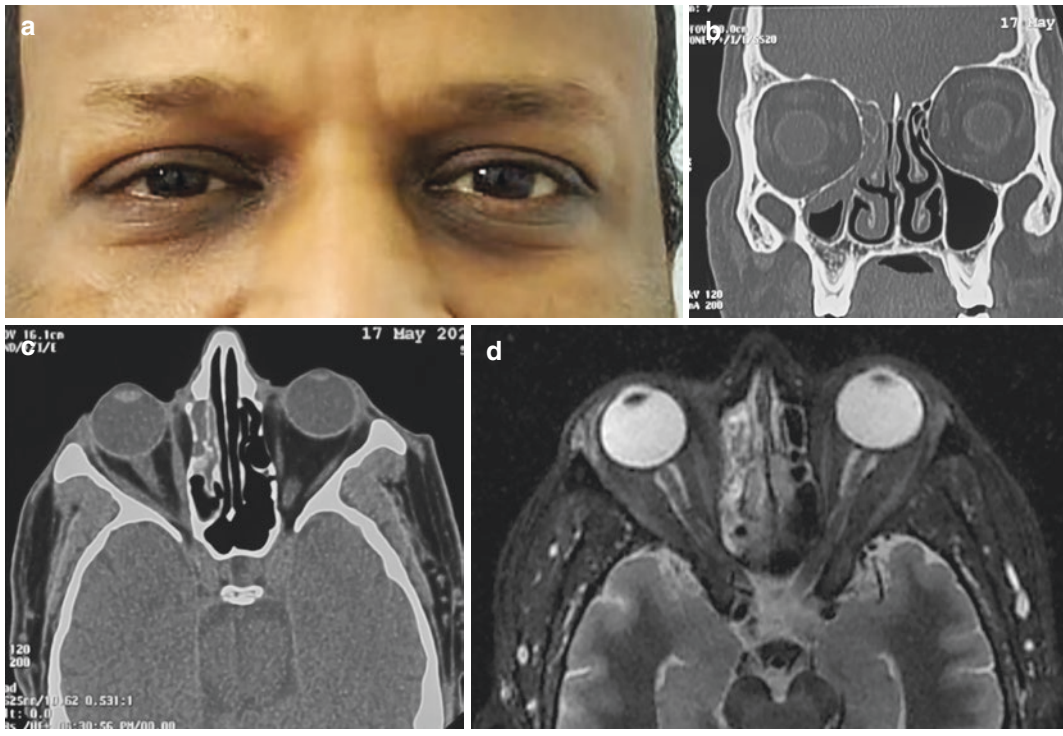

Fig. 17.46 (**a**) Mild periorbital oedema right eye. (**b**) CT-PNS coronal view; mucosal thickening in right maxillary and ethmoid sinuses and focal erosion of right lamina papyracea, (**c**) CT-PNS axial view—mucosal thickening in right ethmoid cells and erosions in lamina papyracea, (**d**) Axial STIR images through orbit show mucosal thickening in ethmoid air cells, more on the right side and mild fat stranding in the medial compartment of right orbit

Fig. 17.47 (**a**) Clinical picture of patient 45 days after surgery note periorbital swelling reduced. (**b**) MRI coronal view of the same patient 45 days after surgery; complete clearance of disease

Nasal endoscopy was done, and eschars were sent for KOH wet mount, which revealed broad aseptate hyphae.

17.9.8.3 Radiological Investigations

Radiological investigations were performed as per protocol and included CT scans of paranasal sinuses and orbit, T1W, T2W and T1W with gadolinium contrast MRI images of paranasal sinuses, orbit and brain.

CT scan of paranasal sinuses revealed opacification in the left maxillary sinus and left anterior ethmoids with air pockets. It also showed hyperdensities within the sinus cavity. T2w MRI PNS showed hyperintense shadows in the left maxillary sinus, hypointense areas in the left ethmoid sinus, medial wall of the maxillary sinus and left nasal cavity. Periorbital tissue appears bulky, which could be correlated clinically with proptosis. Premaxillary soft tissue is hyperintense suggestive of inflammation.

In STIR sequences, hyperintense areas are noted in left maxillary sinus mucosa, periorbital and premaxillary soft tissue, suggesting inflammation. Left extraocular muscles, intraconal and extraconal orbital fat appear hyperintense, which points towards extensive orbital involvement. On post-contrast T1W images, fungal invasion is suggested by hypointense non-enhancing areas in left maxillary sinus mucosa, medial wall and floor of the maxilla along with non-enhancing left inferior turbinate.

17.9.8.4 Radiological Findings

Figures 17.48, 17.49, 17.50, 17.51, 17.52, 17.53 and 17.54.

17.9.8.5 Treatment of COVID

Symptomatic treatment was started by a physician, including subcutaneous injection of low molecular weight heparin in the dose of 0.4 units once a day. No steroids and immunosuppressants were given, and the patient was reviewed regularly by the physician.

17.9.8.6 Treatment for Diabetes Mellitus

Patient had uncontrolled diabetes and was started on regular insulin with blood sugar monitoring. Strict controls were maintained to avoid Ketoacidosis.

17.9.8.7 Treatment for Mucormycosis

After the diagnosis of the mucormycosis was confirmed on KOH mount, the patient was immedi-

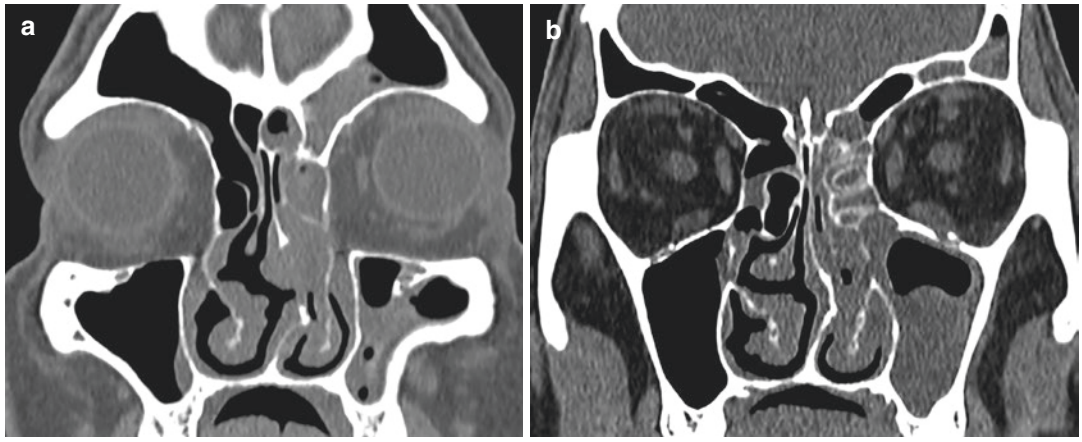

Fig. 17.48 (**a**, **b**) CT PNS images in the coronal plane show nodular mucosal thickening in the left maxillary sinus, left ethmoid air cells and left nasal cavity. Hyperdense areas are seen within the sinus cavity

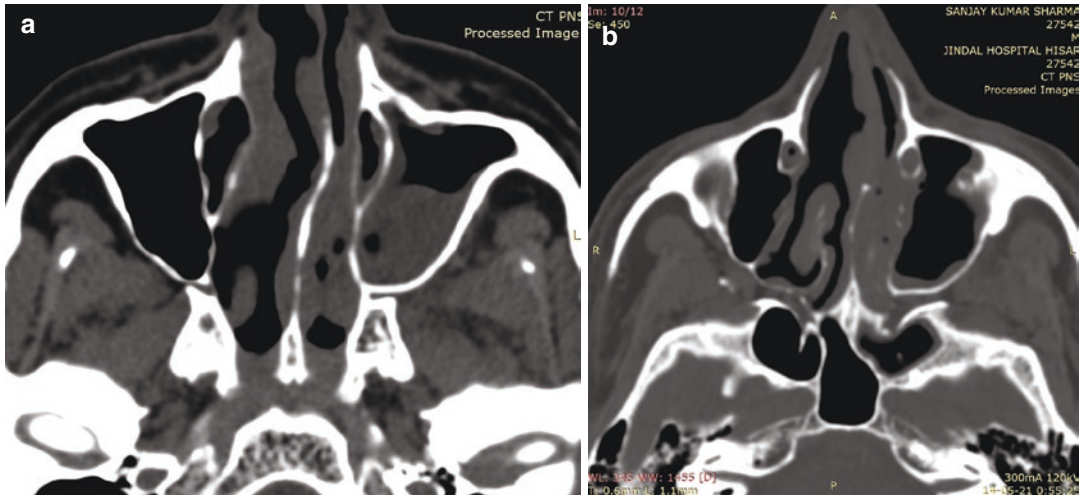

Fig. 17.49 (**a**, **b**) CT PNS images in the axial plane show nodular mucosal thickening in the left maxillary sinus, left ethmoid air cells and left nasal cavity

ately started on intravenous Liposomal Amphotericin-B (5 mg/kg/day). He tolerated antifungal drugs, and his renal functions test were maintained within normal limits during the treatment. Liposomal amphotericin-B was administered for 14 days along with tab Posaconazole 300 mg twice a day for 21 days. Later on, the patient was switched to the maintenance dose of tablet Posaconazole 300 mg once a day for a month.

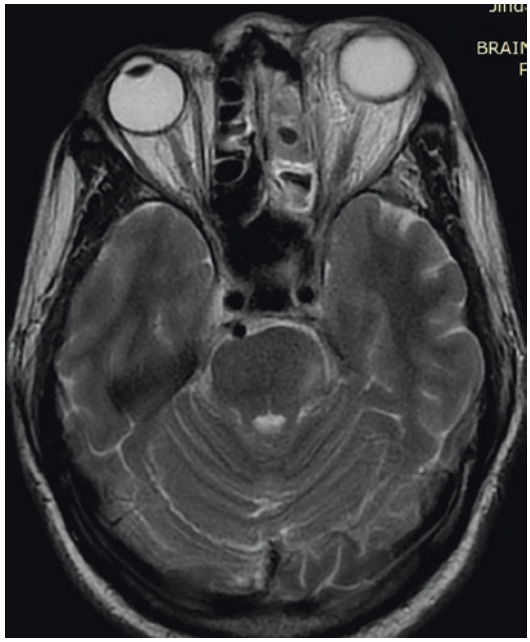

Fig. 17.50 T2W MRI PNS images in the axial plane show mucosal thickening in the left maxillary sinus and ethmoid air cells with T2 hypointense areas. Fat stranding is seen in the left orbit

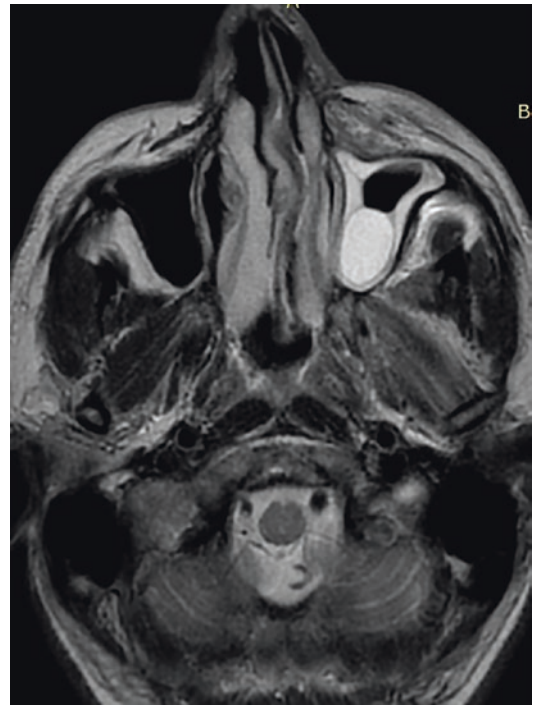

Fig. 17.51 T2W axial images show Inflammation/infiltration in left premaxillary soft tissues

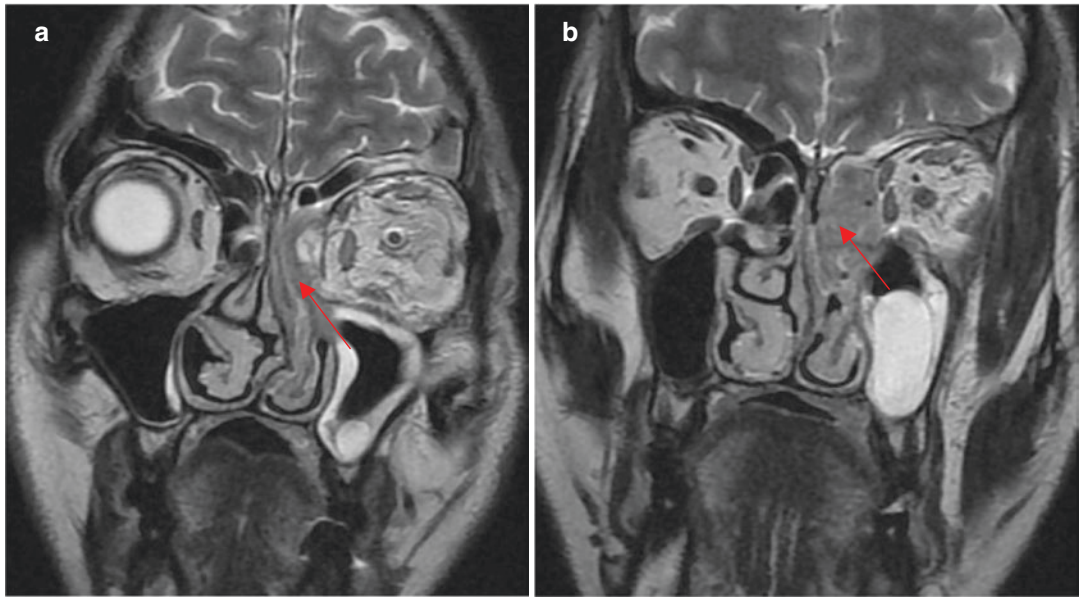

Fig. 17.52 (**a**, **b**) T2W MRI PNS images in the coronal plane show hyperintense mucosal thickening in the left maxillary sinus. T2 hypointense areas are seen in the left nasal cavity, left ethmoid air cells and along the medial wall of the left maxillary sinus suggesting fungal infection (red arrow)

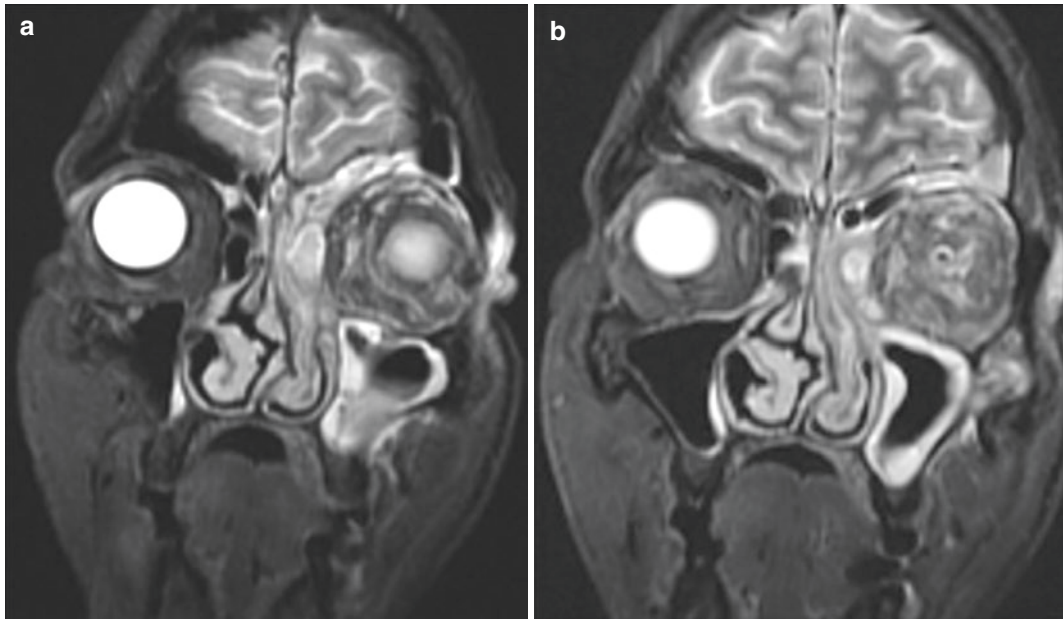

Fig. 17.53 (**a**, **b**) STIR images in MRI PNS in coronal plane show hyperintense mucosal thickening in left maxillary sinus, left nasal cavity and left fronto-ethmoid air cells. There is inflammation of intraconal and extraconal fat in the left orbit. Left orbital muscles are bulky and hyperintense

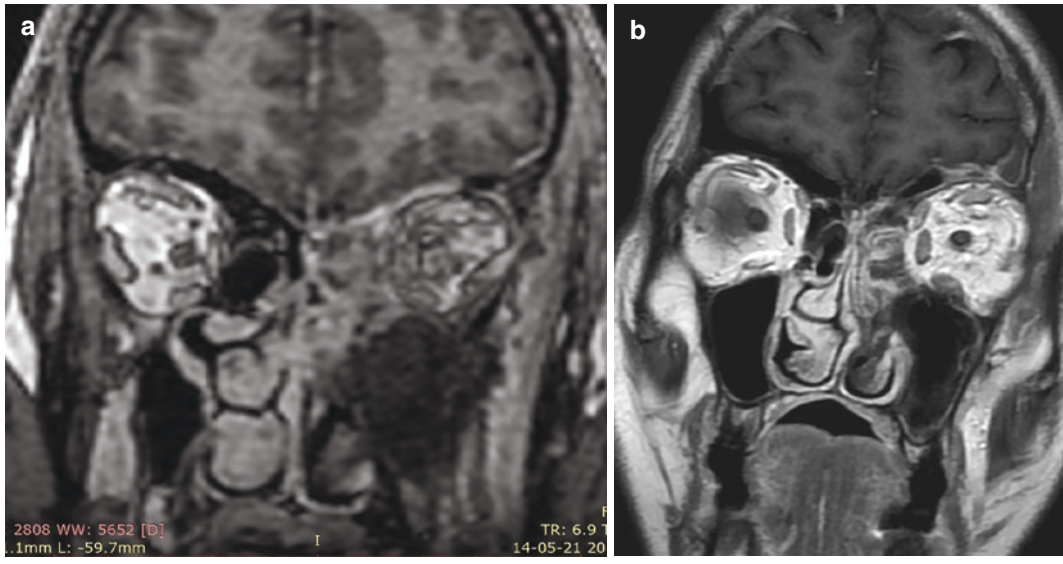

Fig. 17.54 (**a**) Contrast-enhanced T1W images in coronal plane show non-enhancing sinus mucosa in the left maxillary sinus. (**b**) Non-enhancing areas are seen in the medial wall and floor of the left maxillary sinus. Left inferior nasal turbinate is also non-enhancing

17.9.8.8 Surgical Management (Figs. 17.55, 17.56, 17.57, 17.58, 17.59, and 17.60)

Since the patient had extensive disease in the left-sided sinuses and orbit (complete involvement of the globe with total loss of vision), after discussion with the ophthalmologist, left orbital exenteration along with total left maxillectomy was planned. Orbital exenteration is a procedure performed along with total maxillectomy when a disease has extended through the bony wall, periosteum and involves all layers, including the fat, muscle or entire orbital contents, the eyelids and lacrimal apparatus.

The incision given was a modified Weber-Ferguson incision with a supraciliary extension. As the eyelid skin was lifted, the underlying soft tissue was found to be inflamed and necrosed. The upper cheek flap was elevated to expose the entire anterior and anterolateral wall of the maxilla. On subperiosteal dissection of the orbit, the medial orbital wall and the medial rectus muscle were necrosed, and the ethmoids were also full of disease. Orbital samples were sent separately for histopathology and fungal culture. All the soft tissue attachments of the maxilla, anterior, lateral, in the oral cavity and the orbit were divided. The osteotomies, in this case, included the inferior orbital rim and orbital floor and extended through the frontal process of the maxilla and the lacrimal bone, through lamina papyracea and anterior ethmoid to include the left globe in the specimen.

The rest of the osteotomies were the same as in subtotal maxillectomy explained in case number 6. After completing the osteotomies, soft tissue and muscular attachments on the posterior aspect of the maxilla were divided, and the internal maxillary artery was cauterized. The orbital rim was exposed circumferentially, and the attachment of the orbital periosteum to the orbital rim was incised in its superior half. The extraocular muscles at the apex of the orbit were divided. Optic nerve and accompanying blood vessels were clamped and divided, and the left eye with both eyelids was delivered with the maxillectomy specimen.

Unfortunately, this patient was lost to follow up.

17.9.9 Case 9: Intracranial Spread

A 49-year-old male presented to the neurology department with breathlessness and fever for the last 1 month. He had an episode of generalized tonic-clonic seizure a day before presenting to us. At the time of admission, the patient was conscious and oriented, and his vitals were stable. He was kept under the neurology department and was investigated using blood tests and imaging.

Fig. 17.55 Weber-Fergusson skin incision for maxillectomy

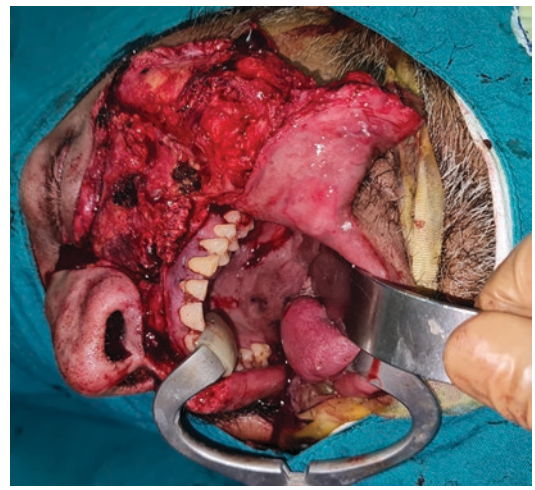

Fig. 17.57 Palatal incision

Fig. 17.56 After lifting the skin flap, the soft tissues of the face are elevated off the anterior and lateral surface of the maxilla

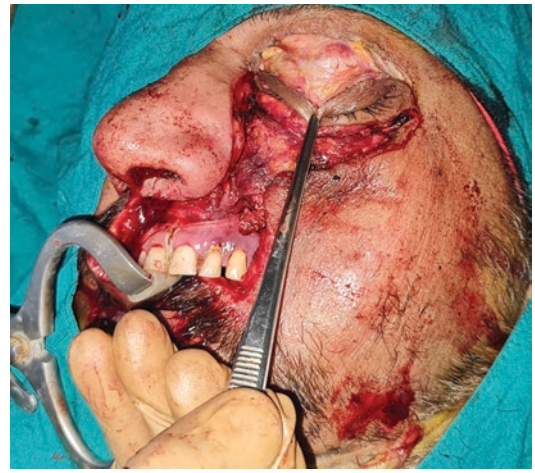

Fig. 17.58 Exenteration of left eye also performed along with maxillectomy

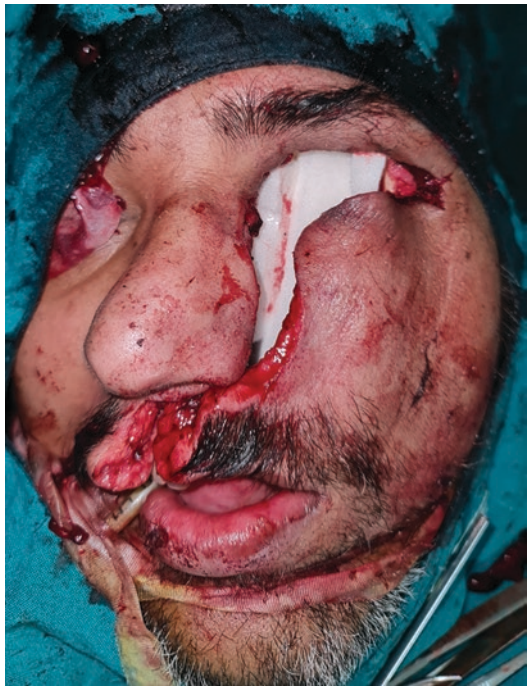

Fig. 17.59 Orbital exenteration with total maxillectomy performed. Skin and soft tissue incision to be sutured back

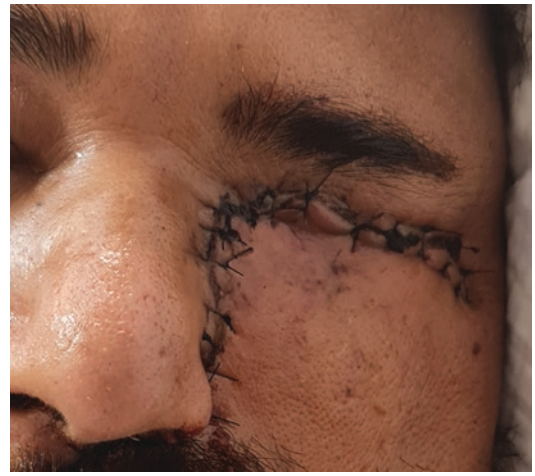

Fig. 17.60 Twenty-four hours post-surgery with sutures of incision line in place

17.9.9.1 Blood Investigations

The routine investigations revealed elevated total lymphocyte count (16.3 × 10^9/L) and CRP (97.9 mg/L), suggesting infection/inflammation.

17.9.9.2 Imaging (Fig. 17.61)

The contrast-enhanced CT scan of the head revealed an ill-defined, hypodense lesion with peripheral enhancement and surrounding oedema in the right inferior and medial temporal region, suggesting a temporal lobe abscess. A Lumbar puncture revealed lymphocytic meningitis. HRCT Chest showed signs of severe covid pneumonitis with a CT Severity Score of 18/25.

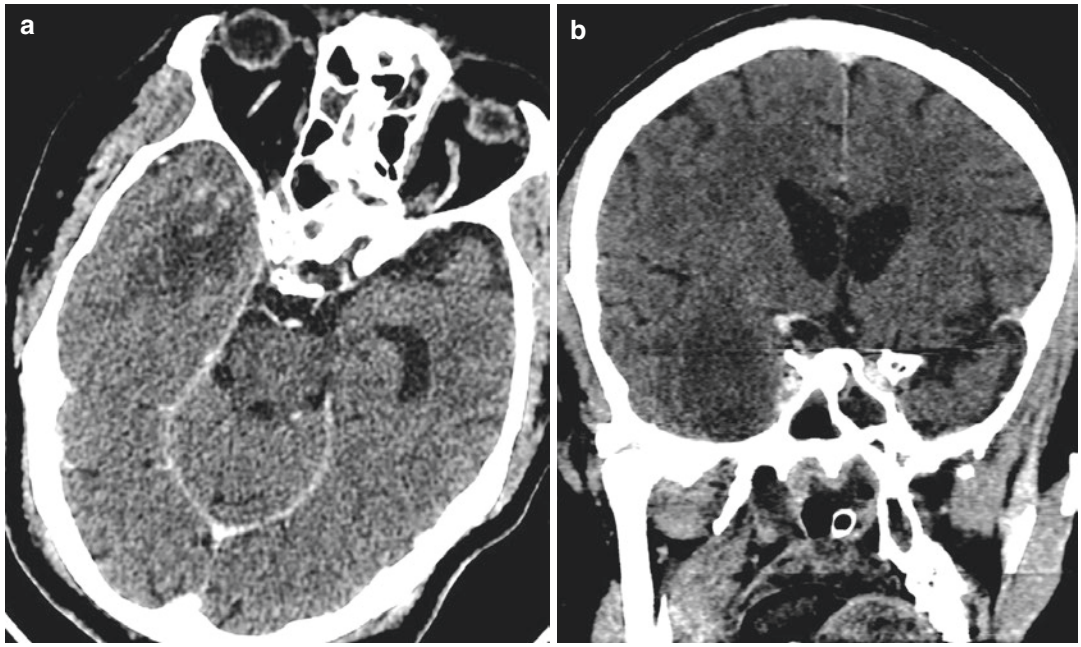

Fig. 17.61 (**a**) Contrast-enhanced CT PNS and brain (**b**) images in axial plane show hypodense lesion with mild peripheral enhancement in right temporal lobe suggestive of the abscess

17.9.9.3 Treatment of COVID

COVID symptoms related to his respiratory system were treated by the physician and an intensivist using broad-spectrum intravenous antibiotics like Cefoperazone with Sulbactam and colistin.

The treating team suspected mucormycosis, and an otorhinolaryngologist was consulted. Detailed bedside ENT examination was conducted, including nasal endoscopy, swabs were collected and sent for KOH mount. The smear showed occasional pseudohyphae. Therefore, the radiological investigations, including various sequences of MRI of paranasal sinuses, orbit and brain, were performed (Figs. 17.62, 17.63, and 17.64). The right inferior turbinate showed loss of contrast with no enhancement indicating the 'Black turbinate sign'. The patient was immediately put on intravenous amphotericin-B in a dose of 5 mg/kg/day. In the meantime, a detailed ophthalmological examination was also carried out.

17.9.9.4 Surgical Steps and Findings

A team of otorhinolaryngologist and neurosurgeon was involved in the surgical management of this patient. The drainage of the temporal abscess was carried out by a neurosurgeon (Fig. 17.65), and in the same stage, endoscopic right medial maxillectomy was performed with complete clearance of necrotic tissue filling the maxillary along with its lateral recess. The disease was also cleared from all around the orbital apex area (Fig. 17.66).

The necrotic tissue was sent for KOH wet mount and revealed aseptate broad fungal hyphae. As his general condition was not satisfactory, the patient was kept on mechanical ventilator support for 3 days. Check endoscopy and clearance were done on day three and after that, every 24 h, the patient was weaned off the ventilator support.

17.9.9.5 Further Neurological Management

To prevent a rise in intracranial pressure patient was given intravenous Mannitol

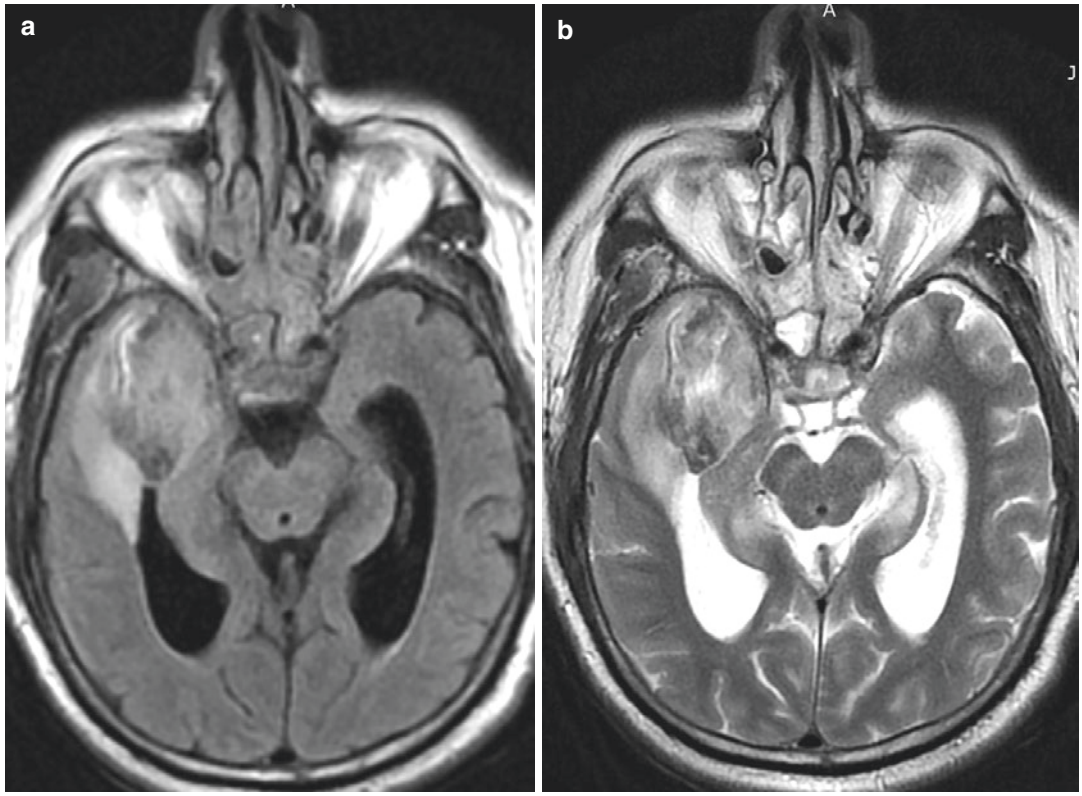

Fig. 17.62 (**a**) FLAIR and (**b**) T2W MRI images in axial plane show intra-axial altered signal intensity lesion in right temporal lobe with hydrocephalus. Sinus disease is evident in the bilateral ethmoid and sphenoid sinuses

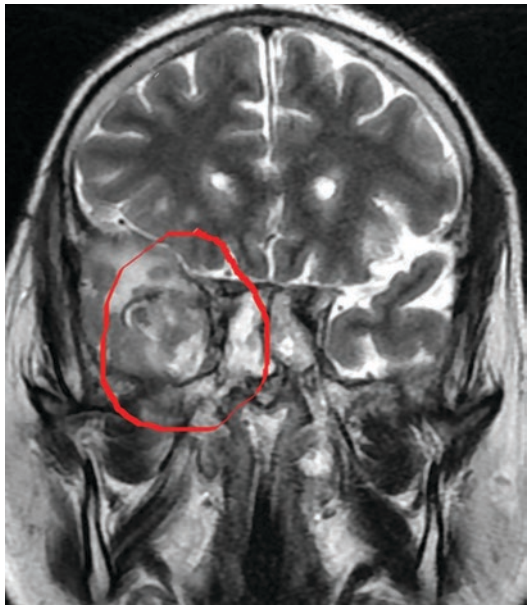

Fig. 17.63 T2W MRI image in coronal plane shows disease extending from sphenoid sinus and orbital apex to right temporal lobe in the region of orbital apex

100 mL 8 hourly and antiepileptic medication in the form of Phenytoin Sodium 100 mg 8 hourly. A post-operative NCCT head was done, and the ventricles were found to be dilated. Hence Ventriculoperitoneal shunting was done. Despite all our efforts, the patient's general condition did not improve, and the patient succumbed.

17.10 Lessons Learnt in COVID-19-Associated Mucormycosis

- The deadly triad of Ketoacidosis, low oxygen tension and hyperglycaemia in diabetics, provide the most favourable medium for the fungus to grow due to the active ketone reductase system in the organism.

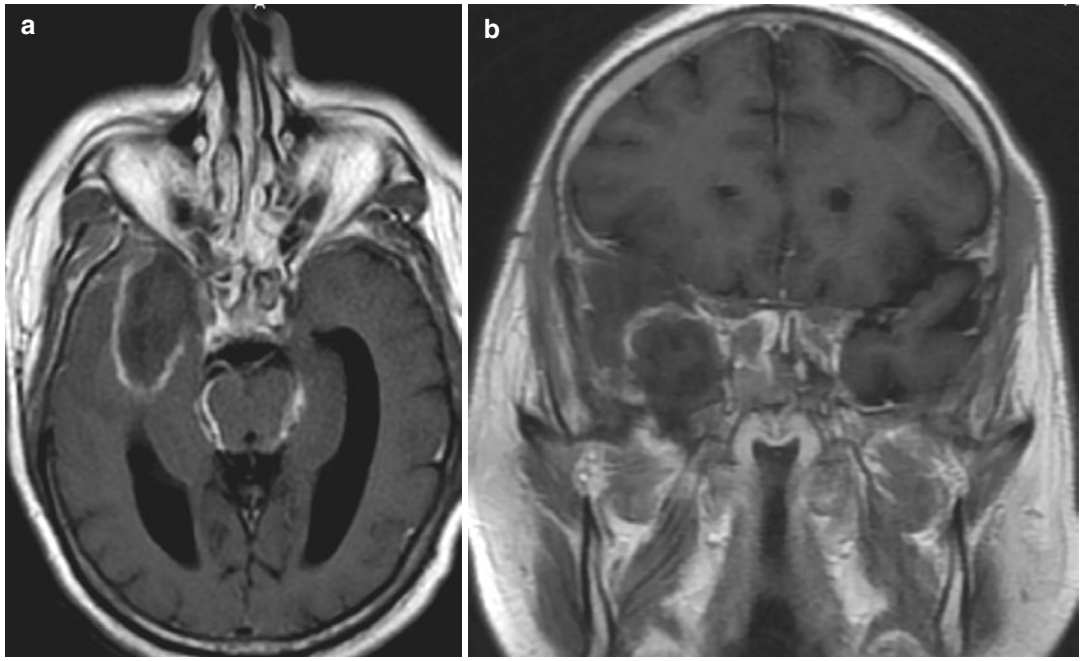

Fig. 17.64 Contrast-enhanced T1W images in (**a**) axial and (**b**) coronal plane show peripherally enhancing lesion in right temporal lobe suggestive of brain abscess. There is evidence of disease spread from the floor of the sphenoid sinus/pterygomaxillary fissure

Fig. 17.65 Craniotomy is done to drain temporal lobe abscess

- Role of a multidisciplinary team including Otorhinolaryngologist, Physician, Ophthalmologist, Neurosurgeon, Nephrologist, Pathologist and Intensivists/ICU specialists is mandatory for complete management of rhino-orbital-cerebral mucormycosis.
- Staging the disease is very important for accurate and in time treatment of different stages of ROCM.
- Multimodality imaging is helpful in prompting an early diagnosis
- Treatment primarily is medical. Surgery is to debride the infected tissue to eliminate the fungal load, to make the drug available to viable tissue and prevent further complications
- The shortage of Liposomal Amphotericin B showed us the way to newer and equally effective antifungals like Isovuconazole with lesser side effects.

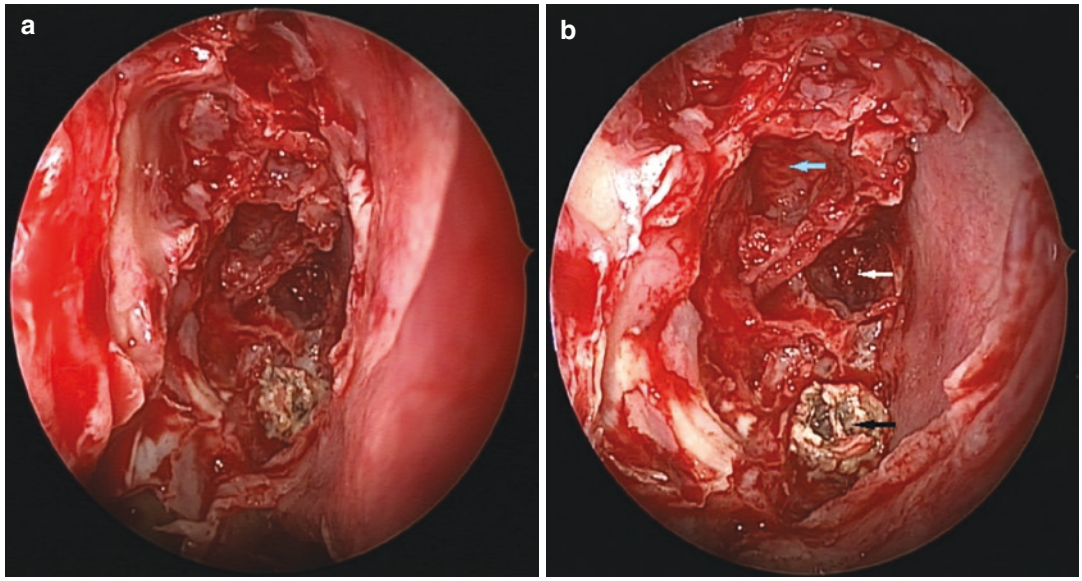

Fig. 17.66 (**a**, **b**) Localization of necrotic tissue in sphenoid sinus and orbital apex after uncinectomy, medial maxillectomy ethmoidectomy, sphenoidotomy and following the disease in orbital apex. All diseased tissue excised from a sphenoid sinus (white arrow) and orbital apex (black arrow) till fresh bleeding started. Posterior ethmoidectomy (blue arrow)

- Along with ROCM, treatment includes control of hyperglycaemia, COVID and its related complications.
- In orbital involvement, exenteration is to be avoided. Mostly endoscopic decompression and clearing the disease is good enough to save the vision and the eyeball. Intraorbital irrigation of injection Amphotericin B helps to save exenteration. Loss of vision is never an indication for exenteration of the eyeball.
- Repeated endoscopic clearance and nasal douching gives faster recovery.
- Progressive and rapid involvement of the cavernous sinus, vascular structures and intracranial contents is a sign of grave prognosis despite radical surgery and antifungals.
- It must be recognized early and treated aggressively.

References

1. Sreshta K, Dave TV, Varma DR, Nair AG, Bothra N, Naik MN, Sistla SK. Magnetic resonance imaging in rhino-orbital-cerebral mucormycosis. Indian J Ophthalmol. 2021;69(7):1915–27. https://doi.org/10.4103/ijo.IJO_1439_21.
2. Hosseini SMS, Borghei P. Rhinocerebral mucormycosis: pathways of spread. Eur Arch Otorhinolaryngol. 2005;262:932–8. https://doi.org/10.1007/s00405-005-0919-0.
3. Goyal P, Lee S, Gupta N, Kumar Y, Mangla M, Hooda K, Li S, Mangla R. Orbital apex disorders: imaging findings and management. Neuroradiol J. 2018;31(2):104–25. https://doi.org/10.1177/1971400917740361.
4. Han Q, Escott EJ. The black turbinate sign, a potential diagnostic pitfall: evaluation of the normal enhancement patterns of the nasal turbinates. Am J Neuroradiol. 2019;40(5):855–61. https://doi.org/10.3174/ajnr.A6037.

18 Analysis of Orbital Involvement in 562 Cases of Rhino-Orbito-Cerebral Mucormycosis

Mohnish Grover, Tanmaya Kataria, and Madhav Goel

Mucormycosis is a rare, fulminant fungal infection caused by a mould of the order Mucorales. It mainly occurs in immunocompromised patients. An inflammatory reaction in the blood vessels after fungus enters the tissue through blood vessels leads to formation of thrombus. This thrombus can increase in size and ultimately compromise the blood supply of tissues and cause ischaemic necrosis. It can be of the following types depending upon the site of involvement; Rhino-orbital-cerebral mucormycosis (ROCM), Cutaneous mucormycosis, Pulmonary mucormycosis, Gastrointestinal mucormycosis, Renal mucormycosis, and Disseminated mucormycosis [1].

In this chapter, the authors report their experience of analyzing 209 cases of orbital involvement seen in total 562 cases of ROCM reported to the Department of Otorhinolaryngology at SMS medical college Jaipur, Rajasthan. Orbital involvement was seen in 209 cases (37.2%) cases, out of which 48 (23%) patients had unilateral complete vision loss, and 6 (2.9%) had complete bilateral blindness on both sides.

18.1 Various Types of Orbital Presentation

The site and extent of orbital involvement depend on the route of the spread of the disease to the orbit. The chapter on imaging in mucormycosis has explained the various routes of spread to the orbit, the most accepted ones include [2]:

- Ethmoid sinus to orbit via the thinness of the lamina papyracea.
- Congenital dehiscences are often present along the medial wall of the orbit.
- The perforations of the medial wall by arteries and veins.
- Through the pterygopalatine fossa/infratemporal fossa. The disease can reach the orbit through the inferior orbital fissure and thereby involve the orbital apex.
- From the orbital apex, the disease can spread to the cavernous sinus via superior orbital fissure.

18.2 Signs and Symptoms

Early presentations of orbital involvement include eye pain, ptosis, chemosis, periorbital oedema (Fig. 18.1a–d), proptosis, decreased vision, and ocular muscle palsy resulting in diplopia. Blindness, complete ophthalmoplegia, and optic atrophy are other late features of orbital involvement.

M. Grover (✉) · T. Kataria
SMS Medical College, Jaipur, India

M. Goel
Maulana Azad Medical College, New Delhi, India

N. Gupta, S. G. Honavar (eds.), *Rhino-Orbito-Cerebral Mucormycosis*,
https://doi.org/10.1007/978-981-16-9729-6_18

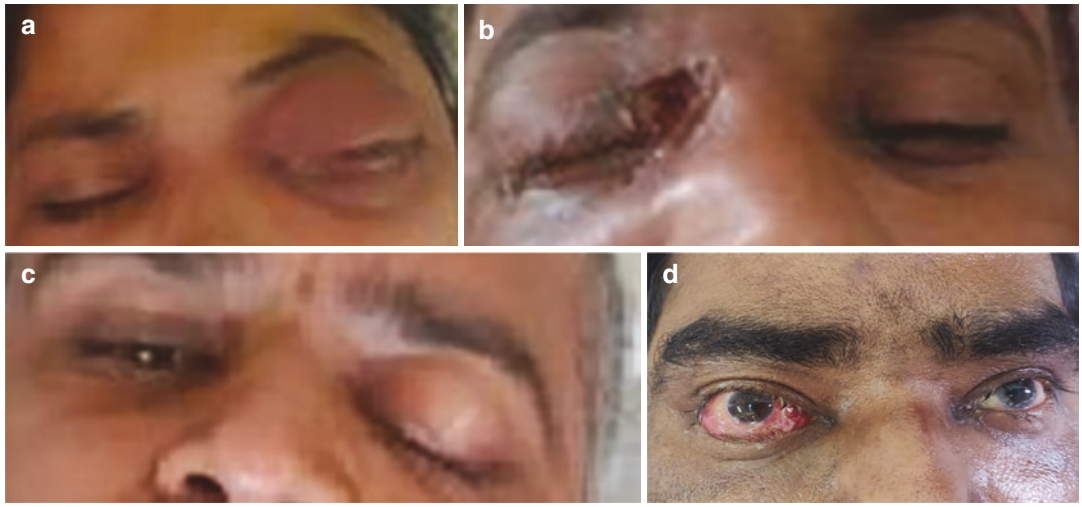

Fig. 18.1 (**a**) Left periorbital oedema, (**b**) Right eyelid involvement, (**c**) Ptosis, (**d**) Chemosis

Development of disease to contralateral side or cavernous sinus thrombosis can be suspected when signs and symptoms start developing in the opposite eye resulting in bilateral proptosis, chemosis, vision loss, and ophthalmoplegia.

18.3 Vision Loss in ROCM [3]

Vision loss in ROCM may occur due to:

1. Orbital Apex Syndrome (OAS)
2. Central Retinal Artery Occlusion (CRAO)
3. Optic nerve involvement
4. Cavernous sinus thrombosis

Vascular tropism of the fungus in orbit leading to arteriolar thrombosis in the orbit wall, oculomotor, and optic nerve explains orbital symptoms like blindness with or without thrombosis of ophthalmic artery. It is unilateral and marked by orbital pain, diplopia, ophthalmoplegia, periorbital oedema, chemosis, exophthalmos, or blindness. Eye fundus is a crucial examination for the diagnosis of ROCM. It may reveal venous congestion or thrombosis of the artery or the retina's central vein, optic atrophy, or panophthalmitis [4].

Occlusive vasculitis and thrombosis because of vascular invasion of hyphae leads to tissue necrosis [5].

Orbital apex syndrome is a common presentation of ROCM. It is characterized by ptosis, proptosis, total ophthalmoplegia, pain along the course of the ophthalmic division of the trigeminal nerve and visual impairment of variable extent and unfortunately, blindness is permanent, and the risk of mortality is increased at this stage of progression [6].

The ominous manifestations like Central Retinal Artery Occlusion (CRAO), cavernous sinus thrombosis, and endophthalmitis have been variably reported. In their published study, Bhansali et al. and Yohai et al. reported that the visual loss in ROCM usually has been attributed to CRAOs and cavernous sinus thrombosis. The unfortunate eventuality of CRAO bears an incidence of 16%–20% [7, 8].

Ferry and Abedi described an exenteration specimen of rhino-orbital-cerebral mucormycosis with thrombosed ciliary arteries next to a necrotic optic nerve [9]. Brown et al. reported one of eight cases and Bullock et al. one of two cases with acute obstruction of the retinal and choroidal circulations in orbital mucormycosis [10, 11].

The optic nerve may be affected, resulting in vision loss. Optic nerve infarction and necrosis may follow invasion of fungus in blood vessel walls causing thrombosis of optic nerve sheath or ophthalmic artery. Direct involvement of the optic nerve can also occur. The fungus may gain

access to the cavernous sinus and the brain parenchyma with further posterior extension, causing vascular thrombosis, and infarction. It can also spread via inferior orbital fissure, superior orbital fissure, infratemporal fossa, or orbital apex. Involvement of the superior orbital fissure and its contents, such as cranial nerves III, IV, and VI, and branches of V1 and V2, may cause diplopia, ophthalmoplegia, and sensory loss to the corresponding areas of the cornea and face [12].

18.4 Diagnosis

Diagnosis of ROCM is made by clinical features, radiology, and identification of fungal hyphae on tissue staining/culture.

Contrast-Enhanced Computed Tomography (CECT) and MRI (Magnetic Resonance Imaging) can help make an early diagnosis of ROCM. Contrast-enhanced MRI is considered the best investigation, especially for extra sinus involvement. Radiology will show the pathway of the spread of the disease to the orbit. This will include erosion of lamina papyracea, fat orbital involvement, extraocular muscle involvement, and orbital apex involvement. MRI provides better visualization of invasion/involvement of orbital soft tissue, perineural invasion and vascular obstruction because of increased soft tissue resolution than CT. MRI signal intensity of mucormycosis lesions tends to be isointense or hypointense in all sequences. After the administration of gadolinium, the lesions are typically non-enhancing, which helps differentiate fungus from surrounding inflammation. To distinguish between fungus and orbital fat T2-weighted fat-suppressed sequences (with and without contrast) are considered the best [13] (Figs. 18.2 and 18.3).

Diffusion-weighted MRI demonstration of ischemic optic neuropathy confirms the infarction of the optic nerve as high signal intensity along the optic nerves, with corresponding low signal on apparent diffusion coefficient map with normal fluid-attenuated inversion recovery (FLAIR) and gadolinium-enhanced images. These imaging findings and ensuing blindness may result from the organisms' invasion of the blood vessel walls, leading to occlusion or thrombosis of the central retinal artery or ophthalmic artery or direct optic nerve infiltration by mucormycosis. Enhancement around the optic nerve

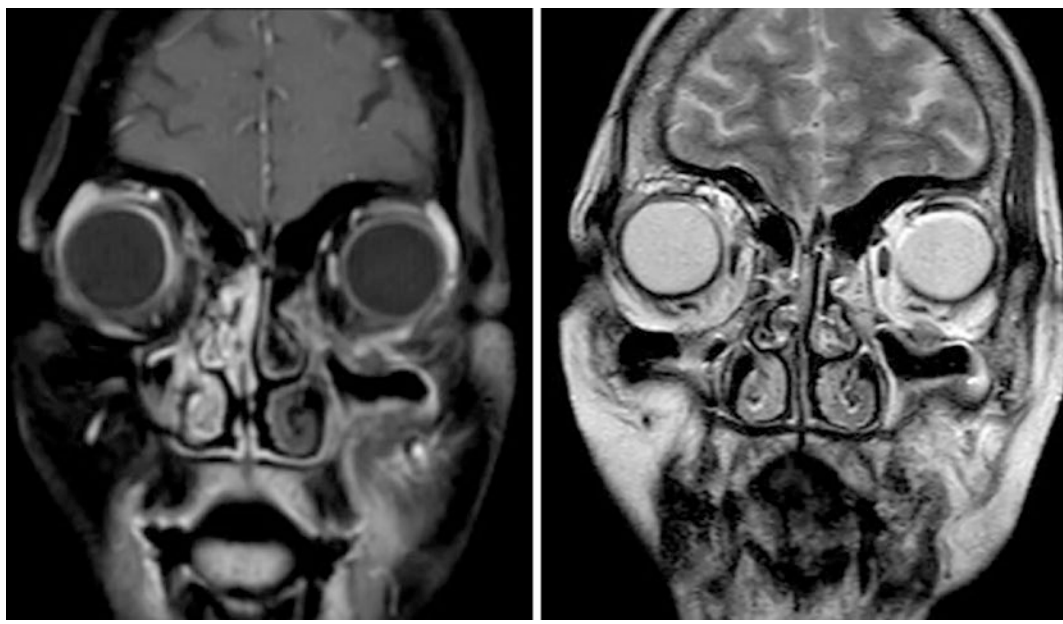

Fig. 18.2 Coronal post-contrast fat-suppressed and coronal regular T2 images show enlarged enhancing left infraorbital nerve with enlargement of the infraorbital canal

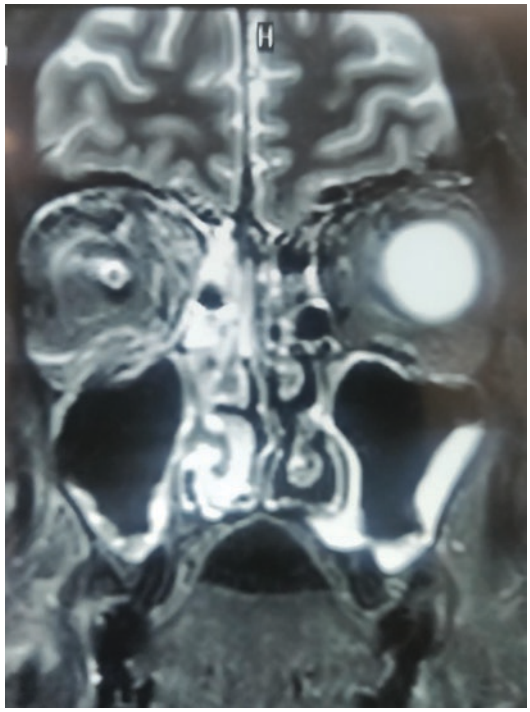

Fig. 18.3 Coronal T2 fat-suppressed image showing diffuse hyperintensity and stranding in the right intraconal compartment. Right optic nerve also appears mildly enlarged and hyper intense

indicates perineuritis on postcontrast T1-weighted magnetic resonance imaging (Figs. 18.4 and 18.5). Diffusion-weighted Imaging is vital for early diagnosis of ischemic optic neuropathy, and it shows the abnormality when other MR sequences are normal [14].

18.5 Surgical Management

The detailed surgical steps of the endoscopic debridement or the globe sparing transnasal endoscopic globe sparing orbital exenteration have been discussed in separate chapters. Therefore, this chapter will discuss the cases of orbital involvement and their management based on the comprehensive radiological evaluation.

Radiology in the form of various sequences of MRI plays a crucial role in mapping the intraorbital disease. On Gadolinium-enhanced MRI, the loss of contrast enhancement represents a necrotic, unsalvageable nidus of fungal elements [15–17]. It is therefore reasonable to immediately debride this necrotic tissue.

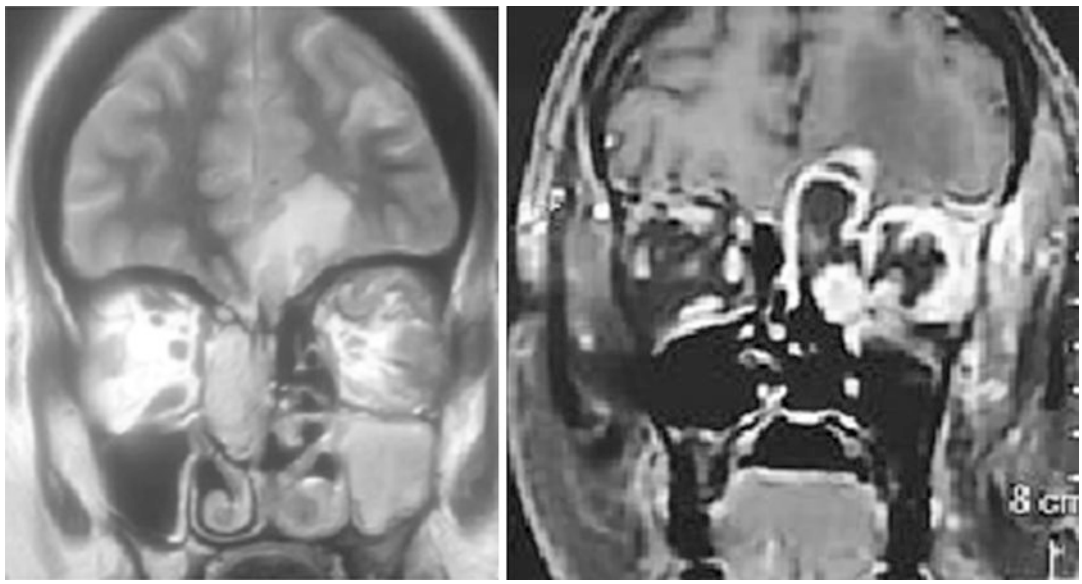

Fig. 18.4 Coronal post-Gadolinium-enhanced MRI image shows significant enhancement of left basifrontal dura with a small enhancing lesion in the left frontal lobe, suggestive of meningeal involvement. Diffuse enhancement of left periorbital and extraocular muscles is also seen

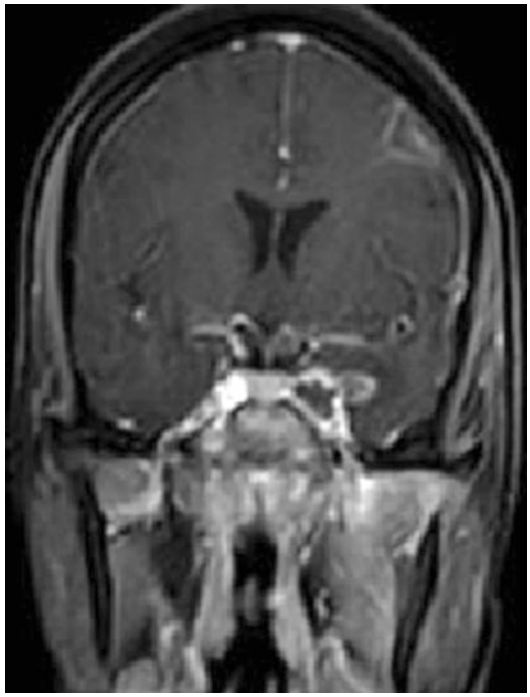

Fig. 18.5 Coronal postcontrast MRI images showing diffuse enlargement, thickening, and enhancement of optic chiasma. The right optic nerve shows thickening and enhancement

Following debridement, local site irrigation via an orbital drain or transcutaneous Amphotericin-B injections helped contain the current series's disease.

The various surgical options for treating orbital involvement in ROCM are listed below:

1. Endoscopic orbital decompression
2. Transcutaneous Amphotericin B injections (TRAMB)
3. Endoscopic orbital clearance
4. Orbital exenteration

18.5.1 Endoscopic Orbital Decompression

Do's and Don't's for endoscopic orbital decompression in ROCM depend on the presence or absence of disease inside the orbit and the integrity of the lamina papyracea.

1. If on imaging there is no intraorbital disease, removal of any of the orbit walls is not needed. If the ethmoid sinus infection is responsible for orbital inflammation, then radical clearance of ethmoids is done with the clearance of other sinuses keeping the lamina intact. Lamina acts as a barrier to the spread of mucormycosis from the sinuses to the orbit.
2. However, in all the cases with suspected or impending orbital involvement or disease progression, it is necessary to clear the pterygopalatine fossa. Pterygopalatine fossa acts as a reservoir of infection, as mentioned in the previous chapters. Therefore, it must be addressed in cases with orbital symptoms to minimize the chances of orbital disease progression. However, a strict postoperative check for progression of symptoms or emergence of new endoscopic findings must be kept.
3. If there are features of post-septal orbital cellulitis (without any intraorbital fungal disease) not responding to injectable antibiotics, endoscopic orbital decompression is performed. Patients with intraorbital fungal disease will require orbital clearance/debridement (as discussed in a later section).

Out of 209 patients of ROCM with orbital involvement, 5 (2.3%) patients underwent endoscopic orbital decompression. Endoscopic exploration in these five cases was planned based on the radiological evidence of the disease. However, on removing the lamina papyracea and teasing out the fat, the orbit looked healthy. Therefore no fat was debrided, and the clearance of ethmoids and all other sinuses led to the complete resolution of cellulitis and periorbital oedema with an excellent symptomatic relief in these patients.

18.5.2 Transcutaneous Retrobulbar Amphotericin B (TRAMB)

TRAMB has the advantage of being a bedside procedure, obviating the need for general anaesthesia in often physically vulnerable patients. But there is

little literature available about TRAMB. Possibly TRAMB can be considered when there is focal involvement of orbit without visual disturbances or when there is a shortage of intravenous amphotericin-B for patients with orbital involvement. The amount of amphotericin-B injected ranges from 1 to 1.5 mL at concentrations ranging from 1 to 3.5 mg/mL daily to weekly.

The authors administered TRAMB in four patients in their series. Out of these four patients, three patients had vision limited to just the perception of light, and one patient had no perception of light. After administration, 2(50%) patients showed improvement and the vision improved to finger counting at a distance of 6 ft. One patient (25%) showed noncompliance after the first injection, and one (25%) patient with a negative perception of light showed no improvement. The only noted side effect was pain at the injection site.

18.5.3 Endoscopic Orbital Clearance

Quite a few patients with ROCM have fungal disease extending into orbit. Most of the time, it is a contiguous spread. However, unlike malignancy, this does not mean that these patients require orbital exenteration. In the present era, with advanced equipment, most areas of orbit can be approached endoscopically. Patients with intact or diminished vision (not complete loss of vision) were included in the indication for endoscopic orbital clearance.

Those patients with complete vision loss but no involvement of orbital apex also underwent endoscopic orbital clearance of the disease. They were, however, clearly explained about the need for a repeat cleaning/exenteration in case any further disease progression was noted in future follow-up.

Out of 209 patients with orbital involvement, 192 (91.8%) patients underwent endoscopic orbital decompression. Six out of 192 (3.1%) needed orbital exenteration at a later date.

18.5.4 Orbital Exenteration

The most crucial decision in the management of orbital mucormycosis is whether the orbit should be exenterated. Authors selected those cases for orbital exenteration where the patient had a disfigured blind eye with no light perception and disease did not respond to endoscopic orbital clearance and intravenous administration of antifungal drugs.

Cases with partial or intact vision having only ophthalmoplegia, where extensive intracranial spread had already taken place, were also the candidates for radical orbital debridement with clearance of pterygopalatine fossa using Denkers modified medial maxillectomy as described in the chapter on surgical management of ROCM. Exenteration is not likely to improve the survival outcome in such cases and hence be avoided.

At our institute, out of 209 patients, only 14 (6.6%) patients underwent orbital exenteration. The mortality rate was 21% after exenteration. Patients with preoperative intracranial extension showed no improved outcome after surgery.

Acknowledgments This chapter and the work done regarding ROC mucormycosis in our institute would not have been possible without visionary leadership of Prof Sudhir Bhandari, Principal, SMS Medical College, Jaipur and the work done by various members of Mucormycosis Board including Dr Shruti Bhargava (Associate Professor Pathology), Dr Sunil Samdhani (Professor and Head ENT), Dr Shashank Nath Singh (Associate Professor ENT), Dr Maya Hada (Associate professor Ophthalmology), Dr Aruna Vyas (Professor Microbiology), Dr Amitabh Dube (Senior Professor Physiology), Dr Shivankan Kakkar (Assistant Professor Pharmacology).

References

1. Prakash H, Chakrabarti A. Epidemiology of mucormycosis in India. Microorganisms. 2021;9:523. https://doi.org/10.3390/microorganisms9030523.
2. Jiang N, Zhao G, Yang S, et al. A retrospective analysis of eleven cases of invasive rhino-orbito-cerebral mucormycosis presented with orbital apex syndrome initially. BMC Ophthalmol. 2016;16:10. https://doi.org/10.1186/s12886-016-0189-1.

3. Goyal P, Lee S, Gupta N, Kumar Y, Mangla M, Hooda K, Li S, Mangla R. Orbital apex disorders: imaging findings and management. Neuroradiol J. 2018;31(2):104–25. https://doi.org/10.1177/1971400917740361.
4. Anders UM, Taylor EJ, Martel JR, Martel JB. Acute orbital apex syndrome and rhino-orbito-cerebral mucormycosis. Int Med Case Rep J. 2015;8:93–6. https://doi.org/10.2147/IMCRJ.S83036.
5. Thurtell MJ, Chiu AL, Goold LA, Akdal G, Crompton JL, Ahmed R, Madge SN, Selva D, Francis I, Ghabrial R, Ananda A, Gibson J, Chan R, Thompson EO, Rodriguez M, McCluskey PJ, Halmagyi GM. Neuro-ophthalmology of invasive fungal sinusitis: 14 consecutive patients and a review of the literature. Clin Exp Ophthalmol. 2013;41(6):567–76.
6. Bhansali A, Bhadada S, Sharma A, Suresh V, Gupta A, Singh P, et al. Presentation and outcome of rhino-orbital-cerebral mucormycosis in patients with diabetes. Postgrad Med J. 2004;80:670–4.
7. Yohai RA, Bullock JD, Aziz AA, Markert RJ. Survival factors in rhino-orbital-cerebral mucormycosis. Surv Ophthalmol. 1994;39:3–22.
8. Ferry AP, Abedi H. Diagnosis and management of rhino-orbito-cerebral mucormycosis. A report of 16 personally observed cases. Ophthalmology. 1983;90:1096–104.
9. Brown GC, Magargal LE, Sergott B. Acute obstruction of the retinal and choroidal circulations. Ophthalmology. 1986;93:1373–82.
10. Bullock JD, Jampol LM, Fezza AJ. Two cases of orbital phyconiycosis with recovery. Am J Ophthalmol. 1974;78:811–3.
11. Kahloun R, Abroug N, Ksiaa I, Mahmoud A, Zeghidi H, Zaouali S, Khairallah M. Infectious optic neuropathies: a clinical update. Eye Brain. 2015;7:59–81. https://doi.org/10.2147/EB.S69173.
12. Lone PA, Wani NA, Jehangir M. Rhino-orbito-cerebral mucormycosis: Magnetic resonance imaging. Indian J Otol. 2015;21:215–8.
13. Ghuman MS, Kaur S, Bhandal SK, Ahluwalia A, Saggar K. Bilateral optic nerve infarction in rhino-cerebral mucormycosis: a rare magnetic resonance imaging finding. J Neurosci Rural Pract. 2015;6(3):403–4. https://doi.org/10.4103/0976-3147.158790.
14. Gorovoy IR, Vagefi MR, Russell MS, et al. Loss of contrast enhancement of the inferior rectus muscle on magnetic resonance imaging in acute fulminant invasive fungal sinusitis. Clin Exp Ophthalmol. 2014;42:885–7.
15. Horger M, Hebart H, Schimmel H, et al. Disseminated mucormycosis in haematological patients: CT and MRI findings with pathological correlation. Br J Radiol. 2006;79:e88–95.
16. Kim JH, Kang BC, Lee JH, et al. The prognostic value of gadolinium-enhanced magnetic resonance imaging in acute invasive fungal rhinosinusitis. J Infect. 2015;70:88–95.
17. Gorovoy IR, Kazanjian M, Kersten RC, et al. Fungal rhinosinusitis and imaging modalities. Saudi J Ophthalmol. 2012;26:419–26.

19 Decision-Making in Orbital Mucormycosis: Conservative Versus Orbital Exenteration

Santhosh G. Honavar and Rolika Bansal

19.1 History of Orbital Exenteration

George Bartisch, a German physician, considered by many as the "father of modern ophthalmology," first reported orbital exenteration in 1583 [1]. The modern total orbital exenteration was reported by Golovine [2], and Coston and Small in 1981 simplified the technique [3]. Since then, several variations in the surgical procedure have been reported [4–14].

19.2 Changing Trends in Orbital Exenteration

Orbital exenteration is a potentially lifesaving yet mutilating surgery with permanent cosmetic blemish leaving the patients socially uncomfortable. It has been primarily reserved for extensive and infiltrative eyelid, ocular surface, adnexal, and intraocular malignancies with orbital extension and for advanced primary orbital malignancies where conservative treatment is not feasible [15–17]. Non-neoplastic conditions including ROCM constituted only a minority of indications in the previously published reports [4–14].

The COVID-19 pandemic led to an unfortunate rapid rise in the number of cases of ROCM undergoing orbital exenteration. It is possible that some of these patients could be conservatively managed without compromising on life salvage. On the contrary, inappropriate attempts at conservation may have implications on life salvage. Therefore, the treating clinicians need to understand the thin line between adopting conservative management and resorting to radical surgical interventions. The decision to conserve versus exenterate becomes logical if we were to follow a system of staging to evaluate the severity and triage the patients for management as appropriate.

19.3 Stages of ROCM

ROCM typically follows a sequence of evolution from the point of entry (nasal mucosa) to the point of proliferation (paranasal sinuses) with contiguous progression to involve the orbit and intracranial structures. There are non-contiguous routes of spread as well, though rare. Before outlining the management protocol, the clinicians must understand the stages of ROCM as described in Fig. 19.1 [18] which provides a logical

S. G. Honavar (✉) · R. Bansal
Department of Ophthalmic and Facial Plastic Surgery and Ocular Oncology Service, Centre for Sight, Hyderabad, India

N. Gupta, S. G. Honavar (eds.), *Rhino-Orbito-Cerebral Mucormycosis*,
https://doi.org/10.1007/978-981-16-9729-6_19

Proposed Staging of Rhino-Orbito-Cerebral Mucormycosis (ROCM)

Staging of Rhino-Orbito-Cererbral Mucormycosis	Symptoms	Signs	Primary Assessment	Confirmation of Diagnosis
Stage 1: Involvement of the nasal mucosa 1a: Limited to the middle turbinate 1b: Involvement of the inferior turbinate or ostium of the nasolacrimal duct 1c: Involvement of the nasal septum 1d: Bilateral nasal mucosal involvement	Nasal stuffiness, nasal discharge, foul smell, epistaxis	Foul-smelling sticky mucoid or black-tinged, or granular or haemorrhagic nasal discharge, nasal mucosal inflammation, erythema, violaceous or blue discoloration, pale ulcer, anaesthesia, ischmia, eschar	Diagnostic nasal endoscopy, Contrast-enhanced MRI (preferred) or CT-scan	Deep nasal swab or endoscopy-guided nasal swab or nasal mucosal biopsy for direct microscopy, culture and molecular diagnostics; nasal mucosal biopsy for rapid histopathology with special stains
Stage 2: Involvement of paranasal sinuses 2a: One sinus 2b: Two ipsilateral sinuses 2c: > Two ipsilateral sinuses and/or palate/oral cavity 2d: Bilateral paranasal sinus involvement or involvement of the zygoma or mandible	Symptoms in Stage 1 + facial pain,facial edema, dental pain, systemic symptoms (malaise, fever)	Signs in Stage 1 + unilateral or bilateral, localized or diffuse facial edema, edema localized over the sinuses, localized sinus tenderness	Diagnostic nasal endoscopy, Contrast-enhanced MRI (preferred) or CT-scan	Same as Stage 1 + sinus biopsy for direct microscopy, culture and molecular diagnostics and rapid histopathology
Stage 3: Involvement of the orbit 3a: Nasolacrimal duct, medial orbit, vision unaffected 3b: Diffuse orbital involvement (>1 quadrant or >2 structures), vision unaffected 3c: Central retinal artery or ophthamic artery occlusion or superior ophthalmic vein thrombosis; involvement of the superior orbital fissure, inferior orbital fissure, orbital apex, loss of vision 3d: Bilateral orbital involvement	Symptoms in Stage 1 and 2 + painin the eye, proptosis,ptosis, diplopia, loss of vision, infraorbital and facial V1 V2 nerve anesthesia	Signs in Stage 1 and 2 + conjunctival chemoses, isolated ocular motility restriction, ptosis, proptosis, infraorbital nerve anesthesia, central retinal artery occlusion, features of ophthalmic artery occlusion and superior ophthalmic vein thrombosis. V1 and V2 nerve anesthesia, and features of III, IV and VI nerve paisy indicating Orbital apex/superior orbital fissure involvement.	Diagnostic nasal endoscopy, Contrast-enhanced MRI (preferred) or CT-scan	Same as Stage 2 + orbital biopsy if indicated and if feasible (if the disease i predominantly orbital) for direct microscopy, culture and molecular diagnostics and rapid histopathology
Stage 4: Involvement of the CNS 4a: Focal or partial cavernous sinus involvement and/or involvement of the cribriform plate 4b: Diffuse cavernous sinus involvement and/or cavernous sinus thrombosis 4c: Involvement beyond the cavernous sinus, involvement of the skull base, internal carotid artery occlusion, brain infarction 4d: Multifocal or diffuse CNS disease	Symptoms in Stage 1 to 3 + bilateral proptosis paralysis, altered consciousness, focal seizures	Signs in Stage 1-3 (some features overlap with Stage 3) + V1 and V2 nerve anesthesia, ptosis, and features of III, IV and VI nerve palsy indicate cavernous sinus involvement. Bilaterality of these signs with contralateral orbital edema with no clinico-radiological evidence of paranasal sinus or orbital involvement on the contralateral side indicate cavernous sinus thrombosis. Hemiparesis, altered consciousness and focal seizures indicate brain invasion and infarction.	Diagnostic endoscopy, Contrast-enhanced CT Scan, MRI (preferred)	Same as Stage 3

Fig. 19.1 Stages of ROCM 18

representation of clinical severity. Stage 3 and stage 4 constitute orbital mucormycosis.

Optimal management of ROCM requires concerted action and rapid response by a multidisciplinary team of experts in diagnosis (radiology, microbiology, pathology, molecular biology), and medical (infectious disease, neurology, critical care), and surgical (otorhinolaryngology, ophthalmology, neurosurgery) care. Establishing a clinico-radiological assessment to ascertain the extent of disease and confirmation by direct microscopy are the primary steps that help plan the management approach.

19.4 Medical Management of ROCM

Comprehensive guidelines for the medical management of ROCM have been issued by the European Confederation of Medical Mycology (ECMM) and the Mycoses Study Group Education and Research Consortium (MSGERC) [19]. Immediate induction therapy includes intravenous liposomal Amphotericin B 5–10 mg/kg BW with strict metabolic control. In cases with contraindication to Amphotericin B due to impaired renal function, Isavuconazole IV 200 mg thrice a day on days 1–2, 200 mg once a day from day 3; or Posaconazole IV 300 mg twice a day on day 1, 300 mg once a day from day 2 must be given. Continuation of induction therapy with intravenous liposomal Amphotericin B 5–10 mg/kg BW is required for a minimum of 4 weeks, followed by step-down treatment (oral Isavuconazole 200 mg thrice a day on days 1–2, 200 mg once a day from day 3; or oral Posaconazole 300 mg twice a day on day 1, 300 mg once a day from day 2) for 3–6 months or a minimum of 6 weeks following clinico-radiological regression or stabilization [18]. Amphotericin B Deoxycholate or Amphotericin B Lipid Complex may be utilized in patients with good renal function.

19.5 Recommended Treatment Protocol for ROCM with Orbital Involvement

Aggressive debridement of the involved paranasal sinuses constitutes the primary surgical management in cases of ROCM [20]. It can be combined with conservative management of the orbital component, primary orbital exenteration, or deferred orbital surgical intervention. Stage-wise management of orbital mucormycosis has been depicted in Fig. 19.2.

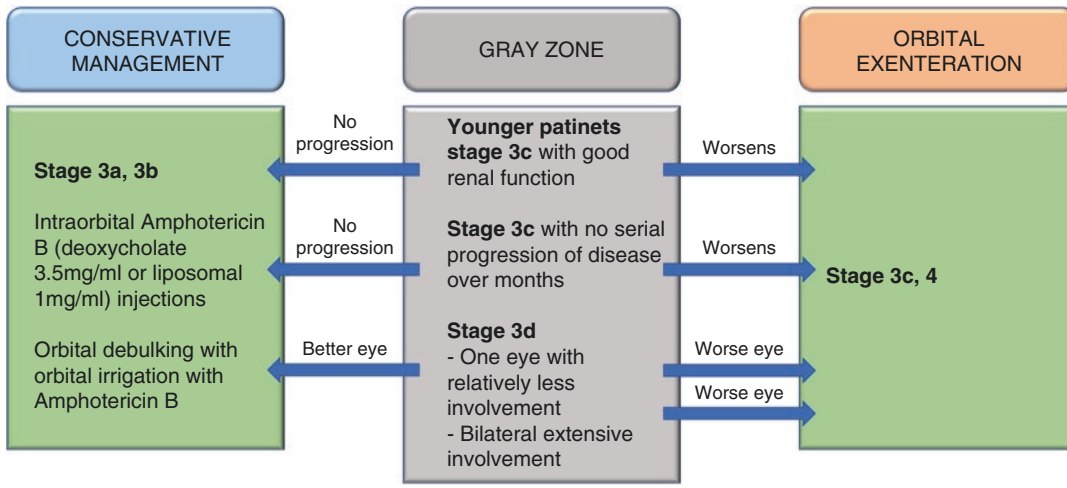

Fig. 19.2 Stage-wise management of orbital mucormycosis

19.6 Conservative Management in ROCM

There are clear indications for conservative management of the orbital disease as follows:

Stage 3a (involvement of the nasolacrimal duct and medial orbit, with unaffected vision): Stage 3a as shown in Fig. 19.3 describes localized orbital involvement, in which it is possible to treat the disease conservatively with medical management as described above along with intraorbital Amphotericin B injection (Deoxycholate Amphotericin B 3.5 mg/mL, Liposomal Amphotericin B 1 mg/mL) specifically to the area of involvement as confirmed by imaging. A series of 7 injections are provided daily or on alternate days depending on clinical severity and response, with clinico-radiological monitoring of response.

Stage 3b (diffuse orbital involvement, >1 quadrant or >2 structures, and unaffected vision): Stage 3b as seen in Fig. 19.4 was managed with intraorbital amphotericin B injections to the areas involved along with concomitant medical management and assessment of response clinico-radiologically and has responded remarkably well. In patients with a suboptimal response after 7 injections, limited orbital debulking is recommended, along with orbital irrigation with Amphotericin B 1 mg/mL.

Results of this approach are variable. Kohn and Helper have established that timely and accurate diagnosis of the extent of involvement attributes to favorable outcomes with conservative management thus avoiding mutilating surgeries and preserving visual acuity [22], and the same has been supported by Pelton et al. [23]. As per Sen et al., in the orbit, diffuse involvement predominated in 40% (674 of 1731) followed by involvement of the medial orbit in 27% (469). Orbital apex was involved in 21% (371) patients [21]. Kashkouli et al. have reported that out of the 34 eyes without exenteration, 41% progressed to complete loss of vision with a final vision survival of 25% in their series [24]. We believe that an accurate assessment of the extent of involve-

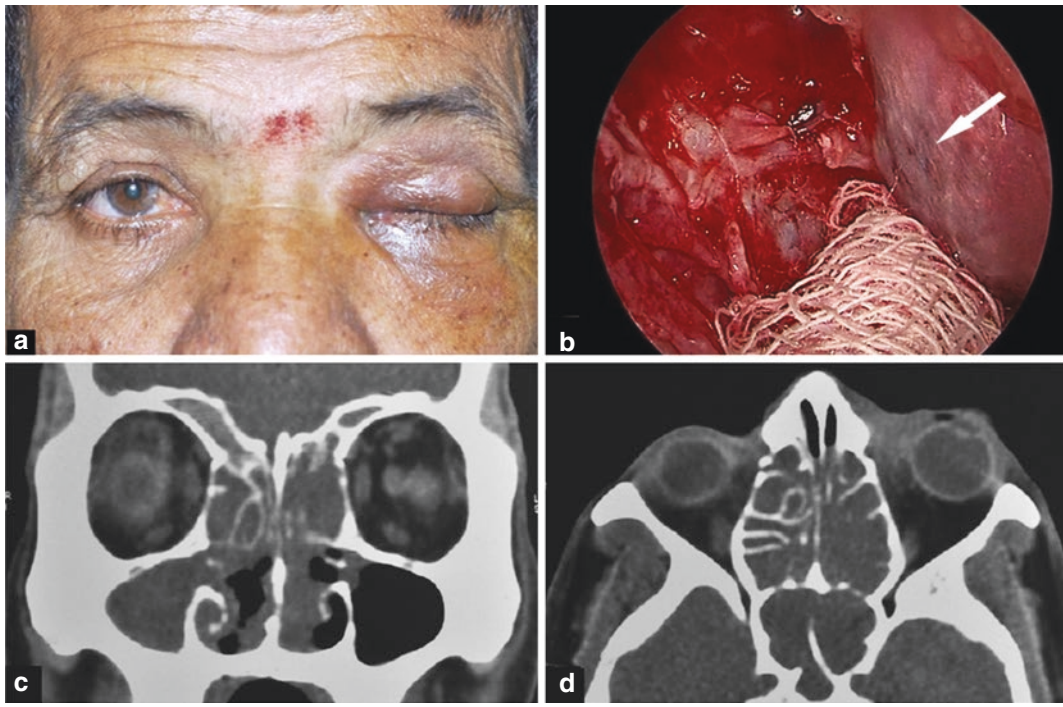

Fig. 19.3 Stage 3a ROCM (**a**) Clinical picture showing left periocular edema, ptosis and proptosis. (**b**) Endoscopy picture showing necrosed left periorbita (arrow). (**c**, **d**) Coronal and axial CT, respectively, showing left eye proptosis with diffuse bilateral paranasal sinus and left medial orbital involvement (Courtesy: Sen M et al. [21])

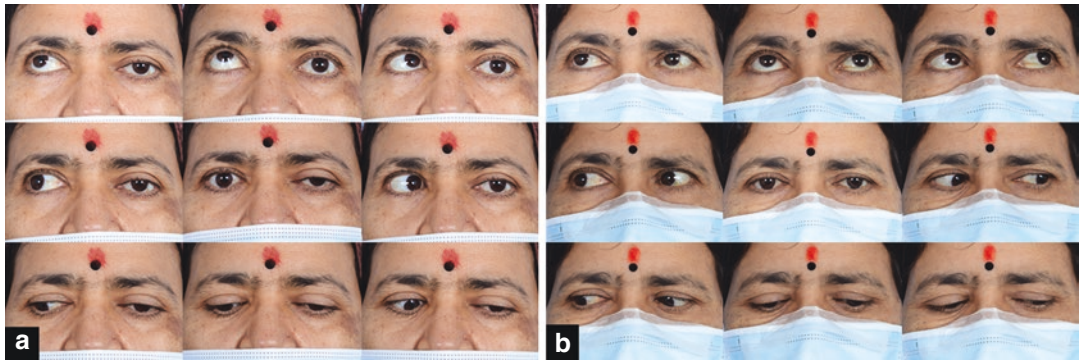

Fig. 19.4 Stage 3b ROCM: (**a**) A 56-year-old lady presented to us with left eye BCVA of light perception only, ptosis of 3 mm, restriction of movements in all directions with radiological evidence of involvement in the superomedial and inferomedial aspect. (**b**) After a series of seven injections of intraorbital Amphotericin B, she had complete resolution of symptoms and signs along with BCVA of 20/40 at the latest follow-up 5 months and interval decrease in the medial orbital involvement on MRI

ment and intraorbital Amphotericin B targeted to the area of involvement, early identification of poor responders and orbital exenteration in that subset are the keys to the success of this approach. Murthy et al. have reported 111 cases of ROCM treated conservatively with no recurrence for 3 months and not requiring orbital exenteration despite complete loss of vision (in five cases), thus avoiding mutilating surgeries [25].

19.7 Orbital Exenteration in ROCM

There are specific indications for orbital exenteration as follows:

Stage 3c (central retinal artery or ophthalmic artery occlusion or superior ophthalmic vein thrombosis; involvement of superior orbital fissure, inferior orbital fissure, orbital apex, loss of vision): This stage (Fig. 19.5) is a specific indication for orbital exenteration with continued medical management. Moorthy et al. have ascertained that an aggressive surgical approach reduces disease burden in these cases with irreversible blindness [26].

Stage 3d (bilateral orbital involvement): This stage requires a comparative analysis of orbital involvement (Fig. 19.6). Bilateral exenteration is not recommended and therefore, intraorbital Amphotericin B to the relatively better orbit along and exenteration of the more severely involved orbit is advised. Kashkouli et al. have reported four such patients in whom two cases were operated on for unilateral exenteration and another eye was left as blind eye and in the other two cases both eyes were left without any surgical intervention [24].

Stage 4 (central nervous system involvement): Sen et al. noted that in the CNS, cavernous sinus was most commonly involved in 53% (285 of 539), bilateral CNS involvement in 5% (133 of 2669) cases with cavernous sinus being the most common route of spread (70%, 299 of 430).

Even though in these cases (Fig. 19.7), the disease has progressed to involve the central nervous system, it has been observed that timely orbital exenteration results in faster recovery and halts the disease progression as is shown by Kashkouli et al. in their series of 79 eyes of 63 patients [24]. Jung et al. have stated that control of the underlying predisposing illness, prompt medical management, and aggressive surgical intervention decreases mortality [27].

19.8 Gray Zone

There are certain situations where cautious conservative measures can be employed:

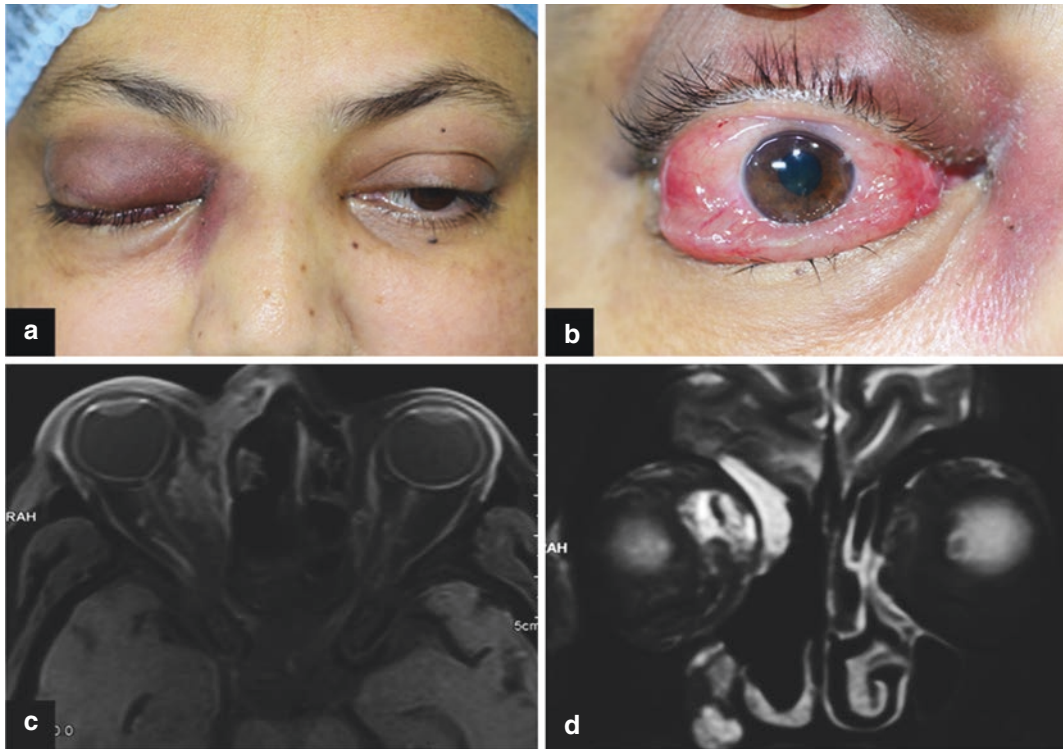

Fig. 19.5 Stage 3c ROCM (**a**) Clinical picture showing right eye ptosis, periocular edema, and ecchymosis. (**b**) Severe conjunctival congestion and chemosis. (**c**) Axial MRI (T1) of orbit and paranasal sinuses showing diffuse orbital involvement along with diffuse paranasal sinus involvement (s/p right paranasal sinus debridement and turbinectomy). (**d**) Coronal MRI (T2) showing unilateral diffuse right orbital involvement (Courtesy: Sen M et al. [21])

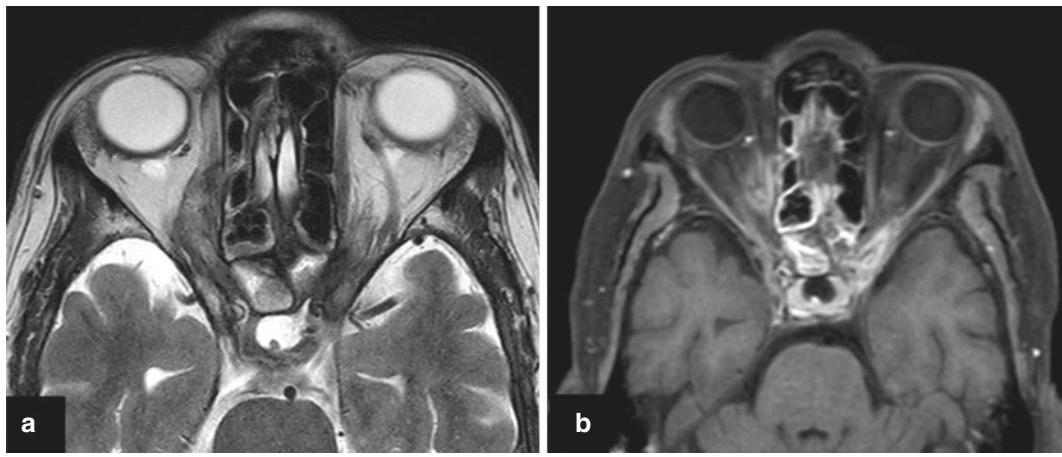

Fig. 19.6 Stage 3d ROCM (**a**) Axial MRI (T2) and (**b**) contrast enhanced (T1) of the orbit and paranasal sinuses showing bilateral orbital apical involvement, more extensive on the right side (Courtesy: Sen M et al. [21])

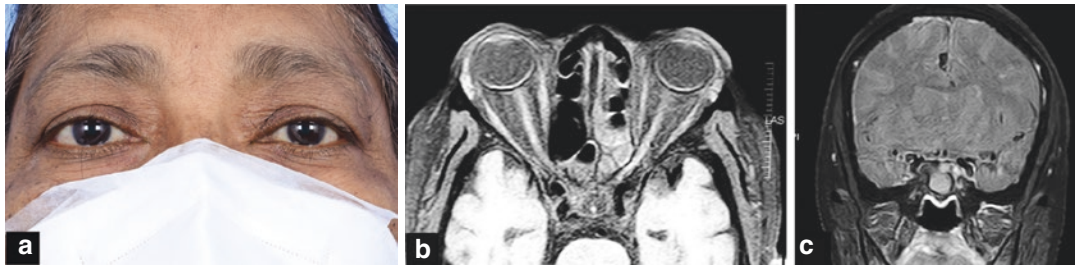

Fig. 19.7 Stage 4b ROCM (**a**) Clinical picture showing no significant ocular manifestation, however, (**b**) Axial MRI (T1) of the orbit, paranasal sinuses and brain showed diffuse paranasal sinus involvement along with (**c**) Coronal view (T1) showing extension into the cavernous sinus via the pterygopalatine fossa (Courtesy: Sen M et al. [21])

1. Younger patients with stage 3c or 3d with good renal function can be treated conservatively with intraorbital Amphotericin B, limited orbital debulking with close clinico-radiological monitoring, which on worsening can be triaged to orbital exenteration. Those improvement or stability can be continued on conservative treatment.
2. Young patients with bilateral orbital involvement (stage 3d) can be treated conservatively with intraorbital Amphotericin B, limited orbital debulking with close clinico-radiological monitoring.
3. Patients with extensive orbital invasion who cannot undergo immediate orbital exenteration due to coexistent uncontrolled comorbidities or continuing COVID-19-associated respiratory derangements.

Sen et al. reported that ROCM covers a wide range of age groups with a mean of 51.9 years (range, 12–88 years) [21], therefore, the decision about radical surgical interventions becomes difficult for the clinicians as well as for the families. It is imperative to weigh the advantages and disadvantages before making a decision (Fig. 19.8).

19.9 Prognosis

Hargrove et al. in an extensive literature review have stated that patients with ROCM with age >46 years, frontal sinus involvement, and fever had bleak chances of survival whereas patients treated with Amphotericin B had a better survival rate and that exenteration increases the likelihood of survival [28]. We have observed that out of 2826 cases assessed, the ocular outcome was available for 1838 patients, 16% (289) had orbital exenteration and in 84% (1549), the eye could be salvaged. With the protocol mentioned above, eye salvage was achieved in 100% (50 of 50) in stage 3a, 98% (81 of 83) in 3b, 83% (97 of 117) in 3c, 77% (10 of 13) in 3d, 71% (24 of 34) in 4a, 79% (11 of 14) in 4b, 82% (22 of 27) in 4c, and 67% (8 of 12) in 4d [21].

Multiple case series have reported a variable outcome including no effect to increased patients' survival [4, 23, 29, 30] to a significant decrease in survival rate [27, 28].

19.10 Challenges in Future

As the treatment entails a significant financial burden due to prolonged hospital stay, repeated radiological investigations, long recovery burden, maintenance therapy, and reconstructive surgeries, it leaves a major impact on the family. Psychological and cosmetic rehabilitation in patients undergoing orbital exenteration due to ROCM has to be handled delicately [31]. Dedicated counseling sessions are recommended for the ROCM survivors as they undergo multiple surgeries with long-term health-related issues within a short period [32].

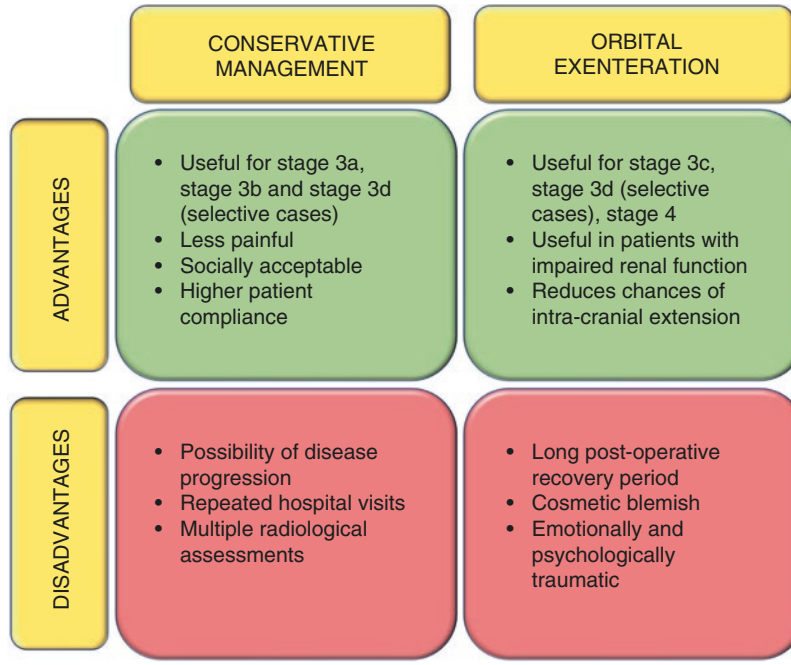

Fig. 19.8 Advantages and disadvantages of conservative treatment versus orbital exenteration

19.11 Conclusion

Among the cases of ROCM, a stage-based treatment protocol has been advocated which includes conservative management for stage 3a, stage 3b, and orbital exenteration for cases with stage 3c, stage 3d, and stage 4. There is, however, a gray zone, wherein for young patients with stage 3c and 3d ROCM, a cautious conservative approach can be considered. A balanced approach must be followed which comprises of a multidisciplinary team, accurate primary assessment of the extent of the disease, close monitoring of treatment response and disease progression by clinico-radiological assessment coupled with holistic consideration of psychological, social, and economical aspects helping in taking the decision for conservative treatment versus orbital exenteration.

References

1. Bartisch G. Ophthalmodouleia-das ist Augendienst. Matthes Sto¨ckel, Dresden 1583.
2. Golovine SS. Orbito-sinus exenteration. Ann Ocul. 1909;141:413–31.
3. Coston TO, Small RG. Orbital exenteration--simplified. Trans Am Ophthalmol Soc. 1981;79:136–52.
4. Bartley GB, Garrity JA, Waller RR, Henderson JW, Ilstrup DM. Orbital exenteration at the Mayo Clinic. 1967-1986. Ophthalmology. 1989;96(4):468–73.
5. Naquin HA. Exenteration of the orbit. AMA Arch Ophthalmol. 1954;51(6):850–62.
6. Ben Simon GJ, Schwarcz RM, Douglas R, Fiaschetti D, McCann JD, Goldberg RA. Orbital exenteration: one size does not fit all. Am J Ophthalmol. 2005;139(1):11–7.
7. Spaeth EB. Information learned from fifty years of orbital exenteration. Trans Ophthalmol Soc U K. 1971;91:611–34.
8. Rathbun JE, Beard C, Quickert MH. Evaluation of 48 cases of orbital exenteration. Am J Ophthalmol. 1971;72(1):191–9.
9. Nagendran ST, Lee NG, Fay A, Lefebvre DR, Sutula FC, Freitag SK. Orbital exenteration: the 10-year Massachusetts eye and ear infirmary experience. Orbit Amst Neth. 2016;35(4):199–206.
10. Rahman I, Cook AE, Leatherbarrow B. Orbital exenteration: a 13 year Manchester experience. Br J Ophthalmol. 2005;89(10):1335–40.
11. Mohr C, Esser J. Orbital exenteration: surgical and reconstructive strategies. Graefes Arch Clin Exp Ophthalmol Albrecht Von Graefes Arch Klin Exp Ophthalmol. 1997;235(5):288–95.
12. Levin PS, Dutton JJ. A 20-year series of orbital exenteration. Am J Ophthalmol. 1991;112(5):496–501.

13. Kasaee A, Eshraghi B, Nekoozadeh S, Ameli K, Sadeghi M, Jamshidian-Tehrani M. Orbital exenteration: a 23-year report. Korean J Ophthalmol KJO. 2019;33(4):366–70.
14. Shields JA, Shields CL, Demirci H, Honavar SG, Singh AD. Experience with eyelid-sparing orbital exenteration: the 2000 Tullos O. Coston lecture. Ophthal Plast Reconstr Surg. 2001;17(5):355–61.
15. Hoffman GR, Jefferson ND, Reid CBA, Eisenberg RL. Orbital exenteration to manage infiltrative sinonasal, orbital adnexal, and cutaneous malignancies provides acceptable survival outcomes: an institutional review, literature review, and meta-analysis. J Oral Maxillofac Surg. 2016;74(3):631–43.
16. Maheshwari R. Review of orbital exenteration from an eye care centre in Western India. Orbit Amst Neth. 2010;29(1):35–8.
17. Ackuaku-Dogbe E. Review of orbital exenterations in Korle-Bu teaching hospital. Ghana Med J. 2011;45(2):45–9.
18. Honavar SG. Code mucor: guidelines for the diagnosis, staging and management of rhino-orbito-cerebral mucormycosis in the setting of COVID-19. Indian J Ophthalmol. 2021;69(6):1361–5.
19. Cornely OA, Alastruey-Izquierdo A, Arenz D, Chen SCA, Dannaoui E, Hochhegger B, et al. Global guideline for the diagnosis and management of mucormycosis: an initiative of the European Confederation of Medical Mycology in cooperation with the Mycoses Study Group Education and Research Consortium. Lancet Infect Dis. 2019;19(12):e405–21.
20. Sundaram N, Bhende T, Yashwant R, Jadhav S, Jain A. A review on outbreak of Mucormycosis in the COVID-19 patients. Indian J Ophthalmol. 2021;69(12):3728–33.
21. Sen M, Honavar SG, Bansal R, Sengupta S, Rao R, Kim U, et al. Epidemiology, clinical profile, management, and outcome of COVID-19-associated rhino-orbital-cerebral mucormycosis in 2826 patients in India – collaborative OPAI-IJO study on mucormycosis in COVID-19 (COSMIC), report 1. Indian J Ophthalmol. 2021;69(7):1670–92.
22. Kohn R, Hepler R. Management of limited rhino-orbital mucormycosis without exenteration. Ophthalmology. 1985;92(10):1440–4.
23. Pelton RW, Peterson EA, Patel BC, Davis K. Successful treatment of rhino-orbital mucormycosis without exenteration: the use of multiple treatment modalities. Ophthal Plast Reconstr Surg. 2001;17(1):62–6.
24. Kashkouli MB, Abdolalizadeh P, Oghazian M, Hadi Y, Karimi N, Ghazizadeh M. Outcomes and factors affecting them in patients with rhino-orbito-cerebral mucormycosis. Br J Ophthalmol. 2019;103(10):1460–5.
25. Murthy R, Bagchi A, Gote YS. Role of medial orbital wall decompression in rhino-orbital mucormycosis management. Indian J Ophthalmol. 2021;69(12):3795–6.
26. Moorthy A, Gaikwad R, Krishna S, Hegde R, Tripathi KK, Kale PG, et al. SARS-CoV-2, uncontrolled diabetes and corticosteroids-an unholy trinity in invasive fungal infections of the maxillofacial region? A retrospective, multi-centric analysis. J Maxillofac Oral Surg. 2021;6:1–8.
27. Jung S-H, Kim SW, Park CS, Song CE, Cho JH, Lee JH, et al. Rhinocerebral Mucormycosis: consideration of prognostic factors and treatment modality. Auris Nasus Larynx. 2009;36(3):274–9.
28. Hargrove RN, Wesley RE, Klippenstein KA, Fleming JC, Haik BG. Indications for orbital exenteration in mucormycosis. Ophthal Plast Reconstr Surg. 2006;22(4):286–91.
29. Peterson KL, Wang M, Canalis RF, Abemayor E. Rhinocerebral mucormycosis: evolution of the disease and treatment options. Laryngoscope. 1997;107(7):855–62.
30. Ketenci I, Unlü Y, Kaya H, Somdaş MA, Kontaş O, Oztürk M, et al. Rhinocerebral mucormycosis: experience in 14 patients. J Laryngol Otol. 2011;125(8):e3.
31. Ackuaku-Dogbe EM, Biritwum RB, Briamah ZI. Psycho-social challenges of patients following orbital exenteration. East Afr Med J. 2012;89(12):385–9.
32. Sikka K, Goel G, Sharma N, Thakar A. Initial and ongoing challenged with COVID-19 associated Mucormycosis. Indian J Ophthalmol. 2021;69(12):3391–3.

20 Debates in Rhino-Orbito Cerebral Mucormycosis (ROCM): Classification Dilemmas

Nishi Gupta, Satish Jain, and Poonam Singla

Rhino-orbito-cerebral mucormycosis (ROCM) is an invasive fungal infection often found in immunocompromised individuals. The mucor is thought to inoculate the nasal cavity first and then spread to the sinuses, orbit and intracranial space [1–5]. Orbital apex allows further intracranial dissemination and cavernous sinus involvement [1]. Several classifications of ROCM have been published by various authors based on this premise [6–10]. They proposed varying degree of resection based on individual criteria. However, the recommendations lack uniformity, and the surgical management remains difficult due to frequent residual/recurrent disease that need multiple debridements. In the current outbreak, surgical debridement sessions ranged from one to seven. (More information about the pattern of the residual or recurrent disease have been provided in a separate chapter).

As a result, staging based on the anticipated route of spread has proved ineffective. Each author classified ROCM into several stages with each step being further subdivided [6–10]. The authors have provided evidence to support their classification, resulting in various classifications, and confusion among the readers.

Our recent experience with ROCM cases has shown us that different classifications lack practical utility in the management of ROCM. Because of the disease's perineural dissemination and angioinvasive nature, the staging system may not provide a clear management approach due to many paths of transmission and normal intervening areas.

There are many unanswered questions in the proposed route of spread on which the staging systems are based. The proposed route of spread does not explain why the retrobulbar space is primarily occupied with the disease with no mucor in the maxillary or ethmoid group of sinuses. It does not explain why there are acute orbital signs in the absence of any sinonasal manifestations. It fails to explain why there is facial numbness, pain and edema. This suggested route of mucor dissemination fails to explain why intensive debridement fails in some cases [1].

As a result in ROCM surgery, evidence-based decisions are more important than predetermined resections based on multiple classifications. In the patients of ROCM mapping was performed on various MRI sequences. The MRI parameters tested were consistent with what has been described in the chapter on imaging in ROCM. Pterygopalatine fossa (PPF) was found to be involved in the majority of our cases. This was consistent with the findings of Hosseni et al. who identified PPF to be the major reservoir of mucor in 100 percent of their

N. Gupta (✉) · P. Singla
Dr Shroff's Charity Eye Hospital, New Delhi, India

S. Jain
Jain ENT Hospital, Jaipur, India

N. Gupta, S. G. Honavar (eds.), *Rhino-Orbito-Cerebral Mucormycosis*,
https://doi.org/10.1007/978-981-16-9729-6_20

cases [1]. It acts as an area for the hidden disease but has been ignored in most classifications. The involvement of PPF has its own implication that must be carefully examined. The involvement of the nasal mucosa in the form of blackish discoloration for example is considered an early sign of the disease, placing it in the lower stage. This black necrosis on the other hand does not necessarily indicate the disease inoculation at this location. It could be caused by thrombosis of the sphenopalatine artery in the pterygopalatine fossa culminating in terminal vessel necrosis [1].

These limited symptoms of nasal cavity and sinuse involvement could be the only symptoms of Isolated involvement of the pterygopalatine fossa [1]. It is possible that putting it in stage 1 and planning a limited resection may leave the residual disease that will likely progress. It highlights the importance of PPF debridement particularlly in situations involving orbits.

20.1 Prognostic Parameters in ROCM

Because ROCM is a non-classifiable angioinvasive disease, stage-based resection is not recommended. We can only have really useful prognostic parameters. These criteria are based on the areas that serve as a control point between a favourable and unfavourable prognosis in extracranial and Intracranial spread.

Extracranial Spread:

1: Orbital involvement (orbital apex spared).
2: Orbital apex involvement (one of the gateways to the intracranial space).
3: Sphenoid wing/clivus (one of the gateways to meningitis and chances of deep skull base infiltration). Extracranial areas other than those mentioned above have better prognosis provided pterygopalatine fossa is cleared wherever needed. Those areas mentioned here need to be handled meticulously to prevent spread of disease into the brain.

Intracranial spread:

1: Initial dural involvement.
2: Isolated intracranial abscess.
3: Disseminated intracranial spread.

In intracranial disseminated involvement has worst prognosis. This method of classifying the condition offers a number of advantages. It allows us to focus on the most important areas that are sometimes overlooked during primary surgery. PPF is a crucial structure that needed clearance in a majority of cases during the current outbreak. Therefore Denker's modified medial maxillectomy is a critical surgical step that every otorhinolaryngologist interested in the management of ROCM must learn [11]. A stepwise approach to PPF has been described in the chapter on the surgical management of ROCM; approach to PPF, pterygoid process, and infratemporal fossa.

The involvement of the orbital apex, sphenoid wing, and clivus marks the transition from good to guarded/bad prognosis. This is because direct invasion of the skull base and intracranial structures occurs in all of these sites. The surgeon is guided by the requirement to analyse these critical areas to perform essential radiological investigations, including various MRI sequences. In ROCM precise drilling enhances results significantly. The steps of drilling have been mentioned in the chapter on surgical management of ROCM: drilling beyond sinuses.

ROCM's recommended classifications do not work, and stage-based management may complicate the situation. The above-mentioned prognostic factors were developed based on the extensive experience with primary and revision ROCM cases during this pandemic.

The PPF and the bone of the sphenoid sinus floor were main sites left untreated during earlier procedures. During endoscopic debridement, the shenoid sinuses are frequently cleared, and at the end, a clean looking sinus cavity is left with no indication of the bone involvement.

The same patient's preoperative MRI revealed that there were subtle signs of bone erosion in this area prior to the first surgery as well.

However, the condition progressed and postoperative MRI revealed that the sphenoid wing was implicated. This became a priority region for us to search for on MRI in subsequent cases so that it could be cleared in the first sitting itself.

This prognostic classification highlights some crucial areas allowing us to look for them on various CT and MRI sequences to assist complete the debridement of necrotic areas. One may argue that there are other areas of the spread of disease to the intracranial structure; however, each one has a different dimension and has been described separately in various chapters on the area-by-area management of various case-based scenarios.

The involvement of sphenoid wing and orbital apex in extracranial spread indicates that these two locations should be cleared in the first sitting by a more experienced surgeon.

20.2 Why Doesn't a Fixed Classification Based on a Fixed spread Route Work?

The following are the reasons for this:

- Staging can lead to bias because it's a medical disease. It has angioinvasive spread and cannot be resected based on dissemination.
- It is not like malignancy which has a well defined path of spread. There are multiple pathways of spread in ROCM that are difficult to predict, so they cannot be classified.
- Consider disorders such as Juvenile nasopharyngeal angiofibroma. Its classification is useful because the disease progression follows a predictable pattern that guides the surgical planning [12]. For example, in stage 1 no Denker's medial maxillectomy is needed [11, 12], and no embolization is required (as it is Limited to the nasopharynx and nasal cavity). Stage 2, requires Denker's surgery (because the disease has spread to the pterygopalatine fossa), stage 3 requires embolization (because the disease has spread to the infratemporal fossa or orbital region with intracranial extradural involvement), and stage 4 is more extensive with Intracranial intradural spread with or without infiltration of the cavernous sinus, pituitary fossa, or optic chiasma [12, 13]. As a result neurosurgeon as well as an interventional radiologist are required. In contrast to mucormycosis angiofibroma always grows in the same direction.
- Mucor has a hematogenous spread; the outcome is determined by drug sensitivity and penetration rather than stage. Even third and fourth stage disorders will recover if drug sensitivity is present. The prognosis is excellent in cases where mucor is responsive to amphotericin B even in advanced disease. If mucor is resistant to amphotericin B, the prognosis is bad even in the early stages of disease. As a result classification-based surgical planning is not useful when it comes to selecting how to treat ROCM surgically.
- Each drug's minimal inhibitory concentration is different, which the treating surgeon is unaware of. There are 21 species of the mucor, but only three medicines are available: amphotericin, posaconazole, and isavuconazole. As described in the chapter on future directions in the management of ROCM, Amphotericin B is the most potent drug against mucormycetes, with MICs lower than 0.5 mg/L and [14]. Posaconazole is the second-line drug that has the highest activity among the azoles, with a MIC value of 0.5 mg/L [14]. However, drug resistance was noted in our cases, like reported by Drogari-Apiranthitou et al. [14].
- Drug resistance in mucormycosis leads to poor outcomes. Drogari-Apiranthitou et al. found resistance to amphotericin B in five Rhizopus species with minimum inhibitory concentrations of ≥2 mg/L (against the usual 0.5 mg/L). Resistance to posaconazole was observed in three *Rhizopus* species with minimum inhibitory concentrations ≥4 mg/L (against the usual0.5 mg/L), of which one was also resistant to amphotericin B [14]. In a series of 409 cases of ROCM, we found drug resistance in about 10% of cases.

20.3 Reason for Prognosis-Based Parameters and Ways to Improve Outcomes

- This disease can spread at anytime from Grade 1 to Grade 4.
- The disease does not always manifest in the nose and sinuses after inoculation. To begin with it can directly damage any structure, such as the eye, palate, and brain. It can strike any of these places any moment, and each patient's pattern will be unique.
- Although prognosis depends on the crucial areas affected; the species of the mucor involved and its sensitivity to amphotericin B are equally important. Therefore, based on current classifications, stage 1 may have a poorer prognosis than stage 2.
- An adequate clearance is required for better prognosis, and an expert surgeon is required to access difficult locations such as the floor of the sphenoid sinus, pterygoid process, and clivus. Because surgeons will be hesitant to clear this area for the fear of injuring the internal carotid artery, a full debridement may not be possible leading to poor prognosis.
- The difference in intracranial and extracranial spread is that the drug penetration is questionable in the brain due to the blood–brain barrier.

It is feasible to take specific aspects from each classification and evaluate their advantages and disadvantages in detail. However, that is not our goal; rather, we want to provide some best practises for dealing with this disease. Based on MRI findings, the surgeons are expected to be much more aggressive with this condition. For most of us this epidemic has been a completely new experience as well as an opportunity to work as a team. The mainstay of treatment remains MRI knowledge, thorough debridement and medication susceptibility and sensitivity.

References

1. Hosseini SMS, Borghei P. Rhinocerebral mucormycosis: pathways of spread. Eur Arch Otorhinolaryngol. 2005;262:932–8. https://doi.org/10.1007/s00405-005-0919-0.
2. Hussain S, Salahuddin N, Ahmad I, Salahudin I, Jooma R. Rhinocerebral invasive mycosis: occurrence in immunocompetent individuals. Eur J Radiol. 1995;20:151–5.
3. Pelton RW, Peterson EA, Patel BC, Davis K. Successful treatment of rhino-orbital mucormycosis without exenteration: the use of multiple treatment modalities. Ophthal Plast Reconstr Surg. 2001;17:62–6.
4. Onerci M, Gursel B, Hosal S, Gulekon N, Gokoz A. Rhinocerebral mucormycosis with extension to the cavernous sinus. A case report. Rhinology. 1991;29:321–4.
5. Raj P, Vella EJ, Bickerton RC. Successful treatment of rhinocerebral mucormycosis by a combination of aggressive surgical debridement and the use of systemic liposomal amphotericin B and local therapy with nebulized amphotericin—a case report. J Laryngol Otol. 1998;112:367–70.
6. Honavar SG. Code mucor: guidelines for the diagnosis, staging and management of rhino-orbito-cerebral mucormycosis in the setting of COVID-19. Indian J Ophthalmol. 2021;69(6):1361–5. https://doi.org/10.4103/ijo.IJO_1165_21.
7. Naik MN, Rath S. The ROC staging system for COVID-related rhino-orbital-cerebral mucormycosis. Semin Ophthalmol. 2021; https://doi.org/10.1080/08820538.2021.1946094.
8. Shah K, Dave V, Bradoo R, Shinde C, Prathibha M. Orbital exenteration in rhino-orbito-cerebral mucormycosis: a prospective analytical study with scoring system. Indian J Otolaryngol Head Neck Surg. 2019;71(2):259–65. https://doi.org/10.1007/s12070-018-1293-8.
9. Talmi YP, Goldschmied-Reouven A, Bakon M, Barshack I, Wolf M, Horowitz Z, Berkowicz M, Keller N, Kronenberg J. Rhino-orbital and rhino-orbito-cerebral mucormycosis. Otolaryngol Head Neck Surg. 2002;127(1):22–31. https://doi.org/10.1067/mhn.2002.126587.
10. Wali U, Balkhair A, Al-Mujaini A. Cerebro-rhino orbital mucormycosis: an update. J Infect Public Health. 2012;5(2):116–26. https://doi.org/10.1016/j.jiph.2012.01.003.
11. Upadhyay S, Dolci RL, Buohliqah L, Prevedello DM, Otto BA, Carrau RL. Endoscopic endonasal anterior maxillotomy. Laryngoscope. 2015;125(12):2668–71. https://doi.org/10.1002/lary.25205.

12. Andrews JC, Fisch U, Valavanis A, Aeppli U, Makek MS. The surgical management of extensive nasopharyngeal angiofibromas with the infratemporal fossa approach. Laryngoscope. 1989;99(04):429–37.
13. Safadi A, Schreiber A, Fliss DM, Nicolai P. Juvenile angiofibroma: current management strategies. J Neurol Surg B Skull Base. 2018;79(1):21–30. https://doi.org/10.1055/s-0037-1615810.
14. Drogari-Apiranthitou M, Mantopoulou FD, Skiada A, Kanioura L, Grammatikou M, Vrioni G, Mitroussia-Ziouva A, Tsakris A, Petrikkos G. In vitro antifungal susceptibility of filamentous fungi causing rare infections: synergy testing of amphotericin B, posaconazole and anidulafungin in pairs. J Antimicrob Chemother. 2012;67(8):1937–40. https://doi.org/10.1093/jac/dks137.

21 Debates in Rhino-Orbito-Cerebral Mucormycosis: Orbital Disease Management Dilemma

Nishi Gupta, Satish Jain, and Poonam Singla

Management of the orbital disease in rhino-orbito-cerebral mucormycosis (ROCM) remains a dilemma. With the endoscopic method, restricted debridement of the affected area is more feasible. Managing orbital disease in a large series of ROCM cases gave us some useful information.

The extent of orbital clearance is still up for debate. Literature supports aggressive surgical management to improve survival [1–6] except for some authors who support no orbital intervention in a few selected cases [3, 7]. The decision to exenterate is difficult when vision is preserved or the ophthalmoplegia is not complete [1, 8–10].

A team of surgeons and radiologists can map the full extent of disease with good imaging facilities. The spread of disease from the orbit to the cavernous sinus is a serious concern that has a substantial impact on the prognosis. That is why the issue over no intervention versus limited orbital debridement or orbital exenteration is so important [11]. Any disease in orbit that is not treated will inevitably increase the chance of involvement of the cavernous sinus. Contiguous spread from the sinuses and orbits cause involvement of the central nervous system (CNS) [11] or it might manifest as isolated CNS involvement with hematogenous spread from distant places [11]. The orbital apex on the other hand is a clear path for the disease to travel from orbit to the brain.

The orbital apex (OA) is the narrowest part of the orbit connecting it to intracranial structures [12]. The superior orbital fissure and the optic canal make up the bony OA (Fig. 21.1). The optic nerve and the ophthalmic artery are housed in the optic canal, which is located in the superomedial region of the orbital apex. Optic strut is a piece of bone that separates superior orbital fissure from the optic nerve [12] (Fig. 21.2).

The important structures related to the orbital apex are the cavernous sinus that is located posterior to the superior orbital fissure (SOF). Cranial nerves III, IV, VI & ophthalmic (VI) branch of

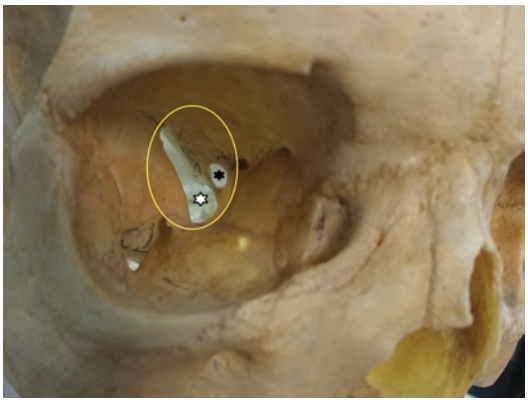

Fig. 21.1 Skull photograph demonstrating the orbital apex (OA) consisting of the superior orbital fissure (SOF) (white star) and the optic canal (black star)

N. Gupta (✉) · P. Singla
Dr Shroff's Charity Eye Hospital, New Delhi, India

S. Jain
Jain ENT Hospital, Jaipur, India

N. Gupta, S. G. Honavar (eds.), *Rhino-Orbito-Cerebral Mucormycosis*,
https://doi.org/10.1007/978-981-16-9729-6_21

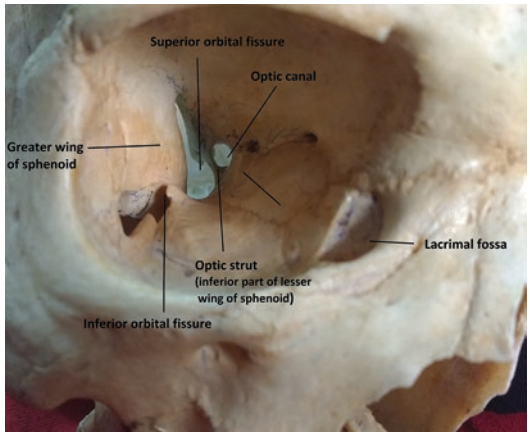

Fig. 21.2 Skull photograph demonstrating optic strut, a bony ledge that separates SOF from the optic canal

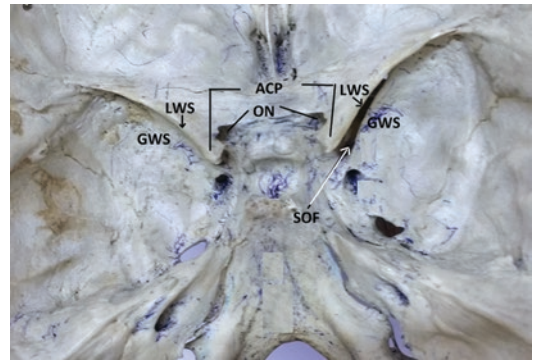

Fig. 21.4 Intracranial surface of the skull showing OA and its relation. *ACP* Anterior clinoid process, *ON* Optic nerve canal, *LWS* Lesser wing of sphenoid, *GWS* Greater wing of the sphenoid

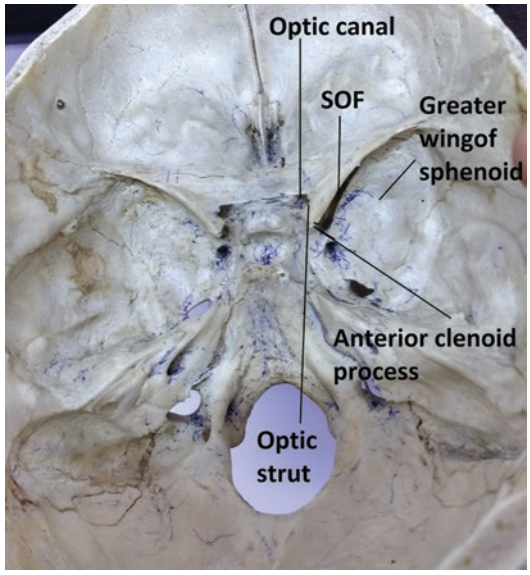

Fig. 21.3 Skull photograph, intracranial surface showing the OA, the relation of SOF, optic canal, greater wing of the sphenoid and cavernous sinus area

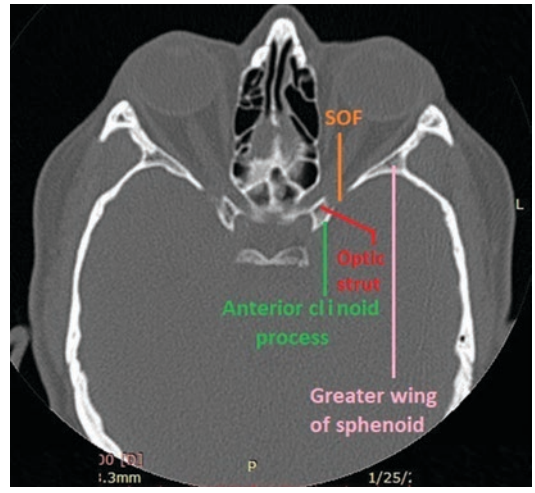

Fig. 21.5 CT scan axial section showing OA and its relations

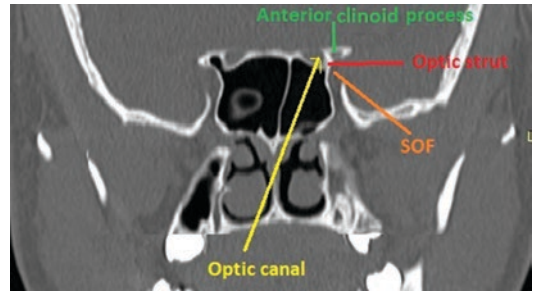

Fig. 21.6 Coronal CT showing SOF, optic canal, anterior clinoid process, and optic strut

trigeminal nerve pass through superior orbital fissure [13]. The symptoms of orbital apex syndrome include vision loss and ophthalmoplegia. Because SOF, OA (SOF + optic canal), and cavernous sinus are so close together, the disease from SOF to OA to cavernous sinus happens quickly, with overlapping symptoms resulting in three syndromes, SOF syndrome, cavernous sinus syndrome, and OA syndrome [13, 14] (Figs. 21.3, 21.4, 21.5, and 21.6). OA is the most crucial area that is often The most important factor to consider when deciding whether to debride the orbit radically or conservatively is OA.

Endoscopic debridement of sinuses is the most critical part of ROCM surgery. The need for orbital clearance during the same sitting raises some of the questions listed below.

21.1 Should the Lamina Papyracea Be Opened

This question arises in circumstances of extremely limited ocular disease, because in cases of severe orbital disease, the answer is obvious. In case of restricted disease, the patient may have little or no eye symptoms, yet an MRI of the orbit reveals illness. If an MRI indicates that a disease is present in the orbit, the lamina papyracea must be opened. However, it is necessary to be able to distinguish basic inflammation/infection from fungal disease in the orbit. The best way to diagnose ocular illness is to use a contrast-enhanced MRI that detects loss of contrast. T2W MRI will reveal enhancement in infection, whereas contrast enhanced MRI will show loss of enhancement, suggesting the need to open up the lamina payracea. The lamina papyracea can be removed easily using a blunt dissector and, the periorbita is incised. Allow the fat to prolapse; this helps identifying the diseased tissue much easier. The fat can be teased; the orbital tissues are retracted laterally by the assistant, and an angled endoscope is employed. If there is a disease in orbit on MRI in areas with loss of contrast, they should be identified and looked for intraoperatively. In case of a limited disease, distinguishing between the healthy and unhealthy fat may be difficult. MRI on the other hand provides information on disease's location in the orbit.

21.2 Mapping of the Orbital Disease on MRI

Orbital disease can be detected in three ways

1. Perioptic cerebrospinal fluid space
2. T2W fat-suppressed imaging
3. Diffusion-weighted MRI.

21.2.1 Perioptic Cerebrospinal Fluid Space

Perioptic cerebrospinal fluid space is the area between the optic nerve and the meningeal sheath covering it (Fig. 21.7). Enhancement of this space on the T2W sequence indicates a normal optic

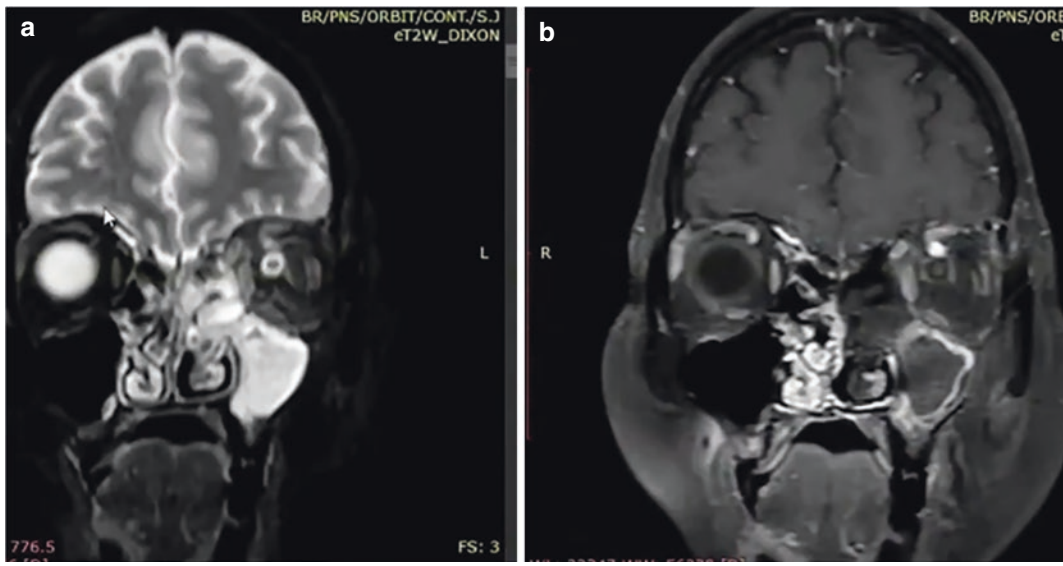

Fig. 21.7 (**a**) T2W fat-suppressed MRI showing left perioptic space enhancement. (**b**) Extensive disease on the left side involving ethmoids, left orbit, reaching up to the skull base

nerve. This space should be looked for from the anterior to the posterior as sometimes this perioptic space is normal in anterior cuts. As we go posteriorly, the space enhancement disappears in massive orbital disease (Fig. 21.8). The best MRI sequences for orbital disease mapping are T2W FS. After the fat is suppressed, any area that shows enhancement indicates disease. It is easy to distinguish between minimal disease and a massive orbital disease, making it easy to determine the extent of debridement (Figs. 21.9 and 21.10).

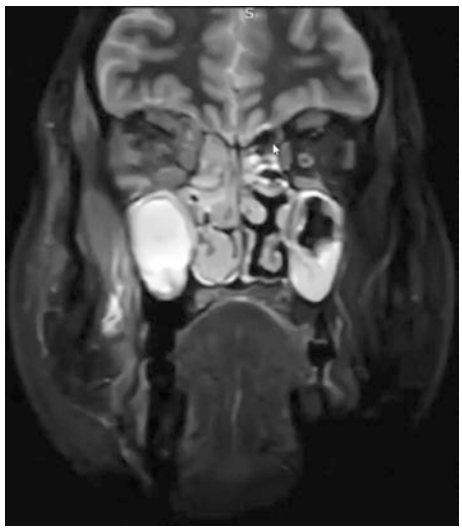

Fig. 21.8 Extensive disease in the right orbit, suggests the need for an endoscopic orbital debridement

21.2.2 Diffusion-Weighted MRI

DW MRI sequences can pick up the infarct at the earliest. In Fig. 21.11, the left optic nerve has infarct and even if the patient clinically has some vision, he could lose it the next day so warn him before he is operated. Infarcts are developing on the right side (Figs. 21.12 and 21.13) of the same patient, indicating bilateral involvement with eventual blindness.

21.3 Indications of Traditional Orbital Exenteration vs, Endoscopic Orbital Clearance

Clinical pictures in Figs. 21.14 and 21.15 show patients who are a clear case for traditional orbital exenteration and an open surgical technique for the treatment of ROCM. Patients with

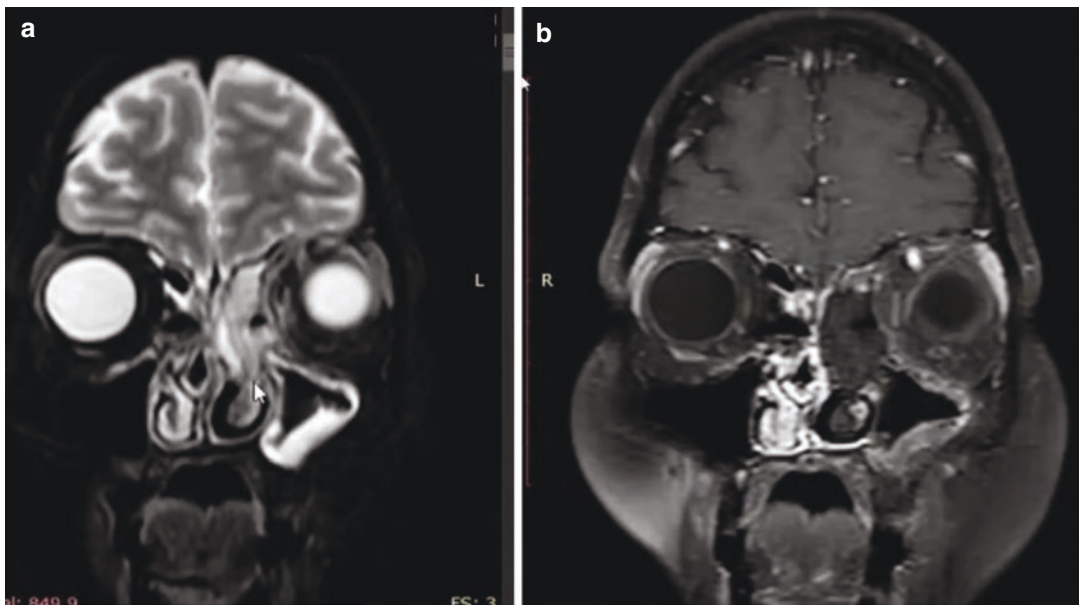

Fig. 21.9 (**a**) T2W FS MRI showing enhanced area of disease in the left orbit. (**b**) Contrast-enhanced MRI showing dark area with loss of contrast in ethmoids, pterygopalatine fossa, ethmoids, and left orbit

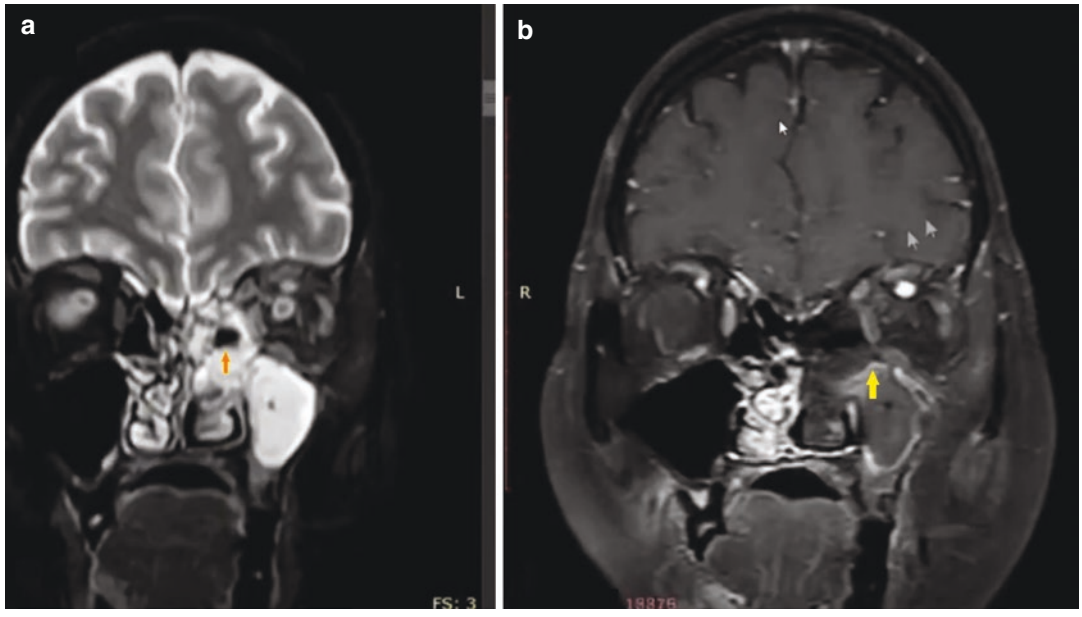

Fig. 21.10 (**a**) T2W FS MRI showing involvement of the left maxillary antrum, ethmoids, and orbit. (**b**) Contrast-enhanced MRI showing dark areas in the pterygopalatine fossa (arrow)

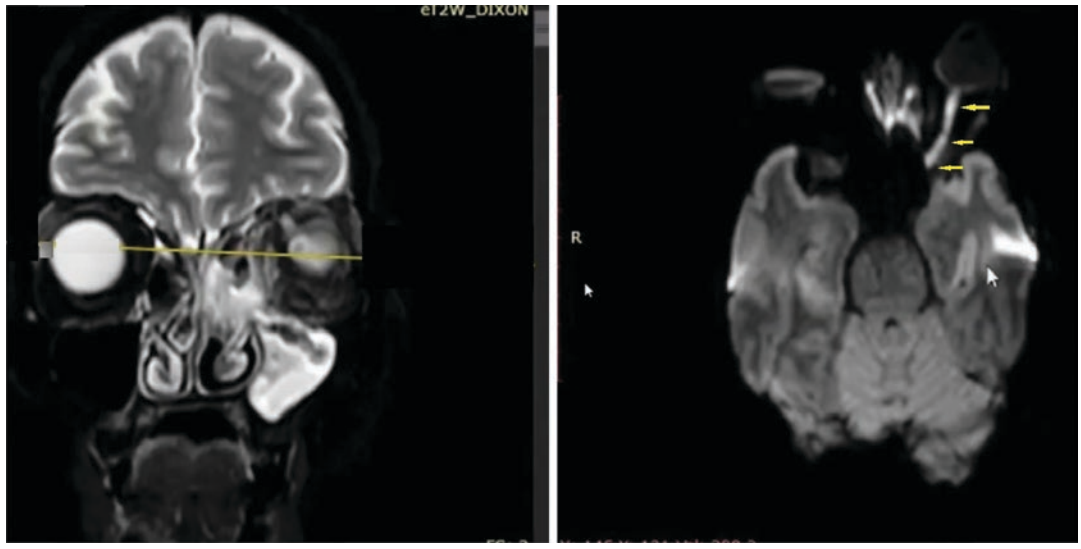

Fig. 21.11 Left orbital disease with infarct in the left optic nerve on DW MRI (arrows)

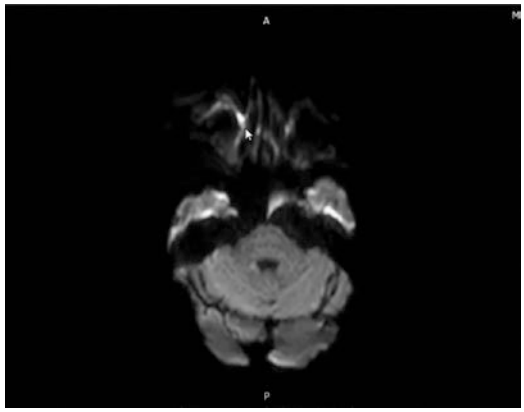

Fig. 21.12 Infarct in both the optic nerve indicating impending vision loss

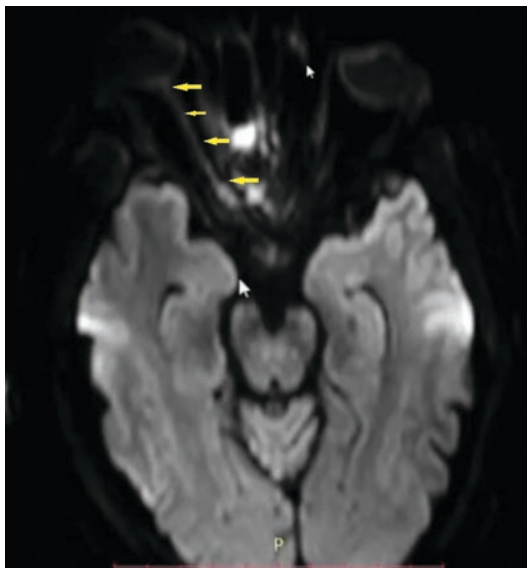

Fig. 21.13 Right optic nerve infarct (arrows) seen on DW MRI

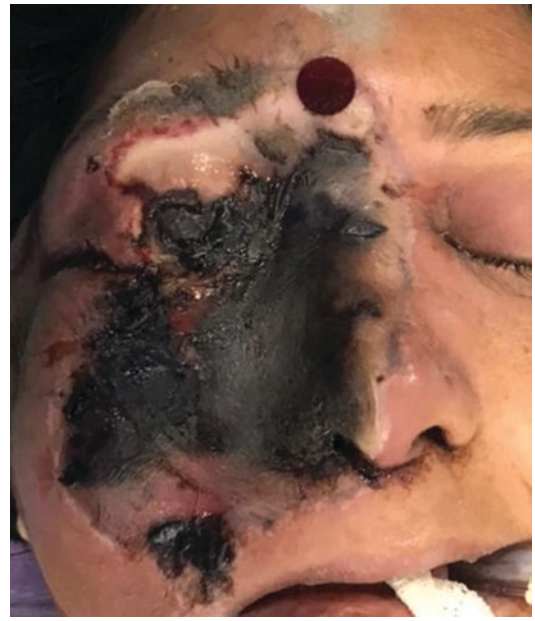

Fig. 21.14 Clinical image of a patient showing extensive involvement of the skin and eyelids, indicating orbital exenteration with an the open approach for the remainder of the disease clearance

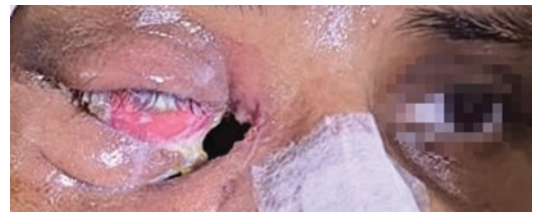

Fig. 21.15 Clinical image of a patient with severe corneal, conjunctival, eyelid, and cheek skin involvement, indicating traditional orbital exenteration

merely ptosis (Fig. 21.16) and no involvement of anterior structures of the eye on the other hand, are candidates for endoscopic orbital clearance. The disease area can be classified on MRI as confined or large (Figs. 21.17 and 21.18). Transnasal endoscopic clearance can be done in the orbit irrespective of the extent of disease on MRI. It may vary from a limited clearance to exenterating most of the diseased part except optic nerve and globe. Endoscopic clearance however, has no role in cases of massive disease involving cheek, skin, lids, cornea and conjunctiva etc.

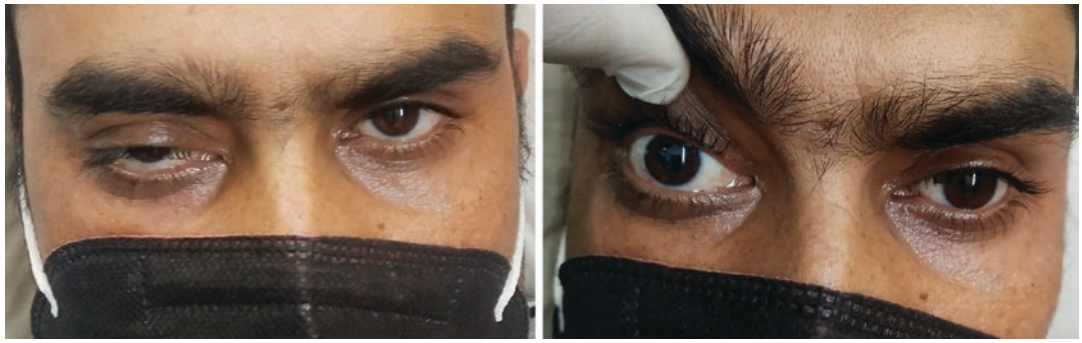

Fig. 21.16 Clinical photograph of a patient with right ptosis and normal anterior contents of the orbit, an indication of endoscopic debridement

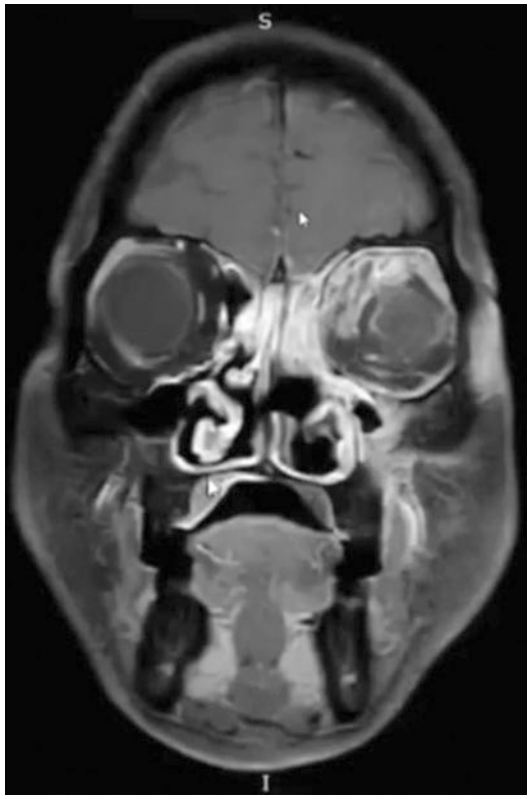

Fig. 21.17 Left orbital disease on T1W MRI

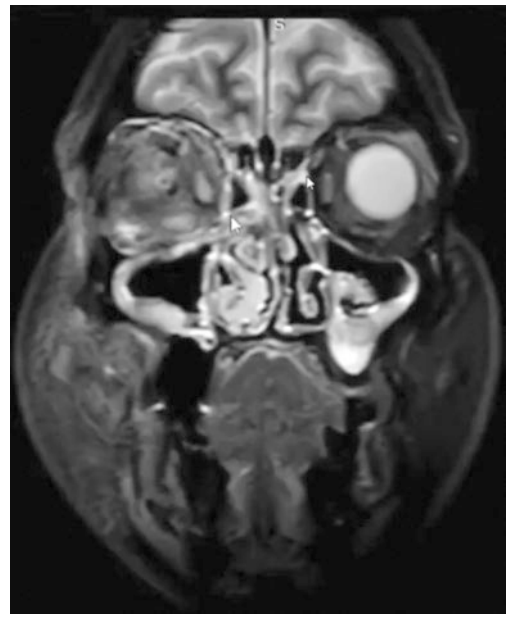

Fig. 21.18 T2W FS MRI showing extensive right orbital disease

21.4 What to Do If You Have Severe Ocular Signs with Normal Nasal Endoscopy

During the current Covid pandemic, majority of ROCM patients presented with severe ocular signs, there were no nasal symptoms and the nasal endoscopy was within normal limits [15–17] (Fig. 21.19). In such cases, a biopsy from the nasal mucosa should be obtained at the earliest, even if there are no black discoloration or necrosis. The biopsy is often positive and helps in clinching the diagnosis. Despite the fact that clinical characteristics of mucor are often diagnostic, orbital intervention requires a proven diagnosis due to medicolegal concerns. If the diagnosis is confirmed, the next step is to evaluate many MRI sequences in detail to distinguish between infection and tissue fungal infiltration.

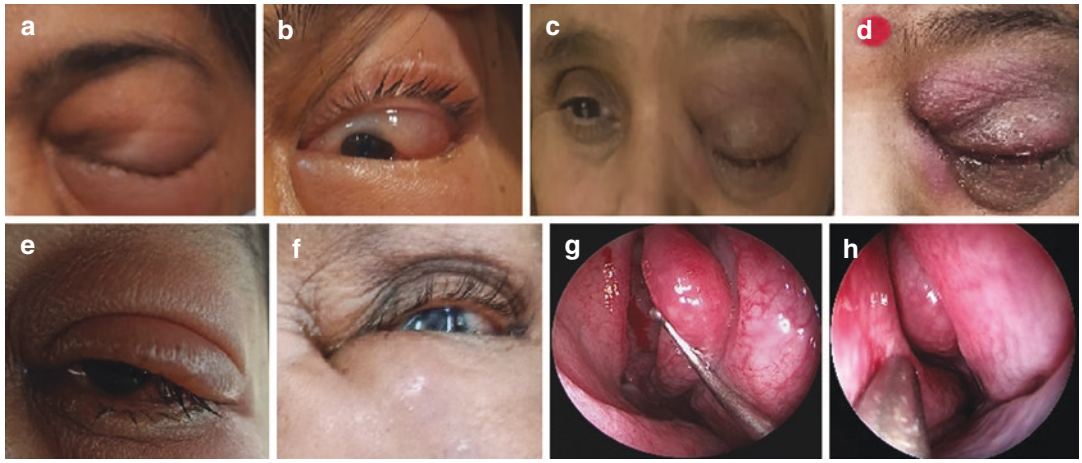

Fig. 21.19 Acute ocular involvement with lid odema (**a**), conjunctival chemosis (**b**), ptosis (**c**) and lid excoriation (**d**), lid odema with congestion (**e**), cheek swelling (**f**) in a series of patients with normal nasal endoscopy (**g** and **h**)

After obtaining a guarded visual prognosis consent, endoscopic orbital debridement is performed. The reason for isolated orbital involvement with no sino nasal disease is direct spread of mucor through the sphenopalatine foramen to the PPF, inferior orbital fissure, and to the orbit, bypassing the sinuses.

Following confirmation of the diagnosis, additional endoscopic orbital clearance or exenteration is performed based on the characterstics stated in the indications.

21.5 Should Patients with Cerebral Involvement Have Orbital Exenteration

Orbito-cerebral involvement in mucormycosis carries a poor prognosis [18–20]. Once the cerebral involvement has already taken place, orbital exenteration may not improve the overall survival [20]. There is significant morbidity attached to the orbital exenteration, and if the vision is normal, it becomes considerably more difficult to exenterate the eye.

This, however, does not mean the orbital disease load should not be decreased. This situation definitely needs intervention, and the option to choose an intervention depends on the disease's extent and the skill set's available to do a complete endoscopic debridement of the orbital apex area. The wide opening of the sinuses, an endoscopic medial maxillectomy and clearance of PPF are all needed to clean the orbital apex area.

In the case of extensive orbital disease with cerebral involvement, exenteration may help reduce the disease burden and prolong the survival of patients with cerebral disease. Endoscopic globe sparing orbital exenteration is a safe, successful, and effective procedure with minimal low-morbidity operation that can be performed in cases when the anterior structures are not affected. If there is severe orbital disease with infiltration of the cornea and conjunctiva, a traditional orbital exenteration should be performed.

Endoscopic orbital debridement can be performed without compromising vision in cases with mild orbital disease and preserved vision, as discussed, in the surgical management of ROCM chapter. Although the results of endoscopic orbital clearance have been highly encouraging, a consent for vision compromise must be taken from those who have normal or partial loss of vision. A globe sparing transnasal orbital exenteration may be performed in cases of massive disease where the patient has total blindness, ophthalmoplegia, and orbital apex involvement. An excellent view of OA is obtained by endoscopic approach, as well as an adequate clearance (Fig. 21.20).

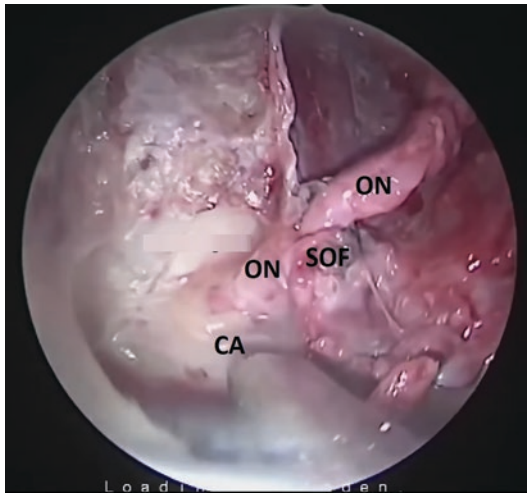

Fig. 21.20 Endoscopic view of the orbital apex including the optic nerve, SOF, and carotid artery in the lateral wall of the sphenoid

It is not recommended to do orbital exenteration or clearance without first clearing the PPF. Despite the fact that it is an aggressive necrotizing infection that spreads from the nose to the sinuses, orbit, and CNS, orbital and cerebral involvement may occur through diverse paths [21]. These occur via the routes of numerous affected and via the lamina papyracea or cribriform plate; the pterygopalatine fossa is the most likely route to orbital dissemination, followed by inferior orbital fissure, retrobulbar area and ultimately, the cavernous sinus involvement. Hoseni et al. found no evidence of orbital invasion via the ethmoid sinus in any of these patients. The lamina papyracea was intact in all the cases [15].

21.6 Mortality

In the literature, many points of view have been provided with some arguing, that the orbital involvement may not be a sign of poor prognosis [1]. Others on the other hand, indicated that when orbital involvement was present, the mortality rate increased by more than 2-fold in their study [7].

Hargrove et al. similarly found that exenteration of the eyeball resulted in a higher survival rate in patients with same symptoms and risk factors [22–24]. In some circumstances, debridement without exenteration, according to various writers allows for eyesight preservation [25, 26]. They also noted that globe invasions are uncommon and have only been observed in one of their cases [27, 28].

Key Points

- Even if the eyesight is normal, if there is a disease in orbit, it must be endoscopically debrided.
- Globe sparing endoscopic exenteration is a preferrable method if the competence is available otherwise traditional orbital exenteration is the best option.
- Endoscopic clearance of the orbital apex disease is possible.
- If the patient refuses to consent to orbital intervention, it is best to postpone the surgery while outlining the benefits and drawbacks.

References

1. Talmi YP, Goldschmied-Reouven A, Bakon M, Barshack I, Wolf M, Horowitz Z, Berkowicz M, Keller N, Kronenberg J. Rhino-orbital and rhino-orbito-cerebral mucormycosis. Otolaryngol Head Neck Surg. 2002;127(1):22–31. https://doi.org/10.1067/mhn.2002.126587.
2. Rangel Guerra RA, Martinez HR, Saenz C, et al. Rhinocerebral and systemic mucormycosis: clinical experience with 36 cases. J Neurol Sci. 1996;143:19–30.
3. Blitzer A, Lawson W, Meyers BR, et al. Patient survival factors in paranasal sinus mucormycosis. Laryngoscope. 1980;90:635–48.
4. Rangel Guerra R, Martinez HR, Saenz C. Mucormycosis. Report of 11 cases. Arch Neurol. 1985;42:578–81.
5. Bullock JD, Jampol LM, Fezza AJ. Two cases of orbital phycomycosis with recovery. Am J Ophthalmol. 1974;78:811–5.
6. Anand A, Anand N. Rhinocerebral mucormycosis: cure without surgery? Arch Intern Med. 1996;156:2262–9.
7. Peterson KL, Wang M, Canalis RF, et al. Rhinocerebral mucormycosis: evolution of the disease and treatment options. Laryngoscope. 1997;107:855–62.

8. Yohai RA, Bullock JD, Aziz AA, et al. Survival factors in rhino-orbital-cerebral mucormycosis. Surv Ophthalmol. 1994;39:3–22.
9. Schwartz JN, Donnelly EH, Klintworth GK. Ocular and orbital phycomycosis. Surv Ophthalmol. 1977;22:3–28.
10. Pillsbury HC, Fischer ND. Rhinocerebral mucormycosis. Arch Otolaryngol. 1977;103:600–4.
11. Chikley A, Ben-Ami R, Kontoyiannis DP. Mucormycosis of the central nervous system. J Fungi. 2019;5(3):59. https://doi.org/10.3390/jof5030059.
12. Engin Ö, Adriaensen GFJPM, Hoefnagels FWA, et al. A systematic review of the surgical anatomy of the orbital apex. Surg Radiol Anat. 2021;43:169–78. https://doi.org/10.1007/s00276-020-02573-w.
13. Goyal P, Lee S, Gupta N, Kumar Y, Mangla M, Hooda K, Li S, Mangla R. Orbital apex disorders: imaging findings and management. Neuroradiol J. 2018;31(2):104–25. https://doi.org/10.1177/1971400917740361.
14. Badakere A, Patil-Chhablani P. Orbital apex syndrome: a review. Eye Brain. 2019;11:63–72. https://doi.org/10.2147/EB.S180190.
15. Hosseini SMS, Borghei P. Rhinocerebral mucormycosis: pathways of spread. Eur Arch Otorhinolaryngol. 2005;262:932–8. https://doi.org/10.1007/s00405-005-0919-0.
16. Galetta SL, Wulc AE, Goldberg HI, Nichols CW, Glaser JS. Rhinocerebral mucormycosis: management and survival after carotid occlusion. Ann Neurol. 1990;28:103–7.
17. Vessely MB, Zitsch RP 3rd, Estrem SA, Renner G. Atypical presentations of mucormycosis in the head and neck. Otolaryngol Head Neck Surg. 1996;115:573–7.
18. Apinhasmit W, Chompoopong S, Methathrathip D, Sansuk R, Phetphunphiphat W. Supraorbital notch/foramen, infraorbital foramen and mental foramen in Thais: anthropometric measurements and surgical relevance. J Med Assoc Thail. 2006;89(5):675–82.
19. Becker M, Masterson K, Delavelle J, Viallon M, Vargas MI, Becker CD. Imaging of the optic nerve. Eur J Radiol. 2010;74(2):299–313.
20. Belotti F, Ferrari M, Doglietto F, et al. Ophthalmic artery originating from the anterior cerebral artery: anatomo-radiological study, histological analysis, and literature review. Neurosurg Rev. 2016;39(3):483–93.
21. Fisher EW, Toma A, Fisher PH, Cheeseman AD. Rhinocerebral mucormycosis: use of liposomal amphotericin B. J Laryngol Otol. 1991;105:575–7.
22. Hargrove RN, Wesley RE, Klippenstein KA, et al. Indications for orbital exenteration in mucormycosis. Ophthal Plast Reconstr Surg. 2006;22:286–91.
23. Bergstrom L, Hemenway WG, Barnhart RA. Rhinocerebral and otologic mucormycosis. Ann Otol Rhinol Laryngol. 1970;79:70–81.
24. Greenberg MR, Lippman SM, Grinnell VS, et al. Computed tomographic findings in orbital mucor. Western J Med. 1985;143:102–3.
25. Blazquez R, Pinedo A, Cosin J, et al. Nonsurgical cure of isolated cerebral mucormycosis in an intravenous drug user. Eur J Clin Microbiol Infect Dis. 1996;15:598–9.
26. Kohn R, Hepler R. Management of limited rhino-orbital mucormycosis without exenteration. Ophthalmology. 1985;92:1440–4.
27. Sponsler TA, Sassani JW, Johnson LN, et al. Ocular invasion in mucormycosis. Surv Ophthalmol. 1992;36:345–50.
28. Ferry AP, Abedi S. Diagnosis and management of rhinoorbitocerebral mucormycosis (phycomycosis): a report of 16 personally observed cases. Ophthalmology. 1983;90:096–104.

22 Profile of Rhino-Orbito-Cerebral Mucormycosis Patients Reporting after Multiple Debridement and Antifungal Treatment

Nishi Gupta, Shruti Ogra, and Shreya Aggarwal

Despite surgical debridement and a full course of antifungals six months after the initial cases of rhino-orbito-cerebral mucormycosis (ROCM) began flooding, the disease refuses to leave us with the patients coming with persistent symptoms and significant morbidity. It is uncertain whether it's a residual disease or recurrent disease, which puts clinicians in a dilemma?

This chapter discusses several recent cases residual/recurrent disease reported despite multiple debridements. A detailed analysis of these cases was done regarding the initial presentation of these cases, the number of debridements, the extent of debridement, availability of amphotericin B, patient compliance, and so on were all thoroughly examined.

Let us take a look at each of these conditions one by one using appropriate instances.

Case 1

After right orbital exenteration and endoscopic sinus debridement, a 37-year-old man presented with recurrent symptoms. At the time of presentation his orbital socket was oozing eschar, indicating an inadequate debridement (Figs. 22.1 and 22.2). He had a minor non-healing gingival ulcer that wasn't there when he undewent primary surgery (Figs. 22.3 and 22.4).

Patient's preoperative contrast-enhanced MRI scans were reviewed. On preoperative scans there was loss of enhancement in the palate on the right (red circle, Fig. 22.5), indicating that the palate was involved, a finding which is commonly overlooked if not explicitly sought for. Leaving this disease untreated might lead to palatal disease progression, as seen in this example who also had disease in the right right pterygopalatine fossa (star, Fig. 22.6).

CT scan of the same patient showed intact walls of the maxilla, indicating that a modified medial maxillectomy was not performed during the previous surgery resulting in the residual disease in the pterygopalatine fossa (PPF). Such patients frequently continue to have symptoms with further progression of the disease.

N. Gupta (✉)
Dr Shroff's Charity Eye Hospital, New Delhi, India

S. Ogra
Central Railway Hospital, Connaught Place, New Delhi, India

S. Aggarwal
All India Institute of Medical Sciences, New Delhi, India

N. Gupta, S. G. Honavar (eds.), *Rhino-Orbito-Cerebral Mucormycosis*,
https://doi.org/10.1007/978-981-16-9729-6_22

Complete bilateral spheno-ethmoidectomy, bilateral modified medial maxillectomy, clearance of both sides PPF, and alveolar bone debridement were all part of the revision surgical plan. The PPF is the reservoir of infection that should essentially be cleaned in all the cases of ROCM undergoing orbital clearance or exenteration. Median maxillectomy does not give any morbidity to the patient. Instead it allows more access to the orbit and postoperative inspection. Failure to clear PPF can lead to further involvement of the palate due to the involvement of vessels in the pterygopalatine fossa with further progression of the disease, like a gingival ulcer in this case.

An oozing socket with eschar from an exenterated eye implies a lack of preliminary workup, clearance, and presence of a disease reservoir. In mucormycosis orbital exenteration should never be performed without PPF clearing.

Fig. 22.1 Case 1: A 37-year-old male with a post exenteration orbital cavity oozing eschar

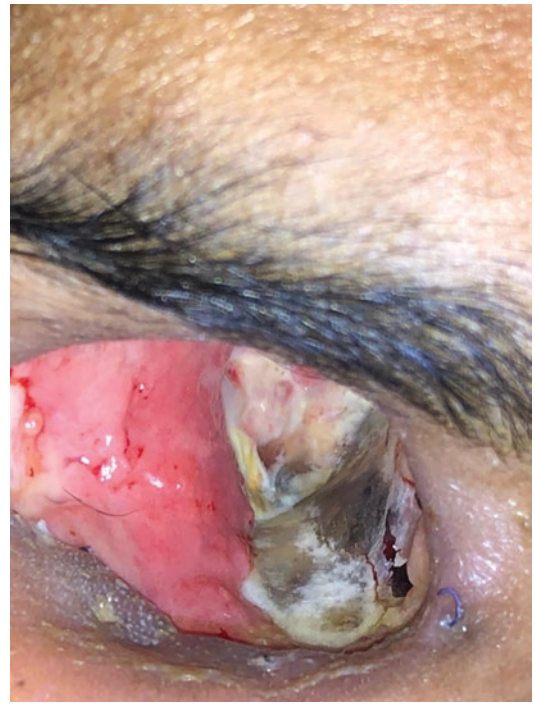

Fig. 22.2 Case 1: Close-up view of the socket filled with necrotic material and has bluish discoloration of the medial canthal skin indicating an impending fistula

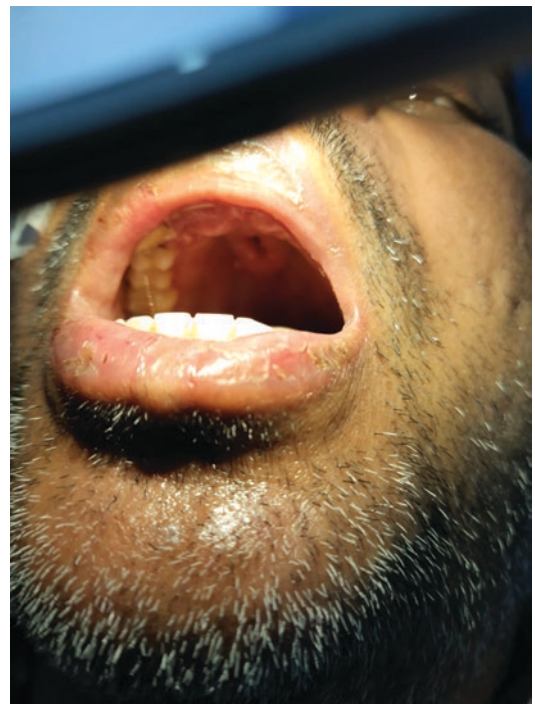

Fig. 22.3 Case 1: Same patient as in Fig. 22.2, has palatal bogginess in postoperative period indicaing early palatal involvement

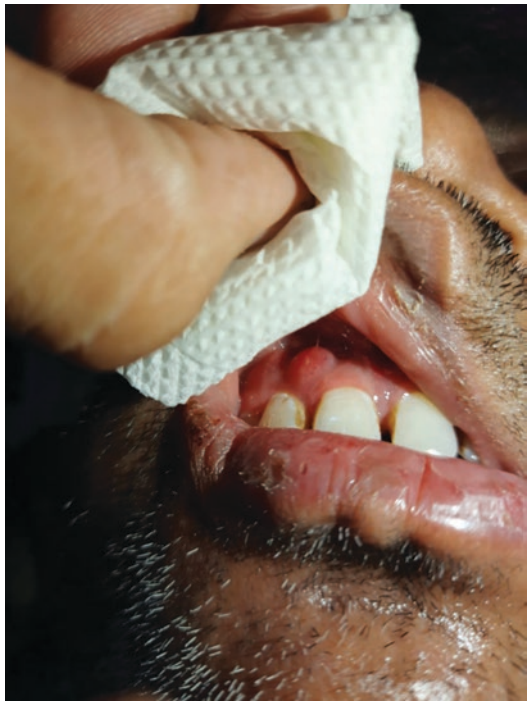

Fig. 22.4 Case 1: A tiny non-healing gingival ulcer that indicates disease spread

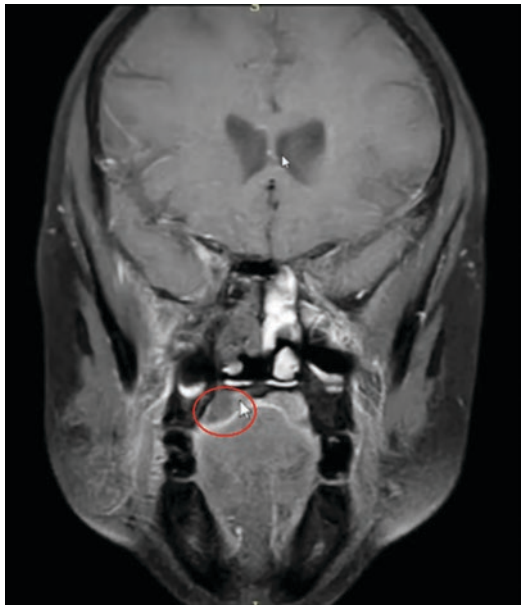

Fig. 22.5 Contrast-enhanced MRI reveals loss of enhancement in the right palate (red circle) indicating palatal disease (Courtesy Dr Satish Jain, Jaipur)

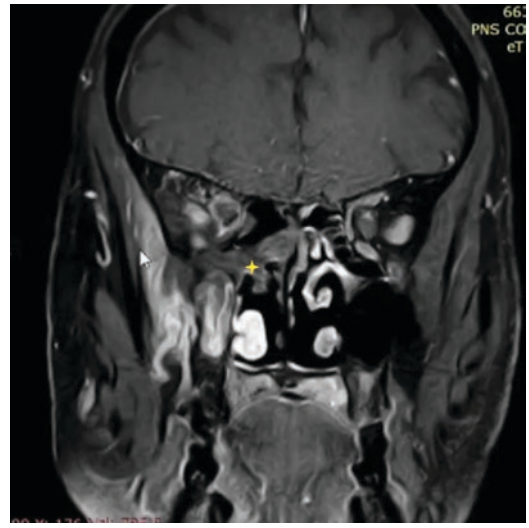

Fig. 22.6 Contrast-enhanced MRI reveals intermittent areas of non-enhancement in right pterygopalatine fossa (star) (Courtesy Dr Satish Jain, Jaipur)

Case 2

A 35-year-old woman presented with proptosis, severe conjunctival chemosis, a melting cornea, a big fistula in the medial canthal area and pustules over the skin of the cheek (Fig. 22.7). She'd had an endoscopic sinus debridement as well as a palatal excision and was feeding through a Ryle's tube. Patient's unwillingness to consent to an orbital clearance, which is a typical example of residual disease flaring up to this extent, contributed to the rapid advancement of eye symptoms.

Large lesions in the right medial wall and apex of the orbit were seen on MRI with contrast enhancement (Figs. 22.8 and 22.9). Postoperative changes were seen on the right with the lack of medial wall of maxilla and formation of a single cavity (Fig. 22.10). Significant involvement of ethmoids, sphenoid, and orbit was seen. Involvement of the greater wing of sphenoid and bilateral ethmoids was also present (Figs. 22.11, 22.12, and 22.13).

The next step in the treatment strategy included a total maxillectomy, orbital exenteration and excision of the involved skin. The patient was emphatic about refusing to submit to orbital exenteration. Because the team refused to adjust the plan to her liking, she was not operated.

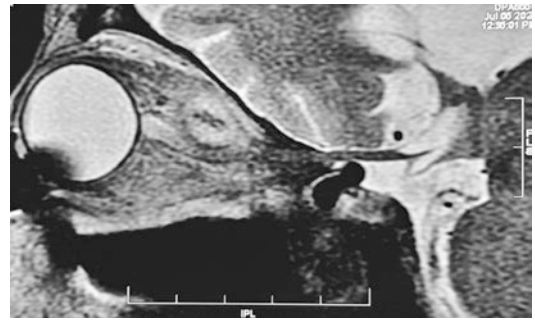

Fig. 22.9 Case 2: The sagittal section of a contrast MRI of the paranasal sinuses reveals large lesions in right orbital apex

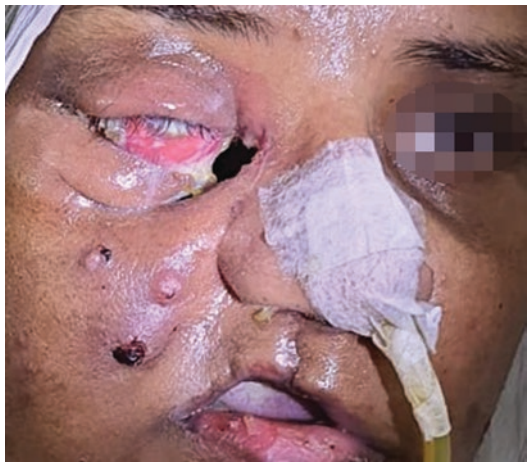

Fig. 22.7 Case 2: Right eye proptosis, ptosis with severe conjunctival chemosis, melting cornea, fistula in the medial canthal area and pustules on the right maxillary skin area. Ryle's tube can also be seen in place

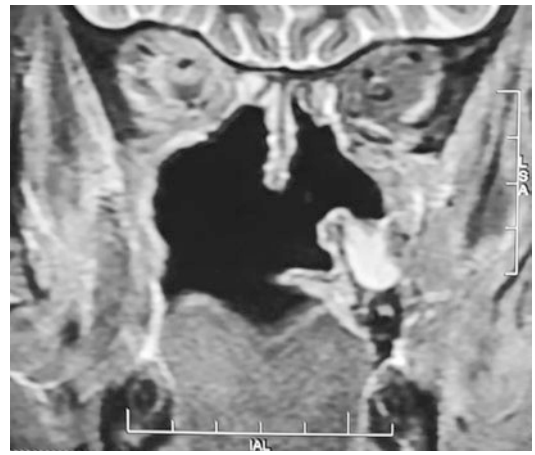

Fig. 22.10 Case 2: A big postoperative cavity reveals the missing medial wall of the maxilla and a common cavity formation between the nose and the maxilla

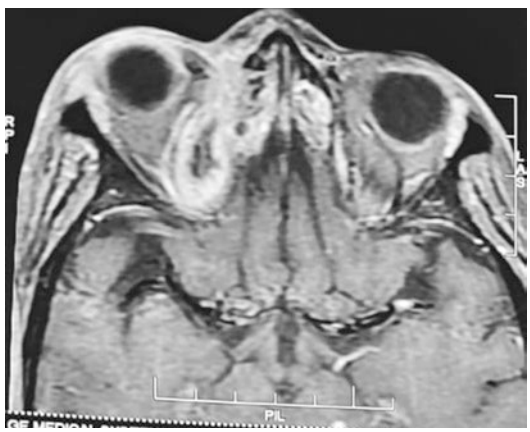

Fig. 22.8 Case 2: Contrast MRI of paranasal sinuses axial section reveals extensive lesions in right orbital apex

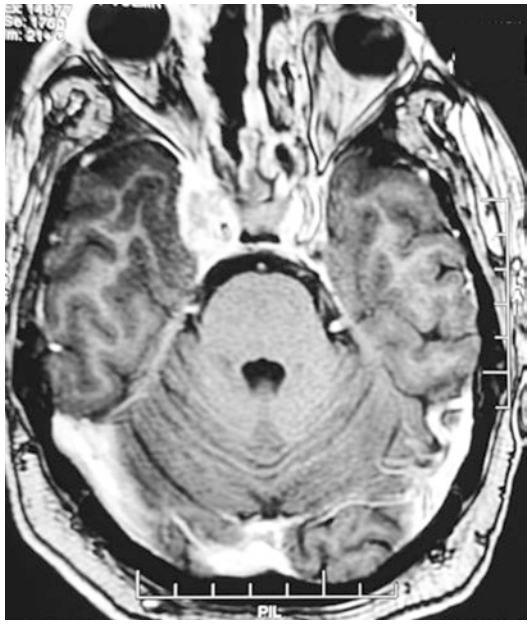

Fig. 22.11 Case 2: Contrast MRI of PNS, axial view reveals a lesion in medial orbital wall and ethmoids as well as orbital apex with extension into the right cavernous sinus

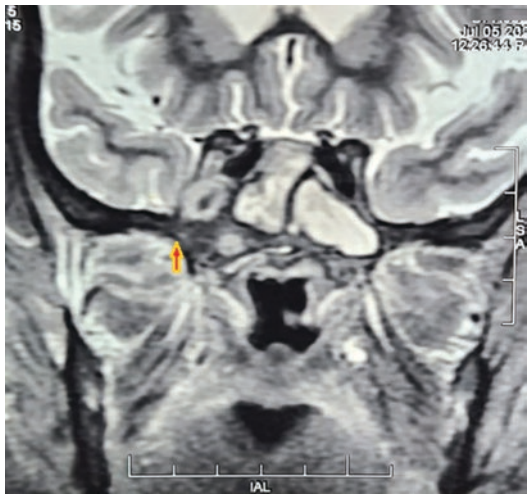

Fig. 22.12 Case 2: The right orbital apex and greater wing of the sphenoid (arrow) are involved in T2W MRI

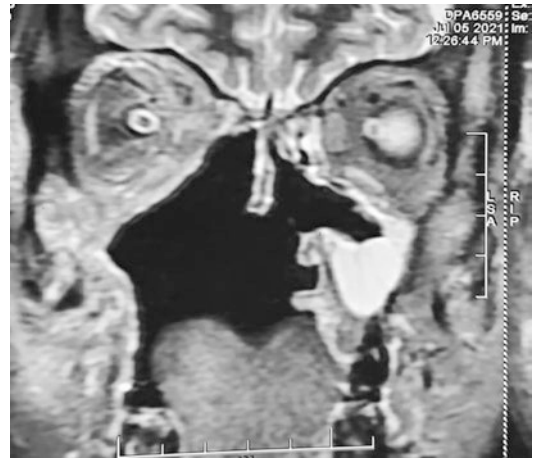

Fig. 22.13 Case 2: T2W Fat-suppressed MRI of right orbits reveals areas of enhancement indicating significant disease

Case 3

The third patient was a 57-year-old man who had previously undergone two ROCM procedures. He developed conjunctival chemosis, ophthalmoplegia, and partial vision loss, a month after the second surgery (Figs. 22.14, 22.15, and 22.16). T2W fat-saturated and T1W with contrast-enhanced scans were done in axial, coronal, and sagittal planes. There was evidence of heterogeneously enhancing T2 hyperintense contents in the left frontal, ethmoid, and sphenoid sinus, which extends into the medial wall of the left orbit with the destruction of lamina papyracea. The soft tissue is seen to extend into the left orbital apex and left cavernous sinus that appears heterogeneous. However, flow voids within are maintained. The extraocular muscles appeared bulky and showed altered signal intensity with both intra and extraconal fat stranding. Optic nerve appeared bulky and showed altered signal and heterogeneous enhancement. There was evidence of post-operative changes in the form of non-

visualization of the medial wall of the left maxillary sinus with a common cavity formation with the nasal cavity. Signs of residual disease were present (Figs. 22.17, 22.18, 22.19, 22.20, and 22.21).

This patient underwent revision surgery with orbital exenteration at a higher center (Fig. 22.22). Orbital exenteration was performed because of the involvement of anterior structures of the eye, including the conjunctiva. Amphotericin B injection were given after a complete debridement of the pterygopalatine fossa with orbital exenteration. Patient is doing fine one month after the surgery. To achieve good results, complete compliance and well-understood consent as well with meticulous surgery are required.

In this patient, the probable cause of the recurrence of the symptom was the residual disease in the orbit that progressed gradually. In case 1 residual disease in the pterygopalatine fossa led to an exuding socket. In this case, the residual disease in orbit and probably the incomplete clearance of PPF led to the slow progression of symptoms. These cases showed significantly improved outcomes following thorough debridement and antifungal medication.

Fig. 22.14 Case 3: Clinical photograph of a 57-year-old man with ophthalmoplegia and a history of ROCM surgery

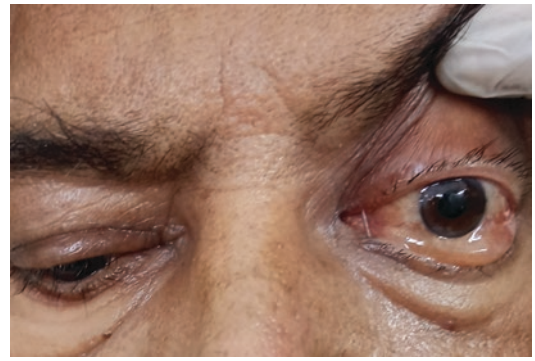

Fig. 22.15 Case 3: Postoperative image of the same patient as in Fig. 22.14 showing conjunctival chemosis

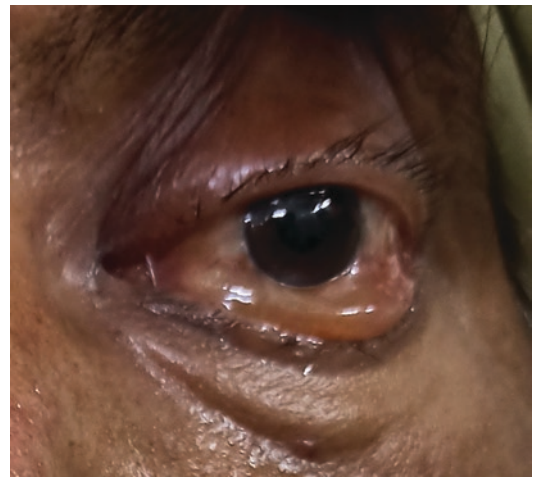

Fig. 22.16 Case 3: Close-up view of the same patient as in Fig. 22.15

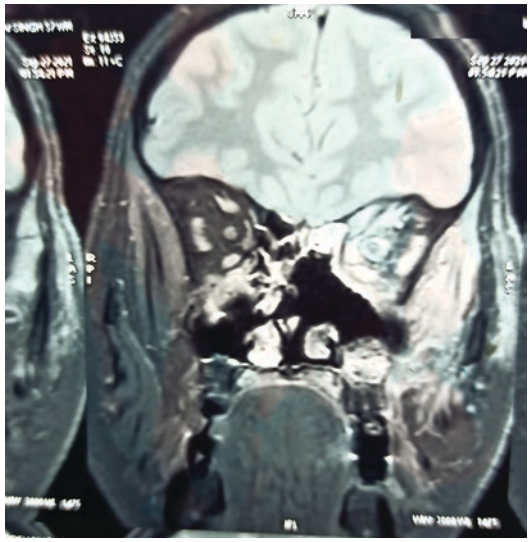

Fig. 22.17 Case 3: Heterogeneously enhancing T2 hyperintense contents in the left ethmoids, which extends into the medial wall of the left orbit with the destruction of lamina papyracea

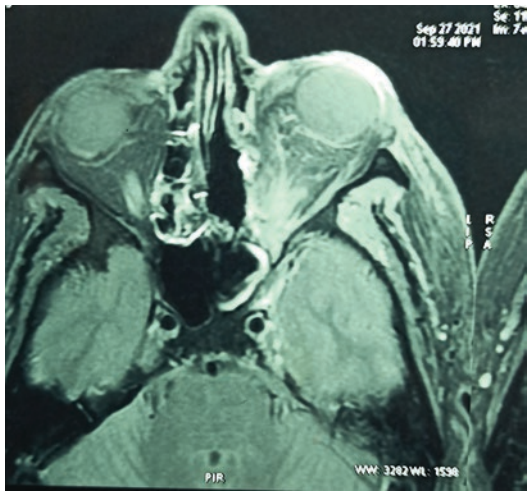

Fig. 22.18 Case 3: Reveals T2W fat-saturated axial MRI paranasal sinus with hyperintense contents in the left ethmoid and sphenoid sinus with the destruction of the left lamina papyracea

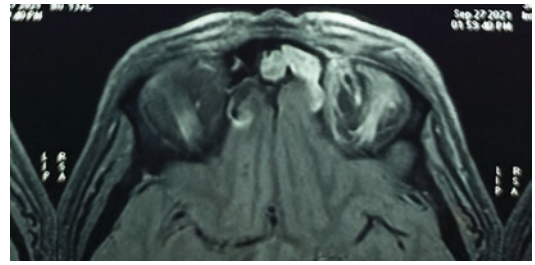

Fig. 22.19 Case 3: Contrast-enhanced T1W MRI paranasal sinus with hyperintense contents in left frontal sinus

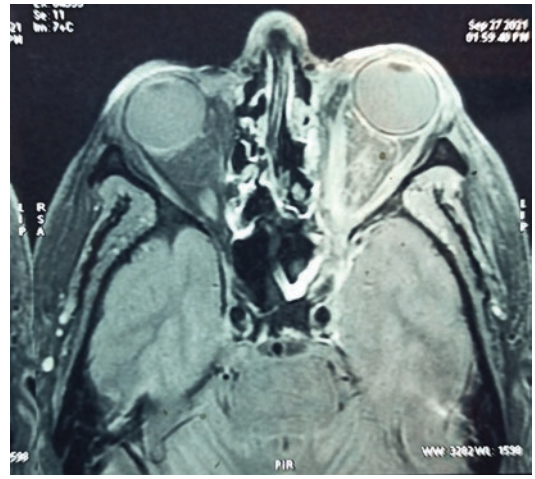

Fig. 22.20 Case 3: Contrast-enhanced T1W MRI paranasal sinus with soft tissue extension into the left orbital apex and left cavernous sinus, and extraocular muscles appear bulky and show altered signal intensity

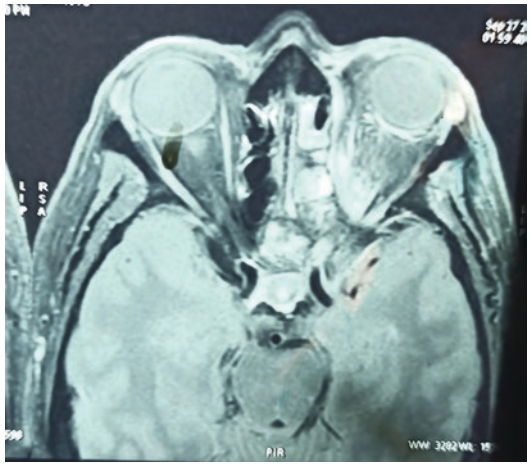

Fig. 22.21 T2W MRI paranasal sinus axial view showing bulky extraocular muscles with hyperintense contents in left orbit, sphenoid, and ethmoids

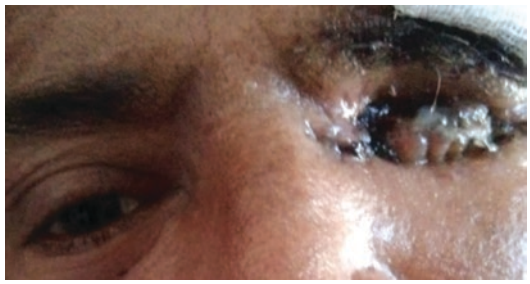

Fig. 22.22 Case 3: Clinical image of patient after left orbital exenteration

Case 4

A 55-year-old woman, presented with a 2-month history of two ROCM surgeries with left orbital exenteration (Fig. 22.23). She was fine for the first two months, but then she began to lose vision in her right eye, for which she was given a transcutaneous retrobulbar amphotericin B injection. Nasal endoscopic examination showed a well-healed cavity (Fig. 22.24).

MRI Study revealed postoperative changes in left orbit and sinonasal cavity (Figs. 22.25 and 22.26). Homogeneously enhancing T2W and T1W isointense soft tissue was noted in the periphery of the left orbital socket. No non-enhancing areas were seen within the left orbit.

Moderate to extensive mucosal thickening was seen involving bilateral ethmoids, bilateral frontal and right sphenoid sinuses, with mild mucosal thickening in the rest of the paranasal sinuses. Heterogenous enhancement was seen in bilateral maxillary sinuses with a non-enhancing retention cyst in the right maxillary antrum, measuring approximately 1.5 × 1.1 cm (Fig. 22.27). The rest of the mucosa showed relatively homogenous enhancement.

Ill-defined STIR hyperintensity is noted in the right masticator space with heterogeneous post-contrast enhancement. Heterogenous enhancement was seen in the right pterygopalatine fossa abutting the orbital apex. No definite compromise of the right orbital apex is seen. The right middle cranial fossa floor appeared thinned out and irregular, with dural thickening measuring approximately 2.3 mm in thickness (Figs. 22.27, 22.28, and 22.29).

The cavernous sinus appeared normal. The right optic nerve and extraocular muscles were normal in signal intensity on all sequences. The extraocular muscles show homogenous post-contrast enhancement.

All these abnormalities were absent during the preoperative assessment. Following the initial procedure the endoscopy showed a well healed nasal cavity. They were classified as new instances of illness.

At the time of presentation, The patient was taking transcutaneous retrobulbar amphotericin B and at the time of presentation. Her prescription was changed to include anticoagulants to her medication and she was given a follow-up appointment.

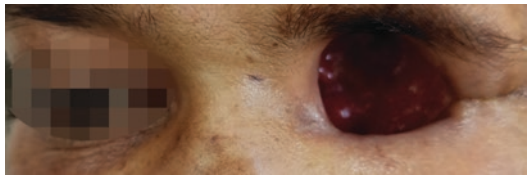

Fig. 22.23 Clinical photograph of a patient who underwent left orbital exenteration with symptoms of partial vision loss appearing in the right eye after 2 months, indicating recurrent disease

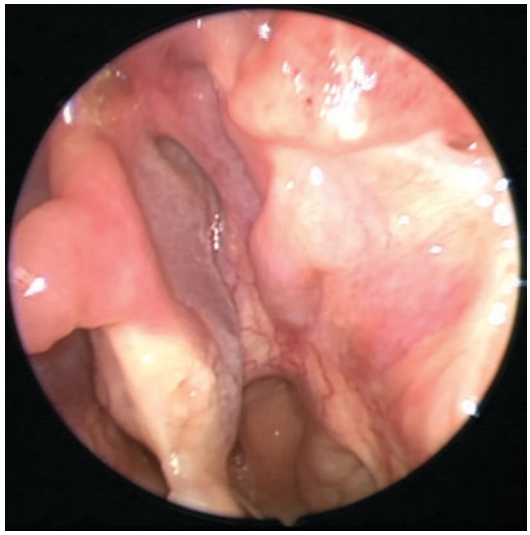

Fig. 22.24 Case 4: Endoscopic view of the same patient in Fig. 22.23 reveals a well healed cavity

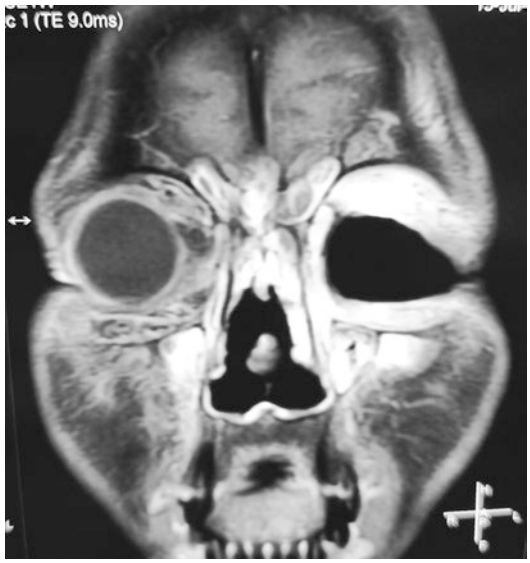

Fig. 22.25 Case 4: MRI PNS showing postoperative changes in the left orbit and sinonasal area

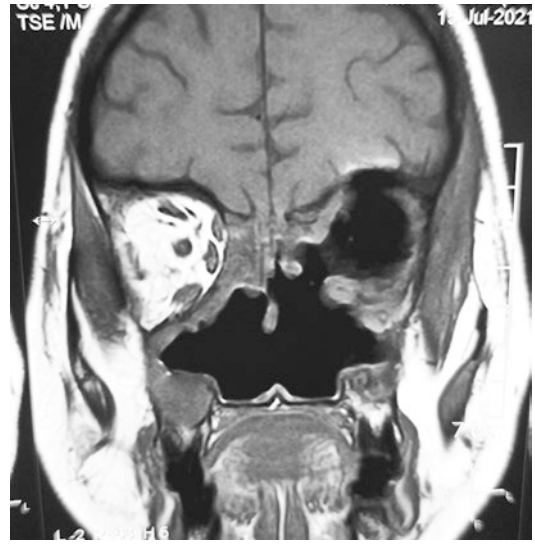

Fig. 22.26 Case 4: The left orbit and sinonasal cavity reveal postoperative changes in contrast-enhanced MRI paranasal sinuses coronal view

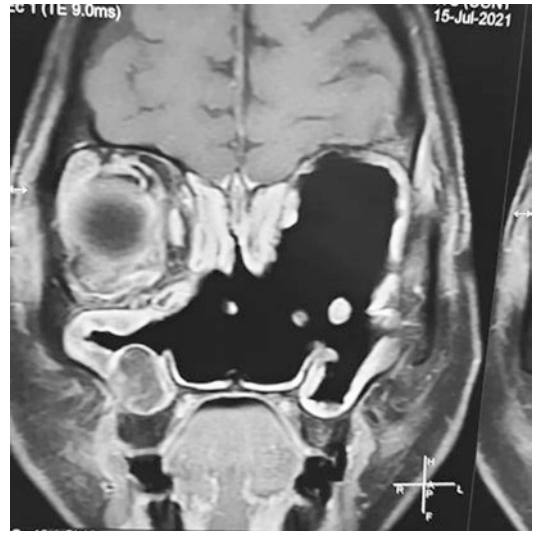

Fig. 22.27 Case 4: Contrast-enhanced MRI paranasal sinuses showing soft tissue in the periphery of the left orbital socket. Mucosal thickening was seen in bilateral maxillary and ethmoids. Note a non-enhancing retention cyst in the right maxillary sinus

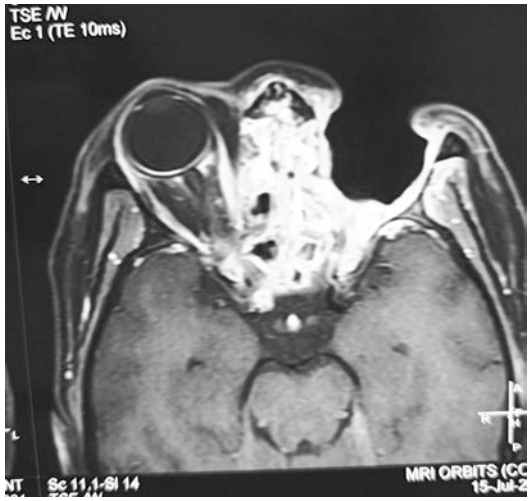

Fig. 22.28 Case 4: T2W MRI showing a postoperative cavity with hypodense areas in the right ethmoids

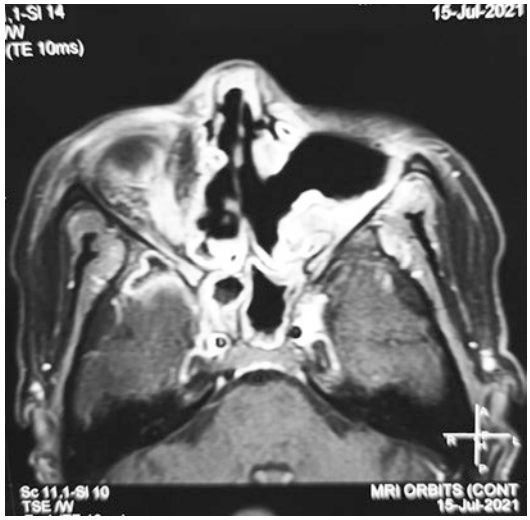

Fig. 22.29 Case 4: Contrast-enhanced MRI paranasal sinuses axial view shows postoperative changes and mucosal thickening in bilateral ethmoids

Case 5

A 40-year-old man had two surgical debridements and had completed a full course of antifungal medication. He was alright for 2 months, before developing symptoms of recurrent disease. At the time of reporting to us he had developed weakness on the right side of his face and right hemiparesis and he was wheelchair-bound (Fig. 22.30). Hemiparesis and intracranial involvement necessitated. MR angiography (Figs. 22.31, 22.32, 22.33, and 22.34). Both internal carotid arteries were obstructed on MR angiography with the disease in the vicinity. However, collateral from the external carotid artery were forming. He had extensive intracranial disease with pontine hemorrhage. Greater wings of sphenoid were also infiltrated with the disease on both sides. The surgery carried a risk of paraplegia, and the chances of recovery from anesthesia were grim, given the pontine involvement.

The patient was put on anticoagulants and antifungals and were looked after by a team of an intensivist and an otorhinolaryngologist. Periodic nasal endoscopy with disease clearance was performed. After 15 days of treatment patient's hemiparesis was gone, and he was able to walk without assistance. He tolerated amphotericin B well, and he is doing well two months, after he was diagnosed with significant intracranial disease. We do not know how the future will pan out for him, but for the time being, the conservative approach appears to be working well.

The return of symptoms, despite the fact that the patients had a symptom-free interval, signal either persistent silent damage or the emergence of a new thromboembolic phenomenon. Identifying trends can aid in better scenario management.

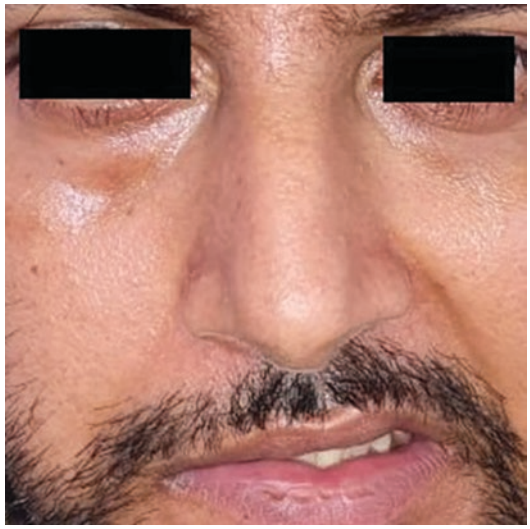

Fig. 22.30 Case 5: Clinical photograph of a patient presenting with right facial paresis with a normal intervening period of 2 months following surgery for ROCM

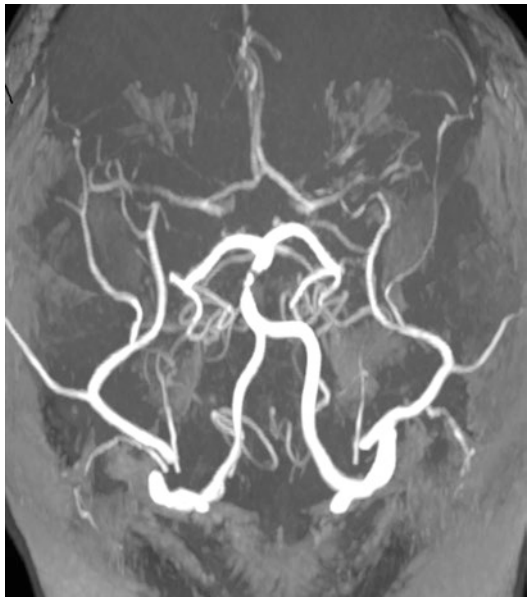

Fig. 22.31 Maximum intensity projection (MIP) MR angiography brain showing focal stenosis of mid-segment of the basilar artery

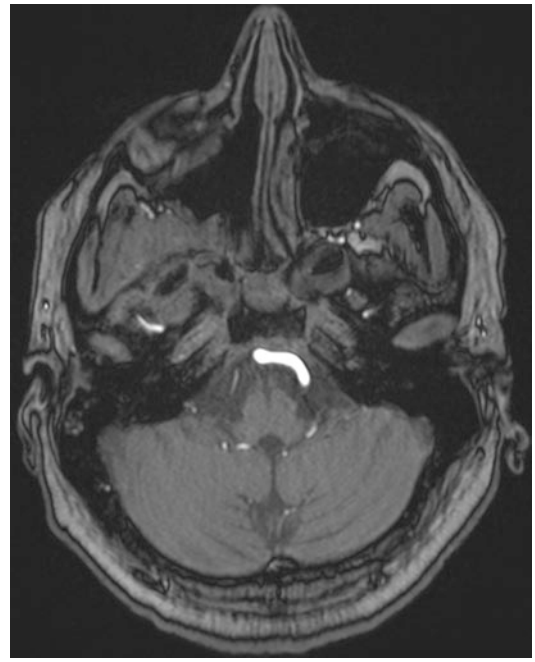

Fig. 22.32 MR angiography brain showing absence of flow-related signal in petrous segments of bilateral internal carotid arteries

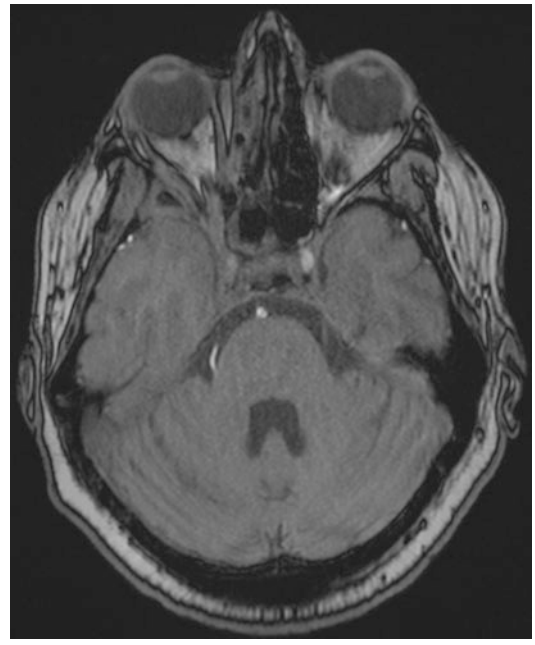

Fig. 22.33 MR angiography brain showing attenuated signal in cavernous segments of bilateral internal carotid arteries

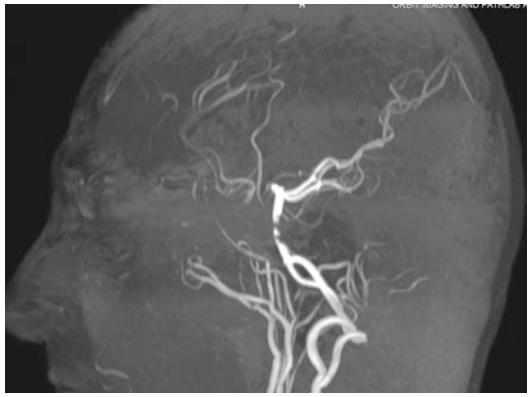

Fig. 22.34 Maximum intensity projection (MIP) MR angiography brain showing attenuated anterior cerebral circulation and focal basilar artery stenosis

22.1 Residual/Recurrence Disease: What Causes it and How to Prevent It

Recurrent or residual disease can happen for a variety of causes.

- A rapid increase in ROCM cases and a lack of infrastructure to deal with the problem.
- There is a critical scarcity of life-saving drugs such as amphotericin B.
- Due to a tremendous influx of patients, there aren't imaging facilities. As a result, due to the scarcity of comprehensive imaging modalities, disease mapping was not possible. Imaging facilities involving CT, MRI, simple, contrast, fat-suppressed, diffusion-weighted, and MR angiography were required but locating even a simple CT in a high volume COVID facility for all of the patients was very difficult. It made it impossible to undertake a thorough initial debridement.
- The pterygopalatine fossa, which is a disease reservoir, was not cleared in the vast majority of patients.
- The disease spread so quickly and aggressively, that even though an if MRI was performed 72 hours before surgery, the disease was discovered intraoperatively, to be present in places not visible on MRI.
- In the instance of partial vessel occlusion, there is a risk of progression as the thrombus gradually obstructs the vessels until they are completely blocked, with the symptoms appearing after the primary surgery. As a result, it is critical to check for notorious areas on MRI and get diffusion-weighted MRI or MR angiography, as mentioned in the chapter on imaging. It is preferrable to read MRI sequences on your own and compare them. However, collaborating with a radiologist and discussing MRI findings in depth is beneficial for improved surgical planning.
- Last but not least, was the difficulty in obtaining patients' consent regarding the orbital exenteration and palatal excision. Failures resulted from the residual disease that was left due to a lack of permission.

The novel thromboembolic phenomenon, drug resistance, continual immunocompromised condition and other factors all contribute to the uncertain results in ROCM.

The patient must be aware that the high-cost antifungal drugs may be needed for a longer period than anticipated. The risk of further progression of the recurrent disease to the intracranial structures may occur despite our best efforts. Given India's current trend of medicolegal difficulties, obtaining record video permission during the dialogue with the patient to convey the benefits and drawback of the treatment is critical. Medical treatment can improve life span in patients with extensive intracranial involvement. We provide our expertise based on diverse circumstances because there is no consensus on the optimum technique. It is upto the readers to come out of best practises.

Recurrence can be prevented by thorough debridement of disease in ROCM based on MRI evaluation of the preferential sites as described in the chapters on surgical management Strict glycemic control, adequate antifungal drugs with species identification, drug sensitivity and susceptibility are all important factors to consider.

23 Future Directions in the Management of Rhino-Orbito-Cerebral Mucormycosis

Nishi Gupta

There are several unmet needs in managing rhino-orbito-cerebral mucormycosis (ROCM), especially after the cerebral involvement of mucormycosis takes place [1]. The future lies in solving the challenges that lie ahead. These include free availability of quick and reliable diagnostic tests including PCR and molecular tests, decision-making in surgical debridement, drug sensitivity and susceptibility, minimal inhibitory concentration (MIC) level, and combination drug trials of antifungal drugs.

23.1 Quick and Reliable Diagnostic Tests, Including PCR and Molecular Tests

The key to treating mucormycosis successfully lies in early intervention. As a result, early diagnosis and institution of prompt therapy in ROCM leads to improved outcomes [1]. Currently, there are no available biomarkers of mucormycosis [2]. Definitive diagnosis is based on the microbiological assessment of the biopsy material. A preliminary diagnosis can be made on direct microscopic examination aided by fluorescence microscopy that enhances the sensitivity [3]. The Mucorales hyphae are highly fragile and may get damaged during processing leading to poor culture results. Some stains that highlight hyphae like Grocott methenamine silver (GMS) and periodic acid Schiff (PAS) should be used for histopathological examination. Mucorales species need to be stained for a longer duration than other fungi [3].

However, having a culture-independent technique for the early identification of species is critical. PCR-based assays, using Mucorales specific primers such as CotH [4], can add to the diagnosis. PCR-sequencing for the internal transcribed spacer (ITS) region is the recommended molecular method for identifying *Mucorales* [5].

This technique's use is limited due to its availability only at the reference laboratories. There is a need for the free availability of this technique at major centers treating mucormycosis. The molecular technique is helpful in cases where culture fails to grow *Mucorales* or in cases of concurrent infection due to *Aspergillus* and *Mucorales* or where histopathological differentiation is difficult due to the sparse fragments in tissue [6–9].

The molecular method is a quicker and takes <48 h compared to the culture that takes more than (72–144 h) and histopathological (72–96 h) [6]. Immunohistochemical staining of tissue specimens shows good sensitivity and specificity for *Mucorales* sp., and enables differentiation between mucormycosis and aspergillosis [10]. *Mucorales* DNA can be detected in the serum of patients 3–68 days before the routine diagnosis [11, 12]. This can help predict patients at risk of

N. Gupta (✉)
Dr Shroff's Charity Eye Hospital, New Delhi, India

N. Gupta, S. G. Honavar (eds.), *Rhino-Orbito-Cerebral Mucormycosis*,
https://doi.org/10.1007/978-981-16-9729-6_23

progression and can help in instituting early therapy.

The absence of commercially available methodologies to test the analytical sensitivity of molecular methods is one of the many challenges in doing molecular testing in the current situation. A commercially available kit, MucorGenius (Pathonostics, Maastricht, The Netherlands), is a real-time PCR assay. It can provide results in as early as 3 h with a sensitivity of 75%. However, it is not an FDA-approved kit [5, 12–15].

23.2 Decision-Making in Surgical Debridement

Surgical debridement is the cornerstone of mucormycosis treatment and it improves survival [1, 16–18]. The majority of ROCM cases are treated by Otorhinolaryngologists with endoscopic sinus surgery. However, the extent of resection can range from simple endoscopic debridement to radical surgery involving orbital exenteration, palatal resection, and intracranial intervention. The decision is based on the disease mapping on multiple MRI sequences, but the extent of resection is still up for debate.

There is adequate evidence to show that major surgery for intracranial involvement has a poor prognosis [19–23]. High mortality was seen despite intervention in patients with intracranial involvement while those on conservative management remained stable for much longer than anticipated.

The collaterals developing from the external carotid artery were detected in those who were unsuited for anesthesia and had areas of infarction in the brain with engulfment of both internal carotid arteries. They were kept on antifungals and anticoagulants. The collateral circulation kept improving with time. Some of them recovered from hemiparesis and were stable at the time of writing this. However, the future course remains uncertain in these cases.

As a result, after consulting with the patient and their families, a team of neurosurgeons, otorhinolaryngologists, radiologists, and intensivists decides to operate on cases with intracranial involvement [24]. Intracranial intervention should focus solely on assisting the patient in reducing intracranial pressure. Radical excision of intracranial fungal lesions is not recommended [25].

23.3 Drug Sensitivity, MIC Level and Combination Drug Trials, and the Cost of Antifungal Drugs

Some of the important aspects of antifungal treatment in mucormycosis are as follows:

- The Ideal antifungal drug
- Drug resistance/Minimal Inhibitory Concentration/drug susceptibility
- Combination antifungal drugs
- Duration of antifungal drugs
- Blood–brain barrier
- Antifungal drugs for invasive antifungal infections; Cost regulation

23.3.1 The Ideal Antifungal Drug

The optimal antifungal agent for treating ROCM is the one that has a fungicidal property against that strain, has a good penetration across the blood–brain barrier in (cerebral mucormycosis) to result in a concentration that is more than the minimal inhibitory concentration, and is safe to use for longer periods of time that means it should have low side effects. So, there is no single ideal drug that fulfils all these criteria [1].

23.3.2 Drug Resistance/Minimal Inhibitory Concentration/ Drug Susceptibility

During the care of ROCM endemic surgeons and physicians confronted numerous problems. There was a variation in susceptibility to antifungals. Therefore, mere identification to species level is

not helpful. Antifungal susceptibilities vary across mucormycetes hence antifungal testing is beneficial.

Drug resistance was noted during ROCM management, where some patients on antifungals deteriorated despite a meticulous debridement based on disease mapping on MRI. Poor drug response in these cases was due to the drug resistance with high minimal inhibitory concentration (MICs) of amphotericin B. MICs can be tested by EUCAST methodology (European Committee on Antimicrobial Susceptibility Testing) [26].

Amphotericin B was the most potent drug against mucormycetes, with MICs lower than 0.5 mg/L for most of the strains. However, resistance to amphotericin B was found in five cases of *Rhizopus* strains [26]. Posaconazole is the second-line most potent drug against mucormycosis. It has the highest activity among the azoles, with an MIC value of 0.5 mg/L [26]. It is important to know the strain of mucor on culture as there are 21 clinical isolates of micromycetes. Appropriate antifungal susceptibility tests should be carried out, and susceptibility breakpoints for Mucorales and other common species of mucor should be determined [1].

23.3.3 Combination Antifungal Drugs

There are only a few studies on in vitro susceptibility tests to guide us in our treatment decisions [1]. However, a two-drug regimen (amphotericin B and Posaconazole) right from the beginning has better outcomes in patients with intracranial extension of mucor.

Although a drug of choice for Mucorales species, liposomal amphotericin B, has a poor blood–brain barrier and is highly nephrotoxic [1]. As a result, when used in combination with an azole, like posaconazole or isavuconazole, it may increase the drug concentrations in the brain. Although there haven't been many studies in the past to support this, we have enough evidence of using a combination of antifungal drugs during the mucormycosis endemic with significantly improved outcomes.

Patients were started on amphotericin B and then switched to azoles like posaconazole or isavuconazole over time. Lack of amphotericin B, pressing need to save lives, the necessity to counteract amphotericin B toxicity and in some scenarios, poor response to amphotericin B, prompted us to try various combinations [1].

Since mucormycosis is an emerging invasive fungal infection, antifungals can help manage it. Using a combination of antifungal drugs does not offer any antagonism. It instead offers the synergistic effect of the combination of amphotericin B with other antifungals; consequently, more research is worthwhile [26–30].

23.3.4 Duration of Antifungal Drugs

Patients with CNS manifestation were given amphotericin B for 1 month. However, the duration of antifungals should ideally be determined by the severity of the disease at the time of presentation, extent of surgical debridement, and the patient's systemic condition. Some people have recommended using antifungals for 6 months [1]. However, the high cost, practicality, and toxicity were some of the challenges we encountered.

23.3.5 Blood–Brain Barrier

Amphotericin B crosses the blood–brain barrier poorly and is available in low concentrations in the brain tissue in patients [31–33]. In experimental animals, cerebral spinal fluid and plasma concentration of <0.3 have been achieved [34]. During experimental studies, the azoles showed better penetration while the penetration of amphotericin B remains poor even in meningeal inflammation [33]. Intrathecal administration of amphotericin B using an Ommaya reservoir has been reported to be helpful in a few cases [34].

The patients were shifted to isavuconazole after amphotericin B due to toxicity of amphotericin in some cases and due to better cerebral penetration. The concentration of isavuconazole in the brain and plasma ratio was 1.8 after a single dose and 1 after the repeat dose [35, 36]. With

a typical dose of isavuconazole, a higher concentration of isavuconazole could be obtained in brain tissue, although, its penetration was low in cases of fungal brain abscess and was shown to be nearly zero [35].

Cerebrospinal fluid concentrations of posaconazole are highly variable, with cerebrospinal fluid to plasma ratios ranging from 2.3 to <0.01 [37–39]. Unlike amphotericin B, cerebrospinal fluid penetration of posaconazole increases in meningeal inflammation [38]. Successful treatment with posaconazole was found in 50% of CNS fungal infections [40], making it effective in cerebral mucormycosis [41, 42].

23.3.6 Antifungal Drugs for Invasive Fungal Infections; Cost Regulation

Invasive fungal infections necessitate long-term antifungal treatment. The ROCM endemic faced numerous obstacles. One of them was the high cost of the antifungal medication, which added to the patient's financial hardship. This resulted in low compliance, which resulted in high morbidity and mortality.

The path forward entails resolving present diagnostic constraints, improving sensitivity and susceptibility characteristics, developing combination techniques, and most significantly managing antifungal drug costs.

References

1. Chikley A, Ben-Ami R, Kontoyiannis DP. Mucormycosis of the central nervous system. J Fungi. 2019;5:59. https://doi.org/10.3390/jof5030059.
2. Dadwal SS, Kontoyiannis DP. Recent advances in the molecular diagnosis of mucormycosis. Expert Rev Mol Diagn. 2018;18:845–54.
3. Schelenz S, Barnes RA, Barton RC, Cleverley JR, Lucas SB, Kibbler CC, Denning DW. British Society for Medical Mycology best practice recommendations for the diagnosis of serious fungal diseases. Lancet Infect Dis. 2015;15:461–74.
4. Baldin C, Soliman SSM, Jeon HH, Alkhazraji S, Gebremariam T, Gu Y, Bruno VM, Cornely OA, Leather HL, Sugrue MW, et al. PCR-based approach targeting mucorales-specific gene family for diagnosis of mucormycosis. J Clin Microbiol. 2018;56:e00746–18.
5. Cornely OA, Alastruey-Izquierdo A, Arenz D, Chen SCA, Dannaoui E, Hochhegger B, et al. Global guideline for the diagnosis and management of mucormycosis: an initiative of the European Confederation of Medical Mycology in cooperation with the Mycoses Study Group Education and Research Consortium. Lancet Infect Dis. 2019;19:e405–21.
6. Zaman K, Rudramurthy SM, Das A, Panda N, Honnavar P, Kaur H, et al. Molecular diagnosis of rhino-orbito-cerebral mucormycosis from fresh tissue samples. J Med Microbiol. 2017;66(8):1124–9.
7. Chakrabarti A, Chatterjee SS, Das A, Panda N, Shivaprakash MR, Kaur A, et al. Invasive zygomycosis in India: experience in a tertiary care hospital. Postgrad Med J. 2009;85(1009):573–81.
8. Chakrabarti A, Das A, Sharma A, Panda N, Das S, Gupta KL, et al. Ten Years' experience in zygomycosis at a tertiary care centre in India. J Infect. 2001;42(4):261–6.
9. Chakrabarti A, Das A, Mandal J, Shivaprakash MR, George VK, Tarai B, et al. The rising trend of invasive zygomycosis in patients with uncontrolled diabetes mellitus. Med Mycol. 2006;44(4):335–42.
10. Jung J, Park YS, Sung H, Song JS, Lee SO, Choi SH, Kim YS, Woo JH, Kim SH. Using immunohistochemistry to assess the accuracy of histomorphologic diagnosis of aspergillosis and mucormycosis. Clin Infect Dis. 2015;61:1664–70.
11. Millon L, Larosa F, Lepiller Q, Legrand F, Rocchi S, Daguindau E, et al. Quantitative polymerase chain reaction detection of circulating DNA in serum for early diagnosis of mucormycosis in immunocompromised patients. Clin Infect Dis. 2013;56(10):e95–101.
12. Millon L, Herbrecht R, Grenouillet F, Morio F, Alanio A, Letscher-Bru V, et al. Early diagnosis and monitoring of mucormycosis by detection of circulating DNA in serum: retrospective analysis of 44 cases collected through the French Surveillance Network of Invasive Fungal Infections (RESSIF). Clin Microbiol Infect. 2016;22(9):810.e1–8.
13. Skiada A, Pavleas I, Drogari-Apiranthitou M. Epidemiology and diagnosis of Mucormycosis: an update. J Fungi (Basel). 2020;6(4):265.
14. Guegan H, Iriart X, Bougnoux M-E, Berry A, Robert-Gangneux F, Gangneux J-P. Evaluation of MucorGenius® mucorales PCR assay for the diagnosis of pulmonary mucormycosis. J Infect. 2020;81(2):311–7.
15. Caillot D, Valot S, Lafon I, Basmaciyan L, Chretien ML, Sautour M, et al. Is it time to include CT "reverse halo sign" and qPCR targeting mucorales in serum to EORTC-MSG criteria for the diagnosis of pulmonary mucormycosis in leukemia patients? Open Forum Infect Dis. 2016;3(4):ofw190.
16. Roden MM, Zaoutis TE, Buchanan WL, Knudsen TA, Sarkisova TA, Schaufele RL, Sein M, Sein T, Chiou CC, Chu JH, et al. Epidemiology and outcome of

zygomycosis: a review of 929 reported cases. Clin Infect Dis. 2005;41:634–53.
17. Lanternier F, Dannaoui E, Morizot G, Elie C, Garcia-Hermoso D, Huerre M, Bitar D, Dromer F, Lortholary O, French Mycosis Study Group. A global analysis of mucormycosis in France: the retro zygo study (2005–2007). Clin Infect Dis. 2012;54:S35–43.
18. Skiada A, Pagano L, Groll A, Zimmerli S, Dupont B, Lagrou K, Lass-Florl C, Bouza E, Klimko N, Gaustad P, et al. Zygomycosis in Europe: analysis of 230 cases accrued by the registry of the European Confederation of Medical Mycology (ECMM) Working Group on Zygomycosis between 2005 and 2007. Clin Microbiol Infect. 2011;17:1859–67.
19. Kasapoglu F, Coskun H, Ozmen OA, Akalin H, Ener B. Acute invasive fungal rhinosinusitis: evaluation of 26 patients treated with endonasal or open surgical procedures. Otolaryngol Head Neck Surg. 2010;143:614–20.
20. Gillespie MB, O'Malley BW Jr, Francis HW. An approach to fulminant invasive fungal rhinosinusitis in the immunocompromised host. Arch Otolaryngol Head Neck Surg. 1998;124:520–6.
21. Davoudi S, Kumar VA, Jiang Y, Kupferman M, Kontoyiannis DP. Invasive mould sinusitis in patients with haematological malignancies: a 10 year single-Centre study. J Antimicrob Chemother. 2015;70:2899–905.
22. Turner JH, Soudry E, Nayak JV, Hwang PH. Survival outcomes in acute invasive fungal sinusitis: a systematic review and quantitative synthesis of published evidence. Laryngoscope. 2013;123:1112–8.
23. Zuniga MG, Turner JH. Treatment outcomes in acute invasive fungal rhinosinusitis. Curr Opin Otolaryngol Head Neck Surg. 2014;22:242–8.
24. Ben-Ami R, Halaburda K, Klyasova G, Metan G, Torosian T, Akova M. A multidisciplinaryteam approach to the management of patients with suspected or diagnosed invasive fungal disease. J Antimicrob Chemother. 2013;68:iii25–33.
25. McCarthy M, Rosengart A, Schuetz AN, Kontoyiannis DP, Walsh TJ. Mold infections of the central nervous system. N Engl J Med. 2014;371:150–60.
26. Drogari-Apiranthitou M, Mantopoulou FD, Skiada A, Kanioura L, Grammatikou M, Vrioni G, Mitroussia-Ziouva A, Tsakris A, Petrikkos G. In vitro antifungal susceptibility of filamentous fungi causing rare infections: synergy testing of amphotericin B, posaconazole and anidulafungin in pairs. J Antimicrob Chemother. 2012;67(8):1937–40. https://doi.org/10.1093/jac/dks137.
27. Reed C, Bryant R, Ibrahim AS, et al. Combination polyene-caspofungin treatment of rhino-orbital-cerebral mucormycosis. Clin Infect Dis. 2008;47:364–71.
28. Arikan S, Sancak B, Alp S, et al. Comparative in vitro activities of posaconazole, voriconazole, itraconazole, and amphotericin B against aspergillus and Rhizopus, and synergy testing for Rhizopus. Med Mycol. 2008;46:567–73.
29. Philip A, Odabasi Z, Rodriguez J, et al. In vitro synergy testing of anidulafungin with itraconazole, voriconazole, and amphotericin B against aspergillus spp. and fusarium spp. Antimicrob Agents Chemother. 2005;49:3572–4.
30. Arikan S, Lozano-Chiu M, Paetznick V, et al. In vitro synergy of caspofungin and amphotericin B against aspergillus and fusarium spp. Antimicrob Agents Chemother. 2002;46:245–7.
31. Collette N, van der Auwera P, Lopez AP, Heymans C, Meunier F. Tissue concentrations and bioactivityof amphotericin B in cancer patients treated with amphotericin B-deoxycholate. Antimicrob Agents Chemother. 1989;33:362–8.
32. Collette N, Van der Auwera P, Meunier F, Lambert C, Sculier JP, Coune A. Tissue distribution andbioactivity of amphotericin B administered in liposomes to cancer patients. J Antimicrob Chemother. 1991;27:535–48.
33. Groll AH, Giri N, Petraitis V, Petraitiene R, Candelario M, Bacher JS, Piscitelli SC, Walsh TJ. Comparative efficacy and distribution of lipid formulations of amphotericin B in experimental Candida albicans infection of the central nervous system. J Infect Dis. 2000;182:274–82.
34. Grannan BL, Yanamadala V, Venteicher AS, Walcott BP, Barr JC. Use of external ventriculostomy and intrathecal antifungal treatment in cerebral mucormycotic abscess. J Clin Neurosci. 2014;21:1819–21.
35. Lamoth F, Mercier T, Andre P, Pagani JL, Pantet O, Maduri R, Guery B, Decosterd LA. Isavuconazole brain penetration in cerebral aspergillosis. J Antimicrob Chemother. 2019;74:1751–3.
36. Schmitt-Hoffmann AH, Kato K, Townsend R, Potchoiba MJ, Hope WW, Andes D, Spickermann J, Schneidkraut MJ. Tissue distribution and elimination of isavuconazole following single and repeat oral-dose administration of isavuconazonium sulfate to rats. Antimicrob Agents Chemother. 2017;61:e01292–17.
37. Reinwald M, Uharek L, Lampe D, Grobosch T, Thiel E, Schwartz S. Limited penetration of posaconazole into cerebrospinal fluid in an allogeneic stem cell recipient with invasive pulmonary aspergillosis. Bone Marrow Transplant. 2009;44:269–70.
38. Ruping MJ, Albermann N, Ebinger F, Burckhardt I, Beisel C, Muller C, Vehreschild JJ, Kochanek M, Fatkenheuer G, Bangard C, et al. Posaconazole concentrations in the central nervous system. J Antimicrob Chemother. 2008;62:1468–70.
39. Calcagno A, Baietto L, De Rosa FG, Tettoni MC, Libanore V, Bertucci R, D'Avolio A, Di Perri G. Posaconazole cerebrospinal concentrations in an HIV-infected patient with brain mucormycosis. Antimicrob Chemother. 2011;66:224–5.
40. Pitisuttithum P, Negroni R, Graybill JR, Bustamante B, Pappas P, Chapman S, Hare RS, Hardalo CJ. Activity of posaconazole in the treatment of central nervous system fungal infections. J Antimicrob Chemother. 2005;56:745–55.

41. Tarani L, Costantino F, Notheis G, Wintergerst U, Venditti M, Di Biasi C, Friederici D, Pasquino AM. Long-term posaconazole treatment and follow-up of rhino-orbital-cerebral mucormycosis in a diabetic girl. Pediatr Diabetes. 2009;10:289–93.

42. Davoudi S, Anderlini P, Fuller GN, Kontoyiannis DP. A long-term survivor of disseminated aspergillus and mucorales infection: an instructive case. Mycopathologia. 2014;178:465–70.